INSTRUCTOR & STUDENT RESOURCES

Aircraft Performance

An Engineering Approach

Second Edition

Mohammad H. Sadraey

CRC Press
Taylor & Francis Group

Aircraft Performance

Aircraft Performance: An Engineering Approach, Second Edition introduces flight performance analysis techniques of fixed-wing air vehicles, particularly heavier-than-aircraft. It covers maximum speed, absolute ceiling, rate of climb, range, endurance, turn performance, and takeoff run.

Enabling the reader to analyze the performance and flight capabilities of an aircraft by utilizing only the aircraft weight data, geometry, and engine characteristics, this book covers the flight performance analysis for both propeller-driven and jet aircraft. The second edition features new content on vertical takeoff and landing, UAV launch, UAV recovery, use of rocket engine as the main engine, range for electric aircraft, electric engine, endurance for electric aircraft, gliding flight, pull-up, and climb-turn. In addition, this book includes end-of-chapter problems, MATLAB® code and examples, and case studies to enhance and reinforce student understanding.

This book is intended for senior undergraduate aerospace students taking courses in Aircraft Performance, Flight Dynamics, and Flight Mechanics.

Instructors will be able to utilize an updated Solutions Manual and Figure Slides for their course.

Aircraft Performance
An Engineering Approach

Second Edition

Mohammad H. Sadraey

CRC Press
Taylor & Francis Group
Boca Raton London New York

CRC Press is an imprint of the
Taylor & Francis Group, an **informa** business

Designed cover image: Steve Dreier

Second edition published 2024
by CRC Press
6000 Broken Sound Parkway NW, Suite 300, Boca Raton, FL 33487-2742

and by CRC Press
4 Park Square, Milton Park, Abingdon, Oxon, OX14 4RN

CRC Press is an imprint of Taylor & Francis Group, LLC

First edition published by CRC Press 2017

Library of Congress Cataloging-in-Publication Data
Names: Sadraey, Mohammad H, author.
Title: Aircraft performance: an engineering approach / Mohammad H Sadraey.
Description: Second edition. | Boca Raton, FL : CRC Press, 2023. |
Includes bibliographical references and index.
Identifiers: LCCN 2022060247 | ISBN 9781032245157 (hardback) |
ISBN 9781032245171 (paperback) | ISBN 9781003279068 (ebook)
Subjects: LCSH: Airplanes—Performance. | Aerodynamics.
Classification: LCC TL671.4.S234 2023 | DDC 629.133/34—dc23/eng/20230111
LC record available at https://lccn.loc.gov/2022060247

ISBN: 978-1-032-24515-7 (hbk)
ISBN: 978-1-032-24517-1 (pbk)
ISBN: 978-1-003-27906-8 (ebk)

DOI: 10.1201/9781003279068

Typeset in Times
by codeMantra

Access the Instructor Resources: routledge.com/9781032245157

To Fatemeh Zafarani, Ahmad, and Atieh for all their love and understanding

Contents

Preface to the Second Edition

Flight is the process in which a vehicle moves through the air without any direct mechanical support from the ground. In physics, the science of the action of forces on material bodies is referred to as mechanics. Mechanics is divided into two branches: (1) dynamics and (2) statics. The branch of mechanics that deals with the motion of objects in relation to force, mass, momentum, and energy is referred to as dynamics. Flight mechanics (or flight dynamics) is the study of the motion of flying objects (e.g., aircraft, missile) through the air. It covers two main areas: (1) flight performance and (2) flight stability and control.

As an aircraft does not usually have a static motion (except for the case of a VTOL aircraft during hovering flight), we mostly deal with flight dynamics. On the other hand, there are two types of aircraft motions: (1) steady-state motion and (2) perturbed-state motion. It is customary that steady-state motion is studied in a course called flight dynamics I, and perturbed-state motion is studied in flight dynamics II. In some institutions, flight mechanics is referred to as flight dynamics I; flight stability and control is referred to as flight dynamics II.

The first topic (flight dynamics I) includes subjects such as cruising flight, maximum speed, absolute ceiling, rate of climb, range, endurance, turn rate, turn radius, and takeoff/landing run. The second topic (flight dynamics II) is mainly to examine subjects such as aircraft trim, control, stability, aircraft response to pilot input and gust, and flying qualities. The subject of aircraft performance mainly deals with the forces applied to the aircraft, but the subject of flight dynamics concentrates on various moments (either aerodynamic or non-aerodynamic) that determine the trajectory. Time span in "aircraft performance" is mostly in the range of hours, whereas time span in "flight stability and control" is primarily in the range of seconds/minutes.

The objective of this book is to introduce flight performance analysis techniques of fixed-wing air vehicles, particularly heavier-than-air craft. This subject will be interesting for aeronautical/mechanical engineers, aircraft designers, pilots, aircraft manufacturing companies, airlines, air forces, and primarily students of the field of aeronautical/aerospace engineering.

This group of individuals often faces the following questions:

1. How fast can this airplane fly on a cruising flight?
2. How high can this airplane fly?
3. How far can this airplane fly?
4. How long is the runway for takeoff?
5. How long is the runway for landing?
6. How long can this airplane be airborne?
7. How fast can this airplane climb to a certain altitude?
8. How fast can this airplane turn?
9. How tight can this airplane turn?
10. How capable is this aircraft in a maneuver?
11. What are the limits of this airplane in flight?
12. How much does it cost for this airplane to fly over a certain distance?

And, in one sentence, what is the performance of this airplane?

If one has access to a manufactured airplane, the answers to all these questions can be found through flight tests. However, the primary objective of this book is to enable the reader to answer these questions without having access to the aircraft itself. Therefore, an aircraft designer can predict the performance of an airplane during the design process, before manufacturing it. In addition, an aircraft buyer can calculate and evaluate the performance of an aircraft prior to its purchase. In this way, the buyer can compare the performances of different aircraft and choose the best one.

The performance of a military airplane is of high importance, since in an aerial mission, the fighter aircraft that has a high performance will always fulfill the mission's purpose and will win a fight. The result of an air fight depends not only on aircraft weight, configuration, cost, pilot experience, and so on but also on its capabilities, that is, flight performance. This book presents techniques and methods that enable the reader to analyze the performance and flight capabilities of an aircraft by utilizing only aircraft weight data, geometry, aerodynamic characteristics, and engine data.

Chapter 1 is devoted to the atmosphere as the flight condition. The methods to calculate atmospheric variables such as pressure, temperature, and air density as a function of altitude are presented. In Chapter 2, the flight governing equations of motion and of an air vehicle are presented, and the concept of airspeed is defined. The four major forces acting on an aircraft are weight, engine thrust, lift, and drag (i.e., aerodynamic forces). Drag and engine thrust need detailed considerations, so the techniques to calculate these forces are presented in Chapters 3 and 4.

Chapters 5–9 cover all aspects of flight performance analysis for propeller-driven and jet aircraft. Both constant-speed flights and accelerated flights are covered. In every case, we start with a mathematical equation that governs that specific flight condition. Then, an applicable algebraic equation is derived in order to perform the analysis of various flight performance areas such as maximum speed, maximum range, maximum ceiling, maximum rate of climb, and maximum endurance. Takeoff and landing performance is particularly addressed in Chapter 8. In Chapter 9, turn performance and related topics such as pull-up are covered. The technique to plot the flight envelope (i.e., *V-n* diagram) in order to find the maximum g-load on an air vehicle is presented in this chapter. In addition, advanced materials in flight mechanics such as fastest turn, tightest turn, turn rate, turn radius, and flight maneuvers are investigated.

There are complex performance cases and flight missions where analysis requires a long and complex mathematical solution. A popular and powerful technique for such cases is numerical methods. Chapter 10 is devoted to the performance analysis of aircraft using numerical methods, mainly using the MATLAB® software package (i.e., MATLAB codes).

The appendices are devoted to real statistics of current aircraft and flight records throughout the history of flight. This information gives the readers an insight and a criterion to compare their calculated and achieved results. This book is prepared such that it can be covered as an undergraduate course in aerospace/aeronautical engineering programs at the junior level. Solutions manual and figure slides are available for qualified instructors adopting the text.

Currently, the International System of Units (SI), or metric units (Newton, kilogram, meter, second, Watt, and Kelvin) is the standard system of units used around the world, except in the United States. The English Engineering System, or British/Imperial Units (pounds, slug, feet, second, and Rankine), is still the primary system of units in the USA. In addition, many Federal Aviation Regulations (e.g., stall speed and altitude) are written using British units. This situation is gradually changing, particularly in the aerospace community.

The United States is making progress toward the voluntary implementation of SI units in engineering. Several NASA (National Aeronautics and Space Administration) laboratories have made SI units mandatory for all technical publications, although units can be shown in duplicate sets. Moreover, the AIAA (American Institute of Aeronautics and Astronautics) has a policy of encouraging the use of SI units in papers published in its journals. Hence, in this edition, the unit is more consistent, and more SI units are implemented in examples, case studies, and problems.

Hence, familiarity with both systems of units is still necessary for engineers and engineering students. Current engineering students should be familiar and be able to work professionally with both systems. For this reason, both unit systems are employed in worked examples and end-of-chapter problems in this book. The readers are encouraged to familiarize themselves with both unit systems. Readers are expected to have basic knowledge of dynamics, calculus, and aerodynamics.

I am enormously grateful to the Almighty for the opportunity to serve the aerospace community by writing this book. I acknowledge many contributors and photographers who contributed to this book. I am especially grateful to those who provided great aircraft photos to this text: Alex Snow (Russia); Ryosuke Ishikawa (Japan); Kas van Zonneveld (the Netherlands); Daniel Mysak (Austria); Gustavo Corujo (Canada); Steve Dreier (United Kingdom); Jan Selig (Germany); Georgi Petkov (Bulgaria); Maurice Kockro (Germany); Fabian Dirscherl; Capenti Fabrizio (Italy); and Weimeng (China); and www.airliners.net. In addition, my effort was helped immeasurably by many insights and constructive suggestions provided by students and instructors in the past 26 years. Unattributed figures are held in the public domain and are either from the U.S. government departments and agencies or from Wikipedia.

In this second edition, the entire manuscript was extensively revised and updated, new materials were added, and a few topics were deleted. All chapters have been brought up to date to introduce some of the new terminology, concepts, and specific aircraft systems that have appeared over the past 7 years. Furthermore, this edition provides real-life case studies (e.g., Cessna 208 Caravan, Cessna Citation, Cessna 560, DC-9-30, Pilatus PC-9, Embraer EMB 312 Tucano, Hawker 800, Cessna 172, Boeing 737, Boeing 747-400, Boeing 777-200, Gulfstream G-650, Lockheed Martin F-16 Fighting Falcon, and Boeing F/A-18) that link theory to industry application, as well as historical and future perspectives with regards to aviation. The revisions made some of the materials clearer and easier to understand. The typos and errors have been corrected.

Putting a book together requires the talents of many people, and talented individuals abound at CRC Press - Taylor & Francis Group. My sincere gratitude goes to Kyra Lindholm, Editor for Aerospace/Aviation, for initiating and coordinating the publication process of the second edition. I especially owe a large debt of gratitude to my students, colleagues, and reviewers. Their ideas, suggestions, and criticisms have

helped me to write more clearly and accurately and have influenced markedly the evolution and revision of this edition.

Mohammad H. Sadraey
October 30, 2022

Author

Dr. Mohammad H. Sadraey is a Professor in the School of Engineering, Technology, and Aeronautics at the Southern New Hampshire University, and the national president of Sigma Gamma Tau honor society. Dr. Sadraey's main research interests are in aircraft design techniques, robust nonlinear control, autopilot, design and automatic control of unmanned air vehicles, and manned–unmanned aircraft teaming. He received his M.Sc. in Aerospace Engineering in 1995 from RMIT, Australia, and his Ph.D. in Aerospace Engineering from the University of Kansas, USA, in 2006. He is a senior member of the American Institute of Aeronautics and Astronautics (AIAA), and is in Who's Who in America for many years. He has over 26 years of professional experience in academia and industry. He is also the author of eight textbooks including *Aircraft Design: A Systems Engineering Approach, Design of Unmanned Aerial Systems*, published by Wiley Publications in 2012, and 2019, and *Aircraft Performance Analysis* by CRC in 2016 and "Flight Stability and Control" by Springer Nature in 2022.

List of Symbols

Symbols	Names	Units
a	Speed of sound	m/s, ft/s
a	Acceleration	m/s^2, ft/s^2
a	Lift curve slope	1/rad
ac	Aerodynamic center	—
a_c	Centripetal acceleration	m/s^2, ft/s^2
AR	Aspect ratio	—
b	Wing span	m, ft
C	Specific fuel consumption	lb/h/lb, N/h/kW, lb/h/hp, 1/s, 1/m
C	Mean aerodynamic chord	m, ft
C_D	Drag coefficient	—
C_{D_o}	Zero-lift drag coefficient	—
C_{Di}	Induced drag coefficient	—
C_{D_w}	Wave drag coefficient	—
C_f	Skin friction coefficient	—
C_L	Lift coefficient	—
$C_{L_{max}}$	Maximum lift coefficient	—
cp	Center of pressure	—
D	Drag force, drag	N, lb
E	Endurance	hour, second
e	Oswald span efficiency factor	—
F	Force, friction force	N, lb
FAA	Federal Aviation Administration	
FAR	Federal Aviation Regulations	
F_C	Centrifugal force	N, lb
g	Gravity constant	$9.81\,m/s^2$, $32.2\,ft/s^2$
G	Fuel weight fraction	—
GA	General Aviation	—
h	Altitude	m, ft
i_t	Tail incidence	deg, rad
i_T	Engine incidence	deg, rad
I	Moment of inertia	$kg\,m^2$, $slug\,ft^2$
I	Current	Ampere
ISA	International Standard Atmosphere	—
K	Induced drag factor	—
KEAS	Knot Equivalent Airspeed	knot
KTAS	Knot True Airspeed	knot
knot	Nautical mile per hour	nmi/h
L	Fuselage length	m, ft
L	Lift force, lift	N, lb

(*Continued*)

Symbols	Names	Units
L	Lapse rate	0.0065°C/m, 0.002°C/ft
$(L/D)_{max}$	Maximum lift-to-drag ratio	—
M	Mach number	—
m_f	Fuel mass	kg, slug
m_{TO}	Takeoff mass	kg, slug
MTOW	Maximum takeoff weight	N, lb
MAC	Mean aerodynamic chord	m, ft
n	Load factor	—
ω	Turn rate	rad/s, deg/s
P	Pressure	N/m^2, Pa, lb/in^2, psi
P	Power	kW, hp
P_R	Required power	kW, hp
P_A	Available power	kW, hp
P_{Ex}	Excess power	kW, hp
q	Dynamic pressure	N/m^2, Pa, lb/in^2, psi
Q	Fuel flow rate	kg/s, lb/s
R	Range	m, km, ft, mile, mi, nmi
R	Turn radius	m, ft
R	Air gas constant	287.26 J/kg K
R	Radius of action	km, ft
Re	Reynolds number	—
ROC	Rate of climb	m/s, ft/min, fpm
ROD	Rate of descent	m/s, ft/s
rpm	Revolutions per minute	Rev/min
S	Gross wing area	m^2, ft^2
S_{exp}	Exposed wing area	m^2, ft^2
S_A	Airborne section of the takeoff run	m, ft
S_G	Ground roll	m, ft
S_L	Landing run	m, ft
S_{ref}	Reference wing area	m^2, ft^2
S_t	Tail area	m^2, ft^2
S_{TO}	Takeoff run	m, ft
S_w	Wing area	m^2, ft^2
S_{wet}	Wetted area	m^2, ft^2
SFC	Specific fuel consumption	N/h kW, lb/h·hp, lb/h/lb
t	Time	Second, hour
T	Engine thrust	N, lb
T	Temperature	°C, °F, K, °R
T_{req}	Required thrust	N, lb
T_{av}	Available thrust	N, lb
V^*	Corner speed	knot, m/s, ft/s
V	Velocity, speed, airspeed	m/s, ft/s, km/h, mi/h, knot
V_A	Maneuver speed	m/s, ft/s, km/h, mi/h, knot
V_D	Dive speed	m/s, ft/s, km/h, mi/h, knot
V_E	Equivalent airspeed	m/s, ft/s, km/h, mi/h, knot

(*Continued*)

Symbols	Names	Units
V_{ft}	Fastest turn airspeed	knot, m/s, ft/s
V_{LOF}	Liftoff speed	m/s, ft/s, km/h, mi/h, knot
V_g	Gust speed	ft/d, m/s, knot
V_G	Ground speed	m/s, ft/s, km/h, mi/h, knot
V_{max}	Maximum airspeed	m/s, ft/s, km/h, mi/h, knot
$V_{max\ E}$	Maximum endurance airspeed	m/s, ft/s, km/h, mi/h, knot
$V_{max\ R}$	Maximum range airspeed	m/s, ft/s, km/h, mi/h, knot
V_{mc}	Minimum controllable speed	m/s, ft/s, km/h, mi/h, knot
$V_{min\ D}$	Minimum drag airspeed	m/s, ft/s, km/h, mi/h, knot
$V_{min\ P}$	Minimum power airspeed	m/s, ft/s, km/h, mi/h, knot
V_{NE}	Never exceeded airspeed	m/s, ft/s, km/h, mi/h, knot
V_R	Rotation speed	m/s, ft/s, km/h, mi/h, knot
$V_{ROC_{max}}$	Maximum rate of climb airspeed	m/s, ft/s, km/h, mi/h, knot
V_s	Stall airspeed	m/s, ft/s, km/h, mi/h, knot
V_T	True airspeed	m/s, ft/s, km/h, mi/h, knot
V_{TO}	Takeoff speed	m/s, ft/s, km/h, mi/h, knot
V_{tt}	Tightest turn airspeed	knot, m/s, ft/s
V_W	Wind speed	m/s, ft/s, km/h, mi/h, knot
W	Weight	N, lb
W_{TO}	Takeoff weight	N, lb
W_f	Fuel weight	N, lb
Y	Side force	N, lb
x, y, z	Displacement in x, y, and z direction	m, ft
Greek Symbols		
α	Angle of attack	degree, radian
β	Sideslip angle	degree, radian
γ	Climb angle	degree, radian
θ	Pitch angle, pitch attitude	degree, radian
θ	Temperature ratio	—
ϕ	Bank angle	degree, radian
δ	Pressure ratio	—
δ_f	Flap deflection	degree, radian
σ	Air density ratio	—
ρ	Air density	kg/m^3, slug/ft^3
μ	Dynamic viscosity	kg/m s, lb s/ft^2
μ	Friction coefficient	—
η_P	Propeller efficiency	—
Λ	Sweep angle	degree, radian
ω	Angular velocity	rad/s, deg/s, rpm
ψ	Yaw angle, heading angle	degree, radian

1 Atmosphere

1.1 INTRODUCTION

An aircraft, as the name implies, is a vehicle that moves (flies) in air (i.e., atmosphere). The environment is the medium in which an aircraft is flying. Hence, air is a significant parameter of an aircraft's flight. Aerospace vehicles are divided into two major groups: (1) aerial vehicle, aircraft, or airplane; (2) space vehicle, spacecraft, or space plane. An aircraft is capable of flight inside a gas medium (i.e., air) but not in vacuum (i.e., space); otherwise, it would be called a spacecraft. A spacecraft is designed to fly in space, but in order to do that, it must be launched into space. Spacecraft sometimes returns to Earth, such as the Space Shuttle. In such cases, a spacecraft is an aircraft as well.

Air is the primary constituent of the atmosphere. To study the performance of an aircraft, we must comprehend the properties of air. Since there are several parameters of air that influence an aircraft's performance, we have to examine the atmosphere. The major parameters of air are density, pressure, and temperature. These parameters are functions of altitude, time of year, and location. In this chapter, we examine the relationship between these parameters as functions of altitude and time of year. These calculations are a prerequisite for aircraft performance analysis. Since there must be a benchmark for analysis, we will introduce a standard atmosphere called the *International Standard Atmosphere* (ISA). If you are able to analyze an aircraft's performance in an ISA condition, it should be easy to determine the performance in a nonstandard condition.

The atmosphere is a dynamic system that is continuously changing. There are several phenomena that influence an aircraft's performance: wind, gust, disturbance, lightning, rain, snow, hail, hurricane, tornado, and humidity. Although these are parameters of meteorology, both the pilot and the aircraft performance engineer must be familiar with atmospheric conditions for a safe flight. This information helps pilots to decide whether or not to take off in a specific flight condition. For these reasons, atmospheric phenomena are also briefly presented.

One of the duties of an aircraft performance engineer is to prepare an instruction manual for pilots that include tables, charts, graphs, and data. To perform this job, one must determine and specify the limits of an aircraft and guide pilots to a safe flight. The major limits of a safe flight are imposed by the atmosphere; hence, several hints are emphasized to assist the reader in distinguishing safe from unsafe atmospheric flight conditions.

The certification program of a transport aircraft usually requires the aircraft to be tested in a variety of atmospheric conditions. For instance, in 2014, an Airbus A350 test aircraft headed to Canada for "cold-weather testing" as part of the A350-900 certification program. Atmospheric research is an ongoing program for NASA. For example, since 2010, NASA and NOAA scientists have been using a Global Hawk

DOI: 10.1201/9781003279068-1

unmanned aerial vehicle (UAV) to conduct atmospheric research over Guam as part of the Airborne Tropical Tropopause Experiment.

Two important performance parameters are speed of sound and altitude. Speed of sound is mostly stated in terms of Mach number. Altitude has several applications and implications. These two variables are dealt with in more depth and explained in more detail in this chapter. They are used in a variety of performance problems throughout this book.

1.2 GENERAL DESCRIPTION OF ATMOSPHERE

The Earth is surrounded by a thin gaseous envelope called the atmosphere. The atmosphere is a dynamic system, with a number of active subsystems. Life on Earth is supported by the atmosphere, solar energy, and the planet's magnetic fields. The atmosphere absorbs energy from the Sun, recycles water and other chemicals, and works with electrical and magnetic forces to provide a moderate climate. The atmosphere also protects us from high-energy radiation and the frigid vacuum of space. The energy exchange that continually occurs between the atmosphere and the Earth's surface and between the atmosphere and space produces a phenomenon called weather.

The atmosphere is a gaseous layer surrounding the Earth and is held by the Earth's gravity. The atmosphere has a mass of about 5×10^{18} kg, three-quarters of which are within about 11 km (36,000 ft) of the Earth's surface. More than 99% of the atmosphere [1] is within 30 km of the sea level. This thin gaseous blanket is an integral part of the planet. The thickness of the atmosphere is about 100 km or 62 miles, beyond which the sky is not blue anymore, it is black. Figure 1.1 illustrates the Earth, its atmosphere, an aircraft in an atmospheric trajectory, and a satellite in a space orbit. When one views the atmosphere from the ground, it seems to be extremely deep.

FIGURE 1.1 The Earth, aircraft trajectory, and satellite orbit.

But when the thickness of its visible section is compared to the radius of the Earth (6,371 km), the atmosphere is seen to be a shallow layer.

The major component of the atmosphere is air. It not only provides the air that we breathe but also acts as a shield to protect us from dangerous radiation emitted by the Sun. If, like the Moon, the Earth had no atmosphere, our planet would not only be lifeless, but many of the processes and interactions that make the surface such a dynamic place could not operate.

There is no definitive answer to the question, "how much is the thickness of the atmosphere?" since the atmosphere gets thinner at a higher altitude. The atmosphere does not abruptly end at any given altitude but becomes progressively thinner with altitude. At altitudes of about 300 km, there is about one molecule of air per cubic kilometer. There is no universally accepted definition of how much air in a given volume constitutes the presence of an atmosphere. However, there are two answers to this question. From the astronautic point of view, the atmosphere thickness is 100 km (62 miles).

By international convention, the Karman line marks the beginning of space where human travelers are considered astronauts. This is the commonly accepted border of space (and is called Karman line), since the sky is black beyond this altitude. However, air may be found even up to an altitude of 1,000 km [2] from the Earth's surface, so the atmosphere thickness may be assumed to be 1,000 km.

Aerial vehicles are able to fly only in lower sections of the atmosphere. The aerodynamic forces and moments by which an aircraft is able to suspend and move are generated only in the presence of air. The knowledge of properties of air enables the reader to analyze an aircraft's performance accurately.

1.3 MAJOR COMPONENTS

The major component of the atmosphere is called air. Even today, the term "air" is sometimes used as if it were a specific gas, which, of course, it is not. The envelope of air is a mixture of many discrete gases, each with its own specific physical properties, in which varying quantities of tiny solid particles and water droplets are suspended. The composition of air is not constant; it varies from time to time, and from place to place. If the water vapor, dust, and other variable components were removed from the atmosphere, we would find that its makeup is very stable up to an altitude of about 80 km. In general, the concentration of the gas in the atmosphere exists in a steady-state condition.

The air is primarily composed of nitrogen (N_2, 78%), oxygen (O_2, 20.9%), and argon (Ar, 0.93%). A myriad of other very influential components are also present, which include water (H_2O, 0%–4%), "greenhouse" gases or ozone (O_3, 0.01%), and carbon dioxide (CO_2, 0.01%–0.1%). In the following sections, the major components of air and their features are introduced.

1.3.1 Oxygen and Nitrogen

Two gases, nitrogen and oxygen, make up 99% of the volume of clean, dry air. Although these gases are the most plentiful components of the atmosphere and are

of great significance to life on Earth, they are of little or no importance in affecting weather phenomena. The remaining 1% of dry air is mostly the inert gas argon (0.93%) plus tiny quantities of a number of other gases. Oxygen is the most important element of air in generating the engine thrust for air-breathing engines. Even though nitrogen makes up more than 78% of the atmosphere, it is relatively unimportant in terms of thrust generation. The concentration of nitrogen and oxygen in the atmosphere is almost stable.

1.3.2 Carbon Dioxide

Carbon dioxide, although present in only minute amounts (0.04%), is nevertheless a meteorologically important constituent of air. The concentration of carbon dioxide in the atmosphere is not stable, and it varies from time to time and location to location. Natural sources of generation of carbon dioxide are volcanos and burning trees (wildfire). Although the proportion of carbon dioxide in the atmosphere is relatively uniform, its percentage has been rising steadily for more than a century. This overall rise is attributed to the burning of fossil fuels, such as coal and oil. Parts of the additional carbon dioxide are absorbed by the waters of the ocean or is used by plants, but nearly a half remains in air.

Carbon dioxide is of great interest to meteorologists because it is an efficient absorber of energy emitted by Earth (through ground surface radiation) and thus influences the heating of the atmosphere. The precise impact of the increased carbon dioxide is difficult to predict, but most atmospheric scientists believe that it will bring about the warming of the lower atmosphere (i.e., global warming) and thus will trigger global climate change. Carbon dioxide has a negative impact on aircraft performance as it causes an air-breathing engine to generate less thrust.

1.3.3 Water Vapor

The amount of water vapor in air varies considerably, from practically none at all up to about 4% by volume. Water vapor is the source of all clouds and precipitation. However, water vapor has other roles. Like carbon dioxide, it has the ability to absorb heat radiated by Earth as well as some solar energy. When water changes from one state (e.g., liquid) to another (e.g., vapor), it absorbs or releases heat. Water vapor in the atmosphere transports this latent heat from one region to another, and it is the energy source that helps drive many atmospheric hazardous phenomena such as storms and hurricane.

Because the source of water vapor in the atmosphere is evaporation from the Earth's surface (such as lakes and oceans), its concentration usually decreases rapidly with height, and most water vapor is found in the lowest 5 km of the atmosphere. Near the Earth's surface, the water vapor content ranges from a fraction of 1% over deserts and polar regions to about 4% in tropical regions. Water vapor affects the air density as discussed in Section 1.7. The aircraft aerodynamic forces and moments, which influence the flight performance, are directly proportional to the air density.

1.3.4 Aerosols

The movements of the air are sufficient to keep a large quantity of particles suspended within it. Although visible dust sometimes clouds the sky, these relatively large particles are too heavy to stay in air for very long. Still, many particles are microscopic and remain suspended for considerable periods of time. They may originate from many sources, both natural and human made, and include sea salts, fine soil blown into air, smoke and soot from fires, pollen from trees and plants, and ash and dust from volcanic eruptions. These tiny solid and liquid particles are called aerosols.

Aerosols are most numerous in the lower atmosphere near their primary source. However, the upper atmosphere is not free of them because some dust is carried to high altitudes by rising currents of air, and other particles are contributed by meteoroids that burn and disintegrate as they enter the atmosphere.

Aerosols can absorb and reflect incoming solar light and radiation. For example, when ash fills the sky following volcanic eruption, the amount of sunlight reaching the Earth's surface will be significantly reduced. In addition, many act as surfaces on which water vapor may condense; this is an important function in the formation of clouds and fog. Furthermore, aerosols contribute to an optical phenomenon we have all observed – the varied hues of red and orange at sunrise and sunset. Aerosols affect aircraft performance and can cause flight hazards to aircraft, such as shutting down aircraft engines and reduced visibility. For instance, on May 5, 2013, in an area important to air traffic between North America and Asia, thousands of flights canceled or diverted after Alaska's Mount Cleveland volcano eruptions spew ash nearly 15,000 ft.

1.4 ATMOSPHERIC LAYERS

The blanket of air that surrounds the Earth reaches over 500 km [3], and its envelope changes from the ground. Various organizations [4] and countries have different classifications of atmospheric layers, which have been grouped [5] into four to seven layers. In practice, these classifications are based on aviation, astronautics, and meteorology. The International Civil Aviation Organization (ICAO) is a civilian body that administers the civil flights and airlines. The ICAO has named the five layers of the atmosphere as follows: (1) troposphere, (2) stratosphere, (3) mesosphere, (4) thermosphere or ionosphere, and (5) exosphere. Figure 1.2 shows the features of these layers. These five distinct layers have been identified using thermal characteristics, chemical composition, movement, and density. No aircraft can fly in the mesosphere, ionosphere, and exosphere due to lack of sufficient air. This section introduces mainly the first two layers.

An altitude of 18,000 ft is the altitude after which oxygen is not enough for breathing. Any aircraft that is flying beyond this altitude must be equipped with the air pressure system. According to Federal Aviation Regulations (FAR) [6] Part 91 (Section 91.211), no person may operate a civil aircraft at cabin pressure altitudes above 12,500 ft unless they use supplemental oxygen.

In a civil transport aircraft, a section of fuselage is pressurized to provide a comfortable place for pilots, crew, and passengers. An air-conditioning system increases

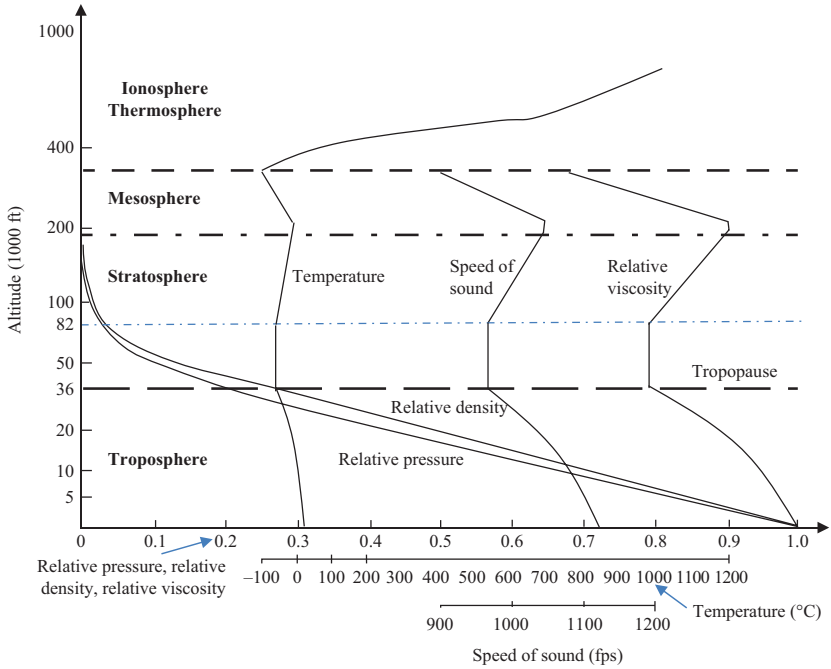

FIGURE 1.2 Atmospheric parameters of various layers.

the air pressure from about 0.2 atm up to about 0.85 atm. In military fighters, instead of a pressurized cabin, pressurized air is provided through a special hose just for the pilot. Above 120,000 ft altitude, there is not enough air (to be mixed with fuel) for combustion of the aircraft engine. Thus, this altitude is assumed to be the absolute ceiling of all types of air vehicles.

1.4.1 Troposphere

The troposphere (the first layer) starts at the Earth's surface and extends up to a mean of about 11 km high (36,089 ft). This part of the atmosphere is densest. As you climb higher in this layer, the temperature drops from about 15°C to −56°C. The troposphere is known as the lower atmosphere. The troposphere is the region where almost all weather phenomena take place and the region of rising and falling packets of air. The air pressure at the top of the troposphere is only 10% of that at sea level (0.1 atm). The troposphere is thicker over the tropics than over the polar regions and thicker during the summer than winter. The average decrease of temperature in the troposphere is about 6.5°C per 1,000 m or 3.5°F per 1,000 ft.

There is a thin buffer zone between the troposphere and the next layer called the *tropopause*. Almost all general aviation (GA) and turboprop aircraft fly within this region. Most large jet transport aircraft fly close to this zone due to the reasons discussed in later sections. Despite being the shallowest of the atmosphere's five layers, the troposphere contains 80% of the atmosphere's mass.

1.4.2 Stratosphere

Above the troposphere is the stratosphere (the second layer), where airflow is mostly horizontal. The stratosphere starts just above the troposphere (11 km; or 36,000 ft) and extends to 50 km high. Compared to the troposphere, this layer is dry and less dense. The temperature in the lower region of the stratosphere (up to 20 km) remains relatively constant at −56°C and then increases gradually from −56°C to −3°C in the upper region, due to the absorption of UV radiation. The ozone layer, which absorbs and scatters the solar UV radiation, is in this layer. The *stratopause* separates the stratosphere from the next upper layer. The stratosphere contains about 19.9% of the total mass of the atmosphere. Therefore, 99% of "air" is located in the troposphere and the stratosphere.

In the upper stratosphere, heating is almost exclusively the result of UV radiation being absorbed by the ozone layer. In the lower stratosphere where temperature does not vary with height, heating is the result of both absorption of solar UV radiation and absorption of thermal radiation from the Earth's surface. The temperature characteristics of the stratosphere avoid vertical motions of the air masses. The stratosphere has very low moisture content and features strong horizontal winds.

Modern jet transport aircraft cruise in the lower stratosphere. The turbojet-powered supersonic passenger airliner Aerospatiale-BAC Concorde (retired on November 26, 2003) used to fly in the stratosphere well above the tropopause. When early aircraft first started to fly at a high altitude, conditions were very uncomfortable for the crew. The low density and pressure meant that oxygen masks had to be worn, and, at low temperatures, even the heavy fur-lined clothing was barely adequate. Nowadays, the cabins of high-altitude airliners are pressurized, and air is heated so that passengers are unaware of the external conditions.

Above every seat in an airliner, there is an emergency oxygen mask to be used in the event of a sudden failure of the pressurization system. Despite the low external air temperature in the stratosphere, supersonic aircraft has a problem that surface friction heats the aircraft up during flight, so it is important to provide a means to keep the cabin cool enough. An altitude of 65 km is where aerodynamic heating of NASA's Space Shuttle became important during re-entry into the Earth's atmosphere from space.

1.5 INTERNATIONAL STANDARD ATMOSPHERE

Any aircraft is expected to perform in a variety of air and flight conditions (i.e., altitudes, temperature, and pressures). These consist of various temperature and pressure values that the aircraft is desired to fly in its lifetime. On any given day, it is very likely that the atmosphere will not be standard. When an aircraft is taking off from an airport and lands on another airport, the air conditions at both places are not necessarily the same. One of the requirements that are given to an aircraft designer is aircraft flight conditions. To provide a common basis for comparing the performance features of various aircraft, it is desirable to establish standards for atmospheric properties. The standards will also allow for the calibration of mechanical altimeters.

In addition, for flight tests of an aircraft, the results would be different, if the tests were performed on different days of a year. However, the results can become comparable when they reduced to standard conditions.

Although the aircraft is designed to fly in a variety of flight conditions, when it comes to performance specifications, they must be defined so that other people can evaluate the aircraft's performance. Therefore, there must be a flight condition in which the performance of several aircraft could be compared. In a specific country, this could be a major city in a dominant atmospheric condition (i.e., the first day of spring).

Most aircraft are designed to be sold to other countries or are expected to be able to fly under the atmospheric conditions in other countries. In addition, the atmospheric condition varies throughout the year. This necessitates the definition of a unified atmospheric condition. The ICAO has defined a unique atmospheric condition that is internationally accepted. It is called the International Standard Atmosphere [7], which is based on the 1959 ARDC Model Atmosphere [8]. It is noticeable that the U.S. standard atmosphere is the same as the ICAO atmosphere for altitudes below 20,000 m. The difference is due to the specific latitudes of the United States.

When we consider the ISA condition, we do not need to know what the season of the year is or where the flight place is located. Thus, the performance of all aircraft could be compared based on this unified and internationally accepted flight condition. The standard ISA atmospheric conditions seldom exist.

One of the reliable sources of statistics for an aircraft's performance is *Jane's All the World's Aircraft* [9]. It is published yearly and introduces the latest aircraft data that are produced by all countries in the world. The data include aircraft type, manufacturer, year of production, details of wing, tail, landing gear, powerplant, geometry, weight, and the most important one – performance specifications. It is notable that the performance specifications of most aircraft in Reference [9] are defined frequently in ISA condition. This standard leads to having a unique criterion among airlines, pilots, designers, performance engineers, and even marking and sales representatives.

There are considerable variations in those properties of the atmosphere with which an aircraft's performance is concerned, namely, temperature, pressure, and density. Since the performance of aircraft and engine depends on these three factors, it will be obvious that the actual performance of an aircraft does not give a true basis of comparison with other airplanes. This is another reason that the ISA has been adopted.

The properties assumed for this standard atmosphere in temperate regions are those given in Figure 1.3. If the actual performance of an airplane is measured under certain conditions of temperature, pressure, and density, it is possible to determine what would have been the performance under the conditions of the standard atmosphere. Thus, it can be compared with the performance of some other airplane that has been similarly reduced to standard conditions.

The cornerstone of the standard atmosphere is a defined variation of temperature with altitude, based on experimental evidence. It consists of a series of straight lines, some vertical and some inclined. The ISA condition is defined as the atmospheric condition at the altitude of sea level (0 m) as follows:

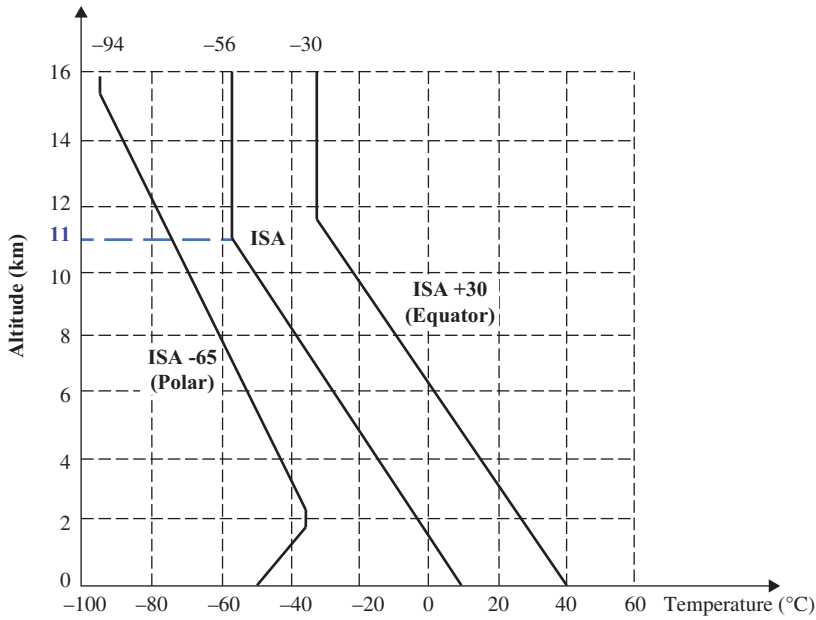

FIGURE 1.3 Difference in temperature variations at three locations.

Pressure:

$$P_o = 101{,}325\,\text{N/m}^2 = 14.7\,\text{psi} = 2{,}116.2\,\text{lb/ft}^2 = 760\,\text{mm Hg} = 29.92\,\text{in. Hg}$$
$$\textit{Temperature}: \; T_o = 15°\text{C} = 288.15\,\text{K} = 518.69°\text{R} = 59°\text{F}$$
$$\textit{Air density}: \; \rho_o = 1.225\,\text{kg/m}^3 = 0.002378\,\text{slug/ft}^3 \tag{1.1}$$

Air: Dry perfect gas

Temperature gradient: From sea level to the start of the second layer (i.e., tropopause) at which the temperature is −56°C, it is −0.002°C per foot.

These are the base values [10] for the standard atmosphere. The subscript *o* indicates that these parameters are defined at sea level. Pressure, temperature, and air density at higher altitudes are calculated by the mathematical models that are presented in the next section. It must be clarified that the term "sea level" is the level of the free seas or oceans, not other seas. The levels of seas that are not connected to oceans are higher or lower than free sea level. Moreover, the term "sea level" does not mean that the aircraft must necessarily fly by having flown exactly at this level, since it is not safe to fly while part of the aircraft has contact with water.

Figure 1.3 illustrates temperature variations at three locations of the Earth, namely, standard (ISA), tropical (nonstandard) or ISA + 30, and polar (nonstandard)

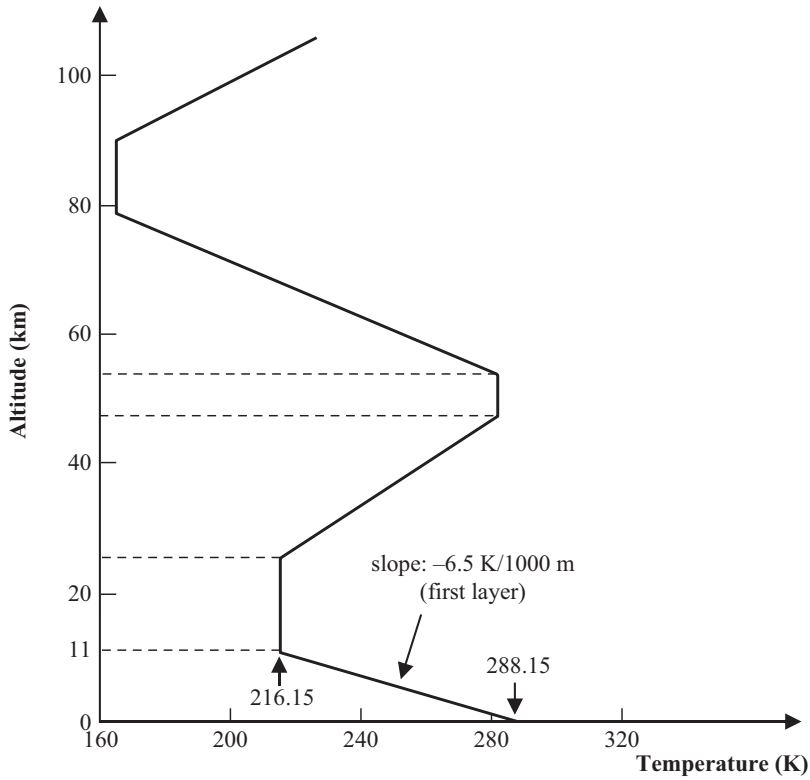

FIGURE 1.4 Temperature distribution in the standard atmosphere.

or ISA − 70 weather for the first two layers. The middle graph shows the variation of the temperature in ISA condition. Based on this graph, the temperature is 15°C at sea level, then decreases with a linear rate up to 11,000 m altitude, and then remains constant at −56°C above this altitude. The right graph demonstrates the variation of the temperature in tropical condition that is 45°C at sea level and decreases with a linear rate up to about 11,540 m at −30°C. Then, the temperature remains constant in the second layer. The left graph is for polar condition and starts at −50°C. This figure shows the highest and lowest temperatures at sea level. Figure 1.4 illustrates the variations of temperature for all atmospheric layers up to 100,000 km.

Since there could be infinite numbers of nonstandard conditions, we first have to specify their differences and then all parameters are calculated. In most cases, pressure in any condition (standard and nonstandard) may be assumed as constant and only a function of altitude, not of location on Earth. The main difference between standard and nonstandard conditions is their temperatures [11]. Other parameters could be readily found through calculations. For instance, when we say an aircraft is flying at ISA + 12, we mean that the temperature at sea level is 15°C + 12°C or 27°C. Then, the pressure is the same for standard cases, but the air density must be calculated through the tools that are presented in the next section.

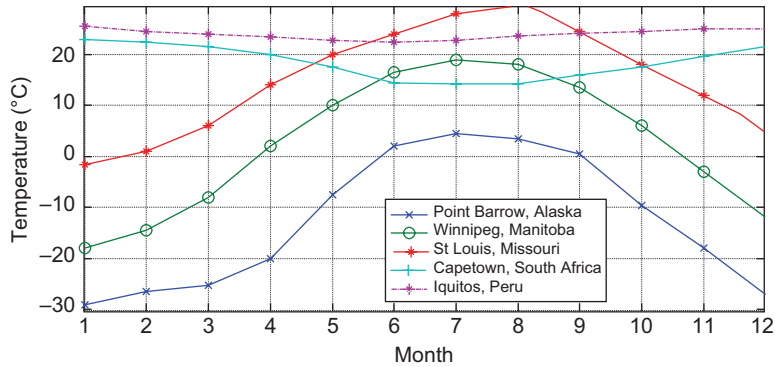

FIGURE 1.5 Mean monthly temperatures for five cities located at different latitudes.

Figure 1.5 illustrates the mean monthly temperatures [12] for five cities located at different latitudes. Note that Cape Town, South Africa, and Iquitos, Peru experience winter in June, July, and August, since they are located at the southern hemisphere. These cities only have a few days in ISA condition in a year.

Such a table is given in Appendix A for SI units and in Appendix B for English engineering units. Look at these tables carefully and become familiar with them. They are the data for the standard atmosphere. The first column gives the geometric altitude. The second, third, and fourth columns give the corresponding standard values of temperature, pressure, and density, respectively, for each altitude. We emphasize again that the standard atmosphere is a reference atmosphere only and does not certainly predict the actual atmospheric properties that may exist at a given time and place.

1.6 ATMOSPHERIC PARAMETERS

Aircraft performance depends heavily on atmospheric parameters. All atmospheric parameters could be measured at any altitude and location through flight test by using an appropriate measurement device. This book is about analysis and calculation; thus, we are going to calculate atmospheric parameters by employing the engineering techniques and mathematical calculations. This section introduces the tools to calculate temperature (T), pressure (P), air density (ρ), and viscosity (μ). Since current air vehicles are able to fly only up to about the middle of the second layer, we will discuss how to calculate these four atmospheric parameters only for the first two atmospheric layers (troposphere and stratosphere).

1.6.1 Temperature

Although we are all familiar with temperature as a means of hotness or coldness, it is not easy to provide a definition for it. Even thermodynamics textbooks such as

Reference [2] do not provide an exact fundamental physical definition for temperature. The temperature of a body is often explained as a quantity that indicates how hot or cold the body is. The temperature is an indication of the amount of heat energy stored inside a control volume of gas, liquid, or solid. The temperature is related to the mean velocity of free molecules of a body. By virtue of the molecular motion, a molecule's kinetic energy is sensed as the temperature of the body. Due to this definition, the mean velocity of free molecules at absolute zero temperature is zero. The heat is transferred from a body at a higher temperature to the one at a lower temperature.

Air is a type of gas; when the thermal energy is added (i.e., heat is transferred), its temperature increases. As air moves from place to place, its temperature varies based on the amount of heat that is transferred into or out of it. The main source of the air energy is the Sun; since the Earth absorbs the Sun's energy faster than the atmosphere, the Earth's heat energy is also transferred into air. During the day, air absorbs thermal energy from the Sun's radiation, and heat is also transferred from the Earth to air. During the night, the Earth's energy and air's thermal energy are transferred out to space through radiation. Thus, the air temperature changes throughout the day and night, and also place to place.

As Figure 1.3 shows, the air temperature varies as we climb. In the first layer (up to 11,000 m or 36,000 ft), the temperature is constantly decreasing. At the lower region of the second layer (from 11,000 m up to 21,000 m altitude, or from 36,000 ft up to 70,000 ft altitude), the temperature is constant at −56°C (in ISA condition). In addition, in the upper region of the stratosphere (from 21,000 m up to 47,000 m altitude, or from 70,000 ft up to 155,000 ft altitude), the temperature increases again and approaches 1°C at 47,000 m (155,000 ft) altitude. Therefore, in the first layer, the temperature is linearly decreased but is constant at the lower region of the second layer.

A number of different temperature scales have been introduced; two popular choices in the SI system are the *Celsius* (formerly Centigrade) and *Kelvin* scales. The Kelvin temperature and the Celsius temperature are related by

$$T(\mathrm{K}) = T(^{\circ}\mathrm{C}) + 273.15 \tag{1.2}$$

In the British unit system, the Rankine scale is related to the Fahrenheit scale by

$$T(\mathrm{R}) = T(^{\circ}\mathrm{F}) + 460 \tag{1.3}$$

The temperature scales in the two unit systems are related by

$$T(\mathrm{R}) = 1.8\,T(\mathrm{K}) \tag{1.4}$$

$$T(^{\circ}\mathrm{F}) = 1.8T(^{\circ}\mathrm{C}) + 32 \tag{1.5}$$

In engineering calculations, we only use the Kelvin scale or Rankine scale, since they are absolute temperature scales.

Based on the atmospheric empirical values (linear variation in the first layer), the temperature of the first layer (troposphere) in ISA condition is mathematically modeled by the following equation:

$$T_{\text{ISA}} = T_o - Lh \tag{1.6}$$

In the lower region of the second layer (stratosphere), the temperature will be

$$T_{\text{ISA}} = -56°\text{C} \tag{1.7}$$

where h denotes altitude, T_{ISA} temperature in ISA condition, T_o temperature at the sea level and ISA condition, and L represents the rate of temperature change with altitude or lapse rate that is 0.0065°C/m or 0.0065 K/m or 0.002°C/ft or 0.0035 °R/ft or 0.0035 °F/ft.

As the name implies, lapse rate is the rate of decrease of temperature with altitude. The lapse rate is to show that the temperature is decreased 6.5° (in °C or K) every 1,000 m or 2° (in °C or K) every 1,000 ft.

However, in the upper region of the stratosphere (from 21,000 m up to 47,000 m altitude, or from 70,000 ft up to 155,000 ft altitude), the temperature increases at a rate of 2.1°C per 1,000 m, or 7°C per 1,000 ft, and approaches 1°C at an altitude of 47,000 m (155,000 ft).

The ratio between the temperature (in ISA condition) at any altitude and that at the sea level is called temperature ratio (θ) and is

$$\theta = \frac{T_{\text{ISA}}}{T_o} = \frac{T_{\text{ISA}}}{288.15\,\text{K}} \tag{1.8}$$

The temperature in non-ISA condition is

$$T = T_{\text{ISA}} + \Delta T \tag{1.9}$$

where ΔT is the temperature difference between non-ISA and ISA conditions. Appendices A and B provide the temperature for any altitude in ISA condition.

Example 1.1

Determine the temperature at 20,000 and 50,000 ft altitudes assuming ISA conditions.

Solution

At sea level, the temperature is 518.69°R = 59°F

a. *20,000 ft*
This altitude is located in the first layer (troposphere), so

$$T_{\text{ISA}} = T_o - Lh = 518.7 - \left(0.0035 \times 20{,}000\right)$$
$$= 447.7°\text{R} = -12°\text{F} = -24.4°\text{C} \tag{1.6}$$

b. *50,000 ft*
This altitude is located in the lower region of the second layer (stratosphere), so

$$T_{\text{ISA}} = -56°\text{C} = -68.8°\text{F} \tag{1.7}$$

Example 1.2

The temperature in a city on a summer day is ISA + 32 and on a winter day is ISA − 25. Determine the temperature on both days in Celsius. This city has an elevation of 3,000 m.

Solution

$$T_{\text{ISA}} = T_o - Lh = 15 - \left(0.0065 \times 3{,}000\right) = -4.5°\text{C} \tag{1.6}$$

a. Summer day:

$$T = T_{\text{ISA}} + \Delta T = -4.5 + 32 = 27.5°\text{C} \tag{1.9}$$

b. Winter day:

$$T = T_{\text{ISA}} + \Delta T = -4.5 - 25 = -29.5°\text{C} \tag{1.9}$$

1.6.2 Pressure

Pressure is another important atmospheric variable that influences an aircraft's performance. Pressure is basically defined as a normal force exerted by a fluid (gas or liquid) per unit area on which the force acts. Pressure has the unit of Newton per square meter (N/m^2 or Pascal) or pound per square inch (lb/in^2 or psi).

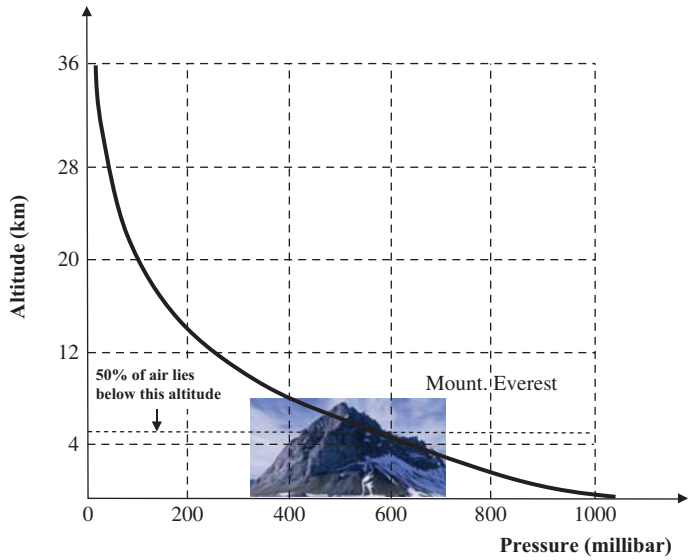

FIGURE 1.6 Atmospheric pressure variation with altitude.

The weight of air (i.e., force) above any surface produces pressure at that surface. The higher we ascend in the atmosphere, the less will be the weight of air above us, so the less will be pressure. The average pressure at sea level due to the weight of the atmosphere is 101,325 N/m^2, a pressure which causes the mercury (Hg) in a barometer to rise about 760 mm. This pressure is sometimes referred to as "one atmosphere" (i.e., 1 atm), and high pressures are then spoken of in terms of "atmospheres".

Another common metric unit of pressure is the millibar (mb), which is 1/1,000th of a bar: a bar being $10^5 N/m^2$. One bar is very close to the standard atmospheric pressure at sea level. It had been adopted by meteorologists many years before the metric SI unit system was introduced, and the reader may often encounter atmospheric pressure given in millibars. However, for most straightforward performance calculations, we will use N/m^2.

Pressure with altitude is not decreased linearly (Figure 1.6). The rate at which pressure decreases is much greater near the Earth's surface than at altitude (i.e., nonlinear). Rather, the pressure decreases rapidly near the Earth's surface and more gradually at greater heights. Between sea level and 10,000 ft, pressure has been reduced from 1,013 to 697 mb, a drop of 316 mb; for the corresponding increase of 10,000 ft (between 20,000 and 30,000 ft), the decrease of pressure is from 466 to 301 mb, a drop of only 165 mb; between 70,000 and 80,000 ft, the drop is only 17 mb. The pressure at an altitude of 16 km is about 1/10th of the atmosphere, at an altitude of 31 km is about 1/100th of the atmosphere, and at an altitude of 48 km is about 1/1,000th of atmosphere.

This is because air is compressible; the air near the Earth's surface is compressed by the air above it, and, as we climb higher, the air becomes less dense, so the pressure becomes less. Air would become thinner from the Earth's surface upward; the

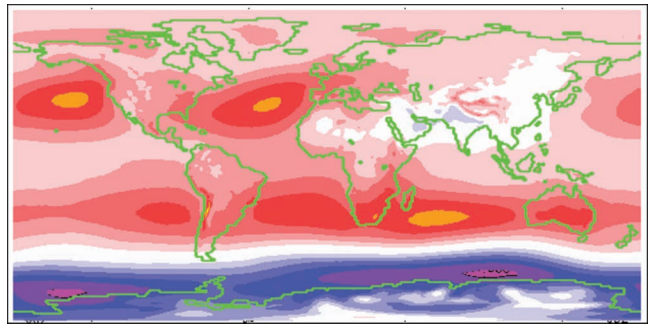

FIGURE 1.7 Mean sea level pressure for June–July–August.

final change from the atmosphere to space being is so gradual such that it is indistinguishable. In this respect, air differs from liquids such as water; in liquids, there is a definite dividing line or surface at the top; and beneath the surface of a liquid, the pressure increases in direct proportion to the depth because the liquid, being practically incompressible, remains of the same density in all depths. In the following sections, a few equations are presented to calculate pressure in the first layer (troposphere) and the second layer (stratosphere).

Figure 1.7 illustrates the mean sea level pressure for June–July–August. Note that the mean sea level pressure is varying throughout the year and at various locations. However, the difference between the highest and lowest mean sea level pressures is ignorable (about 3%).

1.6.2.1 First Layer

To derive a relationship for pressures as a function of altitude, we use the thermodynamics energy equation and notice physics laws. The rate of change of pressure with respect to a change in altitude (h) is mainly a function of the air density. Air is assumed to be in hydrostatic equilibrium, so it will satisfy the differential equation:

$$dP = -\rho g dh \tag{1.10}$$

where g is the gravitational constant. For calculating pressures below 30 km (100,000 ft), it has been customary to assume g to be constant. In addition, the air density (ρ) is a function of pressure and temperature as stated by ideal gas law or *gas equation of state*:

$$P = \rho RT \tag{1.11}$$

In this equation, R is referred to as *gas constant* and for air $R = 287$ J/kg K. By dividing Equation 1.10 by Equation 1.11, we obtain

$$\frac{dP}{P} = -\frac{gdh}{RT} \tag{1.12}$$

Differentiation of Equation 1.6 yields

$$dT = -Ldh \Rightarrow dh = -\frac{dT}{L} \tag{1.13}$$

Substitution of this equation into Equation 1.12 results in

$$\frac{dp}{P} = \frac{g}{RL}\frac{dT}{T} \tag{1.14}$$

This equation may be integrated between the pressure at any altitude and the pressure at a reference altitude (i.e., sea level). The integration yields the following expression:

$$\frac{P_2}{P_1} = \left(\frac{T_2}{T_1}\right)^{g/LR} \tag{1.15}$$

Since three parameters of g, L, and R are known to have constant values (as defined earlier), the power of Equation 1.15 (in SI units) will be $g/LR = 9.81/(0.0065 \times 287) = 5.256$. With the substitution of this number and generalizing Equation 1.15 for the ISA condition, we have

$$\frac{P}{P_o} = \left(\frac{T}{T_o}\right)^{5.256} = (\theta_{\text{ISA}})^{5.256} \tag{1.16}$$

Please note, in this equation, temperature is in terms of the absolute scale (i.e., Kelvin [not Celsius] or Rankine [not Fahrenheit]). Moreover, both pressure and temperature are in ISA condition. The pressure in ISA and non-ISA conditions is assumed to be the same. To find the pressure at any altitude, one must first calculate temperature from the technique offered in Section 1.6.1, or read the value from standard tables (e.g., Appendix A or B), and then determine pressure from Equation 1.16.

1.6.2.2 Second Layer

Since in the lower region of the second layer (stratosphere), the temperature is constant (isothermal region at −56°C), we directly integrate Equation 1.12 to obtain

$$\ln\left(\frac{P}{P_{\text{ref}}}\right) = -\frac{g(h - h_{\text{ref}})}{RT_{\text{ref}}} \Rightarrow \frac{P}{P_{\text{ref}}} = \exp\left(\frac{g(h_{\text{ref}} - h)}{RT_{\text{ref}}}\right) \tag{1.17}$$

where P_{ref}, T_{ref}, and h_{ref} are the values of pressure, temperature, and altitude at the start of the isothermal region (i.e., tropopause). By taking the reference altitude (h_o) to be sea level, the following is obtained for sea level pressure or P_o:

$$\frac{P}{P_o} = \frac{P}{P_{\text{ref}}}\frac{P_{\text{ref}}}{P_o} \tag{1.18}$$

The reference temperature (T_{ref}) at the tropopause is −56°C or 217 K. Thus, the pressure ratio (using Equation 1.16) at the tropopause is

$$\frac{P_{ref}}{P_o} = \left(\frac{T_{ref}}{T_o}\right)^{5.256} = \left(\frac{-56+273}{15+273}\right)^{5.256} = 0.2234 \tag{1.19}$$

However, at the tropopause, the altitude is 11,000 m or 36,089 ft. By inserting Equation 1.19 into Equation 1.18, the pressure is referenced to sea level as

$$\frac{P}{P_o} = 0.2334 \exp\left(\frac{11{,}000-h}{6{,}342}\right) \tag{1.20}$$

$$\frac{P}{P_o} = 0.2234 \exp\left(\frac{36{,}089-h}{20{,}807}\right) \tag{1.21}$$

The altitude (h) is in terms of meters in Equation 1.20 and in feet in Equation 1.21. The subscript o refers to the sea level, and h is measured from sea level.

Example 1.3

Determine the pressure of air at 40,000 ft and in ISA condition.

Solution

Since this altitude belongs to the second layer, and its unit is in feet, we use Equation 1.21:

$$\frac{P}{P_o} = 0.2234 \exp\left(\frac{36{,}089-h}{20{,}807}\right) = 0.2234 \exp\left(\frac{36{,}089-40{,}000}{20{,}807}\right) = 0.1851 \quad (1.21)$$

The pressure at sea level is 14.7 psi = 2,116.2 lb/ft² = 29.92 in. Hg. Hence,

$$P = 2116.2 \times 0.1851 = 391.7 \frac{\text{lb}}{\text{ft}^2} = 5.538 \text{ in. Hg} = 18{,}757.2 \text{ Pa}$$

The ratio between the pressure at any altitude and the pressure at sea level is assigned a symbol of δ as follows:

$$\delta = \frac{P}{P_o} \tag{1.22}$$

Appendices A and B provide the pressure ratio at any altitude. This is an alternate and easier way to find pressure, since the results are calculated based on the equations of this section. The actual pressure at different points in the flow without any dynamic effect is called static pressure. When we use the word "pressure", it always means static pressure unless otherwise stated.

In all of our previous discussions so far, the pressures have been static pressures. The other two types of pressure that are commonly utilized in aircraft performance are dynamic pressure and total pressure. The thermodynamic properties of a flow such as pressure, temperature, and density, of the fluid element would change as we bring the element to rest. When a flow isentropically is slowed down to zero velocity, the pressure will be changed to total pressure.

Indeed, as the fluid element is isentropically brought to rest, pressure would increase above its original static value. The value of this pressure is called *total pressure* P_t. The difference between total pressure and static pressure is referred to as *dynamic pressure*.

For the special case of a gas that is not moving, that is, the fluid element has no velocity in the first place, then static and total pressures are synonymous: $P_t = P$. This is the case in common situations such as stagnant air in the room and gas confined in a cylinder. Total pressure is equal to the sum of static pressure and dynamic pressure. Dynamic pressure will be examined later in this chapter.

1.6.3 Air Density

Another important atmospheric parameter of air is the air density. It has a significant influence on aircraft performance. All aerodynamic forces plus engine thrust are functions of air density; hence, air density's decrease or increase will affect these forces and consequently the flight performance. Air density is defined as the mass of air per unit volume. In general, air density decreases with altitude. For instance, the air density at a 16 km altitude is about 11% of the air density at sea level.

Air density is a function of both temperature and pressure. Equation 1.11, as already introduced, is repeated to calculate the air density:

$$\rho = \frac{P}{RT} \tag{1.23}$$

Therefore, to determine the air density, one must calculate temperature and pressure first. Inserting density from Equation 1.23 into Equation 1.17 and solving for air density (where $h_o = 0$) will result in

$$\rho = \rho_o e^{-g_o h/RT} \tag{1.24}$$

This equation is referred to as the *exponential model atmosphere*. This equation is valid up to about a height of 140 km; above this height, air is very thin. This model – that was adopted by NASA in the early 1960s – can be used to accurately predict the density variation in the standard atmosphere. The air density ratio is defined as the ratio of the air density at any altitude (ρ) to the air density at sea level (ρ_o):

$$\sigma = \frac{\rho}{\rho_o} \tag{1.25}$$

Figure 1.2 demonstrates the variation of air density with altitude. Appendices A and B provide the *air density ratio* at any altitude. In general, most aircraft performance

parameters (e.g., rate of climb and maximum speed) degrade with altitude. However, the drag force is a function of air density (as will be explained in Chapters 2 and 3). As an aircraft flies higher and higher, its drag will be lower since the air density will be lower. That is one of the reasons why transport aircraft prefer to fly at high altitude. The properties of the standard atmosphere (i.e., values of atmospheric pressure, temperature, and air density) are tabulated in Appendices A and B as a function of altitude.

Example 1.4

Determine the air density at a 5,000 m altitude and in ISA condition.

Solution

The air temperature at sea level and ISA condition is 15°C or 288.15 K.

$$T_{\text{ISA}} = T_{5,000} = T_o - Lh = 15 - (0.0065 \times 5{,}000) = -17.3^{\circ}\text{C} = 255.9\,\text{K} \tag{1.6}$$

The air pressure at the sea level is 101,325 Pa.

$$\frac{P}{P_o} = \left(\frac{T}{T_o}\right)^{5.256}$$
$$\Rightarrow P_{5,000} = 101{,}325 \times \left(\frac{255.9}{288.15}\right)^{5.256} = 54{,}271.3\,\text{Pa} \tag{1.16}$$

The air density:

$$\rho = \frac{P}{RT} = \frac{54{,}271.3}{287 \times 255.9} = 0.739\,\text{kg/m}^3 \tag{1.23}$$

Example 1.5

Determine the air density at the sea level and ISA – 15 condition.

Solution

At the sea level and standard condition, the temperature is 15°C. So,

$$T = T_{\text{ISA}} + \Delta T = 15 - 15 = 0^{\circ}\text{C} = 273.15\,\text{K} \tag{1.9}$$

The air pressure at the sea level is 101,325 Pa.

$$\rho = \frac{P}{RT} = \frac{101{,}325}{287 \times 273.15} = 1.29\,\text{kg/m}^3 \tag{1.23}$$

Therefore, as the weather gets colder, the air density is increased.

1.6.4 Viscosity

Another property of air that affects flight performance is its viscosity. Viscosity is a measure of the resistance of one layer of air to movement over the neighboring layer; it is rather similar to the property of friction between solids. It is owing to viscosity that eddies are formed when air is disturbed by a body passing through it. Viscosity is possessed by fluids such as oil and honey to a large degree, and, although the property is much less noticeable in air, it is nonetheless of considerable importance.

Viscosity is defined as a measure of the resistance of a fluid to deform under shear stress. Therefore, it is a property that represents a fluid's internal resistance to flow and may be thought of as a measure of fluid friction. All real fluids (liquid or gas) have some resistance to shear stress, but a fluid that has no resistance to shear stress is known as an ideal fluid or inviscid fluid. The coefficient of viscosity is the ratio of the pressure exerted on the surface of a fluid, to the change in velocity of the fluid as you move in the fluid. Shear stress and drag force (as will be addressed in Chapter 3) are directly proportional to the fluid's viscosity.

The viscosity of air has been found to vary with temperature and to be independent of pressure at low to moderate pressures (from a few percent of 1 atm to several atm). The viscosity is denoted by μ, and its unit is N·s/m^2 or kg/(m·s). The variation of viscosity in terms of temperature by Sutherland correlation (from the U.S. Standard Atmosphere) is [13] modeled as

$$\mu = \frac{a\sqrt{T}}{1 + (b/T)} \tag{1.26}$$

where T is absolute temperature (in Kelvin or Rankine) and a and b are experimentally determined constants.

For air under atmospheric conditions, the values of the constants are $a = 1.485 \times 10^{-6}$ kg/(m·s·K$^{1/2}$) and $b = 110.4$ K. At sea level and ISA condition, 15°C (288.15 K), the dynamic viscosity of air (μ_o) is 1.783×10^{-5} kg/(m·s). The viscosity μ is also referred to as the coefficient of viscosity or the dynamic (or absolute) viscosity. In calculations, the ratio of the dynamic viscosity to the density appears frequently, so it is called kinematic viscosity (ν).

$$\nu = \frac{\mu}{\rho} \tag{1.27}$$

The unit of kinematic viscosity is m^2/s.

1.7 HUMIDITY

One of the ingredients of air is water vapor. As the Sun shines over lakes, seas, and oceans, part of their waters is vaporized. This vapor enters air and produces humidity. Humidity affects air density and air pressure as well. Therefore, humidity influences the aircraft's performance. The amount of water vapor can reach a maximum of about 4% of air. In practice, about 2% of water vapor is pleasant for human life.

Water vapor weighs less than dry air; therefore, a given volume of moist air will weigh less than an equal volume of dry air. The primary result of high humidity is a loss of engine thrust/power (due to a loss of the weight per unit volume of air and a drowning effect on the combustion process). On a very humid day, this effect will decrease takeoff and climb performance by ~7%.

When the level of vapor in air has reached its limit (i.e., *saturation*), if more vapor is added to air, another vapor will be condensed back to water in another place. This limit is a function of air temperature. A parcel of air at the sea level, at a temperature of 25°C, would be completely saturated if there were 20 g of water vapor in every kilogram of dry air.

There are several ways to describe the humidity of air. Four relevant terms to humidity are: (1) *absolute humidity,* (2) *relative humidity*, (3) *vapor pressure*, and (4) *humidity ratio.* They are briefly described in this section and are employed for our analysis.

Absolute humidity expresses the water vapor content of air using the mass of water vapor contained in a given volume of air. It may be measured in grams of vapor per cubic meter of air.

Relative humidity: Relative humidity, ϕ, is defined as the ratio of the mass of water vapor (m_v) to the maximum amount of water vapor that, air can hold at the same temperature (m_g) at saturation.

$$\phi = \frac{m_v}{m_g} \tag{1.28}$$

At a temperature of 20°C, and at sea level, the saturation mixing ratio is 14 g of water per one kilogram of dry air. Relative humidity is given as a percentage; the amount of water vapor is expressed as a percent of saturation. For instance, if 10 g of water vapor were present in each kilogram of dry air, and air would be saturated with 50 g of water vapor per kilogram of dry air, the relative humidity would be 10/50 = 20%.

Using the ideal gas law, one can prove that the mass ratio is equivalent to pressure ratio. In other words, relative humidity is the ratio of water vapor pressure in air (P_v) to the saturation pressure of water (P_g).

$$\phi = \frac{P_v}{P_g} \tag{1.29}$$

Vapor pressure measures the water vapor content of air using the partial pressure of the water vapor in air. The gases in the atmosphere exert a certain amount of pressure. Since water vapor is one of the gases in air, it contributes to the total air pressure. The contribution by water vapor is rather small. The vapor pressure of water in the air at sea level, at a temperature of 20°C, is only about 24 millibar (mb) at saturation.

The pressure at which a pure substance at a given temperature changes phase (e.g., from liquid to gas) is called the *saturation pressure* (P_{sat} or P_g). Likewise, at a given pressure, the temperature at which a pure substance changes phase is called the

TABLE 1.1
Saturated Pressure of Water at Various Temperatures

T (°C)	−10	−5	0	5	10	15	20	25	30	35	40	45	50
P_g (kPa)	0.26	0.4	0.611	0.872	1.227	1.705	2.34	3.17	4.246	5.63	7.384	9.543	12.35

saturation temperature (T_{sat}). At a pressure of 101.325 kPa, T_{sat} is 99.97°C. Table 1.1 [14] shows the saturated vapor pressure at various temperatures.

The total air pressure is equal to the summation of air pressure without vapor (P_a) and vapor pressure (P_v) as follows:

$$P = P_a + P_v \tag{1.30}$$

Relative humidity varies between 0 and 1, or 0%–100%. For example, if relative humidity is said to be 70%, it means that the vapor pressure at this condition is 70% of partial pressure of the water vapor. Since the water vapor density is lower than oxygen and nitrogen densities, the existence of humidity reduces the air density. Thus, humidity directly impacts the aircraft's performance.

Humidity ratio: Humidity ratio (also referred to as *specific humidity*) – commonly used by meteorologists – measures the water vapor content using a measure of mass. It may be measured in grams of water vapor per kilogram of dry air. Humidity ratio (ω) is defined as the ratio of the mass of water vapor (m_v) to the mass of dry air (m_a):

$$\omega = \frac{m_v}{m_a} \tag{1.31}$$

Using the ideal gas law for air and water vapor, one can obtain:

$$\omega = 0.622\frac{P_v}{P_a} = 0.622\frac{\phi \cdot P_g}{P_a} \tag{1.32}$$

For a given mass of water vapor in the air, the humidity ratio (ω) remains constant, but relative humidity (ϕ) varies as the temperature varies. By knowing relative humidity, one can determine the air density by using Equation 1.32 and Table 1.1. The following two examples illustrate the applications.

Example 1.6

The air at 25°C and 100 kPa in a 150 m^3 room has a relative humidity of 60%. Calculate: (1) humidity ratio, (2) mass of water vapor in air.

Solution

The saturation pressure P_g at 25°C from Table 1.1 is 3.17 kPa. By using Equation 1.29:

$$\phi = \frac{P_v}{P_g} \Rightarrow P_v = P_g\phi = 3.17 \times 0.6 = 1.9\,\text{kPa} \tag{1.29}$$

Partial pressure of air is

$$P_a = P - P_v = 100 - 1.9 = 98.1\,\text{kPa} \tag{1.30}$$

The humidity ratio is

$$\omega = 0.622\frac{P_v}{P_a} = 0.622 \times \frac{1.9}{98.1} = 0.01205\ \frac{\text{kg-H}_2\text{O}}{\text{kg-dry-air}} \tag{1.32}$$

From the definition of the humidity ratio, the mass of water vapor is

$$m_v = \omega m_a = \omega\frac{P_aV}{RT} = (0.01205)\left[\frac{98.1 \times 150}{0.287 \times (25 + 273.15)}\right] = 2.07\,\text{kg} \tag{1.31}$$

If we convert this much mass of vapor into volume fraction of water, it demonstrates that air with 60% relative humidity is about 2% water vapor by volume.

Example 1.7

The temperature of a city located at sea level is 20°C and relative humidity is 70%. Calculate the air density.

Solution

From Table 1.1, $P_g = 2.339$ kPa, so

$$\phi = \frac{P_v}{P_g} \Rightarrow P_v = P_g\phi = 2.339 \times 0.7 = 1.637\,\text{kPa} \tag{1.29}$$

Partial pressure of air is

$$P_a = P - P_v = 101.325 - 1.637 = 99{,}688\,\text{Pa} \tag{1.30}$$

Air density is

$$\rho = \frac{P}{RT} = \frac{99{,}688}{287 \times (273.15 + 20)} = 1.185\,\text{kg/m}^3 \tag{1.23}$$

1.8 ALTITUDE AND ITS MEASUREMENT

Altitude, or height, is the vertical distance from any point (e.g., a flying aircraft) to a reference point. A reference point must be on a point on Earth. In aeronautics, this point is mean free sea level, and, in astronautics, this point is the center of the Earth.

In aerospace terms, there are several types for altitude depending on how it is determined: (1) geometric altitude, (2) pressure altitude, (3) indicated altitude, and (4) absolute altitude. The geometric altitude (h or h_g) is the physical (true) altitude measured directly above sea level. This altitude can be measured by radar and global positioning system (GPS) and is read from Appendices A or B. Airport, terrain, and obstacle elevations on aeronautical charts are true altitudes. The absolute altitude is the physical altitude measured directly above ground level (AGL).

The *pressure altitude* h_p, is the altitude on a standard day for which the pressure is equal to the existing atmospheric (or ambient) pressure. Current mechanical altimeters are pressure instruments and are therefore calibrated to read the pressure altitude, which is based on pressure measurement. This altitude can also be determined indirectly (in fact, calculated). In reality, there is only one physical altitude, but depending on how the altitude is measured, pressure altitude may or may not be the same as real altitude.

An altimeter is an active instrument used to measure the altitude of an object above a fixed level. The three main types of altimeters are: (1) pressure altimeter; (2) radio or radar altimeter; and (3) GPS. The pressure altitude is often measured by pitot static tube, which is a mechanical altimeter. However, with the recent advance in technology and the application of GPS, the altitude can be determined fairly accurately.

1.8.1 Pressure Altimeter

The pressure altimeter (aneroid barometer) approximates altitude above sea level by measuring atmospheric pressure. This traditional mechanical altimeter, found in most GA aircraft, works by measuring the air pressure from a static port of *pitot tube* in the aircraft. The measurement of airspeed and static pressure can be made by this instrument. The pitot tube is one of the most fundamental measurement devices employed in almost any aircraft. The schematic of a pitot tube and its mechanism is presented in Chapter 2, Section 2.4.3.

It mainly consists of tube, diaphragm, spring, display, and pointer. The altimeter is calibrated to show the pressure directly as altitudes, in accordance with a mathematical model defined by the ISA. When it is set to the proper barometric pressure, it measures the altitude of the aircraft above sea level.

These altimeters must be calibrated for each aircraft against position error, scale error, compressibility error, and apply altitude correction factor. Without the radar altimeter or GPS, the measured altitude by a pressure altimeter is subject to various errors. Because altitude measured in this manner is also subject to changes in local barometric pressure, altimeters are provided with a barosetting that allows the pilot to compensate for weather changes, the sea-level air pressure to which the altimeter is adjusted. A pressure altimeter is unable to measure the local altitude (e.g., the height above a terrain).

Flights below 18,000 ft must constantly contact the nearest control tower to keep the altimeters updated. Flights above 18,000 ft and over international waters utilize a constant altimeter setting of 101,325 Pa or 29.92 in. Hg, so that all high-flying aircraft have the same reference and will be interrelated to provide a margin of safety. Pressure altimeter is the least accurate altimeter among various altitude measurement devices. However, pressure altimeters are much less expensive than radar altimeters.

1.8.2 Radar Altimeter

A radar altimeter uses electromagnetic waves to measure the altitude of an aircraft above the local ground. Radar altimeters are often used in aircraft during bad-weather landings. Radar altimeters are much more accurate and more expensive than pressure altimeters. They are an essential part of many blind-landing and navigation systems and are used over mountains to indicate terrain clearance. Special types are used in surveying for quick determination of profiles.

The altimeter measures height (absolute altitude or distance above land or water) by determining the time required for a radio wave to travel to and from a target. If the Earth were a perfectly flat horizontal plane, the signal would come only from the closest point and would be a true measure of altitude. However, the Earth is not smooth, and energy is scattered back to the radar from all parts of the surface illuminated by the transmitter. A radar altimeter is unable to measure the altitude from sea level (unless the aircraft is above ocean/free-water).

1.8.3 Global Positioning System

The GPS uses the satellite constellation and is fairly accurate in measuring altitude. The GPS has almost no direct effect from atmospheric conditions. The GPS provides specially coded satellite signals that can be processed in a GPS receiver, enabling the receiver to determine their position and velocity. At least four GPS satellite connections are needed to compute their positions in three dimensions. The positions in x, y, and z are converted within the receiver to latitude, longitude, and height. Velocity is computed from the measured change in position over time.

The space segment of the system consists of the GPS satellites, which send radio signals (electromagnetic waves) from space to Earth. The orbit altitude (20,200 km, 55° inclination) is such that the satellites repeat the same ground track and configuration over any point approximately each 24 hours.

While there are hundreds of millions of civil users of GPS worldwide, the system was designed for and is operated by the U.S. military [15]. Civil users worldwide can utilize a civil version of GPS signal without charge or restrictions. The predictable accuracy of this signal is a few meters. No matter, if an aircraft is flying in an ISA or non-ISA condition, its altitude is measured precisely through GPS. All modern aircraft are currently equipped with a GPS receiver.

1.9 SPEED OF SOUND

Speed of sound is another parameter involved in aircraft performance analysis. The aircraft speed in many cases is presented in terms of speed of sound. The speed of sound (a) is determined through the following equation:

$$a = \sqrt{\gamma RT} \tag{1.33}$$

where γ is the ratio of specific heats (1.4 for air at the sea level and ISA condition), R is the gas constant, and T is air temperature in absolute scale (e.g., Kelvin). The speed of sound at sea and ISA condition is about 340 m/s and decreases with altitude.

The speed of sound leads to another vital definition for high-speed flight, namely, the Mach number. By definition, the Mach number (M) of an aircraft is the true airspeed (i.e., aircraft velocity with respect to the surrounding air) divided by the speed of sound:

$$M = \frac{V}{a} \tag{1.34}$$

Parameter M is a nondimensional parameter and is one of the most widely used quantities in aircraft performance. Figure 1.2 illustrates the variation of the Mach number with altitude. Using such a scale for airspeed, five flight regimes with distinct features are defined:

1. If $M < 0.8$, the flight is referred to as subsonic.
2. If $M = 1$, the flight is referred to as sonic.
3. If $0.8 < M < 1.2$, the flight is referred to as transonic.
4. If $M > 1.2$, the flight is referred to as supersonic.
5. If $M > 5$, the flight is referred to as hypersonic.

The borderline between various flight regimes is not fixed, but they are defined and agreed upon between aerodynamicists and flight dynamicists. It will be shown in Chapter 3 that drag force is increased dramatically in transonic and supersonic speeds compared with subsonic speeds. Aircraft performance depends on the Mach number as the shock wave (at supersonic speeds) has a significant impact on it. Figure 1.8 demonstrates three aircraft: (1) subsonic aircraft Airborne Windsports XT-912, (2) transonic transport aircraft Airbus A340, and (3) the supersonic fighter – McDonnell Douglas F-18C Hornet.

Another important parameter of the aircraft's performance is *dynamic pressure* (q). Dynamic pressure is in fact not a pressure by nature, but has the unit of pressure indeed. It is a function of air density, aircraft speed, static pressure, and Mach number.

(a)

(b)

(c)

FIGURE 1.8 Three aircraft with three flight regimes: subsonic, transonic, and supersonic aircraft. (a) Subsonic aircraft Airborne Windsports XT-912. (Courtesy of Gustavo Corujo.) (b) Transonic transport aircraft Airbus A340. (Courtesy of Jan Seler.) (c) Supersonic fighter – McDonnell Douglas F-18C Hornet. (Courtesy of Maurice Kockro.)

$$q = \frac{1}{2}\rho V^2 = \frac{1}{2}\gamma P M^2 = 0.7 P M^2 \tag{1.35}$$

In the end of this section, two speed-of-sound-related terms are briefly described. *Sound barrier* is introduced when an aircraft is flying faster than the speed of sound (i.e., flying from the subsonic to supersonic regime). Passing from a sonic barrier (i.e., aircraft airspeed faster than the sound propagation speed) creates a huge sound, which acts like an explosion.

Sonic boom is a trail of the shock wave that may reach the ground. If the shock wave is powerful enough, it may damage whatever it can directly hit; for instance, it will break window glasses. For this reason, supersonic aircraft are required not to fly under a supersonic regime in the proximity of residential regions and cities.

Example 1.8

A jet transport aircraft is cruising at an altitude of 3,000 m with a velocity of 100 m/s in ISA + 15 atmospheric conditions. Determine: (1) the airspeed in terms of the Mach number. (2) static pressure and dynamic pressure at this flight condition.

Solution

a. *Mach number*
Temperature is

$$T = T_{\text{ISA}} + \Delta T \tag{1.9}$$

$$T_{\text{ISA}} = T_o - Lh \tag{1.6}$$

Thus

$$T = T_o - Lh + 15 = 288.15 - \left(0.0065 \times 3{,}000\right) + 15 = 283.8\,\text{K}$$

The speed of sound is obtained by

$$a = \sqrt{\gamma RT} = \sqrt{1.4 \times 287 \times 283.8} = 337.7\,\text{m/s} \tag{1.33}$$

Aircraft's Mach number is

$$M = \frac{V}{a} = \frac{100}{337.7} = 0.296 \tag{1.34}$$

From this Mach number, it is concluded that this aircraft is flying under a subsonic regime.

b. Static and dynamic pressure
Static pressure:

$$P = P_o\left(\frac{T}{T_o}\right)^{5.256} = 101{,}325\left(\frac{283.8}{288.15+15}\right)^{5.256} = 71.622\,\text{Pa} \tag{1.16}$$

Dynamic pressure:

$$q = 0.7PM^2 = 0.7 \times 71{,}622 \times \left(0.296\right)^2 = 6{,}721\,\text{Pa} \tag{1.35}$$

It is observed that the dynamic pressure at this subsonic speed is much lower than the static pressure.

1.10 ATMOSPHERIC PHENOMENA

The atmosphere is a dynamic system that produces several phenomena. This section briefly reviews these phenomena. These phenomena are significant in aircraft design and performance analysis. Through the process of preparing a flight manual by aircraft performance engineer, the pilot is guided that, in what atmospheric conditions, a flight is safe and allowed. The atmospheric phenomena include (1) rain, (2) icing, (3) snow, (4) wind, (5) gust, (6) turbulence, (7) hurricane, (8) tornado, (9) thunderstorm, (10) lightning, and (11) hail [16]. The detailed descriptions of these atmospheric phenomena are out of scope of this book.

Interested readers are encouraged to consult references such as [1,2]. Of these phenomena, only three topics are briefly reviewed here to demonstrate how they influence aircraft performance. The jobs of pilots when they encounter these phenomena in flight are also explained. In general, pilots are recommended to avoid flying in or near regions with turbulence, tornado, thunderstorm, hurricane, and lightning.

1.10.1 Wind

Wind is the air flowing horizontally with respect to the Earth's surface. It is one of the almost permanent phenomena of the atmosphere. Wind is very significant in aircraft performance and influences most aspects of performance (particularly range and takeoff run). We know the upward movement of air and its importance in cloud formation. As important as vertical motion is, far more air is involved in the horizontal movement, and this phenomenon is called wind.

Wind is the result of horizontal differences in air pressure. Air flows from areas of higher pressure to areas of lower pressure. Wind is the nature's solution to balance the inequalities in air pressure (i.e., circulation). Because unequal heating of the Earth's surface continually generates these pressure differences, solar radiation is the ultimate energy source for most winds. The direction of a wind at a specific location is not constant throughout the year. But the prevailing wind could be measured at every location.

If the Earth did not rotate and there was no friction, air would flow directly from areas of higher pressure to areas of lower pressure. However, because both factors exist, wind is controlled by a combination of (1) pressure-gradient force, (2) Coriolis force, and (3) friction. Currently, the prevailing wind direction in every region of the world is known. For instance, easterly flow occurs at low and medium latitudes globally. However, in the mid-latitudes, westerly winds are the rule, and their strength is largely determined by the polar cyclone.

The pressure-gradient force is the primary driving force of wind that results from pressure differences that occur over a given distance. A steep pressure gradient creates strong winds, and a weak pressure gradient generates light winds. There is also an upward-directed vertical pressure gradient, which is often balanced by gravity (i.e., hydrostatic equilibrium).

When the gravitational force exceeds the vertical pressure-gradient force, it will result in slow downward airflow. Conversely, on those occasions when the vertical pressure gradient exceeds the gravitational force, it will result in slow upward airflow (i.e., thermal). Friction, which significantly influences airflow near the Earth's

surface, is negligible at high altitude. Near the surface, friction plays a major role in redistributing air within the atmosphere by changing the direction of airflow. The result is a movement of air at an angle across the isobars toward the area of lower pressure.

The Coriolis force produces a deviation in the path of wind due to the Earth's rotation (to the right in the northern hemisphere and to the left in the southern hemisphere). The amount of deflection is greatest at the poles and decreases to zero at the equator. The amount of Coriolis deflection also increases with wind speed. At high altitude, as the wind speed increases, the deflection caused by the Coriolis force also increases. Winds in which the Coriolis force is equal to and opposite the pressure-gradient force are called geostrophic winds. Geostrophic winds flow in a straight path, with velocities proportional to the pressure-gradient force.

The prevailing wind is the wind that blows most frequently across a particular region. Different regions on the Earth have different prevailing wind directions, which are dependent upon the nature of the general circulation of the atmosphere and the latitudinal wind zones. Wind speed (see Figure 1.9) is lower at low altitude (about 50 km/h) and higher at high altitude (up to 200 km/h). The highest wind speed has been recorded over the White Mountains in New Hampshire, the United States.

If an aircraft encounters a headwind, its ground speed (thus the range) is decreased; however, its airspeed does not change. On the other hand, if an aircraft encounters a tailwind, its ground speed (thus the range) is increased; however, its airspeed does not change again. The crosswind changes the heading of flight, so the pilot must correct its heading by using a rudder. Every aircraft can tolerate a maximum amount of wind speed. If the wind is faster than that, the aircraft is not allowed to fly. An aircraft performance engineer must calculate this speed and include it in the flight manual. Therefore, any pilot must consult with a meteorologist to predict the weather in its trajectory (including wind speed and direction).

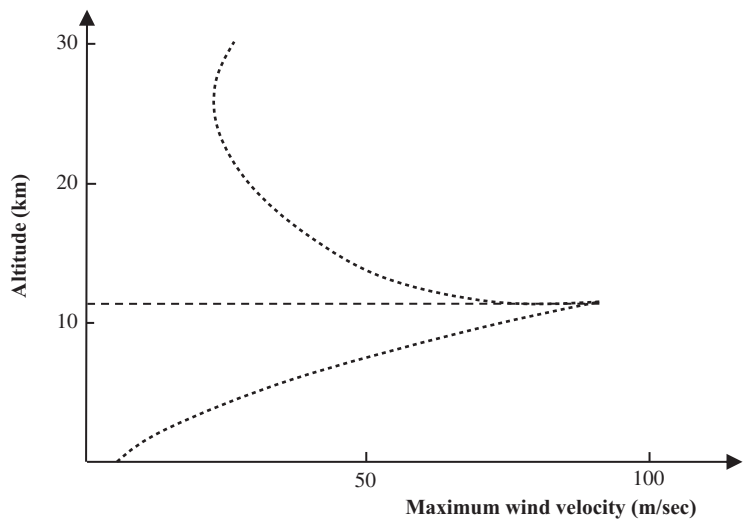

FIGURE 1.9 A typical statistical maximum wind speed curve.

1.10.2 Gust and Turbulence

Two effective atmospheric phenomena in flight dynamics are gust and turbulence. Gust is the most important and famous type of atmospheric disturbance that almost every aircraft is experiencing. Gust is a sudden wind-speed increase of 4.6 m/s (10.3 mph) or more, to a peak speed of 8 m/s (about 18 mph) or more. It is briefer than a squall and usually lasts 20 s or less. Air turbulence around an obstacle causes gusts; they occur frequently over buildings, irregular ground, and mountains and are generally absent over water.

The study on gust is mainly useful in aircraft stability and control, rather than aircraft performance. In case of severe weather, when gust speed is high, aircraft flight is not assumed as safe; thus, the flight must be postponed or the route must be changed. A mathematical representation of gust can be found in References [17,18]. NASA *sounding rockets* [19] are still launched in an effort to better understand and visualize turbulent air currents in the upper atmosphere. Gust considerably influences the aircraft structural loads, which will be discussed in Chapter 9. The terrible T_s (i.e., Turbulence, Thunderstorms, and Tornadoes) can unleash enormous amount of destructive energy that is perilous for aircraft.

1.10.3 Icing

Icing is a harmful atmospheric phenomenon that is often generated in the winter. However, even during the summer, it may be produced over the aircraft body at high altitudes. Ice can physically form on any surface at 0°C (32°F) or colder when liquid water or water vapor is present. Most icing tends to occur at temperatures between 0°C and −20°C. Ice usually accumulates on the leading edge, upper surface of the wing, around patio-tube, antennas, flap hinges, control horns, fuselage nose, windshield wipers, wing struts, and fixed landing gear. Ice can disturb the flow of air over the wing; hence, it significantly reduces the lift and increases the drag. The solutions to icing are special surface protection, cleaning of the surface prior to the flight, and *deicing*.

According to an American Institute of Aeronautics and Astronautics, AIAA report [20], pilots of an Etihad Airways Airbus A340 (Figure 1.8) diverted to Singapore after a sudden encounter with turbulent weather during cruise generated unreliable airspeed data and left the jet unable to maintain altitude separation requirements. A preliminary inquiry into the incident highlights that the aircraft suffered *icing* on its pitot system, which is notably the cause of unreliable airspeed indications at high altitude.

All modern transport aircraft, including the Boeing 777, have a capable anti-ice system that includes the leading edges of the horizontal and vertical stabilizers. The system usually operates full time, with no cycling between the wings and tail for *anti-ice* air. Icing considerably influences the aircraft drag, which will be discussed in Chapter 3.

PROBLEMS

Note: In the following problems, if altitude, pressure, or temperature is not given, assume sea-level ISA condition, and if humidity is not given, assume zero:

1.1 Determine the temperature, pressure, and air density at 5,000 m and ISA condition.
1.2 Determine the pressure at 5,000 m and ISA − 10 condition.
1.3 Calculate air density at 20,000 ft altitude and ISA + 15 condition.
1.4 An aircraft is flying at an altitude at which its temperature is −4.5°C. Calculate
   a. Altitude in ISA condition
   b. Altitude in ISA + 10 condition
   c. Altitude in ISA − 10 condition
1.5 Determine relative density (σ) in ISA − 20 condition and 80,000 ft altitude.
1.6 Determine the temperature at 70,000 ft and ISA condition.
1.7 An aircraft is flying at an altitude at which its temperature and pressure are 255 K and 4.72×10^4 Pa. Calculate
   a. Pressure altitude
   b. Temperature altitude
   c. Density altitude
1.8 An aircraft is flying at an altitude at which its pressure altitude and density altitude are 4,000 and 4,200 m. Calculate the temperature at this altitude.
1.9 If the lapse rate (L) is 3°C per 1,000 ft, what is the temperature at 15,000 ft altitude?
1.10 An aircraft is flying at 20,000 ft altitude with a speed of 400 km/h and ISA condition. What is the aircraft's Mach number?
1.11 Calculate air density at the sea level and ISA condition when humidity is 100%.
1.12 Determine the speed of sound at sea level and (1) ISA condition, (2) ISA + 12, and (3) ISA − 18.
1.13 What is the dynamic pressure when an aircraft is cruising at an altitude of 8,000 m and the Mach number of 0.6?
1.14 The elevation of Lake Michigan at Chicago, IL, is 581 ft from the sea level. On a summer day, the temperature is ISA + 20; determine pressure and air density.
1.15 Fighter aircraft MiG-31 is able to fly with Mach 2.2 at an altitude of 60,000 ft. What is the dynamic pressure if it is flying in ISA + 20 condition?
1.16 The temperature at the summit of a mountain in ISA condition is −5°C. What is the height of this summit from the sea level?
1.17 The highest peak of Mount Everest has an elevation of 29,035 ft. Calculate temperature, pressure, and air density at this peak.
1.18 The fighter aircraft F-15C is capable of flying at an altitude of 12,000 m with the speed of 2,443 km/h. What is its speed in terms of the Mach number in ISA condition?
1.19 A gas balloon has a volume of 2,800 m^3 and a mass of 140 kg. The gas inside the balloon is hydrogen (with the density of 0.11 kg/m^3), determine how high this balloon can climb. Assume the volume of the balloon remains fixed, as it climbs.

1.20 An aircraft is flying with the speed of Mach 1.8 at 20,000 ft altitude. Calculate its speed in terms of mile/h for
   a. ISA condition
   b. ISA + 20 condition
   c. ISA − 20 condition
1.21 Determine the air viscosity for an altitude of 10,000 m and ISA condition.
1.22 The Earth is rotating around itself once a day. Calculate its velocity in a city at the equator in terms of the Mach number, if speed of sound is assumed to be 340 m/s. The average radius of Earth is about 6,400 km.
1.23 A Boeing 767 is flying at an altitude of 40,000 ft. How much air pressure must be increased by its air pressure system to provide a pressurized air of 0.8 atm for the passengers inside cabin and cockpit?
1.24 Humans can climb up to a 12,000 ft altitude without the help of pressurized air. Determine the temperature and pressure ratio at this altitude.
1.25 The condition at a polar air base is ISA − 70. Calculate the air density at this air base.
1.26 The humidity is 80% in a room with the volume of 160 m^3 on a summer day. Determine the water vapor content (in kg) of this room in ISA + 30 condition, if located at a 2,000 ft altitude.
1.27 A transport aircraft is flying at an altitude of 25,000 ft, ISA condition. The pilot observes that the ice has been formed on the leading edge of the wing. How much deicing system must increase the temperature of the leading edge to melt the ice?
1.28 The temperatures of a city on a summer day and a winter day are 115°F and 15°F, respectively. Find the ratio between air densities on the summer day and the winter day.
1.29 The humidity of a city on a summer day (ISA + 20) is 100%, and on a winter day (ISA − 20) is 10%. Find the ratio between air densities on the summer day and the winter day.
1.30 The reconnaissance aircraft Lockheed SR-71 Blackbird can fly with Mach 3 at a 75,000 ft altitude. What is aircraft speed in terms of mile/h?
1.31 What is the dynamic pressure when an aircraft is cruising at an altitude of 14,500 m and a Mach number of 0.6, in ISA − 12 flight condition?
1.32 An aircraft is cruising at an altitude of 12,000 m and a Mach number of 0.93, in ISA + 15 flight condition. Determine the dynamic pressure.
1.33 Determine the air viscosity for an altitude of 30,000 ft and ISA + 20 condition.
1.34 Determine temperature, pressure, and air relative density in ISA + 30 condition and 50,000 ft altitude.
1.35 A Reconnaissance aircraft is able to fly with Mach 4 at an altitude of 80,000 ft. Determine the dynamic pressure, if flying in ISA condition.
1.36 The Northrop Grumman high-altitude, remotely piloted surveillance aircraft RQ-4 Global Hawk is cruising at 18,000 m with a cruise speed of 570 km/h. Determine the dynamic pressure for ISA condition.

2 Equations of Motion

2.1 INTRODUCTION

In general, equations of motion represent the mathematical description of the behavior of a dynamic system (e.g., the motion of an object under the influence of a force/moment) as a function of time. Sometimes, the term refers to the differential equations that the system satisfies (e.g., Newton's second law) and sometimes to the solutions to those equations. The equations of motion are the equations that govern the motion of a vehicle. Newton's laws of motion are the important bases for aircraft performance analysis. Among the three laws, the second law is the most significant; it describes the relationship between applied forces and the consequent motion of the vehicle.

We can predict what happens in terms of motion variables (e.g., displacement, speed, and acceleration), if several forces act on a vehicle simultaneously. Newton's second law states that the sum of the forces (F) results in a change in the linear momentum of an object/vehicle.

$$\sum F = \frac{d}{dt}(mV) \tag{2.1}$$

where m is the mass, and V is the velocity of the object.

The term mV is referred to as the linear momentum, where m is the vehicle's mass and V is the velocity of the vehicle. The d/dt represents a differentiation of the product of mass and velocity. If the mass of the vehicle remains unchanged during the motion, Newton's second law is stated as follows: the acceleration of a body is directly proportional to, and in the same direction as, the net force acting on the body and inversely proportional to its mass.

A vehicle in this book is an air vehicle (aircraft) that moves in the atmosphere (air). The mass could be considered constant through the flight operation (as it is the case for most aircraft in a short period of time) or varying (as it is the case for air vehicles that have rocket engines, such as missiles). We will consider both cases in the following sections. Equation 2.1 will be expanded for every class of air vehicles and for every major flight operation.

Based on Newton's first law, a change in the motion status of any object requires a force. Newton's first law states that an object at rest remains at rest and an object in motion remains in motion (at a constant linear/angular velocity) unless compelled by a net force/moment. The aircraft is not an exception. Several forces are simultaneously applied on an aircraft, but the net force determines its motion status. If the net force is zero, the aircraft will continue its current motion status (e.g., cruise); otherwise, the motion status will be changed (e.g., velocity). Since the force/moment is a vector, the direction of change will be in the direction of the net force/moment.

DOI: 10.1201/9781003279068-2

One of the early steps in recognizing an aircraft's motion is to identify the forces acting on the aircraft. These forces will add up and determine the direction and status of the motion, velocity, and acceleration. In general, there are three groups of forces that act on an airborne aircraft at all times: (1) gravitational force or weight, (2) propulsive force or engine thrust, and (3) aerodynamic forces/moments.

The combination of these forces/moments determines the future of aircraft motion. Due to the fact that the scope of this text is not about aircraft control or stability, aerodynamic moments, although very effective in motion status, are ignored in this chapter. Aircraft performance can be analyzed without referring to aerodynamic moments (e.g., pitching moment and rolling moment).

Weight is always downward toward the center of the Earth. The direction of this force does not change under any circumstances, unless it goes in the vicinity of another planet, such as the Moon or Sun. Weight (W) is simply mass (m) times the gravitational constant, g (9.81 m/s^2). The unit of force in the SI or metric system is Newton and in the British system is pound (lb). In addition, the unit of mass is slug in the British system and kilogram in the metric system.[1] In some references, the pound-force (lbf) is also employed as the unit of force.

$$W = mg \tag{2.2}$$

For simplicity, we consider the aircraft as a point mass. This allows us to simplify the equations of motion and see the aircraft as a rigid body. In this assumption, we do not consider aeroelasticity as an effective phenomenon in aircraft performance.

The second force, on any heavier-than-air craft and some lighter-than-air craft, is thrust. Thrust is generated by the propulsion system or powerplant as a result of fuel combustion. Gliders or sailplanes do not have an engine, and thus their thrust is zero. The motion of these air vehicles is under the influence of only two other forces (i.e., weight and aerodynamic forces) unless they find thermal force to climb. The direction of thrust is always forward and is independent of engine location. Engine thrust is not responsible for lifting the aircraft as it may seem at the first glance. If the engine has a setting angle (α_T), the direction of thrust has an angle of α_T with respect to the aircraft fuselage body axis. This angle is very small (about $<5°$). Figure 2.1 illustrates an aircraft with two non-aerodynamic forces (weight and thrust).

The third group of forces is called aerodynamic force and is produced when any air vehicle is moving in the atmosphere. Thus, the combination of aircraft configuration and aircraft motion is responsible for this force. There are two forces in this category: lift force or simply lift, and drag force or drag. Every external (i.e., aerodynamic) component of aircraft contributes to the aerodynamic force. The primary factor responsible for generation of lift is the wing, but the wing is only accountable for about 30% of the drag. The generation of considerable lift is one of the main differences between aircraft and other vehicles such as car, ship, and train.

The major problem for aircraft designers is how to conquer aircraft weight in an efficient way. They solve this problem with a combination of a powerful engine and an aerodynamic configuration. Thus far, the four forces, namely, weight, thrust, lift,

[1]Reference [9] mistakenly uses kg as the unit of aircraft weight.

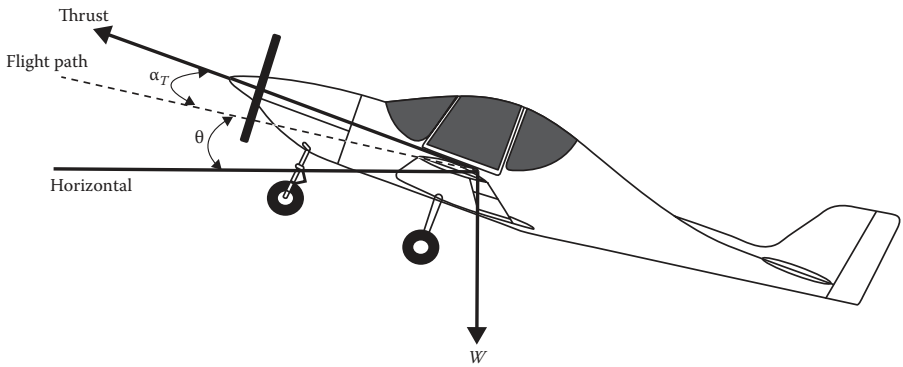

FIGURE 2.1 An aircraft with two non-aerodynamic forces (weight and thrust).

and drag, have been briefly introduced in this chapter, but drag and thrust are covered again in more detail in Chapters 3 and 4, respectively. The performance feature of any aircraft depends on how these four forces behave.

Since the Earth has a spherical shape, we need to consider an aircraft's motion as a circular one. However, the Earth's radius is about 6,400 km, and it is too large when compared with a typical distance that is covered by an aircraft flight in a typical mission. For this reason and for simplicity, we ignore the circular motion of the aircraft. In this book, we consider the aircraft-cruising flight as a linear motion and apply the equation of motion for a linear motion; thus, we assume flat earth. Therefore, the assumption of linear aircraft motion is reasonable and does not considerably affect our analysis. One must consider the Earth's radius when dealing with space flight. The interested reader is recommended to refer to Flight Dynamics references such as [21,22] for the expansion of Equation 2.1 to see the details for inclusion of all related motion parameters.

2.2 AERODYNAMIC FORCES

Every force has an origin and is applied to one point. Weight originates from the Earth's gravitational force and is applied at the aircraft's center of gravity. Thrust is generated by the engine and applied at the engine thrust line. However, what is the origin of the aerodynamic force and where is it applied? The origin of aerodynamic force is air pressure distribution over the entire aircraft plus friction between air and aircraft external components. Therefore, the simple answer is that the aircraft configuration is the main origin of the aerodynamic forces. The aircraft must be designed to produce the aerodynamic forces (lift and drag) in such a way that they support the aircraft's motion as much as possible in the most efficient way. Lift force is upward and is the primary force for lifting the aircraft and holding it in the air; thus, it must be maximized. Drag force always acts as a counter motion force; thus, it must be minimized. The aerodynamic forces are originally applied at the center of pressure, but, via a process, they are assumed to be applied at the aerodynamic center. A brief description of the process follows, but, for more details, the reader is encouraged to consult aerodynamic texts such as [23].

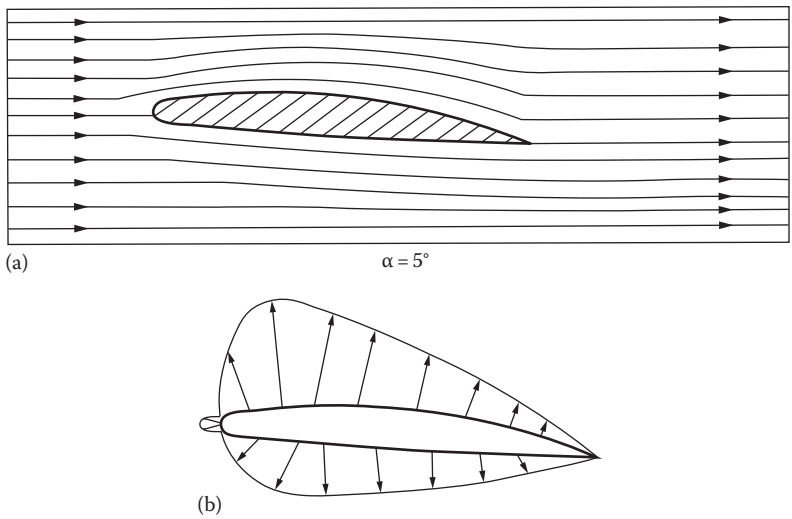

FIGURE 2.2 A typical pressure distribution over an airfoil with 5° of angle of attack. (a) Streamlines and (b) pressure distribution.

Aerodynamicists are those who study and research to improve the production of aerodynamic forces. With the advancement of science of aerodynamics and its impact on efficiency and cost of flight, other vehicle designers such as car designers and train designers are trying to apply the aerodynamic principles in order to minimize cost and maximize the vehicle efficiency. To analyze aircraft performance, one should know how to determine aerodynamic forces. In this section, the technique to calculate the lift is presented. Chapter 3 is devoted to the process and techniques to determine the aircraft drag.

Figure 2.2 shows an asymmetrical airfoil experiencing a free air stream with a velocity of *V*. The description of the process of generation of lift is beyond the scope of this text, since it involves several laws and theories such as energy equation, momentum equation, continuity (conservation of mass) equation, circulation theorem, Kutta condition, and boundary layer. For instance, according to the Kutta–Joukowski theorem, the lift per unit span is directly proportional to circulation. In addition, in an airfoil with positive camber and positive angle of attack, the upper surface has a lower pressure, and the lower surface has a higher pressure than the ambient pressure. Figure 2.2 also illustrates the pressure distribution over an airfoil.

The energy of any molecule around the airfoil (in unit of pressure) consists of kinetic energy plus static pressure or pressure energy[2] and will remain constant along a streamline.

$$E = \frac{1}{2}\rho V^2 + P \tag{2.3}$$

[2] The potential energy is ignored because of small mass of a molecule and small change in its height over the airfoil.

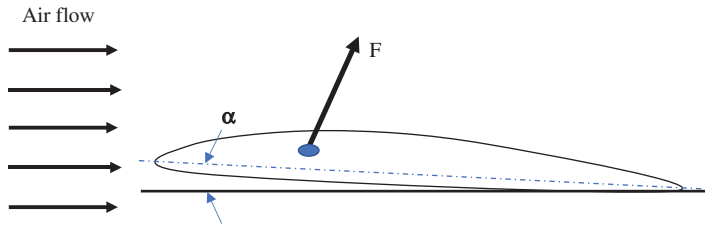

FIGURE 2.3 The resultant force out of integration of pressure distribution.

In a subsonic inviscid flow, when the compressibility effect is ignored, *Bernoulli's* equation confirms this result. Therefore, the pressure at the upper surface is lower than the pressure at the lower surface. Figure 2.2b illustrates a typical pressure distribution over an airfoil, with an angle of attack, α. The length of each arrow shows the magnitude of the pressure (normal to the surface) compared to the ambient local pressure. The directions of lower/upper arrows are outward to indicate that they decrease the local pressure at both surfaces.

Pressure and shear stress are defined as force divided by the area that the force is exerted on. To have an area, we consider a lifting surface (e.g., wing or tail) with a unit span and a cross section as an asymmetric airfoil. Thus, we move from a three-dimensional object instead of a two-dimensional airfoil.

We can integrate pressure and shear stress over the entire surface of the lifting surface (e.g., wing) to have one resultant force. The location of this resultant force (see Figure 2.3) is referred to as the center of pressure (cp). The location of this center depends on aircraft speed and the airfoil's angle of attack. In subsonic speeds, as the angle of attack is increased, the center of pressure moves forward (below stall angle). At supersonic speeds, the center of pressure moves toward the mid-chord, since the airfoil is often biconvex or bi-wedge.

Since the center of pressure is moving, it is hard to be used in aerodynamic calculations. Hence, a new center is invented that has almost a fixed location. This imaginary center or point, referred to as "*aerodynamic center* (ac)", is a useful concept for the study of aircraft performance analysis. This location on the airfoil also has significant features in aircraft aerodynamics, stability, and control.

It is convenient to move the location of the resultant force from the center of pressure to this new location (aerodynamic center). The process is as follows. Two opposite but equal forces (see Figure 2.4) are considered at the aerodynamic center. The magnitude of these forces is equivalent to the resultant force at the pressure center. Now, the resultant force at the center of pressure plus the force in the opposite direction at the aerodynamic center are replaced with a couple (moment). Thus, an aerodynamic force at the center of pressure is equivalent to an aerodynamic force at the aerodynamic center, plus a pitching moment. The next step is to divide this aerodynamic force into two components: vertical component or lift, and axial component or drag (Figure 2.4). So, the force at the aerodynamic center is divided into two components: one force along the free stream (called lift) and one force perpendicular to the free stream (called drag).

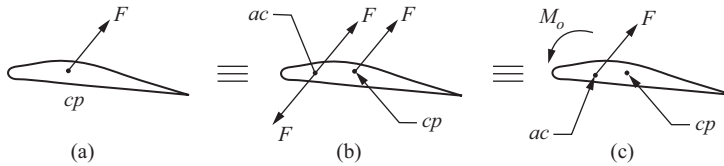

FIGURE 2.4 The movement of resultant force to the aerodynamic center. (a) Original force, (b) adding two equal and opposite forces, and (c) resultant force.

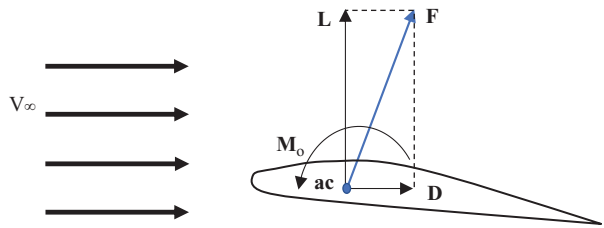

FIGURE 2.5 Lift, drag, and pitching moment.

In practice, this moment can be taken about any arbitrary point (the leading edge, the trailing edge, the quarter-chord, etc.). The moment can be visualized as being produced by the aerodynamic force acting at a particular distance back from the leading edge (center of pressure). It is proved in aerodynamics (see Reference [23]) that there exists a particular point about which the moment is independent of the angle of attack. This point is defined as the *aerodynamic center* of the wing. Therefore, it is concluded that the pressure and shear stress distributions over a wing produce two aerodynamic forces (lift and drag) plus a pitching moment. Indeed, the forces and moments system on a wing can be completely specified by the lift and drag acting on the aerodynamic center, plus the moment about the aerodynamic center, as sketched in Figure 2.5.

Based on this technique, the lift acts at a point on the airfoil that is at 25% of the chord aft of the leading edge. For most conventional airfoils, the aerodynamic center is close to, but not necessarily exactly at, the quarter-chord point. In wind tunnel tests, the "ac" is usually within 1% or 2% chord of the quarter-chord point until the Mach number increases to within a few percent of the "drag divergence" Mach number.[3] The aerodynamic center then slowly moves aft as the Mach number is increased further.

Therefore, there is an aerodynamic force created by the pressure and shear stress distributions over the wing surface. The resultant forces (L and D) are depicted by the vector in Figure 2.5. The aerodynamic force can be resolved into two forces: parallel and perpendicular to the relative wind. The drag is always defined as the component of the aerodynamic force parallel to the relative wind. The lift is always defined as the component of the aerodynamic force perpendicular to the relative wind.

[3] The interested reader is referred to *Aerodynamics* textbooks for more details.

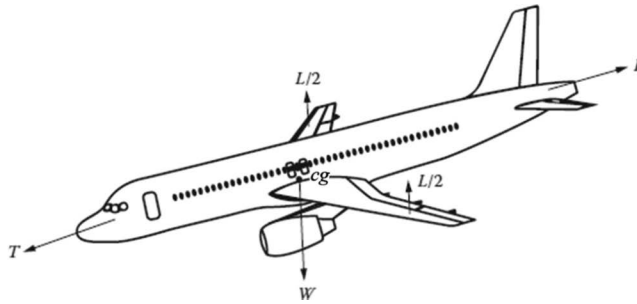

FIGURE 2.6 The major forces on an airplane.

So, in addition to lift and drag, the surface pressure and shear stress distributions also create a moment that tends to rotate the wing. Since in most cases, the center of pressure is located aft of the aerodynamic center, this moment is negative. Thus, this moment is sometimes referred to as nose-down pitching moment. The main application of the nose-down pitching moment is in analysis of aircraft stability and control, so we do not apply this moment in our performance analysis. It is assumed that the aircraft is stable and controllable; therefore, the influence of this moment on aircraft performance is ignored.

We can now summarize that we have the following four[4] main forces acting on an airplane during a cruising flight: (1) Weight (W), (2) Thrust (T), (3) Lift (L), and (4) Drag (D).

Figure 2.6 shows these forces on an airplane. Please note that since a wing has two sections, right and left, we can assume that one-half of the lift ($L/2$) is generated by each half-wing. The aerodynamic forces of lift and drag are functions of the following factors: (1) aircraft configuration, (2) aircraft angle of attack, (3) aircraft geometry, (4) airspeed (V), (5) air density (ρ), (6) Reynolds number of the flow, and (7) air viscosity.

To consider other factors and to convert the proportionalities to equations, two coefficients are introduced: (1) lift coefficient (C_L) and (2) drag coefficient (C_D).

Then

$$L = \frac{1}{2}\rho V^2 S C_L \tag{2.4}$$

$$D = \frac{1}{2}\rho V^2 S C_D \tag{2.5}$$

[4]Indeed, there are five forces; the fifth one is an aerodynamic force, called side force. The side force is mainly produced by the vertical tail, and is in the direction of y axis. For the sake of simplicity, we did not include this force in our analysis, since it is zero most of the times. However, it is an important force in the topic of "Stability and control analysis", which is beyond the scope of this text.

Using Equation 1.35, these two forces also have two new forms as follows:

$$L = 0.7PM^2SC_L \tag{2.6}$$

$$D = 0.7PM^2SC_D \tag{2.7}$$

In the above equations, S represents wing reference area (gross), M is the flight Mach number, and P is air pressure. Both lift and drag coefficients are functions of several parameters including aircraft configurations. Precise calculations of these two coefficients need aerodynamics background or flight test results. However, Chapter 3 presents a technique to calculate drag coefficient for any aircraft configuration.

Since in most aircraft, the major contributor of aircraft lift is the wing,[5] we can assume that wing lift (L_w) is almost equal to aircraft lift (L).

$$L \cong L_w \tag{2.8}$$

As a consequence, we can assume that the aircraft lift coefficient is almost equal to the wing lift coefficient:

$$C_L \cong C_{L_w} \tag{2.9}$$

In linear theory, lift coefficient is equal to lift curve slope (a or $C_{L\alpha}$) times wing angle of attack, or (α):

$$C_{L_\alpha} = a = \frac{dC_L}{d\alpha} \quad (\text{aircraft}) \tag{2.10}$$

$$C_{L_{\alpha_w}} = a_w = \frac{dC_{L_w}}{d\alpha_w} \quad (\text{wing}) \tag{2.11}$$

In a general case, where the aircraft or wing has an asymmetrical airfoil (has a non-zero lift angle of attack), we have

$$C_{L_w} = C_{L_{\alpha_w}}(\alpha_w - \alpha_o) = C_{L_{\alpha_w}}(\alpha_f + i_w - \alpha_o) \tag{2.12}$$

where α_w is the wing angle of attack, α_f is the fuselage angle of attack, i_w is the wing incidence, and α_o is the zero lift angle of attack of the wing. For a three-dimensional lifting surface (e.g., wing or tail), the lift curve slope can be obtained [23] through

$$a = C_{L_{\alpha_w}} = \frac{a_o}{1 + \frac{a_o}{\pi \cdot \text{AR}}} \tag{2.13}$$

[5] The fuselage usually contributes about 5%–10% to the aircraft lift.

where aspect ratio (AR) is the lifting surface aspect ratio (will be defined in Equation 3.9), and a_o is its two-dimensional (airfoil cross section) lift curve slope. According to the thin airfoil theory, the lift curve slope of a typical airfoil is about 2π (1/rad). If you do not have access to the airfoil graphs, or wind tunnel data, you may use the following approximation:

$$a_o = 2\pi\ (1/\text{rad}) = 0.11\ (1/\text{deg}) \tag{2.14}$$

Example 2.1

Aircraft Beech Baron 58 is cruising at sea level with a speed of 80 m/s and 3° of angle of attack. The wing area is 18.51 m^2 and its AR is 7.2. Determine the aerodynamic forces (lift and drag) that this aircraft is producing. Assume that the aircraft drag coefficient is 0.05, and wing zero lift angle of attack is zero ($\alpha_o = 0$).

Solution

Since the wing airfoil is not given, we will assume a theoretical lift curve slope:

$$a_o = 2\pi\ (1/\text{rad}) \tag{2.14}$$

$$a = C_{L_{\alpha_w}} = \frac{a_o}{1+\left(\frac{a_o}{\pi \cdot \text{AR}}\right)} = \frac{2\pi}{1+\frac{2\pi}{3.14\times 7.2}} = 4.9\ (1/\text{rad}) \tag{2.13}$$

$$C_{L_w} = C_{L_{\alpha_w}}(\alpha_w - \alpha_o) = 4.9\times\frac{3-0}{57.3} = 0.22 \tag{2.12}$$

$$C_L \cong C_{L_w} = 0.22 \tag{2.9}$$

$$L = \frac{1}{2}\rho V^2 S C_L = 0.5\times 1.225\times(80)^2\times 18.51\times 0.22 = 15{,}963\,\text{N} \tag{2.4}$$

$$D = \frac{1}{2}\rho V^2 S C_D = 0.5\times 1.225\times(80)^2\times 18.51\times 0.05 = 3{,}628\,\text{N} \tag{2.5}$$

2.3 GENERAL GOVERNING EQUATIONS OF MOTION

This section is devoted to deriving the aircraft general governing equations of motion. In doing so, we need to define coordinate system, typical mission, and flight operation phases. In the next section, the general governing equations are applied to each flight phase to come up with specific governing equations of motion. Aircraft motion can be classified in various ways. Here, we introduce three classifications based on (1) the motion acceleration, (2) the flight phase, and (3) the nature of the motion. In each classification, we will apply Newton's second law (Equation 2.1) and derive a final equation that can be employed for motion analysis.

2.3.1 Coordinate System

A coordinate system should be defined prior to the derivation of equations of motion. To describe the motion of an object that moves relative to a given fixed point, it is convenient to use a reference frame that moves with the moving object.

Such a reference frame is body-fixed and moves with the aircraft (*Cartesian* coordinates). The best option for the origin is the aircraft's center of gravity (cg). In this definition, we define x-axis to be in the forward direction, z-axis to be perpendicular to the x-axis and downward, and finally y-axis to be perpendicular to the x–z plane and to the right of the pilot, if seen from the pilot position.

The x-axis has two options. This originates from the fact that the aircraft has a fuselage reference line and at the same time has a flight path. The angle between these two is called fuselage angle of attack (α). In aircraft performance analysis, we prefer to have x-axis along the flight path (i.e., relative wind). This choice allows the calculation to be simpler and more convenient. Please note that this coordinate system will rotate with aircraft rotation about x-axis (roll).

In Figure 2.7, a body-fixed reference frame xyz with its origin at a fixed point of the rigid body (cg) on General Dynamics F-16 Fighting Falcon is illustrated. There is an exception for this frame. When we are dealing with aircraft altitude, we always use a positive number. This means that the aircraft altitude is measured from a fixed point at sea level. Based on this orientation, the lift will be in the negative z direction, weight in the positive z direction, thrust in the positive x direction, and drag in the negative x direction. A side force could be produced in the y direction in a specific flight condition (such as in a turn).

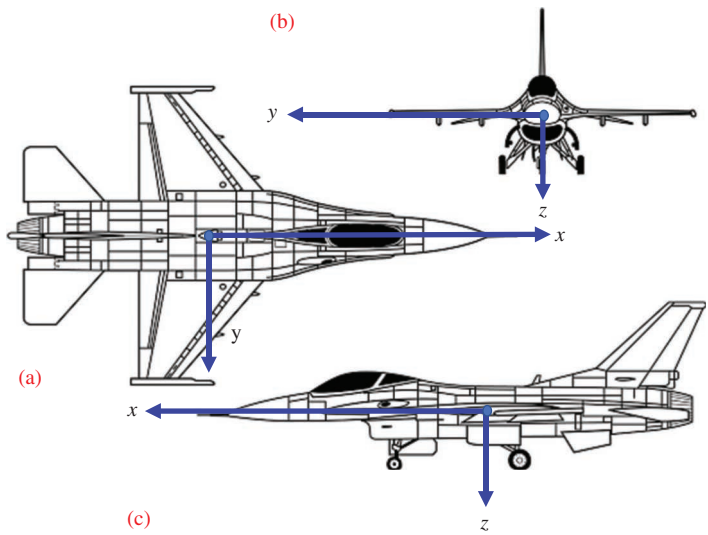

FIGURE 2.7 Aircraft body-fixed coordinate system (F-16): (a) top view, (b) front view, and (c) side view.

2.3.2 Un-accelerated Versus Accelerated Flight

Aircraft motion can be either un-accelerated flight or accelerated flight. An un-accelerated motion (flight) is a flight without acceleration (constant velocity). Recall that speed is a scalar that has only magnitude, but velocity is a vector that has both magnitude and direction. In an un-accelerated flight, not only the velocity does not vary, but also the direction of aircraft does not change. Takeoff and landing are always assumed to be accelerated motions. In a takeoff, the aircraft increases its speed until liftoff and then until climb. In landing, the aircraft decreases its speed from flare to touch down and then until it stops completely (or until taxi speed). A turning flight, even with constant speed, will be considered an accelerated flight, since the direction of flight (velocity vector) constantly varies. In general, the original form of Newton's second law (Equation 2.1) will be used.

If the flight phase duration is short, we can ignore the change in aircraft mass (m). Examples are takeoff and landing (few seconds or about a minute), and turning flight (usually less than minutes in a turning flight other than loiter). The reason is that the change of aircraft mass during these flight operations is less than about 1%. Thus, Equation 2.1 will be simplified to

$$\sum F = m\frac{d}{dt}(V) = ma \tag{2.15}$$

where a is the motion acceleration. If the acceleration is positive (as in the case of takeoff), the speed will be increased, and, if it is negative (as in the case of landing), the speed will be decreased. The analysis of takeoff and landing will be presented in Chapter 8, and the analysis of turning flight will be offered in Chapter 9. In an un-accelerated flight, the velocity remains constant. In this case, the aircraft is said to be in an equilibrium state.

$$\sum F = 0 \tag{2.16}$$

The summation of all forces in any axis will be zero.

$$\sum F_x = 0 \tag{2.17}$$

$$\sum F_y = 0 \tag{2.18}$$

$$\sum F_z = 0 \tag{2.19}$$

The examples of this flight phase would be the cruising flight, and the climbing flight with a constant speed.

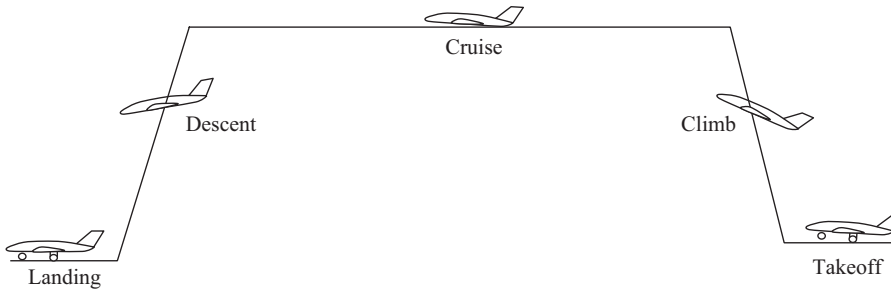

FIGURE 2.8 A basic and typical flight operation of an aircraft.

2.3.3 Flight Phases

Figure 2.8 illustrates a regular flight mission of an aircraft. The flight of an aircraft usually begins with a takeoff from a base (ground or sea) and ends the journey with a landing operation. As shown in Figure 2.8, a typical flight operation consists of the following phases: taxi, takeoff, climb, cruise, turn, descend, approach, and landing. For a civil transport aircraft, the following are the typical phases of a flight:

1. *Taxi*: The aircraft is prepared for takeoff. Passengers are boarded, and their payloads are loaded. The aircraft will move from a gate toward the beginning of the runway at a very low speed. The pilot is ready to take off after permission is received from a control tower.
2. *Takeoff*: The aircraft starts from rest at the beginning of runway. It moves in a straight line along the runway. As time passes, the aircraft speed will be increased toward liftoff speed. At the same time, the lift is increased until it is equal to the aircraft weight and allows the aircraft to leave the ground. Then aircraft will clear an obstacle and retract its landing gear when airborne. The details of takeoff will be presented in Chapter 8. Employing the flaps is very crucial and helpful in a successful takeoff.
3. *Climb*: The aircraft begins to gain height and increase the altitude. Since the aircraft has just taken off at low speed, the first part of the climb will be accelerated until a specified speed. Then, the climbing flight will be continued with a constant speed until the aircraft has reached the cruising altitude. In this flight phase, the aircraft will maintain a climb angle of about 10°–40°. This flight operation will be analyzed in Chapter 7.
4. *Cruise*: The aircraft will hold a fixed altitude until the pilot decides to descend. The first part of the cruising flight will be accelerated until the aircraft reaches a predefined cruising speed. Then the flight will be continued toward the destination at a constant cruising speed. If there is no change in the flight plan, the aircraft will continue the flight at a constant speed and constant altitude until the vicinity of the destination airport. Chapters 5 and 6 are devoted to this flight operation.

5. *Maneuver*: This flight phase could be a combination of several flight operations. In the simplest case, the aircraft will turn toward the destination. Based on flight regulations, the aircraft must pass from certain points and contact with various towers in various hubs or countries. The main feature of this phase in a turning flight that the aircraft will experience is a rolling motion plus a yawing motion. The aircraft will be banked up to a certain bank angle (often <45°). In Chapter 9, various maneuvers and turning flights will be described and analyzed.
6. *Descend*: When the aircraft is close to the destination, the aircraft must lose altitude until the aircraft will be able to land safely. In a descending flight, both altitude and speed will be reduced constantly. In a descent, an aircraft will have a negative pitch attitude to have a lift less than weight. Chapter 7 will present the details of a descending flight.
7. *Landing*: The last phase of any civil flight is landing. The landing phase includes an approach, flare, and touchdown, and reduces speed. The pilot has to initially align the aircraft with the runway after he or she receives landing permission from the control tower. The pilot must follow the runway until it reaches a safe speed to turn toward its gate. Most aircraft employ a brake (mechanical, spoiler, or engine reverse) to help reduce the speed as quick as possible. When the aircraft arrives at the gate, passengers will get off the plane (phase 8 in Figure 2.8) and their luggage will be carried to the baggage claim area. The landing analysis will be introduced in detail in Chapter 8.

The analysis of these flight operation phases will be presented in Chapters 5–9.

2.4 AIRSPEED

The airspeed in the relative speed between air and an air vehicle. There are mainly two cases: (1) Aircraft is moving in a calm air, and (2) Aircraft is not moving, but air is moving. The first case is a common case for all flying aircraft, but an example for the second case would be an aircraft model in a wind tunnel. The aerodynamic forces and moments are functions of this airspeed. This section is dedicated to a number of topics related to airspeed.

2.4.1 Airspeed Measurement

In the subsonic regime, energy conservation law – in the form of Bernoulli's equation – gives rise to a simple method of measuring airspeed. The equation states that the summation of static pressure (P_s) and dynamic pressure (P_d) of a low-speed flow remains constant in a tube.

$$P_s + P_d = \text{constant} = P_t \tag{2.20}$$

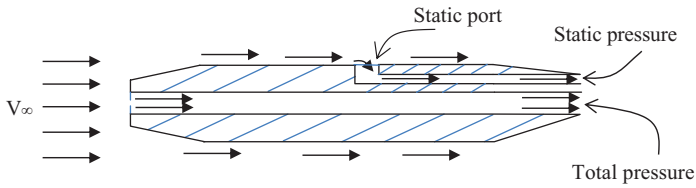

FIGURE 2.9 Schematic of a pitot tube.

The dynamic pressure (as defined in Chapter 1) is related to the density and the airspeed; therefore, if we measure the dynamic pressure and the density, we could determine the speed.

$$P_d = q = \frac{1}{2}\rho V^2 \tag{2.21}$$

There is a convenient way of measuring the dynamic pressure. If a tube is directly pointed into the flow of air, then connect the other end of it to a chamber (pressure measurement device). Thus, the oncoming air is brought to rest relative to the tube as it meets the blocked end of the tube. Since the tube exit is blocked, no air can flow down the tube. Then, the device will read the stagnation or total pressure (P_t). This type of tube is called a pitot tube (Figure 2.9) and provides a means of measuring the stagnation pressure.

Now consider a tube that has a blocked inlet. If we make a hole in the side of a tube and point it into the flow of air and then connect this via a tube to a pressure measurement device, a different result is obtained. The hole will not impede the airflow; thus, the pressure measured will be the local static pressure. A hole used for this purpose is called a *static port*. The pitot tube and static port are sometimes (as an alternative) combined to measure the total pressure and static pressure with one device. Using such a device, the dynamic pressure is readily determined by deducting the static pressure from the total pressure.

The pitot-static tube consists of two co-centric tubes. The inner one is simply a pitot tube, but the outer one is sealed in the front and has a few small holes in the side. By mounting it under the wing or on the fuselage side, it can be arranged so that it is well clear of interference from the flow around the aircraft. Pitot-static tubes are frequently used in wind tunnels.

By measuring the difference in pressure ($P_t - P_s$), we will obtain a measurement of the dynamic pressure (q). Combining Equations 2.20 and 2.21 yields:

$$V = \sqrt{\frac{2(P_t - P_s)}{\rho}} \tag{2.22}$$

Thus, we have a simple means of measuring airspeed. If we could find a way of assessing the air density, we could determine airspeed. The pressure difference

measuring device used on aircraft usually consists of a diaphragm. The stagnation pressure is applied to one side of the diaphragm, and the static pressure is applied to the other side. The resulting deflection of the diaphragm can then either be amplified through a series of levers or gears to cause a dial pointer to move or can be used to produce an electric signal to be fed into an appropriate electronic circuit or processor. So, this instrument generates a reading that is proportional to the dynamic pressure.

The pitot tube and static pressure holes are located at a suitable convenient position (see Figure 3.16) on the aircraft. Some convenient locations include (1) under the wing, (2) at the middle of fuselage nose, and (3) beside fuselage front or middle section. The location of the static tapping is very important because it is essential to select a position where the local static pressure is the same as that in the free stream. The location of the pitot tube is also very important because it is essential to select a position where the local airspeed is the same as that in the free stream and also is not too sensitive to change in the aircraft angle of attack and sideslip angle. The pitot and static holes are normally heated to avoid icing at low temperatures and high altitudes. The location of the holes will usually induce 2%–5% error in reading, so the pressure difference measuring device must be calibrated.

In cases where either the pitot head or static hole becomes blocked, there would be a significant inaccuracy in measuring airspeed. In the past, some deadly aircraft crashes were related to such an incident. On October 2, 1996, shortly after takeoff, the crew of a Boeing 757–200 (Figure 5.8), Aeroperú Flight 603, was confused by false speed [24] and altitude readings and contradictory warnings from the aircraft's air data system. In preparation for an emergency landing, the crew descended the aircraft but relying on false readings the crew went too far causing the aircraft to crash into the water, killing everyone on board. The false readings and contradictory warnings were caused by a duct tape over the static ports; the duct tape was used to protect the ports during the maintenance but was not removed afterward.

2.4.2 True and Equivalent Airspeeds

Speed and its measurement have a significant position in aircraft performance analysis. Although the GPS is a powerful tool in the measurement of several flight variables including aircraft speed, it only measures the ground speed, not the airspeed. In addition, due to safety reasons and FAA regulations, all aircraft use pitot tube to measure the aircraft speed. Airspeed is measured by comparing the difference between the pitot and static pressures (Figure 2.9) and, through mechanical linkages, displaying the resultant on an airspeed indicator.

A static port measures only the static pressure, since the hole is perpendicular to the airflow, and the flow must turn 90° to enter into the tube. In contrast, a pitot tube measures the dynamic pressure, since the hole faces the airflow. When a pitot tube has a static port, it is often referred to as the pitot-static tube.

By employment of the pitot tube and the static port, we deal with three types of aircraft speeds (i.e., airspeed): (1) indicated airspeed (IAS), (2) true airspeed (TAS), and (3) equivalent airspeed (EAS). Before explaining the difference between these three terms, it is beneficial to describe how a pitot tube works.

2.4.3 Airspeed Indicator

As stated in Section 2.4.1, the pitot and static tube combination provides a means of measuring the dynamic pressure. It does not provide speed directly, but we can calculate the speed if we know the air density using Equation 2.22. In an aircraft with no processor, there is no simple method of measuring air density, so all that could be done is to assume a constant value for air density (usually equivalent to sea-level air density). This means that this airspeed would correspond to that at the standard sea-level air density. This instrument is called an airspeed indicator.

Since the instrument is calibrated assuming one constant standard sea-level value of air density (ISA condition), it does not give the TAS, unless the aircraft is flying at a height where the density just happens to be equal to the standard sea-level value. The value of the IAS at which this occurs will always be the same whatever be the height. With the advance of technology, there are devices that can measure the true ground speed (e.g., GPS), but the airspeed indicator described earlier is still an important item on most cockpit instrument panels.

One important feature of this type of airspeed indicator is that it is more convenient in terms of safety and stall speed indication. In reality, stall speed increases with altitude; thus, a pilot must know stall speed at each altitude in order to keep aircraft speed above this speed, if the speed indicator shows the TAS. In other words, if the pilot had only a true speed indicator, he or she would have to know what the stall speed was at any altitude. With such an airspeed indicator, the pilot just has to remember to keep the above-indicated stall speed.

Nowadays, navigation systems have been advanced by the introduction of ground-based radios and satellites that can give very accurate indications of position and speed relative to the ground. Despite these advances, however, pilot students still have to learn the traditional methods of navigation in order to qualify for their license. Old instruments such as the airspeed indicator and the altimeter are simple and reliable and will not break down in the event of an electrical failure or a violent thunderstorm. Even on advanced modern airliners, an old mechanical airspeed indicator and a pressure altimeter are recommended to be employed, since they will continue to work even if all the electrical systems have failed.

2.4.4 Airspeed Indicator Corrections

The airspeed measured by the airspeed indicator (read from the dial) is referred to as the IAS. There are several sources of errors in this reading. The four notable sources of errors in measuring airspeed are (1) Instrument, (2) Pitot tube position, (3) Compressibility, and (4) Air density. The instrument itself may be aged, or a diaphragm may be suffering from some wear. This error is called an instrument error. By recalibrating the instrument, it is possible to determine what the correction should be at every indicated speed. IAS equals TAS only at sea level on a standard day.

There will also be errors due to the positioning of the pitot tube and static tapping on the aircraft. It is very hard to find a position around the aircraft where the static pressure is always exactly the same as the pressure in the free airstream. To determine the correction for such position errors, the aircraft can be flown in formation

with another aircraft with specially calibrated instruments. Once the position error correction has been applied, the speed is known as the calibrated airspeed (CAS). An airspeed correction table is provided by the aircraft manufacturer when the difference between TAS and IAS is significant.

For any aircraft that can fly faster than about Mach 0.3, it is necessary to apply a correction factor for compressibility, since Bernoulli's equation only applies to low subsonic speed incompressible flow.

For high-speed aircraft, the IAS has to be corrected for compressibility, and to do this we need a further instrument, one that indicates the speed relative to the local speed of sound. This instrument is called a Mach meter. Reference [25] is a rich source for various flight tests to determine CAS and the calibration of the airspeed indicator. If the compressibility effect and the real value of the air density are known, the CAS may be converted to real or TAS. Thus, TAS is found by correcting CAS for non-real air density and compressibility.

The instrument IAS may sometimes be more useful to the pilot than the TAS. For purposes of navigation, however, he or she must estimate his or her speed over the ground, and with traditional navigation methods, he or she must first determine the TAS and then make corrections to allow for the speed of the atmospheric wind relative to the ground. The TAS can be determined using the procedure mentioned earlier, but to do this we need to know the true air density. This can be obtained by using the altimeter reading and tables for the variation of relative density. In practice, as an alternative to calculations, the pilot can use tables showing the relationship between TAS and IAS at different heights under ISA conditions.

After all position and compressibility corrections have been applied, the resulting speed is called the EAS. Once the EAS has been obtained, it is quite easy to estimate the TAS that is required for navigation purposes. For a light piston prop aircraft, the corrections will be relatively small, and, for simple navigational estimates, the pilot can assume that the speed (IAS) reading from his or her instrument is about 10% different from the EAS. Table 2.1 summarizes various types of airspeeds used in flight analysis and flight tests.

By referring to the definition of dynamic pressure (Equation 2.21), we can write

$$q = \frac{1}{2}\rho_o V_E^2 = \frac{1}{2}\rho V_T^2 \tag{2.23}$$

TABLE 2.1
Airspeed Classification

No.	Airspeed	Description
1.	Indicated airspeed	The airspeed that is read directly from the dial of the airspeed indicator
2.	Calibrated airspeed	When position error corrections have been applied to indicated airspeed
3.	Equivalent airspeed	When compressibility corrections have been applied to calibrated airspeed
4.	True airspeed	When density corrections have been applied to equivalent airspeed

where ρ_o is the air density at sea level, and ρ is the air density at altitude. Now, we can readily conclude that

$$\left(\frac{V_E}{V_T}\right)^2 = \frac{\rho}{\rho_o} \tag{2.24}$$

Then, the TAS (or V_T) is the EAS (or V_E) divided by the square root of the relative air density (σ):

$$V_T = \frac{V_E}{\sqrt{\sigma}} \tag{2.25}$$

This relationship denotes that the EAS is always equal to or less than TAS. For instance, at 12,200 m, the true airspeed is slightly more than twice the indicated airspeed.

2.4.5 Airspeed and Ground Speed

When we speak of the speed of an airplane, we mean its speed relative to the air, or airspeed as it is usually termed. Now the existence of wind simply means that portions of the air are in motion relative to the Earth, and, although the wind will affect the speed of the airplane relative to the Earth, that is, its ground speed, it will not affect its speed relative to the air.

Similarly, if the wind had been blowing across the path, the pilot would have to incline his or her airplane several degrees toward the wind on both journeys so that it would have traveled crabwise. On both outward and homeward journeys, the airspeed would be the same although the wind would have been a headwind or a tailwind.

An airplane that encounters a headwind equal to its own airspeed will appear to an observer on the ground to stay still, yet its airspeed will be high. A free balloon flying in a wind travels over the ground, yet it has zero airspeed; that is, a flag on the balloon will hang vertically downward. Ground speed is, of course, important when the airplane changes from one medium to another, such as in takeoff and landing, and also in the time taken and the course to be steered when flying cross-country. In terms of aircraft performance, wind will not influence the flight endurance but changes the flight range. Thus, the wind speed will not influence aerodynamic forces and moments; it will change ground speed, aircraft heading, and flight range.

Example 2.2

An airplane is flying from city A (the east) to city B (the west) and then returns. The speed of the airplane (i.e., its airspeed) is 300 km/h, and these two cities are 600 km apart. There is a wind that is blowing from the west to the east at a speed of 40 km/h. Calculate the aircraft's airspeed and ground speed for both flights.

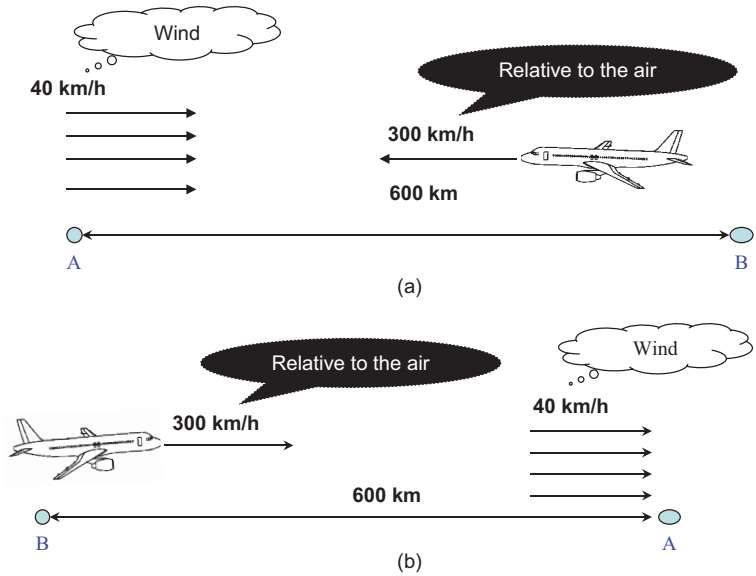

FIGURE 2.10 Airspeed and wind speed: (a) headwind and (b) tailwind.

Solution

If there is a wind of 40 km/h blowing from city B toward city A (see Figure 2.10a), the ground speed of the airplane as it travels from A to B will be 260 km/h, and it will take 2½ hours to reach B, but the airspeed will be 300 km/h.

$$300 - 40 = 260\,\text{km/h}$$

However, when the airplane flies back from city B to city A, the ground speed on the return journey will be 340 km/h (Figure 2.10b).

$$300 + 40 = 340\ \text{km/h}$$

The time to return to city A will be <2 h, but the airspeed will still remain 300 km/h; that is, the wind will strike the airplane at the same speed as on the outward journey.

A wind in the opposite direction of the aircraft direction is called headwind. A wind that has the same direction as the aircraft direction is called tailwind. A wind that blows perpendicular to the aircraft direction is referred to as crosswind. A headwind is beneficial in takeoff and landing, while a tailwind has a negative effect in takeoff and landing. The reason is that a headwind makes the takeoff run and landing run shorter (safer), while a tailwind makes the takeoff run and landing run longer. Since the runway length is limited in every airport, this may be a problem for some aircraft that need long runways. The problem with a crosswind during takeoff and landing is that it pushes the aircraft out of the runway. Thus, pilots need to employ their training skills to hold the aircraft inside and along the runway.

2.4.6 The Unit of Airspeed

The reader may have noticed that we have not been altogether consistent, nor true to the SI system, in the units that we have used for speed; these already include m/s, km/h, and knot. There are good reasons for this inconsistency, the main one being that for a long time to come it is likely to be convenient practice to use knot for navigational purposes, both by sea and by air, km/h for speeds on land, for example, of cars, while m/s is not only the proper SI unit but it must be used in certain formulae and calculations. We shall continue to use these different units throughout the book. The important point to remember is that it is only a matter of simple conversion from one to another unit.

A nautical mile or sea mile is a unit of distance and displacement. It is accepted for use with the SI unit, but it is not an SI unit. The nautical mile is used around the world for maritime and aviation purposes. It is commonly used in international law and treaties, especially regarding the limits of territorial waters. It developed from the geographical or statute mile. The nautical mile is roughly equal to 1 min[6] of angle at the equator. The angular length of the equator is 360° or roughly equivalent to 21,600 nautical miles. There is no official international standard symbol for the nautical mile. The symbols "nm" and "nmi" are commonly used in some areas. Here, we use the symbol "nm".

In terms of speed, one knot is equal to one nautical mile per hour. For cars and trains, statute mile is used in the United States, since statute mile is different from nautical mile. Relationships between various units of speed are as follows:

$$\text{knot} = \frac{\text{Nautical mile}}{\text{Hour}}$$

$$1\,\text{knot} = 0.5144\,\text{m/s} = 1.852\,\text{km/h} = 1.689\,\text{ft/s}.$$

It is often convenient to state the true and equivalent airspeeds in terms of knot; in such cases, knot true airspeed (KTAS) and knot EAS (KEAS) are used, respectively. The term or unit KEAS denotes knot EAS (or equivalent airspeed in knot), and KTAS represents knot true airspeed (or TAS in knot).

Example 2.3

The fighter aircraft F-15 has a mass of 30,845 kg and a wing area of 56.5 m^2. If this fighter is cruising at 15,000 m altitude with the lift coefficient of 0.1, determine its true and EAS in terms of knot.

[6] 1/60 of 1/360 degree of a circle.

Solution

Based on Appendix A, the air density at 15,000 m altitude is $\rho = 0.1935\,\text{kg/m}^3$. In cruising flight, lift is equal to weight, so

$$L = W = \text{mg} = 30{,}845 \times 9.81 = 302{,}589.5\,\text{N} \tag{2.19}$$

TAS is obtained when we use real air density:

$$L = \frac{1}{2}\rho V^2 S C_L \Rightarrow V = \sqrt{\frac{2 \times 302{,}589.5}{0.1935 \times 56.5 \times 0.1}} \Rightarrow V = 744\,\text{m/s(TAS)} \tag{2.6}$$

In terms of knot:

$$V_T = \frac{744}{0.5144} = 1{,}446.3\text{(KTAS)}$$

The EAS is

$$V_T = \frac{V_E}{\sqrt{\sigma}} \Rightarrow V_E = 1446.3 \times \sqrt{0.158} \Rightarrow V_E = 574.9\text{(KEAS)} \tag{2.25}$$

An alternative way is to use Equation 2.6, but employ air density at sea level.

2.5 STALL SPEED

The primary generator of the lift force in an aircraft is the wing. Thus, as the wing lift is increased or decreased, the same thing almost happens in the aircraft lift. In addition, the behavior of a wing (three-dimensional body) is very much similar to the behavior of its cross section (two-dimensional airfoil). As the wing angle of attack (α) is increased, it produces more lift and more non-dimensional lift (i.e., lift coefficient, C_L). As with an airfoil, this is true up to a specific angle.

Figure 2.11 shows a typical variation of lift coefficient with angle of attack. As the angle of attack is increased beyond a certain value, the lift coefficient peaks at some maximum value, $C_{L_{\max}}$, and then drops precipitously as α is further increased. In this situation, where the lift is rapidly decreasing at high α, the wing airfoil is stalled. This behavior reflects non-linearity that must be dealt with. This incidence of stall hurts the aircraft performance and must be prevented. Computer models don't do an accurate job of predicting the behavior of the air flowing around an aircraft when its wings have a high angle of attack in near-stall conditions.

The phenomenon of airfoil stall is of critical importance in aircraft performance. It is caused mainly by flow separation on the upper surface of the wing. The angle at which stall happens is referred to as stall angle (α_s). In practice, the stall angle is the highest angle that a wing may be safe to have in a flight. The magnitude of this angle depends on the aircraft configuration and sometimes can be increased a few degrees by utilizing a high-lift device such as flap. For most aircraft, the stall angle is about 15°. High-lift device systems consist of leading and trailing edge devices whose primary function is to produce a higher $C_{L_{\max}}$. The plain wing of the transport aircraft

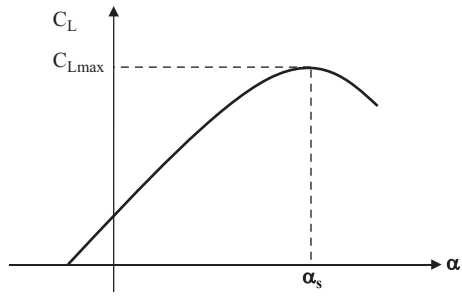

FIGURE 2.11 Wing lift curve slope.

DC-9-30 has a $C_{L_{max}}$ of 2.1, while it is increased to 3 when the high-lift devices are extended.

From the point of view of aircraft performance, a higher angle of attack means a lower speed in a level flight. If a pilot in a cruising flight needs to reduce the aircraft speed, he or she should increase the aircraft angle of attack and reduce the throttle setting. The reason is discussed in Chapter 5. In an aircraft, wing area is fixed, so the only option is to increase the lift coefficient. However, the lift coefficient has a maximum, thus aircraft speed cannot be reduced from a specific value. This speed is called stall speed (V_s), since it corresponds with the stall angle. The stall speed is the lowest speed at which a steady controllable flight of a fixed wing, non-Vertical Takeoff and Landing (VTOL) aircraft can be maintained.

If a pilot continues to reduce the speed further than this speed, it will lose part of its lift and therefore cannot maintain a sustained cruising flight. This means losing height and ending up in a tragic crash. At this speed, the aircraft begins to vibrate and is unstable. In this situation, the aircraft is no longer in trim condition and needs to be recovered. The stall speed is the lowest speed at which a trimmed cruising flight is possible. The VTOL aircraft and helicopters are exception from this phenomenon, and they can have zero speed while flying. When the aircraft speed is reduced to its lowest steady-level value (stall speed), this means that the lift coefficient has reached its maximum value ($C_{L_{max}}$). Therefore, at the stall speed in a trimmed cruising flight, we have

$$L = \frac{1}{2}\rho V_s^2 S C_{L_{max}} \tag{2.26}$$

By substituting lift with aircraft weight (as in Equation 2.19), we obtain an equation for stall speed:

$$V_s = \sqrt{\frac{2W}{\rho S C_{L_{max}}}} \tag{2.27}$$

The stall speed of each aircraft is unique. Table 2.2 demonstrates stall speeds and maximum lift coefficients for several aircraft. From the safety point of view, the

TABLE 2.2
Stall Speed and Maximum Lift Coefficient for Several Aircraft

No	Aircraft	Type	Engine	Mass (kg)	$C_{L_{max}}$	*P* or *T*	V_s (knot)
1.	Cirrus VK30	GA	Piston	1,520	2.51	35 hp	57
2.	Eipper Quicksilver	Ultralight	Piston	259	2	35 hp	24
3.	Mirage celerity	Homebuilt	Piston	828	2.83	160 hp	46
4.	Volmer VJ-23	Hang glider	No engine	136	2.93	0	13
5.	Swiss Aerolight Nimbus	Hang glider	No engine	138	2.57	0	16
6.	Embraer EMB 121A1	Transport	Turboprop	5,670	2.16	2×750 hp	76
7.	DHC-8 Dash-100	Transport	Turboprop	14,968	3.2	2×1,800 hp	72
8.	Grob G115	Light	Piston	680	1.61	115 hp	57
9.	Soko J-22 Orao	Fighter	Turbofan	10,326	1.42	2×17.8 kN	130
10.	Aeritalia G222	Transport	Turboprop	28,000	2.93	2×3,400 hp	84
11.	Siai-Marchetti	Military trainer	Turbofan	2,750	2.2	11.12 kN	74
12.	Sukhoi SU-26M	Racer	Piston	800	1.34	360 hp	55
13.	British Aerospace BAe 146-300	Transport	Turbofan	42,184	3.17	4×31 kN	102
14.	Boeing 737-200	Transport	Turbofan	56,472	2.66	2×71.2 kN	102
15.	Cessna 208	GA	Turboprop	3,311	2.14	600 hp	60
16.	Saab 340A	Transport	Turboprop	12,372	2.1	2×1,735 hp	93
17.	Bell Boeing V-22 Osprey	Tiltrotor VTOL	Turboprop/ turboshaft	21,546	—	2×6,150 hp	110
18.	Cessna citation II	Transport	Turbofan	6,033	1.73	2×11.1 kN	82
19.	Silver Eagle	Ultralight	Piston	251	—	23 hp	24
20.	Falcon 900	Transport	Turbofan	20,640	2.25	3×20 kN	82
21.	Grumman F-14 Tomcat	Fighter	Turbofan	33,724	2.94	2×93 kN	115
22.	Bede BD-17	Sport plane	Piston	430	2.37	60 hp	47
23.	Antonov An-70	Transport	Propfan	145,000	—	4×10,350 kW	61
24.	Pegasus Quantum	Ultralight trike	Piston	409	—	80 hp	33

lower the stall speed, the safer the aircraft in takeoff and landing. Stall speed for ultralight aircraft is about 20–30 knots, for very light aircraft is about 30–50 knots, for light general aviation (GA) aircraft is about 40–60 knots, for large transport aircraft is about 90–110 knots, and for supersonic fighters is about 110–180 knot. Unless

FIGURE 2.12 Aircraft Raytheon Hawker 800XP. (Courtesy of Gustavo Corujo—Gusair.)

stall speed handling is practiced, a non-VTOL aircraft pilot must be careful not to reduce the airspeed below the stall speed. As a margin of safety, pilots are recommended to fly with a speed greater than about 10%–30% of stall speed.

Aircraft designers try hard to lower the stall speed as much as possible by using powerful high-lift devices such as flaps. In Chapter 3, descriptions of several flaps are reviewed. The maximum lift coefficient of typical aircraft is about 1–1.6 without using any high-lift devices. With the application of high-lift devices, the maximum lift coefficient increases up to about 2–3. According to Federal Aviation Regulations (FAR), Part-23 and European Aviation Safety Agency, EASA-VLA (formerly called JAR-VLA[7]), the stall speed must be lower than the following values:

$$V_s \leq 61\,\text{knot}\,(\text{FAR-23}) \tag{2.28}$$

$$V_s \leq 45\,\text{knot}\,(\text{EASA-VLA}) \tag{2.29}$$

Figure 2.12 shows the twin-turbofan business transport aircraft Hawker 800XP with a $C_{L_{\max}}$ of 2.26. Figure 2.13 demonstrates a Eurofighter EF-2000 Typhoon, a single-seat fighter in an angle beyond stall angle.

A Gulfstream G650 test aircraft suffered [26] stall and crashed shortly after takeoff during type certification flights of the design in 2011. The National Transportation Safety Board (NTSB) determined that Gulfstream failed to validate safe takeoff speeds for the test program.

Example 2.4

Transport aircraft DC-9-30 has a mass of 54,884 kg, a wing area of 92.9 m^2, and is equipped with a double-slotted flap. The aircraft has a maximum lift coefficient of 2.1 without flap deflection. When the flap is deflected 50°, the maximum lift coefficient will reach 3. (1) Determine the stall speed in both cases, that is, with and without flap deflection (assume sea level, ISA condition). (2) Determine true and equivalent stall speeds at 20,000 ft altitude, when the flap is deflected.

[7] Joint Aviation Requirements—very light aircraft (FAR equivalent in Europe).

FIGURE 2.13 Eurofighter EF-2000 Typhoon, a single-seat fighter in an angle beyond stall angle. (Courtesy of Fabrizio Capenti.)

Solution

The stall speed without flap is

$$V_s = \sqrt{\frac{2W}{\rho S C_{L_{\max}}}} = \sqrt{\frac{2\times 54{,}884\times 9.81}{1.225\times 92\times 2.1}} \Rightarrow V_s = 67.12\,\text{m/s} = 130.5\,\text{knot(TAS)} \quad (2.27)$$

The stall speed with the flap deflected is

$$V_s = \sqrt{\frac{2W}{\rho S C_{L_{\max}}}} = \sqrt{\frac{2\times 54{,}884\times 9.81}{1.225\times 92\times 3}} \Rightarrow V_s = 56.16\,\text{m/s} = 109.18\,\text{knot(TAS)}$$

The true stall speed with the flap at 20,000 ft ($\rho = 0.653\,\text{kg/m}^3$) is

$$V_s = \sqrt{\frac{2W}{\rho S C_{L_{\max}}}} = \sqrt{\frac{2\times 54{,}884\times 9.81}{0.653\times 92\times 3}} \Rightarrow V_s = 76.92\,\text{m/s} = 149.5\,\text{knot(TAS)}$$

The equivalent stall speed with the flap at 20,000 ft is

$$V_T = \frac{V_E}{\sqrt{\sigma}} \Rightarrow V_{s_E} = \sqrt{\sigma}\ V_{s_T} = \sqrt{\frac{0.653}{1.225}} \times 76.92 = 56.16\,\text{m/s} = 109.18\,\text{knot(EAS)} \quad (2.25)$$

You may have noticed that the equivalent stall speed at 20,000 ft is the same as the true stall speed at the sea level, as we expected.

In Example 2.4, we observed that the equivalent stall speed of DC-9-30 at 20,000 ft altitude is the same as the true stall speed at sea level. This is a correct statement for every aircraft at any altitude and at any speed. In other words, for any aircraft, the equivalent stall speed at any altitude is the same as the true stall speed at sea level. This is correct, whereas the true stall speeds at two different altitudes are not the same.

This is one of the reasons why pilots are happy to use EAS when dealing with stall speed. They only need to remember one number. No matter what the altitude is, the pilot should not reduce the aircraft equivalent speed below a specific equivalent

stall speed. If the pilot uses TAS, he or she must remember true stall speeds for all altitudes, since they are different at every altitude. For this purpose, a speed meter in front of a pilot has a red mark to warn about the stall speed. With this simple technique, pilots are assured not to fly with a speed below stall speed. Furthermore, there is a warning device (e.g., a horn in most GA aircraft) to warn pilots when they are flying near stall speed. Although the equivalent stall speed is not a TAS, it has an important property that simplifies the pilot's job and increases flight safety.

PROBLEMS

In all problems, assume ISA condition, unless otherwise stated.

2.1 Determine the lift coefficient of an aircraft with a 180 ft^2 wing area and a mass of 3,200 kg in a cruising flight when flying at sea level with a speed of (a) 80 knot, (b) 130 knot.

2.2 An aircraft with a mass of 1,200 kg and a wing area of 14 m^2 is cruising at 3,000 ft altitude. Determine its lift coefficient when the TAS is 100 knots.

2.3 Assume that the aircraft in Problem 2.2 has a drag coefficient of 0.05. How much thrust is the engine producing?

2.4 Determine lift curve slope (in 1/rad) of a wing with an AR of 12.5. Then, calculate the lift coefficient of this wing when its angle of attack is 5°. Assume that the zero lift angle of attack is zero and ao is 2π (1/rad).

2.5 Calculate the true and equivalent stall speeds of the aircraft in Problem 2.2, when the maximum lift coefficient is 1.6.

2.6 An aircraft is required to climb with 10° of climb angle. The aircraft has a mass of 30,000 kg and produces 50,000 N of drag. Assume zero angle of attack and zero thrust setting angle.
   a. How much lift must this aircraft generate?
   b. How much thrust must the aircraft engine produce?

2.7 An aircraft that is initially at rest is accelerating on a runway with an acceleration of 10 m/s^2. Consider a moment when other features of this aircraft are

$$S = 30\,m^2,\ m = 6{,}000\,kg,\ C_L = 0.7, C_D = 0.1,\ V = 60\,knot$$

Calculate the engine thrust, assuming that the friction force is constant and equal to 2% of the aircraft weight.

2.8 A cargo aircraft with a weight of 145,000 lb and a wing area of 1,318 ft^2 has a maximum lift coefficient of 2.5. Is this aircraft able to cruise at an altitude of 25,000 ft and ISA + 15 condition with a speed of 150 KTAS?

2.9 A hang glider (Nimbus) has a mass (structure plus pilot) of 138 kg and a wing area of 16.2 m^2 and stall speed of 16 knots. What is the maximum lift coefficient?

2.10 Calculate the wing area of a hang glider Volmer VJ-23. The aircraft geometry and mass information may be taken from Table 2.2. If the pilot mass is 75 kg, what is the mass of the aircraft structure?

2.11 The sport aircraft Butterworth has the following characteristics:

$$m = 635\,\text{kg},\ S = 10.4\,\text{m}^2,\ V_s = 56\,\text{knot}\left(\text{at sea level}\right)$$

Assume that the maximum speed of this aircraft at every altitude is 126 knots (TAS). At what altitude, maximum TAS and stall TAS will be the same?

2.12 The cargo aircraft C-130 has an empty mass of 13,000 kg, a wing area of 85 m^2, and a stall speed of 94 knot (EAS). If the maximum lift coefficient is 2.2, determine the maximum mass of payload (cargo and crew) plus fuel to satisfy this stall speed.

2.13 The bomber B-1B has a maximum takeoff mass of 216,367 kg, a 181 m^2 wing area, and a maximum velocity of Mach 2.2. Assume the drag coefficient of this aircraft at cruise is 0.03, how much thrust do the four engines generate for this flight condition?

2.14 The trainer aircraft PC-7 with a mass of 2,700 kg and a wing area of 16.6 m^2 has a cruising speed of 330 km/h.

a. What is the lift coefficient when cruising at 5,000 m altitude, ISA condition?
b. How much lift coefficient must be increased when cruising on this day and at the same altitude? On a summer day, the temperature at sea level is 42°C.

2.15 A maneuverable aircraft has a mass of 6,800 kg, a wing area of 32 m^2, and a drag coefficient of 0.02. The aircraft is required to climb vertically with a speed of 100 knots. How much thrust does the engine need to produce?

2.16 Calculate the wing area of the aircraft EMB-121A1. The aircraft geometry and weight data may be taken from Table 2.2.

2.17 Is fighter aircraft F-14 able to fly vertically? The aircraft data may be taken from Table 2.2. Assume the drag coefficient to be 0.03.

2.18 The dynamic pressure of an aircraft that is cruising at an altitude is 9,000 N/m^2.

a. Determine the altitude, if the aircraft speed is 389 KTAS?
b. Calculate aircraft EAS in terms of KEAS.

2.19 A transport aircraft is cruising at 20,000 ft altitude with a speed of Mach 0.5. If a 50 m/s headwind is blowing, what is the ground speed and TAS in terms of knot?

2.20 The aircraft Voyager is able to fly around the globe without refueling. In one mission, the aircraft is flying at the equator at an altitude of 15,000 ft with a speed of 110 knots. Assume that there is a 15 m/s wind blowing from the west to the east all the time.

a. How many days does it take to do this mission if cruising from the west to the east?
b. How many days does it take to do this mission if cruising from the east to the west?

Note: The Earth has a diameter of 12,800 km.

2.21 The aircraft Cessna Citation II is climbing with 3° of angle of attack. The geometry and weight data of this aircraft may be taken from Table 2.2.
   a. If the drag coefficient is 0.035, determine its climb angle, when climbing with a speed of 160 knot.
   b. Determine the ratio of lift to weight at this climbing flight.

2.22 A transport aircraft with a wing area of 200 m^2 is cruising with a speed of Mach 0.6 at 35,000 ft altitude, ISA condition.
   a. Determine the mass of aircraft, if the lift coefficient is 0.24.
   b. Determine the engine thrust, if the drag coefficient is 0.035.

2.23 A transport aircraft with a wing area of 420 m^2 is cruising at a constant speed of 550 knots (KTAS) at 38,000 ft altitude. The aircraft has a mass of 390,000 kg at the beginning of a cruising flight and consumes 150,000 kg of fuel at the end of the cruise. Determine the wing angle of attack at the beginning and end of the cruise. Also assume

$$\mathrm{AR} = 8.5,\ a_o = 2\pi(1/\mathrm{rad}),\ \alpha_o = -1°.$$

2.24 The aircraft Falcon 900 is going to take off from a runway on a winter day (ISA-20). It starts from rest and after a few seconds, when speed reaches 0.5 Vs, friction force is 1% of aircraft weight and the drag coefficient is 0.1.
   a. Determine aircraft acceleration for this moment.
   b. How long does it take to come to this point? Assume that the acceleration is constant during this period.
   Note: Aircraft geometry and weight data may be taken from Table 2.2.

2.25 Repeat Problem 2.24, assuming that the aircraft is taking off on a summer day (ISA + 20).

2.26 An aircraft that is initially at rest is accelerating on a runway for a takeoff operation. When the aircraft speed is 35 KTAS, the acceleration is 10 m/s^2. Other features of this aircraft at this time are

$$S = 35\,\mathrm{m}^2,\ m = 6{,}400\,\mathrm{kg},\ C_L = 0.8,\ C_D = 0.037.$$

If the friction coefficient is 0.02, calculate the engine thrust. Assume sea-level ISA condition.

2.27 The aircraft (Figure 2.14) is descending at a constant airspeed and a descent angle of 20°. The aircraft has an angle of attack of 5°, and engines have a setting angle of 3°. Draw forces (weight, aerodynamic forces, and engine thrust) on the aircraft and derive the governing equations for this flight phase.

2.28 A fighter aircraft is climbing with an arbitrary climb angle. The aircraft has two turbofan engines; both engines have positive degrees of setting angle. Draw the side view of the aircraft with an arbitrary angle of attack. Then, derive the governing equations of motion for this climbing flight.

2.29 A non-VTOL fighter aircraft is climbing vertically at sea level. The aircraft has two turbofan engines; both engines have positive degrees of setting angle. Draw the side view of the aircraft with an arbitrary angle of attack. Then, derive the governing equations of motion for this climbing flight.

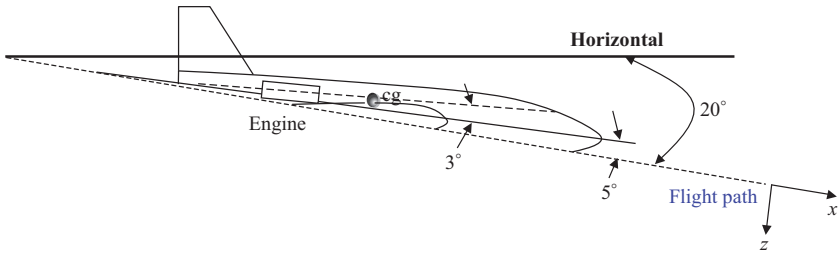

FIGURE 2.14 An aircraft in descending flight.

2.30 A VTOL aircraft is climbing vertically at sea level. The aircraft has two turbofan engines, which during takeoff they are arranged such that, they produce a thrust which is upward. Draw the side view of the aircraft with an arbitrary angle of attack. Then, derive the governing equations of motion for this climbing flight.

2.31 A pilot is planning to fly from the east to the west at 5,000 m altitude such that he or she can watch the sunset for a couple of hours. What must be the flight speed (in Mach number) in order to achieve such an objective? Assume there is a 30-knot headwind during this flight. The radius of Earth at sea level is 6,400 km.

2.32 A transport aircraft Boeing 777 (Figure 7.18) is descending at a velocity of 318 mph at 8,200 ft.

a. After 1 min, the altitude is 4,000 ft, the airspeed is 234 mph, determine the average descent angle.

b. After 1 min, the altitude is the touchdown (sea-level altitude), the airspeed is 180 mph, determine the average descent angle and deceleration. This phase takes one minute.

2.33 The Earth is moving in a circular orbit about the sun, with a radius of 147×109 m. The duration of one turn is 1 year. Determine the velocity of Earth in terms of speed of sound (i.e., the Mach number) at sea level.

2.34 On March 24, 1960, the maximum speed of a Tu-114-the world's fastest propeller-driven aircraft—on a 1,000 km closed circuit with payloads of 0–25,000 kg was recorded to be 871.38 km/h. Determine this velocity in terms of the Mach number. Assume sea level.

2.35 Two aircraft (A and B) are flying with a speed of Mach 0.9. Aircraft A is flying at sea level, while aircraft B is at 40,000 ft. Determine the airspeed of both aircraft. Which one has a faster speed? Then, determine the percentage difference.

2.36 A fighter aircraft with a maximum take of weight of 60,000 lb is accelerating for takeoff from stationary to 150 miles per hour in just two seconds. (a) Determine the aircraft acceleration. (b) Compare the aircraft acceleration with gravity acceleration; find the ratio.

2.37 A fighter aircraft with a maximum take of weight of 50,000 lb is accelerating for takeoff from stationary to 120 knots after traveling 400 ft. (a) Determine the aircraft acceleration. (b) Compare the aircraft acceleration with gravity acceleration; find the ratio.

2.38 A transport aircraft is flying at 11,000 m altitude. From GPS measurement, the aircraft speed is 900 km/hr. However, from pitot tube measurement, the airspeed is 400 KTAS.

a. Assume, there is a tailwind/headwind, calculate the wind speed. Is this a tailwind or a headwind?
b. Determine the total pressure that the pitot tube is measuring.
c. Compare the total pressure and static pressure (in percent).

3 Drag Force and Drag Coefficient

3.1 INTRODUCTION

Drag is the enemy of flight and imposes the major cost. In Chapter 2, major forces that influence an aircraft's motion are briefly introduced. One group of those forces is aerodynamic forces which are classified into lift and drag. A prerequisite to aircraft performance analysis is the ability to calculate the aircraft drag under various flight conditions. One of the jobs of a performance engineer is to determine drag force produced by an aircraft at different altitudes, speeds, and configurations. This is not an easy task, since this force is a function of several parameters, including aircraft configuration and components. As discussed in Chapter 2, drag is a function of aircraft speed, wing area, air density, and its configuration. Each aircraft is designed with a unique configuration; thus, aircraft performance analysis must take this configuration into account. The configuration effect of aircraft drag is represented through the drag coefficient (C_D), plus a reference area that relates to the aircraft.

An aircraft is a complicated three-dimensional vehicle, but, for simplicity in calculation, we assume that the drag is a function of a two-dimensional area, and we call it the reference area. This area could be any area, including tail area, wing area, fuselage cross-sectional area (i.e., fuselage cross section), fuselage surface area, and even aircraft top-view area. No matter what area is selected, the drag force must be the same. This unique drag comes from the fact that the drag coefficient is a function of the reference area.

Therefore, if we select a small reference area, the drag coefficient shall be large; if we choose a large reference area, the drag coefficient shall be small. In an air vehicle with a small wing area (e.g., high-speed missile), the fuselage cross-sectional area (normal to the flow) is often considered as the reference area. However, in an aircraft with a large wing, the top-view planform area (in fact, gross wing area) of the wing is often assumed to be the reference area.

The measurement of this area is easy, and it usually includes the most important aerodynamic part of the aircraft. This simplified reference area is compensated with the complicated drag coefficient, as we discussed in Chapter 2.

$$D = \frac{1}{2}\rho V^2 S C_D \tag{3.1}$$

The drag coefficient (C_D) is a non-dimensional parameter, but it takes into account every aerodynamic configuration aspect of the aircraft, including large components such as wing, tail, fuselage, engine, and landing gear and small elements such as rivets and antenna. This coefficient has two main parts (as will be explained in the next section). The first part is referred to as lift-related drag coefficient or induced drag coefficient (C_{D_i}), and the second part is called zero-lift drag coefficient (C_{D_o}). The calculation

DOI: 10.1201/9781003279068-3

of the first part is not very hard, but it takes a long time and energy to determine the second part. In large transport aircraft, this task is performed by a group of up to 20 engineers for a time period of up to 6 months. For this reason, a large portion of this chapter is devoted to the calculation of (C_{D_o}). This calculation is not only time-consuming but also very sensitive, since it influences every aspect of aircraft's performance.

One of the occasions in which the drag is considered a beneficial factor and is effectively used is in parachutes. A parachute is a device employed to considerably slow the motion of an object/vehicle through an atmosphere (e.g., Earth or Mars) by increasing drag. Parachutes are used with a variety of loads, including people, food, equipment, and space capsules. Drogue chutes are used to sometimes provide horizontal deceleration of a vehicle (e.g., space shuttle after a touchdown). The parachute is utilized by paratroopers to extremely reduce the terminal speed for a safe landing.

One of the primary functions of aerodynamicists and aircraft designers is to reduce this coefficient. Aircraft designers are very sensitive about this coefficient because any change in the external configuration of aircraft will change this coefficient and finally the aircraft's direct operating cost.

As a performance engineer, you must be able to estimate the (C_{D_o}) of any aircraft just by looking at its three views with an accuracy of about 30%. As you spend more time for calculation, this estimation will be more accurate but will never be exact, unless you use an aircraft model in a wind tunnel or flight test measurements with a real aircraft model. The method presented in this chapter is about 90% accurate for subsonic aircraft and 85% for supersonic aircraft. The accurate calculation of drag for aircraft is still a challenge – even with using advanced computational fluid dynamics (CFD) techniques [27]. The reasons lie behind modeling boundary layer, turbulent flow, flow separation, skin friction, interaction between shock wave and boundary layer, and three-dimensional flowfield.

3.2 DRAG CLASSIFICATION

Drag force is the summation of all forces that resist aircraft motion. The calculation of drag of a complete aircraft is a difficult and challenging task, even for the simplest configurations. We will consider the separate sources of drag that contribute to the total drag of an aircraft. The variation of drag force as a function of airspeed looks like a graph of parabola. This indicates that the drag initially reduces with airspeed and then increases as the airspeed increases. It demonstrates that there are some parameters that will decrease drag as the velocity increases and some other parameters that will increase drag as the velocity increases. This observation shows us a nice direction for drag classification.

Although drag and the drag coefficient can be expressed in a number of ways, for reasons of simplicity and clarity, the parabolic drag polar will be used in all main analyses. Different references and textbooks use different terminologies, so it may confuse students and engineers. This section presents a list of definitions of various types of drag and a classification of the drag forces.

Induced drag: The drag that results from the generation of a trailing vortex system downstream of a lifting surface with a finite aspect ratio (AR). In other words, this type of drag is induced by the lift force.

Parasite drag: The total drag of an airplane minus the induced drag. Thus, it is the drag not directly associated with the production of lift. Parasite drag is composed of drag of various aerodynamic components, the definitions of which follow.

Skin friction drag: The drag on a body resulting from viscous shearing stresses (i.e., friction) over its contact surface (i.e., skin). The drag of a very streamlined shape such as a thin, flat plate is frequently expressed in terms of skin friction drag. This drag is a function of the Reynolds number. There are mainly two cases where the flow in the boundary layer is entirely laminar or entirely turbulent over the plate. The Reynolds number is based on the total length of the object in the direction of the velocity. In a usual application, the boundary layer is normally laminar near the leading edge of the object undergoing transition to a turbulent layer at some distance back along the surface.

A laminar boundary layer begins to develop at the leading edge and its thickness grows downstream. At some distance from the leading edge, the laminar boundary becomes unstable and is unable to suppress disturbances imposed on it by surface roughness or fluctuations in the free stream. In a distance, the boundary layer usually undergoes a transition to a turbulent boundary layer. The layer suddenly increases in thickness and is characterized by a mean velocity profile on which a random fluctuating velocity component is superimposed. The distance from the leading edge of the object to the transition point can be calculated from the transition Reynolds number. Skin friction factor is independent of surface roughness in laminar flow but is a strong function of surface roughness in turbulent flow due to the boundary layer.

Form drag (sometimes called Pressure drag): The drag on a body resulting from the integrated effect of the static pressure acting normal to its surface resolved in the drag direction. Unlike the skin friction drag that results from viscous shearing forces tangential to a body's surface, form drag results from the distribution of pressure normal to the body's surface. In an extreme case of a flat plate normal to the flow, the drag is totally the result of an imbalance in the pressure distribution. As with skin friction drag, form drag is generally dependent on the Reynolds number. Form drag is based on the projected frontal area. As a body begins to move through the air, the vorticity in the boundary layer is shed from the upper and lower surfaces to form two vortices of opposite rotation.

A number of symmetrical shapes having drag values [13] at low speed are illustrated in Table 3.1. The drag coefficient values in this table are based on the frontal area. In this table, the flow comes from the left to the right.

Interference drag: The increment in drag resulting from bringing two bodies in proximity to each other. For example, the total drag of a wing–fuselage combination will usually be greater than the sum of the wing drag and fuselage drag independent of each other.

Trim drag: The increment in drag resulting from the (tail) aerodynamic forces required to trim the aircraft about its center of gravity. Trim drag usually is a form of induced and form drag on the horizontal tail.

Profile drag: Usually taken to mean the total of the skin friction drag and form drag for a two-dimensional airfoil section.

Cooling drag: The drag resulting from the momentum lost by air that passes through the powerplant installation for the purpose of cooling the engine.

TABLE 3.1
Drag Coefficient Values for Various Geometries and Shapes

(a) Two-Dimensional Bodies (*L*: Length along Flow, *D*: Length Perpendicular to the Flow)

No	Body	Status	Shape	C_D
1	Square rod	Sharp corner		2.2
		Round corner		1.2
2	Circular rod	Laminar flow		1.2
		Turbulent flow		0.3
3	Equilateral triangular rod	Sharp edge face		1.5
		Flat face		2
4	Rectangular rod	Sharp corner 	$L/D = 0.1$	1.9
			$L/D = 0.5$	2.5
			$L/D = 3$	1.3
		Round front edge 	$L/D = 0.5$	1.2
			$L/D = 1$	0.9
			$L/D = 4$	0.7
5	Elliptical rod 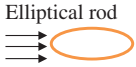	Laminar flow	$L/D = 2$	0.6
			$L/D = 8$	0.25
		Turbulent flow	$L/D = 2$	0.2
			$L/D = 8$	0.1
6	Symmetrical shell	Concave face		2.3
		Convex face		1.2
7	Semi-circular rod	Concave face		1.2
		Flat face		1.7

(b) Three-Dimensional Bodies (*L*: length, *D*; diameter)

No	Body	Laminar/Turbulent	Status	C_D
1	Cube	$Re > 10{,}000$		1.05
2	Thin circular disk	$Re > 10{,}000$		1.1
3	Cone ($\theta = 30^o$)	$Re > 10{,}000$		0.5
4	Sphere	Laminar $Re \leq 2 \times 10^5$		0.5
		Turbulent $Re \geq 2 \times 10^6$		0.2
5	Ellipsoid	Laminar $Re \leq 2 \times 10^5$		0.3–0.5
		Turbulent $Re \geq 2 \times 10^6$		0.1–0.2
6	Hemisphere	$Re \geq 10{,}000$	Concave face	0.4
		$Re \geq 10{,}000$	Flat face	1.2
7	Rectangular plate	$Re \geq 10{,}000$	Normal to the flow	1.1–1.3
8	Vertical cylinder	$Re \leq 2 \times 10^5$	$L/D = 1$	0.6
			$L/D = \infty$	1.2
9	Horizontal cylinder	$Re \geq 10{,}000$	$L/D = 0.5$	1.1
			$L/D = 8$	1
10	Parachute	Laminar flow		1.3

Wave drag: This drag, limited to supersonic flow, is a form of induced drag resulting from non-canceling static pressure components to either side of a shock wave acting on the surface of the body from which the wave is emanating.

The material to follow will consider these various types of drag in detail and will present methods for reasonably estimating their magnitudes. Figure 3.1 illustrates the classification of drag into two major groups.

For a conventional aircraft, the drag is divided into two main parts: lift-related drag and non-lift-related drag. The first part is called induced drag (D_i) because this drag is induced by lift (pressure). The second part is referred to as zero-lift drag (D_o), since it does not have any influence on lift and mainly originates from shear stress.

$$D = D_o + D_i \tag{3.2}$$

a. *Induced drag:* Induced drag is the drag directly associated with the production of lift. This results from the dependency of the lift on angle of attack. As the angle of attack of the aircraft (i.e., lift coefficient) varies, this type of drag is changed. The induced drag in itself consists of two parts. The first part originates from vortices around the wing, tail, fuselage, and other components. The second part is because of air compressibility effect. In low subsonic flight, it is negligible, but, in high subsonic and transonic flight, it must be taken into account. In supersonic flight, wave drag (D_w) is added to the induced drag. The reason is to account for the contribution of shock waves. The wing is the major aircraft component contributor for the lift production. Thus, about 80% of the induced drag comes from the wing, about 10% comes from tail, and the rest originates from other components. The induced drag is a function of airspeed, air density, reference area, and the lift coefficient:

$$D_i = \frac{1}{2}\rho V^2 S C_{D_i} \tag{3.3}$$

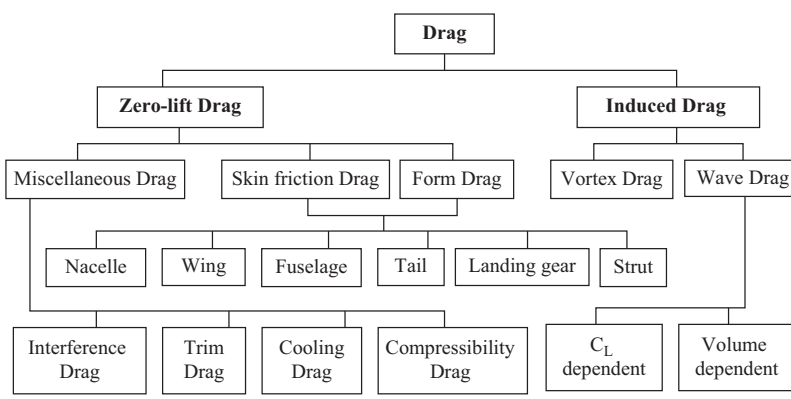

FIGURE 3.1 Drag classification.

In this equation, the coefficient C_{D_i} is called induced drag coefficient. The method to calculate this coefficient will be introduced in the next section. Figure 3.2 shows the behavior of induced drag as a function of airspeed. As the airspeed increases, the induced drag decreases; therefore, the induced drag is inversely a function of airspeed.

b. *Zero-lift drag:* The zero-lift drag includes all types of drag that do not depend on production of the lift. Every aerodynamic component of aircraft (i.e., the components that are in direct contact with flow) generates zero-lift drag. Typical components are wing, horizontal tail, vertical tail, fuselage, landing gear, antenna, engine nacelle, and strut. The zero-lift drag is a function of airspeed, air density, reference area, and the external shape of the components:

$$D_o = \frac{1}{2}\rho V^2 S C_{D_o} \tag{3.4}$$

In this equation, the coefficient C_{D_o} is called zero-lift drag coefficient. The method to calculate this coefficient will be introduced in Section 3.4. Figure 3.2 shows the variations of zero-lift drag as a function of airspeed. As the airspeed increases, the induced drag increases too; therefore, the zero-lift drag is directly a function of airspeed.

From Equations 3.1–3.4, one can conclude that drag coefficient has two components:

$$C_D = C_{D_o} + C_{D_i} \tag{3.5}$$

The calculation of C_{D_i} is not a big deal and will be explained in the next section, but the calculation of C_{D_o} is very challenging, tedious, and difficult. A major portion of this chapter is devoted to the calculation of C_{D_o}. The main idea behind this chapter is about the calculation of C_{D_o}.

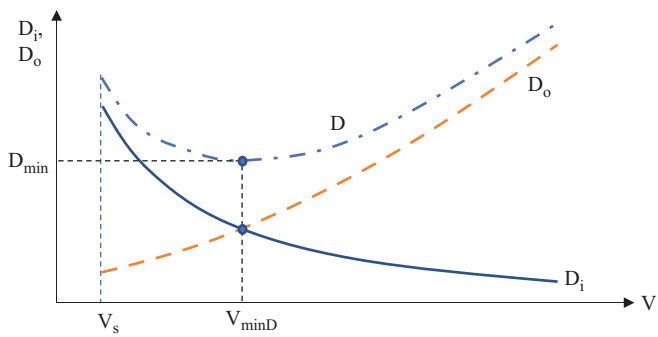

FIGURE 3.2 Variations of D, D_o, and D_i versus velocity.

3.3 DRAG POLAR

The aircraft drag may be mathematically modeled by a variety of methods. It seems natural to seek the similarity of variation of drag due to a flight parameter to a standard figure or geometry. We are looking for an accurate, but simple mathematical model, and a math expression for such curves.

As Figure 3.2 and Equation 3.5 show, drag is composed of two terms: one proportional to the square of airspeed (i.e., V^2) and the other one inversely proportional to V^2. The first term, called zero-lift drag, represents the aerodynamic cleanliness with respect to frictional characteristics, and shape and protuberances such as cockpit, antenna, or external fuel tanks. It increases with aircraft velocity and is the main factor in determining an aircraft's maximum speed. The second term represents induced drag (drag due to the lift). Its contribution is highest at low velocities, and it decreases with increasing flight velocities.

If we combine (indeed add) these two curves (D_i and D_o) in Figure 3.2, we will have a parabolic curve such as what is shown in Figure 3.3. The parabolic drag model is not exact, but accurate enough for performance calculation. A similar behavior is observed for the variation of drag coefficient versus lift coefficient. The plot for variations of drag coefficient as a function of lift coefficient (as shown in Figure 3.3) and its mathematical model is referred to as lift-drag polar or simply drag polar.

Although drag and drag coefficient can be expressed in a number of ways, for reasons of simplicity and clarity, the parabolic drag polar has been selected in the analysis. This is true only for subsonic flight. For the existing supersonic aircraft, drag cannot be adequately described by such a simplified expression. Exact calculations must be carried out using extended equations or tabular data.

However, the inclusion of more precise expressions for drag at this stage will not greatly enhance the basic understanding of performance and, thus, will be included only in some calculated examples and exercises. Note that the curve begins from stall speed, since an aircraft is not able to maintain a sustained level flight at any speed below the stall speed. The same conclusion is true for the variation of drag coefficient (C_D) versus lift coefficient (C_L) as shown in Figure 3.3.

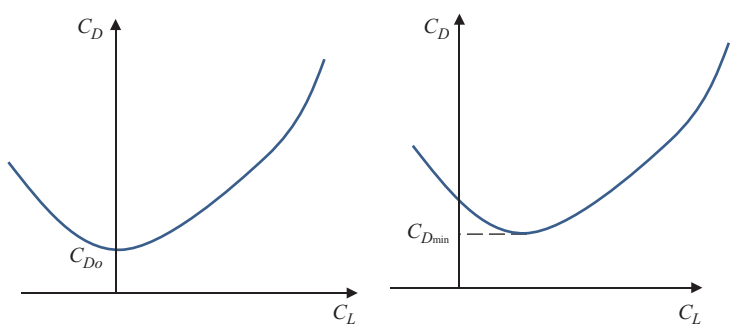

FIGURE 3.3 A typical drag polar (variations of C_D versus C_L).

Figure 3.3 depicts a non-dimensional form of Figure 3.2, the variation of drag coefficient versus lift coefficient. It can be proved that a second-order parabolic curve can mathematically describe such a curve with an acceptable accuracy:

$$y = a + bx^2 \tag{3.6}$$

where y may be replaced with C_D, and x may be replaced with C_L. Therefore, drag coefficient versus lift coefficient is modeled with the following parabolic model:

$$C_D = a + bC_L^2 \tag{3.7}$$

Now, we need to determine the values or expressions for a and b in this equation. In a symmetrical parabolic curve, the parameter a is the minimum value for parameter y. Hence, in a parabolic curve of C_D versus C_L, the parameter a must be the minimum amount of drag coefficient. We refer this value of drag coefficient as C_{D_o} as it means the value of C_D when the lift is zero. Note that, C_{D_o} is not usually equal to $C_{D\min}$.

The corresponding value for b in Equation 3.7 must be found through experiment. Aerodynamicists have represented this parameter with the symbol of K and refer to it as the induced drag correction factor. The induced drag correction factor is inversely proportional to the wing AR and the wing Oswald efficiency factor (e). The mathematical relationship is as follows:

$$K = \frac{1}{\pi \cdot e \cdot \mathrm{AR}} \tag{3.8}$$

The wing AR is the ratio between the wingspan (b) and the mean aerodynamic chord (MAC or $\bar{C}$). The ratio can be reformatted to be a function of the wing area (S) and wingspan as follows:

$$\mathrm{AR} = \frac{b}{C} = \frac{bb}{Cb} = \frac{b^2}{S} \tag{3.9}$$

Note that, for a rectangular wing; $S = b{\cdot}C$. The wing Oswald efficiency factor represents the efficiency of a wing in producing lift and is a function of the wing AR and the leading edge sweep angle, Λ_{LE}. If the lift distribution is parabolic, the Oswald efficiency factor is assumed to be highest (i.e., 100% or 1). The Oswald efficiency factor is usually between 0.7 and 0.9. Reference [28] introduces the following two expressions for the estimation of the Oswald efficiency factor:

$$e = 4.61\left(1 - 0.045\,\mathrm{AR}^{0.68}\right)\left[\cos\left(\Lambda_{\mathrm{LE}}\right)\right]^{0.15} - 3.1 \tag{3.10}$$

$$e = 1.78\left(1 - 0.045\,\mathrm{AR}^{0.68}\right) - 0.64 \tag{3.11}$$

Equation 3.10 is for swept wings with leading edge sweep angles of more than 30°, and Equation 3.11 is for rectangular wings (without sweep). These two formulas are valid only for wings with a high AR (e.g., more than 6).

The wing leading edge sweep angle is the angle between wing leading edge and the aircraft y-axis. Table 3.2 shows the wing Oswald efficiency factor for several aircraft.

TABLE 3.2
Typical Values of C_{D_o} and e for several aircraft

No.	Aircraft type	C_{D_o}	e
1.	Twin-engine piston prop	0.022–0.028	0.75–0.8
2.	Large turboprop	0.018–0.024	0.8–0.85
3.	Small GA with retractable landing gear	0.02–0.03	0.75–0.8
4.	Small GA with fixed landing gear[a]	0.025–0.04	0.65–0.8
5.	Agricultural aircraft with crop duster	0.07–0.08	0.65–0.7
6.	Agricultural aircraft without crop duster	0.06–0.065	0.65–0.75
7.	Subsonic jet	0.014–0.02	0.75–0.85
8.	Supersonic jet	0.02–0.04	0.6–0.8
9.	Glider	0.012–0.015	0.8–0.9
10.	Remote-controlled model aircraft	0.025–0.045	0.75–0.85

[a] This also refers to a small GA with retractable landing gear during takeoff.

The value of e is decreased at a high angle of attacks (i.e., low speed) up to about 30%. The measure values of the Oswald efficiency factor [29] for a couple of aircraft are as follows: Lockheed F-16C Fighting Falcon (Figure 7.6): 0.91; Lockheed Martin F-22A Raptor (Figure 5.10): 0.84; McDonnell Douglas (now Boeing) F-15E Strike Eagle: 0.78; Lockheed L-1011 TriStar: 0.61; Lockheed SR-71 Blackbird (Figure 4.24): 0.51; Boeing 747 (Figure 8.10b): 0.52; Lockheed C-5B Galaxy: 0.51; Northrop Grumman RQ-4A Global Hawk (Figure 2.11): 0.77; Lockheed U-2S: 0.8; Boeing B-52 Stratofortress: 0.57; and Airbus A-340 (Figure 1.8b): 0.62. As you see, these values range from 0.5 to 0.9.

Employing the induced drag correction factor (K), we have a mathematical expression for the variation of drag coefficient versus lift coefficient.

$$C_D = C_{D_o} + KC_L^2 \tag{3.12}$$

This equation is sometimes referred to as aircraft "drag polar". The main challenge in this equation is the calculation of zero-lift drag coefficient. Table 3.2 shows typical values of C_{D_o} for several aircraft. The values in this table are the lowest possible, which means that they were determined at the lowest airspeed (usually low subsonic speeds). Gliders or sailplanes are aerodynamically the most efficient aircraft (with C_{D_o} as low as 0.01), and agricultural aircraft are aerodynamically the least efficient aircraft (with C_{D_o} as high as 0.08). The lift coefficient is readily found in Equation 2.4. Compare the glider Schleicher ASK-21 with a wingspan of 16 m and a C_{D_o} 0.016 (Figure 3.4) with the agricultural aircraft Piper PA-25-260 Pawnee that has a C_{D_o} of 0.058 (Figure 3.5).

Comparison between Equations 3.5 and 3.12 yields the following relationship:

$$C_{D_i} = KC_L^2 \tag{3.13}$$

Therefore, induced drag is proportional to the square of lift coefficient. Figure 3.4 shows the effect of lift coefficient (induced drag) on drag coefficient.

FIGURE 3.4 The glider Schleicher ASK-21. (Courtesy of Fabrizio Capenti.)

FIGURE 3.5 Agricultural aircraft Piper PA-25-260 Pawnee. (Courtesy of Gustavo Corujo, Gusair.)

3.4 CALCULATION OF C_{D_o}

Equation 3.12 implies that the calculation of aerodynamic force of drag is dependent on zero-lift drag coefficient (C_{D_o}). Since the performance analysis is based on aircraft drag, it follows that, the accuracy of aircraft performance analysis relies heavily on the calculation accuracy of C_{D_o}. This section is devoted to the calculation of zero-lift drag coefficient and is the most important section of this chapter. The method by which the zero-lift drag coefficient is determined is called the "build-up" technique.

As Figure 3.6 illustrates, the external aerodynamic components of an aircraft are all contributing to aircraft drag. Although only wing and, to some extent, tail has aerodynamic function (i.e., to produce lift), every component (either of large size such as the wing or of small size such as a rivet) that has direct contact with airflow performs some types of aerodynamic functions (i.e., producing drag). Thus, in order to calculate the zero-lift drag coefficient of an aircraft, we must include every contributing item. The C_{D_o} of an aircraft is simply the summation of C_{D_o} of all contributing components.

$$C_{D_o} = C_{D_{of}} + C_{D_{ow}} + C_{D_{oht}} + C_{D_{ovt}} + C_{D_{o_{LG}}} + C_{D_{o_N}} + C_{D_{o_S}} + C_{D_{o_{\text{HLD}}}} + \cdots \quad (3.14)$$

where $C_{D_{of}}, C_{D_{ow}}, C_{D_{oht}}, C_{D_{ovt}}, C_{D_{o_{LG}}}, C_{D_{o_N}}, C_{D_{o_S}}$, and $C_{D_{o_{\text{HLD}}}}$, respectively, represent fuselage, wing, horizontal tail, vertical tail, landing gear, nacelle, strut, and high-lift device (HLD) (such as flap) contributions to aircraft C_{D_o}. The ellipsis at the end of

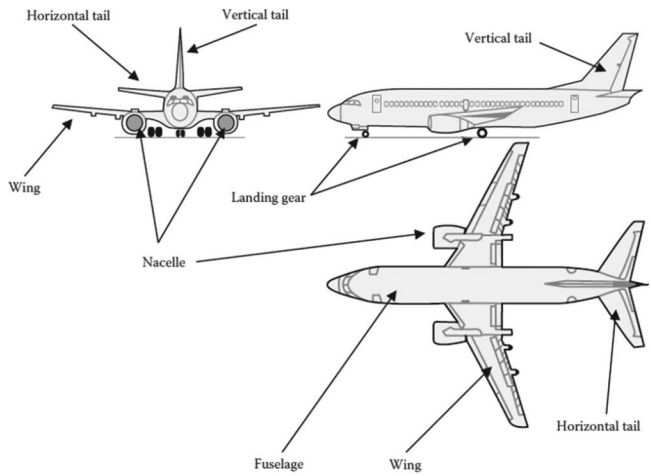

FIGURE 3.6 Major components of a Boeing 737 contributing to C_{D_o}.

Equation 3.14 illustrates that there are other components that are not shown here. They include non-significant components such as antenna, pitot tube, stall horn, wires, interference, and wiper.

Every component has a positive contribution, and no component has a negative contribution. In most conventional aircraft, wing and fuselage each contribute about 30%–40% (totally 60%–80%) to aircraft C_{D_o}. All other components contribute about 20%–40% to C_{D_o} of an aircraft. In some aircraft (e.g., hang gliders), there is no fuselage, so it does not have any contribution to C_{D_o}; instead, the human pilot plays a similar role to fuselage.

In each subsection of this section, a technique is introduced to calculate the contribution of each component to C_{D_o} of an aircraft. The primary reference for all these techniques and equations is Reference [30]. A majority of the equations are based on flight tests data and wind tunnel test experiments, so the build-up technique relies mainly on empirical formulas.

3.4.1 Fuselage

The zero-lift drag coefficient of a fuselage is given by the following equation:

$$C_{D_{of}} = C_f f_{\text{LD}} f_M \frac{S_{\text{wet}_f}}{S} \tag{3.15}$$

where C_f is skin friction coefficient and is a non-dimensional number. It is determined based on the Prandtl relationship as follows:

$$C_f = \frac{0.455}{\left[\log_{10}(\text{Re})\right]^{2.58}} \quad \left(\text{turbulent flow}\right) \tag{3.16}$$

$$C_f = \frac{1.327}{\sqrt{\text{Re}}} \quad \left(\text{laminar flow}\right) \tag{3.17}$$

The parameter Re is called the Reynolds number and has a non-dimensional value. It is defined as

$$\text{Re} = \frac{\rho V L}{\mu} \tag{3.18}$$

where ρ is the air density, V is the aircraft's true airspeed, μ is the air viscosity, and L is the length of the component in the direction of flight. For a fuselage, L is the fuselage length. For lifting surfaces such as wing and tail, and L is the MAC.

Equation 3.16 is for a purely turbulent flow, and Equation 3.17 is for a purely laminar flow. Most aircraft frequently experience a combination of laminar and turbulent flow over fuselage and other components. There are aerodynamic references (e.g., [30,31]) that recommend a technique to evaluate the ratio between laminar and turbulent flow over any aerodynamic component. The transition point from laminar to turbulent flow may be evaluated by these references. For simplicity, they are not reproduced here. Instead, you are recommended to assume that the flow is either completely laminar or completely turbulent. The assumption of complete turbulent flow provides a better result, since overestimation of drag is much better than its underestimation.

In theory, the flow is laminar when the Reynolds number is below 4,000. However, in practice, turbulence is not effective when the Reynolds number is below 200,000, so when it is <200,000, you may assume laminar flow, and when it is higher than 2,000,000, you may assume turbulent flow. Reference [6] suggests that the critical Reynolds number determined from experience is ~500,000. As a rule of thumb, in low subsonic flight, the flow is mostly laminar, but, in high subsonic and transonic speed, it becomes mostly turbulent.

A supersonic and hypersonic flight experiences a complete turbulent flow over every component of aircraft. A typical current aircraft may have laminar flow over 10%–20% of the wing, fuselage, and tail. A modern aircraft such as the Piaggio 180 can have laminar flow over as much as 50% of the wing and tails and about 40%–50% of the fuselage.

The second parameter in Equation 3.15 (f_{LD}) is a function of the fuselage length-to-diameter ratio. It is defined as

$$f_{LD} = 1 + \frac{60}{\left(L/D\right)^3} + 0.0025\left(\frac{L}{D}\right) \tag{3.19}$$

where L is the fuselage length, and D is its maximum diameter. If the cross section of the fuselage is not a circle, you need to find its equivalent diameter. The third parameter in Equation 3.15 (f_M) is a function of the Mach number (M). It is defined as

$$f_M = 1 - 0.08M^{1.45} \tag{3.20}$$

The last two parameters in Equation 3.15 are S_{wet_f} and S, which are the wetted area of the fuselage and the wing reference area, respectively.

Wetted area is the actual surface area of the material making up the skin of the airplane; it is the total surface area that is in actual contact with, that is, wetted by, air in which the body is immersed. Indeed, the wetted surface area is the surface on which the pressure and shear stress distributions act; hence, it is a meaningful geometric quantity when one is discussing aerodynamic force. However, the wetted surface area is not easily calculated, especially for complex body shapes.

A comment seems necessary regarding the reference area, S, in Equation 3.15. The parameter S is nothing other than just a reference area, suitably chosen for the definition of the force and moment coefficients.

The reference area (S) is simply an area as a basis or reference that can be arbitrarily specified. This selection is primarily done for convenience. The reference area (S) for a conventional aircraft is the projected area that we see when we look down on the wing from top view, including the fuselage section between two parts of the wing. For this reason, for wings as well as the entire airplane, the wing planform area is usually used as S in the definitions of C_L, C_D, and C_m. However, if we are considering the lift and drag of a cone, or some other slender, missile-like body, then the reference area S is frequently taken as the base area of the cone or fuselage. Figure 3.7 highlights the difference between the wing net area and the wing gross area. Thus, when we say wing planform area, we mean wing gross area. The assumption of the reference area selection will not incur any error in the calculation of wing drag and aircraft drag. The reason is that the drag coefficient will be automatically adjusted by this selection.

Whether we take the planform area, base area, or any other areas to a given body shape for S, it is still a measure of the relative size of different bodies that are geometrically similar. As long as you are consistent, you may take any significant area as the reference area. What is important in the calculation of C_L, C_D, and C_m is to divide the aerodynamic force/moment to a noticeable area. Whenever aircraft performance engineers take data for C_L, C_D, or C_m from the technical literature, it is imperative that they know what geometric reference area was used for S in the calculation. Then, they should use the same area when making calculations

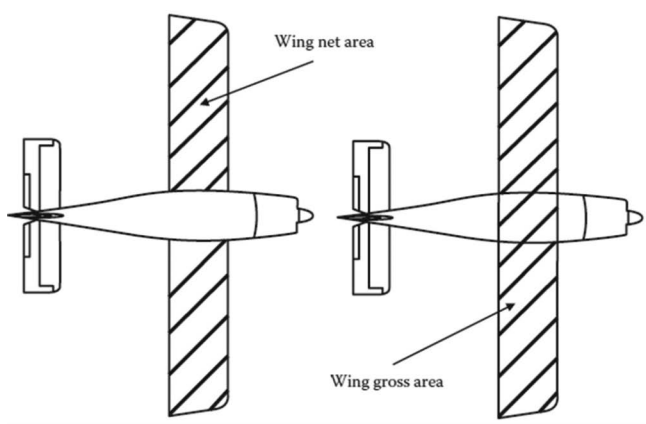

FIGURE 3.7 Wing gross area and wing net (exposed) area.

involving lift, drag, and pitching moment; otherwise, the results will involve significant inaccuracies. In contrast with S_{wet}, it is much easier to calculate the planform area of a wing.

3.4.2 Wing, Horizontal Tail, and Vertical Tail

Since wing, horizontal tail, and vertical tail are three lifting surfaces, they are treated in a similar manner. The zero-lift drag coefficient of the wing ($C_{D_{o_w}}$), horizontal tail ($C_{D_{o_{ht}}}$), and vertical tail ($C_{D_{o_{vt}}}$) are respectively given by the following equations:

$$C_{D_{o_w}} = C_{f_w} f_{tc_w} f_M \left(\frac{S_{\text{wet}_w}}{S}\right)\left(\frac{C_{d_{\min_w}}}{0.004}\right)^{0.4} \tag{3.21}$$

$$C_{D_{o_{ht}}} = C_{f_{ht}} f_{tc_{ht}} f_M \left(\frac{S_{\text{wet}_{ht}}}{S}\right)\left(\frac{C_{d_{\min_{ht}}}}{0.004}\right)^{0.4} \tag{3.22}$$

$$C_{D_{o_{vt}}} = C_{f_{vt}} f_{tc_{vt}} f_M \left(\frac{S_{\text{wet}_{vt}}}{S}\right)\left(\frac{C_{d_{\min_{vt}}}}{0.004}\right)^{0.4} \tag{3.23}$$

In these equations, C_{f_w}, $C_{f_{ht}}$, and $C_{f_{vt}}$ are similar to what we defined for fuselage in formula (3.15). The only difference is that the equivalent values of L in the Reynolds number (Equation 3.24) for wing, horizontal tail, and vertical tail are their MACs (or $\bar{C}$). In other words, the definition of the Reynolds number for a lifting surface (e.g., wing) is

$$\text{Re} = \frac{\rho V \bar{C}}{\mu} \tag{3.24}$$

where the $\bar{C}$ (or MAC) is calculated by

$$\bar{C} = \frac{2}{3} C_r \left[1 + \lambda - \frac{\lambda}{1+\lambda}\right] \tag{3.25}$$

where C_r denotes the root chord (see Figure 3.8), and λ is the taper ratio, the ratio between tip chord (C_t) and root chord (C_r) is:

$$\lambda = \frac{C_t}{C_r} \tag{3.26}$$

The parameter f_{tc} is a function of thickness ratio and is given by

$$f_{tc} = 1 + 2.7\left(\frac{t}{c}\right)_{\max} + 100\left(\frac{t}{c}\right)^4_{\max} \tag{3.27}$$

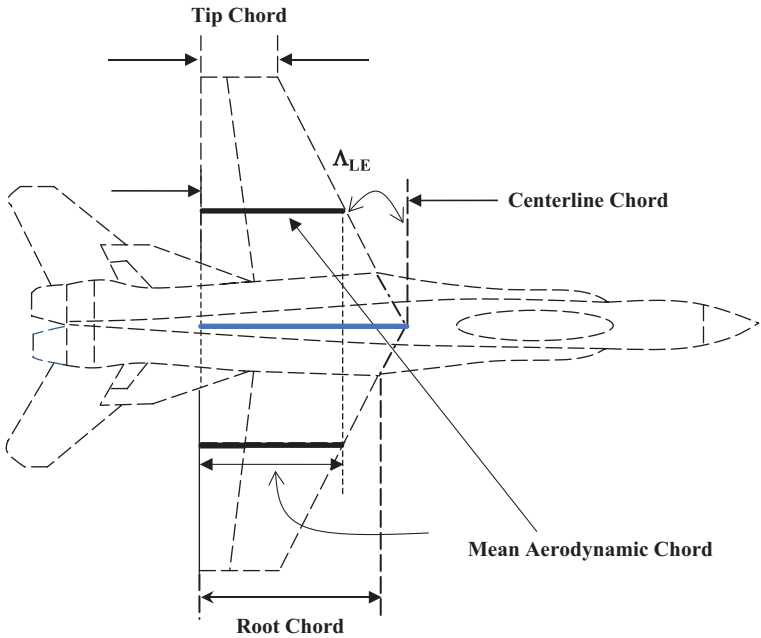

FIGURE 3.8 Wing mean aerodynamic chord (MAC).

where $(t/c)_{max}$ is the maximum thickness-to-chord ratio of the wing or the tail. Generally speaking, the maximum thickness-to-chord ratio for a wing is about 12%–18% and for a tail is about 9%–12%. The parameter S_{wet} in Equation 3.13 is the wing or tail wetted area.

The parameters S_{wet_w}, $S_{wet_{ht}}$, and $S_{wet_{vt}}$ denote the wetted area of the wing, horizontal tail, and vertical tail, respectively. Unlike the reference area, the wetted area is based on the exposed area, and not the gross area. Due to the special curvature of the wing and tail airfoil sections, it may seem time-consuming to calculate the accurate wetted area of a wing or tail. There is a simplified method to determine the wetted area of a lifting surface with an acceptable accuracy. Since the wing and tail are not too thick (average about 15%), it may be initially assumed that the wetted area is about twice that of the net or exposed area (see Figure 3.7). To be more accurate, you may assume the lifting surface as a thin box with its average thickness equal to half of the airfoil thickness. According to this assumption, the wetted area is given as

$$S_{wet} = 2\left[1 + 0.5\left(\frac{t}{c}\right)_{max}\right]bC \tag{3.28}$$

For ultimate accuracy, you need to employ a CAD software package (e.g., AutoCAD and SolidWorks) to calculate the wetted area.

The parameter $(C_{d_{min}})$ in Equations 3.21, 3.22, and 3.23 is the minimum drag coefficient of the airfoil cross section of the wing or tail. It can be readily extracted from a $C_d - C_l$ curve of the airfoil. One example is illustrated in Figure 3.9 for a six-series NACA airfoil 63_1-412. Reference [32] is a rich collection of information for a variety of

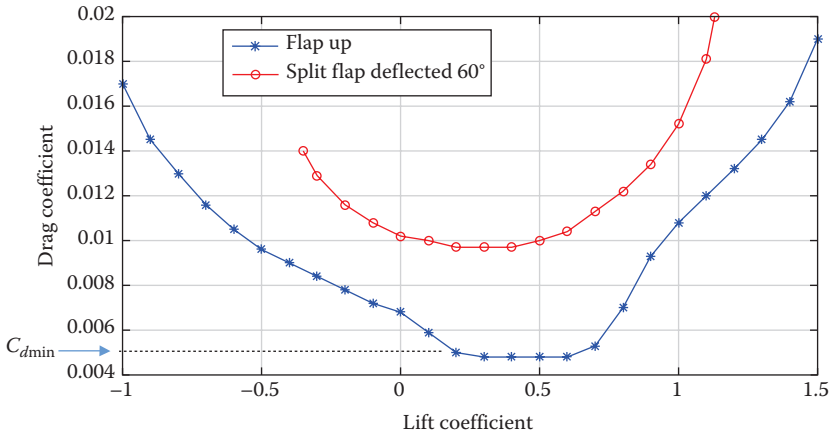

FIGURE 3.9 The variations of lift coefficient versus drag coefficient for airfoil NACA 63_1-412.

NACA four-digit, five-digit, and six-series airfoils. For instance, the NACA airfoil 63_1-412 has a minimum drag coefficient of 0.0048 for the clean or flap-up configuration.

Example 3.1

Consider a cargo aircraft with the following features:

$$m = 380{,}000\,\text{kg}, S = 567\,\text{m}^2, \text{MAC} = 9.3\,\text{m}, (t/c)_{\max} = 18\%, C_{d_{\min_w}} = 0.0052$$

This aircraft is cruising at sea level with an airspeed of 400 knots. Assuming the aircraft C_{D_o} is three times the wing C_{D_o} (i.e., $C_{D_{o_w}}$), determine the aircraft C_{D_o}.

Solution

$$\text{Re} = \frac{\rho V \bar{C}}{\mu} = \frac{1.225 \times (400 \times 0.5144) \times 9.3}{1.785 \times 10^{-5}} = 131{,}334{,}640 = 1.31 \times 10^8 \quad (3.18)$$

$$M = \frac{V}{a} = \frac{400 \times 0.5144}{340} = 0.605 \quad (1.36)$$

Due to the high Reynolds number, the air flow over the wing is turbulent, so

$$C_f = \frac{0.455}{\left[\log_{10}(\text{Re})\right]^{2.58}} = \frac{0.455}{\left[\log_{10}(131{,}334{,}640)\right]^{2.58}} = 0.00205 \quad (3.16)$$

$$f_M = 1 - 0.08M^{1.45} = 1 - 0.08 \times (0.606)^{1.45} = 0.9614 \quad (3.20)$$

$$f_{tc} = 1 + 2.7\left(\frac{t}{c}\right)_{\max} + 100\left(\frac{t}{c}\right)^4_{\max} = 1 + 2.7(0.18) + 100(0.18)^4 = 1.591 \quad (3.27)$$

$$S_{\text{wet}} = 2\left[1 + 0.5\left(\frac{t}{c}\right)_{\max}\right] bC = 2[1 + 0.5 \times 0.18] \times 567 = 1{,}236\,\text{m}^2 \tag{3.28}$$

$$C_{D_{ow}} = C_{f_w} f_{tc_w} f_M \left(\frac{S_{\text{wet}_w}}{S}\right)\left(\frac{C_{d_{\min_w}}}{0.004}\right)^{0.4} \tag{3.21}$$

$$C_{D_{ow}} = 0.00205 \times 1.591 \times 0.9614 \times \frac{1236}{576} \times \left(\frac{0.0052}{0.004}\right)^{0.4} = 0.0759$$

Therefore, the aircraft zero-lift drag coefficient is

$$C_{D_o} = 3C_{D_{ow}} = 3 \times 0.0759 = 0.0228$$

3.4.3 High-Lift Devices

HLDs are parts of the wing to increases lift when employed (i.e., deflected). They are usually employed during takeoff and landing. Two main groups of HLDs are trailing edge HLDs (often called flap) and leading edge HLDs (e.g., slat). There are many types of wing trailing edge flaps such as split flap, plain flap, single-slotted flap, fowler flap, double-slotted flap, and triple-slotted flap. They are deflected down to increase the camber of the wing, in order to increase lift, so the maximum lift coefficient, $C_{L_{\max}}$, will be increased. The most effective method used on large transport aircraft is the leading edge slat.

A variant on the leading edge slat is a variable camber-slotted Kruger flap used on Boeing 747 (Figure 8.10b). The main effect of the wing trailing edge flap is to increase the effective angle of attack of the wing without actually pitching the airplane. The application of HLDs has a few negative side effects, including an increase in aircraft drag (as will be included in C_{D_o}). Flap deflection of up to 15° primarily produces lift with minimal drag.

3.4.3.1 Trailing Edge HLDs

The increase in C_{D_o} due to the application of a trailing edge HLD (flap) is given by the following empirical formula:

$$C_{D_{o\text{flap}}} = A\left(\frac{C_f}{C}\right)\left(\delta_f\right)^B \tag{3.29}$$

where C_f/C is the ratio of average flap chord to average wing chord (see Figure 3.10) at the flap location and is usually about 0.2. In the case where the flap is extended, as in the case of a slotted flap, the C_f represents the extended chord; furthermore, the wing chord (C) is also locally increased. Please do not confuse this C_f with the C_f of skin friction coefficient, which shares the same symbol (Equations 3.16 and 3.17). Equation 3.29 is based on a flap with a flap-span-to-wing-span ratio of 70%. In the case where the flap span is different, the results should be revised accordingly.

The parameters A and B are given in Table 3.3 based on the type of flap. The δ_f is the flap deflection in degrees (usually <50°). Figure 3.10 also illustrates the deflected slotted flap of a McDonnell Douglas MD-11.

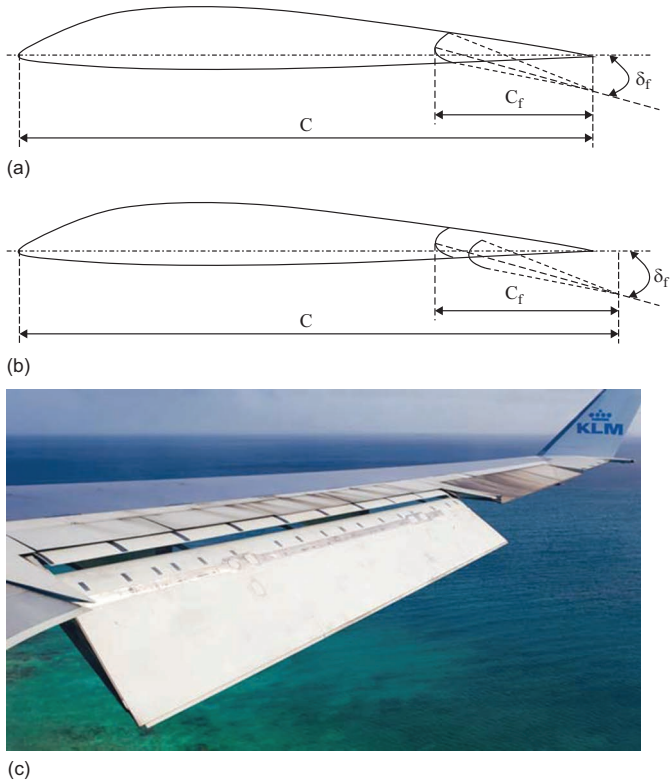

FIGURE 3.10 Wing section at the flap location. (a) Flap; only deflected (plain flap), (b) flap; extended while deflected (slotted flap), (c) slotted flap of a McDonnell Douglas MD-11. (Courtesy of Kas van Zonneveld.)

TABLE 3.3
Values of *A* and *B* for Different Types of Flaps

No.	Flap Type	*A*	*B*
1.	Split flap	0.0014	1.5
2.	Plain flap	0.0016	1.5
3.	Single-slotted flap	0.00018	2
4.	Double-slotted flap	0.0011	1
5.	Fowler	0.00015	1.5

3.4.3.2 Leading Edge HLDs

The increase in C_{D_o} due to application of a leading edge HLD (e.g., slot and slat, *sl*) is given by the following empirical formula:

$$C_{D_{osl}} = \left(\frac{C_{sl}}{C}\right) C_{D_{ow}} \tag{3.30}$$

where C_{sl}/C is the ratio of average extended slat chord to average extended wing chord. The $C_{D_{ow}}$ is the wing zero-lift drag coefficient without extending a HLD (including slat).

3.4.4 Landing Gear

Landing gear (or undercarriage) is the structure (usually struts and wheels) that supports the aircraft weight and facilitates its motion along the surface of the runway when the aircraft is not airborne. Landing gear usually includes wheels and is equipped with shock absorbers for solid ground, but some aircraft are equipped with skis for snow or floats for water, and/or skids. To decrease drag in flight, some landing gears are retracted into the wings and/or fuselage with wheels or concealed behind doors; this is called retractable gear. In the case of retracted landing gear, the aircraft clean C_{D_o} is not affected by the landing gear.

When landing gear is fixed (not retracted) in place, it produces an extra drag for the aircraft. It is sometimes responsible for an increase in the aircraft drag as high as 50%. In some aircraft, a fairing is used to decrease the drag of a non-retracted gear (see Figure 3.11b). The fairing is a partial cover that has a streamlined shape such as an airfoil. The increase in C_{D_o} due to the wheel of the landing gear is given by the following empirical equation:

$$C_{D_{olg}} = \sum_{i=1}^{n} C_{D_{lg}} \left(\frac{S_{lgi}}{S} \right) \tag{3.31}$$

where S_{lg} is the frontal area of each wheel, and S is the wing reference area. The parameter $C_{D_{lg}}$ is the drag coefficient of each wheel that is 0.15, when it has fairing, and 0.30, when it does not have any fairing (see Figure 3.11a). The frontal area of each wheel is simply the diameter (d_g) times the width (w_g).

$$S_{lg} = d_g w_g \tag{3.32}$$

(a) (b)

FIGURE 3.11 Landing gear and its fairing. (a) Gulfstream G-V nose gear without fairing and (b) Cirrus SR-22 landing gear with fairing. (Copyright Gustavo Corujo.)

As it is observed in Equation 3.31, every wheel that experiences air flow must be accounted for drag. For this reason, subscript i is used. The parameter n is the number of wheels in an aircraft. The drag calculation for the strut of landing gear is presented in the next section. Some aircraft are equipped with skid, especially when they have tail gear configuration. Skid is not a lifting surface, but, for the purpose of zero-lift drag calculation, it may be treated as a small wing.

3.4.5 Strut

This section deals with two types of struts: (1) Landing gear strut and (2) wing strut. Landing gear is often attached to the aircraft structure via a strut. In some general aviation (GA)/homebuilt aircraft, wings are attached through a few struts to support wing structure, that is, strut-braced wings (see Figure 3.12). Modern aircraft use advanced material for structure that is stronger, and there is no need for any strut to support their wings, that is, cantilever. In some aircraft (such as hang gliders), the cross section of the wing strut is a symmetrical airfoil in order to reduce the strut drag. In both cases, the strut produces an extra drag for aircraft.

The increase in C_{D_o} due to application of strut is given by the following empirical equation:

$$C_{D_{os}} = \sum_{n}^{i=1} C_{D_{osi}} \left(\frac{S_s}{S} \right) \tag{3.33}$$

where S_s is the frontal area of each strut (its diameter times its length), and S is the wing reference area. The parameter $C_{D_{os}}$ is the drag coefficient of each strut that is 0.1, when it is faired (i.e., has an airfoil section). When strut does not have an airfoil section, its drag coefficient is obtained from Table 3.1. The parameter n is the number of struts in an aircraft. It is observed that using an airfoil section for a strut decreases its drag by an order of 10. However, its manufacturing cost is increased too.

FIGURE 3.12 Wing strut and landing gear strut in a Sky Arrow. (Courtesy of Gustavo Corujo.)

3.4.6 Nacelle

If the engine is not buried inside fuselage, it must be in direct contact with air flow. To reduce the engine drag, the engine is often located inside an aerodynamic cover called nacelle. For the purpose of drag calculation, it can be considered that the nacelle is similar to the fuselage, except that its length-to-diameter ratio is lower. Thus, the nacelle zero-lift drag coefficient ($C_{D_{on}}$) will be determined in the same way as that in a fuselage. In the case where the nacelle length-to-diameter ratio is below 2, assume 2. This parameter is used in Equation 3.19. Some aero-engine manufacturers publish the engine nacelle drag in the engine catalog when the installed drag is demonstrated. In such a case, use that manufacturers' data. Determine nacelle drag only when the engine uninstalled thrust is available. The nacelle of an engine for an Airbus A330 is shown in Figure 3.13.

3.4.7 External Fuel Tank

An external fuel tank (such as a wingtip tank) is in direct contact with air flow and is generating drag. An external fuel tank may be modeled as a small fuselage. In the case where the fuel tank length-to-diameter ratio is below 2, assume 2.

3.4.8 Cooling Drag

An aero-engine is a source of heat where it is generated when fuel is burned in the combustion chamber. This heat is initially conducted to the engine's external surface, including cylinder heads via oil/water. To keep the engine efficient and maintain its performance, the heat should be transferred to outside airflow through a convenient technique, usually conduction. The various types of heat exchangers are arranged in an aero-engine that requires a flow of air through them for the purpose of cooling. The source of this cooling air is usually the free air stream possibly augmented to some extent by a propeller slipstream (in a prop-driven engine) or bled from the compressor section (in a turbine engine).

As the air flows through, to extract heat energy from the body, it experiences a loss in the total pressure and momentum. This loss during the heat transfer process may be interpreted as a drag force referred to as the cooling drag.

Turbine engine manufacturers calculate the net power/thrust lost in the flow and subtract this from the engine uninstalled power/thrust. In such a case, no cooling drag increment is added to the aircraft. Piston engine manufacturers often do not provide installed power, so the cooling drag needs to be determined in order to calculate the installed power. For a piston engine, the engine power is typically reduced by as much as approximately 5% to account for the cooling losses.

FIGURE 3.13 The nacelle of an engine for an Airbus A330. (Courtesy of Gustavo Corujo.)

An engine needs to be installed to the aircraft structure (e.g., fuselage and wing) through a special mounting/pylon. An air-cooled engine has a special mounting (see Figure 3.14) to provide the airflow around the engine. The calculation of the cooling drag is highly installation-dependent. It is unfeasible to present a general technique that can be applied to every engine installation. Turbine/piston engine manufacturers use computer software packages for the calculation [33] of installation losses for their engines. Because of the complexity of the engine configuration and the internal flow through a typical engine installation, the current methods for estimating cooling losses are empirical in nature.

For an oil-cooled turbine engine, it is sufficient to consider cooling drag by consulting the engine manufacturer catalog and using installed power/thrust. For an air-cooled engine, the engine cooling drag coefficient ($C_{D_{oen}}$) is given [5] by the following empirical relationship:

$$C_{D_{oen}} = 4.51 \times 10^{-8} \frac{K_e P T^2}{\sigma V S} \tag{3.34}$$

where P is the engine power (in hp), T is the hot air temperature (in K) at exit, σ is the relative density of the air, V is the aircraft airspeed (in m/s), and S is the wing reference area (in m^2). The parameter K_e is a coefficient that depends on the type of engine and its installation. It varies between 1 and 3.

3.4.9 Trim Drag

Basically, trim drag is not different from the types of drag already discussed. It arises mainly as a result of having to produce a horizontal tail load in order to balance the airplane around its center of gravity. Any drag increment that can be attributed to a finite lift on the horizontal tail contributes to the trim drag. Such increments mainly represent changes in the induced drag of the tail.

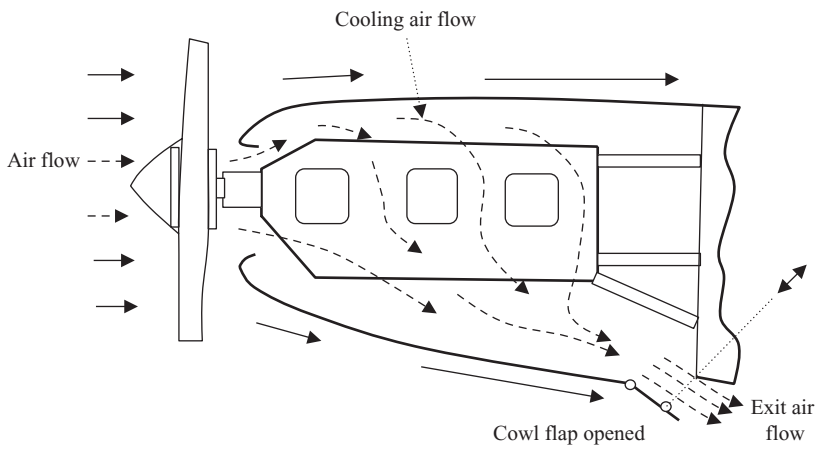

FIGURE 3.14 The use of cowl flaps to control engine cooling air.

To examine this further, we begin with the sum of the lifts developed by the wing and the tail that must be equal to the aircraft weight in a trimmed cruising flight.

$$L_t + L_w = L = W \tag{3.35}$$

where

$$L_w = \frac{1}{2}\rho V^2 S_w C_{L_w} \tag{3.36}$$

$$L_t = \frac{1}{2}\rho V^2 S_t C_{L_t} \tag{3.37}$$

Equation 3.35 is one of the requirements of the aircraft longitudinal trim in cruising flight. Substituting tail and wing lift into Equation 3.35, one can derive the horizontal tail lift coefficient (C_{L_t}) as

$$C_{L_t} = \left(C_L - C_{L_w}\right)\frac{S}{S_t} \tag{3.38}$$

where C_L is aircraft lift coefficient, C_{L_w} is wing lift coefficient, and S_t is horizontal tail area. Then, the trim drag will be

$$C_{D_{o\text{trim}}} = C_{D_{it}} = K_t C_{L_t}^2 \frac{S_t}{S} = \frac{1}{\pi \cdot e_t \cdot \text{AR}_t}\frac{S_t}{S}\left[\left(C_L - C_{L_w}\right)\frac{S}{S_t}\right]^2 = \frac{1}{\pi \cdot e_t \cdot \text{AR}_t}\frac{S}{S_t}\left(C_L - C_{L_w}\right)^2 \tag{3.39}$$

where e_t is the horizontal tail span Oswald efficiency factor, and AR_t is the horizontal tail AR. The trim drag is usually small, amounting to only 1% or 2% of the total drag of an airplane for the cruise condition. Reference [34], for example, lists the trim drag for the Learjet Model 25 as being only 1.5% of the total drag for the cruise condition.

3.4.10 Other Parts and Components

So far, we have introduced techniques to calculate C_{D_o} of aircraft major components. There are other components, parts, factors, and items that produce drag and contribute to the total C_{D_o} of an aircraft. These items are introduced in this section.

3.4.10.1 Interference

When two bodies intersect or are placed in proximity, their pressure distributions and boundary layers can interact with each other, resulting in a net drag of the combination that is often higher than the sum of the separate drags. This increment in the drag is known as interference drag. Except for specific cases where data are available, interference drag is difficult to calculate accurately, for example, (1) placing an engine nacelle in proximity to a rear pylon (e.g., Gulfstream *V*),

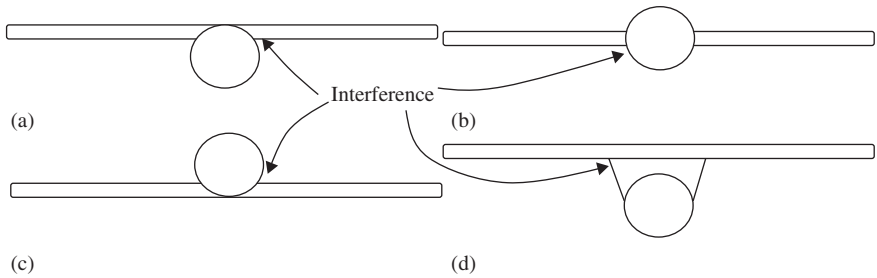

FIGURE 3.15 Wing–fuselage interference drag. (a) High wing, (b) mid wing, (c) low wing, and (d) parasol wing.

(2) the interference drag between the wing and fuselage in a mid-wing configuration, (3) horizontal tail aft of a jet engine exhaust nozzle, and (4) wing leading edge aft of a propeller wake.

Figure 3.15 shows a wing attached to the side of a fuselage. At the fuselage–wing juncture, a drag increment results as the boundary layers from the two components interact and thicken locally at the junction. This type of drag penalty will become more severe if surfaces meet at an angle other than 90°. Reference [35] shows that the interference drag of a strut attached to a body doubles as the angle decreases from 90° to ~60°. Avoid acute angles; if not, filleting should be applied at the juncture to reduce interference drag.

In the case of a high-wing configuration, interference drag results principally from the interaction of the fuselage boundary layer with that on the wing's lower surface. The latter layer is relatively thin at positive angles of attack. In addition, it is the boundary layer on the upper surface of a low wing that interferes with the fuselage boundary layer. The upper surface boundary layer is relatively thicker than the lower surface boundary layer. Thus, the wing–fuselage interference drag for a low-wing aircraft is usually greater than for a high-wing aircraft.

The available data on interference drag are limited; References [11,12] present a limited amount. Based on reference [36], an approximate drag increment caused by the wing–fuselage interference is estimated to equal 4% of the wing's zero-lift drag for a typical AR and wing thickness.

The theoretical accurate calculation of interference drag is impossible unless you utilize a high-fidelity CFD software package. For example, a wing protruding from a fuselage just forward of the station where the fuselage begins to taper may trigger a flow separation over the rear portion of the fuselage. Sometimes, interference drag can be favorable, for example, when one body operates in the wake of another. The most accurate technique to determine interference drag is to employ wind tunnel or flight tests.

3.4.10.2 Antenna

The communication antennas of many aircraft are located outside the aircraft. They are in direct contact with the air, and hence they produce drag. There are mainly two types of antennas: (1) rod/wire/whip and (2) blade or plate. Both types of antennas should be in an open space (below or above the fuselage) for better communication. During a flight, airstream flows around an antenna, so it will generate drag. In the older aircraft, a whip or wire was employed, while in the modern aircraft a vertical plate is utilized. The antennas are frequently located on top of or under the fuselage.

For instance, the reconnaissance aircraft U-2S Dragon Lady has a thin whip that acts as an ADF (Automatic Direction Finder) antenna and a large plate antenna as the UHF (Ultra High Frequency) radio antenna. The whip was originally straight. Later on, the bend in the upper portion of the whip antenna was introduced to provide clearance for the senior span/spur dorsal pod. In addition, the Boeing Vertol CH-113 Labrador had various antennas and plates under the fuselage section, namely, two blade antennas, two whip antennas, and a towel-rack "Loran" antenna. Figure 3.19 (see later in this chapter) illustrates the antennas of a Saab JAS-39C Gripen: one on top of the fuselage and the other inside the vertical tail.

To calculate C_{D_o} of an antenna, the rod antenna is treated as a strut and the blade antenna is considered as a small wing. The very equations that are introduced for the strut (Section 3.4.5) and the wing (Section 3.4.2) may be employed to determine the C_{D_o} of the antenna.

3.4.10.3 Pitot Tube

The mechanism of a pitot tube as a pressure/velocity measurement instrument is presented in Chapter 2 (Section 2.4.2). Since a pitot tube is in direct contact with outside air, it follows that it has a contribution to aircraft drag (i.e., C_{D_o}). If the aircraft is in subsonic regime, the horizontal part of the pitot tube may be assumed as a little fuselage and its vertical part as a strut. In a supersonic flight, a shock wave is formed around the pitot tube and creates additional wave drag. For supersonic flow, Section 3.5 introduces a technique to account for the zero-lift drag coefficient (C_{D_o}) of pitot tube. Figure 3.16 illustrates a pitot tube on the vertical tail of a Boeing KC-135R Stratotanker and a pitot tube mounted under the wing of a Cessna 172. In addition, the pitot tube of the NASA aircraft Global Hawk can be visualized in Figure 5.21.

3.4.10.4 Surface Roughness

The outer surface of an aircraft structure (skin) has a considerable role in aircraft drag. For this reason, the aircraft skin is often finished and painted. The paint not only protects the skin from atmospheric hazards (e.g., rusting) but also reduces its drag. As the surface of the skin is more polished, the aircraft drag (surface friction) will be reduced. The interested reader is referred to specific aerodynamic references and published journal papers to obtain more information about the effect of surface roughness on the aircraft drag. For aerodynamic analysis of surface roughness, the interested reader is referred to References [37,38].

(a) (b)

FIGURE 3.16 Pitot tube. (a) Pitot tube mounted under the wing of a Cessna 172 and (b) Boeing KC-135R Stratotanker vertical tail with a pitot tube. (Courtesy of Steve Dreier.)

3.4.10.5 Leakage

There are usually gaps between control surfaces (such as an elevator, aileron, and rudder), flaps, and spoilers and the lifting surfaces (such as wing and tails). Air flows through these tiny gaps and thus produces extra drag. This is called leakage drag, which usually contributes about 1%–2% to total drag. The reader is referred to specific aerodynamic references and published journal papers to gain more information about the influence of these gaps on the aircraft drag.

3.4.10.6 Rivet and Screw

The outside of the aircraft structure (fuselage and wing) is covered with a skin. The skin, if it is from metallic materials, is attached to the primary components of an aircraft structure (such as spar and frame) via parts such as rivets or screws. For instance, the aircraft Fairchild Republic A-10 Thunderbolt has non-flush button head rivets on the aft fuselage, nacelle, and vertical tail. They are stronger and less expensive to install than flush rivets. The composite structures have the advantage that they do not require any rivet or screw and are often attached together through techniques such as bonding.

In the case of the screw, the top part of the screw could be often hidden inside the skin. But the heads of most types of rivets are out of the skin; therefore, they produce extra drag. Figure 3.18a illustrates both rivet and screw on wing of Cessna-172. Rivets and screws usually contribute about 2%–3% to total drag. The author did not find any reference that demonstrates the technique to calculate the contribution of rivet to aircraft drag. For aerodynamics analysis of imperfections (e.g., rivet), the interested reader is referred to Reference [37]. You may also use flight tests to measure this type of drag.

3.4.10.7 Pylon

A podded turbine engine (e.g., turbofan engine) is usually mounted to the airplane wing or fuselage with a pylon. Pylon is mainly a structural component but may be designed such that it contributes to aircraft lift. Although pylon is not fundamentally a lifting surface, but for the purpose of zero-lift drag calculation, it may be treated as a small wing. The pylon of an engine for a Canadair CC-144 Challenger can be noticed in Figure 8.15. Furthermore, the pylon of engines for Scaled Composites 348 White Knight 2 can be seen in Figure 5.13.

3.4.10.8 Fairing for the Flap Mechanism

A HLD needs to be deflected at takeoff and landing and retracted under other flight conditions. A mechanical device (i.e., mechanism) is employed to adjust the flap setting. In a long flap (as in a large transport aircraft), multiple mechanisms are needed for each side. To reduce the drag of such mechanism, a shell-shaped fairing housing is utilized with at least partly U-shaped profile with an open side. This is not a structural element and does not carry the stress. For the purpose of zero-lift drag calculation, each fairing may be treated as a small vertical tail. The fairing for the flap mechanism for an Airbus A330 can be seen in Figure 3.13. In addition, the fairing for the flap mechanism and the pylon for a Boeing 777 are depicted in Figure 3.17.

FIGURE 3.17 Miscellaneous items that contribute to drag. (a) Fairing (red arrow) for the flap mechanism and pylon (blue arrow) for a Boeing 777 and (b) underwing mounting of stores for a McDonnell Douglas EAV-8B Matador II. (c) Step (arrow) of a Bell-Boeing MV-22B Osprey. ((a): Courtesy of Fabrizio Capenti; (b): Courtesy of Weimeng; (c): Courtesy of Maurice Kockro.) (d) Engine exhaust pipe (arrow) of a Cessna 172. (e) Aerial refueling hose (arrow) of an McDonnell Douglas KDC-10 and (f) detachable in-flight refueling nose probe of a Vickers VC10. ((d): Courtesy of Gustavo Corujo; (e): Courtesy of Fabrizio Capenti; (f): Courtesy of Steve Dreie.) (g) Antennas (arrows) of a Saab JAS-39C Gripen and (h) windshield wiper of a Lockheed L-1011 TriStar. ((g): Courtesy of Fabrizio Capenti; (h): Courtesy of Steve Dreier.)

3.4.10.9 Compressibility

Compressibility effects on aircraft drag have been important since the advent of high-speed aircraft in the 1940s. Compressibility is a property of the fluid; when a fluid is compressed, its density will be increased. Liquids have very low values of compressibility, whereas gases have high compressibility. In real life, every flow of every fluid is compressible to some greater or lesser extent. A truly constant density (incompressible) fluid is a myth. However, for almost all liquids (e.g., water), the density changes are so small that the assumption of constant density can be made with reasonable accuracy.

As fluid is compressible, the flow of fluid may be compressible too. Incompressible flow is a flow where the density is assumed to be constant throughout. Compressible flow is a flow in which the density varies. A few important examples are the internal flow through rocket and gas turbine engines, high-speed subsonic, transonic, supersonic, and hypersonic wind tunnels, the external flow over modern airplanes designed to cruise faster than Mach 0.3, and the flow inside the common internal combustion reciprocating engine. For most practical problems, if the density changes by more than 5%, the flow is considered to be compressible. Figure 3.18 shows [30] the effect of compressibility on drag for three configurations. The wing-body on the right has a smaller fuselage diameter in the center section (i.e., coke-bottling).

Flow velocities higher than Mach 0.3 are associated with considerable pressure changes, accompanied by correspondingly noticeable changes in density. The aircraft drag at high subsonic speed (e.g., $M = 0.9$) is about twice that at low subsonic speed (e.g., Mach 0.2). Consider a wing with a free stream. The lift is created by the occurrence of pressures higher than free stream on the lower surface of the wing and lower than free stream on the upper surface. This usually coincides with the occurrence of velocities higher than free stream on the upper surface of the wing [39] and lower than free stream on much of the lower surface.

As the airspeed approaches the speed of sound (i.e., $M > 0.85$), due to a positive camber, the higher local velocities on the upper surface of the wing may reach and even substantially exceed local sonic speed, $M = 1$ (see Figure 3.19). The free stream Mach number at which the maximum local Mach number reaches 1 is referred to as the critical Mach number.

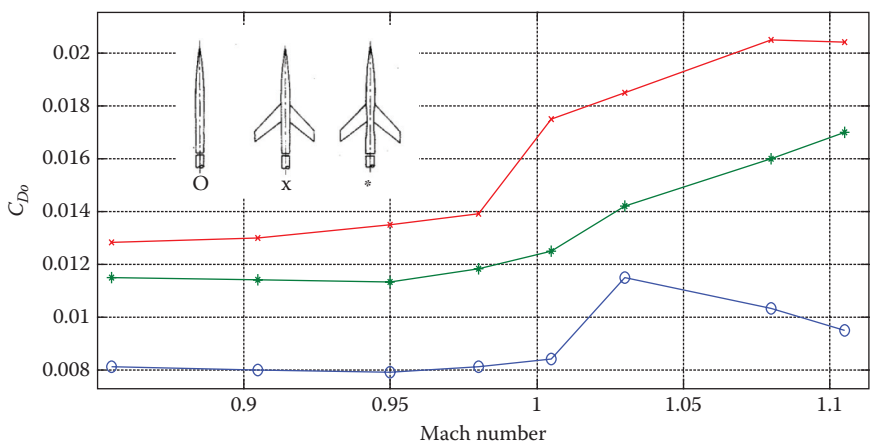

FIGURE 3.18 Effect of compressibility on drag for three configurations.

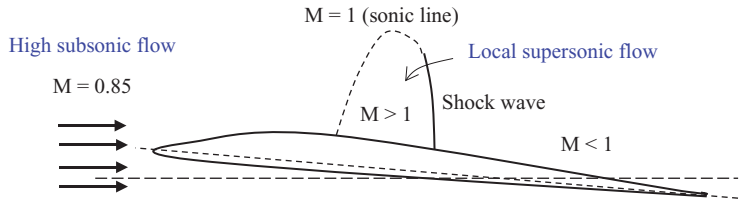

FIGURE 3.19 Local supersonic speed with a high subsonic flow.

The existence of sonic and supersonic local velocities on a wing is associated with an increase in drag. The extra drag is due to a reduction in total pressure through an oblique shock wave, which causes local adverse pressure gradients. In addition, when an oblique shock interacts with the boundary layer, the boundary layer gets thicker and may even separate. This is referred to as compressibility drag.

A cambered airfoil has typically a crest, and a lifting surface with such an airfoil has a crestline. The crest is the point on the airfoil upper surface to which the free stream is tangent. The crestline is the locus of airfoil crests along the wingspan. The drag increase due to compressibility is generally not large, until the local speed of sound occurs at or behind the crest of the airfoil. Empirically, it is found for all airfoils except the supercritical airfoil that at a 2%–4% higher Mach number than that at which $M = 1$ at the crest, the drag rises abruptly. The Mach number at which this abrupt drag rise begins is called [10] the drag divergence Mach number.

However, the occurrence of substantial supersonic local velocities well ahead of the crest does not lead to a significant drag increase, provided that the velocities decrease again below the sonic speed forward of the crest. The incremental drag coefficient due to compressibility is designated ΔC_{D_c}. Table 3.4 demonstrates the incremental drag coefficient due to compressibility for several aircraft.

3.4.10.10 Icing

Ice usually accumulates on the leading edge, the upper surface of the wing, around pitot tube, antennas, flap hinges, control horns, fuselage nose, windshield wipers, wing struts,

TABLE 3.4
Drag Increase Due to Compressibility Effects for Several Aircraft

No.	Aircraft	C_{D_o} at Low Subsonic Speed	C_{D_o} at High Subsonic Speed	Incremental Drag Coefficient Due to Compressibility (ΔC_{DC}) (%)
1.	Boeing 727	0.017	0.03	76.5
2.	North American F-86 Sabre	0.014	0.04	207.7
3.	Grumman F-14 Tomcat	0.021	0.029	38.1
4.	McDonnell Douglas F-4 Phantom	0.022	0.031	40.9
5.	Convair F-106 Delta Dart	0.013	0.02	54

and fixed landing gear. Ice can disturb the flow of air over the wing; hence, it significantly reduces the lift and increases the drag. Wind tunnel tests have shown that an ice on a wing no thicker or rougher than a piece of coarse sandpaper can increase drag up to 40%.

3.4.10.11 Refueling Boom, Receptacle, Hose, Probe, and Drogue

Military aircraft, mainly fighters, are equipped with a refueling system that allows them to refuel in air from a fuel tanker aircraft. Currently, the Air Force fixed-wing aircraft [40] refuel with a flying boom. The boom is a rigid, telescoping tube that an operator on the tanker aircraft extends and inserts into a receptacle on the aircraft being refueled. Air Force helicopters, all Navy and Marine Corps aircraft, and the NATO countries and other allies refuel using the hose-and-drogue. This refueling method employs a flexible hose that trails from the tanker aircraft.

A drogue (a small windsock) at the end of the hose stabilizes it in flight and provides a funnel for the aircraft being refueled, which inserts a probe into the hose. Refueling boom, hose, probe, and drogue will create a significant amount of drag. The calculation is a challenging task, but some simplified models may allow an approximate result. Figure 3.17 illustrates an aerial refueling hose of a McDonnell Douglas KDC-10 and a refueling nose probe of a Vickers VC10 C1K.

3.4.10.12 External Store

Fighter aircraft have a variety of external store arrangements. The types and arrangements of external stores are not the same for all airplanes but differ as to the purpose for which the airplane is used; some examples are missiles, bombs, and cannons, usually mounted under the wing or at the wingtips. Every store will create an extra drag, the magnitude of which is a function of its geometry and size. Two external stores (fuel tanks) of a McDonnell Douglas EAV-8B Matador II are depicted in Figure 3.17.

3.4.10.13 External Sensors

Many manned aircraft and any modern large unmanned aerial vehicles are equipped with a number of sensors and measurement devices such as cameras, and electro-optical and infrared sensors. For instance, NASA's Armstrong Flight Research Center operates one Northrop Grumman Global Hawk unmanned aircraft for Earth science missions to measure, monitor, and observe remote locations on Earth not feasible or practical with piloted aircraft, or space satellites. The two pods under the wings of Global Hawk house atmospheric measurement probes (13 instruments were installed). Every external sensor will create an extra drag, the magnitude of which is a function of its geometry and the configuration.

3.4.10.14 Miscellaneous Items

There are other items that produce drag but, due to their variations, are not listed in this section. These items include (1) footstep in small GA aircraft that allows the pilot or technician to climb up; (2) small plate on tails to balance the manufacturing unbalances, (3) catapult hook, (4) wiper blades, (5) angle of attack meter vane, (6) non-streamlined fuselage, (7) deflector cable, (8) chemical sprayer in agricultural aircraft, (9) vortex generator, (10) navigation lights, (11) fitting, (12) engine exhaust pipe, (13) external fuel tank, (14) underwing station/mounting/hardpoint for stores, (15) landing gear bay door, (16) window cutout, (17) structural wires (see Figure 3.11a), (18) cable

to pull an unpowered glider by a powered aircraft, (19) wingtip (see Figure 3.17a), and (20) spoiler.

The calculation of drag of such minor items is out of scope of this text. However, some items can be modeled as a small wing or a fuselage. For instance, a pitot tube may be modeled as a small fuselage, and a pylon can be modeled as a small wing.

Behind a paywall, Aviation Week (4/21/2020) reports [41] that the US Air Force "has discovered that vertically mounted wiper blades on the KC-135 Stratotanker reduce aircraft drag by about 1% during cruise conditions, potentially saving the service $7 million".

Figure 3.17 illustrates the following eight miscellaneous items that contribute to drag: (1) fairing for the flap mechanism and wingtip for an Airbus A319, (2) underwing mounting/hardpoint for stores for a McDonnell Douglas EAV-8B Matador II, (3) step of a Bell-Boeing MV-22B Osprey, (4) engine exhaust pipe of a Cessna 172K, (5) aerial refueling hose of a McDonnell Douglas KDC-10, (6) refueling nose probe of a Vickers VC10 C1K, (7) antennas of a Saab JAS-39C Gripen, and (8) windshield wiper of a Lockheed L-1011 TriStar. Reference [42] provides a great collection of aircraft photos in which various aircraft details may be observed and identified.

3.4.11 Overall C_{D_o}

Based on the build-up technique, the overall C_{D_o} is determined readily as the sum of C_{D_o} of all aircraft components and factors. The calculation of C_{D_o} contribution due to factors as introduced in Section 3.4.10 is complicated. These factors are sometimes responsible for an increase in C_{D_o} up to about 50%. Thus, we will resort to a correction factor in our calculation technique. Then, the overall C_{D_o} of an aircraft is given by

$$C_{D_o} = K_c\left[C_{D_{o_w}} + +C_{D_{of}} + C_{D_{o_{ht}}} + C_{D_{o_{vt}}} + C_{D_{o_s}} + C_{D_{o_{lg}}} + C_{D_{o_n}} + C_{D_{o_{fi}}} + \cdots\right] \tag{3.40}$$

where K_c is a correction factor and depends on several factors such as the type, year of fabrication, degree of streamline of fuselage, configuration of the aircraft, and number of miscellaneous items. Table 3.5 yields the K_c for several types of aircraft.

TABLE 3.5
Correction Factor (K_c) for Equation 3.40

No.	Aircraft Type	K_c
1.	Jet transport	1.1
2.	Agriculture	1.5
3.	Prop-driven cargo	1.2
4.	Single-engine piston	1.3
5.	General aviation	1.2
6.	Fighter	1.1
7.	Glider	1.05
8.	Remote-controlled	1.2

TABLE 3.6
C_{D_o} of Major Components of Gates Learjet 25

No.	Component	C_{D_o} of Component	Percent from Total C_{D_o} (%)
1.	Wing	0.0053	23.4
2.	Fuselage	0.0063	27.8
3.	Wingtip tank	0.0021	9.3
4.	Nacelle	0.0012	5.3
5.	Engine strut	0.0003	1.3
6.	Horizontal tail	0.0016	7.1
7.	Vertical tail	0.0011	4.8
8.	Other components	0.0046	20.4
9.	Total C_{D_o}	0.0226	100

Each component has a contribution to the overall C_{D_o} of an aircraft. Their contributions vary from aircraft to aircraft and from configuration to configuration (e.g., cruise to takeoff). Table 3.6 illustrates [36] the contributions of all major components of Gates Learjet 25 to aircraft C_{D_o}. Note that row 8 of this table shows the contributions of other components as high as 20%.

Table 3.7 illustrates C_{D_o} of several aircraft at low speeds [43]. The retired airliner Boeing 707 was a very aerodynamic aircraft with a C_{D_o} of 0.013 at low subsonic speeds. You may have noticed that Cessna 185 has a lower C_{D_o} compared with Cessna 172 (Figure 3.17) and Cessna 182 (Figure 4.4). The reason is that Cessna 172 and Cessna 182 are equipped with fixed tricycle landing gear, while Cessna 182 has a fixed tail dragger.

3.5 WAVE DRAG

In supersonic airspeeds, a new type of drag is produced and referred to as "shock wave drag" or simply "wave drag". When supersonic flow experiences an obstacle (e.g., wing leading edge or fuselage nose), it is turned into itself and a shock wave is formed. A shock wave is a thin sheet of air across which abrupt changes occur in flow parameters such as pressure, temperature, density, speed, and Mach number. In general, air flowing through a shock wave experiences a jump toward higher density, higher pressure, higher temperature, and lower Mach number. The effective Mach number approaching the shock wave is the Mach number of the component of velocity normal to the shock wave. This component Mach number must be >1.0 for a shock wave to exist. The wave drag - the new source of drag - is inherently related to the loss of the stagnation pressure and increase of entropy across the oblique and normal shock waves.

In general, a shock wave is always required to bring supersonic flow back to subsonic regime. In a subsonic free stream, whenever the local Mach number becomes >1 over the surface of a wing or body, the flow must be decelerated to a subsonic speed before reaching the trailing edge. If the surface could be shaped such that the surface Mach number is reduced to 1 and then decelerated subsonically to reach the trailing edge at the surrounding free-stream pressure, there would be no shock wave and no shock drag. A major goal of transonic airfoil design is to reduce the local supersonic Mach number to as close to 1 as possible before the shock wave. One of the main functions of sweep angle in a swept wing is to reduce wave drag at transonic and supersonic airspeeds.

TABLE 3.7
C_{D_o} of Several Aircraft at Low Speed

No.	Aircraft	Type	Landing Gear	m_{TO} (kg)	S (m^2)	Engine	C_{D_o}
1.	Cessna 172	Single-engine GA	Fixed	1,111	16.2	Piston	0.028
2.	Cessna 182	Single-engine GA	Fixed	1,406	16.2	Piston	0.029
3.	Cessna 185	Single-engine GA	Fixed	1,520	16.2	Piston	0.021
4.	Cessna 310	Twin-engine GA	Retractable	2,087	16.6	Piston	0.026
5.	Boeing F/A-18 Hornet	Fighter	Retractable	23,541	38	Turbofan	0.017
6.	Learjet 25	Business jet	Retractable	6,804	21.53	Turbojet	0.0226
7.	Gulfstream II	Business jet	Retractable	29,711	75.21	Turbofan	0.023
8.	Saab 340	Transport	Retractable	29,000	41.81	Turboprop	0.028
9.	McDonnell Douglas DC-9-30	Airliner	Retractable	49,090	92.97	Turbofan	0.021
10.	Boeing 747-400	Airliner	Retractable	412,000	525	Turbofan	0.018
11.	Boeing 767-200	Airliner	Retractable	142,880	283.3	Turbofan	0.0135
12.	Airbus 340-200	Airliner	Retractable	275,000	361.6	Turbofan	0.0165
13	Boeing C-17 Globemaster III	Transport	Retractable	265,350	353	Turbofan	0.0175
14	Pilatus PC-9	Trainer	Retractable	3,200	16.29	Turboprop	0.022
15	Embraer EMB 312 Tucano	Trainer	Retractable	3,175	19.4	Turboprop	0.021
16	Lockheed C-5 Galaxy	Military transport	Retractable	381,018	580	Turbofan	0.019

In supersonic airspeeds, the following three main types of waves are created: (1) oblique shock wave, (2) normal shock wave, and (3) expansion waves. In general, an oblique shock wave brings a supersonic flow to another supersonic flow with a lower Mach number. A normal shock wave brings a supersonic flow to a subsonic flow (i.e., Mach number < 1). However, an expansion wave brings a supersonic flow to another supersonic flow with a higher Mach number. In supersonic airspeeds, a shock wave may happen at any place in the aircraft, including wing leading edge, horizontal tail leading edge, vertical tail leading edge, and engine inlet. All these aircraft component locations will create an extra drag when a shock wave is formed. Thus, in supersonic speed, the drag coefficient is expressed by

$$C_D = C_{D_o} + C_{D_i} + C_{D_w} \tag{3.41}$$

FIGURE 3.20 Mikoyan MiG-29 supersonic fighter. (Courtesy of Maurice Kockro.)

where C_{D_w} is referred to as "wave drag coefficient". The precise calculation of C_{D_w} is time-consuming, but, to give the reader the guidance, we present two techniques: one for a lifting surface leading edge and the other for the whole aircraft. For a complicated geometry aircraft configuration, the drag may be computed with aerodynamic techniques such as the vortex panel method and "computational fluid dynamics" techniques. Figure 3.20 illustrates the Mikoyan MiG-29 supersonic fighter and attack aircraft, with a top speed of Mach 2.25.

3.5.1 Wave Drag for Wing and Tail

This section presents the wave drag of a wing. In an aircraft with a supersonic maximum speed, the locations where they have the first impact on airflow (such as wing leading edge, horizontal tail leading edge, vertical tail leading edge, fuselage nose, and engine inlet edge) are usually made sharp. One main reason for this initiative is to reduce the number of shock waves created over the aircraft components during a supersonic flight. Two airfoil cross sections that are frequently employed for wing, horizontal tail, and vertical tail are double wedge and biconvex (see Figure 3.21).

In this section, a wave drag calculation technique is introduced that is applicable to any component that has a corner angle (e.g., double wedge and biconvex) and experiences a shock wave. Then wave drag coefficient C_{D_w} for such a component is calculated separately and then all are summed together.

Consider the front top half of a wedge with a sharp corner that experiences an oblique shock in a supersonic flow (as illustrated in Figure 3.22). The wedge has a wedge angle of θ, and the free-stream pressure and the Mach number are P_1 and M_1, respectively. When the supersonic flow hits the corner, an oblique shock with an angle of β to the free stream is generated.

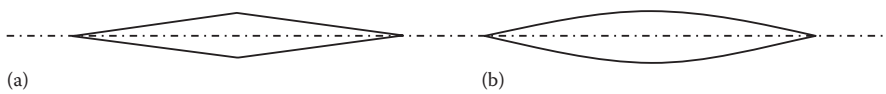

FIGURE 3.21 Supersonic airfoil sections. (a) Double wedge and (b) Biconvex.

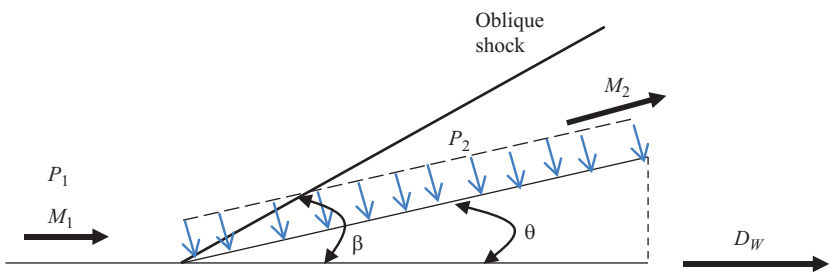

FIGURE 3.22 Geometry for drag wave over a wedge.

For each component with such configuration, the wave drag coefficient is given by

$$C_{D_w} = \frac{D_w}{(1/2)\rho V_\infty^2 S} = \frac{D_w}{(1/2)\gamma \cdot M^2 PS} \tag{3.42}$$

where subscript infinity (∞) means that the parameters are considered in the infinity distance from the surface. Please note that this does not really mean infinity, but it simply means a distance out of the effect of shock and the surface (i.e., free stream). The parameter S is the surface of a body at which pressure is acting (i.e., planform area).

D_w is the wave drag and is equal to the axial component of the pressure force. In supersonic speeds, the induced drag may be ignored, since it has a negligible contribution, compared to the wave drag. In supersonic speeds, the lift coefficient has a very low value. Since the wedge has an angle, θ, the drag force due to flow pressure acting on a wedge surface with an area of A is given by

$$D_w = P_2 A\left(\sin\theta\right) \tag{3.43}$$

where P_2 represents the pressure behind an oblique shock wave, and θ is the corner angle (see Figure 3.22). Please note that, in this particular case, the pressure at the lower surface is not changed. The relationship between upstream and downstream flow parameters may be derived using the energy law, mass conservation law, and momentum equation. The relationship between upstream pressure (P_1) and downstream pressure (P_2) is given [44] by

$$P_2 = P_1\left[1 + \frac{2\gamma}{\gamma+1}\left(M_{n1}^2 - 1\right)\right] \tag{3.44}$$

where γ is the ratio of specific heat at constant pressure and constant volume ($\gamma = c_p/c_v$). For air in standard condition, γ is 1.4. The variable M_{n1} is the normal component of the upstream Mach number and is given by

$$M_{n1} = M_1 \sin\beta \tag{3.45}$$

The parameter β (oblique shock angle) is a non-linear function of upstream Mach number and wedge corner angle (θ):

$$\tan\theta = 2\cot\beta\left[\frac{M_1^2 \sin^2\beta - 1}{M_1^2\left(\gamma + \cos 2\beta\right) + 2}\right] \tag{3.46}$$

Equation 3.46 is called the θ−β−M relation. For any given θ, there are two values of β predicted for any given Mach number. Take the lower value that is the representation of the weak shock wave that is favored by nature.

Pressure may also be non-dimensional as follows:

$$P_2 - P_\infty = \frac{1}{2}\rho_\infty V_\infty^2 C_p = \frac{1}{2}\gamma M_\infty^2 P_\infty C_p \tag{3.47}$$

where C_p is the pressure coefficient.

Now, consider another more general case, where a supersonic airfoil has an angle of attack, or when the second half of a wedge is considered. In such a case, where a supersonic flow is turned away from itself, an expansion wave is formed (see Figure 3.23). Expansion waves are the antithesis of shock waves. In an expansion corner, the flow Mach number is increased, but the static pressure, air density, and temperature decrease through an expansion wave. The expansion wave is also referred to as the Prandtl–Meyer expansion wave.

For a wing with a wedge airfoil section shown in Figure 3.23, the drag force is the horizontal component of the pressure force, so

$$D = P_2 A \sin\theta - P_3 A \sin\theta \tag{3.48}$$

where A is the surface area and is equal to

$$A = b\frac{C/2}{\cos\theta} \tag{3.49}$$

where b is the wingspan (not shown in the figure). Plugging Equation 3.48 into Equation 3.49, the following result is obtained

$$D = (P_2 - P_3) b \frac{C/2}{\cos\theta} \sin\theta = \frac{1}{2}(P_2 - P_3) bC \tan\theta \tag{3.50}$$

If the wing has a different geometry, use this basic technique to determine the wing wave drag. The pressure behind the expansion wave is given [44] by the following equation:

$$P_3 = P_2 \left[\frac{1 + \frac{\gamma - 1}{2} M_2^2}{1 + \frac{\gamma - 1}{2} M_3^2} \right]^{\gamma/(\gamma-1)} \tag{3.51}$$

where the flow Mach number behind expansion wave (M_3) and the flow Mach number behind expansion wave (M_2) are related through the turn angle, θ:

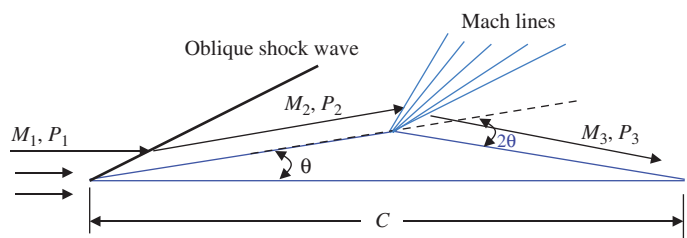

FIGURE 3.23 Oblique shock and Prandtl–Meyer expansion waves.

$$\theta = \nu(M_3) - \nu(M_2) \tag{3.52}$$

The $\nu(M)$ is referred to as the Prandtl–Meyer function and is given by

$$\nu(M) = \sqrt{\frac{\gamma+1}{\gamma-1}}\tan^{-1}\left[\sqrt{\frac{\gamma+1}{\gamma-1}\left(M^2-1\right)}\right] - \tan^{-1}\left[\sqrt{M^2-1}\right] \tag{3.53}$$

Equation 3.53 should be employed twice in the calculation: once to calculate M_2, and once to determine M_3. Example 3.3 indicates the application of the technique.

Example 3.2

Consider a rectangular wing with a span b (not shown in the figure) of 5 m and a chord C of 2 m in a Mach 2 air flow (the side view is sketched in Figure 3.24). The airfoil section is a 10° half-angle wedge at zero angle of attack. Calculate the wave drag coefficient. Assume that the expansion over the corners of the base is such that the base pressure is equal to the free-stream pressure. The experiment is performed at the sea-level ISA condition.

Solution

At sea-level ISA condition, the free-stream pressure is 1 atm (i.e., 101,325 Pa) and air density is 1.225 kg/m^3. The ratio of specific heat at constant pressure and constant volume for air, γ is 1.4. Since the supersonic flow turns to itself, it follows that an oblique shock wave is produced both on top and bottom surfaces. Pressure is increased behind the shock wave (P_2). In order to determine the pressure P_2, we need to first calculate the shock wave angle (β):

$$\tan\theta = 2\cot\beta\left[\frac{M_1^2\sin^2\beta - 1}{M_1^2\left(\gamma + \cos 2\beta\right) + 2}\right] \Rightarrow \tan(10) = 2\cot\beta\left[\frac{2^2\sin^2\beta - 1}{2^2\left(1.4 + \cos 2\beta\right) + 2}\right] \tag{3.46}$$

The solution of this non-linear equation yields an angle of 39.3° (β = 39.3°). The normal component of the shock, M_{n1} is

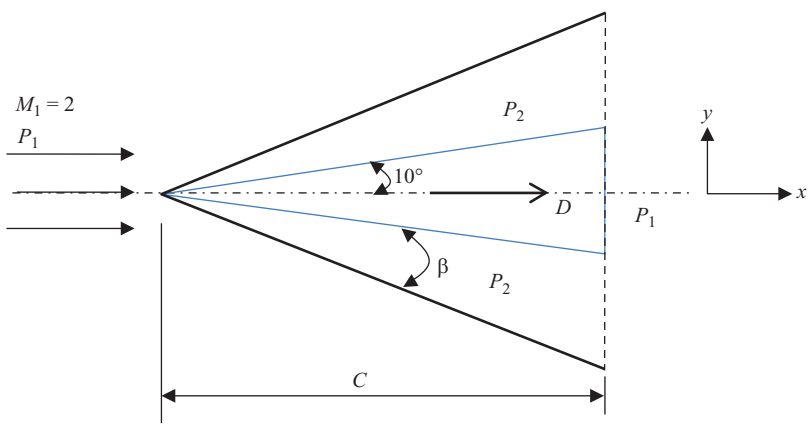

FIGURE 3.24 Geometry for Example 3.2 (side view).

$$M_{n1} = M_1 \sin\beta = 2\sin(39.3) = 1.27 \tag{3.45}$$

The static pressure behind the shock wave is

$$P_2 = P_1\left[1+\frac{2\gamma}{\gamma+1}\left(M_{n1}^2-1\right)\right] = 101{,}325\left[1+\frac{2(1.4)}{1.4+1}\left(1.27^2-1\right)\right] \tag{3.44}$$
$$\Rightarrow P_2 = 172{,}364\,\text{Pa}$$

The wave drag is the net force in the x direction; P_2 is exerted perpendicular to the top and bottom surfaces. The force due to P_1 exerted over the base is in the direction opposite to the x-axis. S is the planform area (the projected area seen by viewing the wedge from the top); thus, $S = C \times b$. The drag, D_w, is the summation of two top and bottom pressure force (see Figure 3.25) components in x direction, minus the force from base pressure:

$$D_w = 2P_2A_2(\sin\theta) - P_1A_1 \tag{3.43}$$

where A_2 is the base area, A_1 are the top and bottom surfaces, and $A_1 = 2bC\tan(10)$, and $A_2 = b\dfrac{C}{\cos(10)}$. Thus:

$$D_w = 2P_2\left[b\frac{C}{\cos(10)}\right]\sin(10) - P_1b\left[2C\tan(10)\right]$$

$$D_w = 2\times172{,}364\times5\times2\times\tan(10) - 2\times110{,}325\times5\times2\times\tan(10) = 251{,}670\,\text{N}$$

By definition, the wave drag coefficient is

$$C_{D_w} = \frac{D_w}{(1/2)\gamma\cdot M_\infty^2 P_\infty S} = \frac{251{,}670}{0.5\times1.4\times2^2\times101{,}325\times5\times2} \tag{3.42}$$
$$\Rightarrow C_{D_w} = 0.089$$

Note that, this drag coefficient is based on the shock wave, and it includes the contribution of the base.

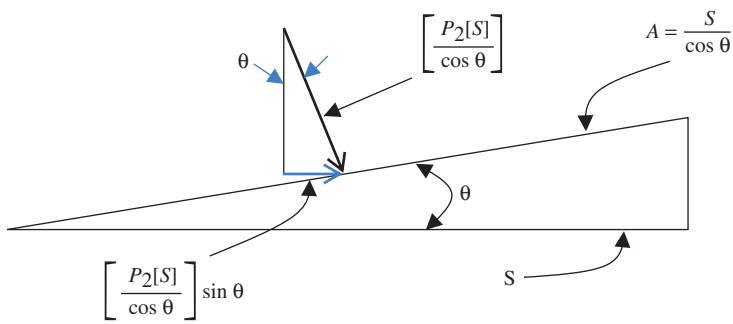

FIGURE 3.25 Wave drag, the component of pressure force in x direction.

Example 3.3

Consider a very thin flat plate wing with a chord of 2 m and a span of 5 m. The wing is placed at a 5° angle of attack in a Mach 2.5 air flow (Figure 3.26). Determine the wave drag coefficient. Assume sea-level ISA condition.

Solution

In the lower surface, an oblique shock is formed. The pressure P_3 is determined as follows:

$$\tan\theta = 2\cot\beta\left[\frac{M_1^2\sin^2\beta-1}{M_1^2(\gamma+\cos 2\beta)+2}\right]\Rightarrow \tan(5)=2\cot\beta\left[\frac{2.5^2\sin^2\beta-1}{2^2(1.4+\cos 2\beta)+2}\right] \quad (3.46)$$

The solution of this non-linear equation yields an angle of 27.4° (β = 27.4°). The normal component of the shock M_{n1} is

$$M_{n1} = M_1\sin\beta = 2\sin(27.4)=1.15 \quad (3.45)$$

The static pressure behind the oblique shock wave is

$$P_3 = P_1\left[1+\frac{2\gamma}{\gamma+1}\left(M_{n1}^2-1\right)\right]=101{,}325\left[1+\frac{2(1.4)}{1.4+1}\left(1.15^2-1\right)\right]=139{,}823\,\text{Pa} \quad (3.44)$$

In the upper surface, expansion waves are formed. The pressure P_2 is determined as follows:

For forward Mach line:

$$\nu_1(M)=\sqrt{\frac{\gamma+1}{\gamma-1}}\tan^{-1}\left[\sqrt{\frac{\gamma+1}{\gamma-1}\left(M_1^2-1\right)}\right]-\tan^{-1}\left[\sqrt{\left(M_1^2-1\right)}\right] \quad (3.53)$$

$$\nu_1(M)=\sqrt{\frac{1.4+1}{1.4-1}}\tan^{-1}\left[\sqrt{\frac{1.4+1}{1.4-1}\left(2.5^2-1\right)}\right]-\tan^{-1}\left[\sqrt{\left(2.5^2-1\right)}\right]=39.1^\circ \quad (3.53)$$

$$\theta=\nu(M_2)-\nu(M_1)\Rightarrow\nu(M_2)=\nu(M_1)+\theta=39.1+5=44.12^\circ \quad (3.52)$$

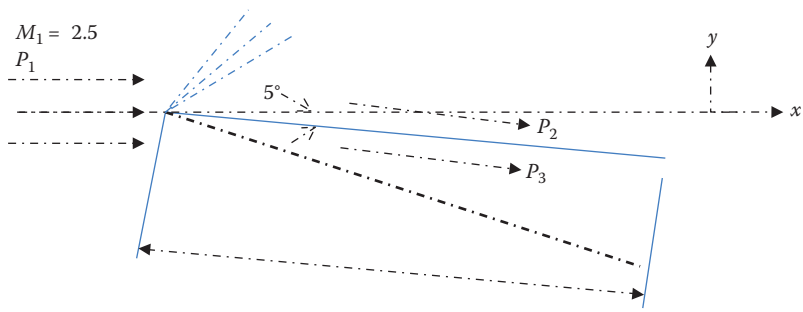

FIGURE 3.26 Geometry for Example 3.3 (side view).

For rearward Mach line:

$$\nu_2(M) = \sqrt{\frac{\gamma+1}{\gamma-1}}\tan^{-1}\left[\sqrt{\frac{\gamma+1}{\gamma-1}\left(M_2^2-1\right)}\right] - \tan^{-1}\left[\sqrt{\left(M_2^2-1\right)}\right] \quad (3.53)$$

$$44.12 = \sqrt{\frac{1.4+1}{1.4-1}}\tan^{-1}\left[\sqrt{\frac{1.4+1}{1.4-1}\left(M_2^2-1\right)}\right] - \tan^{-1}\left[\sqrt{\left(M_2^2-1\right)}\right] \quad (3.53)$$

Solution of this non-linear equation yields

$$M_2 = 2.723$$

The static pressure behind the expansion wave is

$$P_2 = P_1\left[\frac{1+\frac{\gamma-1}{2}M_1^2}{1+\frac{\gamma-1}{2}M_2^2}\right]^{\gamma/(\gamma-1)} = 101{,}325\left[\frac{1+\frac{1.4-1}{2}(2.5)^2}{1+\frac{1.4-1}{2}(2.723)^2}\right]^{1.4/(1.4-1)} = 71{,}742\,\text{Pa} \quad (3.51)$$

The wave drag force is the x-component of the pressure force:

$$D_w = (P_3 - P_2)bC\sin\alpha = (139{,}823 - 71{,}512)\times 5\times 2\times\sin(5) = 59{,}336\,\text{N} \quad (3.43)$$

The wave drag coefficient is

$$C_{D_w} = \frac{D_w}{\frac{1}{2}\gamma\cdot M_1^2 P_1 S} = \frac{59{,}336}{0.5\times 1.4\times 2.5^2\times 101{,}325\times 5\times 2} = 0.0134 \quad (3.42)$$

where $S = b\cdot C = 5\times 2 = 10\,\text{m}^2$.

3.5.2 Aircraft Wave Drag

An aircraft has usually a complex geometry and various components. In the previous section, a mathematical technique was introduced to calculate the wave drag where the object has a very simple (e.g., flat plate, wedge) configuration. Every aircraft component contributes to wave drag. This section presents a technique to determine the wave drag of a complete aircraft.

In this approach, we consider an aircraft as a whole and we will not divide it into several components. This is an approximate and empirical technique [31]. The aircraft wave drag coefficient consists of two parts: volume-dependent wave drag $C_{D_{w_v}}$ and lift-dependent wave drag $C_{D_{w_l}}$. The volume-dependent wave drag is a function of aircraft volume and much greater than the lift-dependent wave drag. The reason is that, at supersonic speeds, the lift coefficient (C_L) is very minimal.

$$C_{D_w} = C_{D_{w_l}} + C_{D_{w_v}} \quad (3.54)$$

The lift-dependent wave drag is given by

$$C_{D_{wl}} = \frac{K_{wl} S C_L^2 \left(M^2 - 1\right)}{2\pi L^2} \tag{3.55}$$

where L represents the aircraft fuselage length, S is wing reference area, b is the wingspan, and K_{wl} is a parameter given by:

$$K_{wl} = 2\left(\frac{S}{bL}\right)^2 \tag{3.56}$$

The volume-dependent wave drag is given by

$$C_{D_{wv}} = \frac{128 K_{wv} V^2}{\pi S L^4} \tag{3.57}$$

where V is the total aircraft volume, and K_{wv} is a factor given by:

$$K_{wv} = 1.17\left(\frac{1 + 0.75\beta(b/L)}{1 + 2\beta(b/L)}\right) \tag{3.58}$$

and β is a function of the Mach number as follows:

$$\beta = \sqrt{M^2 - 1} \tag{3.59}$$

In general, wave drag is significant, such that it will increase the aircraft drag up to about two to three times compared with subsonic drag. For instance, the zero-lift drag coefficient (see Figure 3.27) of the fighter aircraft Grumman F-14 Tomcat at a Mach number of 1.2 (supersonic) is about 0.045, while its C_{D_o} at a Mach number of

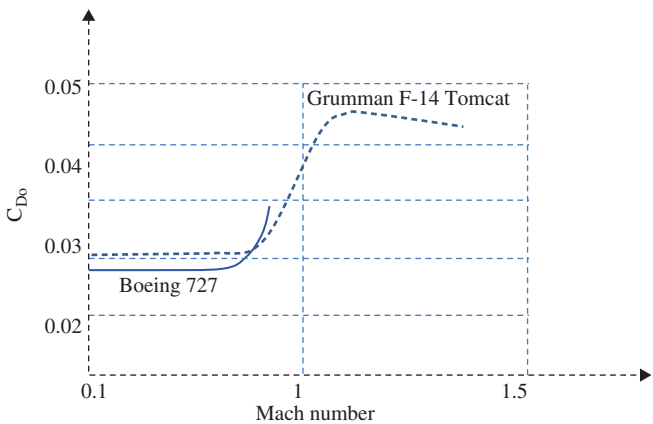

FIGURE 3.27 Variations of drag coefficient for two aircraft.

0.5 (subsonic) is about 0.021. Furthermore, the zero-lift drag coefficient of the transport aircraft Boeing 727 at low subsonic speed is about 0.018, while at high subsonic speed is about 0.03.

3.6 C_{D_o} FOR VARIOUS CONFIGURATIONS

Any individual aircraft will often take various configurations in flight phases. When an aircraft retracts its landing gear, deflects its flap, rotates its control surfaces, exposes any external component (such as gun), releases its store (e.g., missile), or opens its cargo door, it changes configuration. In general, there are three configuration groups that an aircraft may adopt: (1) clean configuration, (2) takeoff configuration, and (3) landing configuration.

Clean configuration is an aircraft configuration employed at flight phases such as cruise, climb, and turn. As the names imply, takeoff and landing configurations are the aircraft configurations that are adopted during takeoff and landing, respectively. In an aircraft with a retractable landing gear, the landing gear is employed during takeoff and landing and retracted during cruising flight. Furthermore, the flaps are extended in takeoff and landing operations. The flap deflection angle is a function of aircraft payload weight and atmospheric conditions.

3.6.1 Clean Configuration

Clean configuration is the configuration of an aircraft when it is in a cruise flight condition. At this configuration, no flap is deflected and landing gear is retracted (if it is retractable). Therefore, the drag polar is

$$C_{D_{\text{clean}}} = C_{D_{o_{\text{clean}}}} + K\left(C_{L_C}\right)^2 \tag{3.60}$$

Thus, clean C_{D_o} of the aircraft $C_{D_{o_{\text{clean}}}}$ includes every component (such as wing, tail, and fuselage) and excludes flap and landing gear (if retractable). If the landing gear is not retractable (e.g., as in Cessna 172, Figure 3.17), the C_{D_o} includes landing gear too. The parameter C_{L_C} is the cruise lift coefficient.

3.6.2 Takeoff Configuration

Takeoff configuration is the configuration of an aircraft when it is in a takeoff condition. In this configuration, the aircraft has a high angle of attack, flap is deflected for takeoff, and landing gear is not retracted (even if it is retractable). In a takeoff condition, the flaps are usually deflected down about 10°–30°. The takeoff C_{D_o} depends on the type and the deflection angle of the flaps. As the flap deflection increases, the takeoff C_{D_o} increases too. The drag polar at a takeoff configuration is

$$C_{D_{\text{TO}}} = C_{D_{o_{\text{TO}}}} + K\left(C_{L_{\text{TO}}}\right)^2 \tag{3.61}$$

where the takeoff zero-lift drag coefficient is given by

$$C_{D_{o\text{TO}}} = C_{D_{o\text{clean}}} + C_{D_{o\text{flap-TO}}} + C_{D_{o\text{LG}}} \tag{3.62}$$

where $C_{D_{o\text{flap-TO}}}$ represents the zero-lift drag coefficient of flap in a takeoff condition. In addition, the parameter $C_{D_{o\text{LG}}}$ represents the zero-lift drag coefficient of the landing gear. Moreover, $C_{L\text{TO}}$ represents the lift coefficient at takeoff. This coefficient does not have a constant value during takeoff due to the accelerated nature of the motion. The $C_{L\text{TO}}$ in the liftoff condition (where the nose wheel is just detached from the ground) is given by

$$C_{L\text{TO}} \cong 0.9\frac{2\,\text{mg}}{\rho S(V_{\text{LO}})^2} \tag{3.63}$$

where V_{LO} represents the aircraft liftoff speed. A factor of 0.9 is added due to the contribution of the engine thrust during takeoff in the vertical direction. The aircraft liftoff speed is often about 10%–30% higher than the aircraft stall speed.

$$V_{\text{LO}} = K_{\text{LO}}V_S \tag{3.64}$$

where $K_{\text{LO}} = 1.1–1.3$. In Chapter 8, the takeoff performance will be discussed in great detail. In general, the $C_{D_{o\text{TO}}}$ for a GA aircraft is about 0.03–0.05 and that for a jet transport aircraft is about 0.025–0.04. The large transport aircraft Boeing 747 (Figure 8.10b) in a zero flap deflection has a $C_{D_{o\text{TO}}}$ of 0.028.

3.6.3 Landing Configuration

Landing configuration is the configuration of an aircraft when it is in a landing condition. In this configuration, the aircraft has a high angle of attack (even more than takeoff condition), flap is deflected (even more than takeoff condition), and landing gear is not retracted (even if it is retractable). In the landing condition, the flaps are usually deflected down about 30°–60°. The landing C_{D_o} depends on the deflection angle of the flaps. As this angle increases, the landing C_{D_o} increases too. The landing zero-lift drag coefficient ($C_{D_{oL}}$) is often greater than the takeoff zero-lift drag coefficient ($C_{D_{o\text{TO}}}$). If there is another means of HLD for the aircraft, such as slat, you need to add it to this equation. The drag polar at a landing configuration is given by

$$C_{D_L} = C_{D_{oL}} + K\left(C_{L_L}\right)^2 \tag{3.65}$$

where C_{L_L} is the lift coefficient at landing and is given by

$$C_{L_L} \cong \frac{2\,\text{mg}}{\rho S(V_L)^2} \tag{3.66}$$

where V_L is the aircraft landing speed. The landing speed (V_L) is often about 10%–30% greater than the stall speed.

$$V_L = K_L V_S \tag{3.67}$$

where $K_L = 1.1–1.3$. The landing zero-lift drag coefficient is given by

$$C_{D_{oL}} = C_{D_{o\text{clean}}} + C_{D_{o\text{flap\_L}}} + C_{D_{o\text{LG}}} \tag{3.68}$$

where $C_{D_{o\text{flap\_L}}}$ represents the zero-lift drag coefficient of the flap in a landing condition. In general, the $C_{D_{oL}}$ for a GA aircraft is about 0.035–0.055 and that for a jet transport aircraft is about 0.03–0.045. The fighter aircraft General Dynamics (now Lockheed Martin) F-16 Fighting Falcon (Figure 7.6) has a $C_{D_{oL}}$ of 0.032. Both $C_{D_{o\text{flap\_TO}}}$ and $C_{D_{o\text{flap\_L}}}$ are functions of flap deflection. In Chapter 8, the landing performance will be presented.

3.6.4 The Effect of Speed and Altitude on C_{D_o}

The aircraft zero-lift drag coefficient is a function of a number of flight parameters. The Reynolds number is one of the influential parameters on the zero-lift drag coefficient. As the Reynolds number increases, the boundary layer thickness decreases and thus C_{D_o} decreases as well. As Equation 3.18 indicates, the Reynolds number is a function of true airspeed. Since the true airspeed is a function of altitude (indeed, air density), it can be concluded that the Reynolds number is also a function of altitude. Another factor affecting C_{D_o} is the compressibility that is significant at speeds higher than Mach 0.7. The third important factor is the wave drag as discussed in Section 3.5. Considering these factors, it is concluded that the C_{D_o} is a function of the Mach number and altitude:

$$C_{D_o} = f(M,h) \tag{3.69}$$

At low subsonic Mach numbers, C_{D_o} is increased due to an increase in the Reynolds number. As compressibility factor shows up at higher subsonic speeds, the C_{D_o} increases at a higher rate. At transonic speeds, a shock wave is formed and a jump (sudden increase) in C_{D_o} will be experienced. Therefore, the C_{D_o} is directly proportional to speed; as speed (Mach number) is increased, the C_{D_o} increases. Figure 3.28 illustrates typical variations of drag coefficient versus lift coefficient at various subsonic Mach numbers.

The second factor that affects the C_{D_o} is altitude. For a specific Mach number, as the altitude increases, the true airspeed decreases. For instance, consider an aircraft flying with a speed of Mach 0.5 at sea level. The true airspeed at this altitude 170 m/s ($0.5 \times 340 = 170$). If this aircraft is flying with the same Mach number at 11,000 ft altitude, the true airspeed will be 147 m/s ($0.5 \times 294 = 147$). In addition, the air density decreases with altitude at a higher rate. Thus, the higher altitude means the lower Reynolds number (Equation 3.24) and therefore the higher C_{D_o}. Figure 3.29 illustrates the variations of drag force for a light transport aircraft with turbofan engines at various altitudes. This transport aircraft has a stall speed of 90 knots and a maximum speed of 590 knots.

In conclusion, it can be assumed that at Mach numbers <0.7, the variation of C_{D_o} is not significant such that it can be considered constant. At higher Mach numbers, the compressibility effect and wave drag must be taken into account. The second conclusion is that, at higher altitude, total drag force is reduced. The reason is that, although at higher altitude, the C_{D_o} is increased, but the air density decreases. The rate of

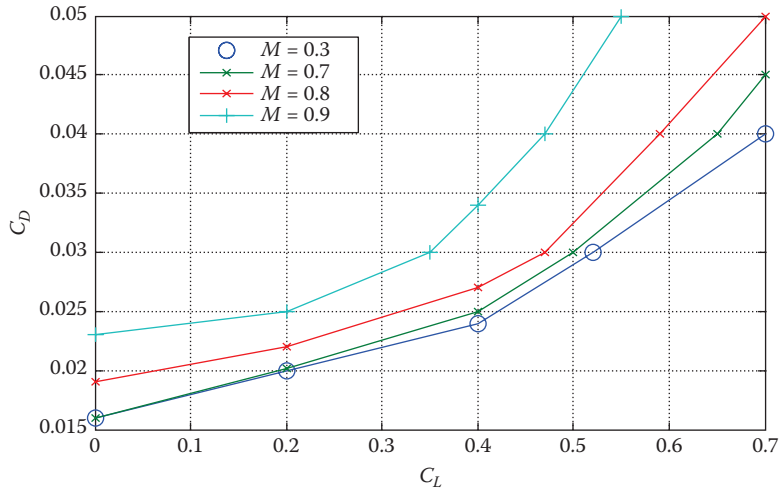

FIGURE 3.28 Drag coefficient versus lift coefficient for various Mach numbers.

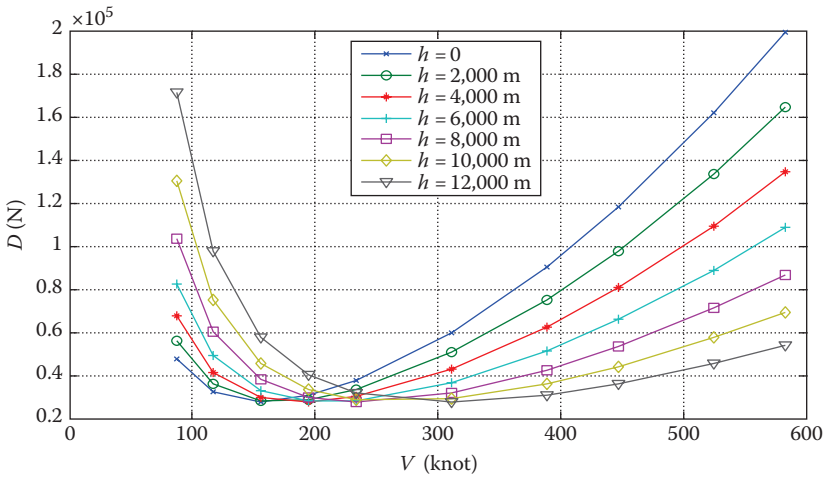

FIGURE 3.29 Variations of drag force without considering the compressibility effects.

change (decrease) in air density is faster than the rate of change (increase) of C_{D_o}. This is one of the reasons why airlines choose to fly at higher altitudes despite the need and cost of climb.

Example 3.4

Consider that the aircraft in Example 3.1 is equipped with a single-slotted flap with an average flap chord of 2.3 m. The aircraft takes off with a flap angle of 20° and lands with a flap angle of 35°. Assume the C_{D_o} of landing gear is 0.01, induced drag

correction factor K is 0.052, and both takeoff and landing speeds are 130 knots. Determine the aircraft C_{D_o} at takeoff and landing configurations.

Solution

The C_{D_o} of the flap is given by

$$C_{D_{o\text{flap}}} = \left(\frac{C_f}{C}\right) A \cdot \left(\delta_f\right)^B \tag{3.28}$$

From Table 3.3, $A = 0.00018$ and $B = 2$, so
The C_{D_o} of flap at takeoff is

$$C_{D_{o\text{flap}}} = \left(\frac{2}{9.3}\right) \times 0.00018 \times (20)^2 = 0.0178 \tag{3.29}$$

The C_{D_o} of the flap at landing is

$$C_{D_{o\text{flap}}} = \left(\frac{2}{9.3}\right) \times 0.00018 \times (35)^2 = 0.0545 \tag{3.29}$$

The takeoff C_{D_o}:

$$C_{D_{o\text{TO}}} = C_{D_{o\text{clean}}} + C_{D_{o\text{flap\_TO}}} + C_{D_{o\text{LG}}} = 0.023 + 0.0178 + 0.01 = 0.051 \tag{3.62}$$

The lift coefficient at takeoff:

$$C_{L_{\text{TO}}} \cong 0.9 \frac{2\,\text{mg}}{\rho S \left(V_{\text{LO}}\right)^2} = \frac{0.9 \times 2 \times 380{,}000 \times 9.81}{1.225 \times 567 \times (130 \times 0.5144)^2} = 2.16 \tag{3.63}$$

The induced drag coefficient

$$C_{D_i} = K\left(C_{L_{\text{TO}}}\right)^2 = 0.052 \times 2.16^2 = 0.242 \tag{3.13}$$

So, $C_{D_{\text{TO}}}$ is

$$C_{D_{\text{TO}}} = C_{D_{o\text{TO}}} + C_{D_i} = 0.051 + 0.242 \ = 0.293 \tag{3.61}$$

For the landing:

$$C_{L_L} \cong \frac{2\,\text{mg}}{\rho S \left(V_{\text{LO}}\right)^2} = \frac{2 \times 380{,}000 \times 9.81}{1.225 \times 567 \times (130 \times 0.5144)^2} = 2.4 \tag{3.54}$$

$$C_{D_i} = KC_L^2 = 0.052 \times 2.4^2 = 0.3 \tag{3.13}$$

$$C_{D_{oL}} = C_{D_{o\text{clean}}} + C_{D_{o\text{flap\_L}}} + C_{D_{o\text{LG}}} = 0.023 + 0.0545 + 0.01 = 0.088 \tag{3.49}$$

$$C_{D_L} = C_{D_{oL}} + K\left(C_{L_L}\right)^2 = 0.088 \ + \ 0.3 \ = \ 0.388 \tag{3.61}$$

PROBLEMS

Note: In all problems, assume ISA condition, unless otherwise stated.

3.1 A GA aircraft is flying at 5,000 ft altitude with a velocity of 100 knots. The length of the fuselage is 7 m, wing MAC is 1.5 m, horizontal tail MAC is 0.8 m, and vertical tail MAC is 0.6 m. Determine the Reynolds number of fuselage, wing, horizontal tail, and vertical tail.

3.2 Figure 3.30 depicts a top view of Boeing 757 (Figure 5.8) transport aircraft that has a wingspan of 38.05 m. Using a proper scale and using a series of measurements, determine the wing reference (gross) area, and wing net area of this aircraft.

3.3 Estimate the wing wetted area of Boeing 757 (Problem 3.2). Assume the wing has a maximum thickness of 12%.

3.4 The MAC of a trainer aircraft is 3.1 m. This trainer is cruising at sea level at a speed of Mach 0.3. Determine the skin friction coefficient of the wing when the flow over the wing is (a) laminar and (b) turbulent.

3.5 A business jet aircraft with a 31 m^2 wing area and a mass of 6,500 kg is flying at 10,000 ft altitude with a speed of 274 knots. If $C_{D_o} = 0.026$, $K = 0.052$, $C_{L_{max}} = 1.8$, calculate and plot the following items:
   a. Drag polar
   b. Variations of drag force with speed.

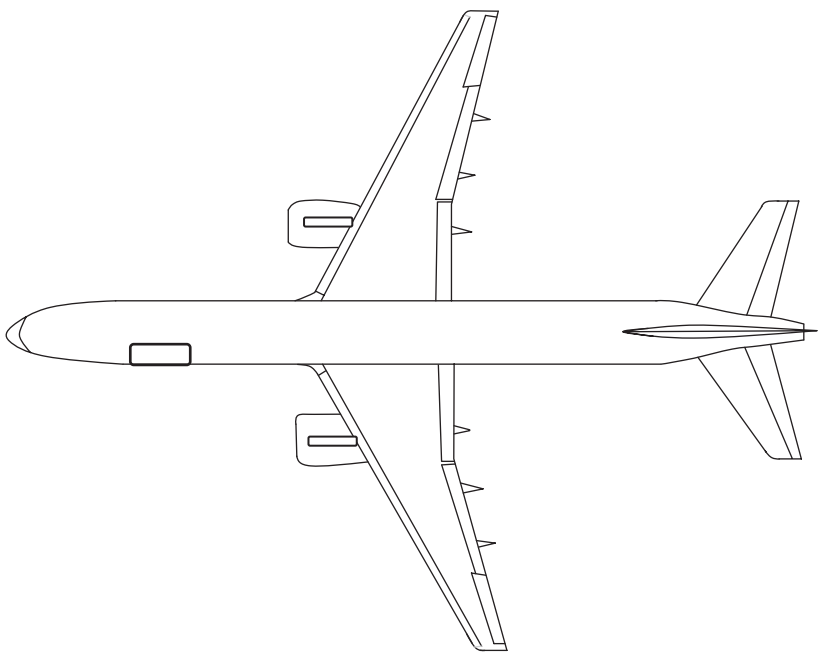

FIGURE 3.30 Top view of Boeing 757 transport aircraft.

3.6 The tip chord of a wing is 6 m and its root chord is 9 m. What is the mean aerodynamic chord?

3.7 The attack aircraft Thunderbolt II (Fairchild A-10) has the following features:

$m_{TO} = 22{,}221\,\text{kg},\ S = 47\,\text{m}^2,\ K = 0.06,\ C_D = 0.032,\ V_{max} = 377$ knots, $V_{TO} = 120$ knots.

Assume that the C_{D_o} is constant throughout all speeds.

a. Plot the variation of zero-lift drag (D_o) versus speed (from takeoff speed to maximum speed)
b. Plot the variation of induced drag (D_i) versus speed (from takeoff speed to maximum speed)
c. Plot the variation of total drag (D) versus speed (from takeoff speed to maximum speed)
d. At what speed, the drag force is minimum?

3.8 The wing of the twin-turbofan airliner Boeing 777 (Figure 7.18) has 31.6° of leading edge sweepback, a span of 60.93 m, and a planform area of 427.8 m^2. Determine Oswald efficiency factor (e) and induced drag correction factor (K) for this wing.

3.9 Determine the Oswald efficiency factor of a rectangular wing with an AR of 14.

3.10 A single-engine trainer aircraft with a wing area of 26 m^2 has a fixed landing gear with three similar tires. Each tire has a diameter of 25 cm and a thickness of 7 cm. Each tire is connected to the fuselage with a strut with a diameter of 4 cm and a length of 15 cm. The landing gear does not have fairing; determine zero-lift drag coefficient of the landing gear.

3.11 A cargo airplane is cruising at the speed of Mach 0.47, is taking off at a speed of 95 knots, and is landing at a speed of 88 knots. The plain flap with a 20% chord ratio is deflected down 22° during takeoff and 35° during landing. The aircraft has a mass of 13,150 kg, a wing area of 41.2 m^2, and induced drag correction factor, K, is 0.048. The zero-lift drag coefficients of all components are

$$C_{D_{o_w}} = 0.008, C_{D_{of}} = 0.006, C_{D_{o_{ht}}} = 0.0016, C_{D_{o_{vt}}} = 0.0012, C_{D_{o_n}} = 0.002,$$
$$C_{D_{o_{LG}}} = 0.015, C_{D_{o_s}} = 0.004.$$

Determine drag force at (a) Cruise, (b) Takeoff, and (c) Landing.

3.12 A Swedish aircraft designer is designing a fuselage for a 36-passenger aircraft to cruise at a Mach number of 0.55. He is thinking of two seating arrangement options: (a) 12 rows of three passengers and (b) 18 rows of two passengers. If he selects option a, the fuselage length would be 19.7 m with a diameter of 2.3 m. In option (b), the fuselage length would be 27.2 m with a diameter of 1.55 m. What option yields the lowest fuselage zero-lift drag coefficient?

3.13 The amphibian airplane Lake LA-250 (Figure 3.31) has a wing with the following features:

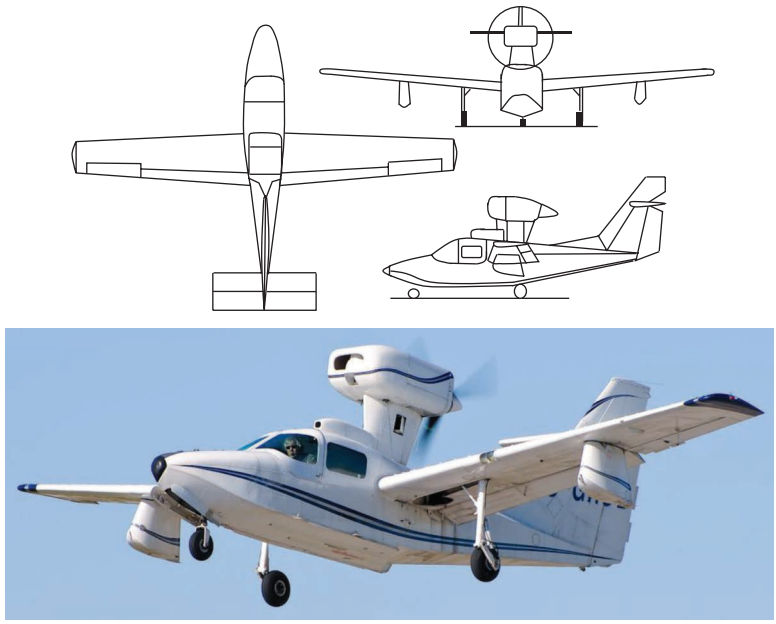

FIGURE 3.31 Three views of amphibian airplane Lake LA-250. (Courtesy of Gustavo Corujo, Gusair.)

$$S = 15.24\,\text{m}^2,\ b = 11.68\,\text{m},\ \text{MAC} = 1.65\,\text{m},\ (t/c)_{\max} = 15\%,\ \text{airfoil}: \text{NACA}\,4415,$$

$$C_{d_{\min_w}} = 0.0042.$$

The aircraft has a mass of 1,678 kg and is cruising at a speed of 155 knots. Determine the wing zero-lift drag coefficient. For other information, use the aircraft's three views that are provided.

3.14 The GA aircraft Moony M20TN (Figure 3.32) has a wing with the following features:

$$S = 16.3\,\text{m}^2,\ b = 11.11\,\text{m},\ (t/c)_{\max} = 15\%,\ \text{airfoil: NACA 63-215},\ C_{d_{\min_w}} = 0.0042.$$

The aircraft has a mass of 1,528 kg and is cruising at a speed of 237 knots. Determine (1) wing zero-lift drag coefficient and (2) fuselage zero-lift drag coefficient. For other information, use the aircraft's three views that are provided.

3.15 Assume that the aircraft in Problem 3.13 has a plain flap with a chord ratio of 0.2. Determine the flap C_{D_o}, when it is deflected 30° during a takeoff operation.

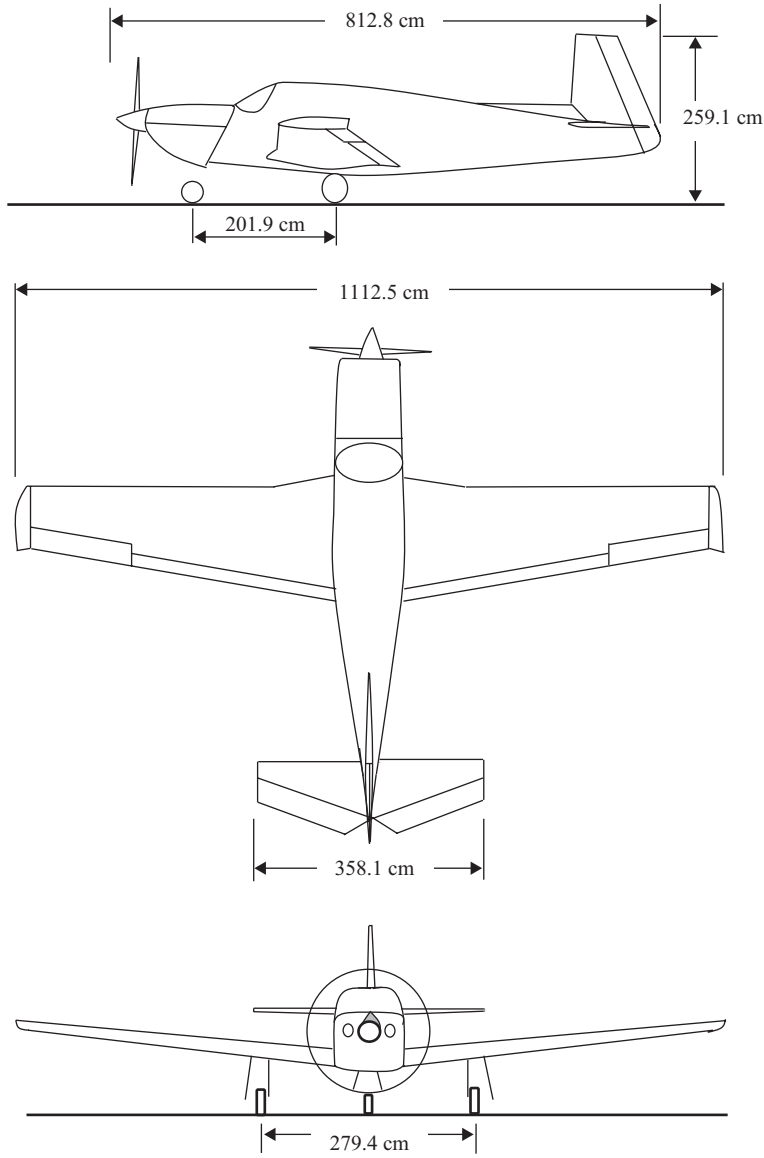

FIGURE 3.32 Three views of GA aircraft Moony M20TN [45].

3.16 A 12-seat commuter airplane has a vertical tail with the following features: $S_{vt} = 4.3\,\text{m}^2$, $b_{vt} = 5.4\,\text{m}$, $(t/c)_{\max_{vt}} = 10\%$, $C_{d_{\min_{vt}}} = 0.005$. The aircraft has a wing area of $29.4\,\text{m}^2$ and is cruising at a true airspeed of 160 knots at an altitude of 18,000 ft ISA condition. Determine the vertical tail zero-lift drag coefficient.

3.17 The four-seat light airplane Piper PA-34 has a horizontal tail with the following features:

$$S_{ht} = 3.6\,\text{m}^2,\ b_{ht} = 4.14\,\text{m},\ (t/c)_{\max_{ht}} = 12\%,\ C_{d_{\min_{ht}}} = 0.0047$$

The aircraft has a mass of 2,154 kg, a wing area of 19.39 m^2, and is cruising at 171 knots at an altitude of 18,500 ft. Determine the horizontal tail zero-lift drag coefficient.

3.18 A jet trainer with a retractable landing gear has the following features:

$$m_{\text{TO}} = 5{,}360\,\text{kg},\ S = 25.1\,\text{m}^2,\ b = 17.4\,\text{m},\ e = 0.85,\ V_c = 270\,\text{knot},\ C_{L_{\max}} = 2.2,$$

$$V_{\text{TO}} = 1.2V_s,\ V_{\text{Land}} = 1.3V_s,\ C_{D_{o_{\text{clean}}}} = 0.032,\ C_{D_{o_{\text{flapTO}}}} = 0.02,\ C_{D_{o_{\text{flapLand}}}} = 0.035,$$

$$C_{D_{o_{\text{LG}}}} = 0.01$$

Determine the aircraft drag under three flight conditions: (a) clean (cruise speed), (b) takeoff, and (c) landing.

3.19 The wings of the Y-5B agricultural biplane are connected together through two struts. Each strut has a circular cross section with a length of 1.2 m and a diameter of 4 cm. The total planform area of both wings is 38 m^2; determine the zero-lift drag coefficient of struts.

3.20 A single-engine small aircraft has a wing area of 260 ft^2 and a turboprop engine that has a power of 600 hp. The aircraft is cruising at 25,000 ft altitude at a speed of 182 knots. Determine the engine cooling drag coefficient. The air temperature at the exit is 400 K; and assume $K_e = 2$.

3.21 A business jet aircraft with a wing area of 45 m^2 is equipped with two turbofan engines. Each engine is podded in a nacelle with a diameter of 62 cm and a length of 110 cm. Determine nacelle zero-lift drag coefficient, provided the aircraft is cruising at a speed of 320 knots at an altitude of 28,000 ft.

3.22 A maneuverable aircraft has two fuel tanks at the wingtips. Each fuel tank has a shape of an ellipsoid with a diameter of 20 cm and a length of 130 cm. Determine fuel tank zero-lift drag coefficient, provided the aircraft is cruising at a speed of 190 knots at an altitude of 18,000 ft.

3.23 The F-16 supersonic jet fighter (Figure 3.33) with a mass 12,331 kg and a wing area of 27.8 m^2 is cruising at an altitude of 40,000 ft at Mach number 2.1. The wingspan is 9.45 m and the length of the fuselage is 15.3 m. Determine the wave drag of the aircraft, assuming the aircraft volume is 21.3 m^2.

3.24 Assume that F-16 in Problem 3.23 is flying at a Mach number of 1.2 at the given altitude. What is the wave drag of this fighter in this flight condition? Compare the result with the result of Problem 3.23 and comment about your finding.

3.25 The fuselage of a large transport aircraft has a diameter of 3.8 m and a length of 43 m. Determine the fuselage zero-lift drag, assuming the wing area to be 180 m^2 and the cruising speed to be 350 knots at 35,000 ft.

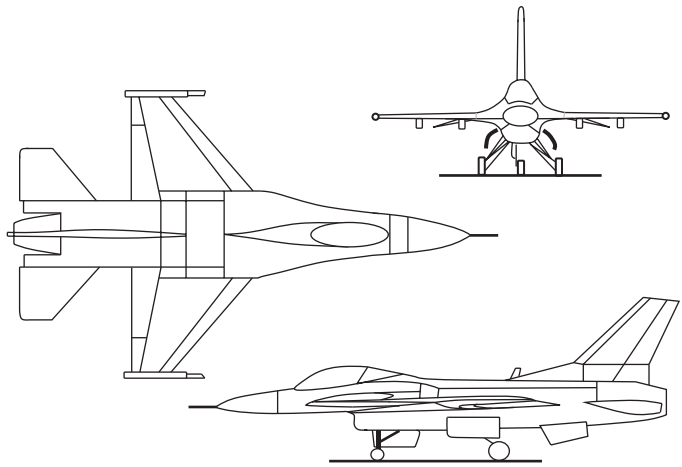

FIGURE 3.33 Three views of the F-16A fighter jet.

3.26 Determine the terminal velocity of a water droplet, assuming it has a shape of a sphere with a radius of 2 mm. The density of water is 998 kg/m^3.

3.27 You are required to design a parachute for the safe landing of a paratrooper with a mass of 85 kg. Determine the diameter of the parachute, if the terminal velocity is required to be 1 m/s at 5,000 ft altitude. Ignore the drag of the paratrooper and strings. The mass of the parachute is 6 kg.

3.28 Felix Baumgartner, an Austrian daredevil, fell to Earth from more than 24 miles high, becoming the first human to break the sound barrier under his own power, on October 14, 2012. He made the highest and fastest jump in history after ascending in a helium balloon to an altitude of 128,100 ft, reaching a maximum speed of Mach 1.24. Assume the terminal velocity was at 70,000 ft, and his frontal area while descending is 0.12 m^2, determine the drag coefficient of his body. Assume a mass of 90 kg.

3.29 Consider a very thin flat plate wing with a chord of 0.4 m and a span of 3.6 m. The wing is placed at a 6° angle of attack in a Mach 1.3 airflow. Determine the wave drag coefficient.

3.30 Consider a 2% thickness flat plate wing with a chord of 1.2 m and a span of 4.5 m. The wing is placed at a 3° angle of attack in a Mach 1.7 airflow. Determine

a. Wing zero-lift drag coefficient
b. Induced drag coefficient
c. Wing wave drag coefficient.

Assuming the aircraft has a mass of 1,000 kg and is cruising at an altitude of 12,000 ft. The wing may be assumed to be 0.003 and Oswald efficiency factor to be 0.8.

3.31 Consider a rectangular wing with a span of 15 m and a chord of 3 m in a Mach 2.6 airflow (the side view as sketched in Figure 3.24). The airfoil section is a 7° half-angle wedge at zero angle of attack. Calculate the wave drag

coefficient. Assume that the expansion over the corners of the base is such that the base pressure is equal to the free-stream pressure.

3.32 Consider a tapered wing with a span of 12 m and a chord of 2.5 m in a Mach 1.5 airflow (the side view as sketched in Figure 3.24). The airfoil section is a 4° half-angle wedge at zero angle of attack. Calculate the wave drag coefficient. Assume that the expansion over the corners of the base is such that the base pressure is equal to the free-stream pressure. The wing taper ratio is 0.4.

3.33 The high-altitude, remotely piloted surveillance aircraft Northrop Grumman RQ-4 Global Hawk is cruising at 18,000 m with a cruise speed of 570 km/h. The fuselage length is 14.5 m, determine the fuselage Reynold number.

3.34 A small, unmanned aircraft with a 0.5 m^2 wing area and a mass of 1.9 kg is flying at 1,000 m altitude with a speed of 60 km/h. Assume $C_{D_o} = 0.024$, $K = 0.1$, $C_{L_{\max}} = 1.4$, calculate and plot the following items:

a. Drag polar
b. Variations of drag force with speed.

4 Engine Performance

4.1 INTRODUCTION

The most influential force in aircraft performance is the force that the engine generates, that is, thrust. Other forces such as drag, lift, side force, and weight contribute to flight dynamics, but thrust is the one that can satisfy every performance requirement, provided the right magnitude of it is available. A fighter pilot can perform any military mission if the fighter possesses a very powerful engine. A powerful engine compensates any deficiency that an aircraft may have in terms of high drag or heavy weight. To analyze the performance of an aircraft, we need to model the engine or powerplant and calculate the engine performance characteristics.

Even a very powerful/thrustful propulsion system will lose its thrust/power at high altitude. Furthermore, any engine will perform differently under various flight conditions. Thus, the question is how to include the variations of engine power or engine thrust in aircraft performance analysis. Engine power, engine thrust, and the techniques by which they are produced are the subjects of this chapter. This chapter emphasizes only those aspects of propulsion that are necessary for our subsequent discussion of aircraft's performance.

An aircraft engine is very similar to a road transportation vehicle engine in many ways. Both engines convert the chemical energy of fuel into mechanical energy. There are a few differences as well. Unlike cars, there is no reverse gear in an aircraft, since there is no direct mechanical connection between the propulsion system and the landing gear.

Therefore, an aircraft is recommended not to independently move backward, so it needs an external force (e.g., tug) to help in its movement. A tug is a small truck that attaches a tow bar to the aircraft nose landing gear. Once attached, it can then push or pull the aircraft. The reverse gear on an aircraft is reverse thrust. This is used only when the plane has landed and is braking to a safe taxi speed on the runway.

In addition, some propeller aircraft can reverse by changing the pitch of the propellers. Although many jet aircraft are capable of moving themselves backward on the ground using reverse thrust (i.e., power-back); in airports, a mechanical tractor (i.e., tug) helps aircraft to taxi around and get out of the boarding gates. For jet aircraft, the reverse thrust is not used in a standstill situation because it is not permitted by the FAA. Two reasons are that it poses a risk of the aircraft tipping over and it creates hazards and safety problems for ground staff.

Jet engines produce thrust mainly based on Newton's third law. Newton's third law states, "For every action, there is an equal and opposite reaction". The aircraft jet engine usually generates a backward force to displace the airflow; thus, the aircraft, in reaction, is pushed forward. In a prop-driven aircraft, the thrust is, indeed, the net lift on the propeller (when considered as a lifting surface). The main converter of the chemical energy of fuel in the propulsion system into power or thrust is a mechanical

DOI: 10.1201/9781003279068-4

(or aerodynamic) part called a fan, or propeller. In Section 4.6, we briefly examine the propeller performance and its features.

Some types of air vehicles such as hang gliders or sailplanes are engineless. They do not have an engine or propulsion system at all. They use combinations of other forces (drag, lift, side force, and weight) to fly around. Sometimes, if they are lucky, they can utilize the energy of rising warm air to climb. Because of this reason, these aircraft are not able to take off without external help. To take off, they have to be towed or pulled by a car or mechanical winch. When they gain enough altitude, they can disconnect themselves from the puller and start to glide.

This chapter begins with aircraft engine classification, followed by more details of each category. Then a comparison between the performances of various engines is presented. The performance-related section of this chapter is Section 4.6, which enables the reader to calculate thrust-related parameters in different atmospheric situations and flight conditions. At the end of this chapter, a brief discussion about propeller performance is introduced.

4.2 AIRCRAFT ENGINE CLASSIFICATION

The first powered flight in an airplane was made by the Wright brothers on December 17, 1903. Thus, the first successful gasoline engine for an aircraft was the engine used in the Wright Flyer. Nowadays, various types of engines are manufactured and employed in aircraft. Aircraft engines are classified into three categories: (1) air-breathing engines, (2) non-air-breathing engines or rocket engines, and (3) unconventional engines. Figure 4.1 illustrates this classification.

Three important unconventional engines are (1) man-powered engines, (2) sun-powered engines, and (3) electrically powered engines. Indeed, the aircraft that uses a man-powered engine has no engine other than the muscular power of the pilot. The sun-powered or solar-powered aircraft uses solar energy that is absorbed through its solar cells. An electrically powered aircraft uses an electric battery that is powerful enough for its entire flight. The sun-powered engine may also be categorized as an electric engine where its battery is charged by using solar cells.

To perform aircraft performance analysis, we employ another engine classification. This classification is based on the type of direct output of the engine.

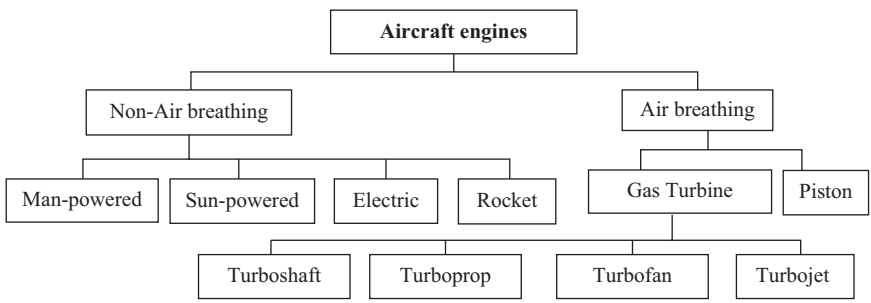

FIGURE 4.1 Air vehicle's aero-engine classification.

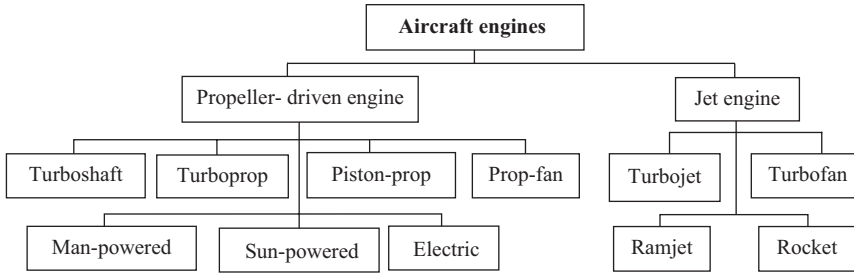

FIGURE 4.2 Output-based aero-engine classification.

Thus, engines are divided into two major categories: (1) power-producing engines and (2) thrust-producing engines. Power-producing engines have a propeller, and the power of the engine is converted into thrust force through the propeller. Thrust-producing engines do not have a propeller and directly generate thrust. Figure 4.2 demonstrates this classification. For this reason, we categorize the ramjet engine as a type of jet engine. The reason for this classification is the way we treat these aircraft for the sake of performance analysis. For instance, Chapter 5 is dedicated to jet aircraft and Chapter 6 is specific for propeller-driven aircraft.

In general, a propeller-driven (or simply prop-driven) engine produces power (P), but a jet engine generates thrust (T). These aerial engines have extensive applications in various types of aircraft. Most small general aviation (GA) aircraft employ piston engines, while most small transport aircraft have turboprop engines. Almost all large modern passenger airplanes and most fighter airplanes utilize turbofan engines, but few fighters use turbojet engines. The performance characteristics of every engine are usually published by the engine manufacturer. However, many engines that are in the same category show a similar performance. For precise engine performance, the reader is referred to the manufacturer's catalog. Currently, major turbine engine manufacturers are Pratt and Whitney (P&W), General Electric, Turbomeca, CFM, and Rolls-Royce. Major piston aero-engine manufacturers are Teledyne Continental (TCM), Continental, Hirth, Limbach, PZL, Rotax, VOKBM, Honeywell, and Textron Lycoming. A brief description of various conventional aero-engines is presented in the following sections.

4.3 PISTON OR RECIPROCATING ENGINE

A piston engine, also known as a reciprocating engine, is a heat engine that employs one or more pistons to release fuel energy through a combustion process and to convert it to rotating mechanical energy. Each piston is inside a cylinder, into which the air–fuel mixture is supplied, either already hot (i.e., external combustion) and under pressure (e.g., steam engine) or heated inside the cylinder (i.e., internal combustion). The combustion (ignition of the fuel–air mixture) in the cylinder is initiated either by the spark plug or by compression (i.e., diesel, where the heated air ignites fuel when injected). The combustion process generates a high-pressure gas while it increases the temperature of the gas.

The very hot gases (combustion products) expand, pushing the piston to the bottom of the cylinder (bottom-dead-center). The piston is returned to the cylinder top (top-dead-center) by either a flywheel or the power from other pistons connected to the same shaft [46]. Then, the expanded hot gases are exhausted from the cylinder through valves. Currently, most aero-engines are using a spark plug; however, recent advances in piston engines have made the application of compression–ignition efficient.

The displacement of a piston along the cylinder to/from top-dead-center from/to bottom-dead-center is often called *stroke*. Usually, one-/two-cylinder piston engines have two strokes, while four- and more-cylinder piston engines have four strokes. The cycle of a four-cylinder piston engine includes four strokes, while the cycle of a one-cylinder piston engine has only two strokes. Some small *radio/*remote-controlled (RC) aircraft with a very low output power (e.g., <1 hp) utilize one-cylinder engines.

The linear movement of the piston is usually converted to a rotating motion through a connecting rod and a shaft (i.e., crankshaft). The more cylinders a reciprocating engine has, the more vibration-free it can operate. The higher the piston displacement volume (i.e., the piston area multiplied by its displacement) is, the more mechanical power it is capable of producing. Figure 4.3 shows the sketch of a simplified two-stroke and four-stroke piston engine. The power production in a four-cylinder piston engine takes place in a process with mainly four strokes (i.e., stages): (1) intake, (2) compression, (3) power, and (4) exhaust.

An aircraft piston engine is similar to an automobile engine with a few slight differences. The aircraft-weight-to-engine-power ratio is generally lower for an aircraft engine as compared to an automobile engine of a comparable size. Today's piston engines' output power ranges from <1 hp to more than 2,000 hp. Figure 4.4 illustrates a four-seat, single-engine light aircraft, Cessna 182, that is equipped with

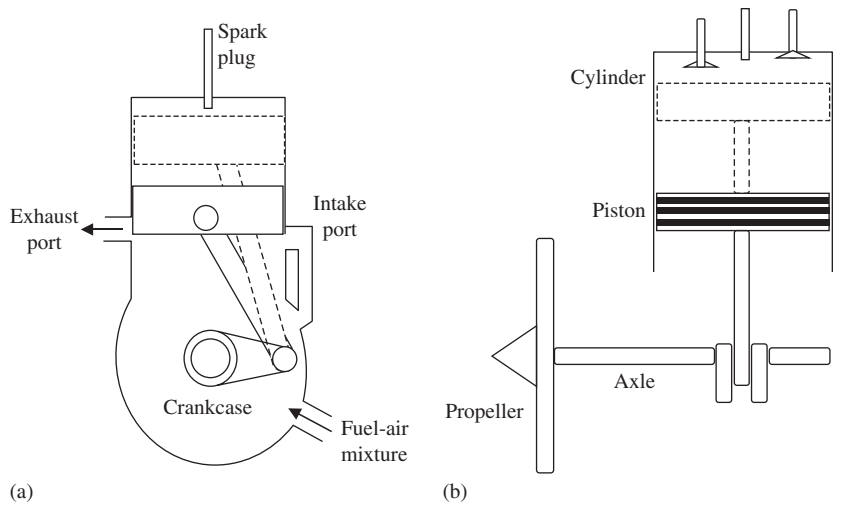

FIGURE 4.3 Schematic of a piston engine. (a) Two-stroke engine; (b) Four-stroke engine.

FIGURE 4.4 GA aircraft Cessna 182T Skylane with a single-piston engine. (Courtesy of Gustavo Corujo.)

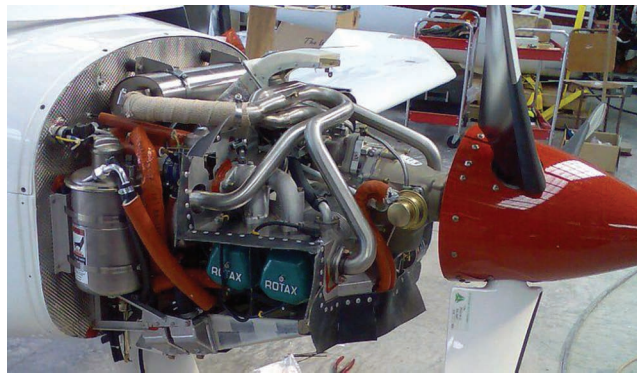

FIGURE 4.5 Piston engine Rotax 912s DynAero connected to a three-blade propeller.

a piston-prop engine. The engine is a Lycoming IO-540 with a three-blade propeller and generates a maximum of 230 hp (172 kW).

The following briefly provides characteristics of a few piston engines. The nine-cylinder four-stroke radial [9] engine PZL K-9 (Poland) with a bore of 155 mm, stroke of 174 mm, and dry mass of 580 kg generates a maximum of 860 kW (1,170 hp). The two-cylinder two-stroke Rotax 447 UL-2V (Austria) with an in-line configuration has a bore of 67.5 mm, stroke of 61 mm, and a dry mass of 26.8 kg, and generates 29.5 kW (39.6 hp). The 18-cylinder 4-stroke rotary (Wankel) diesel engine (Italy) with a bore of 150 mm, a stroke of 180 mm, and a dry mass of 1,700 kg produces a maximum of 1,380 kW (1,850 hp).

The Lycoming O-360-A horizontally opposed, four-cylinder, four-stroke air-cooled engine that generates 180 hp at 2,700 rpm is employed in Piper Cherokee 180. The Wright brothers' Flyer was equipped with a piston engine that had eight cylinders, weighed 200 lb, and generated ~89 hp.

Figure 4.5 shows a four-stroke piston engine Rotax 912s DynAero, which is producing 100 hp. In the United States, two major manufacturers of aircraft reciprocating engines are Continental and Textron Lycoming.

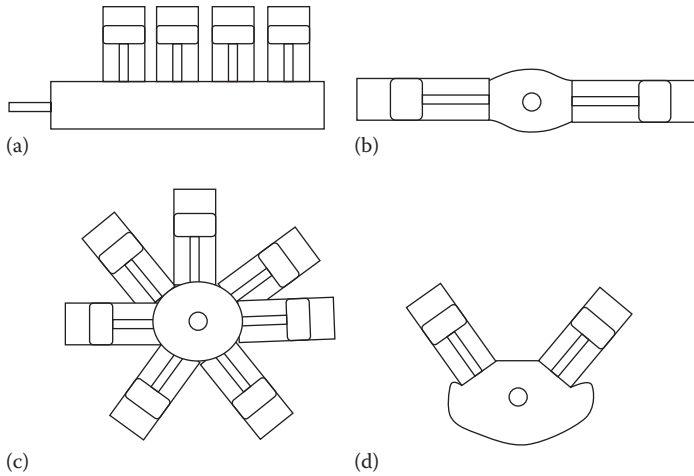

FIGURE 4.6 Basic engine configurations. (a) Inline; (b) flat or horizontally opposed; (c) radial; (d) V-type.

4.3.1 Piston Engine Configurations

When there is more than one cylinder in a piston engine, as is usually the case, they must be connected through a certain order. It is often common for piston engines to be classified by the number and alignment of cylinders and also by the total volume of displacement of gas by the pistons moving in the cylinders. A few commonly used variants of piston engines (Figure 4.6) are introduced briefly here.

1. *In-line engines*: The cylinders of an in-line engine are arranged in a single row parallel to the crankshaft. The cylinders are either upright above the crankshaft or inverted, that is, below the crankshaft. The inverted configuration is generally employed. Rotax 447 is a piston engine with two cylinders, in-line, and two strokes.
2. *Vee-type engines*: The V-type engine has the cylinders arranged on the crankcase in two rows, forming the letter V, with an angle usually between the rows of 45° and 60°. There is always an even number of cylinders in each row. French FAM-200 is a piston engine with six cylinders, in Vee form, and four strokes.
3. *Radial engines*: A radial engine has an odd number of cylinders extending radially from the centerline of the crankshaft. The cylinders are arranged evenly in the same circular plane, and all pistons are connected to a 360° crankshaft, thus reducing both the number of working parts and the engine weight. The cylinders are installed around the crankshaft to form a circle; the pistons move in and out of the circle along the radius. PZL K-9 (Poland) is a piston engine with nine cylinders, in radial form, and four strokes.
4. *Horizontally opposed or flat engine*: The opposed-type engine is usually mounted with the cylinders horizontally and the crankshaft horizontally;

however, in some helicopters, installation of the crankshaft is vertical. Teledyne Continental IO-520-L is a piston engine with six cylinders, horizontally opposed, and four strokes.

The opposed-type engine is most popular [36] for light conventional aircraft and is manufactured in various sizes. This configuration is the most fuel-efficient and economic. Figure 4.6 illustrates four basic piston engine configurations. The in-line engine is shown from the side, while the rest is from the front. The aero-engines are cooled by air, oil, or liquid, or a combination. In general, a majority of aero-piston engines are air-cooled. For instance, Teledyne Continental IO-360-KB and Textron Lycoming IO-540-K are both air-cooled piston engines, while Rotax 582 is a liquid-cooled piston engine. The single-seat kit-built sport plane Bede BD-17 Nugget is equipped with one 60 hp two-cylinder four-stroke piston engine.

4.3.2 Propeller Engine Performance

The shaft power of a propeller-driven engine (e.g., piston) is a function of two input parameters: (1) fuel (that is controlled by the pilot through engine throttle) and (2) inlet air pressure/density (that is a function of the flight altitude). The throttle directly determines the engine shaft's number or revolution per unit time.

The product of a piston engine is a shaft torque at a specific rotational speed that can be stated in terms of power (P). The unit of power in the SI system is kilowatt (kW) and in the British system is horsepower (hp). The output power of the engine is the input power (Figure 4.7) to the propeller (P_{in}) and is converted into the thrust through the propeller. Therefore, the output power (P_{out}) that is received by the aircraft is equal to the input power (P_{in}) multiplied by the prop efficiency (η_P).

$$\eta_P = \frac{P_{out}}{P_{in}} \tag{4.1}$$

In practice, a propeller cannot convert all the shaft input power into propulsive thrust, since part of the input power is wasted due to the prop drag and mechanical friction. A propeller is essentially a type of lifting surface (such as a wing) that transforms

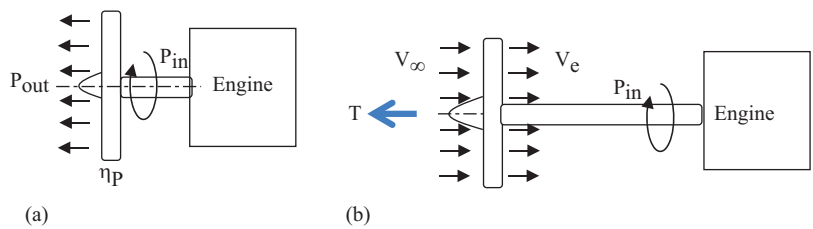

FIGURE 4.7 Propeller efficiency and engine thrust. (a) Propeller efficiency; (b) thrust and propeller.

energy by converting mechanical energy (i.e., rotational motion) into an aerodynamic force (or lift) through the air. The direction of the forward component of this aerodynamic force is forward; we rename it as *thrust*. The mechanism of generating thrust through a propeller is presented in Section 4.8.

Power is defined as force that produces a motion multiplied by the speed of the motion. In an aircraft, the required power for a steady-state motion is equal to the engine thrust multiplied by aircraft speed (TV). Hence, the ratio of the output thrust multiplied by aircraft forward speed to the shaft (i.e., input) power of the propeller is the propeller's efficiency (η_P).

$$\eta_P = \frac{TV}{P_{\text{in}}} \tag{4.2}$$

where P_{in} represents engine power, T is the output thrust, and V is the aircraft airspeed. Please note that this equation cannot be used for a non-airborne flight operation, such as takeoff.

A well-designed propeller typically has an efficiency of around 80% when operating in the best flight condition (e.g., cruise). Changes to a propeller's efficiency are produced by a number of factors, mainly adjustments to the helix angle (θ), the angle between the resultant relative velocity and the blade rotation direction, and to blade pitch. The best output is created provided that the prop angle of attack at all stations is close to its optimum value. Table 4.1 shows power and other features of several piston engines.

Figure 4.8 shows a typical propeller's efficiency versus aircraft speed. The reason for the efficiency falling after the Mach number around 0.5 is the tip shock wave. As the aircraft Mach number increases, the Mach number at the tip of the propeller approaches 1. At Mach number higher than 1, a series of shock waves are generated at the tip of the propeller. The generation of shock waves means the production of wave drag that results in a reduction of propeller's thrust. The condition for reaching Mach 1 depends on the propeller diameter and its rotational speed. In general, when the aircraft forward speed is passing Mach 0.6, the flow at the tip of the propeller is close to becoming supersonic.

Example 4.1

A GA airplane is traveling at sea level with a speed of 180 knots. The piston engine of this aircraft is producing 200 hp, while the propeller delivers 270 lb of thrust. Determine the efficiency of the propeller in this flight condition.

Solution

One horsepower is equivalent to 550 lb ft/s, and 1 knot is equivalent to 1.688 ft/s. Thus

$$\eta_P = \frac{TV}{P_{\text{in}}} = \frac{270 \times (180 \times 1.688)}{200 \times 550} = 0.746 \tag{4.2}$$

Therefore, the propeller's efficiency is 74.6%.

TABLE 4.1
Characteristics of Several Piston Engines

No.	Code	Manufacturer	Country	Power (hp)	SFC (lb/hp/h)	rpm	Mass (kg)	No. of Cylinder	Type	Length	Width	Height
1.	1.7–50	Dragon	USA	50	0.55	2,500	35.4	6	Radial	0.438	0.526	0.5
2.	Wale 342	NGL	Britain	25	0.8	7,000	8.5	2	Opposed	0.237	0.39	—
3.	Saturn 500	Jakowski	Poland	25	0.7	4,000	27	2	Opposed	0.43	0.515	—
4.	PZL A52-62R	WSK-PZLKALISZ	Poland	1,000	0.661	2,200	579	9	Radial	1.13	—	1.375
5.	GT250	Arrow	Italy	34	0.88	6,800	26	1	—	0.46	0.37	0.38
6.	M 137 A	Avia	Czech Republic	180	0.54	2,750	141.5	6	In-line	1.334	0.443	0.63
7.	O-235-C	AVCO Lycoming	USA	115	—	2,800	97.5	4	Opposed	0.751	0.812	0.569
8.	IO-360-C	AVCO Lycoming	USA	200	—	2,700	134	4	Opposed	0.855	0.87	0.495
9.	VO-540-C	AVCO Lycoming	USA	305	—	3,200	200	6	Opposed	0.882	0.88	0.649
10.	TIO-540-C	AVCO Lycoming	USA	250	—	2,575	205	6	Opposed	1.026	0.848	0.77
11.	IO-720-D	AVCO Lycoming	USA	400	—	2,650	259	8	Opposed	1.189	0.87	0.562
12.	IO-520-CB	Continental	USA	285	—	2,700	205	6	Opposed	1.087	0.852	0.502
13.	TSIO-520-E	Continental	USA	300	—	2,700	219	6	Opposed	1.01	0.852	0.527
14.	LTSIO-520-AE	Continental	USA	250	—	2,400	172	6	Opposed	0.967	0.846	0.543
15.	Voyager 550	Continental	USA	350	—	2,700	229	6	Opposed	—	—	—
16.	L-550	Limbach	Germany	45	—		15.5	4	Opposed	Capacity: 548 cc; bore: 66 mm		
17.	IO-520-F	TCM	USA	285	—	—	187	6	Opposed	Capacity: 8,500 cc; bore: 133 mm		
18.	447 UL-1V	Rotax	Austria	39.6	—	—	26.8	2	In-line	Capacity: 436.5 cc; bore: 67.5 mm		

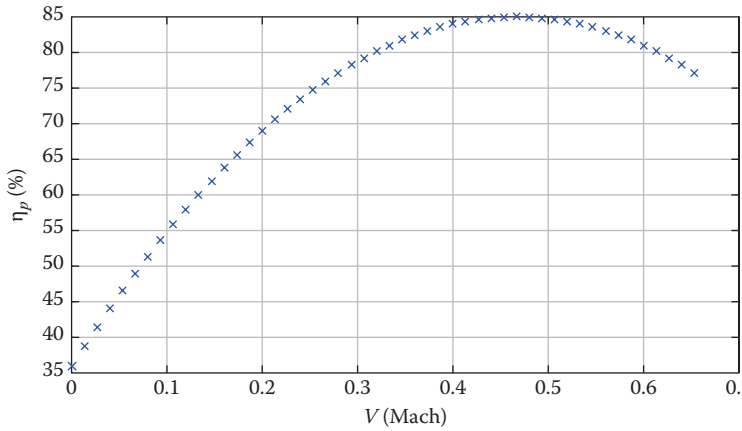

FIGURE 4.8 A typical variation of propeller's efficiency versus aircraft airspeed.

4.3.3 Supercharged Piston Engines

As an aircraft climbs, the air density and air pressure decrease. For instance, at 18,000 ft, air is at half the pressure of sea level. Therefore, the available air for the combustion in an engine is decreased at altitude. Thus, the engine does not have sufficient air to consume and produce power. Therefore, the available power at altitude is reduced and consequently the aircraft's performance is degraded.

The performance of a piston engine at high altitude may be improved by a process called supercharging. This involves compressing air before entering the manifold by means of a compressor (e.g., gas turbine). A *super-charger* is primarily an air compressor [5] used to force more air into the cylinder of a piston engine that can be achieved at ambient atmospheric pressure. The additional mass of air that is forced into the engine improves its efficiency, which allows it to burn more fuel, which results in the production of more power.

A supercharger (i.e., compressor) can be driven mechanically by belt, gear train and shaft, or chain-drive from the piston engine's crankshaft. It can also be powered by a gas turbine that is rotated by the exhaust gases from the piston engine. A turbine-driven supercharger is referred to as a turbo-supercharger or more commonly as *turbocharger*. Manifold pressure is normally the static pressure in the inlet of the engine. Without a super/turbocharger, the maximum manifold pressure is the ambient pressure around the aircraft, with a slight loss due to the throttle plate.

In a piston engine, the more air you can add into the engine, the more fuel is burned, so the more power it produces. Engines are rated to produce power at a certain rpm and pressure. When the added air (due to supercharger) is coming into the manifold, the manifold pressure will be above ambient pressure, and even above the standard sea level (usually 101,325 kPa or 29.9 in. mercury). For instance, a supercharged piston engine may run at 40 in. mercury at takeoff, and 35 in. mercury in cruise at 25,000 ft. This engine is producing more power than a normally aspirated engine would.

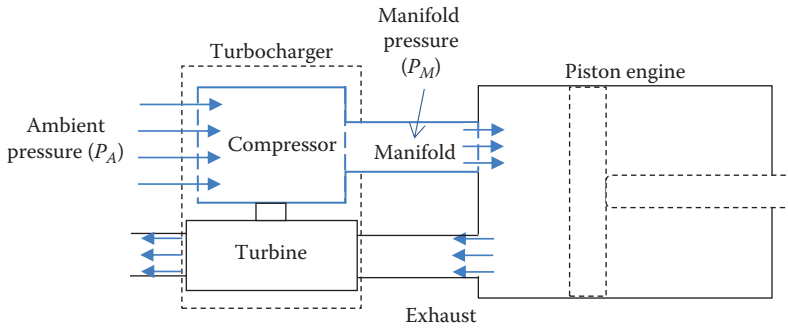

FIGURE 4.9 Pressure in turbocharger and piston engine ($P_M \gg P_A$).

A supercharger requires some energy to be extracted from the engine. For instance, on the supercharged Rolls-Royce Merlin engine, the supercharger uses up to about 150 hp. However, the benefits outweigh the costs. The engine delivers 1,000 hp when it would otherwise deliver 750 hp, an increase of 250 hp.

An engine equipped with a supercharger is generally limited by the intake pressure, so the pilot cannot operate at full throttle at sea level. As the pilot climbs to altitude, the throttle is opened progressively, holding a constant manifold pressure. The engine power will increase slightly until an altitude at which the throttle is wide open is reached. Above this altitude, known as the *critical altitude*, the power decreases linearly with density ratio in the same relative way as a non-supercharged engine.

Most currently operating supercharged piston engines utilize a turbine-driven compressor powered by the engine's exhaust (Figure 4.9). This configuration is referred to as an exhaust *turbo-supercharger.* The small number of modern piston engines designed to run at high altitudes generally use a turbocharger rather than a supercharger. The advantage of this type of supercharger as compared to the shaft-driven type is twofold. First, the compressor does not extract power from the engine but uses hot air energy that would normally be wasted. Second, the turbo-supercharger is able to maintain sea-level-rated power up to much higher altitudes than the shaft-driven supercharger.

Figure 4.10 compares the performance of a piston engine with and without a supercharger. Figure 4.10b presents a typical full-throttle performance chart for a supercharged piston engine. In contrast, Figure 4.10a demonstrates the variations of a shaft power as a function of altitude and shaft rotational speed for hypothetical piston engine. This engine provides 165 hp at sea level when the shaft is spinning at 2,700 rpm.

Thus, a supercharger/turbocharger is a device that helps the engine to hold its power constant up to a specific altitude (see Figure 4.10b). Today, most GA aircraft are naturally aspirated (i.e., have no supercharger).

Figure 4.11 demonstrates the variations of power [47] with altitude for two Lycoming piston engines. The Lycoming IO-360 engine is a regular engine, while the TO-360 is a turbocharged one. The power lapse rate for these two piston engines is not the same; the slope of TO-360 is higher than the lapse rate of IO-360. This

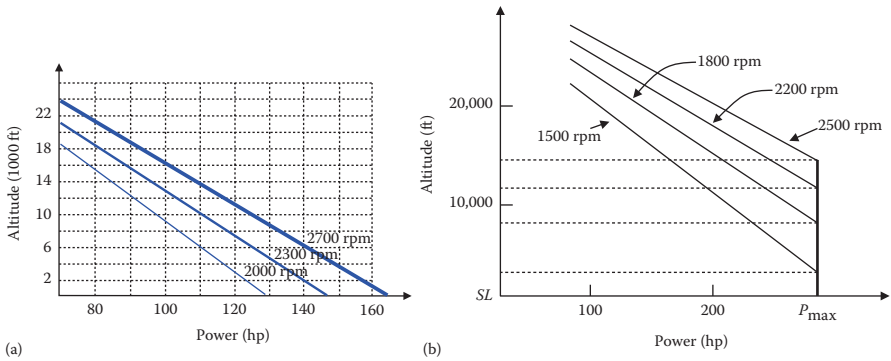

FIGURE 4.10 Performance of a piston engine with and without supercharger. (a) Engine without supercharger, and (b) engine with a supercharger.

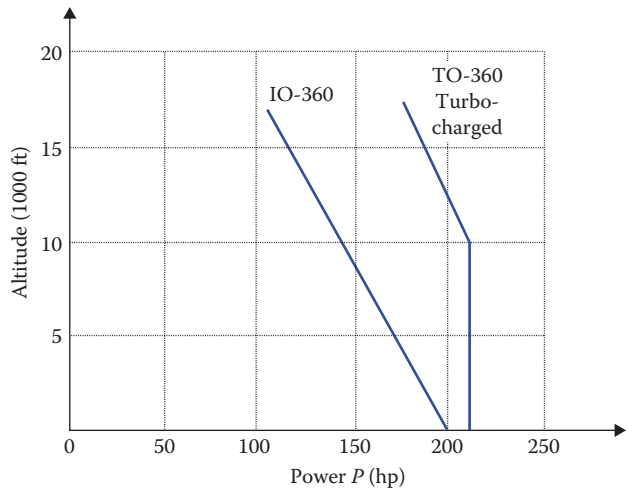

FIGURE 4.11 Variations of power with altitude for **two** piston engines.

engine family Lycoming IO-360 has been employed by thousands of aircraft, including the Cessna 172 (Figure 3.17), Piper Cherokee, and many homebuilt craft.

In general, superchargers maintain three advantages over turbochargers: (1) smaller size, (2) requires less piping, and (3) does not require high-temperature materials in the turbine.

4.4 TURBINE ENGINE

A group of aero-engines such as turbojet, turbofan, and turboprop engines are classified as gas turbine engines or simply turbine engines in which a turbine is used instead of the piston-cylinder to produce shaft power. The science of jet propulsion is

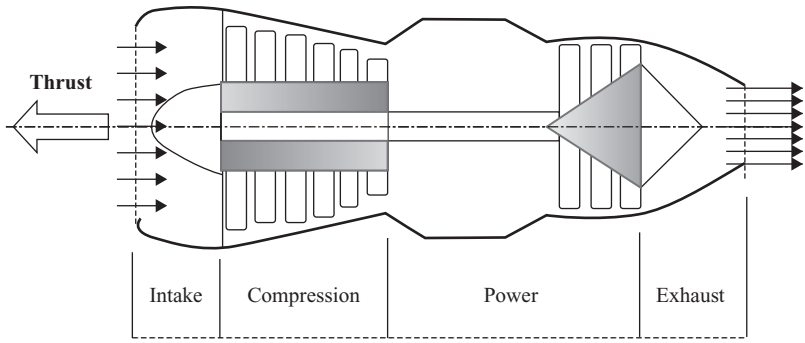

FIGURE 4.12 Schematic diagram of a turbine engine with four stages.

based on Newton's third law: to every action, there is an equal and opposite reaction. The aircraft engine pushes the gas backward, and the gas pushes back on the engine wall, creating thrust.

During World War II, the demand for increased speed and thrust expedited the progress that was already taking place in the development of propulsion systems. As a result, researchers simultaneously in Germany (Von Ohain) and England (Frank Whittle) designed, manufactured, and tested the first turbine engine in 1939. The first flight by an airplane powered with an operational jet engine was made in Germany on August 27, 1939. The aircraft was Heinkel He-178 and was powered by a Heinkel He.S3B turbojet engine.

The thermodynamic process in which thrust is produced in a jet engine is very similar to that of a piston engine. The power production in a turbine engine (see Figure 4.12) is very similar to that in a piston engine with mainly four stages: (1) intake, (2) compression, (3) power, and (4) exhaust.

The free-stream air is taken in through an inlet, compressed in a rotating compressor, heated in a combustion chamber, and expanded through a turbine. The gas then leaves through a nozzle at a velocity much greater than the free stream. The reaction to the ejection of this mass of gas is a forward force on the engine and aircraft: thrust.

Various types of turbine engines have been developed to meet the overall propulsion needs of the aviation community. The gas turbine engine can be used in several configurations: turbojet engine, turbofan engine, turboprop engine, and turboshaft engine. The turbofan and turbojet engines are grouped in a subclass of turbine engines, which is referred to as the jet engines, where they produce thrust directly. A jet engine is an aero-mechanical device that produces forward thrust by forcing the movement of a mass of gases rearward. Small gas turbine engines called auxiliary power unit (APU) have also been developed to supply transport aircraft with electric power.

The amount of force or thrust produced depends on the amount of mass of air moved through the engine per unit time (i.e., mass flow rate) and the extent to which this air can be accelerated. A small percentage of this power output of the turbine is utilized to drive the turbine/compressor and any mechanical load, such as electrical generators and hydraulic pumps, connected to the drive shaft.

4.4.1 Turbojet Engine

The basic type of a turbine engine is the turbojet engine. A pure gas turbine engine that mainly generates thrust through its nozzle is called a turbojet engine. The available energy in the exhaust gases is converted to the kinetic energy of the jet through its nozzle (i.e., thrust). In a turbojet engine, the energy that is added to air by a compressor (high pressure) and by a combustion chamber (high temperature) is divided into two parts. One part returns to the compressor and the other one goes to the nozzle.

The energy that is supposed to be transferred into the compressor is first absorbed by the turbine and converted into mechanical energy. Thus, all the mechanical energy that is produced by the turbine is transferred into the compressor through a shaft to increase the incoming air pressure. The remaining energy of the high-temperature, high-pressure air is transferred into the nozzle.

In an ideal case, part of the incoming air compression occurs in the inlet diffuser, prior to the compressor, which greatly slows the air velocity. The total or stagnation temperature and pressure is a representative of the static values. As the flight Mach number increases, the inlet total temperature rises. Then the air temperature after passing through the compressor is also increased. The basic components of a turbojet engine are illustrated in Figure 4.13.

In a turbojet engine, based on Newton's second and third laws, the summation of all forces including thrust (T) and pressure force (F_P) is equal to the rate of change of linear momentum (mV):

$$\sum F = \frac{d}{dt}(mV) \Rightarrow T + F_P = \dot{m}\ V + m\dot{V} \tag{4.3}$$

After a few algebraic steps, the output thrust of a turbojet engine is given [48] by

$$T = \dot{m}(V_e - V_i) + A_e(P_e - P_a) \tag{4.4}$$

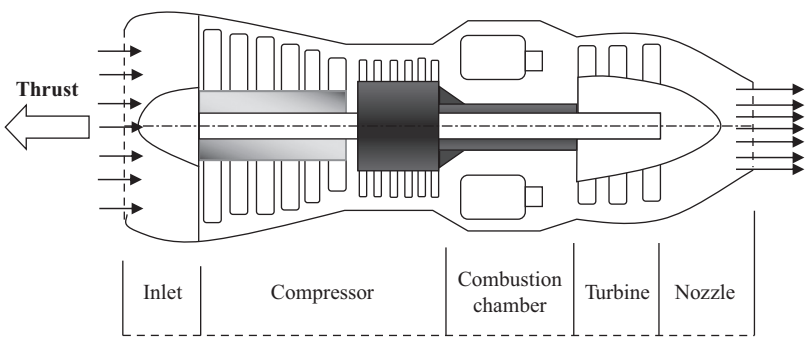

FIGURE 4.13 Schematic diagram of a turbojet engine.

FIGURE 4.14 Lockheed U-2 Dragon Lady reconnaissance aircraft with a turbojet engine.

where $\dot{m}$ represents the air mass[1] flow rate into the engine, V_e is the gas exit velocity from the engine, V_i is the velocity of the incoming air to the engine, A_e is the cross-sectional area of the engine nozzle, P_e is the static pressure of the gas exiting the nozzle, and P_a is the ambient pressure that the aircraft is flying. The incoming air to the engine may have any speed and depends on the aircraft airspeed, but, under ideal conditions, this speed is close to the aircraft airspeed.

Few military airplanes such as U-2 and few civil transport aircraft such as Concorde have turbojet engines. The General Electric J79 is an axial-flow turbojet engine built for use in several fighter and bomber aircraft. The first flight of the engine was in 1955 where the engine was placed in the bomb bay of a North American B-45 Tornado. The first series of F-4 fighters also had a J79 turbojet engine. The F-4 cruises at Mach 1.8 at 55,000 ft altitude. The aircraft's two turbojet engines produce a thrust of 51.4 kN at its cruise speed of 1,030 knots. Figure 4.14 shows the Lockheed U-2 Dragon Lady single-jet engine, ultrahigh-altitude reconnaissance spy-plane that has a J57-P-37A P&W turbojet engine with a thrust of 75.6 kN. This spy-plane, despite being hard-to-maneuver [49], still flies plenty of missions because the alternatives are not great.

Nowadays, the application of a turbojet engine is very limited to a few military aircraft. Some military jet fighters are equipped with an afterburner. An addition to a turbojet (also for a turbofan) engine is the second combustion chamber [50] called *afterburner*[2] (with a process of re-heating) placed after the turbine and before the nozzle. Its purpose is to provide a temporary increase in thrust mainly by increasing the temperature of the gas.

On military aircraft, the extra thrust is also useful for combat operations. This is achieved by injecting additional fuel into the duct downstream of (i.e., *after*) the turbine. This fuel is burned by the hot exhaust gases and adds greatly to the thrust of the engine. The advantage of afterburning (or re-heating) is significantly increased thrust; the disadvantage of afterburning is its very high fuel consumption. But this is acceptable for a short period of time in which afterburning is usually used. Jet

[1] Here, we ignored the fuel flow rate, which is about 2% of air flow rate.
[2] In the British literature, afterburning is called reheat.

engines are referred to as operating *wet* when afterburning is being used and *dry* when the engine is used without afterburning.

The GE J79 was replaced in the late 1960s in new fighter designs by afterburning turbofans such as the Pratt & Whitney TF30 used in the F-111 and F-14, and newer-generation turbofans such as the P&W F100 used in the F-15 Eagle [51], which offer better specific fuel consumption (SFC).

Example 4.2

A fighter jet aircraft is cruising at 30,000 ft altitude with a speed of Mach 2.5. The turbojet engine of this aircraft is consuming 300 kg of air per second. The engine exit flow has a pressure of 53,260 Pa with a velocity of 920 m/s. The exit area of the engine nozzle is 1.2 m^2. Assume that the aircraft is flying in ISA condition. How much thrust is this jet engine generating?

Solution

The 30,000 ft altitude is equivalent to 9,144 m. From Appendix A, at this altitude, the ambient pressure is 30,144 N/m^2 and the speed of sound is 303 m/s.

$$M = \frac{V}{a} \Rightarrow V_i = Ma = 2.5 \times 303 = 757.4 \text{ m/s} \tag{1.34}$$

$$T = \dot{m}\left(V_e - V_i\right) + A_e\left(P_e - P_a\right) \tag{4.4}$$

$$\Rightarrow T = 300 \times \left(920 - 757.4\right) + 1.2 \times \left(53{,}260 - 30{,}144\right) = 76{,}519.2\,\text{N} = 76.5\,\text{kN}$$

4.4.2 Turbofan Engine

Two main problems with a turbojet engine are high SFC and low efficiency. In principle, there are two ways to improve the efficiency of a turbojet engine: (1) adding a propeller (i.e., turboprop) and (2) adding a ducted fan, or a series of fans in front of the compressor with its own exit (i.e., turbofan). Both techniques will impact the efficiency as well as the engine thrust. A trade-off between thrust and efficiency will lead to a final solution. Generally, a propeller produces less thrust but with more efficiency, whereas a fan produces more thrust but with less efficiency. The turbofan engine is a propulsive mechanism that combines the high thrust of a turbojet with the high efficiency of a turbo-propeller. A schematic of a turbofan engine is shown in Figure 4.15.

A turbofan engine is a gas turbine engine in which the turbine extracts gas power in excess of that required to drive a fan or low-pressure compressor in a fan (auxiliary) duct, usually annular around the primary duct (core). The turbofan engine imparts momentum to greater volume of air than a turbojet, but the velocity added is less.

A turbojet engine forms the core of the turbofan; the core contains the inlet, compressor, burner, turbine, and nozzle. However, in the turbofan engine, the turbine

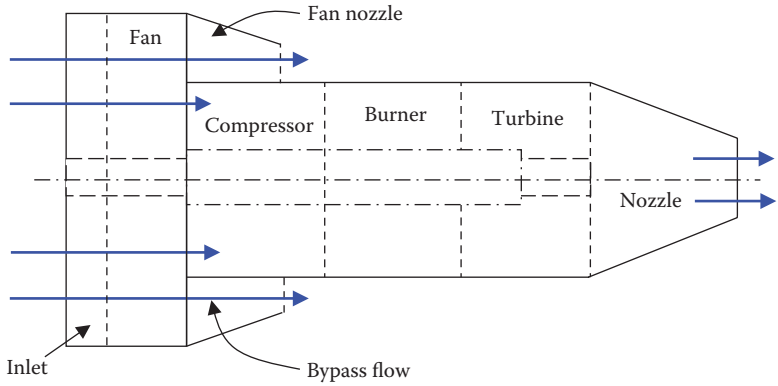

FIGURE 4.15 Schematic diagram of a low-BPR turbofan engine.

drives not only the compressor but also a large fan external to the core. The fan itself is contained in a shroud that is wrapped around the core. The fan is basically a small propeller. Thus, a turbofan engine is a modified version of a turbojet engine to improve a few performance characteristics. In addition, the noise of a turbofan engine is much lower than that of a turboprop engine. The basic principles of the fan and propeller are introduced in Section 4.7. The fan, similar to a propeller, is a producer of thrust through the rotation of fan blades.

The flow through a turbofan engine is split into two paths. One airflow passes through the fan and flows externally over the core; this air is processed only by the fan. The thrust obtained from this flow through the fan is generated with an efficiency similar to that of a propeller. The second airflow passes through the core itself. The thrust obtained from the flow through the core is generated with an efficiency associated with a turbojet. The overall propulsive efficiency of a turbofan engine is therefore a compromise between that of a propeller and that of a turbojet. A vast majority of jet airplanes today are powered by turbofan engines.

An important parameter of a turbofan engine is the bypass ratio (BPR). The BPR is defined as the ratio of the air mass flow passing through the fan to the air mass flow passing through the core. Everything else being equal, the higher the BPR, the higher the propulsive efficiency. A BPR < 1 is referred to as a low BPR, while a BPR higher than 1 is referred to as a high BPR.

Low-BPR turbofan engines are used on many high-performance jet fighter aircraft, such as the McDonnell Douglas F-15. High-BPR turbofan engines are used on many large transport aircraft, such as the Boeing 777 (Figure 7.18). For example, for the large turbofan engines that power large transport airplanes such as the Boeing 747 (Figure 8.10b), the Rolls-Royce RB211, and the Pratt and Whitney JT9D; the bypass BPRs are on the order of 5.

During recent decades, the high-bypass turbofan engine has become one of the major sources of thrust for large transport aircraft. Among such engines are the Pratt and Whitney JT9D, the General Electric CFG, and the Rolls-Royce RB 211. These engines are used, respectively, in Boeing 747 (Figure 8.10b), Douglas DC-9, and

TABLE 4.2
Comparison between Two Similar Jet Engines

No.	Parameter	TFE731 Turbofan Engine	Rolls-Royce Viper Turbojet Engine
1.	Thrust	16.8 kN	16.7 kN
2.	Mass	334 kg	356 kg
3.	Specific mass	0.199 lb/lb, 0.05 kN/kg	0.21 lb/lb, 0.053 kN/kg
4.	Width	869 cm	—
5.	Height	100.8 cm	—
6.	Diameter	—	62.5 cm
7.	Length	126.3 cm	164.1 cm
8.	Specific fuel consumption	0.818 lb/h/lb (20.8 mg/Ns)	0.94 lb/h/lb (25.2 mg/Ns)
9.	Bypass ratio	2.8	–
10.	Gearing ratio	0.555	—

Lockheed L-l0ll aircraft. Typical values of the SFC[3] for these turbofan engines are 0.6 lb/lb/h, much lower than that of a turbojet engine.

To derive an equation that governs the thrust of a turbofan engine, we revise Equation 4.4. By doing so, the thrust of an *ideal*[4] turbofan engine [52] is given by

$$T = \dot{m}_C \left(V_{eC} - V\right) + \dot{m}_F \left(V_{eF} - V\right) \tag{4.5}$$

where $\dot{m}_C$ represents the core airflow rate, V_{eC} is the exit velocity of the core gas flow, $\dot{m}_F$ is the fan airflow rate, V_{eF} is exit velocity of the fan airflow, and the parameter V denotes the aircraft airspeed. In deriving Equation 4.5, it is assumed that the exit (fan and core) pressure is equal to the ambient pressure.

The low-BPR Allison turbofan engine AE 3007A generates a thrust of 31.3 kN. The Allison turbofan engine AE 3007A has been installed in many military aircraft such as Northrop Grumman RQ-4A unmanned aircraft Global Hawk (Figure 5.21). The F110 is an afterburning turbofan engine produced by General Electric. The F110 is part of a family of engines that includes fighter and bomber engines.

Engines in this family—also the F101, F108, and F118 engines—power the fighter aircraft Grumman F-14 Tomcat, McDonnell Douglas F-15 Eagle, General Dynamics F-16 Fighting Falcon (Figure 7.6), and bomber aircraft B-1 and B-2. Figure 1.8b illustrates the civil transport aircraft Airbus 340 that has two turbofan engines. Table 4.2 compares geometries and performance characteristics of two similar jet engines, one turbofan engine and one turbojet engine. Figure 4.16 illustrates the Honeywell Aerospace Lycoming ALF 502 turbofan engine, which powers the British Aerospace 146.

[3] Specific fuel consumption will be defined later in this chapter.
[4] Ideal condition is when the flow pressure at the exit is equal to the ambient pressure.

FIGURE 4.16 Honeywell Aerospace Lycoming ALF 502 turbofan engine.

4.4.3 Turboprop Engine

The turboprop engine is essentially propeller-driven by a gas turbine engine, in which the turbine absorbs power in excess of that needed to drive the compressor. The excess power is used to drive a propeller. Although most of the energy in the hot gases is absorbed by the turbine, the turboprop engine still has slight jet thrust generated by the exhaust gas in its nozzle. Thus, most of the gas energy is extracted by the turbine to drive the propeller.

A schematic of a turboprop engine is shown in Figure 4.17. Similar to the turbojet, the inlet air is compressed by an axial-flow compressor, mixed with fuel and burned in the combustor, expanded through a turbine, and then exhausted through a nozzle.

In a twin-spool arrangement, the compressor is divided into two stages: low-pressure and high-pressure, where each stage is driven by a separate turbine; the low-pressure turbine and high-pressure turbine. The high-pressure turbine drives the high-pressure compressor. But, the low-pressure turbine drives both the low-pressure compressor and the propeller. Most of the available energy in the gas flow is extracted by the turbine, leaving little available for exit nozzle thrust. For most turboprop engines, only about 10% of the total thrust is associated with the jet exhaust, and the remaining 90% comes from the propeller.

With regard to the thrust and efficiency trade-off, the turboprop falls in between the piston-prop engine and the turbofan engine. The turboprop engine generates more thrust than a reciprocating piston-prop engine, but less than a turbofan or turbojet. On the other hand, the turboprop engine has a higher SFC than the reciprocating piston-prop engine but lower SFC than a turbofan or turbojet.

A major problem with the turboprop engine is the very loud noise, which makes it undesirable for carrying passengers. In addition, the maximum flight speed of a turboprop-powered aircraft is limited to that at which the propeller efficiency becomes seriously degraded by shock wave formation on the propeller tip, usually around Mach 0.6.

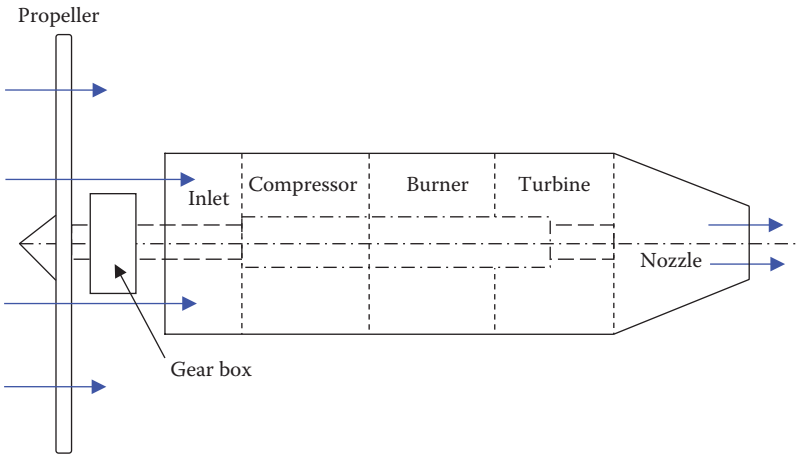

FIGURE 4.17 Schematic diagram of a typical turboprop engine.

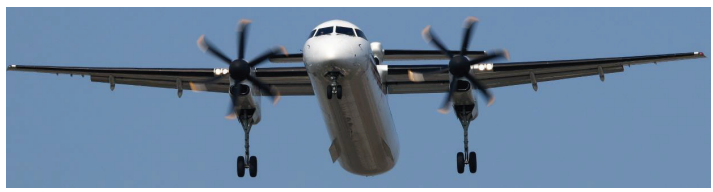

FIGURE 4.18 Transport aircraft Bombardier DHC-8 Q400 with two turboprop engines. (Courtesy of Fabian Dirscherl.)

The Allison AE2100 D3 turboprop engine is employed in a variety of aircraft, including the military transport aircraft Lockheed Hercules C-130 (Figure 8.3). The aircraft is equipped with four turboprop engines and can cruise at a speed of 348 knots with a maximum takeoff mass of 70,305 kg. As a comparison, each turboprop engine Allison AE2100 D3 of a Lockheed Martin C-130 Hercules (Figure 8.3) is rated at 4,591 hp, while the piston engine of a Cessna 172 (Figure 3.17) generates 180 hp.

Aircraft powered by turboprop engines have usually an optimum speed below about 380 knots (195 m/s). Figure 4.18 demonstrates a transport aircraft Bombardier DHC-8 Q400 with two turboprop Pratt & Whitney Canada PW100 engines. The aircraft has a maximum takeoff mass of 29,260 kg, and each engine generates a power of 3,782 kW. Each propeller has six blades, and the cruising speed is 360 knots.

In the past decades, a number of research institutions and companies have tried to combine positive aspects of turbofan engine and turboprop engine and invented a new kind of engine, called *turbo-prop-fan* or simply *propfan* engine. This engine has a unique prop that has a smaller diameter as compared with regular turboprop engine and a larger chord as compared with a turbofan engine. The propfan also is named as an unducted fan or an ultrahigh bypass fan and is gearless. The propfan

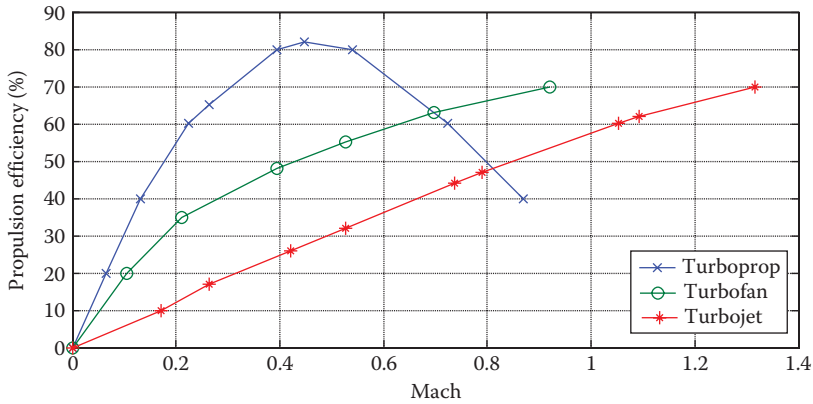

FIGURE 4.19 Typical propulsion efficiencies.

possesses a carefully designed airfoil to reduce the prop noise and increase the propulsive efficiency. Propfans are also known as ultrahigh bypass (UHB) engines and, most recently, open rotor jet engines.

The propfan concept was first introduced by Carl Rohrbach and Bruce Metzger of United Technologies [53] in 1975. So far, the propfan has been installed in only a few transport aircraft (e.g., Antonov An-70 and McDonnell Douglas MD-80 demonstrator). Although the performance results of this engine are satisfactory, the new propfan engine is not still popular. General Electric GE36 and Allison-Pratt and Whitney 578-DX are two engines that employed a propfan. The GE36 had an overall diameter of 11.67 ft, with either eight or ten blades in front and eight blades in back. Figure 4.19 shows typical propulsion efficiencies of various engines including the propfan engine. In general, the efficiency of the turbofan and turbojet engines are increasing with airspeed, while the efficiency of a turboprop engine has a maximum value at about M = 0.5 to 0.7.

The Antonov An-70 (Figure 4.20), a four-engine medium-range transport aircraft, is the first large aircraft powered by propfan engines. Each propfan engine, for example, Progress D27, generates a power of 10,350 kW.

4.4.4 Turboshaft Engine

A gas turbine engine that delivers power through a shaft to operate something other than a propeller is referred to as a turboshaft engine. Turboshaft engines are very similar to turboprop engines. The turbine that extracts energy from gas flow is primarily designed to produce shaft power. The turboshaft engine has the same basic components found in a turbojet engine, with the addition of a turbine shaft to absorb the power of the hot gases of combustion.

The general layout of a turboshaft is similar to that of a turboprop, the main difference being the latter produces some residual propulsion thrust to supplement that produced by the shaft-driven propeller. Another difference is that with a turboshaft

FIGURE 4.20 Antonov An-70 with four propfan engines. (Courtesy of Weimeng.)

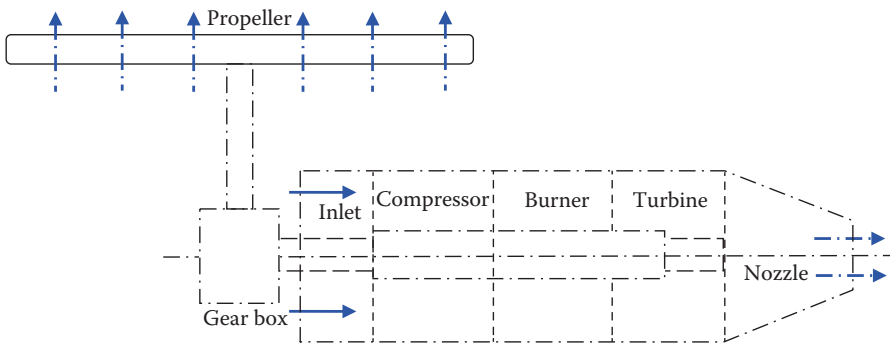

FIGURE 4.21 Schematic diagram of a turboshaft engine of a helicopter.

the main gearbox is part of the vehicle (e.g., helicopter rotor reduction gearbox), not the engine. In practice, all turboshaft engines have a free power turbine, although this is also generally true for modern turboprop engines.

Both types have been successfully employed in helicopter applications; however, the free turbine is the most popular one in use today. Another use of turboshaft engines is the APU. These small gas turbine engines are mostly used on large transport aircraft for providing auxiliary power either on the ground or in flight when needed. They are designed to provide the aircraft with electrical energy or pneumatic power, making the aircraft more independent of ground support equipment. Figure 4.21 shows a schematic diagram of a turboshaft engine that drives a helicopter blade. Figure 4.22 illustrates a Sikorsky HH-60M Black Hawk with a maximum takeoff mass of 10,660 kg and two General Electric T700-GE-710C turboshaft engines, each generating 1,410 kW.

FIGURE 4.22 A Sikorsky HH-60M Black Hawk with a turboshaft engine. (Courtesy of Daniel Mysak.)

4.4.5 Ramjet Engine

In high supersonic speeds (Mach numbers beyond 3), a new type of jet engine, ramjet, is more efficient than turbojet and turbofan engines. The ramjet engine has a simple structure and has no moving part (no turbine). A ramjet is basically a duct with the front end shaped to be the inlet, the aft end designed as a nozzle, and the combustion chamber in the middle. This type of engine is using engine's forward motion to compress incoming air. Since the high-speed flow has a high stagnation pressure, this pressure will be converted to static pressure in the inlet duct in a slow-down process. Located in the combustion chamber are flame holders, fuel injection nozzles, and an igniter.

The main drawback of the ramjet engine is that it is initially assisted to accelerate and attain a velocity in excess of about Mach 0.5 before it can be self-sufficient. Once this speed is reached, there is sufficient combustion pressure to continue firing the engine. The flame holders located in the combustion chamber provide the necessary blockage in the passage to slow down the airflow so that the fuel and air can be mixed and ignited. The combustion product is then passed through a nozzle to accelerate it to supersonic speeds. This acceleration generates forward thrust. For a supersonic flight Mach number, acceleration is typically achieved through a convergent-divergent nozzle (see Figure 4.23). It is interesting to know that, beyond Mach 3, 54% of the propulsive thrust is produced by the inlet.

Practical use of ramjets has been limited to a few missile and aircraft applications. Ramjets are also used as augmenters or afterburners on turbojet engines. In such a case, the augmenter is attached to the rear of the turbojet engine so that the jet exhaust passes through it.

An important variant of the ramjet engine is scramjet engine. As flight Mach number increases in the hypersonic region, the temperature rise due to inlet compression (through shock wave) becomes excessive. The high static temperature can cause dissociation and ionization of air within the combustor, a process that absorbs energy and reduces the temperature increase sought from the burning of the fuel. To solve this problem, the supersonic combustion ramjet, or *scramjet*, has been developed. The inlet flow is decelerated only as much as required to obtain the necessary pressure rise, reducing the static temperature increase. Thus, the flow remains supersonic passing through the combustion chamber.

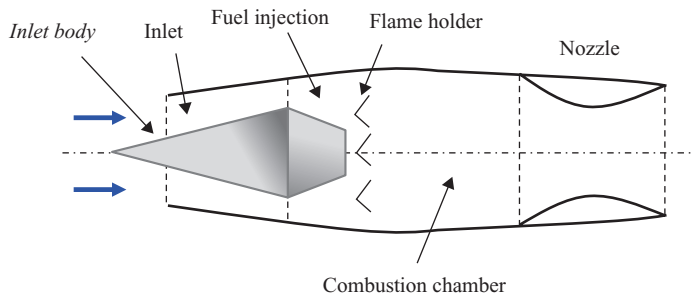

FIGURE 4.23 Schematic diagram of a ramjet engine.

FIGURE 4.24 The Lockheed SR-71 Blackbird high-altitude reconnaissance aircraft.

One of the military aircraft that employed a ramjet engine was the Lockheed SR-71 Blackbird (Figure 4.24). The SR-71 was an advanced, long-range, Mach 3 strategic reconnaissance aircraft developed by the Lockheed. The SR-71 aircraft was in service from 1964 and retired in 1998.

The Pratt and Whitney J58-P4- a single-spool turbojet engine – used in the Blackbird were the only military engines ever designed to operate continuously on an afterburner. The J58 engine – generates a static thrust of 145 kN – was unique in that it was a hybrid jet engine. It could operate as a regular turbojet at low speeds, but at high speeds, it became a ramjet. The engine can be considered as a turbojet engine inside a ramjet engine. At lower airspeeds, the turbojet provides most of the compression and most of the energy from fuel combustion. At higher airspeeds, the turbojet is inactive and just sat in the middle of the engine.

4.5 OTHER ENGINES

Other than piston engines and turbine engines, there are a number of engines that produce thrust or power: (1) rocket engines, (2) solar-powered engines, (3) electric engines, and (4) human-powered engines. In this section, these engines are briefly described.

4.5.1 Rocket Engine

When the free ambient air is not available to combust with fuel in the engine burner, another propulsive device is employed that does not breathe air; rocket engine. A rocket engine is a reaction engine that can be used for aircraft and spacecraft propulsion as well as terrestrial uses, such as missiles. Rocket engines take all their reaction mass from internal tanks and form it into a high-speed gas, producing thrust. Therefore, a rocket engine is a self-contained jet engine that carries both the fuel and the oxidizer (e.g., oxygen). The relative simplicity and manufacturing cost of a rocket engine as compared with an air-breathing engine have made rockets the popular choice for space vehicle application and space propulsion.

Thrust is typically created by high combustion pressure (2–200 bar), high-temperature (1,000–4,700 K) combustion of solid or liquid propellants, consisting of fuel and oxidizer components, within a combustion chamber. The rocket fuel could be of liquid or solid type.

The liquid-fuel rocket (Figure 4.25) typically pumps separate fuel and oxidizer components into the combustion chamber, where they burn. Solid propellants are prepared as a mixture of fuel and oxidizing components, and the propellant storage chamber becomes the combustion chamber. Hybrid rocket engines use a combination of solid and liquid or gaseous propellants.

The thrust of a rocket engine [48] is given by

$$T = \dot{m}(V_e) + A_e\left(P_e - P_a\right) \tag{4.6}$$

where $\dot{m}$ is exit gas mass flow rate (fuel plus oxidizer), V_e is gas exit velocity, A_e is the nozzle exit cross-sectional area, P_e is the exit pressure, and P_a is the ambient pressure.

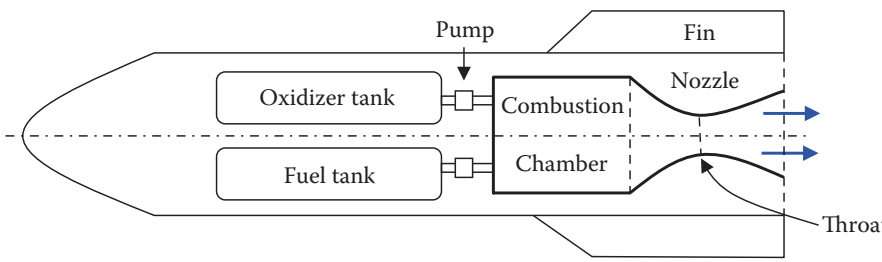

FIGURE 4.25 A flight vehicle with a liquid-fueled rocket engine.

Since ambient pressure is exponentially decreased with altitude, the rocket engine thrust is exponentially increased with altitude, reaching a constant value at higher altitudes (above 100,000 ft).

Another customary way to determine the rocket thrust is the product of the chamber pressure (P_c) and the throat area (A_{th}):

$$T = P_c A_{th} C_F \tag{4.7}$$

where C_F is known as the thrust coefficient. Using the relationship for the total temperature in an isentropic perfect expansion (i.e., the exit pressure is equal to the ambient pressure), one can derive an expression [54] for the C_F as follows:

$$C_F = \sqrt{\left(\frac{2\gamma^2}{\gamma-1}\right)\left(\frac{2}{\gamma+1}\right)^{\frac{\gamma+1}{\gamma-1}}\left[1-\left(\frac{P_2}{P_c}\right)^{\frac{\gamma-1}{\gamma}}\right]} \tag{4.8}$$

where P_2 is the exit pressure and γ is the gas ratio of specific heats. The variable γ is 1.4 for air at sea level. The typical value for the thrust coefficient is from 1.3 to 2.2.

Example 4.3

A rocket engine has a chamber pressure of 220 atm and the throat area is 0.2 m^2. Assuming that the nozzle is perfectly expanded with a gas ratio of specific heat of 1.3 and the ambient pressure is 1 atm, calculate the engine thrust.

Solution

We first determine the thrust coefficient:

$$C_F = \sqrt{\left(\frac{2\gamma^2}{\gamma-1}\right)\left(\frac{2}{\gamma+1}\right)^{\frac{\gamma+1}{\gamma-1}}\left[1-\left(\frac{P_2}{P_c}\right)^{\frac{\gamma-1}{\gamma}}\right]}$$

$$= \sqrt{\left(\frac{2(1.3)^2}{1.3-1}\right)\left(\frac{2}{1.3+1}\right)^{\frac{1.3+1}{1.3-1}}\left[1-\left(\frac{1}{220}\right)^{\frac{1.3-1}{1.3}}\right]} \tag{4.8}$$

$$\Rightarrow C_F = 1.949$$

Then, the rocket engine thrust is (Figure 4.26)

$$T = P_c A_{th} C_F = 220 \times (101{,}325) \times 0.2 \times 1.949 = 8{,}687{,}488\,\text{N} = 8{,}687.5\,\text{kN} \tag{4.7}$$

FIGURE 4.26 Space Shuttle Atlantis on the launch pad prior to the STS-115 mission.

Example 4.4

A spacecraft with a liquid-fuel rocket engine is operating at 200 km above the sea level. The engine is exerting 950 kg of hot gas per second from its exit nozzle. The gas has an exit pressure of 30 kPa and exit velocity is 2,458 m/s. The exit area of the nozzle is 0.8 m^2. Determine the net thrust produced by this rocket engine.

Solution

The 200 km altitude is referred to as space, so the ambient pressure is assumed as zero ($P_a = 0$). Thus, the rocket engine thrust is

$$T = \dot{m}(V_e) + A_e(P_e - P_a) = 950 \times 2{,}458 + 0.8 \times 30{,}000 = 2{,}359{,}100\,\text{N} \qquad (4.6)$$

4.5.2 Electric Engine

An electric propulsion system includes an electric motor, battery, and propeller. Therefore, in electric-powered aircraft, the powerplant is a battery-powered electric motor. Since batteries have limited power and a limited life, this type of propulsion system is not widely used in GA and transport aircraft. However, they are very popular and widely employed in model or radio-controlled (RC) small planes and quadcopters.

The main feature of the electric propulsion system is that they are most appropriate for aircraft with a mass of less than about 30 kg. The highest feasible capacity of the best Li-ion battery may provide is about 300 Wh/kg. For a battery pack with a mass of 200 kg, this is equivalent to providing about 80 hp for 1 h.

The main advantages of an electric-powered engine are its independence from fuel, and from mechanical engine, no vibration, compact size, the near-silent motor, constant center of gravity, as well as low cost. However, the main disadvantages originate from a limit in the electric energy storage that include a low cruising speed (<100 knots), a low range (<400 km), a low endurance (<1 h), a low ceiling (<15,000 ft), a very low rate of climb (<15 m/min).

The technology of electric motors and high-capacity batteries has finally reached the level of development where pure electric flight is now possible. There are a few manned aircraft with an electric engine. The ElectraFlyer ULS by Electric Aircraft Corporation with a maximum takeoff weight of 525 lb and a 20 HP electric engine has 2 h duration and a cruising velocity of 35 knots.

An electric motor converts electrical energy to mechanical energy. The operation of electric motors is based on the electromagnetic principle. In the motor, the current is passed through a loop that is immersed in a magnetic field. In addition, when electric current flows through a coil, it generates a magnetic field. When two magnets get close together the North and the South poles attract, whereas the same poles will repel each other. Thus, the magnetic field and coil currents produce force, and consequently a torque to rotate the rotor is generated. There are two main different motor types used in model aircraft: (1) brushed and (2) brushless.

From another aspect, electric motors are divided into two groups: (1) direct current (DC) motors and (2) alternating current (AC) motors. The electric motor of an aircraft with an electric propulsion system is usually of DC type.

The typical engine-power-to-airplane-mass ratio for the RC airplane is 100–200 W/kg. The typical voltage of electric engines that are employed by RC aircraft is 3–12 V. The maximum engine power is determined through the power of the battery, which provides electric energy to the engine. The electric motor is frequently operated at a much higher voltage, which is provided by a single battery. Hence, a couple of batteries are usually connected in series to add up the voltages. For instance, if an electric motor requires 60 V to operate, five batteries of 12 V can be connected in series. Moreover, as the number of batteries is increased, the maximum power that can be provided to an electric motor will be increased.

As batteries improve, all-electric aircraft are emerging in the world. The aircraft PC-Aero Electra One with one seat and a maximum mass of 300 kg has an electric engine with a lithium-polymer battery that can generate an engine power of 160 kW. This aircraft has a maximum range of 400 km and a maximum endurance of 3 h. The electric self-launching glider Lange Antares 20E uses lithium-ion batteries and a 42 kW brushless DC electric motor.

4.5.3 Solar-Powered Engine

A sun-powered (or solar-powered) aircraft employs a propeller and electric motors that are powered by solar arrays/cells/panels. A solar cell (also called a photovoltaic cell) is an electrical device that converts the energy of light (in this case, sunlight) directly into electric energy by the photovoltaic effect. A sun-powered engine is surely quieter than a piston-prop engine.

The main advantages of this propulsion system are the unlimited endurance, unlimited range, high ceiling, and independence from fuel. The major disadvantages are low speed (<30 knots), low rate of climb (<5 m/min), and dependence on sunlight. Since the sun is always available (above the clouds), the aircraft has theoretically an unlimited endurance and an unlimited range.

NASA's remotely piloted flying wing aircraft Pathfinder and Switzerland-based *Solar Impulse* are the two examples of aircraft that employ solar-powered engines. The aircraft Pathfinder with a wing span of 29.5 m had a cruising velocity of about 17 knots. The aircraft was manufactured by AeroVironment, but the project was canceled later. However, the aircraft Solar Impulse with a wingspan 63 m (longer than that of the Boeing 747; Figure 8.10b) and a cruising velocity of 44 knots is still under development and flight tests.

A successful sun-powered unmanned aircraft is the NASA Pathfinder (Figure 4.27), which was powered by eight electric motors—later reduced to six. The Pathfinder has a 98.4 ft wing span with a weight of 560 lb and is a remotely piloted flying wing aircraft that demonstrates the technology of applying solar power for long-duration and high-altitude flight. The Pathfinder flies with an airspeed of only 15–25 mph. This UAV can fly without an onboard human pilot but instead is controlled remotely

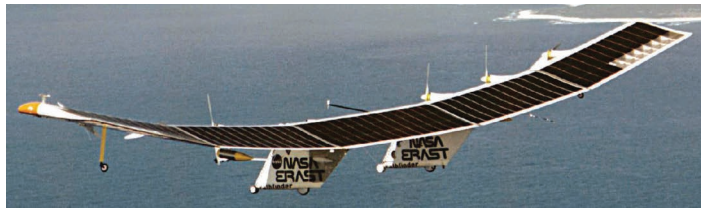

FIGURE 4.27 Pathfinder solar-powered aircraft.

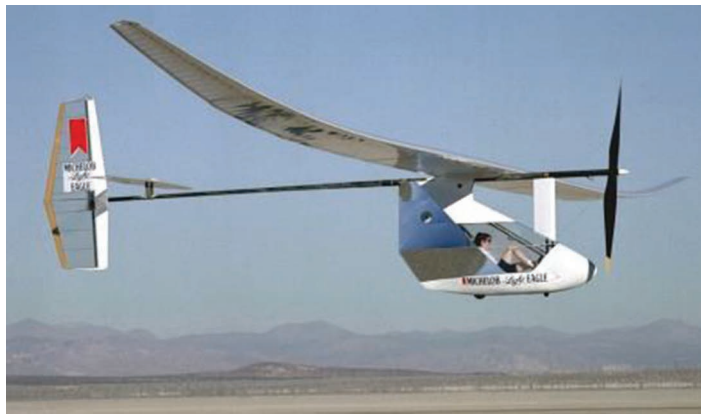

FIGURE 4.28 Light Eagle human-powered aircraft (Michelob Light Eagle).

from a ground station. However, the aircraft structure broke at high altitude and crashed into the ocean due to structural problems in 1997.

4.5.4 Human-Powered Engine

A human-powered aircraft employs the physical power of a human (pilot) to generate thrust through a propeller. Hence, the human is assumed as part of the propulsion system. The pilot will first turn a shaft through his/her hand/leg, and then a propeller converts the shaft rotational motion into thrust. The first successful human-powered aircraft was Gossamer Albatross in 1979. The aircraft was powered using pedals to drive a large two-bladed propeller and completed the 35.8 km crossing in 2 h and 49 min, achieving a top speed of 29 km/h and an average altitude of 1.5 m. Afterward, several successful human-powered aircraft were designed and flown.

The average "in shape" cyclist can produce about 3 W/kg per an hour (e.g., around 200 W for a 70 kg rider). The first successful human-powered aircraft was Gossamer Albatross built by Paul McCready. On June 12, 1979, it completed a successful crossing of the English Channel to win the second Kremer prize. The aircraft was powered using pedals to drive a large two-bladed propeller. Piloted by amateur cyclist

Bryan Allen, it completed the 35.8 km crossing in 2 h and 49 min, achieving a top speed of 29 km/h and an average altitude of 1.5 m.

Two other successful human-powered aircraft are the Michelob Light Eagle and Daedalus (Figure 4.28) which were test beds for flight research conducted at the NASA Dryden Flight Research Center between January 1987 and March 1988. These unique aircraft were designed and constructed by a group of students, professors, and alumni of the Massachusetts Institute of Technology within the context of the Daedalus project.

4.6 ENGINE PERFORMANCE CRITERIA

This section presents the performance of various engines and compares several performance parameters of aero-engines. The performance parameters that we are interested in are primarily engine power, thrust, SFC, and efficiency in terms of altitude and Mach number. Although the aircraft piston/turbine engines are very complex pieces of equipment, the basic tools for mathematical modeling of their performance are discussed in this chapter. They allow performance calculations for existing and proposed similar engines.

The best source of analysis of engine performance is the published catalog of engines by engine manufacturers.

For instance, Figure 4.29 demonstrates [48] thrust of the JT9D-70 high-bypass turbofan engine (with a maximum thrust of 222 kN) as functions of Mach number and air temperature. This turbine engine that was the Pratt and Whitney company's first high-BPR turbofan is utilized in several large transport aircraft, including Boeing 747 (Figure 8.10b), Boeing 767, Airbus 300, Airbus 310, and McDonnell Douglas DC-10 (Figure 3.17). Based on this figure, the thrust of this turbofan engine decreases as the Mach number decreases. Moreover, the thrust decreases with a decrease in the air temperature.

Note the rapid falloff of thrust with rising Mach number that is a typical characteristic of this engine. Frequently, a turbine engine has a lower performance at an

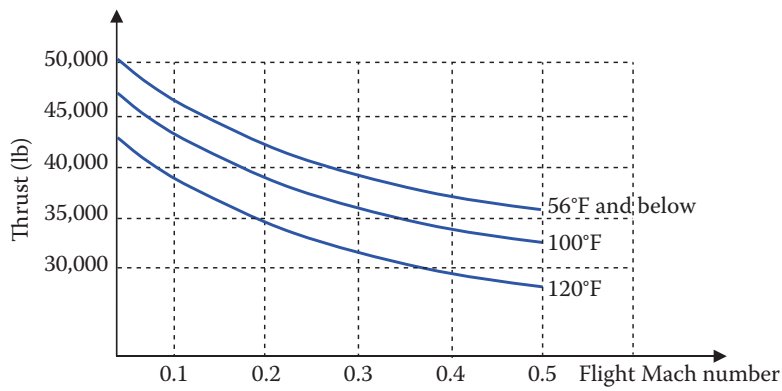

FIGURE 4.29 Pratt and Whitney JT9D-70 turbofan engine thrust versus Mach number and air temperature.

airport, which is located in a high-temperature city (e.g., Phoenix, Arizona) compared with a high-temperature region (e.g., Toronto, Canada).

4.6.1 Engine Performance at Various Altitudes and Speeds

Engine performance varies based on many factors, including flight altitude and aircraft speed. In general, as the aircraft climbs, the power or thrust of an air-breathing engine is decreased, since the available air is dropping. This is true for both jet and prop-driven aircraft. Furthermore, the performance of two different engines (e.g., turbofan) is not completely the same. Turbine engines are capable of operating at higher altitude than piston engines. Similarly, jet engines are capable of operating at higher Mach numbers as compared with piston engines.

4.6.2 Specific Fuel Consumption

The specific fuel consumption (SFC or C) is a technical figure of merit for an engine that indicates how efficiently the engine is burning fuel and converting it to the net thrust. In propeller-driven engines (piston, turboprop, and turboshaft), SFC measures the mass of fuel needed to provide a unit of power for a unit time. The common unit of measure in British unit is lb/hp/h (i.e., lb/(hp·h)), that is, pounds of fuel consumed for every horsepower generated during 1 h of operation, (or kg/kW/h in SI units). Therefore, a lower number indicates a higher efficiency.

The SFC for jet engines (turbofan or turbojet) is defined as the weight (sometimes mass) of fuel needed to provide a unit thrust for a unit time (e.g., lb/h/lb or lb/(h·lb) or g/s/N in SI units). SFC is dependent upon engine design, but differences in the SFC between different engines using a similar underlying technology tend to be very minimal.

For propeller-driven engines:

$$\text{SFC} = \frac{Q_f}{P} = \frac{\text{Weight of consumed fuel}}{\text{Unit time} \times \text{unit power}} \left(\text{piston-prop and turboprop engines}\right) \tag{4.9}$$

For jet engines:

$$\text{SFC} = \frac{Q_f}{T} = \frac{\text{Weight of consumed fuel}}{\text{Unit time} \times \text{unit thrust}} \left(\text{turbofan and turbojet engines}\right) \tag{4.10}$$

where Q_f denotes the fuel flow rate. A typical piston engine will have a SFC of about 0.5 lb/hp/h (or 0.3 kg/kW/h or 83 g/MJ), regardless of the design of any particular engine.

For instance, if a piston engine consumes 400 lb of fuel to produce 200 hp for 4 h, its SFC will be

$$\text{SFC} = \frac{400\,\text{lb}}{4\,\text{h} \times 200\,\text{hp}} = 0.5\ \text{lb/(h} \cdot \text{hp)} = 2.98\ \text{N/(h} \cdot \text{kW)} \tag{4.9}$$

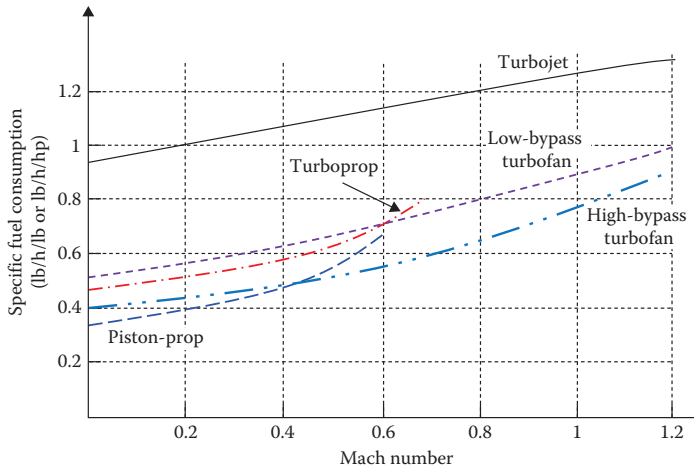

FIGURE 4.30 Typical variations of SFC of typical engines versus flight Mach number.

TABLE 4.3
Typical Values of SFC for Various Engines

No.	Engine Type	SFC	Unit
1.	Turbojet	0.8–0.9	lb/h/lb
2.	Low bypass ratio turbofan	0.7–0.8	lb/h/lb
3.	High-bypass ratio turbofan	0.4–0.5	lb/h/lb
4.	Turboprop	0.5–0.8	lb/h/hp
5.	Piston (fixed pitch)	0.4–0.8	lb/h/hp
6.	Piston (variable pitch)	0.4–0.8	lb/h/hp

A Rolls-Royce (Allison) T56 turboprop engine – which is employed by the Lockheed C-130 Hercules military transport aircraft – is consuming 0.47 lb/h/hp or 79.43 μg/J of fuel at takeoff. A Pratt and Whitney PW2000 turbofan engine – which is employed by Boeing 777 and C-17 – is consuming 9.69 mg/Ns (0.342 lb/h/lb) at takeoff, while 15.95 mg/Ns (0.563 lb/h/lb) at cruise.

It should be noted that SFC varies with throttle setting, aircraft speed, and altitude and flight condition. Although the nominal SFC is a useful measure of fuel efficiency, the total fuel burn is of more importance to the customer.

Figure 4.30 compares the typical SFC of several engines as a function of aircraft speed (Mach number). In this figure, the SFC of prop-driven aircraft is normalized to be comparable with the SFC of jet engines. In general, piston engines have lower SFC compared with jet engines.

Due to advances in technology, modern engines entering service are expected to have cruise fuel consumptions lower by about 5%–10% in every decade. Table 4.3 shows typical values of SFC for various engines.

The Learjet 70/75 at 41,000 ft, ISA + 3°C (5°F) and Mach 0.78 for 462 knots (856 km/h), has an hourly fuel burn of 1,000 lb (450 kg), while 1,400 lb (640 kg) at Mach 0.80.

Example 4.5

The SFC of a turboprop engine is 0.5 lb/(h·hp). (a) Determine the SFC of this engine in terms of 1/nm and 1/km. (b) How much fuel per hour is consumed if the engine power is 900 hp?

Solution

a. We know the following relationship among various units:

$$1\,\text{hp} = 550(\text{ft}\cdot\text{lb})/\text{s}$$

$$1\,\text{h} = 3{,}600\,\text{s}$$

$$1\,\text{nm} = 6{,}080\,\text{ft} = 1{,}853\,\text{m} = 1.853\,\text{km}$$

Now, we substitute the numbers:

$$C = 0.5\,\text{lb}/(\text{h}\cdot\text{hp}) = 0.5\times\frac{6{,}080}{3{,}600\times 550} = 0.001535\,\text{nm}^{-1}$$

Similarly

$$C = 0.5\,\text{lb}/(\text{h}\cdot\text{hp}) = 0.5\times\frac{6{,}080}{3{,}600\times 550\times 1.853} = 0.000828\,\text{km}^{-1}$$

The fuel flow rate (Q_f) is the SFC times the engine power:

$$Q_f = C\cdot P = 0.5\times 900 = 450\,\text{lb/h} = 203.85\,\text{kg/h} \tag{4.9}$$

Thus, this engine will consume 450 lb (203.85 kg) of fuel per hour if the aircraft is flying with maximum engine power.

4.7 ENGINE PERFORMANCE CALCULATIONS

To analyze an aircraft's performance, we need to have a lot of information and charts. One of the required data is the engine model and its performance features. Every engine manufacturer publishes engine charts that help the performance engineer. In this section, we discuss how to extract data from manufacturer's chart and how to apply them in our aircraft performance calculations. The materials in this section present flat rating, variations of power and thrust with aircraft speed and altitude, and variations of SFC with aircraft speed and altitude. In addition, the power calculations for electric engines are briefly presented.

4.7.1 Flat Rating

Most turbine engines (turbojet/turbofan/turboprop) have three frequently published power/thrust values or ratings: (1) nominal or uninstalled rating, (2) installed rating,

and (3) takeoff allowed rating. When an engine is installed, about 3%–8% of the thrust/power is lost and is not recoverable. The reasons include ram drag, nacelle drag, and installation drag and location losses.

For example, the turbofan engine Rolls-Royce Turbomeca F405-RR-401 has a nominal rating (thrust) of 26 kN but an installed rating of 24.59 kN, which implies a 5.4% loss of thrust after installation. Moreover, a Pratt and Whitney PW2000 turbofan engine is launched with TO rating of 170.1 kN (38,250 lb) to 30.55°C (87°F).

Every turbine engine has an operating envelope that requires the pilot not to exceed the limits. Turbine engines essentially have three limits: (1) an internal pressure limit, (2) a combustion temperature limit, and (3) an engine shaft rotational speed limit.

Most turbine engines are not allowed to produce their maximum power or thrust at low altitudes with high temperatures (e.g., summer days). However, they are allowed to generate their maximum power or thrust at high altitudes, where the ambient temperature is low enough.

A limiting factor in the advance of turbine engines is the temperature at the turbine inlet (which is the hottest point in the turbine engine). This means that the turbine blades are not capable of handling beyond a specific temperature; otherwise, they are melted due to the high thermal stress. The best/strongest blade material (e.g., ceramic/tungsten composite) cannot handle beyond 3,000°C. The maximum thrust/power that may be used at takeoff will be the one at which the first of the three limits are reached.

An engine designer has two options: (1) To design the engine based on the worst operating conditions and provide the pilot the freedom to use the throttle at will and (2) to design the engine based on ideal conditions while mandating the pilot not to extract the maximum power/thrust under some non-ideal conditions. The second option is often selected, which means that the engine designer usually considers the ideal operating condition of the standard sea level, which means at an ambient temperature of 15°C (or 59°F).

If the operating condition has a temperature beyond 15°C, the rating of the engine needs to be constrained/restricted. This restriction is referred to as de-rating or flat rating. When an engine is flat rated, it means that an engine of high power/thrust rating is constrained to a lower rating (i.e., de-rated) under some particular conditions. Above that temperature the engine is flat rated; below that temperature, it is "full rated".

The P&W turbine engine manufacturer rates their engines to an ambient temperature. Some non-P&W engines are rated to a compressor shaft rotational speed. For instance, the EuroProp International turboprop engine TP400-D6 (used in Airbus Military A400M) can provide a maximum of 13,000 hp. However, its thermodynamic power is de-rated to 10,700 hp for takeoff at sea level. The maximum power of the Pratt and Whitney PT6A-62 turboprop engine (used in the two-seat trainer Pilatus PC-9) at sea level is 1,150 hp but is flat rated at 950 hp. This implies that the pilot is allowed to extract only 82.6% of the maximum power at sea level.

In a "flat rated" condition, the power/thrust available is kept constant (i.e., flat). The altitude at which the engine is flat rated is called flat rating altitude. Figure 4.31 demonstrates the flat-rated altitude and power of a turboprop engine. Flat rating

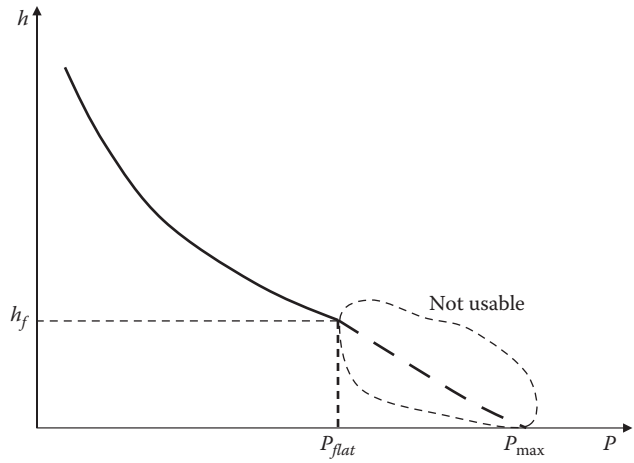

FIGURE 4.31 Flat-rated turboprop engine.

increases the operating life of a turbine engine, but results in a slower acceleration on the runway, a longer takeoff roll, and a reduced initial climb rate.

Since the ambient condition is not always standard (i.e., ISA condition), the flat-rated condition is often stated in terms of outside air temperature. In addition, in terms of the pilot application, the flat-rated temperature must be converted to flight altitude. For instance, if a turbofan engine is rated to a thrust of 10 kN at 15°C and the outside temperature is 35°C, the pilot is not allowed to use the maximum thrust unless the aircraft is flying above 10,000 ft. At 10,000 ft, the outside temperature is decreased by 20°C compared with the sea level (i.e., $35 - 20 = 15$).

In terms of mathematical modeling of the flat-rated condition, the flat rating temperature is not a real temperature but is a virtual one. When the flat rating condition is expressed in terms of temperature, this temperature is substituted in the following relationship to find the flat rating air density (and, subsequently, the corresponding altitude).

$$\rho_f = \frac{P_{SL}}{RT_f} \tag{4.11}$$

where ρ_f is the flat rating air density, T_f is the flat rating temperature, P_{SL} is sea-level ambient pressure (101,325 Pa), and R is the gas constant. The corresponding altitude to this temperature (from Appendix A or B or relationships from Chapter 1) is the flat rating altitude (h_f).

Example 4.6

A turbofan engine is flat rated at 30°C to a thrust of 8,500 N. Determine the flat rating altitude of this engine.

Solution

$$\rho_f = \frac{P_{SL}}{RT_f} = \frac{101{,}325}{278 \times (273.15 + 30)} = 1.1644\ \text{kg/m}^3 \tag{4.11}$$

By referring to Appendix A, the corresponding altitude to the air density of 1.164 kg/m^3 is 500 m. Therefore

$$h_f = 500\ \text{m}$$

Thus, this engine is allowed to produce at most 8,500 N from sea level up to 500 m altitude, which implies a partial throttle. Afterward, a full throttle is allowed.

4.7.2 Variations of Power and Thrust with Aircraft Speed

4.7.2.1 Piston-Prop Engine and Turboprop Engine

As the airplane's airspeed is changed, the pressure of air entering the engine manifold is varied due to the stagnation of the airflow in the inlet lip. Sometimes, this is called a *ram effect*. In effect, as the airspeed increases, this "ram pressure" is increased too, which in turn increases the engine power. For a high-velocity prop-driven acrobatic aircraft, this effect is considerable. However, the reciprocating engines are used mainly on low-speed GA aircraft, and the ram effect is not significant. The same reasoning can be made, and it is true for turboprop engines.

Furthermore, as the airplane airspeed is increased, the mass flow rate of the air entering the engine is increased, which also increases the engine power. Due to two changes in the airflow (pressure, mass flow rate), as a consequence of change in airspeed, it is reasonable to conclude that the engine power is increased as the airspeed is increased. Thus, a prop-driven engine generates more power in cruise than in takeoff. The calculation of accurate variations of engine power is not easily predictable and beyond the scope of this text. Thus, it is reasonable to consider that the power (both piston engines and turboprop engines) is constant with aircraft speed. The interested reader is referred to the engine operating manual for more details.

4.7.2.2 Turbojet Engine

The thrust generated by a turbojet is given by Equation 4.4. Based on the conservation of mass (continuity principle), the mass flow rate ($\dot{m}$) of air entering the inlet is equal to the mass flow rate of air exiting through exit (if the fuel rate is ignored, since it is only about 2%–4%):

$$\dot{m} = \rho A V \tag{4.12}$$

If this is applied on the inlet, the parameter A is the cross-sectional area of an engine (at the inlet). As aircraft speed is increased, airspeed at the inlet stays essentially the

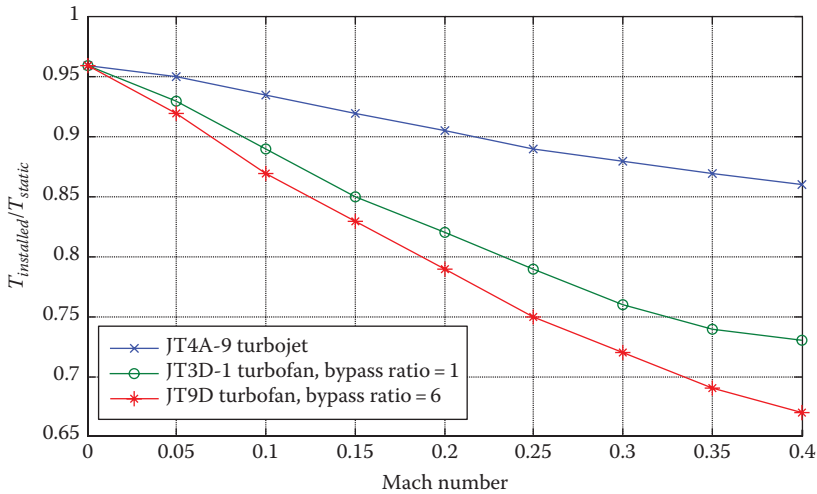

FIGURE 4.32 Variations of installed thrust with Mach number.

same; but the air density at the inlet will be increased due to the internal compression taking place inside the inlet. This results in an increase in the air mass flow rate which implies, the engine thrust will increase too.

However, as the aircraft airspeed is increased, the difference between the exit gas velocity and the aircraft airspeed is decreased. This leads to a decrease in the value of the engine thrust. These two effects tend to cancel in Equation 4.4; therefore, we might expect the thrust generated by a turbojet to be only a weak function of aircraft airspeed. Since these two effects act differently at different rates, the overall effect is sometimes positive and sometimes negative.

This is indeed the case, as shown in Figure 4.32. Here, the thrust for a typical small turbojet is given as a function of flight Mach number for two altitudes, sea level and 40,000 ft, and for three different throttle settings (denoted by different compressor rpm values) at each altitude.

Therefore, the rate of thrust reduction with the Mach number is not large. Hence, to a first approximation, for a turbojet engine, thrust is reasonably constant with speed. Especially at altitude, thrust is a weak function of the Mach number.

4.7.2.3 Turbofan Engine

The thrust generated by a turbofan is governed by Equation 4.5. The high-BPR turbofan engines are the class of turbofan engines that power transport aircraft. The performance of these engines seems to be closer to that of a propeller than that of a turbojet in some respects. The thrust of a turbofan engine has a considerable variation with velocity; thrust decreases as airspeed increases (as Figure 4.32 demonstrates).

The variations of thrust for a turbofan are a strong function of airspeed (or the Mach number) at lower altitudes, and thrust is relatively constant for the narrow Mach number range from 0.7 to 0.95. For instance, a turbofan engine JT9D-70 has a

maximum [54] thrust of 50,000 lb when $M = 0$, but, the thrust decreases to 36,000 lb when $M = 0.45$.

After a small initial decrease at low subsonic Mach numbers, the thrust increases as Mach number increases well above Mach 1. Although the thrust reduction with speed for individual engine types may vary slightly, the effects of BPR are generally significant.

Variations of turbofan engine thrust as a function of aircraft speed – during take-off – may be modeled with a second-order algebraic equation:

$$T = a + bV + cV^2 \tag{4.13}$$

where coefficients a, b, and c are determined through engine performance experiments. For a Rolls-Royce RB211-535E4 turbofan engine (with a maximum thrust of 28,000 lbf), the coefficients have been measured as: $a = 28{,}000$, $b = 22$, and $c = 0.011$, where V is in ft/s, and T is in lbf. For the analysis of an aircraft's performance in the cruise range, it appears reasonable to assume that thrust is constant.

4.7.3 Variations of Power and Thrust with Altitude

The airflow rate is a function of air density, while the air density decreases with altitude. Thus, as the flight altitude increases, the engine power and thrust will decrease. In practice, the variations of engine thrust/power should be provided by the engine manufacturers. Some empirical equations follow.

4.7.3.1 Piston Engine

For a piston engine, there is a strong altitude effect on power. The rate of loss of power in terms of altitude depends on several parameters, including manufacturing technology, configuration, and inlet shape. There is no unique expression for power modeling in terms of altitude; hence, we need to resort to empirical relationships.

Figure 4.11 demonstrates the variations of power with altitude for a IO-360 Lycoming piston engine. Moreover, Figure 4.33 presents the variations of power with altitude for four-cylinder air-cooled horizontally opposed Lycoming O-320 piston engines [55]. This figure also shows the air density ratio variations for the comparison. This figure is an empirical base for deriving a mathematical relationship for power model.

With regard to the altitude variations, the data in Figure 4.33 are reasonably correlated by a mathematical formula. In this figure, the variations of air density ratio (ρ/ρ_o) are also illustrated. It is interesting to note that the behavior of engine power and air density with respect to altitude is very similar.

Indeed, it is reasonable to express the variation of power with altitude in terms of the density ratio (ρ/ρ_o). To a first approximation, we will use the following empirical expression for piston engines:

$$P = P_o\left(\frac{\rho}{\rho_o}\right)^{1.2} \tag{4.14}$$

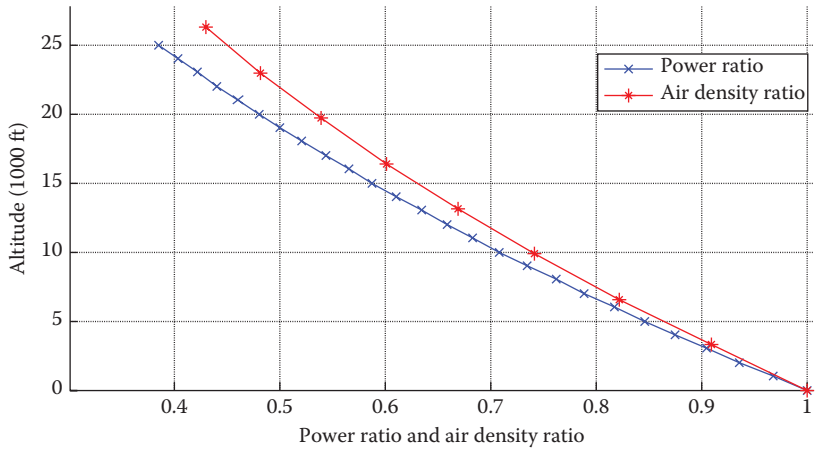

FIGURE 4.33 Variations of power and air density with altitude for Lycoming O-320 piston engine.

where P and ρ are the shaft power output and air density, respectively, at a given altitude and P_o and ρ_o are the corresponding values at sea level.

If the engine has a supercharger, substitute ρ_o with ρ_c (i.e., the altitude up to which the supercharger can hold the power constant; critical altitude) and replace the 1.2 with 0.75. Thus

$$P = P_o\left(\frac{\rho}{\rho_c}\right)^{0.75} \tag{4.15}$$

Case Study - Example 4.7

The piston-prop engine Lycoming A-300E has a maximum power of 300 kW at sea-level ISA condition. Determine its maximum power at sea with ISA + 10 flight condition.

Solution

The air density at this flight condition is

$$\rho = \frac{P_o}{RT} = \frac{101{,}325}{287\times(15+10+273.15)} \Rightarrow \rho = 1.184\,\text{kg/m}^3 \tag{1.23}$$

So the power will be

$$P = P_o\left(\frac{\rho}{\rho_o}\right)^{1.2} = 300\left(\frac{1.184}{1.225}\right)^{1.2} \Rightarrow P = 288\,\text{kW} \tag{4.14}$$

We observe that when the weather is warmer, the engine power is decreased.

4.7.3.2 Turbojet Engine

For a turbojet engine, there is a strong altitude effect on thrust, as can be seen by examining Equation 4.13. In general, the engine thrust decreases with altitude. The variation of thrust with altitude is modeled by two empirical equations: one of troposphere and another one for stratosphere. For the:

$$T = T_o\left(\frac{\rho}{\rho_o}\right)^c \quad (\text{troposphere}) \tag{4.16}$$

where T_o is the sea-level thrust and T is the engine thrust at altitude. Equation 4.21 is an empirical relation that holds for a large number of turbojet engines. The value of c depends on the engine design and configuration; it is usually near 1 but could be less than or greater than 1. Here, we choose 0.9 as it matches with current engine technology. In future, as the engine technology is advanced, this number will be slightly different. For the stratosphere:

$$T = T_{11}\left(\frac{\rho}{\rho_{11}}\right) \quad (\text{stratosphere}) \tag{4.17}$$

where T_{11} and ρ_{11} are engine thrust and air density, respectively, at 11,000 m altitude. This thrust (T_{11}) is readily found from Equation 4.16. If the engine is flat rated (T_{flat}), the relation will be

$$T = T_{\text{flat}}\left(\frac{\rho}{\rho_f}\right)^{0.9} \tag{4.18}$$

This relation is applicable only when the flight altitude (ρ) is greater than flat-rated altitude (ρ_f).

Example 4.8

A turbojet engine of a transport aircraft is flat rated at a thrust of 10,000 N up to 2,000 m altitude. Determine the engine's maximum thrust at 8,000 m altitude.

Solution

The air densities at 2,000 and 8,000 m altitudes are found from Appendix A as follows:

$$\rho_{2000} = 1.0063\,\text{kg/m}^3$$

$$\rho_{8000} = 0.525\,\text{kg/m}^3$$

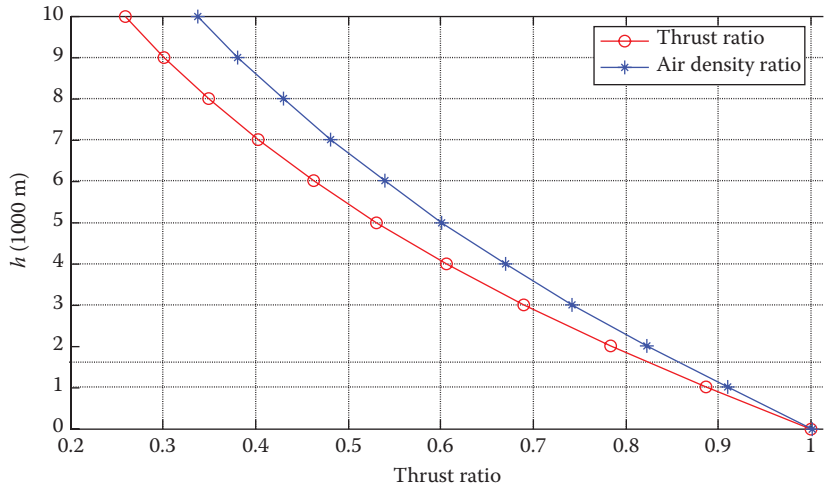

FIGURE 4.34 Variations of uninstalled thrust for a turbofan engine with altitude.

Thus, the maximum thrust at 8,000 m altitude will be

$$T = T_{\text{flat}}\left(\frac{\rho}{\rho_f}\right)^{0.9} \Rightarrow T_{8000} = 10{,}000\left(\frac{0.525}{1.0063}\right)^{0.9} = 5{,}567.8\,\text{N} \tag{4.18}$$

4.7.3.3 Turbofan Engine

The typical drop rate of uninstalled thrust with altitude at Mach 0.85 for a turbofan engine is indicated in Figure 4.34, where thrust curves are shown for altitudes from sea level up to 10 km. In this figure, the variations of air density ratio are also illustrated for comparison.

The variation of turbofan engine thrust with altitude is approximated by the following empirical equations.

$$T = T_o\left(\frac{\rho}{\rho_o}\right)^k \quad \text{(troposphere)} \tag{4.19}$$

$$T = T_{11}\left(\frac{\rho}{\rho_{11}}\right) = T_o\left(\frac{\rho}{\rho_{11}}\right)\left(\frac{\rho_{11}}{\rho_o}\right)^k \quad \text{(stratosphere)} \tag{4.20}$$

where T_o is the sea-level thrust and k is a factor that varies from 0.9 to 1.2, and T_{11} and ρ_{11} are engine thrust and air density, respectively, at 11 m altitude. This thrust (T_{11}) is readily found from Equation 4.19.

$$T = T_{\text{flat}}\left(\frac{\rho}{\rho_f}\right)^k \tag{4.21}$$

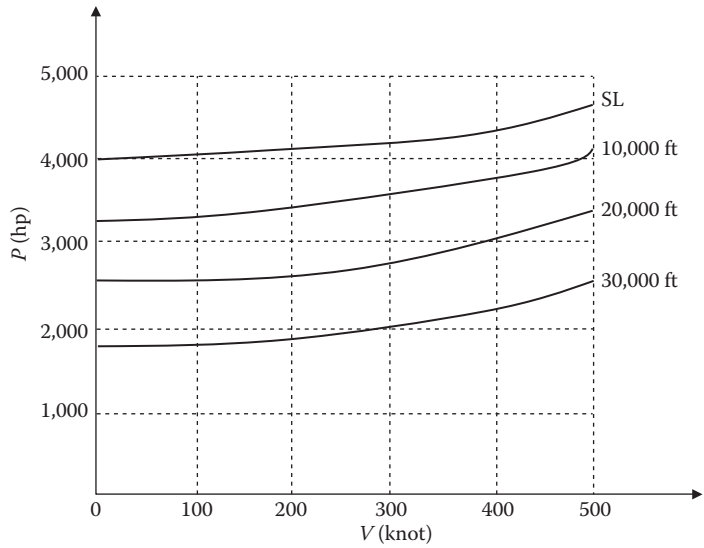

FIGURE 4.35 Variation of maximum available power as a function of Mach number and altitude for a typical turboprop engine.

This relation is applicable only when the flight altitude is greater than flat-rated altitude.

4.7.3.4 Turboprop Engine

A typical variation of shaft available power for a turboprop engine with Mach number and altitude is given in Figure 4.35. Note that, P is the shaft power and does not include the propeller efficiency. As Mach 1 is approached, there is a serious degradation of power because of shock wave formation on the propeller tip. Recall that the propeller tip speed is the vector sum of the aircraft speed and the prop rotational speed.

With regard to the altitude variation, the experimental data are reasonably correlated by the following expression:

$$P = P_o \left(\frac{\rho}{\rho_o} \right)^m \quad \text{(troposphere)} \tag{4.22}$$

The parameter m is a function of engine configuration and installation. A value between 0.9 and 1.1 is recommended [56] for m.

$$P = P_{11} \left(\frac{\rho}{\rho_{11}} \right) \quad \text{(stratosphere)} \tag{4.23}$$

where P_{11} and ρ_{11} are engine power and air density, respectively, at 11,000 m altitude. This power (P_{11}) is readily determined from Equation 4.22. If the turboprop engine is flat rated (P_{flat}), the relation will be

$$P = P_{\text{flat}} \left(\frac{\rho}{\rho_f} \right)^m \tag{4.24}$$

This relation is applicable only when the flight altitude is greater than flat-rated altitude.

Example 4.9

An aircraft is powered with a turboprop engine that has a maximum power of 800 hp at sea level. The aircraft is cruising at 10,000 ft altitude with a maximum speed of 250 knots equivalent airspeed (KEAS). The propeller efficiency is 0.8. How much thrust is this engine plus propeller generating? Assume $m = 0.9$.

Solution

From Appendix B, the specific air density is $\sigma = 0.738$. The 10,000 ft altitude lies in the first atmospheric layer (i.e., troposphere); thus, the engine power at this altitude is

$$P = P_o \left(\frac{\rho}{\rho_o} \right)^{0.9} \Rightarrow P_{10,000} = 800 \times 0.738^{0.9} \Rightarrow P_{10,000} = 608.6\,\text{hp} \tag{4.22}$$

The given airspeed is equivalent airspeed; the true airspeed is

$$V_T = \frac{V_E}{\sqrt{\sigma_{10,000}}} = \frac{250}{\sqrt{0.738}} \Rightarrow V_T = 291\,\text{KTAS} \tag{2.25}$$

One horsepower is equivalent to 550 lb ft/s, and 1 knot is equivalent to 1.688 ft/s. Therefore, the engine thrust is

$$\eta_P = \frac{TV}{P_{\text{in}}} \Rightarrow T = \frac{P\eta_P}{V_T} = \frac{608.6 \times 550 \times 0.8}{291 \times 1.688} \Rightarrow T = 545.1\,\text{lb} \tag{4.2}$$

4.7.3.5 Electric Engine

Electric engines (either with battery or solar-powered) do not breath/consume air to produce the shaft power. However, to convert the shaft power to available power, a propeller is used. As the altitude increases, the air density is decreased, and thus, the available power is decreased too. Electric engines don't suffer a shaft power reduction, they will lose output thrust (i.e., available power). Therefore, electric engine will produce less thrust at altitude, since propellers will have less air to move. This reduction will not be as significant as with internal combustion engines.

With regard to the variation of available power altitude, the experimental data are modeled by Equation 4.22. For the values of m, consult with the engine manufacturer. The parameter *m* is a function of engine configuration, propeller design, and installation. A value between 0.4 and 0.6 is recommended for *m*.

4.7.4 Variations of SFC with Altitude

Turbojet, turbofan, and turboprop engines all have the same core (i.e., gas generator). A gas generator consists of a compressor, a combustion chamber, and a turbine. The SFC of these three types of turbine engines follows a similar trend. Thus, in terms of SFC, turbojet, turbofan, and turboprop engines are grouped together. The piston engine has a completely different configuration.

4.7.4.1 Piston Engine

The SFC of a piston engine is a function of engine power, altitude, shaft rpm, and fuel–air mixture. The typical value of SFC for piston engines is 0.4–0.65 lb/hp/h. The SFC is slightly lower at altitude than at sea level. For simplicity, it is assumed that the SFC is constant with altitude.

4.7.4.2 Turbojet Engine, Turbofan Engine, and Turboprop Engine

The turbine engine thrust is strongly dependent on altitude and considerably affected by airspeed. The minimum SFC is somewhat lower at altitude than at sea level and is quite heavily affected by airspeed. At very high altitudes, the decreasing Reynolds number on the turbine blades may cause a slight increase in SFC. The SFC is raised moderately by higher cruise speeds.

Figure 4.36 shows the variations of SFC for a turbojet engine and a turbofan engine with altitude. The turbojet engine has a compressor pressure ratio of 15, an inlet area of 1 m^2, and an exit temperature of 1,500 K.

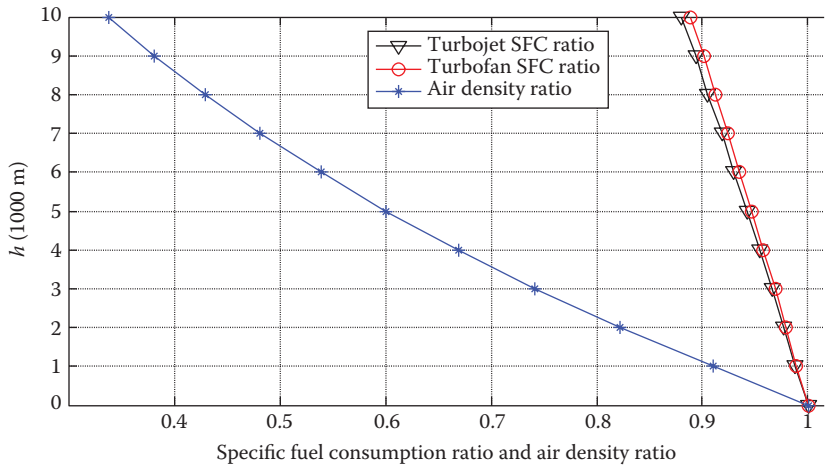

FIGURE 4.36 Variation of SFC ratio with altitude for turbofan and turbojet engines.

Since the fuel-to-air ratio is almost constant, this results in falling of the fuel consumption. Based on Figure 4.36 and Equation 4.23, we model the variations of SFC versus altitude. The variations of SFC in terms of altitude for turbojet, turbofan, and turboprop engines are given by the following empirical relationships:

$$\text{SFC} = \text{SFC}_o \left(\frac{\rho}{\rho_o} \right)^c \quad (\text{troposphere}) \tag{4.25}$$

$$\text{SFC} = \text{SFC}_{11} \quad (\text{stratosphere}) \tag{4.26}$$

where c is 0.1–0.2; it depends on the engine manufacturing technology and configuration. Equation 4.25 is applied for the first layer of the atmosphere, and Equation 4.26 is for the second layer. In these relationships, SFC_o is the SFC at sea level; SFC_{11} is the SFC at 11,000 m altitude (the boundary between the first layer and the second layer). Equation 4.26 states that the SFC in the second layer is constant throughout the layer.

In general, SFC improves at higher altitudes, at a given Mach number, until the second layer is reached. Then, the SFC is generally unaffected by further altitude increase.

4.7.5 Variations of SFC with Speed

4.7.5.1 Piston Engine

Figure 4.37 presents the variations of fuel flow (in gallons of fuel per hour; GPH) with percent rated power for four-cylinder air-cooled horizontally opposed Lycoming O-320 piston engines [55]. This engine has a SFC of 0.64 lb/h/hp at full power and a SFC of 0.29 lb/h/hp at 50% of engine power. There is about a 32% reduction of airspeed when the engine power is increased from full to 50%. This is reflected in the SFC when the fuel density is employed. Figure 4.37 also illustrates the variations of SFC versus engine speed, and fuel–air mixture.

The piston engine Lycoming IO-360-C1C [57] used in the GA aircraft Piper Cherokee Arrow is burning 10.15 gallon per hour (GPH) when 75% of the engine power is employed in a cruising flight. However, for a 65% rated power, the value is 9.16 GPH, and, for a 55% rated power, the value is only 8 GPH. The variations of SFC for piston engines in terms of velocity are given by the following approximate empirical relationship:

$$\text{SFC} = \text{SFC}_R \left(\frac{V}{V_{\max}} \right)^c \tag{4.27}$$

where SFC_R is the SFC at (maximum) rated power, V is the aircraft velocity, and $V_{\max}$ is the aircraft maximum velocity. The value of c depends on the engine design; it is usually near 2 but could be less than or greater than 2. Here, we choose 2 as it matches with current engine technology. In future, as the engine technology is advanced, this number will be slightly different.

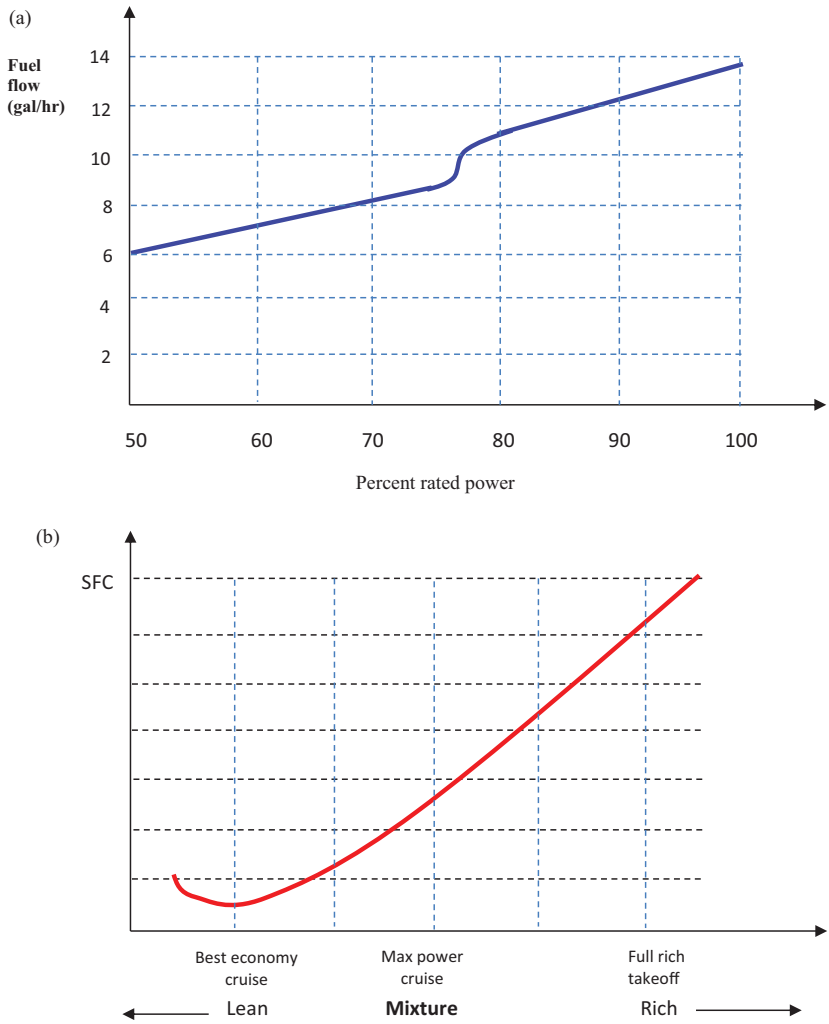

FIGURE 4.37 SFC of Lycoming O-320 piston engine. (a) Variations of fuel flow with percent rated power; (b) SFC versus fuel–air mixture.

4.7.5.2 Turbojet Engine

There is a general trend where the SFC non-linearly increases with flight Mach number. Based on the experimental data we can write a reasonable approximation through curve fitting, such as the following model:

$$\mathrm{SFC} = \mathrm{SFC}_o + kM \tag{4.28}$$

where SFC is the specific fuel consumption at any Mach number and SFC_o is the SFC at zero Mach number.

For this equation, the coefficient k is not introduced because it varies with engine features. The interested reader may use graphical/mathematical data modeling techniques to find k. The factor k is an empirical constant that is found by correlating the data.

4.7.5.3 Turbofan Engine

The SFC of a turbofan engine has a non-linear behavior with respect to speed in both subsonic supersonic regimes. The general trend is that the SFC increases with increases in M. For this reason, a turbojet engine is more fuel-efficient than a turbofan engine at the design Mach number of 2.2 for the *Concorde*.

Based on the experimental data, we can write a reasonable approximation through curve fitting, such as the following model:

$$\text{SFC} = \text{SFC}_o + kM \tag{4.29}$$

where SFC is the specific fuel consumption at any Mach number and SFC_o is the SFC at zero Mach number.

For this equation, the coefficient k is not introduced due to the fact it varies with engine features. The interested reader may use graphical/mathematical data modeling techniques to find k. The factor k is an empirical constant that is found by correlating the data.

For low-BPR turbofan engines, the performance is somewhat different from that for high-BPR engines. The performance of low-BPR turbofan engines is much closer to that of turbojet engines than that of turboprop engines, in contrast to the civil turbofan engine.

4.7.5.4 Turboprop Engine

The variation of SFC with airspeed for a turboprop engine is non-linear and is a function of propeller size, as well as the shaft rpm. The published engine test data show that the SFC is almost constant with velocity. Thus, it is reasonable to assume that SFC is constant with velocity.

4.7.6 Power of Electric Engines

The engine power is varying based on the flight condition and flight operation. For instance, the engine power required in a takeoff is much higher than that in a cruising flight. The power of an electric engine is determined [58] by multiplying the electric current (I) it is consuming by the terminal voltage (V).

$$P = IV \tag{4.30}$$

When the unit of V is voltage (V), and the unit of current is Ampere (A), the unit of power will be Watt (W). Furthermore, the power is the rate of change (consumption) of energy with respect to time.

$$P = \frac{dE}{dt} \tag{4.31}$$

where the unit of time (t) is second (s). Thus, the energy/work supplied by a battery to an electric engine is

$$E = \int_0^{\text{Time}} IVdt \tag{4.32}$$

where 'Time' is the duration of flight operation. When the current and voltage are constant (for instance in a cruising flight), this equation can be reduced to

$$E = IVt \tag{4.33}$$

where the unit of energy will be in Joule (J). For a given battery, the total energy is fixed. In addition, for a given electric engine, the voltage is usually fixed. Hence, the duration for which a battery can supply energy is based on the power, which is consumed by the engine. This implies the current, which is drawn by the electric engine, is adjusted accordingly.

Example 4.10

Determine the total energy supplied by a 4,200 mAh 11.1 V Li-Po (lithium-polymer) battery, and the maximum power that can be provided to an electric engine.

Solution

Based on the description of the battery, a maximum current of 4.2 A (i.e., 4,200 mA) at 11.1 V is provided for 1 h (which is 3,600 s). Thus

Total energy

$$E = IVt = 4.2 \times 11.1 \times 3{,}600 = 167{,}832\,\text{J} = 167.8\,\text{kJ} \tag{4.33}$$

Maximum power

$$P_{\max} = IV = 4.2 \times 11.1 = 46.6\,\text{W} \tag{4.30}$$

4.8 PROPELLER PERFORMANCE

4.8.1 Introduction

Turboprop and piston-prop engines, as well as electric propulsion systems, have a very important component, propeller,[5] that influences their performances. To analyze the performance of an engine, one first needs to be able to determine propeller performance. A propeller is a lifting surface with an airfoil cross section, and it generates an aerodynamic force the same way as a wing. The aircraft propeller

[5] The early literature refers to propeller as "airscrew".

consists of two or more blades and a central hub to which the blades are attached. Aerodynamically, a blade of an aircraft propeller is essentially a rotating wing.

The lift produced at each airfoil section of a blade is perpendicular to the effective resultant air velocity approaching the blade at that point (i.e., forward). The lift vector is therefore inclined at an angle to the flight direction, and it is the component perpendicular to the flight direction that creates most of the torque that the engine must overcome. In addition, the drag of the blades (prop drag) adds to the power the engine must supply. Thus, the process is never 100% efficient. Best propellers' efficiency to date is about 87%.

The power needed to rotate the propeller blades is provided by the engine shaft. The propeller is mounted on a shaft, which may be an extension of the crankshaft of a piston engine; or it is mounted on a propeller shaft that is geared to the turboprop engine. When the engine rotates the blades through air, the propeller transforms the mechanical power of the engine into thrust.

From aerodynamics, the pressure over the top of a lifting wing is lower than the pressure below the wing. In a spinning propeller, the pressure is lower than the free stream in front of the propeller and higher than the free stream behind he propeller. Downstream, the pressure eventually returns to free stream, but at the exit, the velocity is greater than the free stream because the propeller does work on the air.

A propeller's performance suffers if the flow is supersonic. When a blade tip becomes supersonic: (1) shock waves form, (2) blade drag and thus required torque increase suddenly, (3) noise increases sharply, and (4) separating the flow. Aircraft with conventional propellers, therefore, do not usually fly faster than about Mach 0.6.

An unducted fan or *propfan* is a modified turbofan engine, with the fan placed outside the engine nacelle on the same axis as the compressor blades. The design is intended to offer the speed and performance of a turbofan, with the fuel economy of a turboprop. The Progress D27 propfans are used on the four-engine medium-range transport aircraft Antonov An-70 (Figure 4.25).

As an engine's power increased over the years, designers adopted increasingly more propeller blades. Once they ran out of room on the propeller hub, they adopted twin contra-rotating propellers on the same engine, for example, Tupolev four-engine turboprop-powered strategic bomber TU-95 "Bear" (Figure 6.5) and the airliner Tupolev TU-114. These have eight propeller blades per engine. The Tupolev TU-114 with 4× Kuznetsov NK-12MV turboprop engines (11,000 kW [14,800 hp] each) driving contra-rotating props has held the record as the world's fastest propeller-driven aircraft for the past 51 years.

Its maximum speed is 470 knots (870 km/h), and its cruise speed is 415 knots (770 km/h). The Tupolev TU-114 broke several records in the 1960s that still stand today, one of which was on July 12, 1961, when the altitude of 12,073 m (39,610 ft) was achieved with payloads of 25,000–30,000 kg (55,000–66,000 lb).

Figure 4.38 shows a transport aircraft Bell-Boeing MV-22B Osprey with two turboshaft engines. The aircraft is equipped with two Rolls-Royce T406 engines; each can generate 6,150 hp (4,590 kW). This tiltrotor military multi-mission aircraft has a vertical takeoff and landing (VTOL) capability. As you can see, each propeller has three blades; the rotor diameter is 11.6 m.

FIGURE 4.38 Transport aircraft Bell-Boeing MV-22B Osprey with two turboshaft engines. (Courtesy of Weimeng.)

4.8.2 Definitions

Important parameters of a propeller are blades, number of blades, propeller diameter, blade airfoil (cross section) at various locations (e.g., tip and root), blade angle of attack, pitch angle, twist angle, and pitch. Figure 4.39 shows a two-blade propeller and some related variables. To appreciate the advantages of different families of the propeller, we must first define the fundamental characteristics of the propeller. The angle of attack (α) is the angle between the section chord line and the local relative wind. The angle of attack clearly depends on the relative values of forward speed (i.e., V_∞) and linear speed of the prop section (i.e., $R\omega$). Thus, each blade section has a distinct angle of attack.

Each prop section generates a sectional lift and a sectional drag. The sectional lift is perpendicular to the local airflow direction, and the sectional drag is opposing the prop rotation. The thrust is the vector sum of the sectional lifts. The integration of the sectional lift over the blades' spans is the engine thrust (Figure 4.40).

The angle between this relative velocity and the plane of the propeller rotation is called the *helix angle* or angle of advance. For a particular airplane velocity, the helix angle varies from the root to the tip since the propeller tip revolves faster than the root sections; the helix angle approaches 90° at the blade root. Thus, the total angle from the plane of the propeller rotation to the chord line of the blade section is the sum of the helix angle and angle of attack for that section. This is called the *blade angle* or the *pitch angle*.

A propeller blade is typically most effective between station 60% and 90% with peak at 75%. It is this 75% station where the blade angle is usually defined. A propeller blade needs twist due to different angles of attack at different points along its span. The angle between the prop angle of attack at the tip and the prop angle of attack at the root is called *twist angle* (usually between 30° and 60°). Figure 4.41 illustrates a three-blade propeller of a Lockheed L-749 Constellation. Note the size of the hub, and the twist angle.

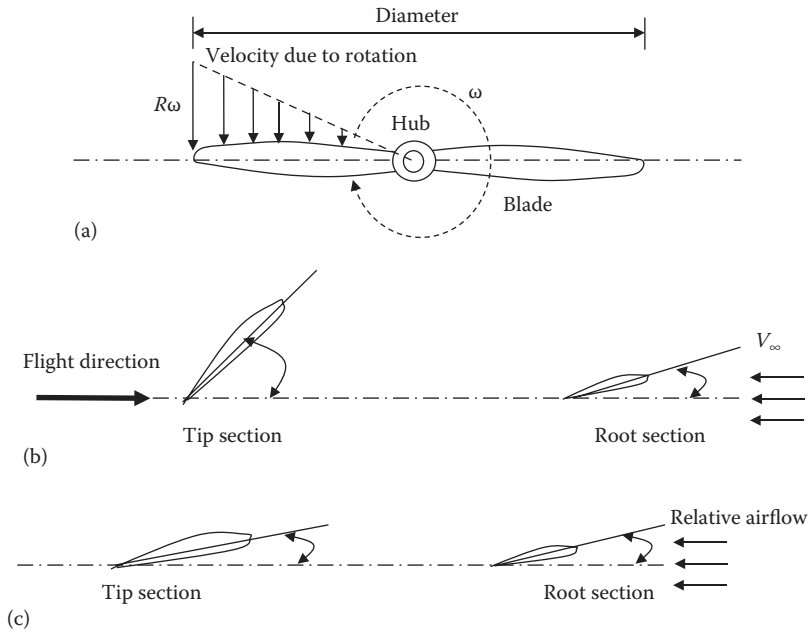

FIGURE 4.39 A two-blade propeller. (a) Propeller; (b) blade angle (different); (c) angle of attack (almost the same).

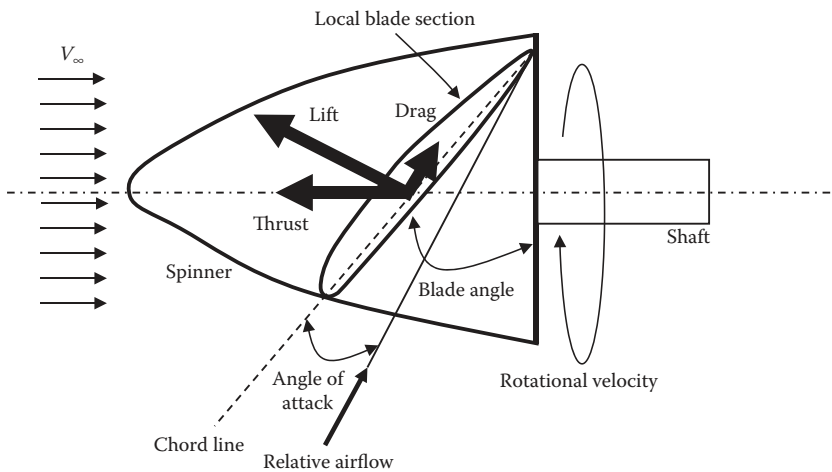

FIGURE 4.40 Propeller angles and aerodynamic forces.

The angle ϕ is the angle of the resultant flow and is determined by the ratio of aircraft airspeed (V) to propeller tip linear speed ($R\omega$).

$$\phi = \tan^{-1}\left(\frac{V}{R\omega}\right) \tag{4.34}$$

FIGURE 4.41 Three-blade propeller of a Lockheed L-749 Constellation. (Courtesy of Kas van Zonneveld.)

A non-dimensional parameter known as the "advance ratio" is defined as

$$J = \frac{V}{nD} \tag{4.35}$$

where D is prop diameter, n is the propeller angular velocity (in rev/s), and V is the aircraft forward speed. The ratio V/n is the distance advanced by the propeller in one revolution and is sometimes referred to as *pitch*. This is made non-dimensional by the prop diameter to yield the dimensionless advance ratio. The propeller pitch angle is a tool in which the *pitch* is controlled that allows us to differentiate between one family of the propeller and another. At a constant rpm and aircraft true airspeed, the speed of air over the airfoil varies with the distance from the center of rotation. The maximum velocity occurs at the point of maximum blade thickness near the propeller tip. To provide an angle of attack close to ideal all along the blade, the blade has "twist" that varies the blade pitch angle from the root to tip.

The angle between the airfoil chord line and the plane of rotation is the pitch angle, β. The pitch angle of a blade (β) is usually defined as the pitch angle measured at 75% of the radial distance from the center of rotation to the prop tip. As aircraft velocity increases, the angle of attack seen by the prop blade of a fixed-pitch prop decreases. This limits the maximum efficiency of a fixed-pitch prop at a given rpm to a single airspeed. If the blade pitch could be varied in flight, the prop efficiency could be very much higher for a wide range of operating conditions.

The pitch angle, β, of the section is sometimes defined relative to the zero-lift line of the airfoil section. The propeller pitch angles are frequently tabulated with respect to the chord line. Geometric pitch or simply pitch is the forward advance of an aircraft per one full rotation of the propeller (Figure 4.42). It is evident that the pitch angle and geometric pitch are related. Pitch is a key element in the classification of propellers. When considering the four families of propellers, it is useful to start with the simple fixed-pitch propeller and look at the enhancements in pitch control that

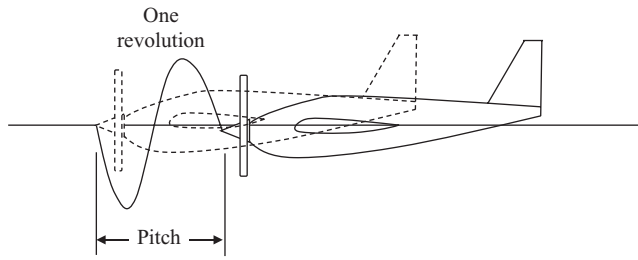

FIGURE 4.42 Propeller geometric pitch.

are gained as we progress through each family to the most advanced, the constant-speed propeller.

A fine pitch propeller has a low blade angle and will try to move forward a small distance through air with each rotation. It requires relatively low power to rotate, allowing high propeller speed to be developed but achieving only limited airspeed. This is like having a low gear in a car. Moreover, a coarse pitch propeller has a high blade angle and will try to advance a long distance through air with each rotation. It requires greater power to rotate, limiting the propeller speed that can be developed but achieving high airspeeds. This is like having a high gear in a car.

4.8.3 Propeller Classifications

There are four common families of the propeller: (1) fixed-pitch, (2) ground adjustable, (3) variable pitch or in-flight adjustable, and (4) constant-speed. The last two are examples of variable-pitch propellers. In the following, a review of the features of these four types is presented.

4.8.3.1 Fixed-Pitch Propeller

The earliest and common type of propeller in GA aviation is the fixed-pitch propeller. For fixed-pitch propellers, which were used exclusively on all airplanes until the early 1930s, the maximum propeller efficiency is achieved at a specific value of aircraft speed. With a fixed-pitch propeller, the pitch of the propeller is fixed from manufacture. The performance of the aircraft is determined on the day the propeller is installed and is limited within the constraints of the propeller.

In an aircraft with a fixed-pitch propeller, the only way to control the engine performance is through throttle, which simultaneously controls the shaft rotational speed, fuel consumption, as well as the manifold pressure. An analogy with a car is as though one had only one gear. Often when choosing a fixed-pitch propeller for the aircraft, manufacturers offer a choice of either a climb or a cruise prop. A climb propeller has a relatively fine pitch, and a cruise propeller has a relatively coarse pitch.

4.8.3.2 Ground Adjustable Propeller

Many propellers for GA aircraft are ground adjustable. These propellers have the advantage of being able to have their pitch set before each flight if started. They are usually used as a low-cost way to try out various pitches and settle on the propeller

pitch that best suits the aircraft. This can be compared to having a gearbox in a car that a driver can change only before setting out on the travel.

4.8.3.3 Variable-Pitch Propeller

The purpose of a variable pitch is to maintain an optimal angle of attack (maximum lift-to-drag ratio) on the propeller blades as aircraft speed varies. Early pitch control systems were pilot-operated, either two-position or manually variable. The pitch of the propeller may be controlled in flight to provide improved performance in each phase of flight.

This is usually done through a mechanical governor that continually adjusts the blade pitch angle. This feature of a variable-pitch propeller will provide the pilot with performance advantages, including shorter takeoff run, improved climb performance, improved fuel efficiency, greater range, higher maximum speed, steeper descent, and shorter landing run. At low speed (e.g., takeoff), the prop has the highest pitch angle, while at high speed (e.g., cruise), the prop has the lowest pitch angle.

Variable-pitch propellers actually come in a variety of versions. These different versions refer to the different ways that they are controlled and include the two-position propeller, in-flight adjustable propeller, automatic propeller, and constant-speed propeller. The in-flight adjustable propeller allows the pilot to directly vary the pitch of the propeller to the desired setting. Combined with the throttle control, this control allows a wide variety of power settings to be achieved. A range of airspeeds can be maintained while keeping the engine speed within limits. The propeller contains a mechanism in the hub to change the overall pitch of the blades in response to a servo command from a control system.

4.8.3.4 Constant-Speed Propeller

The constant-speed propeller is a special case of variable pitch and offers particular operating benefits. Constant-speed propellers allow the pilot to select a specific rpm for optimum engine power or maximum efficiency. A closed-loop controller is employed to control the governor to vary propeller pitch angle to maintain the engine torque, so that the rotational velocity is held constant. In an aircraft with a constant-speed propeller, there are two ways to control the shaft rpm: (1) through throttle setting and (2) through propeller pitch angle. In addition, the fuel consumption can be controlled by a separate knob (i.e., mixture control).

Since at high altitude, less air is available, a constant fuel-to-air ratio means less fuel. These two methods independently control the shaft rotational speed, fuel consumption, as well as the manifold pressure. In practice, engine throttle directly changes the fuel rate, while the rpm is directly impacted by the propeller pitch angle.

After the pilot sets the desired engine/propeller speed, the governor works to keep the propeller speed at the desired value. If the governor detects the propeller speed increasing, it increases the pitch angle accordingly to bring the speed back to the desired value. If the governor detects the propeller speed decreasing, it decreases the pitch angle accordingly to bring the speed again back to the desired value.

A constant-speed propeller will automatically deliver the advantages outlined earlier for variable-pitch propellers, with almost no control required from the pilot. Once a propeller/engine speed is selected, the pilot is able to control the power purely

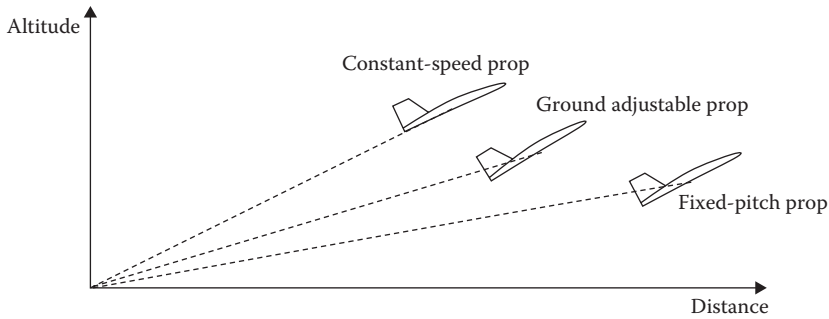

FIGURE 4.43 Comparison of aircraft climb performance for two types of propellers.

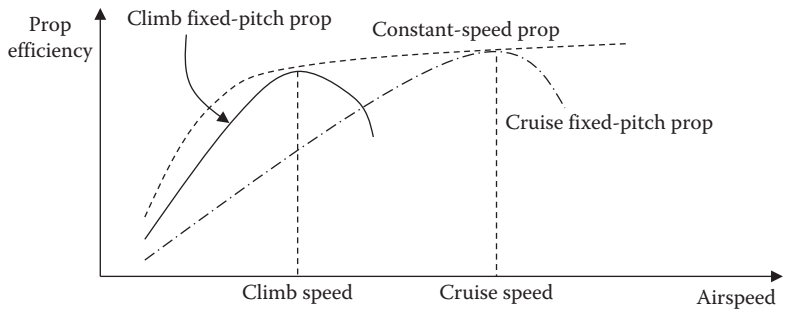

FIGURE 4.44 Comparison between efficiencies of various types of propellers.

with the throttle and the controller will act to keep the propeller/engine speed at the selected setting.

Almost all medium- to high-performance airplanes are equipped with constant-speed propellers. The side-by-side kit-built aircraft Glasair Glastar with a 300 hp piston engine, the four-seat kit-built aircraft Lancair IV with a 350 hp piston engine, the six-seat amphibian aircraft Lake LA-250 (Figure 3.31) with a 250 hp piston engine, the four-seat light plane Cessna 182 SkyLane (Figure 4.4) with a 230 hp piston engine, and fighter aircraft Lockheed P-38 Lightning with two turbocharged piston engines are all equipped with constant-speed propellers.

Figure 4.43 compares the aircraft climb performance for three types of propellers: (1) fixed-pitch prop, (2) ground adjustable prop, and (3) constant-speed prop. When an aircraft employs a constant-speed prop, the prop has the highest efficiency, so it generates the highest possible of thrust; thus, it climbs with a higher climb angle. Figure 4.44 compares the prop efficiencies of various types of propellers.

As observed, the constant-speed prop will provide the almost maximum efficiency at most airspeeds. A fixed-pitch prop at the maximum efficiency only at one airspeed. Its pitch angle is either set for optimum climb or optimum cruise.

4.8.3.5 Special Pitch Modes

Besides the ability to vary the pitch of the propeller to optimize an aircraft's performance, some variable-pitch propellers have some other special modes of operation

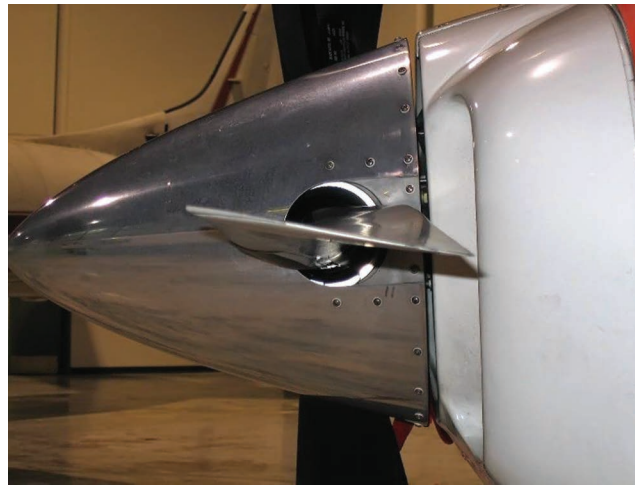

FIGURE 4.45 Feathering.

that can be very useful in certain circumstances. They are feather and reverse and are discussed in this section.

4.8.3.5.1 Feather

Another advantage of being able to vary the propeller pitch is called *feathering* of the propeller. A propeller is feathered when its pitch angle is adjusted so that the drag is minimized, and there is little or no tendency for autorotation when the engine is turned off, but the airplane is still flying. The propeller is feathered when an engine failure occurs in flight, so it also prevents engine damage.

A feathering propeller can alter the pitch angle of the blades up to almost 90° (see Figure 4.45). That is, the blade pitch is changed so that they have their leading edge pointing right into the direction of flight, offering minimum resistance to the airflow. This mode allows the propeller rotation to be stopped, without adding excessive drag to the aircraft. Feather may be used to improve the performance of the aircraft after the failure of an engine, but more usually in light aircraft it is used in motor glider applications. When the engine is switched off, and the propeller feathered, a gliding flight begins.

4.8.3.5.2 Reverse

Some propellers have *reversible pitch* to reverse thrust and thus act as a brake when landing. In this case, negative thrust is obtained by turning the blade to a large negative angle of attack. That is, the blade pitch angle is changed so that they have their leading edge pointing slightly opposite to the direction of flight.

In larger commuter aircraft, this feature is often used to slow the aircraft rapidly after landing, but in sport aircraft it is more usually used to enhance maneuvering on the ground. A popular application is in seaplanes, where the ability to maneuver backward, and sometimes to reduce the thrust to zero, is especially useful. EMB-314 Super Tucano is powered by a PT6A-68A turboprop engine, which drives a Hartzell five-bladed constant speed fully feathering reversible *pitch* propeller.

4.8.3.6 Contra-Rotating Propellers

When a propeller is spinning, a reaction (i.e., opposite) torque is applied to the shaft. At very high rpm, the torque is large and the shaft (i.e., the entire aircraft body) will experience this undesired torque. Thus, this torque must be eliminated. One way to eliminate such torque is to employ two contra-rotating propellers (i.e., rotating about the same axis in opposite directions). Two propellers are arranged one behind the other; propellers each canceling out the opposite's torque. For this purpose, a single-piston or turboprop engine drives two coaxial propellers in contra-rotation through a gearbox.

Furthermore, the prop efficiency at high speeds is improved. Contra-rotating propellers are different from counter-rotation propellers, which are propellers on separate shafts turning in opposite directions (e.g., twin-engine). Figure 4.25 illustrates an Antonov An-70 with four turboprop-fan engines; each engine is equipped with two contra-rotating propellers.

4.8.4 Calculations

4.8.4.1 Propeller Tip Speed

The path of motion of each element of the propeller is a circular path ($R\omega$) plus translational path (V) of the propeller. The airflow at the blade leading edge is the vector sum (see Figure 4.46) of the airplane free-stream velocity and the propeller circumferential velocity at that station. The prop tip speed is given by

$$V_{tip} = \sqrt{V_\infty^2 + V_\theta^2} \tag{4.36}$$

where V_{tip} is the airspeed at the propeller tip, V_∞ is the aircraft forward velocity, and V_θ is the linear velocity of the rotating prop at the tip.

$$V_\theta = R\omega \tag{4.37}$$

where R denotes the prop radius and ω is the prop rotational velocity.

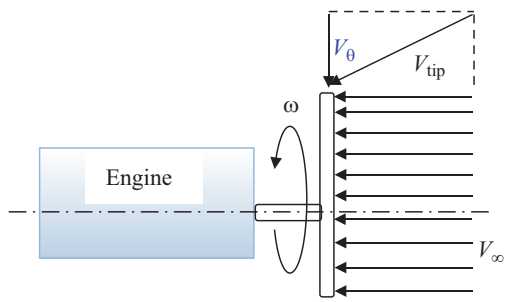

FIGURE 4.46 Propeller tip velocity.

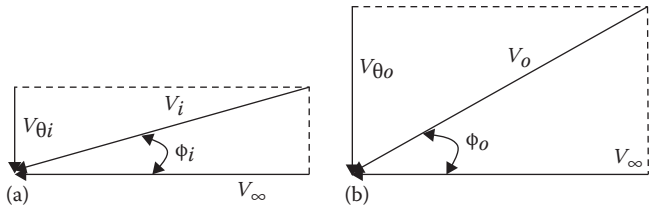

FIGURE 4.47 Relative flow at different blade stations. (a) Inner station; (b) outer station.

If forward speed increases, the relative airflow changes and the angle of attack is reduced. This results in reduced thrust and propeller torque; since engine torque is the same, the engine/propeller *rpm* increases. The tip speed must not approach the speed of sound (i.e., $M = 1$) since it produces vibration and noise due to the shock wave.

4.8.4.2 Propeller Twist Angle

Each airfoil section has a unique angle of attack at which the efficiency is maximum (i.e., the lift-to-drag ratio is maximum). However, since the prop is rotating, at each blade station, the linear velocity is varying. Thus, the local relative airflow is turning direction from the root to tip (i.e., the vector sum of forward speed and linear velocity of the prop [V_θ]). To maintain a constant angle of attack at various blade stations, the blade should be twisted. The helix angle, the angle between the relative airflow and the forward speed (Figure 4.47) at a blade inboard (i) station, is

$$\phi_i = \tan^{-1}\left(\frac{V_{\theta i}}{V_\infty}\right) = \tan^{-1}\left(\frac{R_i \omega}{V_\infty}\right) \tag{4.38}$$

By the same token, the helix angle, the angle between the relative airflow and the forward speed at a blade outboard (o) station, is

$$\phi_o = \tan^{-1}\left(\frac{V_{\theta o}}{V_\infty}\right) = \tan^{-1}\left(\frac{R_o \omega}{V_\infty}\right) \tag{4.39}$$

where ω is the rotational speed of the prop (rad/s) and R is the local radius of the blade station. It is evident that the local radius at the root is zero, and local radius at the tip is equal to half the prop diameter. Thus, the twist angle (α_t) is the difference between relative airflow directions between two stations (mainly root and tip).

$$\alpha_t = \phi_o - \phi_i = \tan^{-1}\left(\frac{R_o \omega}{V_\infty}\right) - \tan^{-1}\left(\frac{R_i \omega}{V_\infty}\right) \tag{4.40}$$

The local blade or pitch angle is the sum of the local angle of attack and the local helix angle:

$$\beta = \phi + \alpha \tag{4.41}$$

Both pitch angle and helix angle are varying (increasing) from the root to tip. The GA aircraft Moony M20TN with a 262 hp piston engine has a constant pitch propeller with 20° of twist angle (blade angles from 17° to 38°). The propeller operating limit is 2,500 rpm.

Example 4.11

A GA aircraft is equipped with a piston engine and a fixed-pitch three-blade propeller. The diameter of the prop is 1.8 m, and the hub assembly diameter is 25 cm. The prop rotates at 2,000 rpm, and the prop airfoil section achieves its best efficiency at an angle of 8°. The aircraft will cruise at 200 knots.

a. Calculate the blade pitch angle from the root to the tip such that the blade angle of attack is 8° along the blade. Plot the variations of pitch angle from hub assembly to the tip.
b. Calculate the blade twist angle.

Solution

a. The blade pitch angle from the root to the tip:
The rotational speed is 2,000 rpm, which is 209.4 rad/s. At the root of the blade (i.e., hub), the blade radius is 25/2 = 12.5 cm = 0.125 m. The helix angle is

$$\phi_r = \tan^{-1}\left(\frac{R_r\omega}{V_\infty}\right) = \tan^{-1}\left(\frac{0.125\times 209.4}{200\times 0.514}\right) = 14.3^\circ \tag{4.38}$$

where 1 knot is equivalent to 0.514 m/s.
The local blade angle at this location will be

$$\beta_r = \phi_r + \alpha = 14.3 + 8 = 22.3^\circ \tag{4.41}$$

At the tip of the blade (i.e., hub), the blade radius is 1.8/2 = 0.9 m. The helix angle is

$$\phi_t = \tan^{-1}\left(\frac{R_t\omega}{V_\infty}\right) = \tan^{-1}\left(\frac{0.9\times 209.4}{200\times 0.514}\right) = 61.4^\circ \tag{4.38}$$

The local blade angle at this location will be

$$\beta_t = \phi_t + \alpha = 61.4 + 8 = 69.4^\circ \tag{4.41}$$

For other radii, the same technique is used. Figure 4.48 illustrates the variations of blade pitch angle from the root to the tip.

b. The blade twist angle

$$\alpha_t = \phi_t - \phi_r = 61.4 - 14.3 = 47.1^\circ \tag{4.40}$$

Thus, the blade twist angle is 47°.

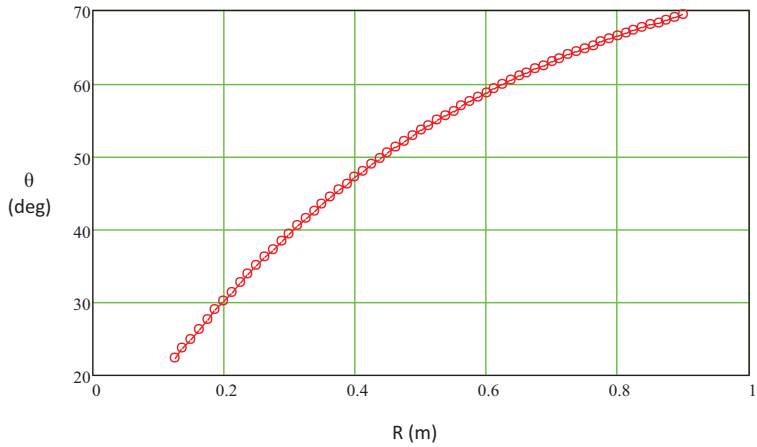

FIGURE 4.48 Blade pitch angle from the root to the tip for Example 4.11.

4.8.4.3 Modified Momentum Theory

A propeller is a rotating wing, but may be considered as an axial-flow machine without a housing. To predict the performance of a propeller, it is necessary to examine the aerodynamics of the blade in detail. The detailed analysis of a propeller is very complex and may be based on theories such as blade element theory, propeller momentum theory, and vortex theory. To calculate the thrust, one must divide a propeller into several elements and calculate thrust of each element and then add them together.

The interaction between the propeller and the airflow may be accurately computed by using high-fidelity techniques such as computational fluid dynamics (CFD) and finite element method (FEM). In practice, you need to write a computer program to predict the performance of a propeller according to the aerodynamic theories.

The modified momentum theory that provides a basic understanding of several aspects of propeller performance is reviewed in this section. This theory is just the classical momentum theory when the effect of fluid rotation is applied. It concentrates on studying the momentum and kinetic energy of the flow system. The theory is based on inviscid, incompressible flow and determines propeller induced velocity and prop efficiency. In addition, the flow velocity and pressure are assumed to be uniform over each cross section of the stream-tube.

Furthermore, the propeller is assumed to have a large number of blades, so that it becomes effectively an "actuator" disk with the thrust uniformly distributed over the disk. The axial velocity of the fluid is continuous in passing through the propeller disk to maintain continuity of the flow. Furthermore, the theory ignores the multiple effects of blade airfoil sections, blade angle of attack, and blade pitch angle.

Three fundamental principles or laws govern this theory: energy conservation, mass conservation (i.e., continuity), and momentum conservation (i.e., Newton's second law). These three laws will be applied to a control volume (stream-tube) that is assumed to extend (Figure 4.49) from a plane infinitely far upstream from the propeller to a plane infinitely far downstream.

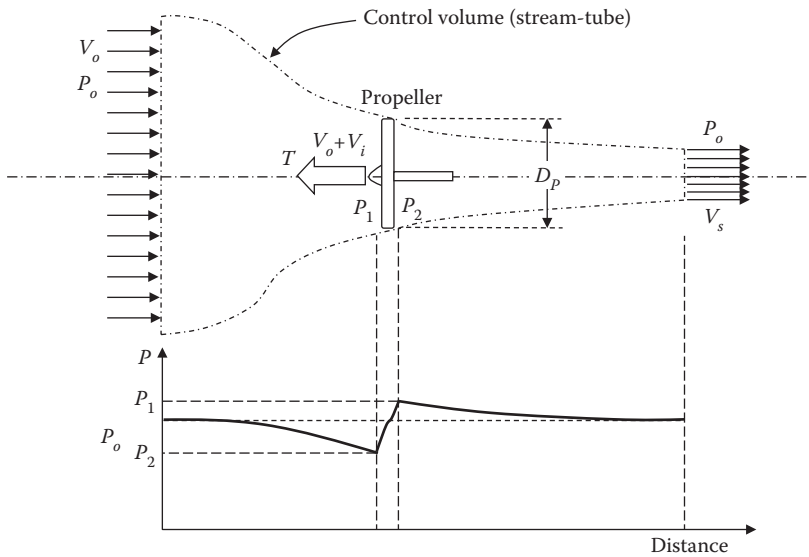

FIGURE 4.49 Momentum theory model and pressure distribution along the flow.

The fluid far upstream from the prop has the pressure P_o and the velocity V_o. The pressure just ahead of the prop is below ambient (P_1), while the pressure just after the prop is above ambient (P_2). Hence, the pressure rises to $(P_1 + \Delta P) = P_2$ immediately behind the disk and then falls to its original value, P_o. The flow velocity just ahead of the prop is increased from V_o to $V_o + V_i$ where V_i is referred to as induced velocity. The flow velocity far downstream of the prop ultimately reaches a steady-state value of stream velocity, V_s. The air density (ρ) and temperature (T) on both sides of the prop are assumed to be unchanged. On application of the conservation of mass to prop disk, we have

$$\dot{m} = \rho V A = \rho\left(V_o + V_i\right) A_P \tag{4.42}$$

where $\dot{m}$ represents the mass flow rate, and A_P is the propeller disk area.

$$A_P = \pi R_P^2 \tag{4.43}$$

where R_P is the prop radius (i.e., $D_P/2$). The assumption of incompressible flow implies that the air density across the prop disk will not change. Moreover, behind the prop, the flow velocity will be $V_o + V_i$. To include the effects of the rotation of the fluid within the slipstream, the angular velocity of the fluid is added to the equations. Due to the prop rotation, the flow behind the prop rotates with the angular velocity of ω. The circumferential velocity of the fluid due to rotation is

$$V_\theta = r\omega \tag{4.44}$$

where r is the radius of a fluid element (see Figure 4.50) from the shaft.

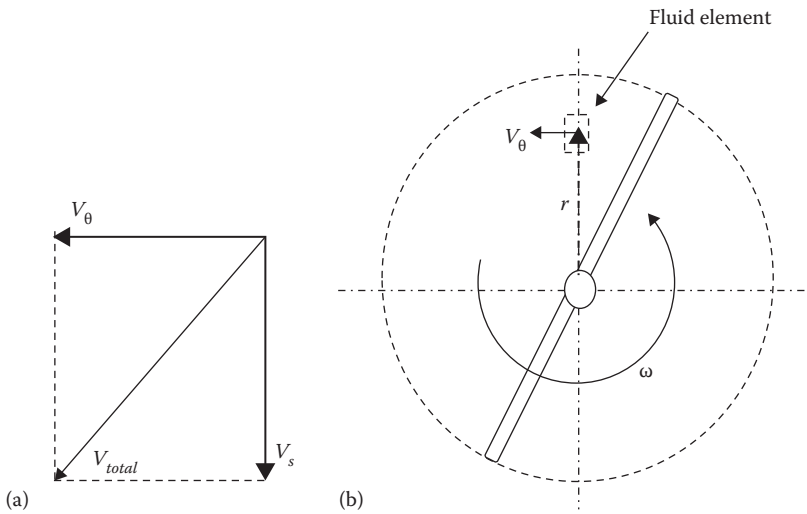

FIGURE 4.50 Circumferential velocity of the fluid. (a) Flow velocity at the exit of stream-tube (top view); (b) front view.

Applying the energy conservation law (i.e., Bernoulli's equation) to the flow before and behind the prop disk separately, but not through the disk, we obtain

$$P_o + \frac{1}{2}\rho V_o^2 = P_1 + \frac{1}{2}\rho(V_o + V_i)^2 \tag{4.45}$$

$$P_o + \frac{1}{2}\rho\left(V_s^2 + (r_s\omega)^2\right) = P_2 + \frac{1}{2}\rho\left[(V_o + V_i)^2 + (R_P\omega)^2\right] \tag{4.46}$$

where r_s is the radius of the stream-tube at the steady-state station. Comparing Equations 4.45 and 4.46 yields

$$P_2 - P_1 = \frac{1}{2}\rho\left[V_s^2 + (r_s\omega)^2\right] - \frac{1}{2}\rho\left[V_o^2 + (R_P\omega)^2\right] \tag{4.47}$$

which is the difference between the static pressure right after and right before the disk. The increase in fluid kinetic energy is the work done on the fluid by the propeller:

$$\dot{E} = \frac{1}{2}\dot{m}\left(V_s^2 - V_o^2\right) \tag{4.48}$$

The pressure of the fluid receives a sudden increment, ΔP, at the propeller disk. ΔP is equal to the axial force on a unit area of the disk, and a slipstream of increased axial velocity is formed behind the propeller.

The momentum equation (i.e., Newton's second law) states that the sum of the forces is equal to the rate of change of fluid linear momentum. Thus, the thrust (the force applied to the fluid) plus the pressure force is equal to the fluid linear momentum increase:

$$T + \int_A (P_o - P_s)\,dA = \int_A (V_s - V_o)\,d\dot{m} \tag{4.49}$$

Reference [59] derives the following expression for the thrust as the result of the integration:

$$T = 2\pi\rho R_P^2 (V_o + V_i) V_i \left[1 - \frac{2(V_o + V_i)V_i}{\omega^2 R_P^2}\right] \tag{4.50}$$

where the induced velocity, V_i, is determined from the following expression:

$$V_i = \left(\frac{V_o^3}{27} + \frac{V_P^3}{2} + \sqrt{\frac{V_P^6}{4} + \frac{V_P^3 V_o^3}{27}}\right)^{1/3} - \frac{2V_o}{3} + \left(\frac{V_o^3}{27} + \frac{V_P^3}{2} - \sqrt{\frac{V_P^6}{4} + \frac{V_P^3 V_o^3}{27}}\right)^{1/3} \tag{4.51}$$

In this equation, V_P is given by the following relationship:

$$V_P = \left[\frac{P}{2\pi\rho R_P^2}\right]^{1/3} \tag{4.52}$$

The P denotes the engine power. The prop efficiency (η_P) is defined as the ratio of the output power to the input power.

$$\eta_P = \frac{P_{\text{out}}}{P_{\text{in}}} \tag{4.53}$$

The power is defined as the applied force multiplied by the linear velocity. Therefore, the propeller output power (i.e., available power, P_A) is the thrust multiplied by the aircraft airspeed. The input power is the engine shaft power.

$$\eta_P = \frac{TV_o}{P} \tag{4.54}$$

By plugging Equations 4.50 and 4.52 into Equation 4.54 and after some manipulations, one can derive the following expression for an ideal efficiency:

$$\eta_P = \frac{V_o}{V_o + V_i} - \frac{2V_o V_i}{\omega^2 R_P^2} \tag{4.55}$$

This equation implies that the greater the percentage increase in the fluid velocity as it passes through the propeller, the lower the efficiency. A large propeller giving a small velocity increase to a large amount of air is more efficient than a small propeller.

Therefore, a propeller is not able to convert all the shaft power into thrust. Thus, part of the engine power is lost during the generation of thrust by the propeller. This engine power loss means that the net power output of the propeller is always less than the shaft power. Hence, the available power, P_A, is always less than the shaft power (i.e., P_{shaft}).

Example 4.12

A constant-speed propeller has three blades and a diameter of 2.5 m. The propeller is operating at standard sea level, and the control system maintains the fuel flow and propeller pitch such that the rotational speed and brake power are held constant at 2,500 rpm and 220 kW, respectively. Use propeller momentum theory to predict the performance of the propeller. Plot:

a. the thrust developed by the propeller and
b. the propulsive efficiency

as a function of airspeed from zero to 100 m/s.

Solution

a. The thrust developed by the propeller
At the velocity of 100 m/s

$$V_P = \left[\frac{P}{2\pi\rho R_P^2}\right]^{1/3} = \left[\frac{220\times 1{,}000}{2\times 3.14\times 1.225\times 1.25^2}\right]^{1/3} = 26.35\,\text{m/s} \tag{4.52}$$

The induced velocity, V_i, is

$$V_i = \left(\frac{V_o^3}{27}+\frac{V_P^3}{2}+\sqrt{\frac{V_P^6}{4}+\frac{V_P^3V_o^3}{27}}\right)^{1/3} - \frac{2V_o}{3} + \left(\frac{V_o^3}{27}+\frac{V_P^3}{2}-\sqrt{\frac{V_P^6}{4}+\frac{V_P^3V_o^3}{27}}\right)^{1/3} \tag{4.51}$$

which yields $V_i = 1.766$ m/s.
The thrust is

$$T = 2\pi\rho R_P^2\left(V_o+V_i\right)V_i\left[1-\frac{2\left(V_o+V_i\right)V_i}{\omega^2R_P^2}\right] \tag{4.50}$$

$$T = 2\times 3.14\times 1.225\times 1.25^2\left(100+1.766\right)\times 1.766\left[1-\frac{2(100+1.766)\times 1.766}{(261.8)^2\times 1.25^2}\right]$$

$$= 2{,}154.6\,\text{N}$$

where the rotational speed (2,500 rpm) is 261.8 rad/s.

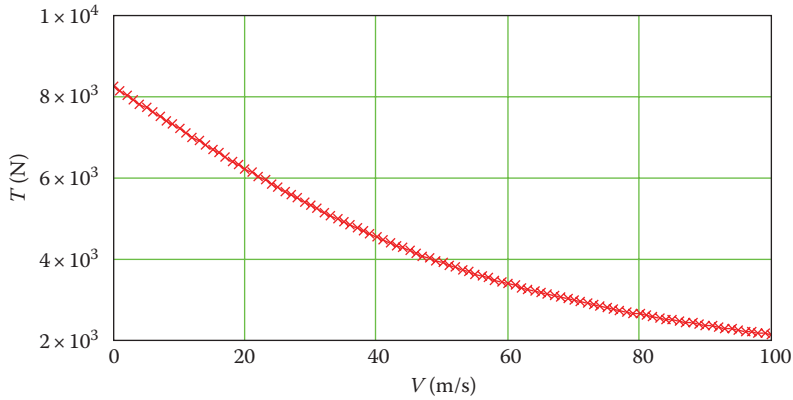

FIGURE 4.51 Variations of thrust versus velocity.

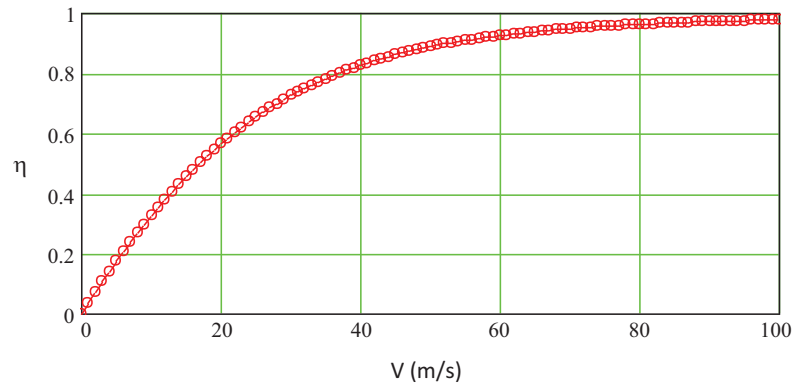

FIGURE 4.52 Variations of prop efficiency versus velocity.

b. Prop efficiency

$$\eta_P = \frac{V_o}{V_o + V_i} = \frac{2V_oV_i}{\omega^2 R_P^2} = \frac{100}{100 + 1.766} - \frac{2 \times 100 \times 1.766}{261.8^2 \times 1.25^2} = 0.979 \qquad (4.55)$$

The same result is achieved by using Equation 4.54. For other velocities, a computer code is written that produces the results as shown in Figures 4.51 and 4.52.

4.8.4.4 Practical Use of Propeller Charts

In practice, propeller performance characteristics are usually measured experimentally and published as charts and graphs. The propeller efficiency can be determined from charts, the basis of which can be a great many detailed calculations or many test points. The performance engineer normally has available both engine and propeller operating charts as supplied by the respective manufacturers. Using these charts together with knowledge of the aircraft aerodynamic characteristics, one is able to estimate the aircraft performance.

Rather than momentum theory, an alternate method is to use pressure distribution over the blade from the tip to root to find sectional lift and drag coefficients (C_l and C_d). Then, dimensionless thrust and power coefficients (C_T and C_P) are given by integration over the prop span:

$$C_T = \frac{\pi}{8}\int_{\text{root}}^{\text{tip}} \left(J^2 + \pi^2 \text{x}^2\right)\left[C_l \cos\left(\phi + \alpha_i\right) - C_d \sin\left(\phi + \alpha_i\right)\right] dx \tag{4.56}$$

$$C_P = \frac{\pi}{8}\int_{\text{root}}^{\text{tip}} x\pi\left(J^2 + \pi^2 \text{x}^2\right)\left[C_l \sin\left(\phi + \alpha_i\right) - C_d \cos\left(\phi + \alpha_i\right)\right] dx \tag{4.57}$$

where α_i is the induced angle of attack due to the angular velocity. The engine thrust, and power are obtained by

$$T = C_T \rho n^2 D^4 \tag{4.58}$$

$$P = C_P \rho n^3 D^5 \tag{4.59}$$

where n is the prop rotational speed in revolutions per second:

$$n = \frac{\omega}{2\pi} \tag{4.60}$$

The propeller efficiency can also be written [60] in terms of the coefficients of power coefficient C_P, thrust coefficient C_T, and the advance ratio J as follows:

$$\eta_P = \frac{C_T}{C_P} J \tag{4.61}$$

Figure 4.53 is a carpet plot that shows [61] variations of power and thrust coefficients (i.e., C_P and C_T) for a three-blade propeller with a Clark Y airfoil section, as a function of advance ratio (J) and blade angle (β). The blade angle in this figure is at 75% of the radius of the propeller. For instance, for advance ratio of 1.4 and blade angle of 35°, C_T and C_P are 0.08 and 0.132 respectively.

Thus, the effective thrust of a given blade is proportional to the advance ratio, J, and blade angle. These two parameters define the geometry of the blade and propeller. From Equation 4.58, the advance ratio J, plays a strong role in propeller performance.

Figure 4.54 illustrates [60] the propeller efficiency of a three-bladed propeller with Clark Y sections as a function of advance ratio for various pitch angles. For each given blade, there is one advance ratio that provide the maximum prop efficiency. For instance, if the blade angle is 40°, the maximum prop efficiency of 0.84 is achieved, when the advance ratio is 1.7.

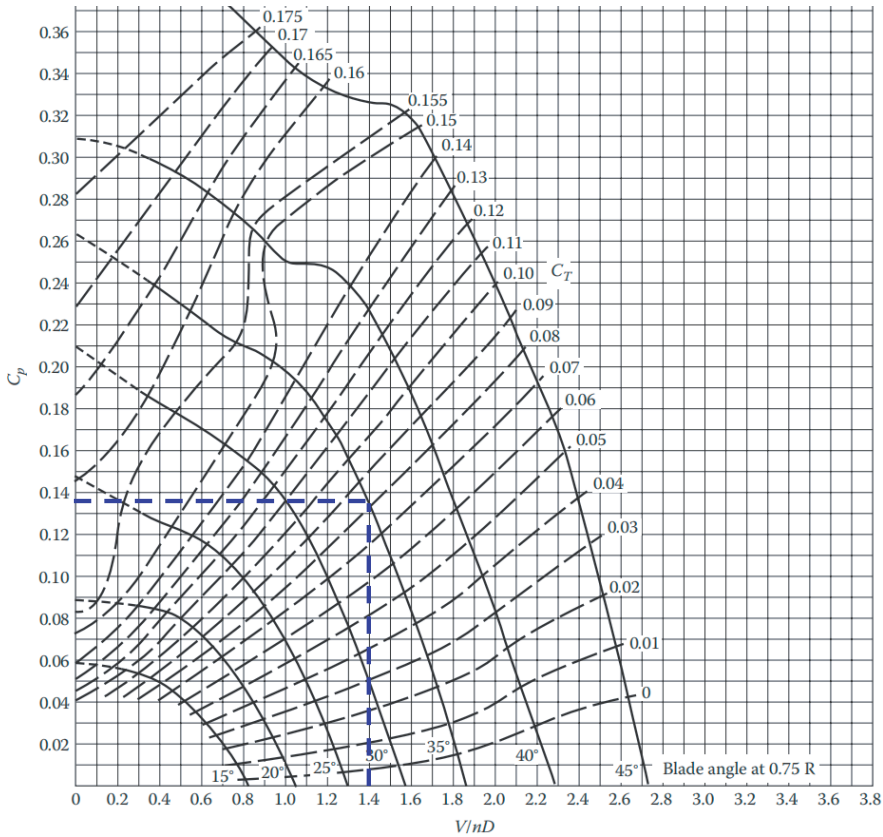

FIGURE 4.53 Power and thrust coefficients for a propeller with Clark Y airfoil section.

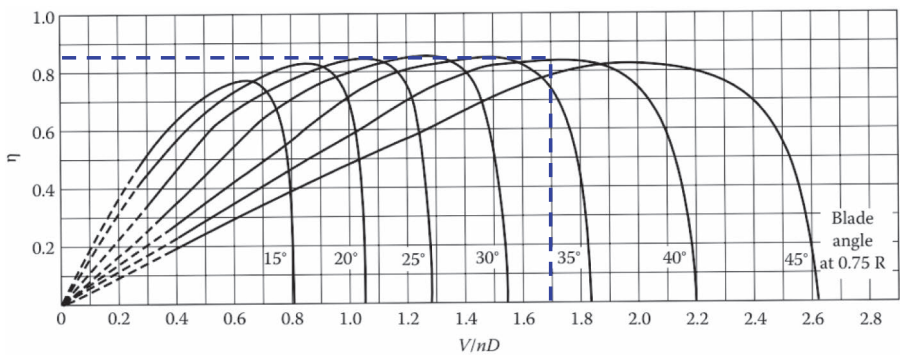

FIGURE 4.54 Propeller efficiency for a propeller with Clark Y airfoil section.

Example 4.13

A sport airplane is cruising at sea level with a speed of 200 knot. A three-blade propeller with Clark Y sections is used for its engine. The propeller with a 7.2 ft diameter is rotating at 1,500 rpm. Engine power is 250 hp.

a. If we are looking to have the maximum propeller efficiency, what should be the blade angle?
b. How much thrust this propeller can deliver at this situation?
c. Determine the propeller tip speed in terms of the Mach number.

Solution

a. Propeller efficiency

$$J = \frac{V}{nD} = \frac{200 \times 1.688}{(1{,}500/60) \times 7.2} \Rightarrow J = 1.87 \tag{4.35}$$

From Figure 4.54, we see that the propeller efficiency will be maximum when the blade angle is 42°. In this case, the propeller efficiency will be 0.85 or $\eta_P = 85\%$.

b. Thrust

$$\eta_P = \frac{TV}{P_{\text{in}}} \Rightarrow T = \frac{P\eta_P}{V} = \frac{250 \times 550 \times 0.85}{200 \times 1.688} \Rightarrow T = 325.5\,\text{lb} \tag{4.2}$$

c. Tip speed

One revolution per minute is equivalent to $2\pi/60$ rad/s.

$$V_{\text{tip}} = \sqrt{(2\pi nR)^2 + V^2}$$

$$= \sqrt{\left(2\pi \times \frac{1{,}500}{60} \times \frac{7.2}{2}\right)^2 + (200 \times 1.688)^2} \Rightarrow V_{\text{tip}} = 565.5\,\text{ft/s} \tag{4.41}$$

The speed of sound at sea level is 1,116 ft/s.

$$M = \frac{V}{a} = \frac{565.5}{1116} = 0.59 \tag{1.34}$$

Therefore, although the aircraft is cruising with a speed of Mach 0.3, the propeller tip experiences a Mach of 0.591.

PROBLEMS

4.1 A single-engine aircraft is cruising at a speed of 200 knot. If the aircraft drag is 270 lb, determine the power that its engine (jet) is generating.

4.2 A turboprop engine of a transport aircraft is providing 596 kW. The propeller is generating 3,200 N of thrust. If the aircraft is cruising at a speed of 280 knot, determine the efficiency of the propeller.

4.3 A twin-turbojet airplane is cruising at 9,000 m altitude with a speed of Mach 1.5. Each engine is consuming 200 kg of air per second. The engine exit flow has a pressure of 32,000 Pa with a velocity of 850 m/s. The exit area of the engine nozzle is 1.4 m^2. Assume that the aircraft is flying under ISA conditions. How much thrust are both engines generating?

4.4 A cargo aircraft with two turbofan engines is cruising with a speed of Mach 0.5 at 10,700 m. The airflow of core of each engine is 80 kg/s and the airflow of fan (bypass) of each engine is 150 kg/s. The flow exit velocity of the core is 400 m/s, and the flow exit velocity of the fan is 300 m/s. Determine the total thrust.

4.5 A solid-fuel rocket engine is operating at 25 km above sea level. The engine is exerting 250 kg of hot gas per second from its exit nozzle. The gas has an exit pressure of 10,000 Pa, and exit velocity is 1,258 m/s. The exit area of the nozzle is 0.3 m^2. What is the net thrust that is produced by this engine?

4.6 A jet aircraft is flying at a speed of Mach 0.85 at 7,600 m altitude. If the exit flow of the jet engine has a velocity of 550 m/s, determine the propulsive efficiency of this engine.

4.7 A fighter aircraft with a turbofan engine is cruising at a speed of Mach 1.4 at 50,000 ft altitude. The aircraft generates 20,000 N of drag, and the engine fuel has a heating value of 52,200 kJ/kg. The airflow rate is 30 kg/s, the fuel flow rate is 0.6 kg/s, and gas exits the nozzle at a velocity of 950 m/s. Determine the thermal, propulsive, and overall efficiencies of this turbofan engine.

4.8 A piston engine of an aircraft is generating 600 hp of power. The aircraft is traveling for 2 h. The engine is consuming 926 lb of fuel for this trip. Calculate SFC of this engine in terms of lb/h/hp.

4.9 A turbofan engine has a maximum thrust of 3,372 lb at sea level. Determine its maximum thrust at 10,000 ft pressure altitude and ISA condition.

4.10 Determine the maximum thrust of the engine of Problem 4.9 at 12,000 m and ISA condition.

4.11 Determine the maximum thrust of the engine of Problem 4.9 at 12,000 m and ISA + 20 condition.

4.12 A turboprop engine with a maximum power of 450 hp is flat rated up to 10,000 ft altitude. Calculate its maximum power at 5,000, 15,000, and 25,000 ft altitudes.

4.13 A turboprop engine is flat rated at 700 kW to 30°C. Calculate its maximum power at 1,200 m and 10°C.

4.14 A piston engine has a maximum power of 450 hp at sea level. What is its maximum power at 5,000 ft and ISA-12 condition?

4.15 A single-engine aircraft has a piston engine with a maximum power of 250 hp. The stall speed is 70 KEAS and propeller efficiency is 0.75. Is this aircraft able to cruise at 20,000 ft altitude if the drag is assumed to be 270 lb?

4.16 A transport aircraft with three turbofan engines is cruising at 40,000 ft altitude with a speed of 480 knots. Each engine generates 22,480 lb of thrust at sea level. The lift and drag coefficients are 0.1 and 0.05, respectively. Determine the aircraft weight.

4.17 The transport aircraft Antonov An-32 with two turboprop engines has the following features:

$$m = 26{,}000\,\text{kg}, S = 75\,\text{m}^2, P_{\text{total}} = 6{,}250\,\text{kW},$$

$$C_{D_o} = 0.028, \text{SFC} = 0.6\,\text{lb/h/hp}, \eta_P = 0.84, b = 29.2\,\text{m}, e = 0.76$$

If the aircraft is cruising at a speed of 250 knots at sea level for 6 h, how much fuel is consumed?

4.18 The fighter aircraft Super Etendard with a turbojet engine has the following features:

$$m = 12{,}000\,\text{kg}, S = 28.5\,\text{m}^2, T_{\text{max}} = 50{,}000\,\text{N}, \text{SFC} = 0.7\,\text{N/h/N}$$

a. Assume the drag coefficient (C_D) – for the maximum speed at 30,000 ft – is 0.04, determine the maximum speed at this altitude?
b. If the aircraft is required to travel a distance of 3,000 km, how much fuel will be needed (in kg) for this velocity?

4.19 The transport aircraft Boeing 747-100 (Figure 8.10b) has four turbofan engines. The variation of the engine thrust versus velocity is modeled using the following relationship:

$$T = 46{,}100 - 46.7\,V + 0.046\,V^2$$

where
T is in terms of pound
V in feet per second

a. Plot the variation of thrust versus velocity up to Mach 0.9 at sea level.
b. If the aircraft is cruising at 35,000 ft with Mach 0.9, how much would the total thrust be?

4.20. A prop-driven aircraft is cruising at a speed of 103 m/s. If the aircraft drag is 1,200 N and prop efficiency is 0.76, determine the power that its engine is providing.

4.21. A GA aircraft is cruising at sea level at a speed of 135 knots. The propeller with a 6.23 ft diameter is rotating at 1,800 rpm. Engine power is 150 hp. The variation of the propeller efficiency versus advance ratio for several blade pitch angles is given in Figure 4.55.

a. If we are looking to have maximum propeller efficiency, what should be the blade angle?
b. What is maximum propeller efficiency?
c. How much thrust this propeller can deliver in this situation?
d. Determine the propeller tip speed in terms of the Mach number.

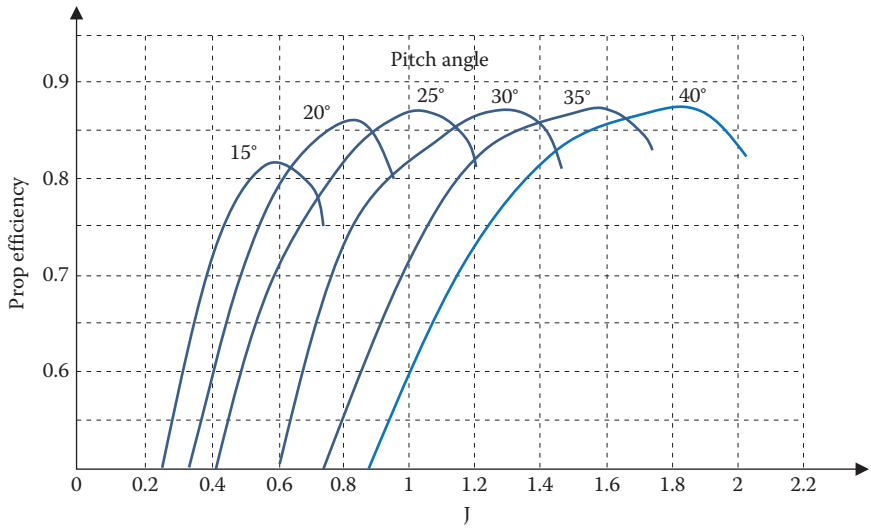

FIGURE 4.55 Propeller efficiency for a GA aircraft as a function of advance ratio and pitch angle.

4.22 A transport aircraft with a weight of 160,000 lbf and a wing area of 4,700 ft^2 has a maximum lift coefficient of 2.1. Is this aircraft able to cruise at an altitude of 16,400 ft and ISA condition with the speed of 270 knot true airspeed (KTAS)? Engine thrust at sea level is 30,000 lbf. Assume that the aircraft drag polar is $0.024 + 0.05\, C_L^2$ and the engine thrust is aligned with the flight path direction.

4.23 A prop-driven aircraft is cruising at 300 knots at 15,000 ft altitude. The propeller has a diameter of 8.2 ft and is rotating at 2,000 rpm. What should be the prop blade angle at the tip in order for the blade to have 7° of angle of attack at the tip?

4.24 An ultralight aircraft is equipped with a piston engine and a fixed-pitch two-blade propeller. The diameter of the prop is 1.2 m, and the hub assembly diameter is 15 cm. The prop rotates at 1,500 rpm, and the prop airfoil section achieves its best efficiency at an angle of 8°. The aircraft will cruise at 46.3 m/s.

a. Calculate the blade pitch angle from the root to the tip such that the blade angle of attack is 4° along the blade. Plot the variations of pitch angle from hub assembly to the tip.
b. Calculate the blade twist angle.

4.25 An amphibian aircraft is equipped with a piston engine and a fixed-pitch two-blade propeller. The diameter of the prop is 1.5 m, and the hub assembly diameter is 20 cm. The prop rotates at 1,700 rpm, and the prop airfoil section achieves its best efficiency at an angle of 5°. The aircraft will cruise at 46.3 m/s.

a. Calculate the blade pitch angle from the root to the tip such that the blade angle of attack is 2° along the blade. Plot the variations of pitch angle from hub assembly to the tip.
b. Calculate the blade twist angle.

4.26 A constant-speed propeller has two blades and a diameter of 5.9 ft. The propeller is operating at standard sea level, and the control system maintains the fuel flow and propeller pitch such that the rotational speed and brake power are held constant at 2,100 rpm and 250 hp, respectively. Use propeller momentum theory (include the effect of slipstream rotation) to predict the performance of the propeller. Including the effect of slipstream rotation, plot
a. the thrust developed by the propeller and
b. the propulsive efficiency
as a function of airspeed from 0 to 160 knots.

4.27 A constant-speed propeller has four blades and a diameter of 2.1 m. The propeller is operating at standard sea level, and the control system maintains the fuel flow and propeller pitch such that the rotational speed and brake power are held constant at 2,300 rpm and 298 kW, respectively. Use propeller momentum theory (including the effect of slipstream rotation) to predict the performance of the propeller. Including the effect of slipstream rotation, plot
a. the thrust developed by the propeller and
b. the propulsive efficiency
as a function of airspeed from 0 to 120 m/s.

4.28 A homebuilt aircraft is cruising at 10,000 ft altitude with a speed of 160 knot. A three-blade propeller with Clark Y sections is used for its engine. The propeller with 5.9 ft diameter is rotating at 1,800 rpm. The engine power is 180 hp.
a. If we are looking to have the maximum propeller efficiency, what should be the blade angle?
b. How much thrust this propeller can deliver in this situation?
c. Determine the propeller tip speed in terms of the Mach number.

4.29 A rocket engine has a chamber pressure of 200 atm and the throat area is 0.3 m^2. Assuming that the nozzle is perfectly expanded with a gas ratio of specific heats of 1.32 and the ambient pressure is 0.85 atm, calculate the engine thrust.

4.30 Determine the total energy supplied by a 50 Ah 3.2 V Li-Po (Lithium Polymer) battery, and the total energy and the maximum power that can be provided to an electric engine.

4.31 Variations of a turbofan engine thrust as a function of aircraft speed – during takeoff – is modeled by the following equation:

$$T = 30,000 + 20V + 0.01V^2$$

where V is in ft/s, and T is in lbf.

a. Plot the variations of engine thrust as a function of speed – from rest up to rotation speed (80 knots = 135 ft/s).
b. Determine the percentage of thrust increment when aircraft reaches the rotation speed.

4.32 Variations of the engine power as a function of altitude for a turboprop engine are given below:

Altitude (ft)	***P* (hp)**
0	1,425
10,000	1050
15,000	860
20,000	725
22,600	630
30,000	450
35,000	400

Assume the variations are modeled with Equation 4.22. Derive the value of m.

4.33 The maximum power of an Allisson V-1710 turbo-supercharged piston-prop of the Lockheed P-38 Lightning at sea level is 1,425 hp. The critical altitude for the turbo-supercharger is 15,000 ft. Determine engine's maximum power at 35,000 ft.

4.34 The SFC of a Rolls-Royce (Allison) T56 turboprop engine – employed by the Lockheed C-130 Hercules military transport aircraft – is 0.47 lb/h/hp or 79.43 μg/J of fuel at takeoff. The C-130J is equipped with four Allison AE2100D3 turboprop engines, each rated at 4,591 shaft horsepower (3,425kW). Consider the average engine power during takeoff is 90% of the maximum engine power, and it takes 40 s to clear the 15 m obstacle. How much fuel (in pound) is consumed during takeoff?

4.35 The SFC of a Pratt and Whitney PW2000 turbofan engine – employed by McDonnell Douglas/Boeing C-17 Globemaster – is 9.69 mg/Ns (0.342 lb/h/lb) at takeoff. The C-17 Globemaster is equipped with four engines, each rated at 40,440 lbf (179.9 kN). Consider the average engine thrust during takeoff is 90% of the maximum engine thrust, and it takes 45 s to clear the 15 m obstacle. How much fuel (in kg) is consumed during takeoff?

4.36 The small, unmanned aircraft AeroVironment RQ-11 Raven is equipped an electric engine with the power 400 W. Determine engine's power at 500 m.

5 Straight-Level Flight – Jet Aircraft

5.1 INTRODUCTION

A regular civil flight operation usually includes takeoff, climb, cruise, turn, descend, and landing (Figure 2.8). A civil aircraft is in cruising flight for much of the duration of its flight. Cruising flight is a major part of an air mission and is defined as a straight-line flight where the velocity and altitude are often kept almost constant. In other words, there will be no climbing and descending in cruising. In this book, we begin the performance analysis of different flight phases from the simplest one, that is, straight-line level flight.

This chapter and Chapter 6 are devoted to the investigation of various flight parameters of an aircraft when it is in cruising flight. In Chapter 4, we classified aircraft engines into two main groups: propeller-driven engines (piston prop and turboprop) and jet engines (turbojet and turbofan). The main difference is that the output of a jet engine is thrust (T), whereas the output of a prop-driven engine is power (P), but the power is converted to thrust by its propeller.

Because of this difference, the derivations of basic relationships and applied equations for these two groups of aircraft are implemented independently, and the results are considerably dissimilar. Therefore, the analysis of aircraft performance in cruising flight is presented in Chapters 5 and 6. The performance of aircraft with turbojet and turbofan engines in straight-line level flight is introduced in this chapter, while in Chapter 6, the performance of aircraft with piston prop and turboprop engines in straight-line level flight is presented.

This chapter is of critical importance, since the conceptual design of major components of powered aircraft such as wing and horizontal tail is based on satisfying the requirements in this flight phase. On the other hand, the easiest flight operation is the cruising flight such that the automatic flight control of civil transport airplane is realizable and currently operational in most transport aircraft. If the reader does not capture the fundamentals of cruising flight, they would find it difficult to understand the other flight phases.

This chapter is organized as follows: First, basic equations in straight-line level flight are introduced and derived. Then, the methods to evaluate the following performance criteria are discussed: (1) specific speeds in straight-line level flight, (2) range, (3) endurance, and (4) ceiling.

The specific speeds in straight-line level flight include maximum speed, cruising speed, minimum drag speed, maximum range speed, speed for absolute ceiling, and maximum endurance speed. These topics are discussed for jet aircraft, and in Chapter 6, they are reintroduced for prop-driven aircraft. In this chapter, several statistical tables have been prepared to illustrate the real data of current aircraft performance

DOI: 10.1201/9781003279068-5

specifications. They provide the reader with a feeling of how a given aircraft is performing. For the purpose of simplicity, we sometimes use "cruising flight" instead of "straight-line level flight". Although, velocity is a "vector" quantity and speed is a "scalar" value, in this book, we use both velocity and speed interchangeably, but we mean a vector quantity in both cases. In majority of the cases, when we use the term "speed" or "velocity", we actually mean aircraft "airspeed".

5.2 FUNDAMENTAL EQUATIONS

This section deals with the fundamental equations and basic parameters that are employed in various performance specifications of cruising flight. They are derived here and then will be applied in later sections to derive various relationships to evaluate cruising flight performance. The equations and parameters are steady-state trim equations, relationship between drag and thrust with speed, relationship between speed and angle of attack, and maximum lift-to-drag ratio.

5.2.1 Steady-State Longitudinal Trim Equations

The most fundamental equations of motion in cruising flight are based on Newton's second law. The straight-line level cruising flight is un-accelerated (e.g., constant cruising speed). In such a case, the equations are simplified as follows:

$$\sum F_x = 0 \tag{5.1}$$

$$\sum F_z = 0 \tag{5.2}$$

In x-z plane, there are mainly four external forces (See Figure 2.6), that include aircraft weight (W), engine thrust (T), drag (D), and lift (L), as derived in Chapters 2–4. Due to equilibrium state, along x and z axes, sum of the forces are zero. Thus, force equations of motion (See Figure 5.1) that govern the straight-line flight are:

$$T\cos(\alpha + i_T) = D \tag{5.3}$$

$$W = L + T\sin(\alpha + i_T) \tag{5.4}$$

where α is the aircraft angle of attack, (shown in Figure 5.1) and i_T is the engine thrust setting angle. Both angles are very small (often $<5°$) and can be neglected. Thus, we can express the equations as:

$$T = D \tag{5.5}$$

$$W = L \tag{5.6}$$

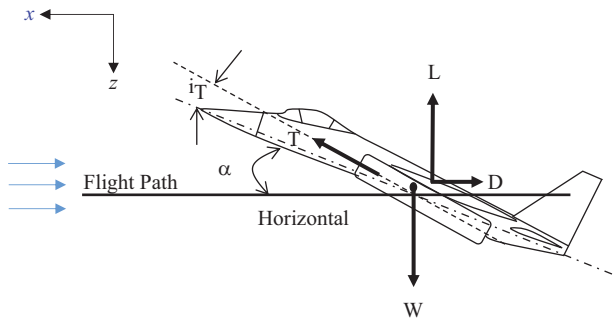

FIGURE 5.1 Equilibrium of forces in a straight-line level flight.

Inserting the relationships for lift and drag from Equations 2.4 and 2.5 yields

$$T = \frac{1}{2}\rho V^2 S C_D \tag{5.7}$$

$$mg = \frac{1}{2}\rho V^2 S C_L \tag{5.8}$$

According to these equations, the engine must produce enough thrust to counteract the drag force, and the aircraft (mainly wing) must generate enough lift force to balance the weight. This implies that the aircraft is in a longitudinal trim or equilibrium state.

Example 5.1

A jet transport aircraft with a mass of 120,000 kg is cruising with a speed of 200 m/s at sea level. If the drag force is 290,000 N, the aircraft angle of attack is 3°, and the engine setting angle is 4°,

How much thrust the engine is producing?

How much lift force the aircraft is providing?

Solution

$$D = T\cos(\alpha + i_T) \Rightarrow T = \frac{D}{\cos(\alpha + i_T)} = \frac{290{,}000}{\cos(3+4)} \Rightarrow T = 292{,}177.8\ \text{N} \tag{5.3}$$

$$W = L + T\sin(\alpha + i_T)$$

$$\Rightarrow L = W - T\sin(\alpha + i_T) = (120{,}000 \times 9.81) - \left(292{,}177.8\ \sin(3+4)\right) \tag{5.4}$$

$$\Rightarrow L = 1{,}141{,}592.5\ \text{N}$$

5.2.2 Drag, Thrust, and Velocity Relationship

When an aircraft is flying in a straight line at a constant-altitude, if the pilot applies more throttle setting, the thrust will be increased and then the aircraft speed will be increased accordingly. In addition, as the velocity is increased, the drag is increased as well. The velocity is increased until the drag and thrust become equal. Therefore, for each value of aircraft weight and engine thrust, there is at least one airspeed (often two) that satisfies the longitudinal trim condition.

The variations of aircraft drag and engine thrust as functions of velocity at a particular altitude are shown in Figure 5.2. It is assumed that the engine thrust is independent of aircraft velocity. As we expect, the aircraft drag is a nonlinear function of velocity (parabolic). The drag curve is a parabola and has a minimum value. Four velocities in this figure are worth noting. The thrust is a required thrust, but the drag is a produced drag in any particular speed. In other words, the thrust is the producer of the velocity, but the velocity is the producer of drag. The following conclusions could be made by considering Equation 5.3 and Figure 5.2:

- There are low engine thrusts such as T_1 that they are not enough for cruising flight. Since there is no intersection between any thrust line and the drag curve, it follows that, the aircraft is not able to have cruising flight at such thrust values.
- At any thrust that is less than the maximum and more than T_2, the thrust line has two intersections with the drag curve. This means that the aircraft may have two cruising velocities at such particular thrust. In other words, there are two different cruising velocities where the aircraft is producing the same drag. The reason for this is that there is a huge increase in induced drag at low velocities due to high lift coefficient.
- The thrust T_2 is a minimum thrust where cruising flight is possible. This velocity is referred to as minimum drag velocity $\left(V_{\min_D}\right)$. In this case, there is only one intersection between the drag curve and thrust lines.
- If the pilot employs the maximum engine thrust ($T_{\max}$) at any particular altitude, the aircraft will have its maximum velocity at that particular altitude.

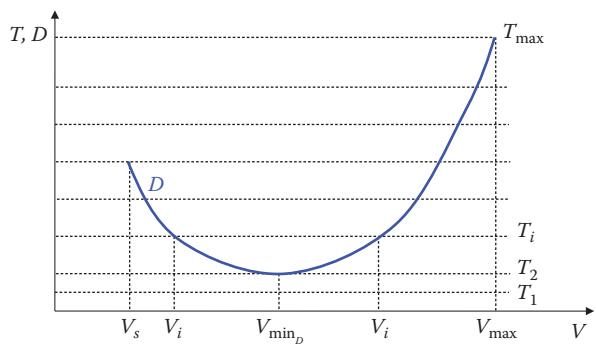

FIGURE 5.2 Variations of drag and thrust as functions of velocity.

Example 5.2

An aircraft with a mass of 2,500 kg, a wing area of 18 m^2, and a drag coefficient of 0.04 is cruising with a speed of 160 knots (82.3 m/s) at a constant-altitude. If the pilot increases the engine thrust by 20%, calculate the initial acceleration and the final velocity. You may assume the drag coefficient is constant throughout this flight and the aircraft is flying at sea-level ISA condition.

Solution

In a cruising flight with a constant-altitude, the thrust is equal to the drag, while the drag is equal to

$$D = \frac{1}{2}\rho V^2 S C_D \tag{3.1}$$

Thus,

$$T_1 = D_1 = \frac{1}{2}\rho V_1^2 S C_D = \frac{1}{2}\times 1.225 \times (160 \times 0.5144)^2 \times 18 \times 0.04 \Rightarrow T_1 = 2{,}987.3N \tag{5.5}$$

When the engine thrust is increased by 20%,

$$T_1 = D_1 = ma \Rightarrow a = \frac{T - D}{m} = \frac{(1.2 \times 2{,}987.3) - 2{,}987.3}{2{,}500} \Rightarrow a = 0.239 \text{ m/s}^2 \tag{5.5}$$

This acceleration will increase the aircraft velocity until the drag is equivalent to the thrust

$$\begin{aligned} T_2 = D_2 \Rightarrow 1.2T_1 &= \frac{1}{2}\rho V_2^2 S C_D \\ \Rightarrow V_2 &= \sqrt{\frac{1.2T_1}{(1/2)\rho S C_D}} = \sqrt{\frac{1.2 \times 2{,}987.3}{0.5 \times 1.225 \times 18 \times 0.04}} \\ &= 90.16 \text{ m/s} = 175.27 \text{ knot} \end{aligned} \tag{5.5}$$

The ratio between the new speed and the previous speed is

$$\frac{V_2}{V_1} = \frac{175.27}{160} = 1.1$$

It means that the aircraft velocity is increased 10%, although the thrust is increased by 20%.

5.2.3 Velocity–Angle-of-Attack Relationship

The straight-line sustained level flight is possible at any permissible velocity. A permissible velocity is defined as any airspeed equal to or higher than the stall speed and

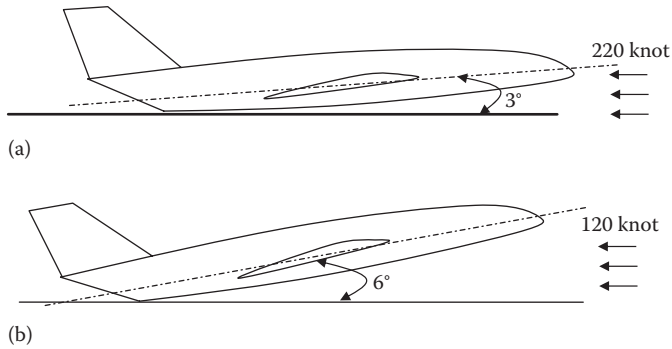

FIGURE 5.3 One aircraft in two different cruising flight conditions. (a) $V = 220$ knot, $\alpha = 3°$; (b) $V = 120$ knot, $\alpha = 6°$.

equal or less than the maximum speed. For an aircraft to stay in the air, it must provide enough lift through its aerodynamic components. The aircraft cannot produce a sufficient lift force if the velocity is less than the stall speed. The aircraft also is not able to generate sufficient thrust to have velocity higher than its maximum velocity. If a pilot needs to maintain the altitude (where air density is constant), he/she must maintain the lift force equal to the weight of the aircraft.

Equation 5.8 implies that to change the airspeed in a cruising flight with a constant aircraft weight, the lift coefficient (C_L) should be inversely varied. To increase the airspeed, the lift coefficient (C_L) needs to be decreased, and to reduce the airspeed, the lift coefficient (C_L) needs to be increased. To vary the lift coefficient in a constant-altitude, the aircraft angle of attack, or flap deflection, must be changed. Thus, lowering the angle of attack (α) increases the airspeed, whereas increasing the angle of attack (α) reduces the airspeed.

Figure 5.3 demonstrates an aircraft in two cruising flight conditions: (1) 3° angle of attack and (2) 6° angle of attack. In both conditions, the aircraft has a constant-altitude but different velocities (220 knots and of 120 knots). In Figure 5.3a, the aircraft has 3° of α (the corresponding C_L is 0.5), since it cruises with the velocity of 220 knots. In Figure 5.3b, the aircraft has 6° of α (the corresponding C_L is 0.8), since it cruises with a lower velocity of 120 knots. Thus, a higher velocity (V) requires a lower lift coefficient (C_L) and subsequently a lower angle of attack (α). The aircraft angle of attack is often equivalent with the fuselage center line. However, the wing angle of attack is measured with respect to a reference line such as the cabin/cockpit floor.

Figure 5.4 demonstrates a typical relationship between the airspeed and the angle of attack for a cruising flight of an aircraft with a mass of 5,100 kg and a reference wing area of 25 m^2. In modern fixed-wing aircraft, the wing setting angle is fixed; therefore, a change in the aircraft angle of attack implies a change in the wing angle of attack. This figure illustrates that as the airspeed is increased, both the lift coefficient and angle of attacked are decreased. For instance, the cruising angle of attack of a supersonic aircraft such as Concorde is about 0.3°–1°, while the cruising angle of attack of a high subsonic aircraft such as Boeing 747 (Figure 8.10b) is about 3°–5°.

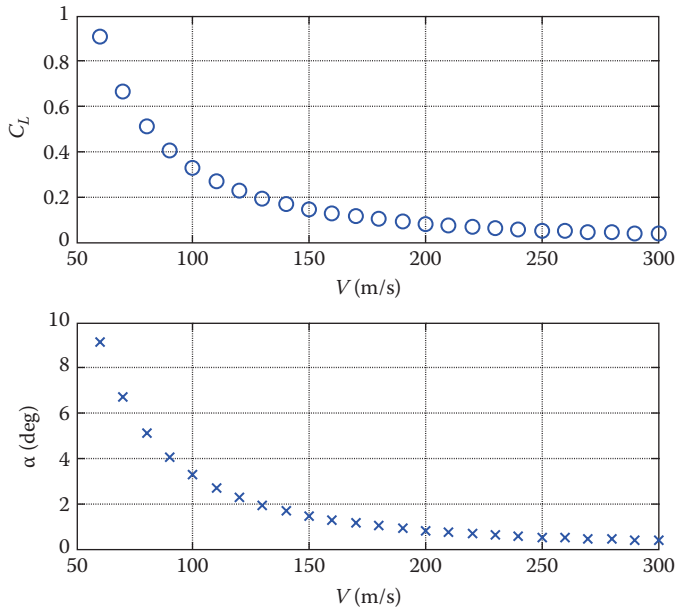

FIGURE 5.4 Typical variations of lift coefficient and angle of attack versus velocity in a cruising flight.

FIGURE 5.5 Comparison between angles of attack of a high-speed aircraft (F-35 Lightning II, left; and a low speed aircraft P-35 Lightning, right). (Courtesy of Ryosuke Ishikawa.)

The maximum allowable angle of attack (α_{max}) that is often referred to as the stall angle (α_s) corresponds with the maximum lift coefficient $\left(C_{L_{max}}\right)$. This maximum lift coefficient (C_L) in turn determines the minimum permissible velocity for a cruising flight. This velocity is referred to as the stall speed (V_s). For the aircraft in Figure 5.4, the stall angle is 9° and the stall speed is 60 m/s. Figure 5.5 compares the angles of attack of a fast supersonic aircraft (Lockheed Martin F-35 lightning II) with a slow subsonic aircraft P-35 Lightning when they are flying at the same speed. As you see, the angles of attack of supersonic aircraft are much higher than that of a subsonic aircraft, since they are designed to cruise supersonically. In this figure, old and new

Lightnings fly at Luke AFB Air Show in 2014. It is claimed that F-35 will be the last manned fighters, and in the near future, the fighters will be unmanned.

The wing is the main component (i.e., major contributor) to produce lift force for the entire aircraft. Therefore, the criterion for the maximum permissible aircraft angle of attack (or aircraft stall angle) is the wing stall angle. The wing is attached to the fuselage with an angle called wing setting angle (i_w). The wing angle of attack (α_w) is the wing setting angle plus fuselage angle of attack (α_f):

$$\alpha_w = \alpha_f + i_w \tag{5.9}$$

In other words, the pilot must always be mindful that the wing angle of attack does not reach/pass its stall angle (α_s).

5.2.4 Maximum Lift-to-Drag Ratio ($(L/D)_{MAX}$)

One of the important parameters in a cruising flight is the lift-to-drag ratio. One of the objectives in aerodynamic design of an aircraft is to design an aircraft that produces the maximum lift with a minimum drag (which corresponds to the maximum aerodynamic efficiency). In this regard, the lift-to-drag ratio plays a significant role in the aircraft design process. This design objective has multiple applications.

From Equations 5.5 and 5.6, we can conclude that for a steady, level flight; the lift-to-drag ratio is simply the reciprocal of the thrust-to-weight ratio. Thus:

$$\frac{L}{D} = \frac{W}{T} \Rightarrow T = W\left(\frac{D}{L}\right) = \frac{W}{\left(L/D\right)} \tag{5.10}$$

Mathematically, to minimize a ratio with a constant numerator, the denominator should be maximized. Recall that the minimum value of D/L is the reciprocal of the maximum value of L/D.

Hence,

$$T_{\min} = \frac{W}{\left(L/D\right)_{\max}} \tag{5.11}$$

This relationship states that if a pilot intends to have a minimum fuel consumption (i.e., minimum thrust), he/she must fly with a configuration that has a maximum lift-to-drag ratio. This configuration for any aircraft is unique, so it must already be calculated and known. In a cruising flight, the lift is equal to the aircraft weight (i.e., constant). So, to maximize the lift-to-drag ratio, simply, the drag should be minimized

$$\left(L/D\right)_{\max} \rightarrow D_{\min} \tag{5.12}$$

In effect, the question for maximizing the lift-to-drag ratio yields a question for minimizing the drag. At the beginning, it may seem that we have to have a flight with a zero angle of attack to minimize the aerodynamic drag of the airplane. This perception is incorrect because the reduction of angle of attack means an increase in the aircraft velocity, and this requires more thrust. Then, it may seem that the solution is to reduce the flight speed. This is incorrect either, because a reduction in the airspeed necessitates an increase in the angle of attack, and this often causes more drag force. Hence, we have to solve this problem analytically. The division of the lift over the drag yields

$$\frac{L}{D} = \frac{(1/2)\rho V^2 S C_L}{(1/2)\rho V^2 S C_D} = \frac{C_L}{C_D} \tag{5.13}$$

By inspection, we can readily conclude:

$$\left(\frac{L}{D}\right)_{\max} = \left(\frac{C_L}{C_D}\right)_{\max} \tag{5.14}$$

Therefore, to maximize the lift-to-drag ratio, one should maximize the ratio of lift coefficient to the drag coefficient. In Chapter 3, the drag polar was defined (Equation 3.12) as

$$C_D = C_{D_o} + KC_L^2 \tag{5.15}$$

This can be plugged into the ratio of lift coefficient to drag coefficient as follows:

$$\frac{C_L}{C_D} = \frac{C_L}{C_{D_o} + KC_L^2} \tag{5.16}$$

The aircraft lift-to-drag ratio is mainly a function of lift coefficient. To find the maximum C_L/C_D, one must differentiate Equation 5.16 with respect to lift coefficient and set the result equal to zero (i.e., zero slope):

$$\frac{d}{dC_L}\left(\frac{C_L}{C_D}\right) = \frac{C_{D_o} + 2KC_L^2 - 2KC_L C_L}{\left(C_{D_o} + KC_L^2\right)^2} \tag{5.17}$$

If we set the right-hand side equal to zero, we obtain

$$C_{D_o} + KC_L^2 - 2KC_L C_L = 0 \tag{5.18}$$

or

$$C_{D_o} = KC_L^2 \tag{5.19}$$

TABLE 5.1
Typical Maximum Lift-to-Drag Ratio for Various Aircraft

No.	Aircraft Type	$(L/D)_{max}$
1.	Sailplane (glider)	30–40
2.	Jet transport	15–20
3.	Light GA	10–15
4.	Subsonic fighter	7–10
5.	Supersonic fighter	4–7
6.	Helicopter	3–5
7.	Quadcopters	2–6
8.	Homebuilt	6–10

Substitution of Equation 5.19 into Equation 5.15 yields

$$C_{D_{(C_L/C_D)_{\max}}} = 2C_{D_o} \tag{5.20}$$

This implies that when the lift-to-drag ratio is at its maximum value, the drag coefficient will be twice the zero-lift drag coefficient. In other words, the zero-lift drag coefficient will be equal to the induced drag coefficient

$$C_{D_o} = C_{D_i} \tag{5.21}$$

Every aircraft has a unique maximum lift-to-drag ratio. Table 5.1 demonstrates the maximum lift-to-drag ratio for several airplane categories.

To calculate this parameter, Equation 5.19 is inserted into Equation 5.16

$$\left(\frac{C_L}{C_D}\right)_{\max} = \frac{C_L}{KC_L^2 + KC_L^2} = \frac{C_L}{2KC_L^2} = \frac{1}{2KC_L} = \frac{1}{2KC_{L_{(C_L/C_D)_{\max}}}} \tag{5.22}$$

Furthermore, when the lift-to-drag ratio is at its maximum value, from Equation 5.23, we obtain

$$C_{L_{(C_L/C_D)_{\max}}} = \sqrt{\frac{C_{D_o}}{K}} \tag{5.23}$$

When this lift coefficient is plugged into Equation 5.17, the following equation is obtained:

$$\left(\frac{C_L}{C_D}\right)_{\max} = \frac{1}{2\sqrt{KC_{D_o}}} \tag{5.24}$$

With this relationship, one is able to evaluate the maximum lift-to-drag ratio of any aircraft. The only necessary information is the aircraft zero-lift drag coefficient $\left(C_{D_o}\right)$ and the induced drag correction factor (K).

Equation 5.23 is a mathematical expression, and the theoretical value of $C_{L(C_L/C_D)_{\max}}$ must be within a practical flight limit. The value of $C_{L(C_L/C_D)_{\max}}$ from Equation 5.23 cannot be more than the aircraft maximum lift coefficient $\left(C_{L_{\max}}\right)$. If the output of the equation is more than $C_{L_{\max}}$, ignore the outcome and select a new value slightly less than $C_{L_{\max}}$. The Northrop Grumman RQ-4 Global Hawk [62], a long-range unmanned aerial vehicle (UAV) with a mass of 11,600 kg and a wing area of 50.2 m^2 has a $\left(L/D\right)_{\max}$ of 33.

The Scaled Composites Model 311 Virgin Atlantic GlobalFlyer, a long-range aircraft for record attempt with a mass of 10,024 kg a wing area of 37.16 m^2 and a wing aspect ratio of 32.6 has a $\left(L/D\right)_{\max}$ of 37. The aircraft first flew a solo nonstop flight by Steve Fossett around the world in slightly more than 67 h (2 days 19 h). The flight speed of 551 km/h set the world record for the fastest nonstop non-refueled circumnavigation, beating the mark set by Voyager aircraft at 9 days 3 min and a top speed of 196 km/h. In February 2006, Fossett flew the GlobalFlyer for the longest aircraft flight distance in history: 25,766 miles (41,466 km).

Case Study - Example 5.3

The aircraft Cessna Citation II has the following features:

$$C_{D_o} = 0.022, e = 0.85, \text{AR} = 8.3,\ m = 6{,}032\,\text{kg},\ S = 30\,\text{m}^2, a = 5.9\ 1/\text{rad},$$
$$V_s = 82\,\text{knot}, T_{\max} = 22{,}240\,\text{N}$$

- Determine the maximum lift-to-drag ratio.
- What is the angle of attack corresponding to the maximum lift-to-drag ratio (at sea level)? Assume $\alpha_o = 0$.
- What is the airspeed corresponding to the maximum lift-to-drag ratio (at sea level)?
- What is the minimum required thrust for this aircraft to fly?

Solution

$$K = \frac{1}{\pi \cdot e \cdot \text{AR}} = \frac{1}{3.14 \times 0.85 \times 8.3} \Rightarrow K = 0.045 \tag{3.8}$$

$$\left(\frac{C_L}{C_D}\right)_{\max} = \frac{1}{2\sqrt{KC_{D_o}}} = \frac{1}{2\sqrt{0.045 \times 0.022}} \Rightarrow \left(\frac{C_L}{C_D}\right)_{\max} = 15.89 \tag{5.24}$$

$$C_L = \sqrt{\frac{C_{D_o}}{K}} = \sqrt{\frac{0.022}{0.045}} \Rightarrow C_L = 0.69 \tag{5.23}$$

$$a = \frac{dC_L}{d\alpha} \Rightarrow 5.9 = \frac{0.69}{\alpha} \Rightarrow \alpha = 0.11\,\text{rad} = 6.7^\circ \tag{2.10}$$

$$W = \frac{1}{2}\rho V^2 S C_L \Rightarrow V = \sqrt{\frac{2W}{\rho S C_L}}$$
$$\Rightarrow V = \sqrt{\frac{2\times 6{,}032\times 9.81}{1.225\times 30\times 0.69}} = 68.3\,\text{m/s} = 132.82\,\text{knot} \tag{5.8}$$

This speed is about two times the stall speed.

$$C_D = 2C_{D_o} = 2\times 0.022 = 0.044 \tag{5.20}$$

$$T = \frac{1}{2}\rho V^2 S C_D = 0.5\times 1.225\times (68.3)^2\times 30\times 0.044 \Rightarrow T_{\min} = 3{,}771.5\,\text{N} \tag{5.7}$$

This implies that the minimum thrust to fly is about 17% of the maximum thrust.

$$\frac{T_{\min}}{T_{\max}} = \frac{3{,}771.5}{22{,}240} = 0.17$$

This example demonstrates that if the Cessna Citation II needs to cruise with the minimum thrust at sea level, the airspeed will be 132.8 knots and that the angle of attack would be 6.7°. In this flight condition, propulsion system employs only 17% of its thrust. The lift-to-drag ratio will be at its maximum value, which is 15.89.

Figure 5.6 shows the generic variations of airfoil C_L/C_D with respect to the angle of attack for an airfoil. The variations curve of airfoil lift-to-drag ratio versus the angle of attack has a similar shape. The variations of drag and lift-to-drag ratio

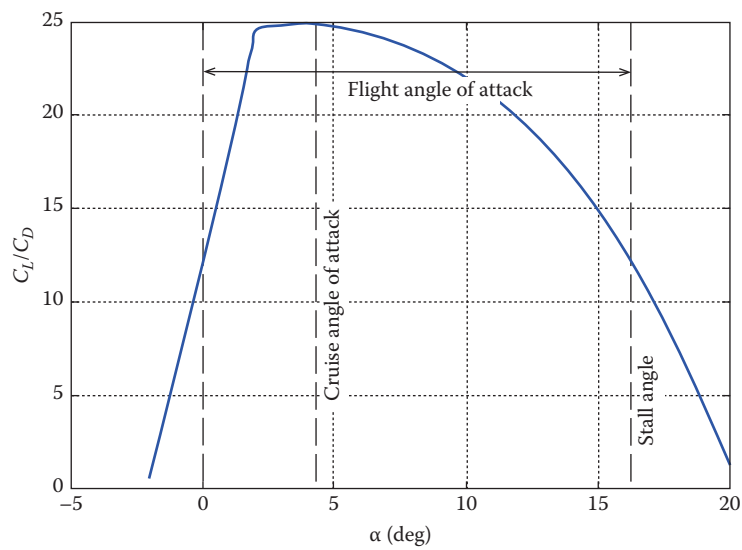

FIGURE 5.6 Typical variations of C_L/C_D with respect to angle of attack for an airfoil.

TABLE 5.2
Variations of Drag, Angle of Attack, and Lift-to-Drag Ratio for a Jet Aircraft

No.	V (knot)	α (°)	Wing L/D	Aircraft L/D	D (N)
1.	100	15	10.7	6	8,330
2.	120	9	17.2	10.6	4,720
3.	140	6	20.6	11.8	4,240
4.	160	4	22.7	12	4,170
5.	180	2.6	23.8	10.7	4,670
6.	200	1.7	22.8	8.5	5,880
7.	220	1	20.8	7.2	6,940
8.	240	0.5	18.8	6	8,330
9.	260	0.2	16.4	5.2	9,615
10.	280	0	13.9	4.5	11,110
11.	300	−0.4	12.8	3.8	13,160

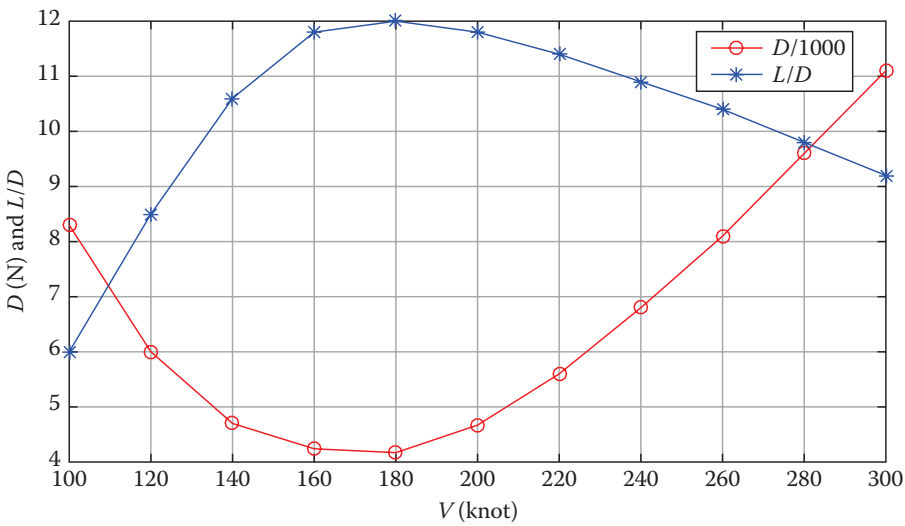

FIGURE 5.7 The variations of drag and lift-to-drag ratio versus speed for a jet aircraft.

versus speed for a jet aircraft with a mass of 5,000 kg are demonstrated in Table 5.2. This graphical representation of this table is sketched in Figure 5.7.

It is noticed that the lift-to-drag ratio reaches a maximum value of 12. In this flight condition, the drag force is at its minimum value (i.e., 4,170 N). This aircraft will have the maximum lift-to-drag ratio if it cruises with 4° of angle of attack. In general, any aircraft has one value for its maximum lift-to-drag ratio. This parameter is usually similar for a group of aircraft with similar configuration.

5.3 SPECIFIC AIRSPEEDS

An aircraft is able to have a sustained cruising flight with various airspeeds from a minimum speed to a maximum speed. The minimum speed – for a fixed-wing aircraft – is usually little more than the stall speed (about $1.1V_s$ – $1.3V_s$). The level flight at the stall speed is challenging (sometimes dangerous), but cruising flight with a velocity less than the stall speed is impossible. The reason is that the lift force would be less than weight, and hence holding altitude at this situation is not realizable. The maximum speed in cruising flight is when the pilot uses the maximum engine throttle. The minimum and maximum speeds of an aircraft depend on aircraft weight, throttle setting, flap setting, and flight altitude.

For a general aviation (GA) aircraft, the maximum speed is often about two to three times the stall speed. This ratio for jet transport aircraft is about 4–5 and for a jet fighter is about 5–15. The specific airspeeds are of significant importance for pilots and are used at specific flight conditions. A few noticeable ones are

- Maximum speed ($V_{\max}$)
- Minimum drag speed ($V_{\min_D}$)
- Speed for maximum lift-to-drag ratio ($V_{(L/D)_{\max}}$)
- Maximum range speed ($V_{\max_R}$)
- Maximum endurance speed ($V_{\max_E}$)
- Speed for absolute ceiling
- Cruise speed (V_C)

Every single airspeed of this list has one or more particular applications, and a pilot adopts one of them based on the desired mission. For instance, a jet transport aircraft is supposed to carry a payload with a minimum cost, while a fighter jet has the mission to fight with enemy fighter, or a surveillance aircraft has to fly over borders to protect it from illegal trespassing. Each aircraft must fly with a specific speed to carry its mission efficiently. Hence, knowing these speeds is a prerequisite of an economic or successful flight for a pilot. Figure 5.8 illustrates a civil transport aircraft

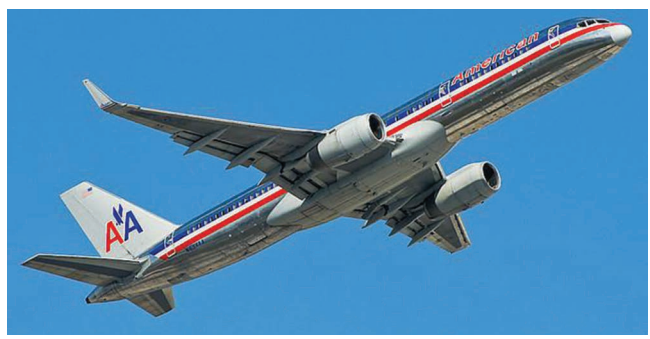

FIGURE 5.8 Boeing 757 with a cruising speed of 458 knots (Mach 0.8). (Courtesy of Gustavo Corujo—Gusair.)

Boeing 757 with two turbofan engines at cruising flight. Note that the angle of attack is considerable by inspection.

In this section, three specific airspeeds of maximum speed (V_{max}), minimum drag speed (V_{min_D}), and speed for maximum lift-to-drag ratio ($V_{(L/D)max}$) are analyzed. Four specific airspeeds of maximum range speed (V_{max_R}), maximum endurance speed (V_{max_E}), speed for absolute, and cruise speed (V_C), ceiling are discussed in Sections 5.4–5.7, respectively.

5.3.1 Maximum Speed (V_{MAX})

One of the most important performance criteria for any aircraft is its maximum speed. The maximum sustained speed in level flight is achieved when the maximum engine thrust is employed. In order for the engine to have a longer life and a lower fuel consumption, it is highly recommended not to fly with the maximum thrust in a long flight. Thus, an aircraft is rarely flown with its maximum speed. However, it is crucial for a fighter jet to succeed/survive in a battle field by flying with its maximum speed. When comparing two aircraft, one with a higher maximum speed is pronounced to have a better cruise performance.

Every year, the record of the maximum speed is registered when it is increased. The experimental aircraft X-15A – with a rocket engine – has achieved the highest maximum speed of 7,297 km/h of Mach of 6.72 on October 3, 1967. It is noticeable that this speed was obtained while X-15A was launched from another mother aircraft. The record of the highest maximum speed for an independent aircraft flight in the 1970s belonged to Lockheed SR-71 Blackbird (Figure 4.24) which achieved a velocity of 1905.8 knots (little more than Mach 3).

The current record for the maximum speed belongs to X-51 Wave Rider. The Boeing X-51 is an unmanned experimental aircraft with a scramjet engine that completed a flight of over 6 min and reached the speed of over Mach 5 for 210 s on May 1, 2013, for the longest-duration hypersonic flight.

The maximum speed of an aircraft depends on several parameters, including the engine thrust, aircraft weight, and the cruising altitude. As the weight of aircraft (e.g., passenger, luggage, cargo, store, or fuel) is decreased, the maximum speed will be increased. Due to this fact, the published value of the maximum airspeed for an aircraft (e.g., by Jane's [3]) is often based on the maximum aircraft weight and the altitude indicated.

Increase in the altitude has several impacts on flight. First, the air density is decreased with altitude, and because of this reduction, the aerodynamic forces of lift, drag, and the engine thrust all are decreased. The reduction of these three forces is not at the same rate. To compensate for the lift reduction at high altitude, the lift coefficient (in effect, the angle of attack) must be increased. But an increase in the lift coefficient will induce an increase in the drag coefficient. Simultaneously, the reduction of air density (with altitude) causes a drag reduction.

This process has dual influence, such that at low altitude, maximum speed is increased, but at high altitude causes a reduction in the maximum velocity. Thus, there is usually a specific altitude that the maximum speed reaches its absolute maximum ($V_{max_{max}}$). This altitude is one of the favorite altitudes to fly when the pilot is

going to absolutely maximize its maximum speed. Therefore, the maximum airspeed is a nonlinear function of the altitude.

Now, let us see how to analyze and calculate this absolute maximum speed and its corresponding altitude. In a cruising flight with a constant velocity, the drag force and thrust must be equal (Equation 5.5). This can be applied for a flight with the maximum speed as follows:

$$T_{\max} = D_{\max} \tag{5.25}$$

where the maximum drag – using Equation 3.1 – is:

$$D_{\max} = \frac{1}{2}\rho V_{\max}^2 S C_D \tag{5.26}$$

We already determined the drag (Equation 3.12) and lift (Equation 5.8) coefficients as

$$C_D = C_{D_o} + KC_L^2 \tag{3.12}$$

$$C_L = \frac{2W}{\rho V_{\max}^2 S} \tag{5.8}$$

By substituting Equations 5.26, 5.8, and 3.12 into Equation 5.25, we obtain

$$T_{\max} = \frac{1}{2}\rho V_{\max}^2 S C_{D_o} + \frac{2KW^2}{\rho V_{\max}^2 S} \tag{5.27}$$

In Chapter 4, the jet engine thrust is introduced as a function of altitude (air density) as follows:

$$T_{\max} = T_{\max_{SL}} \left(\frac{\rho}{\rho_o}\right)^{0.9} \qquad (\text{turbojet; troposhere}) \tag{4.21}$$

$$T_{\max} = T_{\max_{SL}} \left(\frac{\rho_{11}}{\rho_o}\right)^{0.9} \left(\frac{\rho}{\rho_{11}}\right) \quad (\text{turbojet; stratosphere}) \tag{4.25}$$

$$T_{\max} = T_{\max_{SL}} \left(\frac{\rho}{\rho_o}\right)^{1.2} \qquad (\text{turbofan engine}) \tag{4.24}$$

In these expressions, $T_{\max}$ and $T_{\max_{SL}}$ are maximum thrust at any altitude and maximum thrust at sea level, respectively. Using the dynamic pressure equation ($q = \frac{1}{2}\rho V^2$), and Equations 4.21–4.24, Equation 5.27 is expressed as:

$$q^2 S C_{D_o} - q k T_{\max_{SL}} + \frac{KW^2}{S} = 0 \tag{5.28}$$

This is a quadratic equation in q and can be solved to obtain the dynamic pressure:

$$q = \frac{kT_{\max_{SL}} \pm \sqrt{\left(kT_{\max_{SL}}\right)^2 - 4SC_{D_o}\dfrac{KW^2}{S}}}{2SC_{D_o}} = \frac{kT_{\max_{SL}} \pm \sqrt{\left(kT_{\max_{SL}}\right)^2 - 4C_{D_o}KW^2}}{2SC_{D_o}} \tag{5.29}$$

By replacing q with $\frac{1}{2}\rho V^2$ in Equation 5.29, one can obtain:

$$V_{\max} = \sqrt{\frac{kT_{\max} + \sqrt{\left(kT_{\max}\right)^2 - 4C_{D_o}KW^2}}{\rho S C_{D_o}}} \tag{5.30}$$

where factor k is:

$$k = \left(\frac{\rho}{\rho_o}\right)^{0.9} \quad \left(\text{turbojet; troposhere}\right) \tag{5.31}$$

$$k = \left(\frac{\rho_{11}}{\rho_o}\right)^{0.9} \left(\frac{\rho}{\rho_{11}}\right) \left(\text{turbojet; stratosphere}\right) \tag{5.32}$$

$$k = \left(\frac{\rho}{\rho_o}\right)^{1.2} \quad \left(\text{turbofan engine}\right) \tag{5.33}$$

Note that, k (lower case) is not the same as K (upper case).

In these equations, the parameters are as follows: S, wing area; W, aircraft weight; C_{D_o}, aircraft zero-lift drag coefficient; K, induced drag correction factor; ρ, air density at any altitude; ρ_o, air density at sea level; and ρ_{11}, air density at 11,000 m altitude. The only unknown in Equation 5.30 is the maximum speed. This equation is an algebraic nonlinear equation with the order of 4. When solving this equation, we will have four solutions. Only one solution is acceptable that is frequently the highest.

The typical variations of the maximum speed versus altitude for a jet aircraft are such that it increases at the beginning but decreases afterward. For instance, the maximum speed of supersonic heavy bomber Rockwell B-1 Lancer (Figure 5.9) at sea level is 608 knots (Mach 1.25), while at 40,000 ft is 721 knots. The maximum

FIGURE 5.9 Supersonic heavy bomber Rockwell B-1B Lancer.

airspeed has an absolute maximum (i.e., the maximum of the maximum airspeed). Every aircraft has a maximum speed at each altitude; however, the maximum of maximum speed occurs only at one altitude. This altitude depends on such parameters as aircraft weight, engine power and thrust, aircraft zero-lift drag coefficient, and configuration.

One of the reasons why airplanes fly at high altitude is the lower cost of flight. This is due to a lower fuel consumption with higher speed at high altitude, which also leads to a longer range. Table 5.3 demonstrates [3,63,64] the maximum speed of several jet aircraft. With the current technology, the highest speed of supersonic aircraft reaches Mach 3 and in special configuration could pass Mach 5. The maximum speed of a large transport aircraft (e.g., Boeing and Airbus aircraft) is about Mach 0.95.

The supersonic transport (SST) airplane Concorde had a cruising airspeed of Mach of 2.2. It is one of only two SSTs to have entered commercial service, and the other was the Tupolev Tu-144. The Concorde retired in 2003 after a crash during takeoff. On Tuesday, July 25, 2000, the very first fatal accident involving Concorde occurred out bound from Paris to New York. It crashed 60 seconds after takeoff after suffering tire blowout that caused the fuel tank to rupture. This started a sequence of events that caused a fire that eventually led to two engines failing and the aircraft crashing. All 109 people (100 passengers and 9 crew members) on board were killed. Furthermore, four people in a local hotel on the ground were also killed.

Figure 5.10 illustrates the Lockheed Martin F-22A Raptor with a maximum speed of more than Mach 2.25 at altitude. The aircraft has a maximum takeoff mass of 38,000 kg, a wing area of 78 m^2, and two turbofan engines, each generating 116 kN of thrust.

TABLE 5.3
Cruise Speed and Maximum Speed of Several Jet Aircraft

No.	Aircraft	Type	T (kN)	m_{TO} (kg)	Altitude (ft)	V_{max}		V_C (knot)
						Knot	Mach	
1.	Gulfstream G650	Business jet	2×71.6	45,000	41,000	516	0.9	488
2.	Alphajet	Trainer	2×14.1	8,000	32,800	—	0.86	—
3.	Microjet 200B	Trainer	2.6	1,300	18,000	250	—	210
4.	Cessna 525	GA	2×8.45	4,710	33,000	—	0.7	383
5.	Airbus 350	Transport	2×274	277,600	41,000	488	0.89	513
6.	Boeing 777	Transport	2×342	299,370	36,000	—	—	$M=0.87$
7.	Concorde	Transport	4×142	185,000	60,000	—	2.3	$M=2.04$
8.	Rafale	Fighter	2×75	24,000	—	1,032	1.8	$M=1.4$
9.	HondaJet Elite II	Light jet	2×9.1	5,035	43,000	422	0.72	415
10.	Tupolev Tu-144	Transport	4×172	180,000	52,000	—	—	$M=2.35$
11	Aermacchi MB-326	Light trainer	15.17	4,570	—	—	—	430
12.	Lockheed F-16 Fighting Falcon	Fighter	131.6	12,331	40,000	—	2.1	—
13.	Lockheed F-22 Raptor	Stealth Fighter	2×155	272,160	30,000	—	2.25	1.82
14.	Northrop Grumman RQ-4 Global Hawk	UAV	34	14,345	60,000	—	—	310
15.	Eurofighter Typhoon	Fighter	2×60	23,045	55,000	—	2	–
16.	Lockheed F-35	Fighter	125	31,150	50,000		1.6	–
17.	Lockheed SR-71 Blackbird	Reconnaissance	2×110	78,018	80,000	1,910	3.3	–
18.	Rockwell B-1 Lancer	Bomber	4×77.4	212,200	40,000	721	1.25	
19.	Bombardier Global 7500	Business jet	2×84.2	51,090	43,000	623	0.9	0.85
20.	Embraer E190	Airliner	2×82.3	51,800	35,000	–	0.82	–

FIGURE 5.10 Lockheed Martin F-22A Raptor. (Courtesy of Weimeng.)

The ratio between the aircraft weight and the wing area (W/S) is called *wing loading*. The wing loading is an important parameter in aircraft performance evaluation. For example, for an aircraft with a weight of 2,650 lb and wing area of 160 ft^2, the wing loading is 2,650/160 or 17.67 pounds per square foot (lb/ft^2). Another term that appears in many performance equations is T/W, which is called the thrust-to-weight ratio. This ratio for the majority of jet aircraft is <1 (about 0.2–0.3). For a vertical takeoff and landing (VTOL) aircraft, this ratio is more than unity.

Two terms of W/S and T/W are fundamental parameters in aircraft performance and influence many performance parameters such as the maximum speed. As the wing loading and thrust-to-weight ratio are increased, the maximum speed will be improved.

There are two limits for the maximum velocity of an aircraft: lower limit and upper limit. The maximum speed of an aircraft should be always higher than the stall speed, since no non-VTOL, fixed-wing, heavier-than air aircraft may have a sustained level flight with a speed lower than the stall speed. Thus, if you experience such a result in your calculations, it implies that the engine is not powerful enough.

$$V_{max} \geq V_s \tag{5.34}$$

There is no lower limit for the maximum airspeed of a VTOL aircraft and a rotary wing aircraft.

The upper limit of the maximum velocity of an aircraft is often a structural limit. This limit, which is also referred to as the never-exceeded velocity (V_{NE}), restricts an aircraft to fly beyond the point at which the structure will be damaged. At a speed beyond V_{NE}, the bending moment on the structure (e.g., on the tail) will be greater than the design limit of the aircraft structure. Moreover, the temperature at the critical locations of the structure (e.g., wing leading edge or fuselage nose) may exceed the thermal limit.

In 2022, Bombardier claims new Global 8000 (will go into service in 2025) is the world's fastest business jet with a top speed of 623 knots (716 mph, 1,152 km/h) and a range of 8,000 nm (9,200 miles, 14,816 km).

Example 5.4

A large jet transport aircraft with a mass of 165,000 kg, a turbofan engine thrust of 320 kN, and a wing area of 260 m² has a zero-lift drag coefficient of 0.02 and $K = 0.05$. Determine the maximum speed at sea level.

Solution

$$V_{\max} = \sqrt{\frac{kT_{\max} + \sqrt{(kT_{\max})^2 - 4C_{D_o}KW^2}}{\rho S C_{D_o}}} \tag{5.30}$$

where k for turbofan engine is:

$$k = \left(\frac{\rho}{\rho_o}\right)^{1.2} = 1 \quad (\text{sea level}) \tag{5.33}$$

Thus:

$$V_{\max} = \sqrt{\frac{1\times 320{,}000 + \sqrt{(1\times 320{,}000)^2 - 4\times 0.02\times 0.05\times(165{,}000\times 9.81)^2}}{1.225\times 260\times 0.02}} \tag{5.30}$$

$V_{\max} = 312.8\,\text{m/s} = 608\,\text{knot} \Rightarrow M_{\max} = 0.92$

5.3.2 Minimum Drag Airspeed

Another interesting airspeed in a straight-line level flight is the speed at which the aircraft generates the minimum drag. Since in a level flight, the thrust is equal to the aircraft drag, the minimum drag implies the minimum thrust and, subsequently, a lower fuel consumption. Equation 3.1 implies that the drag force is a direct function of the airspeed. A quick look at this equation initially reveals that as the velocity increases, the drag increases. This conclusion is not correct for all speeds.

The reason is as follows. When a pilot is going to increase the speed, the thrust will be increased. If the altitude is held constant, the aircraft angle of attack must be reduced. The reduction in the angle of attack means the reduction in the lift coefficient and, consequently, a reduction in the induced drag coefficient (C_{D_i}). Therefore, as the speed is increased, the induced drag coefficient is decreased.

However, the increase in velocity leads to a more induced drag (D_i), while reduction in the induced drag coefficient results in a reduction in induced drag (D_i). The overall result is usually a reduction in the induced drag. In addition, the increase in the airspeed results in an increase in the zero-lift drag (D_o). Thus, an increase in the airspeed increases the zero-lift drag (D_o) while decreasing the induced drag (D_i). As Figure 5.2 demonstrates, the drag force has a minimum value when the velocity is varied. This speed is called the minimum drag speed ($V_{\min_D}$). It is evident that the flight of an aircraft at this speed needs a minimum thrust for a level flight. Consequently, this flight consumes the minimum fuel and has the lowest cost of flight.

It is concluded that, when the objective of a flight is to minimize the fuel consumption, the pilot must select to fly with this speed. An example of such a mission would be aerial surveillance to monitor a border or a region (i.e., loiter). In this mission, the objective is not to rush to the destination but is just to be in the air as long as possible. Another example is a mission to maximize the endurance. This velocity is unique for any specific aircraft and is a function of flight altitude.

To calculate the minimum drag speed, it suffices to differentiate Equation 3.1 with respect to velocity and set it to zero. To do this derivation, we start with the equation of drag as follows:

$$D = \frac{1}{2}\rho V^2 S C_D \tag{3.1}$$

Since

$$C_D = C_{D_o} + KC_L^2 \tag{3.12}$$

and

$$C_L = \frac{2mg}{\rho V^2 S} \tag{5.8}$$

it follows that, substitution of Equations 3.12 and 5.8 into Equation 3.1 results in

$$D = \frac{1}{2}\rho V^2 S C_D + \frac{2K(mg)^2}{\rho V^2 S} \tag{5.35}$$

By differentiating Equation 5.35 with respect to V, and setting it equal to zero, we obtain

$$\frac{\partial D}{\partial V} = \rho V S C_{D_o} - \frac{4K(mg)^2}{\rho V^3 S} = 0 \tag{5.36}$$

or

$$V^4 = \frac{4K(mg)^2}{(\rho S)^2 C_{D_o}} \tag{5.37}$$

and finally,

$$V_{\min_D} = \sqrt{\frac{2\sqrt{K}(mg)}{(\rho S)\sqrt{C_{D_o}}}} = \sqrt{\frac{2mg}{\rho S\sqrt{C_{D_o}/K}}} = \left(\frac{2mg}{\rho S}\right)^{1/2}\left(\frac{K}{C_{D_o}}\right)^{1/4} \tag{5.38}$$

Comparing this equation with Equation 5.8, we can rewrite Equation 5.42 in the following format:

$$V_{\min_D} = \sqrt{\frac{2mg}{\rho S C_{L_{\min_D}}}} \tag{5.39}$$

The minimum drag speed is the inverse function of air density; hence, the minimum drag speed is increased with altitude. This is a general trend. Equation 5.65 further implies that the minimum drag speed is decreased when the aircraft weight is decreased.

Comparing Equations 5.38 and 5.39, we can conclude that the lift coefficient at the minimum drag speed is equal to the square root of the ratio of the zero-lift drag coefficient (C_{D_o}) and induced drag factor (K). Hence,

$$C_{L_{\min_D}} = \sqrt{\frac{C_{D_o}}{K}} \tag{5.40}$$

Equation 5.40 is a mathematical expression; the theoretical value of $C_{L_{\min_D}}$ must be within a practical flight limit. The value of $C_{L_{\min_D}}$ from Equation 5.40 cannot be more than the aircraft maximum lift coefficient ($C_{L_{\max}}$). If the output of the equation is more than $C_{L_{\max}}$, ignore the outcome and select a new value slightly less than $C_{L_{\max}}$.

It is interesting to find out what the relationship between lift and drag coefficients is when an aircraft is flying with the minimum drag speed. To determine this relationship, we divide lift coefficient to drag coefficient and insert their equivalent terms, which is

$$\left(\frac{C_L}{C_D}\right)_{\min_D} = \frac{\sqrt{C_{D_o}/K}}{C_{D_o} + K\left(C_{D_o}/K\right)} = \frac{\sqrt{\left(C_{D_o}/K\right)}}{2C_{D_o}} \tag{5.41}$$

which is simplified to

$$\left(\frac{C_L}{C_D}\right)_{\min_D} = \frac{1}{2\sqrt{KC_{D_o}}} \tag{5.42}$$

Inserting Equation 5.40 into Equation 3.12 yields the following useful result:

$$C_{D_{\min_D}} = 2C_{D_o} \tag{5.43}$$

This equation implies that the drag coefficient of an aircraft when flying with a velocity that corresponds to the minimum drag is equal to twice the value for C_{D_o}.

If the minimum drag speed is theoretically less than the stall speed, a safe minimum drag speed is selected to be about 10%–20% greater than the stall speed:

$$V_{\min_D} = kV_s \tag{5.44}$$

where

$$1.1 < k < 1.2 \tag{5.45}$$

It is interesting to determine the minimum thrust an aircraft requires to have a steady-level flight. The answer is obtained by inserting the minimum drag velocity (Equation 5.39), the drag coefficient corresponding to the minimum drag velocity (Equation 5.43), and the lift coefficient corresponding to the minimum drag velocity (Equation 5.40), into the drag equation (Equation 3.1):

$$\begin{aligned} T_{\min} = D_{\min} &= \frac{1}{2}\rho V_{\min_D}^2 S C_{D_{\min_D}} \\ &= \frac{1}{2}\rho\left(\frac{2mg}{\rho S C_{L_{\min D}}}\right) S\left(2C_{D_o}\right) = \frac{1}{2}\rho\left(\frac{2mg}{\rho S\sqrt{C_{D_o}/k}}\right) S\left(2C_{D_o}\right) \end{aligned} \tag{5.46}$$

This is simplified to

$$T_{\min} = 2W\sqrt{KC_{D_o}} \tag{5.47}$$

Thus, in order to further reduce the minimum thrust in a cruising flight, one should reduce: (1) aircraft weight, (2) aircraft zero-lift drag coefficient, and (3) induced drag factor.

Example 5.5

A small jet aircraft has the following features:

$$m = 2{,}500\,\text{kg},\ S = 20\,\text{m}^2,\ C_{D_o} = 0.03,\ K = 0.06,\ V_s = 72\,\text{knot}\,(37\ \text{m/s})$$

At what speed this aircraft must cruise, such that the engine produces the minimum thrust at 10,000 ft (3,048 m)? Repeat part a when aircraft is flying at sea level.

Solution

The speed at which the engine is producing a minimum thrust is the minimum drag speed. This speed is determined using Equation 5.38. The lift coefficient for a minimum drag speed is calculated through Equation 5.440 as follows:

$$C_{L_{\min_D}} = \sqrt{\frac{C_{D_o}}{K}} = \sqrt{\frac{0.03}{0.06}} = 0.707 \tag{5.40}$$

a. From Appendix B, the air density at the altitude of 3,048 m is 0.412 kg/m^3. So,

$$V_{\min_D} = \sqrt{\frac{2mg}{\rho S C_{L\min_D}}} = \sqrt{\frac{2\times 2{,}500\times 9.81}{0.412\times 20\times 0.707}} \Rightarrow V_{\min_D} = 91.7\ \text{m/s} = 178.3\ \text{knot} \tag{5.39}$$

b. At sea level,

$$V_{\min_D} = \sqrt{\frac{2mg}{\rho S C_{L\min_D}}} = \sqrt{\frac{2\times 2{,}500\times 9.81}{1.225\times 20\times 0.707}} \Rightarrow V_{\min_D} = 53 \text{ m/s} = 103.4 \text{ knot} \qquad (5.39)$$

It is observed that the minimum drag speed is increased with altitude. For both altitudes, the minimum drag speed is greater than the stall speed, which is OK.

5.3.3 Maximum Lift-to-Drag Ratio Speed

The best aerodynamic efficiency of an aircraft is when it cruises with a velocity such that it delivers the highest value of lift-to-drag ratio ($V_{(L/D)_{\max}}$). This velocity is of interest to a pilot for whom the flight cost is of primary concern. To derive an expression for such velocity, we compare Equations 5.24 and 5.42. The right-hand side of both equations is exactly the same. Therefore, the lift-to-drag ratio at the minimum drag speed is exactly the same as the maximum lift-to-drag ratio:

$$\left(\frac{C_L}{C_D}\right)_{\max} = \left(\frac{C_L}{C_D}\right)_{\min_D} = \frac{1}{2\sqrt{KC_{D_o}}} \qquad (5.48)$$

This implies that the minimum drag speed is the speed at which the lift-to-drag ratio has the maximum value. This relationship is sketched in Figure 5.7. Thus, the velocity for minimum drag (i.e., minimum required thrust) is also the velocity for maximum *L*/*D*:

$$V_{(L/D)_{\max}} = V_{\min_D} \qquad (5.49)$$

Thus, from Equation 5.38, we can write

$$V_{(L/D)_{\max}} = \sqrt{\frac{2mg}{\rho S\sqrt{C_{D_o}/K}}} \qquad (5.50)$$

Comparing this equation with Equation 5.8, we can rewrite Equation 5.50 in the following format:

$$V_{(L/D)_{\max}} = \sqrt{\frac{2mg}{\rho S C_{L(L/D)_{\max}}}} \qquad (5.51)$$

The maximum *L*/*D* airspeed is the inverse function of air density; hence, the maximum *L*/*D* airspeed is increased with altitude. This is a general trend. Equation 5.51 further implies that the maximum *L*/*D* speed is decreased when the aircraft weight is decreased. Comparing Equations 5.49 and 5.51, we can conclude that the lift coefficient at maximum *L*/*D* speed is equal to the square root of the ratio of the zero-lift drag coefficient (C_{D_o}) and induced drag factor, *K* (Equation 5.23).

The definitions and derivations of other specific speeds (i.e., maximum range speed, maximum endurance speed, and the speed for maximum ceiling) are presented in the following three sections.

5.4 RANGE

The range is considered as one of the most important parameters in civil aircraft performance and design. This is the first priority for transport aircraft, but the second priority for fighters. By definition, range is the total distance that an aircraft can fly with full fuel tank and without refueling. This consists of takeoff, climb, cruise, descend, and landing (Figure 5.11) and does not include the wind effect (either positive or negative). Usually, the cruise segment is the longest. The range is measured with respect to the ground. In a civil airplane, the definition is the maximum ground distance with full fuel tank minus the reserve fuel.

The reserve fuel is considered when the situation for destination airport is not safe for landing; thus, the aircraft has to fly to another close airport with the remaining fuel. But for a military airplane, range is defined as two-way flight distance that includes takeoff, climb, cruise, descend, maneuver, mission accomplishment (e.g., fight, bomb, and reconnaissance), climb again, return cruise, descend, and landing (Figure 5.11b). It is also referred to as the radius of operation or radius of action.

The significance of this performance criterion is appreciated when we consider the distance between cities and capitals of different countries. Each aircraft has limited range capabilities with specific speed and specific flight altitude. The flight with different flight conditions (e.g., altitude, speed) results in a different range. Therefore,

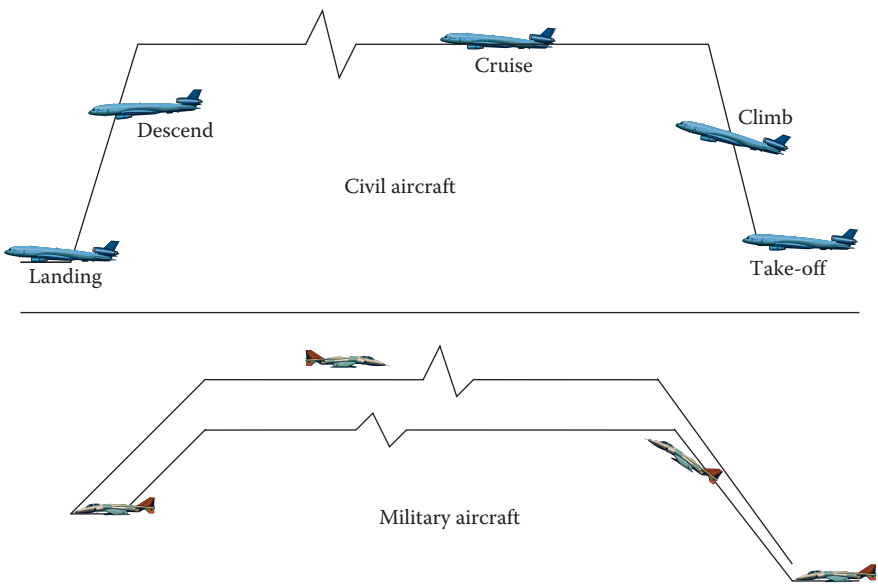

FIGURE 5.11 Range of a civil and a military aircraft.

when we are talking about range, it automatically means that the maximum range is with the best flight condition to provide the maximum range. The range of an aircraft at different altitudes is not the same. Similarly, the range of an aircraft with different speeds is not the same either. However, each aircraft has a unique maximum range with the maximum takeoff weight. This maximum range happens when flying at a specific (optimum) altitude and a specific (optimum) airspeed.

When Charles Lindbergh made his spectacular solo flight across the Atlantic Ocean on May 20–21, 1927, he could not have cared less about maximum velocity, maximum rate of climb, or maximum endurance. Uppermost in his mind was the maximum distance (i.e., range) that he could fly on the fuel carried by the single-piston-engine aircraft Spirit of St. Louis. The range of 5,834 km (distance from New York to Paris) was the main concern to Mr. Lindbergh in this amazing flight (besides navigation and sleep).

Aerial refueling is a technique to increase the range of a fighter. In this case, a tanker aircraft is flying in the region, and when the fighter needs fuel, it must use its probe to connect to tanker's drogue. During Cold War era, several military aircraft [65] such as Lockheed SR-71 Blackbird (Figure 4.24) and Lockheed F-117 Nighthawk had aerial refueling to be able to accomplish their mission in a longer range.

Another technique to increase the range is to use the *external tank*(s). These external tanks are often dropped and left behind when their fuel were consumed, since they are not permanent tanks. The record of the longest range belongs to a two-piston propeller engine aircraft Rutan Model 76 Voyager and a single turbofan engine aircraft Scaled Composites Model 311 Virgin Atlantic GlobalFlyer [64]. Its range is equal to the circumference of the earth (about 38,000 km), since it could circle the globe.

The Scaled Composites Model 311 Virgin Atlantic GlobalFlyer is an aircraft in which Steve Fossett flew a solo nonstop airplane flight around the world in 2 days 19 h and 1 min (67 h 1 min) from February 28, 2005, until March 3, 2005. The flight speed of 590.7 km/h (342.2 mph) set the Absolute World Record for the fastest nonstop unrefueled circumnavigation, beating the mark set by the previous Rutan-designed Voyager aircraft at 9 days 3 min and an average speed of 186.11 km/h (115.65 mph).

Another long-range jet aircraft is Northrop Grumman RQ-4 Global Hawk [62], an UAV with a mass of 11,600 kg and a wing area of 50.2 m^2 is equipped with a turbofan engine with a maximum thrust of 31.4 kN. This surveillance aircraft has a range of over 14,000 km with a cruise speed of 310 knots and service ceiling of 60,000 ft. In this section, we will first review various range definitions and then derive relevant relationships, and finally the application of each equation is discussed.

5.4.1 Definition

There are several types of range with different definitions in the literature (e.g., see Reference [66]). Here, four important types are introduced.

- *Safe range*: Safe range is the maximum distance between two airfields that an aircraft can fly regularly without any problem. The safe range consists of takeoff, climb, cruise, descend, and landing. In this type, the effect of wind

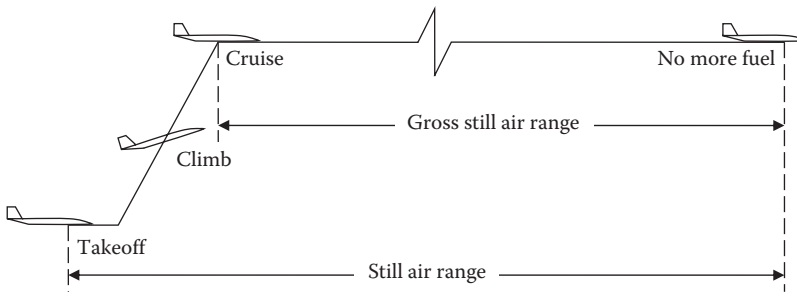

FIGURE 5.12 Net SAR and GSAR.

(headwind or tailwind) is not considered, and it is assumed that the tank is full of fuel at the beginning. For safety reasons, there must be a reserve fuel maintained in the tank at the end (i.e., after landing). Minimum reserve fuel requirements are established by the Federal Aviation Regulations. The reserve fuel is often equivalent to either 20% of the total fuel or 45 min of flight. This is a real case, but since the calculation of safe range is not an easy task, other definitions are offered.

- *Still air range*: In the calculation of still air range (SAR) (or net SAR), it is assumed that the flight begins with takeoff, flight is continued until all fuel is consumed, and there is no landing. It is also imagined that the air is still; that is, there is no wind during the flight. This definition is not a real flight, but instead, the calculation of SAR is more convenient. Figure 5.12 demonstrates this definition. The next type offers a much simpler calculation.
- *Gross still air range:* The gross still air range (GSAR) does not include any segment other than cruising flight, and it is also assumed that the flight begins with a full fuel tank. By definition, this flight ends in the air until the entire fuel is consumed. This is the definition that we are interested in, and the calculation of GSAR is straightforward. Like SAR, the GSAR ignores the influence of wind to the range. The weight of aircraft is constantly decreasing, since the fuel is consumed by the engine. For ease of mathematical derivation, we resort to the fourth definition that is specific range. GSAR is sometimes referred to as "cruise range".
- *Specific range* (SR): Specific range is defined as the distance flown divided by the amount of fuel that is consumed. In simple terms, the value of the miles per pound of fuel is called SR. This is analogous to the mileage of an automobile, especially when it is expressed in miles per gallon.

In terms of flight operations and missions, there are other types of ranges such as combat range, and ferry range. The tiltrotor VTOL aircraft Bell Boeing V-22 Osprey with a maximum takeoff mass of 27,442 kg has a regular range of 1,628 km, combat range of 720 km, and a ferry range of 4,130 km. moreover, the fighter aircraft Boeing F/A-18 Hornet with a maximum takeoff mass of 23,541 kg has a regular range of 2,017 km, combat range of 740 km, and a ferry range of 3,300 km.

To derive an expression for range, we employ the SR. In terms of math language, SR is the differentiation of the flown distance (X) with respect to the aircraft weight (W), or, in effect, fuel weight:

$$\text{SR} = \frac{dX}{dW} \tag{5.52}$$

The units of SR are km/N, nm/lb, and mile/lb. Among the four definitions, the first one is the most accurate but hard to calculate, but the last one is the most unrealistic but easiest to derive. The third definition (GSAR) is relatively easy to handle; thus, we will derive several relationships based on GSAR. At the end of Section 5.4, there is a discussion of how to include the influence of wind on the range.

5.4.2 Calculation of Range

The range is of distance type, and the distance is defined as the velocity times the duration of motion. We begin the derivation of SR with the definition of velocity. The instantaneous velocity is defined as differentiation of the distance traveled with respect to time (t)

$$V = \frac{dX}{dt} \tag{5.53}$$

On the other hand, the fuel mass flow rate (Q_f) is defined as the differentiation of the aircraft weight (W) with respect to time:

$$Q_f = \frac{dW}{dt} \tag{5.54}$$

In Chapter 4, we defined specific fuel consumption (SFC) as the weight of fuel consumed per unit time, per unit thrust, so

$$\text{SFC} = C = \frac{-dW/dT}{t} = \frac{Q_f}{T} \tag{5.55}$$

The minus sign is added because the rate of change of aircraft weight is a negative value and C is always treated as a positive quantity. It is interesting to note that, turbofan engine General Electric GE90 is consuming 2.968 kg/s (6.543 lb/s) at takeoff; but 1.079 kg/s (2.379 lb/s) in cruise. Combining Equations 5.53–5.55, and substituting them into Equation 5.52, yields

$$\text{SR} = \frac{dX}{dW} = \frac{Vdt}{Qdt} = \frac{V}{Q} = -\frac{V}{CT} \tag{5.56}$$

In a cruising flight (with a constant speed), the drag force (D) must be equal to the engine thrust (T); therefore, T is replaced with D:

$$\mathrm{SR} = -\frac{V}{CD} \tag{5.57}$$

Now, we multiply both the numerator and the denominator with lift force (L):

$$\mathrm{SR} = -\frac{V}{CDL} \tag{5.58}$$

Recall that in a cruising flight, the lift force (L) is also equal to the weight of aircraft (W), so the L in denominator is replaced with W

$$\mathrm{SR} = -\frac{V}{CDW} = -\frac{VL/D}{CW} \tag{5.59}$$

This relationship is very informative. It implies that SR is a function of four parameters: velocity, fuel consumption, aircraft weight, fuel weight, and lift-to-drag ratio. Based on the definition of SFC, it is correct to assume that SFC is constant for a jet engine. So, SR is a function of velocity multiplied by lift-to-drag ratio. This implies that to increase SR, both velocity and lift-to-drag ratio must be increased simultaneously. But we know that the lift-to-drag ratio is a function of velocity; and its maximum only happens at only one particular velocity.

Since $V = Ma$, Equation 5.59 can be reformatted as

$$\mathrm{SR} = -a\frac{M}{C}\frac{L}{D}\frac{1}{W} \tag{5.60}$$

The expression $M(L/D)$ is another measure of the SR capability due to the aerodynamic characteristics of a jet aircraft.

Figure 5.13 illustrates a Scaled Composites 348 White Knight 2 with four turbofan engines. This cargo aircraft is used to lift the SpaceShipTwo spacecraft to release altitude. The objective of SpaceShipTwo is to be flown to carry up to six passengers

FIGURE 5.13 Scaled Composites 348 White Knight 2. (Courtesy of Kas van Zonneveld.)

on a high-speed suborbital flight to the fringes of space. In such altitude (service ceiling of 110 km above the earth), six passengers can experience a few minutes of weightlessness and also see the black sky (instead of regular blue) and the earth below. The SpaceShipTwo with a loaded mass of 9,740 kg has a maximum speed of 4,000 km/h.

In general, performance can be evaluated based on two approaches: (1) Instantaneous or *point performance*, and (2) *Mission performance*. The point performance of an aircraft is the performance at a specified point on the flight path or at a specified instant of time. Mission performance primarily lies in determining the overall flight performance. Examples are how far can a particular aircraft fly with a given amount of fuel or, conversely, how much fuel is required to fly a desired range. This can be done by integrating the point performance over the interval between specified initial and final points, usually the start and end of the cruising flight.

The SR is one measure of point performance, but our interest is about the overall range or mission performance. To integrate, we begin with Equation 5.56. Conditions at the start of cruise will be identified by subscript 1 and at the end of cruise by subscript 2. By using the definition of SR, we can write

$$R = \int_0^R dX = \int \mathrm{SR}\, dW \tag{5.61}$$

The specific fuel consumption (C) can be assumed constant for a jet engine, Equation 5.61 can be written as

$$R = -\frac{1}{C}\int_{W_1}^{W_2} V \frac{L}{D}\frac{dW}{W} \tag{5.62}$$

where W_1 is the weight of aircraft at the beginning of the cruising flight, and W_2 is the weight of aircraft at the end of cruising flight. The variable W_1 is usually assumed to be the maximum takeoff weight (W_{TO}) and the variable W_2 as the difference between the maximum takeoff weight and the fuel weight. Equation 5.62 is a general equation for range for a jet aircraft. At any weight and altitude, the speed is associated with an angle of attack and, indeed, with a lift coefficient (C_L) that is

$$C_L = \frac{2W}{\rho S V^2} \tag{5.8}$$

Considering Equation 5.8 in mind, Equation 5.62 has four independent parameters: weight (W), velocity (V), altitude or its corresponding air density (ρ), and angle of attack or its associated lift coefficient (C_L). To solve the integration and come up with a closed-form solution, we need to set a few simplifying assumptions. Since the fuel is consumed during flight, the aircraft weight is constantly decreased during the flight. To maintain a level flight, we have to decrease the lift as well. Of the many possible solutions, only three are more practical which will be examined. In each

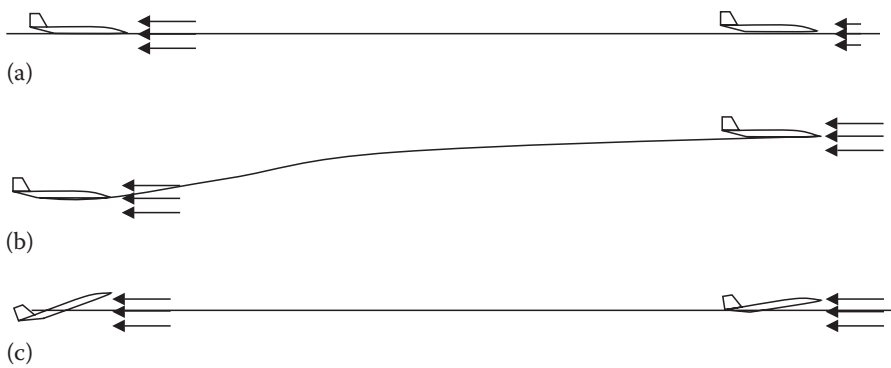

FIGURE 5.14 Three options of interest for a continuous decrease of the lift during cruise: (a) Decreasing flight speed (constant-altitude, constant-lift-coefficient flight). (b) Increasing altitude (constant-airspeed, constant-lift-coefficient flight). (c) Decreasing angle of attack (constant-altitude, constant-airspeed flight).

case, two flight parameters will be held constant throughout cruise. The three options of interest for continuous decrease of the lift during cruise are (Figure 5.14):

1. Decreasing flight speed (constant-altitude, constant-lift-coefficient flight)
2. Increasing altitude (constant-airspeed, constant-lift-coefficient flight)
3. Decreasing angle of attack (constant-altitude, constant-airspeed flight)

For each flight program, the integral Equation (5.62) will be set up, and then only the final range equation will be shown and discussed. In the first option, the velocity must be reduced with the same rate as the aircraft weight is decreased. In the second solution, the air density must be decreased; in other words, the flight altitude must be gradually increased. The third option offers the reduction of aircraft angle of attack, that is, the reduction of lift coefficient.

In terms of pilot operation, the first option is applied through throttle and the third option is implemented through stick/yoke/wheel. In the second option, no action is needed by the pilot and the aircraft will gradually gain height (climbs).

Based on safety regulations and practical considerations, the second option is the option of interest for majority of aircraft. The reason will be explained later. In general, when flight is conducted under the jurisdiction of Federal Aviation Regulations, the accepted flight program is the constant-altitude, constant-airspeed flight program.

5.4.2.1 Flight Program 1: Constant-Altitude, Constant-Lift-Coefficient Flight

In this option, the velocity will be reduced via throttle as the aircraft weight is decreased. This flight program to be examined is the constant-altitude, constant-lift-coefficient flight program. Since the lift coefficient is held constant throughout cruise, the lift-to-drag ratio (L/D) will also be constant. It is convenient, therefore, to express the instantaneous drag as the ratio of the instantaneous weight to the

instantaneous lift-to-drag ratio. Since L/D and C are assumed constant throughout cruise, they are taken out of the integral in Equation 5.68 as

$$R = -\frac{1}{C}\frac{L}{D}\int_{W_1}^{W_2} V\frac{dW}{W} \tag{5.63}$$

Performing the integration using the equation for the velocity (V) yields the range equation as follows:

$$R = -\frac{1}{C}\frac{L}{D}\int_{W_1}^{W_2}\sqrt{\frac{2W}{\rho S C_L}}\frac{dW}{W} = -\frac{1}{C}\frac{L}{D}\sqrt{\frac{2}{\rho S C_L}}\int_{W_1}^{W_2}\frac{1}{\sqrt{W}}dW \tag{5.64}$$

The integration results in

$$R = \sqrt{\frac{2}{\rho S C_L}}\left[2\left(\sqrt{W_1}-\sqrt{W_2}\right)\right] = \frac{2}{C}\frac{L}{D}\sqrt{\frac{2W_1}{\rho S C_L}}\left(1-\sqrt{\frac{W_2}{W_1}}\right) \tag{5.65}$$

which is finally simplified to

$$R_1 = \frac{2}{C}\frac{L}{D}V_1\left(1-\sqrt{1-\frac{W_f}{W_1}}\right) \tag{5.66}$$

where V_1 is the initial airspeed and W_1 is the gross weight of aircraft at the start of cruise. The W_f denotes the fuel weight and is obtained by

$$W_f = W_1 - W_2 \tag{5.67}$$

The aircraft final weight will be

$$W_2 = W_1\left(1-\frac{W_f}{W_1}\right) \tag{5.68}$$

It can be seen from Equation 5.8 that the airspeed must be decreased as fuel is consumed if C_L is to be constant as the weight decreases along the flight path. To determine the final airspeed V_2, we know that the aircraft weight is equal to the lift at the beginning and end of flight

$$W_1 = L_1 = \frac{1}{2}\rho V_1^2 S C_L \tag{5.69}$$

$$W_2 = L_2 = \frac{1}{2}\rho V_2^2 S C_L \tag{5.70}$$

Inserting Equations 5.69 and 5.70 into Equation 5.68 yields

$$\frac{1}{2}\rho V_2^2 S C_L = \frac{1}{2}\rho V_1^2 S C_L \left(1 - \frac{W_f}{W_1}\right) \tag{5.71}$$

which simplifies to

$$V_2 = V_1 \sqrt{1 - \frac{W_f}{W_1}} \tag{5.72}$$

Since lift coefficient (C_L) is held constant, Equation 5.8 implies that the thrust must be constantly decreased (by constantly setting back the throttle) as the fuel is used (i.e., the gross weight decreases).

The lift coefficient is constant throughout the flight, and based on Equations 5.69 and 5.70, it is determined from

$$C_L = \frac{2W_1}{\rho V_1^2 S} = \frac{2W_2}{\rho V_2^2 S} \tag{5.73}$$

For the viewpoint of pilot control, there are three drawbacks to this flight program. The first is the need to continuously compute the airspeed along the flight path and to reduce the throttle setting accordingly. The second is that reducing the airspeed increases the flight times. The third is the fact that air traffic control rules require "constant" true airspeed for cruise flight; currently constant means ±10 knots. The good news is that current autopilot of large transport aircraft has solved part of this problem (i.e., no need for pilot calculation).

5.4.2.2 Flight Program 2: Constant-Airspeed, Constant-Lift-Coefficient Flight

The second flight program to be examined is the constant-airspeed, constant-lift-coefficient flight program, which is commonly referred to as a *cruise-climb* flight. In this option, the air density will be automatically reduced as the aircraft weight is decreased. No pilot intervention is necessary. To evaluate a cruise-climb flight, the level-flight equations are used with the assumption that the flight-path angle is sufficiently small. Thus, the basic operating condition for a cruise-climb flight is that the ratio of the instantaneous weight of the aircraft to the air density is constant.

Since both velocity (V) and lift-to-drag ratio (L/D) are constant, the variables C, V, and L/D will be taken out of the integral, and Equation 5.62 can be written as

$$R = -\frac{1}{C} V \frac{L}{D} \int_{W_1}^{W_2} \frac{dW}{W} \tag{5.74}$$

The result of this integration is

$$R = -\frac{V}{C}\frac{L}{D}\left[\ln(W_2) - \ln(W_1)\right] \tag{5.75}$$

or

$$R = \frac{V}{C}\frac{L}{D}\ln\left(\frac{W_1}{W_2}\right) \tag{5.76}$$

Since the weight of the aircraft at the end of flight is equal to the initial weight minus fuel weight,

$$W_2 = W_1 - W_f \tag{5.77}$$

Therefore, Equation 5.76 can be reformatted in terms of fuel weight as

$$R_2 = \frac{V\left(L/D\right)}{C}\ln\left(\frac{1}{1-\left(W_f/W_1\right)}\right) \tag{5.78}$$

This is the general form of what is known as the *Breguet* range equation. To keep both the airspeed and the lift coefficient constant as the weight of the aircraft decreases, Equation 5.10 demonstrates that air density (ρ) must decrease in a manner so as to keep the ratio of the lift to weight constant. The only way that this can be done is to increase the altitude in an appropriate manner. Consequently, the aircraft will be in a continuous climb (thus the name *cruise-climb*), which appears to violate the level-flight condition of a zero flight-path angle. It will be shown in a subsequent section that the cruise-climb flight-path angle is sufficiently small so as to justify the use of the level-flight equations and solutions for a cruise-climb. The thrust required will decrease along the flight path in such a manner that the available thrust will decrease in an identical manner.

Therefore, a cruise-climb flight requires no computations or efforts by the pilot. In an aircraft equipped with an autopilot, the aircraft cruise control will be implemented by the autopilot. After establishing the desired cruise airspeed, the pilot simply engages the *Mach-hold* mode (or constant-airspeed mode) on the autopilot, and the aircraft will slowly climb at the desired flight-path angle as the fuel is burned. The variations in the flight parameters along the flight path are shown in Figure 5.15.

Only under certain limited conditions, the cruise-climb flight is allowed by air traffic control. Concorde, the SST aircraft, was allowed to employ this program since it was flying at high altitude (above 50,000 ft).

The lift coefficient is constant throughout the flight, and based on the lift equation, it is determined from

$$C_L = \frac{2W_1}{\rho_1 V^2 S} = \frac{2W_2}{\rho_2 V^2 S} \tag{5.79}$$

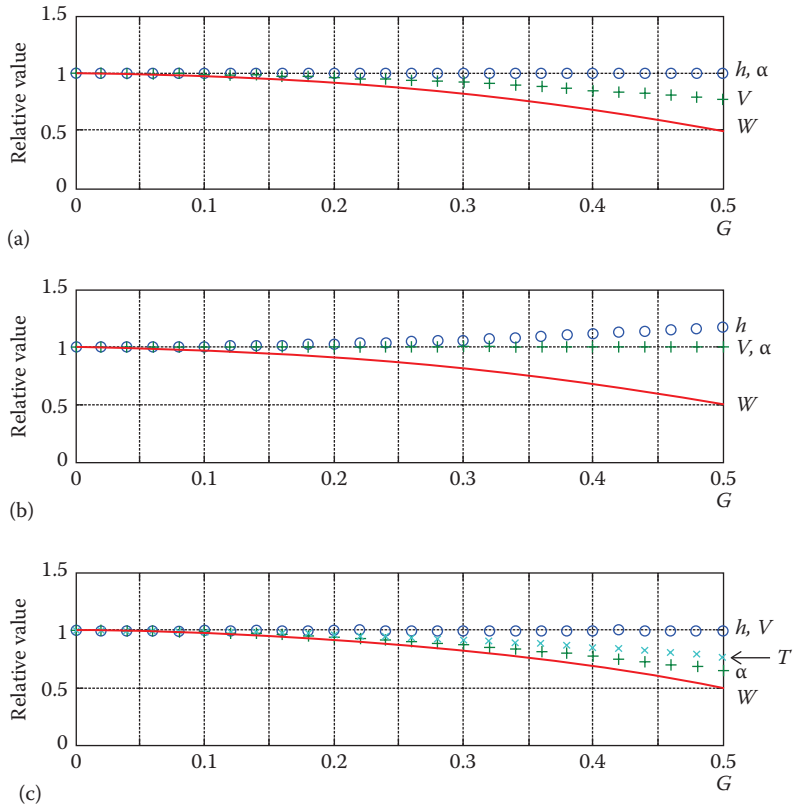

FIGURE 5.15 Variation of flight parameters as a function of fuel weight ratio: (a) constant-altitude, constant-lift-coefficient, (b) constant speed, constant-lift-coefficient, and (c) constant-altitude, constant-airspeed.

The cruise altitude for a cruise-climb flight option is gradually increasing. The altitude at the end of the cruise-climb flight (h_2) can be expressed in terms of both the initial altitude (h_1) and the fuel fraction. The relation between fuel weight, initial weight, and final weight is given as in Equation 5.68.

Plugging Equations 5.69 and 5.70 into Equation 5.68 yields

$$\frac{1}{2}\rho_2 V^2 S C_L = \frac{1}{2}\rho_1 V^2 S C_L \left(1 - \frac{W_f}{W_1}\right) \tag{5.80}$$

or

$$\rho_2 = \rho_1 \left(1 - \frac{W_f}{W_1}\right) \tag{5.81}$$

The ratio of fuel weight to aircraft weight is denoted as G:

$$G = \frac{W_f}{W_1} \tag{5.82}$$

and is sometimes referred to as the fuel weight fraction. The ratio of fuel weight to aircraft weight for RQ-4B Global Hawk UAV is 0.53, since the fuel weight is 17,300 lb, while UAV maximum takeoff weight is 32,500 lb. The ratio of fuel weight to aircraft weight for business jet aircraft Dassault Falcon 6X is 0.43, since the fuel weight is 33,786 lb, while the maximum takeoff weight is 77,459 lb.

The density ratio at the end of the cruise-climb flight (σ_2) can be expressed in terms of both the initial density ratio ($\sigma = \rho/\rho_o$) and the fuel fraction; that is,

$$\sigma_2 = \sigma_1(1-G) \tag{5.83}$$

where σ_1 is the air density ratio at the beginning of the cruise.

The climb angle in cruise-climb is so small that it can be ignored. However, the altitude difference could be considerable (e.g., 10,000 ft). For instance, the aircraft in Example 5.6 with a range of 45,050 km in a cruise-climb flight program has an 8,500 ft increase in altitude and a climb angle of 0.033°. When the air density at the end of the cruise-climb flight (σ_2) is obtained, one can utilize Appendix A or B to determine the final altitude. It should be mentioned that the error in the range from using the level constant-altitude flight range equation instead of the cruise-climb equation is of the order of 1%–2%.

5.4.2.3 Flight Program 3: Constant-Altitude, Constant-Airspeed Flight

In this option, the angle of attack will be reduced via stick/wheel as the aircraft weight is decreased. The integral range Equation 5.62 is repeated here for convenience:

$$R = -\frac{1}{C}\int_{W_1}^{W_2} V\frac{L}{D}\frac{dW}{W} \tag{5.62}$$

Since lift is equal to the weight during cruise, the L from numerator and W from denominator are eliminated. Thus, the equation for this flight program can be simplified as

$$R = -\frac{V}{C}\int_{W_1}^{W_2} \frac{dW}{D} \tag{5.84}$$

Since the altitude and the airspeed are constant in this flight option, the dynamic pressure (q) will be constant:

$$q = \frac{1}{2}\rho V^2 = \text{const} \tag{2.21}$$

Hence, the drag is written in this form:

$$D = qSC_D = qSC_{D_o} + \frac{KW^2}{qS} \tag{5.85}$$

Substituting Equation 5.85 into Equation 5.84 and moving the constant parameters (coefficients) out of the integration yields

$$R = \frac{V}{CqSC_{D_o}} \int_{W_1}^{W_2} \frac{-dW}{1 + \left(KW^2 / \left(q^2 S^2 C_{D_o}\right)\right)} \tag{5.86}$$

The result of integration would be

$$R = \frac{V}{CqSC_{D_o}\sqrt{K/\left(q^2 S^2 C_{D_o}\right)}} \left[\tan^{-1}\left(\sqrt{\frac{K}{q^2 S^2 C_{D_o}}} W_1\right) - \tan^{-1}\left(\sqrt{\frac{K}{q^2 S^2 C_{D_o}}} W_2\right)\right] \tag{5.87}$$

The bracketed term represents the difference between two angles and can be written as

$$\begin{aligned} &\tan^{-1}\left(\sqrt{\frac{K}{q^2 S^2 C_{D_o}}} W_1\right) - \tan^{-1}\left(\sqrt{\frac{K}{q^2 S^2 C_{D_o}}} W_2\right) \\ &= \tan^{-1}\left[\frac{\sqrt{KC_{D_o}} W_1 \left(W_f / W_1\right)}{D_1\left(1 - \left(\left(KC_{L_1} W_1 \left(W_f / W_1\right)\right)/D_1\right)\right)}\right] \end{aligned} \tag{5.88}$$

Since $W_1/D_1 = L_1/D_1 = C_{L_1}/C_{D_1}$, the initial lift-to-drag ratio, and $\sqrt{KC_{D_o}} = 1/\left(2\left(C_L/C_D\right)_{\max}\right)$ for a parabolic drag polar, we can rewrite Equation 5.88 and substitute it in Equation 5.87 to obtain the range equation of this case as

$$R_3 = \frac{2V\left(C_L/C_D\right)_{\max}}{C} \tan^{-1}\left[\frac{\left(C_L/C_D\right)_1 \left(W_f/W_1\right)}{2\left(C_L/C_D\right)_{\max}\left(1 - KC_{L_1}\left(C_L/C_D\right)_1 \left(W_f/W_1\right)\right)}\right] \tag{5.89}$$

Note, in this equation, the angle in the arc tangent term must be expressed in radian. In Equation 5.89, C_{L_1}/C_{D_1} denotes the initial lift-to-drag ratio and C_{L_1} denotes the initial lift coefficient

$$C_{L_1} = \frac{2W_1}{\rho V_1^2 S} \tag{5.90}$$

The final lift coefficient is readily obtained as

$$C_{L_2} = \frac{2W_2}{\rho V_1^2 S} \tag{5.91}$$

where W_2 is the final weight at the end of cruise. Throughout the flight (including at the beginning and at the end of the flight), the lift equals weight:

$$W_1 = L_1 = \frac{1}{2}\rho V^2 S C_{L_1} \tag{5.92}$$

$$W_2 = L_2 = \frac{1}{2}\rho V^2 S C_{L_2} \tag{5.93}$$

where the relation between the aircraft weight at the beginning and at the end of the flight is given by Equation 5.68. Inserting Equations 5.92 and 5.93 into Equation 5.68 yields

$$\frac{1}{2}\rho V^2 S C_{L_2} = \frac{1}{2}\rho V^2 S C_{L_1}\left(1 - \frac{W_f}{W_1}\right) \tag{5.94}$$

which simplifies to

$$C_{L_2} = C_{L_1}\left(1 - \frac{W_f}{W_1}\right) \tag{5.95}$$

which yields the final lift coefficient as a function of the initial lift coefficient.

From the theoretical point of view, all three cases are realizable, but in practice, only the third case is acceptable and approved for transport aircraft by the FAA. This case is hard to follow because the pilot must constantly decrease the angle of attack through the deflection of the elevator. However, for an aircraft equipped with an autopilot, this is an easy task. This case is the safest flight program among three possible programs. Figure 5.15 illustrates variations of several flight parameters as a function of fuel weight ratio (W_f/W_1) for these three cases.

The general variations in the flight parameters for each of the three flight programs are shown in Figure 5.15 as functions of the fuel weight fraction (G), which is a measure of the range flown. As the fuel weight fraction increases, the differences between these three flight programs increase.

The airliner Airbus A320 with a maximum takeoff mass of 77,000 kg has an initial cruise altitude of 37,000 ft, while the maximum certified altitude is 39,800 ft. The business trijet aircraft Dassault Falcon 50 with a maximum takeoff mass of 18,000 kg has an initial cruise altitude of 41,000 ft, while the maximum certified altitude is 49,800 ft. Figure 5.16 illustrates an Airbus A380 with four turbofan engines and a range of 15,200 km. This aircraft is currently the largest civil jet transport aircraft that can carry up to 600 passengers.

Table 5.4 demonstrates a range of several jet aircraft. It is noticeable that the difference in range is directly related to the difference in their fuel capacity.

FIGURE 5.16 Airbus A380 with four turbofan engines and a range of 15,200 km. (Courtesy of Jan Seler.)

TABLE 5.4
Range of Several Jet Aircraft

No.	Aircraft	Country	Type	*T* (kN)	Mass (kg)	Range (km)
1.	Boeing 737–Max 7	United States	Transport	2 × 130	80,000	7,100
2.	Boeing 747-C-19A	United States	Transport	4 × 233.5	235,870	13,520
3.	Alphajet	France	Fighter	2 × 13.24	8,000	4,000
4.	Hawk-200	Britain	Fighter	25.3	5,700	2,433
5.	McDonnell Douglas F-15 Eagle	United States	Fighter	2 × 106.5	13,084	4,631
6.	Concorde	France-Britain	Supersonic Transport	4 × 180	185,056	6,580
7.	Mirage 2000	France	Fighter	95.1	17,000	1,480
8.	Cessna 560	United States	Business jet	2 × 13.55	7,393	3,630
9.	McDonnell Douglas DC-10	United States	Transport	3 × 178	199,580	4,355
10.	Aeromachi MB-326GB	Italy	Trainer	15.2	4,577	1,850
11.	Sukhoi Su-57	Russia	Fighter	2 × 142	35,000	3,500
12.	BAE 125-700	Britain	Business	2 × 16.5	11,566	4,482
13.	Lockheed C-5 Galaxy	United States	Transport	4 × 191.2	379,657	10,411
14.	Global Hawk	United States	Reconnaissance UAV	34	14,628	22,800
15.	McDonnell Douglas F/A-18	United States	Fighter	2 × 71.2	16,500	3,300
16.	Airbus 350-900	Europe	Transport	2 × 374.5	283,000	15,000
17.	Airbus 380-800	Europe	Transport	4 × 348	575,000	14,800
18.	GlobalFlyer	United States	Nonstop flight around the globe	10	10,024	41,466
19.	Lockheed SR-71 Blackbird	United States	Reconnaissance	2 × 110	78,018	22,800
20.	Dassault Falcon 6X	France	Business jet	2 × 60	77,459	10,200

5.4.3 Speed for Maximum Range ($V_{\max_R}$)

In Section 5.4.2, the derivation of Breguet range equation was introduced. This equation allows us to determine the range for jet aircraft. There is a velocity parameter in this equation that must be known prior to range calculation. Maximum range velocity ($V_{\max_R}$) is the aircraft velocity that yields the maximum range. There are basically three programs to reduce lift as the aircraft weight is decreased during a cruising flight.

1. Decreasing flight speed (constant-altitude, constant-lift-coefficient flight)
2. Increasing altitude (constant-airspeed, constant-lift-coefficient flight)
3. Decreasing angle of attack (constant-altitude, constant-airspeed flight)

Since the only variable besides the aircraft weight in the integration of Equation 5.62 is the flight airspeed, these three programs may be classified into two groups: (1) constant-speed cruising flight (programs 2 and 3) and (2) reducing-speed cruising flight (program 1). The mathematical derivations of the cruising speed for these two groups are different; so they are presented separately.

5.4.3.1 Constant-Speed Cruising Flight

This section covers the velocity to gain the maximum range for the second and third flight programs (constant-airspeed, constant-lift-coefficient flight). In a cruising flight for the maximizing range when the airspeed is kept constant, there are two options: (1) reduce the lift coefficient and (2) increase the cruising altitude. For both of these programs, the mathematical solution is developed in the same way. To determine the airspeed, we simply differentiate SR with respect to the velocity and set it equal to zero. Recall that the variation in the SFC with the airspeed is small and can be assumed constant. As defined earlier, the SR (Equation 5.57) is mathematically a ratio of two variables where the denominator (D) is also a function of the other parameter (V).

$$\mathrm{SR} = -\frac{V}{CD} \tag{5.57}$$

For this differentiation, we need to employ the following differentiation technique:

$$\frac{d}{dx}\left(\frac{u}{v}\right) = \frac{(du/x)v - (dv/x)u}{v^2} \tag{5.96}$$

Differentiation of Equation 5.57 with respect to velocity (V) is as follows:

$$\frac{d}{dV}(\mathrm{SR}) = 0 \Rightarrow \frac{d}{dV}\left(\frac{-V}{CD}\right) = -\left[\frac{CD}{(CD)^2} - \frac{CV}{(CD)^2}\left(\frac{dD}{dV}\right)\right] = 0 \tag{5.97}$$

or

$$\frac{d}{dv}\left(\frac{V}{CD}\right)=\frac{1}{CD}-\frac{V}{CD^2}\left(\frac{dD}{dV}\right)=0 \tag{5.98}$$

Thus, the condition for the maximum range becomes

$$\frac{dD}{dV}-\frac{D}{V}=0\Rightarrow\frac{dD}{dV}=\frac{D}{V} \tag{5.99}$$

where we already had

$$D=\frac{1}{2}\rho V^2SC_{D_o}+\frac{2K\left(mg\right)^2}{\rho V^2S} \tag{5.35}$$

and

$$\frac{\partial D}{\partial V}=\rho VSC_{D_o}-\frac{4K\left(mg\right)^2}{\rho V^3S} \tag{5.36}$$

By substitution of Equations 5.35 and 5.36 into Equation 5.99 and after manipulation, we will obtain

$$\frac{2\,mg}{\rho V^2S}\sqrt{\frac{3K}{C_{D_o}}}=1 \tag{5.100}$$

or

$$V_{\max_R}=\sqrt{\frac{2\,mg}{\rho S\sqrt{C_{D_o}/3K}}}=\left(\frac{2\,mg}{\rho S}\right)^{1/2}\left(\frac{3K}{C_{D_o}}\right)^{1/4} \tag{5.101}$$

This is the equation that yields the maximum range speed for a jet aircraft. By comparing this equation with Equation 5.38, we see that the maximum range velocity is always greater than the minimum drag velocity. We note that $V_{\max_R}$ is inversely proportional to the square root of the density ratio and thus increases with altitude. In addition, $V_{\max_R}$ increases in direct proportion to the square root of the wing loading (W/S). A doubling of the wing loading results in a 14% increase in range.

Furthermore, $V_{\max_R}$ is inversely proportional to the ¼ root of the zero-lift drag coefficient and hence decreases with C_{D_o}. Reference [67] illustrates that this velocity minimizes the number of pounds of fuel consumed per mile (i.e., $(dW_f/dX)_{\min}$). Due to this reference, this velocity is sometimes called *Carson's speed*.

In the case of flight program 2, where the lift coefficient is held constant during flight, the following can be concluded by comparing Equation 5.101 with Equation 5.38:

$$C_{L_{\max_R}} = \sqrt{\frac{C_{D_o}}{3K}} = 0.577 C_{L(L/D)_{\max}} \tag{5.102}$$

and

$$C_{D_{\max R}} = \frac{4}{3} C_{D_o} \tag{5.103}$$

The lift-to-drag ratio for the maximum range would be

$$\left(\frac{L}{D}\right)_{\max_R} = \frac{C_{L\max_R}}{C_{D\max_R}} = \frac{\sqrt{C_{D_o}/3\,K}}{4/3C_{D_o}} = \frac{\sqrt{3}}{4\sqrt{KC_{D_o}}} = \frac{\sqrt{3}}{2}\left(\frac{L}{D}\right)_{\max} = 0.866\left(\frac{L}{D}\right)_{\max} \tag{5.104}$$

In other words, lift-to-drag ratio – when flying for the maximum range – is equal to 86.6% of the maximum lift-to-drag ratio.

5.4.3.2 Non-Constant-Speed Cruising Flight

This section covers the velocity to gain the maximum range for the first flight program. In this program, the flight speed is decreasing and is a constant-altitude, constant-lift-coefficient flight. In a cruising flight for the maximizing range when the speed is reduced, there is no unique velocity to maximize the range. In both cases, we have to determine at least two velocities: (1) initial velocity and (2) final velocity.

For both cases, the initial speed is the special speed to deliver the maximum range and is determined as in Equation 5.101:

$$V_1 = V_{\max_R} = \sqrt{\frac{2\,mg}{\rho S\sqrt{C_{D_o/3K}}}} = \left(\frac{2\,mg}{\rho S}\right)^{1/2}\left(\frac{3K}{C_{D_o}}\right)^{1/4} \tag{5.105}$$

The final velocity is found using the following equation, which we derived earlier in this chapter:

$$V_2 = V_1\sqrt{1-\frac{W_f}{W_1}} \tag{5.72}$$

For both cases, the speed throughout cruising flight may be determined accordingly.

5.4.4 Calculation of Maximum Range

This section is devoted to the calculation of the maximum range. As noted earlier, there are three programs during a cruising flight: (1) decreasing flight speed,

(2) increasing altitude, (3) decreasing angle of attack. These three flight programs are discussed separately.

5.4.4.1 Constant-Altitude, Constant-Lift-Coefficient Flight

In the case of constant-altitude, constant-lift-coefficient (flight program 1), substitution of maximum range velocity into Equation 5.66 results in the following maximum range:

$$R_{\max_1} = \frac{1.732 V_{\max_R} \left(L/D\right)_{\max}}{C} \left(1 - \sqrt{1 - \frac{W_f}{W_1}}\right) \tag{5.106}$$

In this equation, $V_{\max_R}$ is set as the initial speed. Thus, the initial speed is determined from Equation 5.105 and the final velocity from Equation 5.101. In addition, the lift coefficient is determined from Equation 5.102.

5.4.4.2 Constant-Airspeed, Constant-Lift-Coefficient Flight

The maximum range equation for flight program 2 is obtained by the substitution of Equations 5.101 and 5.104 into Equation 5.78 as follows:

$$R_{\max} = R_{\max_2} = \frac{0.866 V_{\max_R} \left(L/D\right)_{\max}}{C} \ln\left(\frac{1}{1 - \left(W_f/W_1\right)}\right) \tag{5.107}$$

Note that this equation is based on the constant-velocity, constant-lift-coefficient assumption (cruise-climb). In this flight program, the lift coefficient is determined from Equation 5.102, and the speed is determined from Equation 5.101.

Equations 5.106 and 5.107 indicate that, in order to increase the maximum range, one should: (1) Improve aircraft aerodynamic efficiency, (2) Reduce aircraft weight, (3) Employ an engine with a lower fuel consumption, and (4) Carry more fuel. For instance, in new Bombardier business jet Learjet 40/50, a number of improvements were made: (1) Winglet, (2) Powerful engines that use less fuel, and (3). A 200 lbs less weight in the nose section due to modern avionics. This combination of improvements lowered the aircraft drag by 2%, and resulted in an increased range of 4%.

5.4.4.3 Constant-Altitude, Constant-Airspeed Flight

In the case of constant-velocity, constant-altitude flight (flight program 3), the derivation of maximum range equation begins from Equation 5.89. According to Equation 5.104, the ratio between "lift-to-drag ratio for maximum range" and "the maximum lift-to-drag ratio" is 0.866, and so

$$\frac{\left(C_L/C_D\right)_1}{2\left(C_L/C_D\right)_{\max}} = \frac{0.866}{2} = 0.433$$

Moreover, plugging Equations 5.24 and 5.23 into $KC_{L_1}\left(\frac{C_L}{C_D}\right)_1$ yields

$$KC_{L_1}\left(\frac{C_L}{C_D}\right)_1 = K\left(0.577C_{L_{(L/D)\max}}\right)0.866\left(\frac{L}{D}\right)_{\max}$$

$$= K(0.577)\sqrt{\frac{C_{D_o}}{K}}(0.866)\frac{1}{2\sqrt{KC_{D_o}}} = \frac{0.577\times 0.866}{2} = 0.25$$

In addition, based on Equation 5.102, the initial lift coefficient is

$$C_{L_1} = C_{L_{\max R}} = \sqrt{\frac{C_{D_o}}{3K}} = 0.577C_{L_{(L/D)\max}} \tag{5.108}$$

Furthermore, based on Equation 5.104, the initial lift-to-drag ratio is

$$\left(\frac{C_L}{C_D}\right)_1 = \left(\frac{L}{D}\right)_{\max_R} = 0.866\left(\frac{L}{D}\right)_{\max} \tag{5.109}$$

Inserting these four terms into Equation 5.89, the following is obtained:

$$R_{\max_3} = \frac{2V_{\max_R}\left(L/D\right)_{\max}}{C}\tan^{-1}\left(\frac{0.433\left(W_f/W_1\right)}{1-0.25\left(W_f/W_1\right)}\right) \tag{5.110}$$

In this equation, the angle in the arc tangent term must be expressed in radian. Using the same technique as presented in Section 5.4.2.3, the final lift coefficient as a function of the initial lift coefficient is derived as

$$C_{L_2} = C_{L_1}\left(1-\frac{W_f}{W_1}\right) \tag{5.111}$$

It is emphasized again that among three maximum ranges for three flight programs (Equations 5.106–5.110); the second case (i.e., cruise-climb; Equation 5.107) delivers the absolute maximum range. The following example demonstrates this point.

Example 5.6

A jet transport aircraft with a mass of 100,000 kg, a fuel mass of 30,000 kg, and the following features is flying at 30,000 ft (9,144 m) altitude:

$$S = 341.5\,\text{m}^2,\ C_{D_o} = 0.016,\ K = 0.065,\ C = 0.8\,\text{N/h/N}$$

a. If this aircraft flies with the speed of 325.8 knots (603.4 km/h), how far can it fly without refueling? Determine the range for three following options:
   - Constant-altitude, constant-lift-coefficient flight
   - Constant-airspeed, constant-lift-coefficient flight
   - Constant-altitude, constant-airspeed flight

b. What is the velocity such that the aircraft delivers the maximum range?
c. Determine the maximum range for the same three options.

Solution

a. Regular range

Using Appendix B, at the altitude of 9,144 m, the air density ratio is 0.374. To find lift-to-drag ratio, we have

$$C_L = \frac{2W}{\rho S V^2} = \frac{2\times 100{,}000\times 9.81}{1.225\times 0.374\times 341.5\times(325.8\times 0.5144)^2} \Rightarrow C_L = 0.446 \quad (5.8)$$

$$C_D = C_{D_o} + KC_L^2 = 0.016 + 0.065\times 0.446^2 \Rightarrow C_D = 0.0289 \quad (3.12)$$

$$\frac{L}{D} = \frac{C_L}{C_D} = \frac{0.446}{0.0289} = 15.4 \quad (5.13)$$

The maximum lift-to-drag ratio is

$$\left(\frac{C_L}{C_D}\right)_{\max} = \frac{1}{2\sqrt{KC_{D_o}}} = \frac{1}{2\sqrt{0.065\times 0.016}} = 15.5 \quad (5.24)$$

Now, we calculate range at three different cases:

1. Constant-altitude, constant-lift-coefficient flight

$$R = \frac{2}{C}\frac{L}{D}V_1\left(1-\sqrt{1-\frac{W_f}{W_1}}\right) = \frac{2\times 15.4\times 325.8}{0.8}\left[1-\sqrt{1-\frac{30{,}000\times 9.81}{100{,}000\times 9.81}}\right] \quad (5.66)$$

$$\Rightarrow R = 2{,}048\,\text{nm} = 3{,}794\,\text{km}$$

(Note that the unit of V is nm/h [i.e., knot] and the unit of C is 1 per hour.)

2. Constant-airspeed, constant-lift-coefficient flight

$$R = \frac{V(L/D)}{C}\ln\left(\frac{1}{1-(W_f/W_1)}\right) = \frac{325.8\times 15.4}{0.8}\ln\left(\frac{1}{1-0.3}\right) \quad (5.71)$$

$$\Rightarrow R = 2{,}237\,\text{nm} = 4{,}143\,\text{km}$$

3. Constant-altitude, constant-airspeed flight

$$R_3 = \frac{2V\left(C_L/C_D\right)_{\max}}{C}\tan^{-1}\left[\frac{\left(C_L/C_D\right)_1\left(W_f/W_1\right)}{2\left(C_L/C_D\right)_{\max}\left(1-KC_{L_1}\left(C_L/C_D\right)_1\left(W_f/W_1\right)\right)}\right]$$

$$R = \frac{2\times 325.8\times 15.5}{0.8}\tan^{-1}\left[\frac{15.4\times 0.3}{2\times 15.5\times\left(1-0.065\times 0.446\times 15.4\times 0.3\right)}\right] \tag{5.89}$$

$$\Rightarrow R = 2{,}151.4\,\text{nm} = 3{,}984\,\text{km}$$

Comparison of the range of three flight programs demonstrates that the range of the cruise-climb flight is 4% more than the range of constant-altitude, constant-velocity flight and 9% more than the range of constant-altitude, constant-lift-coefficient flight. However, these ranges are not necessarily maximum ranges.

b. Maximum range velocity

The maximum range velocity is independent of flight program but is a function of the initial flight altitude

$$C_{L_{\max_R}} = \sqrt{\frac{C_{D_o}}{3K}} = \sqrt{\frac{0.016}{3\times 0.065}} = 0.286 \tag{5.102}$$

$$V_{\max_R} = \sqrt{\frac{2\,mg}{\rho S C_{L_{\max_R}}}} = \sqrt{\frac{2\times 100{,}000\times 9.81}{1.225\times 0.374\times 341.5\times 0.286}} = 209.4\,\text{m/s} \tag{5.101}$$

$$V_{\max_R} = 407.1\,\text{knot} \Rightarrow M = 0.69$$

c. Maximum range

We substitute the maximum range velocity into Equations 5.105–5.107 to determine the maximum range in three flight programs:

1. Constant-altitude, constant-lift-coefficient flight

$$R_{\max_1} = \frac{1.732V_{\max_R}\left(L/D\right)_{\max}}{C}\left(1-\sqrt{1-\frac{W_f}{W_1}}\right)$$

$$= \frac{1.732\times 407.1\times 15.5}{0.8}\left(1-\sqrt{1-0.3}\right) \tag{5.106}$$

$$\Rightarrow R_{\max} = 2{,}230\,\text{nm} = 4{,}127\,\text{km}$$

2. Constant-airspeed, constant-lift-coefficient flight

$$R_{\max} = R_{\max_2} = \frac{0.866V_{\max_R}\left(L/D\right)_{\max}}{C}\ln\left(\frac{1}{1-\left(W_f/W_1\right)}\right) \tag{5.107}$$

$$R_{\max} = \frac{0.866\times 407.1\times 15.5}{0.8}\ln\left(\frac{1}{1-0.3}\right) \Rightarrow R_{\max} = 2{,}436\,\text{nm} = 4{,}505\,\text{km}$$

3. Constant-altitude, constant-airspeed flight

$$R_{\max_3} = \frac{2V_{\max_R}\left(L/D\right)_{\max}}{C}\tan^{-1}\left(\frac{0.433\left(W_f/W_1\right)}{1-0.25\left(W_f/W_1\right)}\right)$$
$$= \frac{2\times 407.1\times 15.5}{0.8}\tan^{-1}\left(\frac{0.433\times 0.3}{1-0.25\times 0.3}\right) \tag{5.94}$$
$$\Rightarrow R_{\max} = 2{,}199\,\text{nm} = 4{,}070\,\text{km}$$

It is observed that the maximum range at cruise-climb flight condition is 9% higher than the range with the speed of 325.8 knot. The results of this section are very similar to the results of section (a). The results show that the maximum range for the cruise-climb flight is 1.3% more than the maximum range for constant-altitude, constant-velocity flight, and 9% more than the range of constant-altitude, constant-lift-coefficient flight.

5.4.5 Practical Considerations

5.4.5.1 Optimum Fuel Weight

One of the design applications of the range performance analysis is to determine the optimum fuel weight. It is evident that an aircraft can fly longer with more fuel in tanks. In Example 5.7, we found that the ranges of three flight programs are different. The question we would like to find the answer is that, as we carry more fuel in the tanks, what happens to the difference between the maximum ranges of three flight programs.

The ratio between the maximum range for a cruise-climb flight to that for constant-altitude, constant-lift-coefficient flight is

$$\frac{R_{\max_2}}{R_{\max_1}} = \frac{\left(\left(0.866V_{\max_R}\left(L/D\right)_{\max}\right)/C\right)\ln\left(1/(1-G)\right)}{\left(\left(1.732V_{\max_R}\left(L/D\right)_{\max}\right)/C\right)\left(1-\sqrt{1-G}\right)} = \frac{\ln\left(1/(1-G)\right)}{2\left(1-\sqrt{1-G}\right)} \tag{5.112}$$

Similarly, the ratio between the range for cruise-climb flight and the range for a constant-altitude, constant-speed flight is

$$\frac{R_{\max_2}}{R_{\max_3}} = \frac{\left(\left(0.866V_{\max_R}\left(L/D\right)_{\max}\right)/C\right)\ln\left(1/(1-G)\right)}{\left(\left(2V_{\max_R}\left(L/D\right)_{\max}\right)/C\right)\tan^{-1}\left(0.433G/(1-0.25G)\right)}$$
$$= \frac{0.4331n\left(1/(1-G)\right)}{\tan^{-1}\left[0.433G/(1-0.25G)\right]} \tag{5.113}$$

Recall that G denotes the ratio of fuel weight to aircraft weight. These relative ranges are plotted in Figure 5.17. As the amount of fuel fraction is increased (G increased), the difference among the ranges for the three flight programs becomes wider.

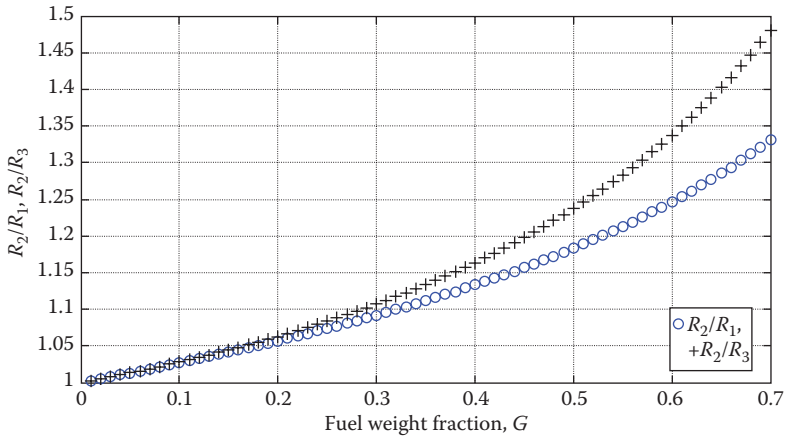

FIGURE 5.17 Relative maximum range as a function of the fuel fraction.

The figure indicates that differences in range among various flight programs are not as important for short-range flight as for long-range flight.

The cruise-fuel weight fraction is a measure of the fuel available for cruise; all of the fuel loaded on the ramp is not available for cruise. A portion of the fuel is used for taxiing, takeoff, and climb to the cruise altitude. Moreover, there must be fuel remaining at the end of cruise for safety reasons. For instance, the wind speed and direction (during cruise) may not be experienced as predicted, or destination may not be open for landing. In the latter case, under instrument flight rules, there must be sufficient fuel to fly to an alternate airport.

For a large transport aircraft, it is reasonable to assume that 3% of the total fuel is consumed prior to the start of cruise and that the reserve is also 10% of the fuel weight, leaving an 87% of the total fuel available for cruise. For a GA aircraft, it may be assumed that 6% of the total fuel (W_f) is consumed to reach cruise altitude, and the same reserve, so that 84% of the total fuel is available for cruise. With these assumptions, the initial cruise weight, W_1, is

$$W_1 = W_{TO} - 0.03W_f \quad (\text{large transport aircraft}) \tag{5.114}$$

$$W_1 = W_{TO} - 0.06W_f \quad (\text{small GA aircraft}) \tag{5.115}$$

If the available fuel for cruise is not needed and not consumed, the performance of the aircraft will be penalized by carrying the fuel as dead weight.

5.4.5.2 Wind Effect

Wind is a permanent feature of the atmosphere which impact range. The range of an aircraft is strongly influenced by the wind. The aerodynamic forces (e.g., lift and drag) are functions of airspeed and not the wind speed. In effect, when an aircraft is

experiencing a headwind, the lift and drag will not change, while the ground speed and range will be reduced. Conversely, when an aircraft is experiencing a tailwind, the ground speed and range will be increased. When an aircraft is cruising into a headwind, the ground speed is

$$V_G = V_W - V_\infty \tag{5.116}$$

In contrast, when an aircraft is cruising with a tailwind, the ground speed is

$$V_G = V_W + V_\infty \tag{5.117}$$

where V_∞ is the aircraft airspeed and V_W is the wind speed.

The prevailing direction of wind in the Northern Hemisphere is from southwest to northeast, while in the Southern Hemisphere it is from northeast to southwest. However, because of the rotation of the earth, and its Coriolis effect, the direction tilts by few degrees. The Coriolis effect is the deflective effect of the Earth's rotation on all free-moving objects, including the atmosphere. The deflection is to the right in the Northern Hemisphere and to the left in the Southern Hemisphere. Furthermore, the wind at high altitude is faster than the wind at low altitude due to the ground friction.

Depending on the direction of the aircraft, wind direction has an angle with aircraft direction (from 0° to 360°). Two important winds for straight-line level flight are those with 0° (headwind or nose-wind) and 180° (crosswind) direction. In these instances, the wind could be either headwind or tailwind. A headwind has an opposite direction compared to the aircraft direction, while a tailwind has the same direction. Consider a 30 knot wind that blows from east to west. This wind is a headwind for an aircraft that is flying from west to east. However, this wind is a tailwind for an aircraft that is cruising from east to west.

The range is calculated relative to the ground, so, the ground speed is employed instead of airspeed.

$$V_G = V_W \pm V_\infty \tag{5.118}$$

Since the wind affects the range, it will consequently influence the flight duration. Due to the three flight operations in a cruising flight, we derived six equations for range so far: three equations for the regular range and three equations for the maximum range. To include the effect of wind on range, in all of the six equations, just replace the V with V_G (i.e., $V_W \pm V_\infty$). For instance, the equations of range and maximum range for the cruise-climb flight operation (i.e., constant-velocity, constant-lift-coefficient) are shown here:

$$R_{W_2} = \frac{(V_\infty \pm V_W)(L/D)}{C} \ln\left(\frac{1}{1-(W_f/W_1)}\right) \tag{5.119}$$

$$R_{\max W} = R_{\max W_2} = \frac{0.866\left(V_{\max R} \pm V_W\right)(L/D)_{\max}}{C} \ln\left(\frac{1}{1-\left(W_f/W_1\right)}\right) \quad (5.120)$$

where R_{W_2} and $R_{\max W_2}$ indicate the range and maximum range, respectively, when the wind effect is included. Other parameters will not be varied.

In 2018, a Norwegian Boeing 787-9 Dreamliner broke the record [68] for the fastest ever transatlantic flight in a subsonic passenger aircraft, flying from New York to London in just over 5 h. The airplane "was able to reach a top speed of 776 mph as it hurtled across the Atlantic Ocean after being pushed by an extra strong jet stream (i.e., wind) that at times reached 202 mph.

Case Study - Example 5.7

The jet transport aircraft DC-9-30 with 100 seats is cruising at 30,000 ft (9,144 m) altitude with the speed of Mach 0.78. This aircraft that has a mass of 44,000 kg at the beginning of cruising flight is planned to descend and then land when 7,000 kg of its fuel is consumed. Turbofan engines of this aircraft (JT8D-1S) have fuel specific consumption of 0.82 N/h/N. Other features of this aircraft are

$$e = 0.82,\ b = 29\,\text{m}, C_{D_o} = 0.02, S = 93\,\text{m}^2$$

a. What is the maximum range of this aircraft at this flight?
b. Determine the range of this flight (i.e., constant-altitude, constant-airspeed).
c. Determine the required thrust of this flight.
d. What is the fuel consumption rate (in kg/h)?
e. Determine the duration of this flight.
f. If the plan is to fly with maximum range objective, determine the altitude at the end of the flight.
g. What is the seat-km capacity of this aircraft per 1 L of fuel?
h. Compare this feature of the aircraft with a car that consumes 10 L of fuel per 100 km.

Assume ISA condition.

Solution

a. Maximum range

$$\text{AR} = \frac{b^2}{S} = \frac{29^2}{93} = 9 \quad (3.9)$$

$$K = \frac{1}{\pi e \text{AR}} = \frac{1}{3.14 \times 0.82 \times 9} = 0.043 \quad (3.8)$$

$$C_{L_{\max R}} = \sqrt{\frac{C_{D_o}}{3K}} = \sqrt{\frac{0.02}{3 \times 0.043}} = 0.394 \quad (5.102)$$

$$V_{\max_R} = \sqrt{\frac{2mg}{\rho S\sqrt{C_{D_o}/3K}}} = \sqrt{\frac{2\times 44{,}000\times 9.81}{1.225\times 0.374\times 93\times 0.394}} = 226.8\,\text{m/s} \quad (5.101)$$

At 9,144 m altitude, the speed of sound is 303 m/s, and so:

$$M_{\max_R} = \frac{226.3}{303} = 0.748 \quad (1.36)$$

$$\left(\frac{C_L}{C_D}\right)_{\max} = \frac{1}{2\sqrt{KC_{D_o}}} = \frac{1}{2\sqrt{0.043\times 0.02}} = 17 \quad (5.24)$$

$$G = \frac{W_f}{W_1} = \frac{m_f}{m_1} = \frac{7{,}000}{44{,}000} = 0.159 \quad (5.82)$$

$$R_{\max} = R_{\max_2} = \frac{0.866 V_{\max_R}(L/D)}{C}\ln\left(\frac{1}{1-(W_f/W_1)}\right)$$
$$R_{\max} = \frac{0.866\times 226.8\times 17\times 3.6}{0.82}\ln\left(\frac{1}{1-0.159}\right) \Rightarrow R_{\max} = 2{,}538.4\,\text{km} \quad (5.107)$$

Note that the number 3.6 is used to convert C to 1/s.

b. Range at the specified flight condition

$$C_L = \frac{2W}{\rho S V^2} = \frac{2\times 44{,}000\times 9.81}{1.225\times 0.374\times 93\times(303\times 0.78)^2} \Rightarrow C_L = 0.363 \quad (5.8)$$

$$C_D = C_{D_o} + KC_L^2 = 0.02 + \left(0.043\times 0.363^3\right) \Rightarrow C_D = 0.0256 \quad (3.12)$$

While the lift-to-drag ratio is

$$\frac{L}{D} = \frac{C_L}{C_D} = \frac{0.363}{0.0256} = 14.13$$

$$R = \frac{2V\left(C_L/C_D\right)_{\max}}{C}\tan^{-1}\left[\frac{\left(C_L/C_D\right)_1\left(W_f/W_1\right)}{2\left(C_L/C_D\right)_{\max}\left(1-KC_{L_1}\left(C_L/C_D\right)_1\left(W_f/W_1\right)\right)}\right] \quad (5.89)$$

$$R = \frac{2\times 0.78\times 303\times 17}{0.82}\tan^{-1}\left[\frac{14.13\times 0.159}{2\times 17\times\left[1-0.043\times 0.363\times 14.13\times 0.159\right]}\right]$$
$$= 2{,}413.18\,\text{km}$$

It is observed that this range is 125 km shorter than the maximum range.

c. Engine thrust

$$D = \frac{1}{2}\rho V^2 S C_D$$

$$D = \frac{1}{2} \times 1.225 \times 0.374 \times (303 \times 0.78)^2 \times 93 \times 0.0256 \tag{3.1}$$

$$\Rightarrow D = 30{,}463\,\text{N} \approx 30\,\text{kN}$$

$$T = D = 30{,}463\,\text{N} \approx 30\,\text{kN}$$

The engine thrust must be equal to aircraft drag, and so the engine must produce about 30 kN of thrust for this flight.

d. Flow rate

$$C = \frac{Q_f}{T} = Q_f = TC = \frac{30{,}463 \times 0.82}{9.81} = 2{,}546\,\text{kg/h} \tag{5.56}$$

e. Flight duration

$$t = \frac{m_f}{Q_f} = \frac{7{,}000}{2{,}546.3} = 2.75\,\text{h} \tag{5.56}$$

f. Maximum range is obtained if the aircraft flies with cruise-climb flight program. Thus, the altitude at the end of this flight would be

$$\sigma_2 = \sigma_1(1 - G) = 0.374 \times (1 - 0.159) = 0.3145 \tag{5.83}$$

Referring to Appendix B, this density ratio belongs to 34,500 ft altitude. Since the aircraft was initially flying at 30,000 ft, the increase in altitude will be 4,500 ft.

g. Seat kilometer

$$\frac{\text{Seat-km}}{\text{kg of fuel}} = \frac{100 \times 0.78 \times 303 \times 3.6}{2546.3} = 33.4$$

h. Comparison with car

A car that can carry 5 passengers has 50 seat-km capacity ($5 \times 100/10 = 50$), and so the ratio of the car capacity to that of this aircraft is

$$\frac{50}{33.4} = 1.497 \approx 1.5$$

This means that a car, compared with an aircraft, has about 50% more seat-km capacity for each kg of fuel.

TABLE 5.5
Summary of Range Equations

Flight Program	Range		Flight Variables						
	Type	Equation	Speed		Altitude		Lift Coefficient		Weight
			Initial	Final	Initial	Final	Initial	Final	Final
1.	Regular	5.66	Given	5.72	Given	Same	5.73	5.73	5.77
	Maximum	5.107	5.105	5.72	Given	Same	5.102	5.102	5.77
2.	Regular	5.78	Given	Same	Given	5.83	5.79	5.79	5.77
	Maximum	5.105	5.101	5.101	Given	5.83	5.102	5.102	5.77
3.	Regular	5.89	Given	Same	Given	Same	5.90	5.95	5.77
	Maximum	5.106	5.101	5.101	Given	Same	5.108	5.111	5.77

5.4.6 Comparison and Conclusion

Table 5.5 presents a summary of range equations with corresponding flight variables. In this table, the word "Given" means that the pilot can select any acceptable airspeed (i.e., a speed from the stall speed to maximum speed) that he/she wishes. In addition, the word "same" indicates that the final value is the same as the initial value.

5.5 ENDURANCE

Another significant aircraft performance item and a design parameter is the endurance. For some aircraft, the most important performance parameter of the mission is to be airborne as long as possible (i.e., the longest endurance). Some examples are as follows:

- An aircraft is ready to land on destination airport, but the airport is not ready or busy. In this case, the pilot must loiter above the airport until the landing permission is issued by the airport control tower.
- An antisubmarine airplane must wait airborne until it can identify an enemy submarine. In this case, the pilot must fly around a specific target area until a submarine is coming up.
- A reconnaissance aircraft must wait airborne in an area close to the target area until it can receive the enemy signal.
- An early warning aircraft (i.e., airborne warning and control system [AWACS], for example, Boeing E-3 Sentry) must hide airborne at a specific area to transmit commanded signals to its team aircraft.
- An aircraft is planned to land on an airfield, but the weather at that area is not favorable for landing for a short time. In this case, the pilot must remain airborne until the weather cooperates and allows the aircraft to be landed.
- A border control aircraft must fly such that the crew can monitor the specific border area as long as possible.

- A relay aircraft is designed to receive a signal from a commander site and then to relay and transmit these signals after amplification to a final receiver (e.g., ground station).

At all of the above flight conditions, the best choice for a pilot is to be airborne with a speed such that it can stay in the air as long as possible. Many basic fundamentals for endurance and range are similar. The only difference is to consider how long (time) the aircraft can fly rather than how far (distance) it can fly. The objective for this flight is to minimize the fuel consumption, because the aircraft has limited fuel. A *loiter* is a flight condition where endurance is its primary objective.

The Scaled Composites Virgin Atlantic GlobalFlyer [9] is an aircraft designed by Burt Rutan in which Steve Fossett flew a solo nonstop airplane flight around the world in a time of 67 h 1 min from February 28, 2005, until March 3, 2005 (world record). The flight speed of 319 knots broke the Absolute World Record for the fastest nonstop unrefueled circumnavigation set by the previous Voyager aircraft at 9 days 3 min and an average speed of 100 knots.

Another long-endurance jet aircraft is Northrop Grumman RQ-4 Global Hawk [62], an UAV with a mass of 14,628 kg and a wing span of 39.9 m is equipped with a turbofan engine with a maximum thrust of 34 kN. This surveillance aircraft has an endurance of 34+ h. According to General Atomics, the newly improved unmanned aircraft Gray Eagle can stay in the air for 25 h and is capable of surveillance over 24 h per mission while carrying 800 lb of payload. In this section, the definition of endurance is presented, and then the techniques to determine the maximum endurance velocity and maximum endurance are discussed.

5.5.1 Definition of Endurance

Endurance (E) is the length of time that an aircraft can remain airborne for a given expenditure of fuel and for a specified set of flight condition. In effect, endurance includes all phases of flight such as takeoff, climb, cruise, descent, and landing. However, due to simplicity, we only consider a level flight portion of the flight (i.e., cruise). For a long-range transport aircraft, about 70%–80% of the flight will be in cruising portion. For instance, a transport aircraft flying from New York City to Seattle spends about 5 h in cruise, while spending about 20 min for takeoff/climb and 30 min for descent/landing.

To develop an expression for endurance, we employ the term "specific endurance" (SE), which is defined as the flight duration (t in h or s) per unit of fuel mass (m in kg or slug) or fuel weight (W in N or lbf). For aircraft with turbofan or turbojet engine, the SE is defined as

$$\mathrm{SE} = \frac{dt}{-dW} \tag{5.121}$$

The minus sign is used to account for a decrease in fuel weight during the flight operation. Recall that we are only considering a level flight, so the lift will be almost

equal to aircraft weight ($L = W$), and engine thrust is approximately equal to aircraft drag ($T = D$).

By employing the definition of specific fuel consumption ($C = Q/T$) and the fuel flow rate ($Q = dW/dt$), we can develop the following:

$$\frac{dt}{dW} = \frac{dt}{Qdt} = \frac{1}{Q} = \frac{1}{CT} = \frac{1}{CD} \tag{5.122}$$

Multiplying both numerator and denominator by lift (L) and replacing one of them with weight (W) results in

$$\frac{dt}{dW} = \frac{1}{CD} = \frac{1}{CDL} = \frac{1}{CDW} \Rightarrow dt = \frac{1}{CD} = \frac{-L}{CD}\frac{dW}{W} \tag{5.123}$$

To derive an equation for endurance, we now integrate the SE for the entire time of cruising flight. It means from the time that aircraft has the initial weight to when the aircraft has consumed its fuel (W_f)

$$E = \int_0^{\text{end}} dt = \int_{W_1}^{W_2} \frac{-L}{CD}\frac{dW}{W} \tag{5.124}$$

where W_1 is the aircraft weight at the beginning of the flight and W_2 at the end of flight. Equation 5.124 is a general equation for endurance for a jet aircraft.

5.5.2 Endurance Calculation

Equation 5.128 is the general expression for the endurance of an aircraft. If the detailed variations of C, L, D, and W are known, one can mathematically integrate to find a closed-form solution for the endurance. The mathematical integration requires an implementation of practical considerations, which will be discussed here. To solve the integration (Equation 5.128) and arrive at a closed-form solution, we need to set a few simplifying assumptions. During the duration of cruising flight (steady level), the lift should be kept equal (if the engine thrust contribution is neglected) to the aircraft weight:

$$L = W = \frac{1}{2}\rho S V^2 C_L \tag{5.8}$$

At any weight, the speed is associated with an angle of attack, and indeed with a lift coefficient (C_L) and an altitude. Assuming specific consumption is constant, and considering Equation 5.10 in mind, Equation 5.124 has independent parameters that are weight (W), velocity (V), altitude or its corresponding air density (ρ), and angle of attack or its associated lift coefficient (C_L).

Since the fuel is consumed during flight, the aircraft weight is constantly decreased during the flight. To maintain a level flight, we have to simultaneously decrease the

lift as well. As discussed in Section 5.4, there are three major flight programs to maintain the cruising flight for the continuous decrease of the lift (Figure 5.14):

1. Decreasing flight speed (constant-altitude, constant-lift-coefficient flight)
2. Increasing altitude (constant-airspeed, constant-lift-coefficient flight)
3. Decreasing angle of attack (constant-altitude, constant-airspeed flight)

For each flight program, the integral Equation (5.124) will be set up and then only the final endurance equation will be shown and discussed. In the first option, the velocity must be reduced with the same rate as the aircraft weight is decreased. In the second solution, the air density must be decreased; in other words, the flight altitude must be increased. The third option offers the reduction of aircraft angle of attack, that is, the reduction of lift coefficient. In terms of pilot operation, the first option is applied through throttle and the third option is implemented through stick/yoke/wheel.

In the second option, no action is needed by the pilot and the aircraft will gradually gain height (climbs). Based on safety regulations and practical considerations, the second option is the option of interest for majority of aircraft. In general, when flight is conducted under the jurisdiction of Federal Aviation Regulations, the accepted flight program is the constant-altitude, constant-airspeed flight program.

5.5.2.1 Flight Program 1: Constant-Altitude, Constant-Lift-Coefficient Flight

In this flight program, the velocity is decreased as the weight is dropped. The drag coefficient is already defined as

$$C_D = C_{D_o} + KC_L^2 \tag{3.12}$$

Plugging this equation into Equation 5.124, and since $L/D = C_L/C_D$ in a cruising flight, we can write

$$E = -\frac{1}{C}\frac{C_L}{C_D}\int_{W_1}^{W_2}\frac{dW}{W} = -\frac{1}{C}\int_{W_1}^{W_2}\frac{C_L}{C_{D_o}+kC_L^2}\frac{dW}{W} \tag{5.125}$$

The ratio of $C_L/\left(C_{D_o} + KC_L^2\right)$ has a constant value and will be taken out of the integration, and so

$$E = -\frac{1}{C}\frac{C_L}{C_{D_o}+KC_L^2}\int_{W_1}^{W_2}\frac{dW}{W} = \frac{1}{C}\frac{C_L}{C_D}\int_{W_1}^{W_2}\frac{dW}{W} \tag{5.126}$$

The result of this integration is

$$E_1 = \frac{C_L/C_D}{C}\ln\left[\frac{W_1}{W_2}\right] = \frac{\left(C_L/C_D\right)}{C}\ln\left[\frac{1}{1-\left(W_f - W_1\right)}\right] = \frac{\left(C_L/C_D\right)}{C}\ln\left[\frac{1}{1-G}\right] \tag{5.127}$$

where $\ln[W_1/W_2]$ is equal to $\ln[W_1] - \ln[W_2]$. The parameter W_f denotes the fuel weight

$$W_f = W_1 - W_2 \tag{5.128}$$

Equation 5.127 implies that endurance is a function of lift-to-drag ratio and fuel weight. It also indicates that the endurance is an inverse function of SFC. As the initial fuel weight and the lift-to-drag ratio increase, the endurance will be increased. Furthermore, as the SFC is decreased, the endurance will be improved.

It can be seen from Equation 5.8 that the airspeed must be decreased as fuel is consumed along the flight path. To determine the final airspeed V_2, we know that the aircraft weight is equal to the lift at the beginning and at the end of flight. As we derived in Section 5.4, this leads to the fact that the velocity at the end of flight is reduced to

$$V_2 = V_1\sqrt{1-\frac{W_f}{W_1}} \tag{5.129}$$

Since C_L is held constant, Equations 5.7, 5.8, and 3.1 imply that the thrust must be constantly decreased (by constantly setting back the throttle) as the fuel is burnt (i.e., the gross weight decreases).

5.5.2.2 Flight Program 2: Constant-Airspeed, Constant-Lift-Coefficient Flight

In this flight program, the altitude is increased as the aircraft weight is dropped (i.e., cruise-climb). By inspection, we notice that this flight option results in the same closed-form solution as the first flight option

$$E_2 = \frac{C_L/C_D}{C}\ln\left[\frac{1}{1-G}\right] \tag{5.130}$$

By inspection, we can conclude that

$$E_2 = E_1 \tag{5.131}$$

Two flight programs of 1 and 2 have similar endurance.

The cruise altitude for a cruise-climb flight option is gradually increasing. The altitude at the end of cruise-climb flight (h_2) can be expressed in terms of both the initial altitude (h_1) and the fuel fraction. The derivation is given earlier. The density ratio at the end of cruise-climb flight (σ_2) in terms of both the initial density ratio and the fuel fraction is given in Equation 5.83, and repeated here for convenience:

$$\sigma_2 = \sigma_1(1-G) \tag{5.132}$$

where σ_1 is the air density ratio at the beginning of the cruise and G is the fuel fraction. The overall climb angle is so small that it can be ignored. When the air density at the end of cruise-climb flight (σ_2) is obtained, one can utilize Appendix A or B to determine the final altitude.

5.5.2.3 Flight Program 3: Constant-Altitude, Constant-Airspeed Flight

In this flight program, the lift coefficient is decreased as the aircraft weight is decreased. Since the lift is equal to the weight during cruise, the L from the numerator and W from the denominator of Equation 5.124 are eliminated. Thus, the endurance equation for this flight program can be simplified as

$$E = \frac{1}{C}\int_{W_1}^{W_2} \frac{dW}{D} \tag{5.133}$$

The variations of drag with respect to aircraft weight are nonlinear. As derived in Equation 5.35, the drag is a function of aircraft weight as follows:

$$D = \frac{1}{2}\rho V^2 S C_{D_o} + \frac{2KW^2}{\rho V^2 S} \tag{5.134}$$

Plugging Equation 5.134 into Equation 5.133 yields

$$E_3 = \frac{1}{C}\int_{W_1}^{W_2} \frac{dW}{(1/2)\rho V^2 S C_{D_o} + \left(2KW^2/\rho V^2 S\right)} \tag{5.135}$$

or

$$E_3 = -\frac{1}{C\left(2K/\rho V^2 S\right)}\int_{W_1}^{W_2} \frac{dW}{\left(\left(\left(\rho V^2 S\right)^2 C_{D_o}\right)/4K\right) + W^2} \tag{5.136}$$

Using a mathematical reference [69], the solution of the integration with a similar form is determined

$$\int \frac{dx}{a^2 + x^2} = \frac{1}{a}\tan^{-1}\left(\frac{x}{a}\right) \tag{5.137}$$

where

$$a = \frac{1}{2}\rho V^2 S\left(\frac{C_{D_o}}{K}\right)^{1/2} \tag{5.138}$$

Therefore, the solution for the integration is

$$E_3 = -\frac{1}{C\left(2K/\left(\rho V^2 S\right)\right)}\frac{1}{\left(1/2\right)\rho V^2 S\left(C_{D_o}/K\right)^{1/2}} \times \left[\tan^{-1}\left(\frac{W}{\left(1/2\right)\rho V^2 S\left(C_{D_o}/K\right)^{1/2}}\right)\right]_{W_1}^{W_2} \tag{5.139}$$

Since the maximum lift-to-drag ratio is related to $\sqrt{KC_{D_o}}$, and $\sqrt{KC_{D_o}} = 1/2\left(C_L/C_D\right)_{\max}$, the equation will be simplified to

$$E_3 = \frac{2\left(L/D\right)_{\max}}{C}\left[\tan^{-1}\left(\frac{2W_1}{\rho V^2 S\sqrt{C_{D_o}/K}}\right) - \tan^{-1}\left(\frac{2W_2}{\rho V^2 S\sqrt{C_{D_o}/K}}\right)\right] \tag{5.140}$$

As derived in Equation 5.40, the term $\sqrt{C_{D_o}/K}$ is equal to the minimum-drag lift coefficient, $C_{L_{\min D}}$.

$$E_3 = \frac{2\left(L/D\right)_{\max}}{C}\left[\tan^{-1}\left(\frac{2W_1}{\rho V^2 S C_{L_{\min D}}}\right) - \tan^{-1}\left(\frac{2W_2}{\rho V^2 S C_{L_{\min D}}}\right)\right] \tag{5.141}$$

The bracketed term represents the difference between two angles (in radian). Equation 5.141 is valid for any given constant-altitude, and any given constant velocity, as long as the altitude and the velocity are permissible (i.e., within the flight envelope of the aircraft). In this flight program, the initial lift coefficient and the final lift coefficient are readily obtained from Equations 5.90 and 5.91, respectively. Inserting the relationship between initial weight, final weight, and fuel weight ($W_2 = W_1(1-G)$) into Equation 6.78 and converting the difference between the tangent of two angles, we may reformat Equation 5.141 as

$$E_3 = \frac{2\left(L/D\right)_{\max}}{C}\tan^{-1}\left[\frac{\left(C_L/C_D\right)_1 G}{2\left(C_L/C_D\right)_{\max}\left(1 - KC_{L_1}\left(C_L/C_D\right)_1 G\right)}\right] \tag{5.142}$$

where C_{L_1} is the initial lift coefficient (Equation 5.90) and $\left(C_L/C_D\right)_1$ denotes the initial lift-to-drag ratio (i.e., $C_{L_1}/\left(C_{D_o} + KC_{L_1}^2\right)$).

From the theoretical point of view, all three flight programs are realizable; but in practice, only the third case is acceptable, and approved for GA and transport aircraft by the FAA. The third case is hard to follow by a human pilot because the pilot must constantly decrease the angle of attack through deflection of the elevator. However, for an aircraft equipped with an autopilot, this is an easy task. This case is the safest flight program among three possible programs.

A comparison between endurance Equations 5.127, 5.130, and 5.142 and range equations (e.g., Equation 5.78) shows that endurance is simply equal to the range divided by airspeed. Three endurance equations (E_1, 5.127; E_2, 5.130; and E_3, 5.142) provide the technique to find the endurance for a jet aircraft while at a cruising flight with given flight conditions. In endurance equations, the unit of endurance is the reciprocal of the unit of specific fuel consumption (C). For instance, if the unit of C is 1/h, the unit of endurance will be in terms of hour.

5.5.3 Maximum Endurance Velocity

As we classified earlier, there are three options in a cruising flight for an endurance mission. These can be regrouped into two groups: (1) constant-speed flight (cases 2 and 3) and (2) non-constant-speed flight (case 1). For cases 2 and 3, the technique to determine the maximum endurance velocity ($V_{\max_E}$) to maximize the endurance is presented.

In a jet aircraft, the SFC is almost constant with speed, so in order to minimize the fuel consumption, the aircraft should fly such that it requires minimum thrust. This implies that we need to fly with an airspeed that produces the minimum drag. Furthermore, Equation 5.130 confirms that in order to maximize the endurance, the aircraft must fly with a speed such that the $(L/D)_{\max}$ is maximized. Therefore, the maximum endurance speed is the same as minimum drag speed as follows:

$$V_{\max_E} = V_{\min_D} = \sqrt{\frac{2\,mg}{\rho S\sqrt{C_{D_o}/K}}} \tag{5.143}$$

We note from Equation 5.143 that the maximum endurance velocity is a function of aircraft weight and altitude, and inverse function of wing area and zero-lift drag coefficient. As noted, the maximum endurance velocity is proportional to the square root of air density (i.e., altitude); it increases with altitude.

By comparing Equations 5.143 and 5.59, we can conclude that the lift coefficient at maximum endurance speed is equal to the square root of ratio of the zero-lift drag coefficient (C_{D_o}) and the induced drag factor (K). Hence

$$C_{L_{\max_E}} = C_{L_{\min_D}} = C_{L_{(L/D)_{\max}}} = \sqrt{\frac{C_{D_o}}{K}} \tag{5.144}$$

The typical value for the maximum endurance lift coefficient ($C_{L_{\max_E}}$) is about 0.3–0.6. In theory, the maximum endurance velocity may become lower than the stall speed or could be greater than the stall speed. However, in practice, only a maximum endurance velocity higher than the stall speed is allowable. For an aircraft whose maximum endurance speed is theoretically lower than the stall speed, a safe maximum endurance speed is selected (considered) to be about 10%–20% higher than the stall speed.

$$V_{\max_E} = kV_s \tag{5.145}$$

where

$$1.1 < k < 1.2 \tag{5.146}$$

It should be emphasized that this velocity has been derived based on the assumption that the SFC is constant with speed.

For a non-constant-speed flight operation (case 1), the velocity at the beginning of flight to maximize the endurance is assumed equal to the maximum endurance velocity, as derived before

$$V_1 = V_{\max_E} = \sqrt{\frac{2\,mg}{\rho S\sqrt{C_{D_o}/K}}} \tag{5.147}$$

To find the final airspeed V_2, we know that the aircraft weight is equal to the lift at the beginning and at the end of flight. As we derived in Section 5.4, this leads to

$$V_2 = V_1\sqrt{1-\frac{W_f}{W_1}} \tag{5.148}$$

Since C_L is held constant, Equation 5.8 implies that the thrust must be constantly decreased (by constantly setting back the throttle) as the fuel is burning (i.e., the gross weight decreases).

5.5.4 Maximum Endurance

Three endurance equations (E_1, 5.127, E_2, 5.130, and E_3, 5.140) provide the technique to find the regular endurance for a jet aircraft. However, we are more interested in determining the maximum endurance. In this section, the technique to determine the maximum endurance ($E_{\max}$) for a jet aircraft is developed.

As we classified earlier, there are three options in a cruising flight for an endurance mission: (1) Constant-altitude, constant-lift coefficient flight; (2) Constant-airspeed, constant-lift coefficient flight; and (3) Constant-altitude, constant-airspeed flight. In Section 5.5.2, three equations were derived for calculations of regular endurance at any flight condition. Moreover, in Section 5.5.3, an equation was developed for the speed to maximize endurance.

Equations 5.127, 5.130, and 5.140 illustrate that in order to maximize the endurance during aircraft design phase the SFC must be minimized, while the fuel weight should be maximized (carry the highest possible fuel). When an aircraft is manufactured, the pilot can maximize endurance with selecting flight conditions. In the derivation process in this section, we assume that the specific fuel consumption (C) is constant with speed and altitude. Table 5.6 presents endurance of several jet aircraft.

TABLE 5.6
Endurance of Several Jet Aircraft

No.	Aircraft	Type	T (kN)	Mass (kg)	Endurance
1.	British Aerospace Harrier II	Close support	105.9	14,061	3 h
2.	BAE Hawk 60	Attack	25.35	5,700	2 h, 42 min
3.	Boeing E-3 Sentry	Airborne warning	2×273.6	171,255	10 h
4.	McDonnell Douglas F/A-18 Hornet	Fighter	2×71.2	25,401	1 h, 45 min
5.	Sukhoi Su-57	Fighter	2×142	35,000	6 h
6.	Mikoyan MiG-31	Interceptor	2×91.3	41,000	3 h, 36 min
7.	Aeromacchi MB-339C	Fighter	19.57	6,350	3 h, 50 min
8.	Northrop Grumman RQ-4 Global Hawk	Reconnaissance UAV	31.4	11,600	28 h
9.	Boeing 737-Max 7	Transport	2×130	80,000	9 h
10.	Airbus 380-800	Transport	4×348	575,000	13 h
11.	Virgin Atlantic GlobalFlyer	Nonstop flight around the world	10	10,024	67 h
12.	Dassault/Dornier Alphajet	Trainer	2×14.1	8,000	3 h, 30 min
13.	Panavia Tornado	Fighter	2×71.2	24,500	2 h
14.	Saai-marchetti S.211	Fighter	11.12	2,750	3 h, 50 min
15.	Lockheed U-2	Reconnaissance	76	18,600	>10 h
16.	Boeing E-6A	Relay	4×97.9	155,128	15 h, 24 min
17.	Mirage F-1	Fighter	70.6	16,200	2 h, 15 min

5.5.4.1 Constant-Altitude, Constant-Lift Coefficient

In this flight program, the velocity is decreased as the weight is dropped. In Section5.5.2.1, the equation to calculate the regular endurance was developed (Equation 5.127). By inspection of Equation 5.127, we notice that the endurance will be maximized when lift-to-drag ratio is at its maximum value (Equation 5.24). Therefore, the maximum endurance is

$$E_{\max_1} = \frac{\left(C_L/C_D\right)_{\max}}{C} \ln\left[\frac{1}{1-\left(W_f/W_1\right)}\right] \tag{5.149}$$

This relationship implies that in order to maximize the endurance (in this flight program), the pilot must always cruise with any combination of lift coefficient, velocity, and altitude such that the flight delivers the maximum lift-to-drag ratio, $(L/D)_{\max}$. This implies that the lift coefficient should always be

$$C_{L_{\max E}} = \sqrt{\frac{C_{D_o}}{K}} \tag{5.150}$$

Since the velocity is reduced during this flight program, the initial velocity will be

$$V_1 = \sqrt{\frac{2W_1}{\rho S\sqrt{C_{D_o}/K}}} \tag{5.151}$$

Similarly, the final velocity will be

$$V_2 = \sqrt{\frac{2W_2}{\rho S\sqrt{C_{D_o}/K}}} \tag{5.152}$$

In theory, this maximum endurance can be achieved at any fixed altitude as long as the flight conditions are practical.

5.5.4.2 Constant-Airspeed, Constant-Lift Coefficient

In this flight program, the altitude is increased as the aircraft weight is dropped (i.e., cruise-climb). In Section 5.5.2.2, the equation to calculate the regular endurance was developed (Equation 5.130). By inspection of Equation 5.130, we notice that the endurance will be maximized when lift-to-drag ratio is at its maximum value (Equation 5.24). Therefore, the maximum endurance is

$$E_{\max_2} = \frac{\left(L/D\right)_{\max}}{C}\ln\left[\frac{1}{1-G}\right] \tag{5.153}$$

This relationship implies that in order to maximize the endurance (in this flight program), the pilot must always cruise with the velocity such that the flight delivers the maximum lift-to-drag ratio; $(L/D)_{\max}$ (i.e., $V_{\max_E}$; Equation 5.143) and a lift coefficient that has a value equal to $\sqrt{C_{D_o}/K}$ (Equation 5.143). The only choice the pilot has is to select the initial altitude and increase it along the flight. It is observed that flight programs 1 and 2 deliver the same endurance (i.e., $E_{\max_1} = E_{\max_2}$).

Due to speed instability, flight at the maximum endurance speed is often not realizable. To resolve this problem, it is recommended to fly at a speed that is 10%–20% higher than the minimum drag speed. This leads to the endurance being lower than the calculated one.

5.5.4.3 Constant-Altitude, Constant-Airspeed Flight

In this flight program, the lift coefficient gradually decreases as the aircraft weight is dropped. In Section 5.5.2.3, the equation to calculate the regular endurance was developed (Equation 5.142). By inspection of Equation 5.142, we notice that the maximum endurance is when the ratio inside the parentheses is maximized:

$$E_{\max_3} = \frac{2\left(C_L/C_D\right)_{\max}}{C} \times \tan^{-1}\left[\frac{\left(C_L/C_D\right)_{\max}\left(W_f/W_1\right)}{2\left(C_L/C_D\right)_{\max}\left(1-KC_{L_{\max_E}}\left(C_L/C_D\right)_{\max}\left(W_f-W_1\right)\right)}\right] \tag{5.154}$$

By inserting Equations 5.24 and 5.146 into Equation 5.154, we obtain:

$$E_{\max_3} = \frac{2\left(C_L/C_D\right)_{\max}}{C} \tan^{-1}\left[\frac{G}{2\left(1-K\sqrt{C_{D_o}/K}\left(1/2\sqrt{KC_{D_o}}\right)G\right)}\right] \tag{5.155}$$

which results in

$$E_{\max_3} = \frac{2\left(C_L/C_D\right)_{\max}}{C} \tan^{-1}\left[\frac{0.5G}{1-0.5G}\right] \tag{5.156}$$

This relationship implies that in order to maximize the endurance (in this flight program), the pilot must always cruise with an initial velocity such that the flight delivers the maximum lift-to-drag ratio; $(L/D)_{\max}$ (i.e., $V_{\max_E}$; Equation 5.143) and an initial lift coefficient that has a value equal to $\sqrt{C_{D_o}/K}$ (Equation 5.143). The only choice the pilot has is to select a fixed altitude and to keep it along the flight. In Equation 5.156, the initial lift coefficient is

$$C_{L_1} = \sqrt{\frac{C_{D_o}}{K}} \tag{5.157}$$

However, the final lift coefficient decreases to

$$C_{L_2} = C_{L_1}\frac{W_2}{W_1} \tag{5.158}$$

where W_2 is the final weight at the end of cruise.

Case Study - Example 5.8

Determine the maximum endurance for the transport aircraft DC-9-30 for a constant-airspeed, constant-lift coefficient flight program. The characteristics of this aircraft are given in Example 5.7. Then, determine the maximum endurance speed if the aircraft cruises at sea level.

Solution

Using the result of Example 5.7, we have

$$\left(L/D\right)_{\max} = 17 \text{ and } G = 0.159$$

This constant-airspeed, constant-lift coefficient flight program is the flight program 2; so $E_{\max} = E_{\max_2}$. Then:

$$E_{\max} = \frac{(L/D)_{\max}}{C}\ln\left[\frac{1}{1-G}\right] = \frac{17}{0.82}\ln\left[\frac{1}{1-0.159}\right] \Rightarrow E_{\max} = 3.59\,\text{h} \tag{5.153}$$

Comparison of this value with the result of section "e" of Example 5.7 reveals that if the pilot flies for the maximum range, the flight duration is 3 h, which is 0.59 h shorter than this case.

To calculate the maximum endurance speed,

$$C_{L_{\max_E}} = \sqrt{\frac{C_{D_o}}{K}} = \sqrt{\frac{0.02}{0.043}} = 0.682 \tag{5.144}$$

$$V_{\max_E} = \sqrt{\frac{2\,mg}{\rho S\sqrt{C_{D_o}/K}}} = \sqrt{\frac{2\times 44{,}000\times 9.81}{1.225\times 0.374\times 93\times 0.682}} = 172.4\,\text{m/s} \Rightarrow M = 0.57 \tag{5.143}$$

Note that the maximum range speed was Mach 0.748. This means that the maximum endurance is about 20% longer than a flight for the maximum range. Also note that the maximum endurance velocity is about 24% slower than the speed for the maximum range.

5.5.5 Practical Considerations

In this section, four topics pertaining to practical considerations on endurance will be discussed briefly: (1) altitude for maximum endurance, (2) comparison between time to maximize range and the maximum endurance, (3) comparison between $V_{\max_E}$ and $V_{\max_R}$, and (4) effect of wind on endurance.

5.5.5.1 Altitude for Maximum Endurance

In Section 5.3.3, we derived three equations for maximum endurance (Equations 5.149, 5.153, and 5.156). Inspection of these equations indicates that the maximum endurance is independent of altitude, assuming specific fuel condition is constant with altitude and velocity. An aircraft cruising at high cruise altitude will have the same endurance as if cruising at sea level, provided that each flight has an appropriate maximum endurance speed. This is because the maximum range speed is faster than the maximum endurance speed at sea level. However, flight at higher altitude yields a longer range.

Please note that in the derivation process in this section we assumed that the SFC (or C) is constant with speed and altitude. However, the SFC varies with airspeed and flight altitude. For a jet aircraft equipped with a turbofan engine, the SFC decreases with altitude, but increases with the Mach number. When this reality is included in our analysis, we can conclude that the maximum endurance will slightly increase with altitude, but slightly decreases with Mach number.

5.5.5.2 Comparison between $t_{\max_R}$ and $E_{\max}$

It is evident that flight duration of a mission to maximize the endurance is longer than that of the maximum range. The difference between these two durations depends on the ratio of their fuel fractions. To have a better idea, we resort to mathematical operation. For instance, consider a constant-altitude, constant-speed flight program (case 3). Equation 5.156 demonstrates the expression for the maximum endurance,

and Equation 5.106 has the relationship for the maximum range. Both equations are repeated here for convenience:

$$E_{\max_3} = \frac{2(L/D)_{\max}}{C} \tan^{-1}\left[\frac{0.5G}{1-0.5G}\right] \tag{5.156}$$

$$R_{\max_3} = \frac{2V_{\max_R}(L/D)_{\max}}{C} \tan^{-1}\left(\frac{0.433G}{1-0.25G}\right) \tag{5.106}$$

The duration of flight when maximizing range is just equal to the maximum range divided by velocity for the maximum range:

$$t_{\max_R} = \frac{R_{\max_3}}{V_{\max_R}} = \frac{2(L/D)_{\max}}{C} \tan^{-1}\left(\frac{0.433G}{1-0.25G}\right) \tag{5.159}$$

If we divide two durations (Equations 5.156 and 5.159), the following is obtained:

$$\left[\frac{E_{\max}}{t_{\max_R}}\right]_{h,V=\text{const}} = \frac{\tan^{-1}\left[0.5G/(1-0.5G)\right]}{\tan^{-1}\left[0.433G/(1-0.433G)\right]} \cong \frac{1.155\times(1-0.25G)}{1-0.5G} \tag{5.160}$$

This relationship illustrates that the more fuel fraction, the larger the difference is between maximum endurance and the duration for the maximum range. The maximum endurance is at least 15.5% longer than the duration for the maximum range. At a fuel weight fraction of 50%, this gap is 34.8% (see Figure 5.18).

5.5.5.3 Comparison between $V_{\max_E}$ and $V_{\max_E}$

It is interesting and beneficial to compare the speed to maximize endurance with the speed to maximize range. To compare the maximum endurance speed with the maximum range speed, Equations 5.143 and 5.101 are used. Figure 5.19 shows these

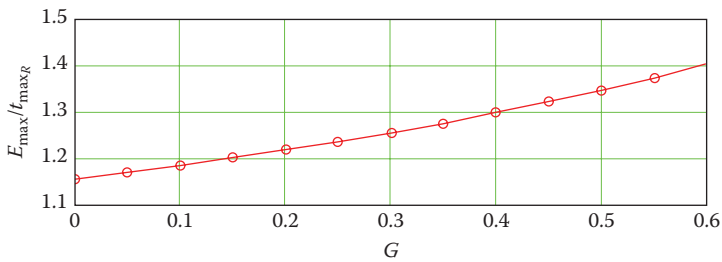

FIGURE 5.18 Comparison between $t_{\max_R}$ and $E_{\max}$ for a constant-altitude, constant-speed flight program.

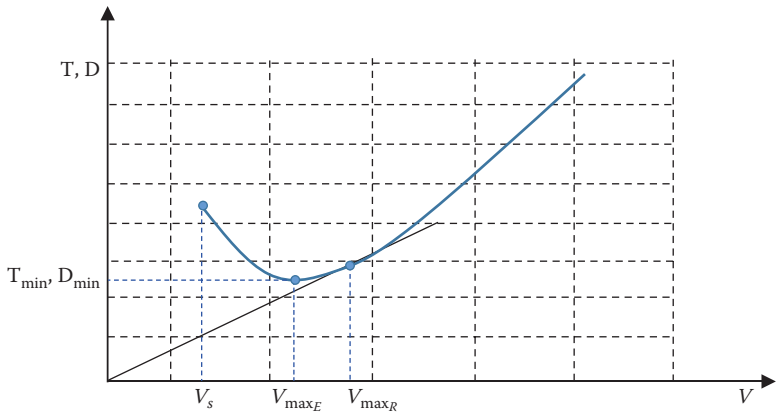

FIGURE 5.19 Comparison between V_{max_E} and V_{max_R}.

two speeds and their relationship with the drag. In a jet aircraft, the maximum range speed is always higher than the maximum endurance speed.

The maximum endurance speed is the same as the minimum drag speed. However, the maximum range speed is graphically determined by passing an asymptote to drag–speed curve (as shown in Figure 5.19).

5.5.5.4 Effect of Wind on Endurance

Aircraft airspeed is not affected by wind speed, while wind affects the ground speed. The endurance is not a function of ground speed which is affected by wind speed. Wind does not affect airspeed or endurance, while it does affect the flight duration to fly over a fixed distance. Wind does not change the aircraft endurance and maximum endurance. The reason is that the endurance is calculated based on the airspeed rather than ground speed. An aircraft with endurance of, say, 10 h will have the same endurance in the presence of a 30 knot tailwind or headwind. By the same token, the maximum endurance of an aircraft will be the same with or without the presence of any wind.

5.6 CEILING

5.6.1 Definition

Another very important criterion for aircraft performance is the ceiling. Ceiling is defined as the highest altitude at which an aircraft can safely have a straight-line level flight. Another definition is the highest altitude that an aircraft can reach by its own engine and have sustained flight. The higher the ceiling, the better the aircraft performance. This performance parameter has limited application in civil airplanes, but is very significant for military aircraft. For instance, if the ceiling of a fighter is higher than the ceiling of missiles in a specific region, this fighter can freely operate

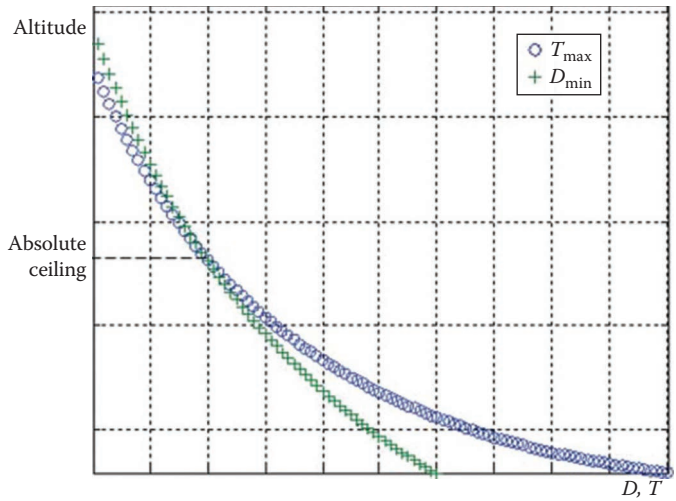

FIGURE 5.20 Variations of engine thrust and aircraft drag with altitude.

on that region and survive. The materials in this section do not apply to an aircraft with rocket engine since there is no limit for their ceilings.

The maximum ceiling of today's aircraft is about 120,000 ft. This record belongs to a Soviet MiG-25 that could fly at 123,523 ft in 1987. The X-15A-3 experimental aircraft could reach the altitude of 314,750 ft after being launched from another aircraft in 1962. In 2014, the first small-scale test flight of a high-altitude balloon and capsule was successfully completed. This project (to let tourists float 20 miles above the earth) broke the world record for highest parafoil flight, lifting a payload to 120,000 ft. It is interesting to know that in 2014, Alan Eustace established a new world parachute altitude record of 135,890 ft, besting the former world record, established by Felix Baumgartner in 2012, by some 7,790 ft.

The primary reason for having ceiling is the air density. At high altitude, there is not sufficient air to be consumed by aircraft engine for combustion; hence, the jet engine thrust drops with altitude. On the other hand, as the air density is decreased, the drag force is decreased too. But the rate of decrease in thrust is higher than the rate of decrease in drag (as shown in Figure 5.20). These two curves have an intersection that is the altitude for ceiling.

As an aircraft flies higher and higher, the amount of available air is decreasing, so the available thrust is decreased too. As a result, at one altitude, the maximum available thrust is barely enough for the aircraft to maintain its level flight. This is the very ceiling. This is true up to about 120,000 ft. Rockets have solved this problem by carrying their own air in a tank as well as fuel. Thus, rockets and missiles with rocket engines do not have any limit in their ceiling. Any fighter that has a ceiling higher than the ceiling of enemy missile in a target area can survive. Otherwise, the fighter must rely on its maneuverability in order to operate on a target airspace.

In general, there are five types of ceiling:

1. *Absolute ceiling* (h_{ac}): As the name implies, the absolute ceiling is the absolute maximum altitude that an aircraft can ever maintain level flight. In other words, the absolute ceiling is the altitude at which the rate of climb* is zero. So, the aircraft is not able to climb higher than the absolute ceiling.
2. *Service ceiling* (h_{sc}): Service ceiling is defined as the highest altitude at which the aircraft can climb with the rate of 100 ft/min (i.e., 0.5 m/s). Service ceiling is lower than absolute ceiling.
3. *Cruise ceiling* (h_{cc}): Cruise ceiling is defined as the highest altitude at which the aircraft can climb with the rate of 300 ft/min (i.e., 1.5 m/s). Cruise ceiling is lower than service ceiling.
4. *Combat ceiling* (h_{cc}): Combat ceiling is defined as the highest altitude at which a fighter can climb with the rate of 500 ft/min (i.e., 2.5 m/s). Combat ceiling is lower than cruise ceiling. This ceiling is defined only for fighter aircraft.
5. *Maximum operating altitude (MOA):* Based on Federal Aviation Regulations (FAR) Part 25 [6] Section 1527, the MOA is defined as "the altitude for which operation is allowed, as limited by flight, structural, powerplant, functional, or equipment characteristics". For instance, at the MOA, the pressurized cabins and compartments must be able to provide a cabin pressure altitude of not more than 8,000 ft (i.e., a 7.8 psi cabin differential pressure). Another requirement is to be able to do an emergency descent to 15,000 ft from MOA in 4 min. The MOA is more of an equipment limitation than a performance limitation.

The MOA in the regional [70] jet airliner Embraer ERJ 145 is 37,000 ft because it is the highest altitude that the plane can go while maintaining a 7.8 psi cabin differential pressure, even though the engines would have no problem climbing higher. The MOA of a Boeing 747-400 airliner (Figure 8.10a) with a normal payload is 41,000, while the service ceiling of the 747-8 is 43,000 ft, and the absolute ceiling is 45,100 ft.

Figure 5.21 depicts three types of ceilings (absolute ceiling, service ceiling, and cruise ceiling) with their features. For a military fighter, the absolute ceiling is one of the primary performance and design criteria, while cruise ceiling is a primary performance and design criterion for civil transport airplane. In majority of airplanes, service ceiling is about 90% of absolute ceiling and cruise ceiling is about 80% of absolute ceiling. In general, the ceiling of a jet aircraft is much higher than the ceiling of a propeller-driven aircraft. Table 5.7 presents [3] the service ceiling for several jet aircraft.

5.6.2 Calculation

In any straight-line steady-level flight (including ceiling), due to the equilibrium of forces along *x*-axis, the engine thrust is equal to drag:

$$T = D \tag{5.5}$$

* Rate of climb is covered in Chapter 7.

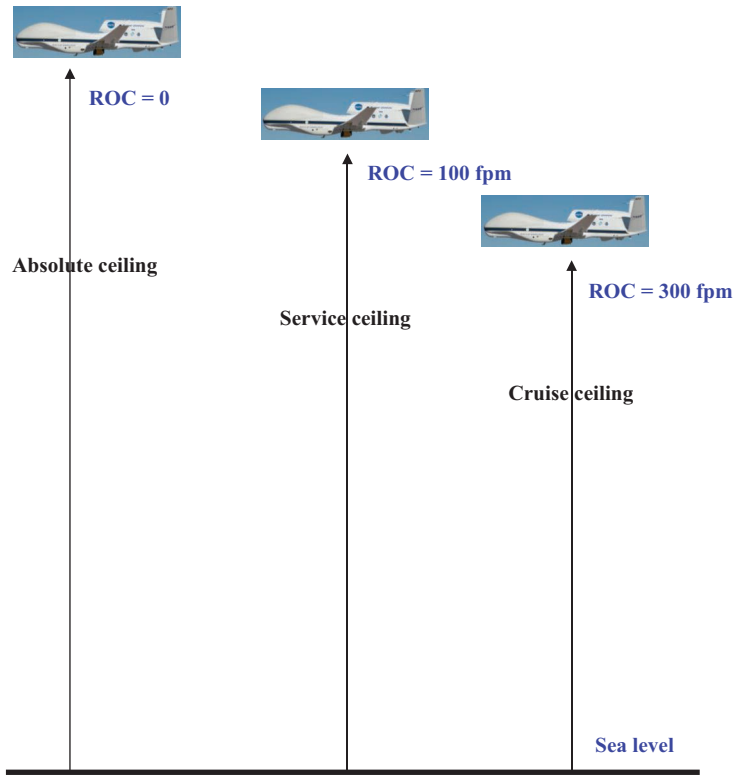

FIGURE 5.21 Three types of ceilings.

As presented in Chapter 4, the available engine thrust for a jet engine is a function of air density. Here, we treat only turbofan engines, and the interested reader may use this technique to develop a similar expression for turbojet engine. The variation of turbofan engine thrust with altitude is approximated by empirical Equations 4.24 and 4.25 and repeated here for convenience. For the troposphere,

$$T_{\max} = T_{\max_{SL}} \left(\frac{\rho}{\rho_o} \right)^{1.2} \quad \text{(troposphere)} \tag{5.161}$$

$$T_{\max} = T_{\max_{SL}} \left(\frac{\rho}{\rho_{11}} \right) \left(\frac{\rho_{11}}{\rho_o} \right)^{1.2} \quad \text{(stratosphere)} \tag{5.162}$$

or

$$T_{\max} = T_{\max_{SL}} \rho \frac{\left(\rho_{11} \right)^{0.2}}{\left(\rho_o \right)^{1.2}} \quad \text{(stratosphere)} \tag{5.163}$$

TABLE 5.7
Service Ceiling of Several Jet Aircraft

No.	Aircraft	Country	Type	Thrust (kN)	Mass (kg)	Service Ceiling (ft)
1.	FAMAIA63 Pampa	Argentina	Trainer	15.57	5,000	42,325
2.	Airbus A-350-900	Europe	Transport	2×374	283,000	43,000
3.	Mitsubishi T-2	Japan	Trainer	2×22.75	12,800	50,000
4.	Lockheed SR-71 Blackbird	USA	Reconnaissance	2×110	78,018	85,000
5.	Dassault Rafale	France	Attack	2×50	24,500	52,000
6.	Dassault Mirage 2000	France	Attack	95.1	17,000	59,000
7.	Microjet 200B	France	Trainer	2.6	1,300	30,000
8.	Dassault/Dornier Alphajet	France-Germany	Reconnaissance	2×14.12	8,000	48,000
9.	Sukhoi Su-57	Russia	Fighter	2×142	35,000	66,000
10.	Eurofighter Typhoon	Europe	Fighter	2×60	23,500	65,000
11.	GlobalFlyer	USA	Long-range record breaker	11.01	10,024	50,669
12.	Aeritalia G91Y	Italy	Fighter	2×12.1	8,700	41,000
13.	Boeing B-52 Stratofortress	United States	Bomber	8×61.2	221,350	55,000
14.	McDonnell Douglas F-15 Eagle	United States	Fighter	2×105.7	30,845	60,000
15.	Lockheed SR-71 Blackbird	United States	Reconnaissance	2×151.3	77,110	85,000
16.	Lockheed U-2C	United States	Reconnaissance	75.6	7,835	90,000
17.	Dassault Falcon 2000	France	Transport	2×26.7	16,238	47,000
18.	Hawker 850	Britain/United States	Business jet	2×20.7	12,700	41,000
19.	Boeing 747-400	United States	Airliner	4×282	396,890	43,000
20.	Embraer ERJ 145	Brazil	Regional jet airliner	2×42	22,000	37,000
21.	F-22 Raptor	United States	Stealth fighter	2×155	39,000	65,000
22.	Global Hawk	United States	Reconnaissance UAV	34	14,628	60,000
23.	Gulfstream G650	United States	Business jet	2×71.6	47,000	51,000

where $T_{\max_{SL}}$ denotes the sea-level maximum thrust, $T_{\max}$ is the maximum thrust at altitude, and ρ_{11} is the air density at 11,000 m altitude. The drag force is also a function of air density:

$$D = \frac{1}{2}\rho V^2 S C_D \tag{3.1}$$

As indicated in Figure 5.20, if an aircraft is planned to fly at ceiling, it must employ its maximum thrust. Furthermore, it should produce a minimum drag. In a technical term, the prerequisite for the absolute ceiling is that the maximum engine thrust is equal to the aircraft minimum drag:

$$T_{\max} = D_{\min} \tag{5.164}$$

As discussed in Section 5.3.3, an aircraft will have its minimum drag if it flies with the minimum drag speed:

$$D_{\min} = \frac{1}{2}\rho V^2_{\min_{DT}} S C_{D_{\min_D}} = \frac{1}{2}\rho_o V^2_{\min_{DE}} S C_{D\min_D} \tag{5.165}$$

Subscript *E* denotes equivalent airspeed and subscript *T* denotes the true airspeed. We previously derived an equation for the minimum drag true airspeed (Equation 5.36). The equivalent minimum drag airspeed is

$$V_{\min_{DE}} = \sqrt{\frac{2m_{\text{ac}}g}{\rho_o S\sqrt{C_{D_o}/K}}} \tag{5.166}$$

where m_{ac} is the maximum aircraft mass at the arrival to the absolute ceiling and

$$C_{D_{\min_D}} = 2C_{D_o} \tag{5.167}$$

We substitute Equations 5.161, 5.163, 5.165, and 5.167 into Equation 5.164. Since air density (ρ) in this equation is at the absolute ceiling (ac), the new parameter ρ_{ac} is used instead:

$$T_{\max_{\text{SL}}}\left(\frac{\rho_{\text{ac}_1}}{\rho_o}\right)^{1.2} = \frac{1}{2}\rho_o V^2_{\min_{DE}} S\left(2C_{D_o}\right)\left(\text{first layer}\right) \tag{5.168}$$

$$T_{\max_{SL}}\rho_{ac_2}\frac{\left(\rho_{11}\right)^{0.2}}{\left(\rho_o\right)^{1.2}} = \frac{1}{2}\rho_o V^2_{\min_{DE}} S\left(2C_{D_o}\right)\left(\text{second layer}\right) \tag{5.169}$$

where ρ_{ac_1} and ρ_{ac_2} represent the air density at the absolute ceiling for the first and second layers of the atmosphere (troposphere and stratosphere), respectively. In this pair of equations, the only unknown is the air density at the absolute ceiling, ρ_{ac}.

Solving these equations for air density at the absolute ceiling (ρ_{ac}), we will obtain a closed-form solution

$$\rho_{ac_1} = \left(\frac{C_{D_o} \left(\rho_o\right)^{2.2} V_{\min_{DE}}^2 S}{T_{\max_{SL}}} \right)^{1/1.2} \quad \left(\text{first layer}\right) \tag{5.170}$$

$$\rho_{ac_2} = \frac{C_{D_o} \left(\rho_o\right)^{2.2} V_{\min_{DE}}^2 S}{T_{\max_{SL}} \left(\rho_{11}\right)^{0.2}} \quad \left(\text{second layer}\right) \tag{5.171}$$

If the theoretical value of the minimum drag velocity is greater than the stall speed, we may further develop the equations. Plugging the minimum drag equivalent velocity (Equation 5.166) into Equations 5.170 and 5.171 yields

$$\rho_{ac_1} = \left(\frac{C_{D_o} \left(\rho_o\right)^{2.2} \left(\left(2m_{ac} g\right) / \left(\rho_o S \sqrt{C_{D_o} / K}\right) \right) S}{T_{\max_{SL}}} \right)^{1/1.2} \left(\text{first layer}\right) \tag{5.172}$$

$$\rho_{ac_2} = \frac{C_{D_o} \left(\rho_o\right)^{2.2} \left(\left(2m_{ac} g\right) / \left(\rho_o S \sqrt{C_{D_o} / K}\right) \right) S}{T_{\max_{SL}} \left(\rho_{11}\right)^{0.2}} \left(\text{second layer}\right) \tag{5.173}$$

which simplify to

$$\rho_{ac_1} = \rho_o \left(\frac{2m_{ac} g \sqrt{K C_{D_o}}}{T_{\max_{SL}}} \right)^{1/1.2} \left(\text{first layer}\right) \tag{5.174}$$

$$\rho_{ac_2} = \frac{2m_{ac} g \sqrt{K C_{D_o}} \left(\rho_o\right)^{1.2}}{T_{\max_{SL}} \left(\rho_{11}\right)^{0.2}} \quad \left(\text{second layer}\right) \tag{5.175}$$

However, the term $2\sqrt{KC_{D_o}}$ is used for the calculation of the maximum lift-to-drag ratio (Equation 5.24). Plugging the equivalent of $2\sqrt{KC_{D_o}}$ into Equations 5.174 and 5.175 and rearranging the terms yields other forms for equations of absolute ceiling

$$\rho_{ac_1} = \rho_o \left(\frac{W_{ac}}{T_{\max_{SL}} \left(L/D\right)_{\max}} \right)^{1/1.2} \left(\text{first layer}\right) \tag{5.176}$$

$$\rho_{ac_2} = \frac{W_{ac} \left(\rho_o\right)^{1.2}}{T_{\max_{SL}} \left(\rho_{11}\right)^{0.2} \left(L/D\right)_{\max}} \left(\text{second layer}\right) \tag{5.177}$$

where W_{ac} is the maximum aircraft mass at the arrival to the absolute ceiling. Recall that the maximum lift-to-drag ratio is given in Equation 5.24. The maximum aircraft mass/weight at the arrival to the absolute ceiling, m_{ac}, is determined by deducting the fuel consumed during takeoff and climb from takeoff mass/weight:

$$m_{ac} = m_{TO} - t_{cl} C \frac{T_{cl}}{g} - m_{f_{TO}} \tag{5.178}$$

$$W_{ac} = m_{ac} g \tag{5.179}$$

where t_{cl} is the time to climb to the absolute ceiling, C is the specific fuel consumption (in 1 per unit time), and $m_{f_{TO}}$ is the mass of fuel burned during the takeoff phase. The parameter T_{cl} denotes the average engine thrust during the climb phase.

Equations 5.174 and 5.176 are employed to determine the absolute ceiling if located at the first layer (troposphere), while Equation 5.175 or 5.177 governs the absolute ceiling at the second layer (stratosphere). Since a non-air-breathing aircraft can fly higher than the second layer, there is no need to develop the absolute ceiling equation for beyond the second layer.

In Equations 5.176 and 5.177, ρ_{ac_1} and ρ_{ac_2} and denote air density at the absolute ceiling for the first and second layers, respectively, $\rho_{11,000}$ denote air density at altitude of 11,000 m, and $T_{max_{SL}}$ is the maximum available engine thrust at sea level. Note that the subscript E denotes equivalent airspeed. When the air density is determined from one of these two equations, we will refer to atmospheric tables (such as Appendix A or B) to find its corresponding altitude, which represents the absolute ceiling.

In practice, it is a wise practice to first assume that the absolute ceiling is located within the first layer. In such a case, first use Equation 5.172 or 5.176. If the calculation yields an answer (ρ_{ac_1}, air density) that corresponds to the second layer, the result is not valid. Thus, you will have to repeat the calculation by using Equation 5.173 or 5.177. The new result (ρ_{ac_2}, air density) would be the correct answer.

Please note that if the minimum drag equivalent airspeed is less than the sea-level stall speed, you cannot use Equations 5.172, 5.173, 5.176, and 5.177. In such a case, assume a value for the minimum drag equivalent airspeed greater than the sea-level stall speed:

$$V_{min_{DE}} = kV_s \tag{5.180}$$

where $1.1 < k < 1.2$. Then, use Equation 5.174 or 5.175.

Equations 5.174 and 5.175 imply that the absolute ceiling is an inverse function of aircraft weight, zero-lift drag coefficient, and induced drag factor. Moreover, the absolute ceiling is a direct function of engine thrust. To increase the absolute ceiling, one must increase a better engine with a higher thrust. In addition, the aircraft mass should be decreased by making the aircraft lighter. Moreover, the aircraft should be more aerodynamic by reducing the zero-lift drag coefficient. Since the induced drag factor is a function of the aspect ratio, we may also conclude that a higher aspect ratio will lead to a higher absolute ceiling.

We may conduct another interesting conclusion regarding the relationships between weather and location with the absolute ceiling. A jet aircraft will have a higher absolute ceiling during a warmer weather (say summer) compared with a colder time (say winter). In addition, a jet aircraft has a higher absolute ceiling when flying over a colder region (i.e., closer to poles), compared to flying over a warmer area (i.e., close to equator). For instance, a jet aircraft will have a higher absolute ceiling when flying over Mexico compared with flying over Alaska.

Equations 5.174 and 5.175 illustrate that the absolute ceiling is not directly a function of wing area and wing loading. This implies that a small aircraft (i.e., small wing area) may have a higher absolute ceiling than a large aircraft, provided it has a sufficient engine thrust. Since the absolute ceiling is a function of the aircraft mass, as the time elapses, the absolute ceiling is gradually increased. This is because the fuel is gradually consumed, and the aircraft weight is gradually decreased.

Equations 5.178 and 5.179 indicate the direction to an aircraft designer the ways to improve the absolute ceiling. To increase the absolute ceiling, one must apply a change such that the density will decrease (i.e., height is increased). First of all, since $T_{\max}$ appears in the denominator, one must employ an engine with a higher thrust. Second alternative is to reduce the C_{D_o} by making the aircraft more aerodynamic. Third technique is to reduce the aircraft mass. The last technique to improve the absolute ceiling is to reduce the induced drag factor (K), which implies an increase in the wing aspect ratio. Thus, the aircraft parameters that positively influence its ceiling are the lower weight, higher engine thrust, and lower drag.

Example 5.9

Consider a business jet aircraft equipped with a turbofan engine, a mass of 11,000 kg 35 m^2, a wing area, and a sea-level engine thrust of 33 kN. Assume the climb to the absolute ceiling takes 25 min, and the average engine thrust during the climb is equal to 90% of the maximum thrust at sea level. Other aircraft specifications are

$$K = 0.055, C_{D_o} = 0.018, C_{L_{\max}} = 2.2, C = 0.8\,\text{N/h/N}.$$

Determine the absolute ceiling for this aircraft in an ISA condition. Ignore the effect of the fuel consumed during takeoff.

Solution

$$m_{\text{ac}} = m_{\text{TO}} - t_{\text{cl}} C \frac{T_{\text{cl}}}{g} - m_{f\text{TO}} = 11{,}000 - 0.2 \times 0.8 \times \frac{0.9 \times 33{,}000}{9.81} - 0 = 10{,}192.4\,\text{kg} \quad (5.178)$$

The minimum drag equivalent airspeed is

$$V_{\min_{DE}} = \sqrt{\frac{2mg}{\rho_o S \sqrt{C_{D_o}/K}}} = \sqrt{\frac{2 \times 10{,}192.4 \times 9.81}{1.225 \times 35 \times \sqrt{0.018/0.055}}} \Rightarrow V_{\min_{DE}} = 90.23\,\text{m/s} \quad (5.38)$$

The stall speed at sea level is

$$V_s = \sqrt{\frac{2mg}{\rho_o S C_{L_{\max}}}} = \sqrt{\frac{2\times 10{,}192.4\times 9.81}{1.225\times 35\times 2.2}} \Rightarrow V_s = 89.5\,\text{m/s} \tag{2.27}$$

The minimum drag speed is greater than the sea-level stall speed, so we can use Equation 5.174 or 5.175. It is initially assumed that the absolute ceiling is located within the first layer

$$\begin{aligned}\rho_{ac_1} &= \rho_o\left(\frac{2mg\sqrt{KC_{D_o}}}{T_{\max_{SL}}}\right)^{1/1.2}\\ &= 1.225\left(\frac{2\times 10{,}192.4\times 9.81\times\sqrt{0.055\times 0.018}}{33{,}000}\right)^{1/1.2} = 0.3078\,\text{kg/m}^3\end{aligned} \tag{5.174}$$

The corresponding altitude to this density ratio from Appendix B is obtained as 12,090 m. This altitude lies within the second layer, but our assumption was to have absolute ceiling within the first layer. Therefore, the result is not valid, and we have to repeat the calculation by using the equation that yields an altitude within the second layer. From Appendix A, the air density at 11,000 m is 0.3638 kg/m^3

$$\begin{aligned}\rho_{ac_2} &= \frac{2mg\sqrt{KC_{D_o}}\left(\rho_o\right)^{1.2}}{T_{\max_{SL}}\left(\rho_{11}\right)^{0.2}}\\ &= \left(\frac{2\times 10{,}192.4\times 9.81\times\sqrt{0.055\times 0.018}\times 1.225^{1.2}}{33{,}000\times 0.3638^{0.2}}\right)\\ &= 0.2977\ \text{kg/m}^3\end{aligned} \tag{5.175}$$

The altitude corresponding to this air density is 12,290 m or 40,321 ft. Therefore, the absolute ceiling of this jet aircraft is 40,321 ft.

5.7 CRUISE PERFORMANCE

Aircraft engines are a major source of pollution and flying with a cruise speed and cruise altitude should achieve national ambient air quality standards. For instance, the Clean Air Act is the comprehensive federal law that regulates air emissions from stationary and mobile sources.

There are four main environmental requirements that impact the flight mission design and the selection of cruise operation: (1) Water issues, (2) Air issues, (3) Waste and land pollution, (4) Climate change. To satisfy these requirements, an aircraft performance engineer should design a flight mission such that it consumes the lowest fuel and have the shortest flight time. This goal will generate the lowest amount of prolusion and emissions from aircraft.

Airliners contribute to climate change by emitting carbon dioxide, nitrogen oxides, contrails, and particulates. The global aviation industry produces around 2.1% of

all human-induced carbon dioxide (the best understood greenhouse gas) emissions. Aviation is responsible for 12% of CO_2 emissions from all transport sources, compared to 74% from road transport. CO_2 emissions from fuel are 3.15 grams per gram of aviation fuel, which gives CO_2 emissions from a Boeing 767 of 115 grams per passenger per kilometer. At a cruising speed of 800 km/h, this is equivalent to 90 kg of CO_2 per passenger per hour.

In 2021, global airlines, convened by the International Air Transport Association, committed to reversing this trend to reach net-zero emissions by 2050. An important step toward this objective is to optimize the cruise performance; that is to determine the optimum cruise altitude and the optimum cruise speed.

As shown in Figure 5.11, the major phase of the mission of a transport aircraft is cruise, which is also the longest phase. For a transport aircraft, the cruise phase of flight consumes the majority of fuel. Due to this reason, transport aircraft are usually designed for an optimum performance at their cruise speed, which frequently means the longest range. The cost of flight for a transport aircraft can be minimized by optimizing the cruising flight. A number of wing parameters such as airfoil section and setting angle are determined primarily based on the cruise performance [71]. Compared with other phases of flight, the cruise is historically the safest phase of a flight. In this section, the analysis of two topics is provided: (1) cruise speed and (2) cruise altitude.

5.7.1 Cruise Speed

In Section 5.3.1, some explanations about the significance and calculation of the aircraft maximum speed were presented. In a long-duration flight, for economic reasons and maintenance considerations, aircraft do not usually fly with the maximum speed. They fly with an efficient speed called *cruise speed*. This speed is lower than (around 70%–90% of) the maximum speed. In this flight condition, full throttle is not utilized. The other reason is to let the engine last longer.

For this topic, an aircraft and a car are similar. The reason for flying with cruise speed is very similar to that of the car driving. For instance, it is recommended to car drivers not to use the maximum throttle on a long trip and to avoid driving at the highest speed for a long time. The reason is that it may hurt the engine due to high temperature and high fuel consumption.

One of the limits on the cruising speed is the shock wave and sonic boom. Since 1973, due to concerns about sonic booms, civil supersonic flights have been forbidden in the United States. However, European and many other countries allow supersonic flight over lands, but they do not permit disturbance caused by sonic booms. In 2003, two European airlines retired the only SST aircraft, Concorde, due to age and safety concerns (after more than 20 years). Hence, it is now more than 20 years that, there is no supersonic civil transport aircraft.

The amount of usage of jet engine thrust in a cruising flight depends on parameters such as aircraft weight, flight altitude, and aircraft mission. This could be from 60% up to about 90% of the maximum thrust. Thus, the cruising speed is always lower than the maximum speed. Table 5.3 demonstrates the cruise speed of several jet aircraft.

Typical cruising airspeed for long-range commercial passenger flights is 440–500 knots (Mach 0.75–0.85). The cruising speed of a large transport aircraft such as Boeing 747 (Figure 8.10b) and Airbus 340 (Figure 1.8) is about Mach 0.85. In transonic speed, particularly close to Mach 1, shock waves are generated and produce wave drag. Therefore, it is undesirable to fly with a cruising speed that is very close to Mach 1.

The cruising speed for the Boeing 747-400 (Figure 8.10b) is Mach 0.8, for the Boeing 787 Dreamliner (Figure 5.26, later in this chapter) is Mach 0.85, and for the Boeing 767 is Mach 0.84. The business trijet aircraft Dassault Falcon 50 with a maximum takeoff mass of 18,000 kg has a maximum operating speed of 350 knots at sea level, while 370 knots at 23,700 ft. It also has a maximum cruising speed of 487 knots (Mach 0.85), a normal cruising speed of 459 knots (Mach 0.8), and a long-range cruising speed of 430 knots (Mach 0.75) at 35,000 ft.

There are two methods to determine the cruise speed: (1) Based on engine performance charts, and (2) Based on range mission. These two methods will be discussed independently.

5.7.1.1 Based on Engine Performance Charts

The first technique to determine the cruise speed is to use engine performance charts which are provided by engine manufacturer. A related chart indicates the variations of engine SCF with respect to engine shaft rotational speed (e.g., rpm). Two important outputs of this chart – which are given as a function of altitude – are: (1) The rpm which requires the minimum SFC, and (2) The range of shaft rpms that are recommended for cruising flight. Each shaft rpm is corresponding to an engine thrust.

Figure 5.22 demonstrates the variation of the drag force versus speed as a parabolic curve. In this figure, several thrust lines are also presented. For simplicity, it is assumed that the engine thrust is constant with respect to airspeed and Mach number. The intersections between each thrust line and drag curve demonstrate two possible solutions. The solution with a higher value (highest speed) is the cruising speed.

Based on the derivation provided in Section 5.3.1 and by considering Equation 5.27, we are able to develop a relationship to determine the cruising speed of an aircraft as follows:

$$AV_C^2 + \frac{B}{V_C^2} - nCT_{\max_{SL}} = 0 \tag{5.181}$$

where the coefficients A, B, and C are found from Equation 5.27. The parameter n is the percentage of usage of engine thrust and is in the following range:

$$0.9 > n > 0.65 \tag{5.182}$$

The coefficient n is a factor of several parameters such as fuel cost, engine type, engine maintenance, flight duration, market necessity, flight mission, aircraft weight, and altitude. It is determined through an optimization process to optimize a few parameters at the same time (i.e., minimize fuel cost, minimize flight duration,

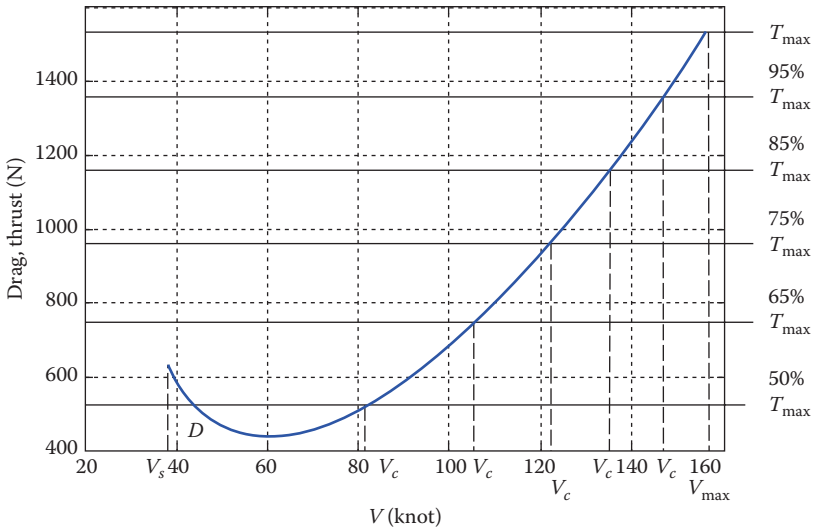

FIGURE 5.22 Cruising speed with various thrust lines.

maximize engine life, minimize engine maintenance cost, and compete in the market). This parameter as a function of altitude and aircraft weight is usually provided to pilots by the aircraft manufacturer (in pilot operating handbook).

Example 5.10

The following jet aircraft is equipped with a turbojet engine and is utilizing 80% of its maximum engine thrust in a cruising flight at 30,000 ft (9,144 m).

$$m = 47{,}000\,\text{kg}, C_{D_o} = 0.022, T_{\max_{SL}} = 103.16\,\text{kN}, S = 127\,\text{m}^2, k = 0.047$$

Determine the cruising speed of this aircraft at 30,000 ft altitude.

Solution

From atmospheric table in Appendix B, the air density at the altitude of 9,144 m ft is $0.458\,\text{kg/m}^3$. So, the air density ratio is 0.458/1.225 = 0.374. The cruising speed can be obtained by using Equation 5.181

$$AV_C^2 + \frac{B}{V_C^2} - 0.8CT_{\max_{SL}} = 0 \tag{5.181}$$

The maximum turbojet engine thrust at 30,000 ft is

$$T = T_{\max_{SL}} \left(\frac{\rho}{\rho_o}\right)^{0.9} = 103{,}160 \times (0.374)^{0.9} = 42{,}569.2\,\text{N} \tag{4.21}$$

The coefficients *A*, *B*, and *C* are (*n* is 0.8):

$$A = \frac{1}{2}\rho S C_{D_o} = 0.5 \times 0.458 \times 127 \times 0.022 = 0.64 \tag{5.27}$$

$$B = \frac{2KW^2}{\rho S} = \frac{2 \times 0.047 \times (47{,}000 \times 9.81)^2}{0.458 \times 127} = 343{,}551{,}924 \tag{5.27}$$

$$C = \left(\frac{\rho}{\rho_o}\right)^{0.9} = (0.374)^{0.9} = 0.3857$$

When the values for *A*, *B*, and *C* are plugged in Equation 5.181, we obtain:

$$0.64V_C^2 + \frac{343{,}551{,}924}{V_C^2} - 0.8 \times 0.3857 \times 103{,}160 = 0 \tag{5.181}$$

Solution of this algebraic equation yields the following acceptable result:

$$V_C = 184.13 \text{ m/s} = 357 \text{ KTAS}$$

5.7.1.2 Based on Range Mission

If the engine performance charts for the optimum performance (best range) are not available, the theoretical value of the cruise speed is determined by using the lift coefficient for the maximum range and the cruising altitude. When an aircraft is cruising to maximize range, the lift is equal to weight:

$$W = L_{\max_R} = \frac{1}{2}\rho_C V_C^2 S C_{L_{\max_R}} \tag{5.183}$$

When the *cruise altitude* is known, we can obtain the cruise velocity based on the velocity to maximize the range (see Equation 5.101) as follows:

$$V_C = \sqrt{\frac{2W}{\rho_C S C_{L_{R_{\max_R}}}}} \tag{5.184}$$

where the cruise lift coefficient (C_{L_C}) is determined by Equation 5.102

$$C_{L_C} = C_{L_{\max_R}} = \sqrt{\frac{C_{D_o}}{3K}} \tag{5.185}$$

Typical values of the cruise lift coefficient for majority of civil subsonic aircraft vary from 0.1 to 0.5. These cruise lift coefficients correspond to the aircraft angle of attacks of about 1°–5°. Most large transport aircraft (e.g., Boeing 747 [Figure 8.10b]

and Airbus 380 [Figure 5.16]) have about 4°–5° of angle of attack at the beginning of cruise, while about 2°–3° of angle of attack at the end of cruising flight. Airbus A320 with a maximum takeoff mass of 77,000 kg has a maximum operating [72] speed of Mach 0.82 (350 knots at ISA condition), while the optimum cruising speed is Mach 0.78. Most airliners are currently cruising at a speed of Mach 0.8–0.9.

Equation 5.184 implies that the cruise speed increases with altitude (via ρ_C) and decreases with aircraft weight. In addition, the value of aircraft cruise speed is dependent on the inverse of wing area (indeed, its square root); as the wing area is decreased, the cruise velocity is increased. Furthermore, the aircraft cruise speed is a direct function of the square root of the wing loading (W/S). Section 5.7.2 provides a technique to determine cruise altitude.

5.7.2 Cruise Altitude

Another important parameter affecting the cruising performance is the cruise altitude, which is the level portion of aircraft travel where the flight is most fuel efficient. Various parameters influence the cruise altitude, including flight operating cost, flight time, flight distance, and competition among airliners. The cost of flight at various altitudes depends on the speed. To optimize the cruise performance, a jet aircraft must be flown with a specific cruising speed at each altitude. The cruising altitudes of different aircraft are not the same. This altitude is a function of several parameters such as aircraft weight, FAR, and the distance to the destination.

In 2014, there were 87,000 daily aircraft flights [73] in the United States. This large number produces great limits and challenges for flight engineers and airliners to determine the safe while economic cruise altitudes for various aircraft. A number of websites (e.g., *FlightAware.com*) provide accurate real-time, historical, and predictive flight insights to all segments of the aviation industry.

In fact, other than practical factors (such as traffic and safety regulations), the cost of flight is the main driver to determine the cruise altitude. The calculation of the cruise altitude is a challenging problem and should take into account a number of parameters simultaneously. In this section, the procedure to determine the cruise altitude is reviewed, and related important charts and figures are discussed.

Since in higher altitudes (above 18,000 ft), the air pressure is not enough for human to have a normal breath, the compressed air must be provided for the pilot, crew, and passengers. Normally at altitude higher than 12,000 ft, the aircraft needs to be provided with an air conditioning system. In busy air traffic, because of safety reasons, all aircraft cannot fly at the same altitude. Thus, aviation regulations determine the cruising altitude of each aircraft (altitude separation requirements).

The selection of cruise or service ceiling is also related to climb performance. In Chapter 7, the climb performance of the business jet aircraft Cessna Citation III is analyzed. Figure 7.26 (in Chapter 7) demonstrates time to climb to the absolute ceiling for the Cessna Citation III with a service ceiling of 51,000 ft and a maximum rate of climb of 3,700 ft/min. It is interesting to see that it takes about 43 min to climb to its service ceiling, while it takes longer (about 50 min) to climb from service ceiling to the absolute ceiling. Hence, it is cost-effective to cruise at service ceiling rather than the absolute ceiling. This is one reason behind such selection.

One of the FAA regulations is the "vertical separation", which states that all Eastbound flying aircraft must use altitude with odd numbers of 1,000 ft, while all returning aircraft (Westbound) are required to fly at altitudes that are even numbers of 1,000 ft. This leads to a safety measure of 1,000 ft altitude difference between two aircraft with opposite directions. The standard rule defines an East/West track split: (1) Eastbound—Magnetic Track 000 to 179°—odd thousands (FL 250, 270, etc.) and (2) Westbound—Magnetic Track 180° to 359°—even thousands (FL 260, 280, etc.).

Between the surface and an altitude of 29,000 ft (8,800 m), no aircraft should come closer vertically than 300 m, unless some form of horizontal separation is provided. Above 29,000 ft (8,800 m), no aircraft shall come closer than 600 m (or 2,000 ft), except in airspace where "reduced vertical separation minimum" can be applied. Above FL 410–2,000 ft, except (1) in oceanic airspace, above FL 450 between a supersonic and any other aircraft—4,000 ft and (2) above FL 600 between military aircraft—5,000 ft.

The cruising altitude of most GA aircraft is about 10,000–20,000 ft altitude. The cruising altitude of most transport aircraft is about 32,000–42,000 ft altitude. The cruising altitude of most fighter aircraft is about 40,000–60,000 ft altitude. Figure 5.23 shows the cruising altitude of transport aircraft Boeing 747 at various aircraft weights.

The airliner Airbus A320 with a maximum takeoff mass of 77,000 kg has [7] an initial cruise altitude of 37,000 ft, while the maximum certified altitude is 39,800 ft. The business trijet aircraft Dassault Falcon 50, with a maximum takeoff mass of 18,000 kg, has an initial cruise altitude of 41,000 ft, while the maximum certified altitude is 49,800 ft. The business jet Embraer Phenom 300 has a MOA of 45,000 ft with a cruising speed of 450 knots.

Higher altitudes are more efficient for additional fuel economy. In general, for operational and air traffic control reasons, the FAA requires each aircraft to fly at a constant-altitude throughout its cruising flight. On long-range flights, the pilot may

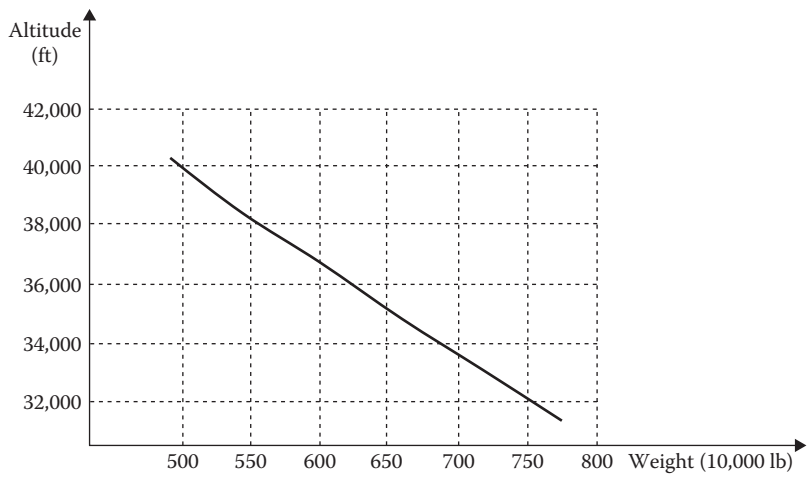

FIGURE 5.23 Cruising altitude of Boeing 747 (with JT9D 7A engine) at various weights.

climb from one flight level to a higher one as permission is requested and given from air traffic control authorities. This operation is called a *step climb*. There is an optimum cruise altitude for a particular aircraft type and each flight condition, including payload weight, air temperature, and flight distance.

Typical cruise altitude for high subsonic large transport aircraft is about 30,000–40,000 ft. The Boeing 747-400 (Figure 8.10b) has an initial cruising altitude of 35,000–38,000, when taking off with the maximum takeoff weight, while the Boeing 777 (Figure 7.21) has an initial cruising altitude of 39,400 ft. The maximum certified altitude for Airbus 320 [7] is 39,800 ft.

As we classified earlier, there are three options in a cruising flight: (1) constant-altitude, constant-lift-coefficient flight, (2) constant-airspeed, constant-lift-coefficient flight, and (3) constant-altitude, constant-airspeed flight. These can be regrouped into two groups: (1) constant-altitude flight (cases 1 and 3) and (2) non-constant-altitude flight (case 2). For cases 1 and 3, the technique to determine the cruising altitude is presented, while for a cruise-climb, the method to calculate the initial cruise altitude will be discussed.

Although a cruise-climb flight can considerably increase the range of an aircraft for long-range flights, it does involve a continuous increase of altitude that is not consistent with safe flight when the presence of other aircraft must be considered. Consequently, the opportunity to use a cruise-climb flight is limited by FAA regulations. However, on long-range flights, *stepped-altitude* flight may be employed, which is a series of constant-altitude, constant-airspeed flight segments conducted at different altitudes (with each step to be about 2,000 ft). Stepped-altitude flight is often used on long-range flights, such as transcontinental and transoceanic flights. This program will place a burden on air traffic control authorities to ensure a safe clearance from any altitude crossed during climb to new cruise altitude.

As we derived in Section 5.6, at absolute ceiling, the lift-to-drag ratio is equal to the aircraft maximum lift-to-drag ratio. Equation 5.104 implies that the lift-to-drag ratio for a constant-speed flight to maximize range is only 15.5% greater than the maximum lift-to-drag ratio, as is required for level flight, but not much more:

$$\left(\frac{L}{D}\right)_{\max} = 1.155\left(\frac{L}{D}\right)_{R_{\max}} \tag{5.186}$$

This indicates that the altitude for the maximum range flight lies below, but close to, the absolute ceiling for the associated throttle setting. As Equation 5.4 demonstrates, at cruise altitude, the lift is almost equal to the weight:

$$W = L + T\sin(\alpha + i_T) \tag{5.187}$$

If the contribution of the engine thrust due to a low angle of attack and low setting angle is ignored, we can write

$$\frac{T_{\max_R}}{W} = \frac{1}{(L/D)_{\max_R}} = \frac{1}{0.866(L/D)_{\max}} = \frac{1.155}{(L/D)_{\max}} \tag{5.188}$$

Equation 5.188 implies that the thrust-to-weight ratio for a constant-speed flight to maximize the range is only 15.5% greater than the reciprocal of the maximum lift-to-drag ratio but not much more. So, the required thrust at cruise altitude will be

$$T_{\max_R} = \frac{1.155W}{(L/D)_{\max}} \tag{5.189}$$

In Chapter 4, the variation of turbofan engine thrust with altitude is approximated by

$$T = T_o\left(\frac{\rho}{\rho_o}\right)^{1.2} \tag{4.24}$$

At cruise altitude, the thrust in Equations 5.189 and 4.24 are the same. Equating these two equations yields

$$\frac{1.155W}{(L/D)_{\max}} = T_o\left(\frac{\rho}{\rho_o}\right)^{1.2} \tag{5.190}$$

The only unknown variable in this equation is the cruise altitude air density, which is obtained as

$$\rho_c = \left(\frac{1.155W\rho_o^{1.2}}{(L/D)_{\max} T_{\text{SL}}}\right)^{1/1.2} \tag{5.191}$$

For an aircraft with the turbojet engine, the reader is encouraged to develop a similar expression. Using Appendix A or B, one can determine the corresponding cruise altitude (h_C).

Equation 5.191 implies that the cruise altitude (via ρ_C) depends on aircraft weight, engine thrust, and maximum lift-to-drag ratio. As the engine thrust and maximum lift-to-drag ratio increase, the cruise altitude would increase. Since the maximum lift-to-drag ratio is an inverse function of aircraft zero-lift drag coefficient (C_{D_o}), the more aerodynamic aircraft result in a higher cruise altitude. This reality drove the design of high- altitude reconnaissance aircraft such as U-2 and Lockheed SR-71 Blackbird (Figure 4.24). Their jet engines should have been powerful enough to support 60,000+ ft cruise altitude. Furthermore, the zero-lift drag coefficient (C_{D_o}) should be low enough to allow the aircraft to fly at very high altitude.

However, as the aircraft weight increases, the cruise altitude will drop due to a decrease in the air density (ρ_C). This indicates the importance of reducing aircraft weight during design phase. We also note that the cruise altitude is the direct function of the thrust-to-weight ratio (T/W). As the thrust-to-weight ratio increases, the cruise altitude increases. This shows the need to have a high thrust-to-weight ratio for a high-altitude flight.

For the maximum range flight, the instantaneous fuel consumption in the weight of fuel per unit time is

$$\left(\frac{dW_f}{dt}\right)_{R_{\max}} = CT_{\max_R} = \frac{1.155CW}{(L/D)_{\max}} \tag{5.192}$$

The SFC decreases slowly with altitude, reaching its minimum value at the tropopause and then increasing even more slowly in the second layer (stratosphere). Furthermore, the thrust-to-weight ratio is greater than the reciprocal of the maximum lift-to-drag ratio, as is required for level flight, but not much more. This indicates that the altitude for the maximum range flight lies below, but close to, the absolute ceiling for the associated throttle setting. Moreover, the absolute ceiling of most large transport aircraft is about 40,000–50,000 ft. Thus, the *maximum range altitude* is a few thousand feet (~5,000 ft) below the absolute ceiling for that particular throttle setting. Therefore, *there is a slight advantage to flying in the vicinity of the tropopause*, all other things being equal.

Another advantage of cruising flight in the vicinity of the tropopause is the lack of strong wind and turbulence. A potential drawback to fly at the vicinity of tropopause is the rare instance of violent, sudden drop in air pressure and severe turbulence, which causes an aircraft to lose altitude rapidly. This will cause the passengers without seatbelt to hit the ceiling, which results in their injury and hospitalization. For instance, on July 21, 2010, 30 passengers injured on United Airlines flight when suddenly the plane lurched into a free-fall due to severe turbulence, sending people literally flying into the cabin ceiling.

For an accurate calculation of the best cruise altitude, the entire mission should be considered [74]. The cruise altitude with lowest cost is theoretically the best altitude (Figure 5.24). When the practical limits and considerations are taken into account, the optimum cruise altitude will be determined. Charts in the aircraft operating handbooks (e.g., References [63,70,72]) allow the pilot to select the best combination of altitude/speed/range/endurance for the intended flight.

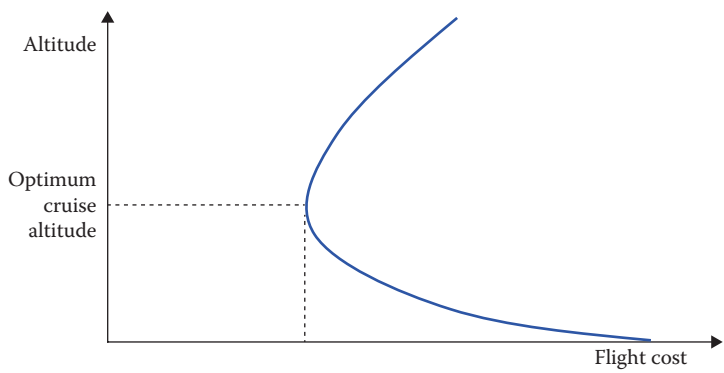

FIGURE 5.24 Variations of flight cost with respect to altitude.

Overall fuel cost (S) of flight is the sum of the cost for five major segments of the flight: (1) takeoff and taxi, (2) climb, (3) cruise, (4) descent, (5) landing

$$S = S_{\text{TO}} + S_{\text{cl}} + S_{\text{cr}} + S_d + S_L \tag{5.193}$$

The cost of fuel for each segment is determined by multiplying the amount of fuel burned per segment by fuel cost per unit weight/mass (f_C)

$$S = W_f f_C \tag{5.194}$$

In 2022, a gallon of jet fuel was estimated to be about \$12, which is about \$3 per L. The amount of fuel burned per segment is calculated by using the definition of SFC (Equation 5.61)

$$W_f = t\,T\,C \tag{5.195}$$

where t is the duration of flight for a segment, T denotes the average engine thrust in the segment, and C is the fuel consumption for the segment.

The regional jet airliner ERJ-145 with a maximum takeoff mass of 20,600 kg [70] has a time to climb 35,000 ft altitude (FL350) of 20 min, while this time for Embraer 175 with a maximum takeoff mass of 37,500 kg is 16 min. The business trijet aircraft Dassault Falcon 50 with a maximum takeoff mass of 18,600 kg has a time to climb 41,000 ft altitude (FL410) of 23 min. The jet fighter Dassault Mirage 2000 has a time to climb 11,000 m (36,080 ft) and Mach 1.8 of ~5 min.

Recall that during cruise, the thrust is almost equal to drag, as we derived earlier (Equation 5.3); it is repeated here for convenience.

$$D = T\cos(\alpha + i_T) \tag{5.3}$$

As the cruise altitude is increased, the cost for climb is increased, but the cost for cruise is decreased. This is due to the fact that the drag and thrust decrease with altitude. In addition, as the cruise altitude is increased, the optimum value for the parameter $M(L/D)$ is increased.

Due to five segments for a flight of a transport aircraft (Figure 5.11), the total consumed weight of fuel is determined by

$$W_f = t_{\text{TO}}\cdot T_{\text{TO}}\cdot C_{\text{TO}} + t_{\text{cl}}\cdot T_{\text{cl}}\cdot C_{\text{cl}} + t_{\text{cr}}\cdot T_{\text{cr}}\cdot C_{\text{cr}} + t_d\cdot T_d\cdot C_d + t_L\cdot T_L\cdot C_L \tag{5.196}$$

Please note that the engine thrust and fuel consumed during descent and landing are minimal and may be neglected for simplicity. Large transport aircraft usually use reverse thrust to reduce the landing run, and thus a minimal amount of fuel is burned during landing. As an approximation, you may consider that about 5% of the total

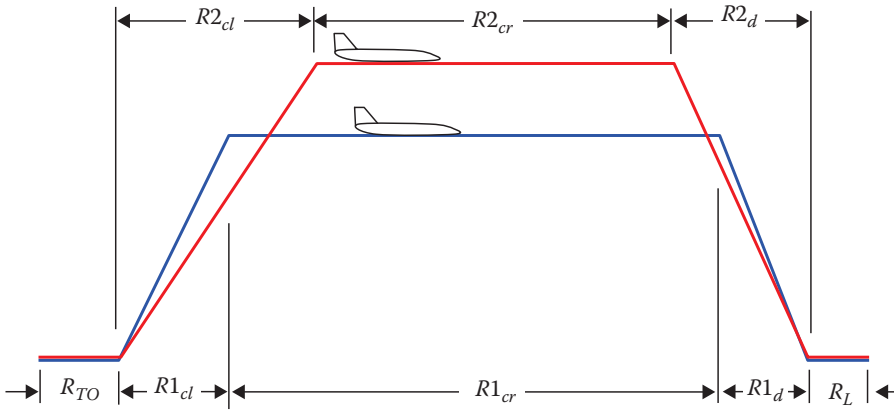

FIGURE 5.25 Comparison between two flight operations with different cruise altitudes.

fuel is being consumed during takeoff, descent, and landing, and thus Equation 5.196 is simplified to

$$W_f = 1.05\left(t_{\text{cl}} \cdot T_{\text{cl}} \cdot C_{\text{cl}} + t_{\text{cr}} \cdot T_{\text{cr}} \cdot C_{\text{cr}}\right) \tag{5.197}$$

Figure 5.25 illustrates a comparison between two flight operations with different cruise altitudes. Both flights have the similar takeoff and landing distances and durations. However, the climb and descent ground distances and durations are different. One reason is that the rate of climb decreases with altitude, so the average climb angle to fly to a higher altitude is less than that for a lower altitude. Similarly, the ground distance to fly to a higher altitude is greater than that for a lower altitude. To determine the optimum cruise altitude, you need to write a computer program to calculate the fuel required to fly for a mission for various cruise altitudes. The altitude that requires the lowest fuel weight for the entire flight is selected as the best cruise altitude.

Parameters that influence the cruise altitude include flight operating cost, number of passengers (i.e., aircraft weight), flight duration, flight distance, and market competition. The cruise flight time for the constant-altitude, constant-airspeed flight program can easily be found by dividing the range by the airspeed. The same procedure can also be used for the cruise-climb flight time.

The time required for any of the maximum range in the cruise segment for constant-lift-coefficient flight programs (either constant-lift coefficient, constant-speed; or constant-lift coefficient, constant-altitude) can be determined by dividing Equation 5.107 by maximum rang speed:

$$t_{\max_R} = \frac{R_{\max}}{V_{\max_R}} = \frac{0.866\left(L/D\right)_{\max}}{C} \ln\left(\frac{1}{1-G}\right) \tag{5.198}$$

The time of flight is the same for all maximum range, constant-lift-coefficient flight programs at any altitude. This implies that the cruise at a higher altitude (which delivers a longer range) will have the same duration when flown at lower altitude (which delivers a shorter range). This indicates that with a full fuel tank the cost for cruise at higher altitude is less than that for a lower altitude. The range of a transport aircraft is about 50% greater at 30,000 ft than at sea level. However, the optimum cruise altitude is determined when the cost for climb is included in the calculation process.

Consider the equation for the maximum range speed (Equations 5.101 and 5.105). We note that $V_{\max_R}$ is inversely proportional to the square root of the air density and thus increases with altitude. We also notice that the thrust required is independent of the altitude itself, being dependent only upon the instantaneous weight of the aircraft and upon maximum lift-to-drag ratio. In other words, the thrust required at sea level is identical (as is the drag) to that required at high altitudes.

It is beneficial to fly at a high altitude (with a low air density) to obtain the range benefits (and the secondary benefits of flying above the atmospheric turbulence) accruing to an increase in the airspeed. As we increase the altitude, however, the available thrust does decrease, and we must be sure that there is sufficient available thrust at the cruise altitude to satisfy Equation 5.7.

The cruise altitude for a cruise-climb flight option is gradually increasing. The altitude at the end of the cruise-climb flight (h_2) can be expressed in terms of both the initial altitude (h_1) and the fuel fraction. The density ratio at the end of the cruise-climb flight (σ_2) can be expressed – as derived earlier – in terms of initial density ratio and the fuel fraction:

$$\sigma_2 = \sigma_1(1-G) \tag{5.83}$$

where σ_1 is the air density ratio at the beginning of the cruise and G is the fuel fraction. The climb angle is so small that it can be ignored. When the air density at the end of the cruise-climb flight (σ_2) is obtained, one can utilize Appendix A or B to determine the final altitude.

The typical flight profile of the Global Hawk unmanned aircraft of NASA consists (See Figure 5.26) of a rapid climb to ~55,000 ft; a subsequent *cruise-climb* at a lower, steady rate – as fuel is expended – until the aircraft reaches its maximum operational altitude of 65,000 ft; and flight at this altitude until the aircraft returns to the operations base and descends for landing.

Figure 5.27 illustrates two jet transport aircraft at their cruising altitudes with their cruising speeds. The jet transport aircraft Boeing 787-8 Dreamliner (the newest Boeing product) with two turbofan engines has a maximum cruising altitude of 43,000 ft. The strategic airlift cargo aircraft Antonov An-225 Mriya with six turbofan engines has a cruising speed of 800 km/h and a service ceiling of 11,000 m. This jumbo aircraft once carried a space shuttle at the Paris Air Show in 1989. Table 5.8 provides [3] the cruise altitude for several jet aircraft.

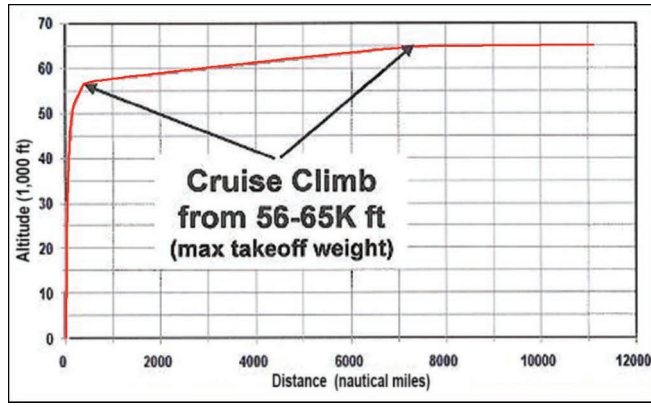

FIGURE 5.26 Illustration of typical flight pattern of a Global Hawk. (Image credit: NASA/DFRC.)

(a)

(b)

FIGURE 5.27 Two jet transport aircraft at their cruising altitudes: (a) Boeing 787 Dreamliner. (b) Antonov An-225 Mriya. (Courtesy of Kas van Zonneveld.)

TABLE 5.8
Service Ceiling of Several Jet Aircraft

No.	Aircraft	Type	Thrust (kN)	TO mass (kg)	Cruise Altitude
1.	Gulfstream G650	Business jet	2×71.6	45,000	51,000 ft (15,545 m)
2.	Boeing 777-300	Transport	2×342	299,370	36,000 ft (10,973 m)
3.	Boeing 787-8	Transport	2×280	227,930	43,000 ft (13,106 m)
4.	Airbus 330-300	Transport	2×316	242,000	41,000 ft (12,653 m)
5.	Concorde	Transport	4×142	185,000	60,000 ft (18,300 m)
6.	Antonov An-225 Mriya	Airlift cargo	6×229.5	640,000	11,000 m
7.	HondaJet Elite II	Light jet	2×9.1	5,035	43,000 ft (13,106 m)
8.	Cessna Citation Latitude	Business jet	2×26.2	13,971	41,000 ft (12,653 m)
9.	Global Hawk	HALE unmanned aircraft	34	14,628	65,000 ft (19,812 m)
10.	Tomahawk	Cruise missile	3.1	1,300	100–300 ft (30–90 m)

Example 5.11

A jet transport aircraft with a mass of 70,000 kg and a wing area of 125 m^2 is equipped with two turbofan engines and has the following characteristics:

$$C_{D_o} = 0.02, K = 0.05, T_{SL} = 2 \times 87\,\text{kN}$$

Determine: (a) Cruise altitude, and (b) Cruising speed in terms of the Mach number. Ignore other phases (including the climb phase) of the flight and assume that this cruise altitude is to maximize the range.

Solution

The maximum lift-to-drag ratio

$$\left(\frac{C_L}{C_D}\right)_{\max} = \frac{1}{2\sqrt{KC_{D_o}}} = \frac{1}{2\sqrt{0.05 \times 0.02}} \Rightarrow \left(\frac{C_L}{C_D}\right)_{\max} = 15.81 \tag{5.24}$$

The cruise altitude air density

$$\rho_c = \left(\frac{1.155 W \rho_o^{1.2}}{(L/D)_{\max} T_{SL}}\right)^{1/1.2} = \left(\frac{1.155 \times (70{,}000 \times 9.81) \times 1.225^{1.2}}{15.81 \times 2 \times 87{,}000}\right)^{1/1.2} = 0.434\,\text{kg/m}^3 \tag{5.191}$$

From Appendix A, this air density corresponds to a cruise altitude of 9,600 m or 31,500 ft. The cruise lift coefficient is determined by the following equation:

$$C_{L_{\max R}} = \sqrt{\frac{C_{D_o}}{3K}} = \sqrt{\frac{0.02}{3 \times 0.05}} = 0.365 \tag{5.102}$$

Then, the cruise velocity is obtained as follows:

$$V_C = \sqrt{\frac{2W}{\rho_C S C_{L_{R_{\max}}}}} = \sqrt{\frac{2\times 70{,}000\times 9.81}{0.434\times 125\times 0.365}} = 263.15\,\text{m/s} \tag{5.184}$$

The speed of sound at this altitude is 301.2 m/s, so the cruise Mach number is

$$M_C = \frac{V_C}{a} = \frac{263.15}{301.2} = 0.874 \tag{1.36}$$

PROBLEMS

5.1 Determine the maximum lift-to-drag ratio of a glider with the following features:

$$\text{AR} = 25, e = 0.9, C_{D_o} = 0.012$$

5.2 A 20,000 kg jet aircraft is flying at sea level with 4° of angle of attack. Determine how much lift and drag this aircraft has produced at this flight condition, if its engine thrust is 50 kN. Assume the thrust line coincides with fuselage center line.

5.3 Consider a jet (turbofan) aircraft with the following features:

$$T_{\max} = 27\,\text{kN}, S = 56\,\text{m}^2, m_{\text{TO}} = 11{,}000\,\text{kg}, C_{L_{\max}} = 1.7, K = 0.05, C_{D_o} = 0.018$$

Determine the following parameters:

a. Stall speed
b. Minimum drag speed
c. Maximum range speed
d. Maximum endurance speed
e. Cruising speed at 20,000 ft altitude (6,096 m) with 75% engine thrust
f. Maximum speed at sea level.

5.4 Consider a jet (turbofan engine) transport aircraft with the following features:

$$T_{\max} = 757\,\text{kN},\ S = 476\,\text{m}^2,\ m_{\text{TO}} = 270{,}000\,\text{kg},\ C_{L_{\max}} = 2.3,\ K = 0.04,$$
$$C_{D_o} = 0.017,\ m_f = 50{,}000\,\text{kg},\ C = 0.7\,\text{lb/h/lb}$$

Determine the maximum range when flying at 25,000 ft (7,620 m) altitude.

5.5 Plot the variation of the maximum speed of the aircraft in Problem 5.3 versus the altitude up to 40,000 ft (12,190 m). At what altitude is the maximum speed the highest ($V_{\max_{\max}}$)?

5.6 Determine the absolute ceiling of the aircraft in Problem 5.4.

5.7 A jet (turbofan engine) fighter aircraft has the following data:

$$T_{\max} = 300\,\text{kN},\ S = 217\,\text{m}^2,\ m_{\text{TO}} = 63{,}000\,\text{kg},\ C_{L_{\max}} = 2.1,\ K = 0.043,\ C_{D_o} = 0.021$$

Is this fighter able to fly with Mach 1.7 at 20,000 ft (6,096 m) altitude?

5.8 Determine whether the fighter in Problem 5.7 can survive from a missile that can reach 40,000 ft altitude.

5.9 What would be the speed if the fighter in Problem 5.7 is required to fly at 25,000 ft (7,620 m) with 70% of its engine thrust?

5.10 Assume that the aircraft in Problem 5.4 has two engines. Is it possible for this aircraft to fly at 24,000 (7,315 m) ft if one engine is inoperative?

5.11 If the aircraft in Problem 5.4 is required to fly with a cruise-climb flight program, what would be its final altitude when the fuel tanks get empty? Ignore the safety of this flight.

5.12 Determine the range of the aircraft in Problem 5.4 if it carries only half of its maximum fuel and is required to fly with a constant-altitude, a constant speed.

5.13 Determine the maximum endurance of the aircraft in Problem 5.4.

5.14 Consider the fighter in Problem 5.7 has a fuel capacity of 20,000 kg and SFC of 0.8 N/h/N. What would be the range of this fighter if it refuels three times in the air from a tanker?

5.15 What would be the maximum range if the fighter in Problem 5.14 carries an external tank with the capacity of 30,000 kg fuel?

5.16 Consider the aircraft in Problem 5.4 that has consumed 70% of its fuel and is ready to land on a runway. The pilot suddenly receives a message from airport control tower that the runway is not ready for landing. The pilot finds out that the nearest alternate airport is 600 km away from the current position. Will this aircraft safely land on its new destination?

5.17 An antisubmarine jet aircraft above the Atlantic Ocean is searching for enemy submarine. This aircraft has the following data:

$$T_{\max} = 64\,\text{kN},\ S = 41\,\text{m}^2,\ m_{\text{TO}} = 17{,}000\,\text{kg},\ C_{L_{\max}} = 2.2,\ K = 0.09,$$
$$C_{D_o} = 0.025,\ m_f = 5{,}000\,\text{kg},\ C = 0.84\,\text{N/h/N}$$

a. How long can this aircraft search for its target?
b. For this duration, what should be its velocity if it flies at 10,000 ft (3,048 m)?

5.18 The aircraft in Problem 5.4 consumes 10% of its fuel during taxi, takeoff, and climb, and is required to have 20 min of reserve fuel. What is its maximum range?

5.19 The aircraft in Problem 5.7 is required to accomplish a mission at 2,000 km distance and 20,000 ft altitude. How much fuel this mission needs if SFC is 0.8 N/h/N? Ignore the fuel needed for takeoff, and climb.

5.20 The aircraft in Problem 5.4 is flying at 20,000 ft or 6,096 m (constant speed) and has a 30 knots (25.43 m/s) headwind. How far can this aircraft fly at this flight condition?

5.21 Between two aircraft of Problems 5.7 and 5.17, which one has higher maximum speed at sea level?

5.22 The aircraft in Problem 5.4 is required to fly 20% faster at sea level. How much more thrust its engine must produce?

5.23 Compare the maximum lift-to-drag ratio of four aircraft in Problems 5.3, 5.4, 5.7, and 5.17.

5.24 The aircraft in Problem 5.7 is required to fly with 200 knots (102.9 m/s) at sea level vertically. What is the required engine thrust?

5.25 Which flight program for the aircraft in Problem 5.4 does deliver a longer range? A flight with the maximum speed or a flight with 1.5 Vs (both at sea level). Consider the constant-altitude, constant-airspeed flight.

5.26 What flight program of the aircraft in Problem 5.25 does deliver a longer endurance?

5.27 Consider the transport aircraft in Problem 5.4 has 200 seats but can carry only 100 passengers. Calculate the maximum range if it flies at 25,000 ft (7,620 m). Assume the average mass of each passenger is 75 kg and each carries a 20 kg bag. Consider a constant-altitude, constant-airspeed flight.

5.28 The stealth aircraft F-117 has a takeoff mass of 23,814 kg, a wing area of 105.9 m^2, and two turbofan engines, each delivering 48 kN of thrust. If the zero-lift drag coefficient is 0.03 and the induced drag factor is 0.1, calculate the following:

a. Maximum speed of this aircraft at 30,000 ft (9,144 m).
b. Absolute ceiling of this aircraft.

Assume the climb to the absolute ceiling takes 7 min, and the average engine thrust during climb is equal to 90% of the maximum thrust at sea level. Ignore the effect of the fuel consumed during takeoff, and assume $C_{L_{\max}} = 2$, $C = 0.9$ N/h/N.

5.29 The fighter aircraft F/A-18 (Hornet) has a takeoff mass of 25,400 kg, a wing area of 37.16 m^2, and two turbofan engines that each produces 71.2 kN of thrust. If AR = 3.5, $e = 0.85$, $C_{D_o} = 0.02$

a. Determine its absolute ceiling. Assume the climb to the absolute ceiling takes 15 min and the average engine thrust during climb is equal to 90% of the maximum thrust at sea level. Ignore the effect of the fuel consumed during takeoff. $C_{L_{\max}} = 1.8$, $C = 0.7$ N/h/N.
b. The mass of aircraft structure is 10,455 kg. If the pilot mass is 95 kg and the aircraft has only 50 kg of fuel, what is its absolute ceiling?

5.30 The fighter Super Etendard has a takeoff mass of 12,000 kg, a wing area of 28.4 m^2, and a jet engine with 49 kN of thrust. Assume it has 5,000 kg of fuel and the following data:

$$\text{AR} = 3.23,\ e = 0.78,\ C_{D_o} = 0.024,\ C = 0.9\ \text{N/h/N}\ C_{L_{\max}} = 1.8$$

If cruising at 35,000 ft (10,670 m); determine

a. Maximum range
b. Maximum endurance

5.31 A designer is designing a jet (turbofan engine) fighter that is required to have 100,000 ft (30,480 m) of absolute ceiling. Its initial data are

$$m_{\text{TO}} = 20{,}000\,\text{kg},\ S = 40\,\text{m}^2,\ C_{D_o} = 0.017,\ K = 0.06$$

Determine how much thrust the engine must be able to produce such that this fighter can fulfill this mission. Assume the climb to the absolute ceiling takes 60 min and the average engine thrust during climb is equal to 90% of the maximum thrust at sea level. Ignore the effect of the fuel consumed during takeoff. $C_{L_{\max}} = 2.1$, $C = 1.1$ N/h/N.

5.32 An experimental aircraft X-31A has a takeoff mass of 6,335 kg, a wing area of 21 m^2, with a wing span of 6.95 m, and a turbofan engine with 47.2 kN of thrust. If $C_{D_o} = 0.016$ and $e = 0.92$, determine the aircraft's absolute ceiling. Assume $C_{L_{\max}} = 1.7$.

5.33 Determine the absolute ceiling of the reconnaissance jet (turbofan engine) aircraft U-2A with the following data:

$$W_{\text{TO}} = 40{,}000\,\text{lb},\ S = 1{,}000\,\text{ft}^2,\ T = 11{,}200\,\text{lb},$$

$$\text{AR} = 11,\ e = 0.94,\ C_{D_o} = 0.018, C_{L_{\max}} = 2,\ C = 0.92\,\text{lb/h/lb}$$

Assume the climb to the absolute ceiling takes 10 min, and the average engine thrust during climb is equal to 90% of the maximum thrust at sea level. Ignore the effect of the fuel consumed during takeoff.

5.34 Determine the maximum speed and absolute ceiling of the reconnaissance jet aircraft Lockheed SR-71 Blackbird (Figure 4.24) with the following data:

$$m_{\text{TO}} = 78{,}000\,\text{kg},\ S = 170\,\text{m}^2,$$

$$T = 2 \times 151\,\text{kN},\ b = 16.94\,\text{m},\ \text{AR} = 1.7,\ e = 0.94,$$

$$C_{D_o} = 0.032\,(\text{at supersonic speeds}),$$

$$C_{D_o} = 0.017\,(\text{at subsonic speeds}),\ C_{L_{\max}} = 2.4,\ C = 1.9\,\text{N/h/N}.$$

Assume the climb to the absolute ceiling takes 12 min and the average engine thrust during climb is equal to 90% of the maximum thrust at sea level. Ignore the effect of the fuel consumed during takeoff. The engines are turbojet (partial ramjet) and have a complex model. In this problem, use Equation 4.16 (for both first and second layers), where $c = 0.37$.

5.35 Determine the maximum range of the unmanned aircraft Global Hawk when it is flying at 60,000 ft (18,290 m), and a constant speed with the following data:

$$m_{\text{TO}} = 14{,}600\,\text{kg},\ S = 50.2\,\text{m}^2,\ T = 31.4\,\text{kN},\ b = 39.9\,\text{m},$$

$$\text{AR} = 22,\ e = 0.94,\ C_{D_o} = 0.018,\ C = 0.6\ \text{L/h},\ m_f = 6{,}590\,\text{kg}$$

5.36 Derive the formulae for the absolute ceiling of an aircraft with a turbofan engine (similar to Equations 5.178 and 5.179), when $V_{\min_D} < V_s$.

5.37 A transport aircraft with twin turbofan engines each generating 3,000 lbf of thrust has the following characteristics:

$$W_{\text{TO}} = 16{,}300 \text{ lbf},\ W_f = 4{,}000 \text{ lbf},\ S = 312\,\text{ft}^2,$$
$$K = 0.025,\ C_{D_o} = 0.038,\ C_{L_{\max}} = 1.2$$

Calculate the absolute ceiling if it takes 30 min to climb that altitude with an average fuel consumption of 1,800 lb/h.

5.38 Consider a single-engine jet (turbofan) aircraft with the following features:

$$m_{\text{TO}} = 7{,}400\,\text{kg},\ S = 110\,\text{m}^2,\ e = 0.92,\ \text{AR} = 9.2,\ C_{D_o} = 0.024$$

Maximum speed at 12,000 ft (3,658 m) is 270 KTAS. You are required to add another engine to this aircraft with the same thrust (to have a twin engine). Determine the maximum speed for the twin-engine configuration at 25,000 ft (7,620 m) in KEAS.

5.39 Consider the following jet aircraft that has a fuel capacity of 10,000 kg and SFC of 0.7 N/h/N.

$$S = 217\,\text{m}^2,\ m_{\text{TO}} = 63{,}000\,\text{kg},\ K = 0.043,\ C_{D_o} = 0.021,\ C_{L_{\max}} = 1.7$$

a. What would be the range (in km) if it flies with a constant speed of 160 m/s and constant angle of attack, assuming that the aircraft begins its flight at 18,000 ft (5,486 m) altitude.
b. What is the new altitude at the end of this flight?

5.40 An antisubmarine jet aircraft with the following characteristics is above the Atlantic Ocean and is searching for a target submarine:

$$m_{\text{TO}} = 17{,}000\,\text{kg},\ m_f = 5{,}590\,\text{kg},\ S = 42\,\text{m}^2,\ C_{L_{\max}} = 2.2,$$
$$C_{D_o} = 0.025,\ e = 0.87,\ b = 20\,\text{m},\ C = 0.84\,\text{N/h/N}$$

a. Determine the maximum duration (in hour) that this aircraft is able to search for a target.
b. For this duration, what should be the velocity if it flies at 10,000 ft (3,048 m)?

5.41 A jet aircraft has a mission to fly 5,000 km (as its maximum range) at 18,000 ft (5,486 m) altitude. The aircraft has the following characteristics:

$$m_o = 11{,}000\,\text{kg},\ S = 32\,\text{m}^3,\ C_{D_o} = 0.021,\ C = 0.6\ \text{N/h/N},\ K = 0.07,$$
$$T_{\max_{\text{SL}}} = 8{,}000\,\text{N},\ C_{L_{\max}} = 1.8$$

a. What percentage of the aircraft's initial weight should be fuel weight to perform this mission successfully?
b. How long this mission will take (in hour)?

5.42 A jet aircraft with the following characteristics has a maximum speed of Mach 0.62 at 12,000 ft altitude or 3,658 m (ISA + 15 flight condition). Determine the aircraft's new maximum speed (in KTAS) if it employs the afterburner that results in a 30% increase in the maximum engine thrust.

$$S = 21\,\text{m}^2,\ m_{\text{TO}} = 13{,}000\,\text{kg},\ C_{D_o} = 0.029,\ \text{AR} = 8.5,\ e = 0.83$$

5.43 Consider the aircraft in Problem 5.40. The aircraft is at 15,000 ft (4,572 m) altitude with a speed of 240 KTAS (123.4 m/s). Determine the range.
a. If the pilot holds the altitude and speed constant throughout the flight.
b. If the pilot holds the lift coefficient and speed constant throughout the flight.
c. If the pilot holds the lift coefficient and altitude constant throughout the flight.

5.44 Consider the aircraft in Problem 5.40. The aircraft is at 25,000 ft (7,620 m) altitude with a speed of 180 KTAS (92.6 m/s). Determine the endurance
a. If the pilot holds the altitude and speed constant throughout the flight.
b. If the pilot holds the lift coefficient and speed constant throughout the flight.
c. If the pilot holds the lift coefficient and altitude constant throughout the flight.

5.45 A very large jet transport aircraft, with a mass of 600,000 kg and a wing area of 900 m^2, is equipped with four turbofan engines and has the following characteristics:

$$C_{D_o} = 0.018,\ K = 0.04,\ T_{\text{SL}} = 4 \times 300\,\text{kN},\ C_{L_{\max}} = 2.7$$

Determine
a. Cruise altitude
b. Cruising speed in terms of the Mach number
Ignore other phases (including the climb phase) of the flight and assume that this cruise altitude is to maximize the range.

5.46 A regional jet airliner, with a takeoff mass of 36,000 kg and a wing area of 83 m^2, is equipped with two turbofan engines and has the following characteristics:

$$C_{D_o} = 0.022,\ K = 0.035,\ T_{\text{SL}} = 2 \times 60\,\text{kN},\ C_{L_{\max}} = 2.6$$

Determine
a. Cruise altitude
b. Cruising speed in terms of the Mach number
Ignore other phases (including the climb phase) of the flight and assume that this cruise altitude is to maximize the range.

5.47 A business jet aircraft (Cessna Citation), with a takeoff mass of 9,000 kg and a wing area of 35 m^2, is equipped with two turbofan engines. Assume the following characteristics:

$$C_{D_o} = 0.022,\ K = 0.042,\ T_{SL} = 2 \times 18\,\text{kN},\ C_{L_{max}} = 1.9$$

Determine
a. Cruise altitude
b. Cruising speed in terms of the Mach number
Ignore other phases (including the climb phase) of the flight and assume that this cruise altitude is to maximize the range.

5.48 A small jet (turbofan engine) aircraft has the following features:

$$m = 24{,}000\,\text{kg},\ S = 24\,\text{m}^2,\ C_{D_o} = 0.02,\ K = 0.05,\ V_s = 80\,\text{knot}\,(41.1\,\text{m/s})$$

Determine the minimum drag velocity and the minimum thrust that the jet engine needs to generate at sea level in order for the aircraft to be airborne for a steady-level flight at 5,000 m.

5.49 A business jet aircraft has the following features:

$$W = 90{,}000\,\text{lb},\ S = 400\,\text{ft}^2,\ C_{D_o} = 0.021,\ K = 0.045,\ V_s = 92\,\text{knot}$$

Determine the minimum drag velocity and the minimum thrust that the jet engine needs to generate at sea level in order for the aircraft to be airborne for a steady-level flight at 30,000 ft.

5.50 Plot the variations of lift-to-drag ratio versus speed for the aircraft in Problem 5.3 when flying at sea level. The speed range is between the stall speed to the maximum speed.

5.51 A fighter aircraft has the following features at subsonic speeds:

$$C_{D_o} = 0.025,\ AR = 2.21, e = 0.81$$

Calculate the maximum lift-to-drag ratio.

5.52 A long-range UAV has the following features:

$$C_{D_o} = 0.016,\ \text{AR} = 32,\ e = 0.92$$

Calculate the maximum lift-to-drag ratio.

5.53 The high-altitude, unmanned surveillance aircraft Northrop Grumman RQ-4 Global Hawk has a wing area of 50.1 m^2, and a wing span of 35.4 m. The aircraft maximum lift-to-drag ratio is 33. Determine zero-lift drag ratio. Assume $e = 0.9$.

6 Straight-Level Flight
Propeller-Driven Aircraft

6.1 INTRODUCTION

In Chapter 5, the straight-level flight performance analysis for jet aircraft was presented. In this chapter, the same topic is explored, but for prop-driven aircraft. As in the case of jet aircraft, the important straight-level flight topics for prop-driven aircraft are as follows: cruising flight, maximum speed, range, endurance, and ceiling. The topics in Chapter 5 are very similar to the topics in this chapter; the only difference is the type of powerplant used, that is, prop-driven engine. As we discussed in Chapter 4, the major difference between jet engine and prop-driven engine is that a jet engine generates the thrust directly, whereas a prop-driven engine produces the power. Then, this power will be converted to thrust via a propeller. Although this difference is not a very important one, this causes a large difference in the straight-level flight performance analysis of the prop-driven aircraft.

This chapter presents techniques to analyze the performance of an aircraft with prop-driven engine(s), either piston engine or turboprop engine, in a steady-state condition. However, some topics such as maximum speed, cruise speed, and ceiling are applicable to fixed-wing aircraft with electric engines.

Since the fundamentals of steady-state level flight were discussed in Chapter 5 for jet aircraft, they are not repeated here. We need to just recapitulate that a straight-level flight is a steady-state condition where all the forces (i.e., thrust, drag, weight, and lift) and moment are in equilibrium.

Although the only difference between the previous chapter and this chapter is the engine type, this leads to a whole new series of techniques and equations and need to be discussed in a separate chapter. However, the analysis techniques are very similar and fundamentals are the same. In general, the straight-level flight performance of a prop-driven aircraft is lower than that for a jet aircraft.

This chapter is organized as follows: First, basic equations in straight-level flight are introduced and derived. Then the methods to evaluate the following performance criteria are discussed: (1) specific speeds in straight-level flight, (2) range, (3) endurance, and (4) ceiling. The specific speeds in straight-level flight include maximum speed, cruising speed, minimum drag speed, minimum power speed, maximum range speed, speed for absolute ceiling, and maximum endurance speed. The performance data for various prop-driven aircraft that are given in several tables are extracted mainly from Reference [9]. Various examples demonstrate the applications of techniques covered in this chapter.

DOI: 10.1201/9781003279068-6

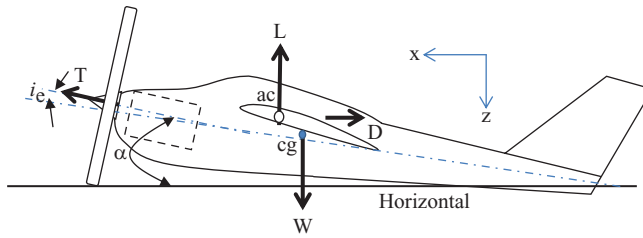

FIGURE 6.1 Equilibrium of forces in a straight-level flight.

6.2 BASIC FUNDAMENTALS

The very basic governing principle in straight-level flight is derived from the equilibrium of forces. As discussed in Chapter 5, the external forces of interest include aircraft weight (W), engine thrust (T), drag (D), and lift (L) which are derived in Chapters 2–4. Hence, in an unaccelerated straight-level flight (i.e., constant airspeed), the governing equations of motion (see Figure 6.1) are

$$\sum F_x = 0 \tag{6.1}$$

$$\sum F_z = 0 \tag{6.2}$$

This implies that the aircraft is in a trim or an equilibrium state. An aircraft in a cruising flight has a low angle of attack (often <5°) and a low engine setting angle. Figure 6.1 shows a cruising aircraft with an angle of attack (α) and engine setting angle. Thus, the trim equations in cruise along z- and y-axes, respectively, will be

$$D = T\cos(\alpha + i_e) \tag{6.3}$$

$$W = L + T\sin(\alpha + i_e) \tag{6.4}$$

where α is the aircraft angle of attack and i_e is the engine setting angle. For simplicity, we ignore the effects of aircraft angle of attack and the engine setting angle in equilibrium. By assuming so, the governing equations of motion in an unaccelerated straight-level flight will reduce to

$$D = \frac{1}{2}\rho V^2 S C_D = T \tag{6.5}$$

$$W = L = \frac{1}{2}\rho V^2 S C_L \tag{6.6}$$

where T, D, W, and L are engine thrust, aircraft drag, aircraft weight, and aircraft lift respectively. According to these equations, the engine must produce enough thrust to balance the drag force, and the aircraft (mainly wing) must generate enough lift force to hold the aircraft against the weight. Equations 6.5 and 6.6 are approximate versions of Equations 6.3 and 6.4. The equations derived for cruise, range, endurance, and ceiling analysis are based on the approximate versions of governing equation.

For an accurate result, the interested reader is encouraged to derive new expressions for cruise, range, endurance, and ceiling, based on Equations 6.3 and 6.4.

The aircraft propulsion system is responsible for the generation of thrust. The engine thrust in a propeller-driven engine is produced through a propeller as a function of engine shaft power (P), aircraft airspeed (V), and prop efficiency (η_P):

$$T = \frac{P\eta_P}{V} \tag{6.7}$$

Please note that this equation is not applicable in a straight-level steady flight, if the airspeed is less than stall speed; such as the takeoff speed, or more than the maximum speed. This means that at the beginning of a takeoff operation, where the aircraft speed is zero, the engine thrust is not infinite. Equation 6.7 is the third basic expression (two other equations are Equations 6.5 and 6.6) that is employed in the aircraft performance analysis of a prop-driven aircraft.

Since the engine thrust is a function of engine power, in order to increase the thrust, one must increase the engine power. When the pilot deflects the engine throttle, the engine power is varied. Then the propeller/shaft rotational velocity (say, in revolutions per minute [rpm]) is varied, so the engine thrust is varied. This causes an acceleration, which eventually results in a greater speed. This simultaneously increases the aircraft drag; thus, the acceleration will be consequently decreased. This process is continued until the aircraft has a new equilibrium airspeed. Figure 6.3 (see later in the chapter) illustrates the typical variations of engine power in prop-driven engines.

The fourth basic equation in this chapter is a relationship for specific fuel consumption (SFC) of a prop engine. As we introduced in Chapter 4, the specific fuel consumption (SFC or simply C) for a prop engine is defined as the amount of fuel weight (w) consumed in a unit time (t) per unit power (P):

$$C = \left(\frac{-dw}{dt}\right)\frac{1}{P} \tag{6.8}$$

The fuel of piston-prop engines is referred to as aviation gasoline, and each gallon weighs about 6 lb or 0.8 kg/L. A typical fuel of most turboprop engines is a kind of kerosene and each gallon weighs about 6.75 lb or 0.82 kg/L. The typical value for C is 0.4–0.7 lb/h/hp.

The relationship between aircraft angle of attack and aircraft speed, the maximum lift-to-drag ratio $(L/D)_{\max}$, and the lift coefficient and drag coefficient when the lift-to-drag ratio has the maximum value, in prop-driven aircraft, is the same as those for jet aircraft (see Section 5.2 for proof). Hence, Equations 5.24, 5.23, and 5.20 are valid for an aircraft with prop-driven engine; so, they are repeated here for convenience:

$$\left(\frac{L}{D}\right)_{\max} = \left(\frac{C_L}{C_D}\right)_{\max} = \frac{1}{2\sqrt{KC_{D_o}}} \tag{6.9}$$

$$C_{L_{(L/D)_{\max}}} = \sqrt{\frac{C_{D_o}}{K}} \tag{6.10}$$

$$C_{D_{(L/D)_{\max}}} = 2C_{D_o} \tag{6.11}$$

Thus, the maximum lift-to-drag ratio of prop-driven aircraft is only a function of aircraft zero-lift drag coefficient (C_{D_o}) and induced drag factor (K).

Example 6.1

Consider an aircraft with a piston-prop engine. The maximum engine power is 200 hp, the SFC is 0.52 lb/h/hp, and the prop efficiency is 0.8. The aircraft is cruising along a straight-level flight with the maximum power and at a constant airspeed of 120 knots for 2 h.

a. Calculate how much fuel has been consumed in 2 h.
b. Determine the aircraft drag.

Solution

a. Fuel mass

$$C = \left(\frac{-dw}{dt}\right)\frac{1}{P} \Rightarrow W = C \cdot P \cdot t = 0.52 \times 200 \times 2 = 208\,\text{lb} \Rightarrow m = 94.4\,\text{kg} \qquad (6.8)$$

b. Aircraft drag

$$T = \frac{P\eta_P}{V} = \frac{200 \times 550 \times 0.8}{120 \times 1.688} = 434.5\,\text{lb} = 1{,}933\,\text{N} \qquad (6.7)$$

$$D = T = 434.5\,\text{lb} = 1{,}933\,\text{N} \qquad (6.5)$$

6.3 SPECIFIC SPEEDS

As we discussed in Section 5.3, a prop-driven aircraft can have straight-level steady flight with all possible, but permissible, airspeeds (i.e., from stall speed to maximum speed). Among the list of infinite speeds, the following speeds are of special interest and have particular applications:

a. Minimum drag speed ($V_{\min_D}$)
b. Minimum power speed ($V_{\min_P}$)
c. Maximum speed ($V_{\max}$)
d. Maximum range speed ($V_{\max_R}$)
e. Maximum endurance speed ($V_{\max_E}$)
f. Maximum (absolute) ceiling speed (V_{ac})
g. Cruising speed (V_C)

From these seven specific speeds, the minimum drag speed is exactly the same as the minimum drag speed of jet aircraft. The technique to determine the maximum speed is addressed in Section 6.3.4. Two speeds of maximum range speed and maximum endurance speed will be introduced in Sections 6.4 and 6.5. The technique to determine the maximum (absolute) ceiling speed will be discussed in Section 6.6. The techniques to determine the cruise speed will be introduced in Section 6.7.

6.3.1 Minimum Power Speed

As discussed in Chapter 4, there are several variables that influence the engine shaft power, such as throttle setting, air density, air temperature, air atmospheric pressure, manifold pressure (for piston-prop engine), fuel-to-air ratio, and aircraft airspeed. One of the interesting speeds in a straight-level flight for a propeller-driven aircraft is the minimum power speed. At this velocity, as the name implies, the required engine shaft power (P_R) will be at its minimum value for a straight-level steady flight. If an aircraft flies at such speed, the minimum engine power will be required.

It is of critical importance to distinguish (see Figure 6.2) the available power (P_A), the required power (P_R), and the shaft power (P_S). The shaft power is the power that is directly produced by the engine shaft to the propeller. The shaft power is simply referred to as the engine power (P). However, the available power is the output power of the engine–propeller combination (i.e., after the propeller). As the throttle is changed, the available power will be changed as well. Please note that the available power is always less than shaft power (P), since the propeller consumes portion (about 10%–30%) of the shaft power/energy for its rotation. In contrast, the required power is the engine power required for a specific mission. If the required power is more than the available power for a required mission, the mission is not possible with the current power.

Thus, the available power is defined as the engine shaft power multiplied by the propeller efficiency:

$$P_A = P\eta_P \tag{6.12}$$

For the sake of simplicity, in this chapter, we assume that the prop efficiency is constant unless otherwise stated. Hence, when we use the term "minimum power" (in this chapter), we mean the minimum required power, not the minimum available power. However, in a straight-level steady flight, the required power is equal to the available power. Hence, the minimum required power is also equal to the minimum available power.

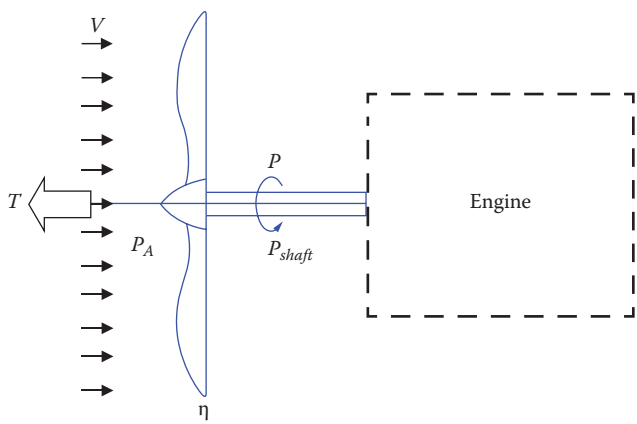

FIGURE 6.2 The propeller and the conversion of power to thrust.

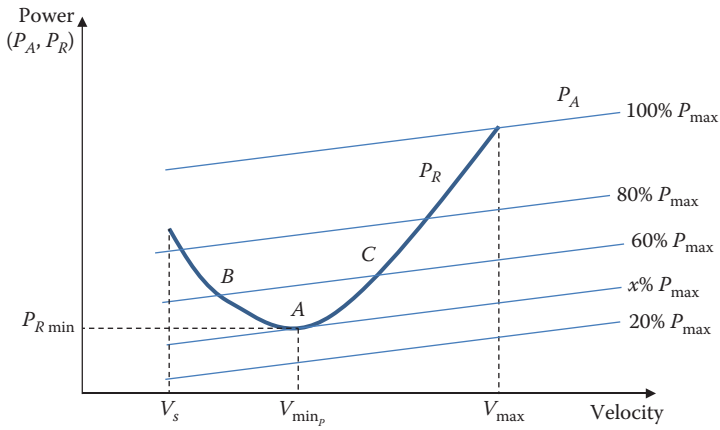

FIGURE 6.3 Minimum power speed, cruise speed, and maximum speed.

The aircraft required power is a function of several parameters, but in this section, we concentrate on airspeed. Both the aircraft required power and the engine available power vary with aircraft airspeed. The variations of the aircraft required power and the engine available power for a steady-level flight are sketched in Figure 6.3. At any given altitude, the power required by the aircraft is a nonlinear function of velocity, and the variation with airspeed looks like a parabola.

In contrast, variations of the engine available power versus velocity are assumed to be linear. In a level flight, when the required power is less than the available power, the aircraft will accelerate. In contrast, in a level flight, when the required power is more than the available power, the aircraft will decelerate. The available power may be from 0% to 100% of the maximum power depending on the throttle setting and airspeed.

As Figure 6.3 demonstrates, with increasing aircraft speed, the power required by aircraft decreases first, but then increases. The lowest point of this curve is an interesting location. The speed corresponding to this point (where the power is at its minimum value) is referred to as the *minimum power speed* (V_{min_P}). The main application of this speed is at high altitude such as absolute ceiling. This velocity is the velocity at which the engine will generate the lowest amount of power to have a steady-level flight. Another implication is that there is no steady-level flight when the engine creates a power that is lower than this value. A typical value of the minimum required power for a steady-level flight is about 30% of the engine maximum available power.

Depending on the throttle setting and airspeed, the P_A and P_R curves may have no, one, or two intersections. If the P_A is too low (e.g., 20% of the maximum engine power), there will be no intersection. When P_A reaches the required value (e.g., 60% of the maximum engine power), there will be two intersections (points B and C). This implies that the aircraft requires the same engine power for two-level flight velocities. However, if the engine power is at a value equal to the minimum required power, there will be only one intersection (point A). This velocity is referred to as the minimum power velocity (V_{min_P}). Now, we are interested in deriving an equation for this velocity.

By using Equations 6.5 and 6.6, we can determine the required power for a steady-level flight at any speed. For an object in motion, the power is basically defined as "applied force" multiplied by "object speed". The required power (P_R) is a function of the required force (i.e., thrust [T_R]). In a steady-level flight, the required thrust/force is equal to the aircraft drag (Equation 6.6). So, the required power for an aircraft to fly at a specific speed in a straight-level flight is defined as follows:

$$P_R = FV = T_R V = DV \tag{6.13}$$

In Chapter 5, we derived the following expression for drag:

$$D = \frac{1}{2}\rho V^2 S C_{D_o} + \frac{2K(mg)^2}{\rho V^2 S} \tag{5.35}$$

By substituting the drag force from Equation 5.35 into Equation 6.13, we obtain

$$P_R = \frac{1}{2}\rho V^3 S C_{D_o} + \frac{2K(mg)^2}{\rho V S} \tag{6.14}$$

This indicates that the required power is a nonlinear function of velocity, as a typical curve of this equation is plotted in Figure 6.3. In a straight-level flight with a constant airspeed, the available power is equal to the required power:

$$P_A = P_R \tag{6.15}$$

So, Equation 6.14 may be reformatted as

$$\frac{1}{2}\rho V^4 S C_{D_o} - P_A V + \frac{2K(mg)^2}{\rho S} = 0 \tag{6.16}$$

When a dependent parameter (e.g., power) is a function of an independent variable (e.g., V), the highest/lowest values of the parameter are determined by differentiating the equation with respect to the variable and setting it equal to zero. Thus, to find the minimum power speed, we differentiate Equation 6.16 with respect to the velocity:

$$\frac{\partial P_A}{\partial V} = \frac{\partial P}{\partial V} = 0 \Rightarrow \frac{1}{2}\rho(3V^2) S C_{D_o} - \frac{2K(mg)^2}{\rho S V^2} = 0 \tag{6.17}$$

To solve for V, we will have

$$V^4 = \frac{4K(mg)^2}{3C_{D_o}(\rho S)^2} \tag{6.18}$$

The equation has a power of 4 for the variable *velocity*; hence, for any given value of P_A, four values of velocity will satisfy this equation. However, only one or two solutions are acceptable, which are only non-negative real values, where they are inside

the aircraft flight envelope. With the application of the square root twice, we will obtain the minimum power speed as

$$V = \pm\sqrt{\frac{2mg\sqrt{K}}{\rho S\sqrt{3C_{D_o}}}} \tag{6.19}$$

or

$$V_{\min_P} = +\sqrt{\frac{2mg}{\rho S\sqrt{3C_{D_o}/K}}} \tag{6.20}$$

By comparing this equation with Equation 6.6, we can write

$$V_{\min_P} = \sqrt{\frac{2mg}{\rho S C_{L_{\min P}}}} \tag{6.21}$$

As will be proven in Section 6.4, one of the main applications of the minimum power speed is to maximize the endurance of a prop-driven aircraft. By comparing Equations 6.21 and 6.20, we derive the aircraft lift coefficient for the minimum power speed as follows:

$$C_{L_{\min P}} = \sqrt{\frac{3C_{D_o}}{K}} \tag{6.22}$$

This is a mathematical expression; the theoretical value of ($C_{L_{\min P}}$) must be within a practical flight limit. The value of $C_{L_{\min P}}$ in Equation 6.22 cannot be more than the aircraft maximum lift coefficient ($C_{L_{\max}}$). If the output of the equation is more than $C_{L_{\max}}$, ignore the outcome and select a new value slightly less than $C_{L_{\max}}$.

By comparing this equation with Equation 6.10 $\left(C_{L_{(L/D)\max}} = \sqrt{C_{D_o}/K}\right)$, we can also derive the following expression as the relationship between the minimum power lift coefficient and the maximum lift-to-drag lift coefficient:

$$C_{L_{\min P}} = \sqrt{3}C_{L_{(L/D)_{\max}}} \tag{6.23}$$

The minimum power drag coefficient using Equation 3.12 is

$$C_{D_{\min P}} = C_{D_o} + KC_{L_{\min P}}^2 = C_{D_o} + K\left(\sqrt{\frac{3C_{D_o}}{K}}\right)^2 = C_{D_o} + 3C_{D_o} \tag{6.24}$$

which results in

$$C_{D_{\min P}} = 4C_{D_o} \tag{6.25}$$

When a prop-driven aircraft is cruising with the minimum power speed, the lift-to-drag ratio is

$$\left(\frac{L}{D}\right)_{\min_P} = \frac{C_{L_{\min P}}}{C_{D_{\min P}}} = \frac{\sqrt{3C_{D_o}/K}}{4C_{D_o}} = \frac{\sqrt{3}}{2}\frac{1}{2\sqrt{KC_{D_o}}} \tag{6.26}$$

Comparing this equation with Equation 6.9, we obtain

$$\left(\frac{L}{D}\right)_{\min_P} = 0.866\left(\frac{L}{D}\right)_{\max} \tag{6.27}$$

The minimum power speed increases with altitude such that at some altitudes, it will be equal to the maximum speed. There is an important flight safety point about minimum power speed, which is related to stall speed. Please note that sometimes minimum power speed that is obtained through Equation 6.20 is less than aircraft stall speed; hence, it is unacceptable. For a prop-driven aircraft in which the minimum power speed is theoretically less than the stall speed, a safe minimum power speed is selected to be about 10%–20% higher than the stall speed:

$$V_{\min_P} = k \cdot V_s \tag{6.28}$$

where

$$1.1 < k < 1.2 \tag{6.29}$$

It is interesting to highlight the connection between the engine's minimum power and the aircraft aerodynamics in order to relate the aircraft performance with aircraft design features. As shown in Equation 6.13, the required power is equal to the required thrust multiplied by the airspeed. In a cruising flight, lift is equal to weight (Equation 6.6), and thrust is equal to drag (Equation 6.5), so we can write the following:

$$P_R = DV = DV\frac{L}{L} = DV\frac{W}{L} = W\frac{D}{L}V = W\frac{1}{L/D}V = W\frac{1}{C_L/C_D}V \tag{6.30}$$

However, the velocity (Equation 6.6) is a function of aircraft weight, air density, wing area, and lift coefficient:

$$V = \sqrt{\frac{2W}{\rho S C_L}} \tag{6.31}$$

Inserting Equation 6.31 into Equation 6.30, we obtain

$$P_R = W\frac{1}{C_L/C_D}\sqrt{\frac{2W}{\rho S C_L}} = \left(\frac{2W^3 C_D^2}{\rho S C_L^3}\right)^{1/2} \tag{6.32}$$

This may be reformatted as follows:

$$P_R = \left(\frac{2W^3}{\rho S}\right)^{1/2}\left(\frac{1}{C_L^3/C_D^2}\right)^{1/2} \tag{6.33}$$

This demonstrates that the required power is the function of the reciprocal of C_L^3/C_D^2; as the ratio C_L^3/C_D^2 is increased, the required power decreases. Hence, we can conclude that the minimum power is an inverse function of the maximum value C_L^3/C_D^2 of the ratio:

$$P_{R_{\min}} \propto \frac{1}{\left(C_L^3/C_D^2\right)_{\max}} \tag{6.34}$$

Employing the drag polar equation (Equation 3.12), one can derive the following expression:

$$P_{R_{\min}} \propto \left(C_L^{3/2}/C_D\right)_{\max} \tag{6.35}$$

Thus, the minimum power required occurs when the aircraft is cruising such that the ratio C_L^3/C_D^2 $\left(\text{or } C_L^{3/2}/C_D\right)$ is at its maximum value $\left(\text{i.e., } \left(C_L^3/C_D^2\right)_{\max} \text{ or } \left(C_L^{3/2}/C_D\right)_{\max}\right)$. We may also conclude that the lift-to-drag ratio, when a prop-driven aircraft is cruising such that engine power is at its minimum value, is

$$\left(\frac{L}{D}\right)_{\min P} = \left(\frac{C_L^3}{C_D^2}\right)_{\max} \tag{6.36}$$

To derive an expression for the aerodynamic ratio $\left(C_L^{3/2}/C_D\right)_{\max}$, we begin with the ratio $C_L^{3/2}/C_D$; then, we replace C_D with its equivalent from drag polar (Equation 3.12):

$$\frac{C_L^{3/2}}{C_D} = \frac{C_L^{3/2}}{C_{D_o} + KC_L^2} \tag{6.37}$$

The maximum value of this ratio is obtained by differentiating Equation 6.37 with respect to lift coefficient (C_L) and setting the result equal to zero:

$$\frac{d\left(C_L^{3/2}/C_D\right)}{dC_L} = 0 \Rightarrow \frac{d}{dC_L}\frac{C_L^{3/2}}{C_{D_o} + KC_L^2} = \frac{\frac{3}{2}C_L^{1/2}\left(C_{D_o} + KC_L^2\right) - 2KC_LC_L^{3/2}}{\left(C_{D_o} + KC_L^2\right)^2} = 0 \tag{6.38}$$

Setting the numerator equal to zero results in (The derivation is left to the reader)

$$C_L = \sqrt{\frac{3C_{D_o}}{K}} \tag{6.39}$$

This is the lift coefficient that maximizes the ratio $C_L^{3/2}/C_D$ and minimizes the required power in a steady-level flight. Inserting Equation 6.39 into Equation 6.37 yields an expression for $\left(C_L^3/C_D^2\right)_{\max}$:

$$\left(\frac{C_L^{3/2}}{C_D}\right)_{\max} = \frac{\left(\sqrt{3C_{D_o}/K}\right)^{3/2}}{C_{D_o} + K\left(\sqrt{3C_{D_o}/K}\right)^2} = \frac{\left(3C_{D_o}/K\right)^{3/4}}{4C_{D_o}} \tag{6.40}$$

which is reduced to

$$\left(\frac{C_L^{3/2}}{C_D}\right)_{\max} = \frac{0.57}{K^{3/4}C_{D_o}{}^{1/4}} \tag{6.41}$$

Note that both powers of K and C_{D_o} at the denominator are less than one. Hence, this expression indicates that the minimum power is inversely proportional to C_{D_o} and K (two variables in the drag polar). As K and C_{D_o} are decreased, the ratio will be increased, and the minimum power (Equation 6.35) will be decreased. Assuming aircraft weight, wing area, and air density to be constant, the more aerodynamic is the aircraft, the lesser is the engine power required for a steady-level flight. Since the induced drag factor, K, is also an inverse function of the wing aspect ratio (AR) and the wing AR is increased, the minimum power will be reduced.

It is also interesting to calculate the minimum required power (point A in Figure 6.3) that a prop-driven aircraft needs to have a steady-level flight. Based on Equation 6.13, the minimum power is determined by multiplying the minimum power drag by the minimum power velocity:

$$P_{\min} = D_{\min_P} V_{\min_P} \tag{6.42}$$

By inserting: (1) the minimum power velocity (Equation 6.21), (2) the drag coefficient corresponding to the minimum power (Equation 6.25), (3) the corresponding lift coefficient (Equation 6.22), and (4) the drag force corresponding to the minimum power (Equation 3.1); into the Equation 6.42, we obtain

$$P_{R_{\min}} = \frac{1}{2}\rho V_{\min_D}^2 S C_{D_{\min D}} \left(V_{\min_P}\right) = \frac{1}{2}\rho \frac{2mg}{\rho S C_{L_{\min P}}} S\left(4C_{D_o}\right)\left(\sqrt{\frac{2mg}{\rho S C_{L_{\min P}}}}\right) \tag{6.43}$$

or

$$P_{R_{\min}} = \frac{4mg}{\sqrt{3C_{D_o}/K}} C_{D_o}\left(\sqrt{\frac{2mg}{\rho S\sqrt{3C_{D_o}/K}}}\right) \tag{6.44}$$

This is further simplified to

$$P_{R_{\min}} = 2.48\frac{(mg)^{3/2}}{\sqrt{\rho S}}\left(\frac{C_{D_o}}{K^5}\right)^{-0.25} \tag{6.45}$$

Since the available power is a function of the propeller efficiency (Equation 6.12), Equation 6.45 is modified as:

$$P_{\min} = 2.48\frac{(mg)^{3/2}}{\eta_P\sqrt{\rho S}}\left(\frac{C_{D_o}}{K^5}\right)^{-0.25} \tag{6.46}$$

This is the absolute minimum power that a prop-driven aircraft needs to be airborne for a steady-level flight. Inspection of this equation implies that as the mass of the aircraft increases, the minimum power increases as well. In contrast, as the wing area increases, the aircraft requires less minimum power to be airborne. In addition, as we expect, the higher the altitude, the higher the minimum power (see Equations 4.15, 4.23, and 4.24) will be.

Please note that if the minimum power velocity is less than the stall speed, it is not allowed to employ Equation 6.46 to determine the minimum power. In such a case, use the new speed to determine the minimum power based on Equation 6.28.

Case Study - Example 6.2

The piston-prop-driven ultralight aircraft Quicksilver MX Sport has a maximum takeoff mass of 238 kg, a wing area of 14.5 m^2, and a wing span of 8.53 m. Assume the aircraft has the following characteristics:

$$C_{D_o} = 0.032, e = 0.8, \eta_P = 0.75, C_{L_{\max}} = 1.8, P_{\max} = 29.8\,\text{kW}$$

Determine the minimum power velocity and the minimum power that the engine needs to generate at sea level in order for the aircraft to be airborne for a steady-level flight at 4,000 m.

Solution

As in Appendix A, at 4,000 m altitude, the air density is 0.819 kg/m^3. We first need to calculate the aspect ratio and the induced drag factor (*K*).

$$\text{AR} = \frac{b^2}{S} = \frac{8.53^2}{14.5} = 5.02 \tag{3.9}$$

$$K = \frac{1}{\pi \cdot e \cdot \text{AR}} = \frac{1}{3.14 \times 0.8 \times 5.02} \Rightarrow K = 0.079 \tag{3.8}$$

The minimum power velocity at 4,000 m is

$$V_{\min_P} = \sqrt{\frac{2mg}{\rho S\sqrt{3C_{D_o}/K}}} = \sqrt{\frac{2 \times 238 \times 9.81}{0.819 \times 14.5 \times \sqrt{(3 \times 0.032)/0.079}}} \tag{6.20}$$

$$= 18.9\ \text{m/s} = 36.74\ \text{knot}$$

The stall speed at 4,000 m is

$$V_s = \sqrt{\frac{2W}{\rho S C_{L_{\max}}}} = \sqrt{\frac{2 \times 238 \times 9.81}{0.819 \times 14.5 \times 1.6}} = 15.67\ \text{m/s} = 30.47\,\text{knot} \tag{2.27}$$

The minimum power velocity is greater than the stall speed, so we can use Equation 6.46. The minimum power at 4,000 m is

$$P_{\min} = 2.48\frac{(mg)^{3/2}}{\eta_P\sqrt{\rho S}}\left(\frac{C_{D_o}}{K^5}\right)^{-0.25} = 2.48\frac{(238\times 9.81)^{3/2}}{0.75\times\sqrt{0.819\times 14.5}}\left(\frac{0.032}{0.079^5}\right)^{-0.25} \tag{6.46}$$

$$P_{R_{\min}} = 10.76\,\text{kW} = 14.4\,\text{hp}$$

At sea level, the engine minimum power should be

$$P = P_{\text{SL}}\left(\frac{\rho}{\rho_o}\right)^{1.2} \Rightarrow P_{\text{SL}} = \frac{P_{\min}}{(\rho/\rho_o)^{1.2}} = \frac{10.76}{(0.819/1.225)^{1.2}} \tag{4.19}$$

$$P_{\text{SL}_{\min}} = 17.45\,\text{kW} = 23.4\,\text{hp}$$

The aircraft has a 29.8 kW piston engine, so the minimum power is about 58.5% of the maximum power.

6.3.2 Minimum Drag Speed ($V_{\min_D}$)

A prop-driven aircraft can fly with a speed such that the aircraft produces a minimum drag. The importance of minimum drag speed for prop-driven aircraft is very similar to that of jet aircraft. For more information, refer to Section 5.3.3. The derivation of minimum drag speed for a prop-driven aircraft is exactly the same as that of a jet aircraft, so it is not repeated here. Thus, only the results (Equations 5.39, 5.40, 5.42, and 5.43) will be copied here for convenience:

$$V_{\min_D} = \sqrt{\frac{2mg}{\rho S\sqrt{C_{D_o}/K}}} \tag{6.47}$$

$$C_{L_{\min_D}} = \sqrt{\frac{C_{D_o}}{K}} \tag{6.48}$$

$$\left(\frac{L}{D}\right)_{\min_D} = \frac{1}{2\sqrt{KC_{D_o}}} \tag{6.49}$$

$$C_{D_{\min_D}} = 2C_{D_o} \tag{6.50}$$

In the application of Equations 6.47 and 6.48, two aircraft operational limits should be considered. There is an important flight safety point about minimum drag speed (Equation 6.47), which is related to stall speed. Please note that sometimes minimum drag speed that is obtained through Equation 6.47 is theoretically less than aircraft stall speed; hence, it is unacceptable. For a prop-driven aircraft in which the minimum drag speed is less than the stall speed, a safe minimum drag speed is selected to be about 10%–20% higher than stall speed:

$$V_{\min_D} = k\cdot V_s \tag{6.51}$$

where

$$1.1 < k < 1.2 \tag{6.52}$$

Equation 6.48 is a mathematical expression; the theoretical value $C_{L_{\min_D}}$ of must be within a practical flight limit. The value of $C_{L_{\min_D}}$ from Equation 6.47 cannot be more than the aircraft maximum lift coefficient $C_{L_{\max}}$. If the output of the equation is more than $C_{L_{\max}}$, ignore the result, and select a new value slightly less than $C_{L_{\max}}$.

6.3.3 Maximum Lift-to-Drag Ratio Speed

The highest aerodynamic efficiency of a prop-driven aircraft is achieved when it is cruising with a velocity that invariably delivers the highest lift-to-drag ratio ($V_{(L/D)_{\max}}$). This velocity is of significant interest to a pilot for whom the flight cost is important. A prop-driven aircraft can fly with a speed such that the aircraft maximum lift-to-drag ratio is at its maximum value. The importance of maximum lift-to-drag ratio speed for a prop-driven aircraft is very similar to that of a jet aircraft. For more information, refer to Section 5.3.3. Derivation of the speed for the highest lift-to-drag ratio for a prop-driven aircraft is exactly the same as that of a jet aircraft, so it is not repeated here. Thus, only the results (Equations 5.48, 5.49, 5.50, and 5.40) will be listed out for convenience:

$$\left(\frac{L}{D}\right)_{\max} = \left(\frac{C_L}{C_D}\right)_{\max} = \frac{1}{2\sqrt{KC_{D_o}}} \tag{6.53}$$

$$V_{(L/D)_{\max}} = V_{\min_D} \tag{6.54}$$

$$V_{(L/D)_{\max}} = \sqrt{\frac{2mg}{\rho S\sqrt{C_{D_o}/K}}} \tag{6.55}$$

$$C_{L_{(L/D)\max}} = \sqrt{\frac{C_{D_o}}{K}} \tag{6.56}$$

In the application of Equations 6.55 and 6.56, two aircraft operational limits should be considered. There is an important flight safety point about maximum lift-to-drag ratio speed (Equation 6.55), which is related to stall speed. Please note that sometimes the maximum lift-to-drag ratio speed that is obtained through Equation 6.55 is less than aircraft stall speed; hence, it is unacceptable. For a prop-driven aircraft in which the maximum lift-to-drag ratio speed is theoretically less than the stall speed, a safe maximum lift-to-drag ratio speed is selected to be approximately 10%–20% higher than the stall speed:

$$V_{(L/D)_{\max}} = k \cdot V_s \tag{6.57}$$

where

$$1.1 < k < 1.2 \tag{6.58}$$

Equation 6.56 is a mathematical expression; the theoretical value $C_{L_{(L/D)\max}}$ of must be within a practical flight limit. The value of $C_{L_{(L/D)\max}}$ calculated using Equation 6.56

cannot be more than the aircraft maximum lift coefficient $C_{L_{max}}$. If the result of this equation is more than $C_{L_{max}}$, ignore it and select a new value that is slightly less than $C_{L_{max}}$.

Comparing Equation 6.20 with Equations 6.47 and 6.55, we obtain

$$V_{\min_P} = 0.76V_{\min_D} \tag{6.59}$$

$$V_{\min_P} = 0.76V_{(L/D)_{max}} \tag{6.60}$$

All three velocities corresponding to the minimum power speed, the minimum drag speed, and the speed corresponding to the maximum lift-to-drag ratio increase in direct proportion with altitude. A comparison between the minimum power speed and the minimum drag speed is depicted in Figure 6.4. It is evident that the minimum power speed is always less than the minimum drag speed.

Example 6.3

The drag polar of a prop-driven aircraft with a mass of 4,500 kg and wing area of 30 m^2 is given as:

$$C_D = 0.025 + 0.06C_L^2$$

The aircraft has a turboprop engine and the maximum lift coefficient is 1.8. Determine (1) the stall speed (V_s), (2) the minimum power speed ($V_{\min_P}$), and (3) the minimum drag speed ($V_{\min_D}$); for seal level ISA condition.

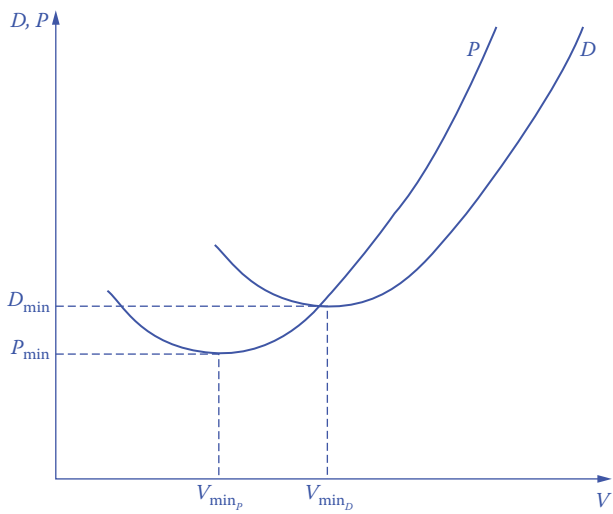

FIGURE 6.4 A comparison between the minimum power speed and the minimum drag speed.

Solution

According to the drag polar, we have $C_{D_o} = 0.025$, $K = 0.06$.

The stall speed is defined as

$$V_s = \sqrt{\frac{2mg}{\rho S C_{L_{\max}}}} = \sqrt{\frac{2\times 4{,}500\times 9.81}{1.225\times 30\times 1.8}} = 36.5\,\text{m/s} = 71\,\text{knot} \tag{2.27}$$

The minimum power speed is given as

$$V_{\min_P} = \sqrt{\frac{2mg}{\rho S\sqrt{3C_{D_o}/K}}} = \sqrt{\frac{2\times 4{,}500\times 9.81}{1.225\times 30\times\sqrt{3\times 0.025/0.06}}} \tag{6.20}$$

$$= 46.35\,\text{m/s} = 90.1\,\text{knot}$$

The minimum drag speed is obtained as

$$V_{\min_D} = \sqrt{\frac{2mg}{\rho S\sqrt{C_{D_o}/K}}} = \sqrt{\frac{2\times 4{,}500\times 9.81}{1.225\times 30\times\sqrt{0.025/0.06}}} \tag{6.47}$$

$$= 61\,\text{m/s} = 118.6\ \text{knot}$$

In this aircraft, both the minimum power speed and the minimum drag speed are greater than the stall speed; so, these are acceptable values.

6.3.4 Maximum Speed

The maximum speed ($V_{\max}$) is another significant performance parameter for prop-driven aircraft. Maximum speed is a function of several variables, including engine power, geometry parameters, and aircraft weight. To achieve the maximum speed, maximum engine power must be utilized. More details about the theoretical background have been provided in Section 5.3.1. When the maximum engine power is applied, the aircraft will eventually reach an equilibrium state at an airspeed that is referred to as the maximum velocity. To obtain an expression for the maximum speed, Equation 6.12 is inserted into Equation 6.14. Since the maximum power is applied, the velocity is replaced with $V_{\max}$.

$$P_{\max}\eta_P = \frac{1}{2}\rho V_{\max}^3 S C_{D_o} + \frac{2K(mg)^2}{\rho V_{\max} S} \tag{6.61}$$

where $P_{\max}$ is the engine shaft power at altitude and ρ is the air density at altitude.

The variations of turboprop and piston-prop engine powers as functions of air density are, respectively, given by Equations 4.27 and 4.19. By substituting these two equations into Equation 6.61, we will have the following for the first layer of the atmosphere (troposphere):

$$P_{\max_{SL}}\eta_P\left(\frac{\rho}{\rho_o}\right)^{0.9} = \frac{1}{2}\rho V_{\max}^3 S C_{D_o} + \frac{2K(mg)^2}{\rho V_{\max} S} \quad (\text{turbo prop}) \tag{6.62}$$

$$P_{\max_{SL}}\eta_P\left(\frac{\rho}{\rho_o}\right)^{1.2}=\frac{1}{2}\rho V_{\max}^3 SC_{D_o}+\frac{2K(mg)^2}{\rho V_{\max}S}\quad(\text{piston prop}) \tag{6.63}$$

where $P_{\max_{SL}}$ is the maximum engine power at sea level. Equations 6.62 and 6.63 are nonlinear functions of the aircraft maximum velocity as the only unknown. Equation 6.62 yields the aircraft maximum speed as a function of the maximum engine power, altitude (air density), wing area, aircraft weight, prop efficiency, and zero-lift drag coefficient for turboprop aircraft. Equation 6.63 can also be solved for aircraft maximum speed for piston-prop aircraft.

Thus, the only unknown in Equations 6.62 and 6.63 is the aircraft maximum speed ($V_{\max}$). The interested reader may derive similar expressions for the second layer of the atmosphere (stratosphere). Each of these equations (Equations 6.62 and 6.63) has theoretically more than one solution. However, in practice, there is only one real answer. Hence, the unacceptable solutions (e.g., negative values and complex numbers) should be ignored.

Since the engine power is a function of altitude, the aircraft maximum speed also varies with altitude. As Figure 5.9 shows, the aircraft maximum speed initially increases with altitude (i.e., decreasing air density), but will decrease afterward. Hence, the maximum speed has an absolute maximum speed at one altitude. This is called the maximum of maximum speeds ($V_{\max}$). For instance, the maximum speed of a Lockheed P-38 Lightning at sea level was flight tested to be 344 mph, while at 20,000 ft, it was 401 mph. Moreover, the maximum speed of a tiltrotor VTOL aircraft Bell Boeing V-22 Osprey at sea level is 275 knots, while at 15,000 ft, it is 305 knots.

The typical maximum speed for a piston-prop aircraft is about Mach 0.3, and for a turboprop aircraft, it is about Mach 0.6. In general, the maximum speed of an aircraft with prop-driven engine is less than that for an aircraft with jet engine.

Table 6.1 shows the maximum speed [9] of several prop-driven aircraft. Because of the presence of propeller, the maximum speed of prop-driven aircraft cannot exceed the speed of sound (i.e., Mach 1). The reason behind this point is not due to the amount of engine power, but due to the propeller tip speed; since the propeller is a weak component [43] to handle the shock waves.

Tupolev Tu-95, one of the fastest prop-driven aircraft, is depicted in Figure 6.5. The aircraft with four turboprop engines has a maximum speed of 499 knots. The retired aircraft Tupolev Tu-114 has held the record as the world's fastest propeller-driven aircraft for the past 51 years. The aircraft with four turboprop engines (each generating 11,000 kW of power) has a maximum speed of 510 knots. All of its records are still valid today. In the world of rotary wing aircraft, in 2013, the Eurocopter X3 helicopter [75] set a speed record of 255 knots during a level flight. This eclipsed the record previously held by the Sikorsky X2.

If the prop tip speed, at any time, reaches the speed of sound, shock waves and prop vibration are generated, and thus the aircraft performance (including the maximum speed) will be degraded. Recall the relationship between linear speed (prop tip speed; V_{tip}) and the rotational speed (revolution per minute; ω[rpm]); that is, $V_{tip}=R\cdot\omega$. The prop tip speed is equal to shaft rotational speed multiplied by prop radius (R). This relationship dictates that as the prop diameter increases, the rotational speed of

TABLE 6.1
Maximum Speed and Cruising Speed of Several Prop-Driven Aircraft

No.	Aircraft	m_{TO} (kg)	Engine Type	P(hp)	Type	V_{max}		V_C (knot)
						knot	Mach	
1.	Dornier DO-128-6	4,350	Turboprop	2 × 400	Transport	183	–	167
2.	Pegasus Quantum	409	Piston-prop	33	Ultralight trike	78	–	52
3.	Pilatus PC-12 Turbo Trainer	4,740	Turboprop	1,200	Trainer	–	–	285
4.	Canadair CL-215T	19,730	Piston-prop	2 × 2,100	Amphibian	–	–	157
5.	Eurocopter SA 365 Dauphin	1,050	Piston-prop	112	Trainer	130	–	116
6.	Embraer/FMA CBA-123	7,800	Turboprop	2 × 1,300	Transport	–	–	360
7.	Harbin Y-12	5,300	Turboprop	2 × 500	Transport	177	–	158
8.	Shaanxi Y-8	61,000	Turboprop	4 × 1,100	Transport	357	–	297
9.	Socata TB 30 Epsilon	1,250	Piston-prop	300	Trainer	205	–	193
10.	Atlantique 2	45,000	Turboprop	2 × 6,100	Patrol	350	–	170
11.	Socata TBM 7006	2,672	Turboprop	700	Business	–	–	300
12.	Piaggio P180 Avanti	4,767	Turboprop	2 × 800	Transport	400	0.67	320
13.	Tupolev Tu-95	188,000	Turboprop	4 × 15,000	Bomber	499	–	380
14.	Lockheed C-130 Hercules	79,380	Turboprop	4 × 4,508	Transport	334	–	320
15.	Beechcraft T-34 Mentor	1,950	Turboprop	400	Trainer	223	–	215
16.	General Atomics MQ-9 Reaper	4,760	Turboprop	900	Hunter UAV	240	–	169
17.	Fairchild C-119 Flying Boxcar	33,778	Piston-prop	2 × 2,500	Transport	257	–	174
18.	Hu-168 Albatross	17,010	Piston-prop	2 × 1,425	Reconnaissance	225	–	195
19.	Saab 340	13,154	Turboprop	2 × 1,870	Regional airliner	–	–	283
20.	Aeritalia G-222	26,500	Turboprop	2 × 3,400	Transport	292	–	238
21.	Silver Eagle	251	Piston-prop	23	Ultralight	55	–	50

FIGURE 6.5 Tupolev Tu-95- fastest prop-driven aircraft. (Courtesy of Alex Snow.)

the shaft must be decreased. For this reason, most turboprop engines have a gearbox to reduce the shaft rotational speed.

Case Study - Example 6.4

The single-engine trainer aircraft Pilatus PC-9 is equipped [76] with a turboprop engine and has the following characteristics:

$$m_{\text{TO}} = 3{,}200\,\text{kg}, S = 16.29\,\text{m}^2, P_{\max_{\text{SL}}} = 857\,\text{kW}, C_{D_o} = 0.02, K = 0.06, \eta_P = 0.8.$$

Determine the aircraft maximum speed at sea level and 5,000 m.

Solution

- At sea level ($\rho = 1.225\,\text{kg/m}^3$, $\sigma = 1$)

$$P_{\max_{\text{SL}}}\eta_P\left(\frac{\rho}{\rho_o}\right)^{0.9} = \frac{1}{2}\rho V_{\max}^3 S C_{D_o} + \frac{2K(mg)^2}{\rho V_{\max} S}$$

$$\Rightarrow 57\times 1{,}000\times 0.8\times 1^{0.9} = 0.5\times 1.225\times 16.29\times V_{\max}^3\times 0.02 + \frac{2\times 0.06\times(3{,}200\times 9.81)^2}{1.225\times 16.29\times V_{\max}}$$

$$\Rightarrow 685{,}600 = 0.199V_{\max}^3 + \frac{5{,}921{,}958}{V_{\max}} \tag{6.62}$$

The only acceptable solution for this nonlinear algebraic equation is 147.9; thus,

$$V_{\max} = 147.9\,\text{m/s} = 287.5\ \text{knot} \Rightarrow M_{\max} = 0.435.$$

- At 5,000 m ($\rho = 0.736\,\text{kg/m}^3$)

$$P_{\max_{\text{SL}}}\eta_P\left(\frac{\rho}{\rho_o}\right)^{0.9} = \frac{1}{2}\rho V_{\max}^3 S C_{D_o} + \frac{2K(mg)^2}{\rho V_{\max} S}$$

$$\Rightarrow 857\times 1{,}000\times 0.9\times\left(\frac{0.736}{1.225}\right)^{0.9} = 0.5\times 0.736\times V_{\max}^3\times 16.29\times 0.02 + \frac{2\times 0.06\times(3{,}200\times 9.81)^2}{0.736\times 16.29\times V_{\max}}$$

$$\Rightarrow 433{,}449 = 0.1199V_{\max}^3 + \frac{9{,}856{,}521}{V_{\max}} \tag{6.62}$$

The only acceptable solution for this algebraic equation is 145. Thus,

$$V_{\max} = 145\,\text{m/s} = 281.8\ \text{knot}.$$

The maximum speed at 5,000 m is slightly less than that for sea level. The published value [9] for the maximum speed is 320 knot, which is about 12.2% different.

6.4 RANGE

6.4.1 Introduction

Range is an important factor in prop-driven aircraft performance, particularly in transport aircraft. As defined in Section 5.4.1, range is the total distance traveled by an aircraft on one load of fuel in fuel tanks. Various types of ranges were already presented in Section 5.4; so, they are not discussed again in this chapter. In this section, the technique to calculate the range for a prop-driven aircraft is given.

Typically, the range of a GA piston-prop aircraft lies between 200 and 5,000 km, and the range of turboprop aircraft lies between 1,000 and 10,000 km. The longest range has grown in the past decades, but the current record is held by Voyager aircraft (Figure 6.6) which achieved a range equal to the circumference of the Earth. In 1985, Voyager took off eastward with two pilots and, after more than eight consecutive days (non-stop flight without refueling) of traveling around the globe, landed safely. Two pilots directed the aircraft taking turns during the days and nights. This historic flight turned a new page with an unconventional aircraft. The Voyager is now on permanent display in the main gallery of the Smithsonian Institution's National Air and Space Museum in Washington, DC, alongside Wright Flyer and Charles Lindbergh's Spirit of St. Louis.

In Section 5.4.1, a few types of range, including safe range, still air range, and gross still air range, are defined for a jet aircraft. The interested reader can refer to that section for more information. These definitions are valid for a prop-driven aircraft as well. As the major difference between jet and prop-driven aircraft is the engine type, the primary difference for range analysis appears in the range equations. In this section, techniques to calculate the range for three distinct flight programs are introduced. Table 6.2 illustrates the maximum range [9] for several prop-driven aircraft.

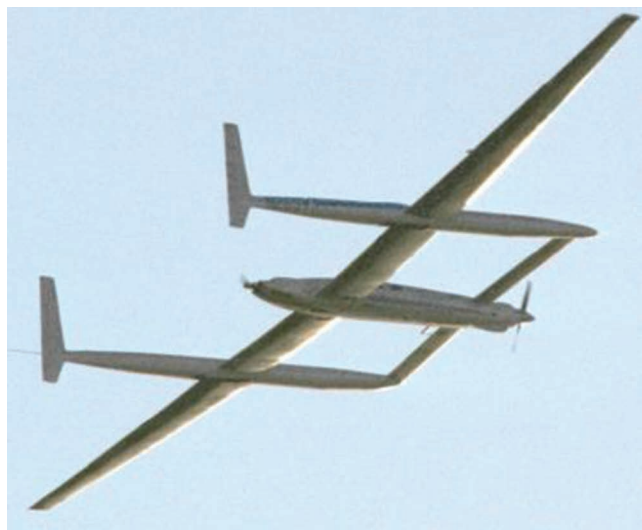

FIGURE 6.6 Rutan Model 76 Voyager. (Courtesy of NASA, Washington, DC.)

TABLE 6.2
Range for Several Prop-Driven Aircraft

No.	Aircraft	Country	m_{TO} (kg)	Engine	Power (hp)	Type	Fuel Volume (L)	Range (km)
1.	BN-2B	England	2,993	Piston	300	Transport	518	1,400
2.	Shorts 330	England	10,387	Turboprop	2 × 1,198	Transport	2,546	1,695
3.	Voyager	United States	4,397	Piston	100 + 130	Record breaker	5,076	40,212
4.	Cessna 172	United States	1,111	Piston	160	Four-seat, single engine	212	1,289
5.	Beech Starship	United States	6,350	Turboprop	2 × 120	Business	1,923	4,032
6.	Thrush S2R-600	United States	2,721	Piston	600	Agriculture	401	648
7.	Mooney 201 LM	United States	1,243	Piston	200	GA	242	1,804
8.	Partenavia AP68TP-600	Italy	2,850	Turboprop	2 × 328	Transport	840	824
9.	Socata TB20B	France–Germany	1,400	Piston	250	GA	326	1,907
10.	Robin R3000	France	1,050	Piston	140	GA	200	1,185
11.	DHC-8 Dash 8-100	Canada	14,968	Turboprop	2 × 1,800	Transport	3,160	1,650
12.	Embraer EMB-110P2A	Brazil	5,670	Turboprop	2 × 750	Transport	1,720	2,001
13.	FAMAIA 58A	Argentina	6,800	Turboprop	2 × 978	Reconnaissance	1,280	3,710
14.	Embraer Tucano	Brazil	2,550	Turboprop	750	Trainer	694	1,844
15.	General Atomics MQ-9 Reaper	USA	4,760	Turboprop	900	Hunter UAV	2,200	1,900
16.	Shin Meiwa SS-2A	Japan	43,000	Turboprop	4 × 3,490	Search and rescue	22,500	3,817
17.	PZL M-24 Dromader	Poland	5,000	Piston	1,000	Agriculture	2,700	1,800
18.	NAC1 Freelance	England	1,225	Piston	180	Utility	280	1,955
19.	Beechcraft super king air 300	United States	6,350	Turboprop	2 × 1,050	Transport	1,438	3,632
20.	Lockheed Hercules C-130J	United States	74,389	Turboprop	4 × 4,591	Medium transport	25,552	5,244

In general, the range of aircraft with turboprop engines is longer than the range of aircraft with piston-prop engines. For instance, the maximum range of the piston-prop aircraft Bonanza is 1,692 km, but the maximum range of the turboprop aircraft Beech Starship [77] is 4,032 km. The record for maximum range for turboprop aircraft is 14,052 km, which is held by Hercules HC-130 [78]. The record for the maximum range of helicopters is 3,561 km, which is held by YOH-6A. Finally, the record

for the maximum range of ultralight aircraft is 1,249 km, which belongs to Quicky. It is interesting to note that the record for maximum range for gliders is 14,608 km and belongs to Schleicher ASW12.

6.4.2 Regular Range Calculation

As defined in Section 5.4.1, the specific range (SR) is the distance traveled by consumption of a unit weight of fuel:

$$\mathrm{SR} = \frac{dX}{dW} \tag{6.64}$$

where the rate of change of aircraft weight is negative, since the fuel weight is decreased. On the other hand, the fuel flow rate (Q) for a prop-driven engine is defined as the SFC (C) multiplied by the engine power:

$$Q = -\frac{dW}{dt} = C \cdot P \tag{6.65}$$

The aircraft speed is defined as the distance traveled in a unit time:

$$V = \frac{dX}{dt} \tag{6.66}$$

When Equations 6.65 and 6.66 are inserted in Equation 6.64, the following is obtained:

$$\frac{dX}{dW} = -\frac{V \cdot dt}{Q \cdot dt} = -\frac{V \cdot dt}{C \cdot P \cdot dt} = -\frac{V}{C \cdot P} \tag{6.67}$$

By using the relationship between engine power and engine thrust (Equation 6.7) and due to the fact, that in a steady-level flight, lift is equal to weight (Equation 6.6) and thrust is equal to drag (Equation 6.5), we can derive the following:

$$\frac{dX}{dW} = -\frac{V}{C \cdot P} = -\frac{\eta_P}{C \cdot T} = -\frac{\eta_P}{C \cdot D} = -\frac{\eta_P L}{C \cdot D \cdot L} = -\frac{\eta_P (L/D)}{C \cdot W} \tag{6.68}$$

Therefore, the distance (X) traveled is

$$dX = -\frac{\eta_P (L/D)}{C \cdot W} dW \tag{6.69}$$

The total distance traveled, that is, range, is obtained by integrating Equation 6.69 between the initial weight, where the fuel tanks are full ($W = W_1$), and the final weight, where the fuel tanks are empty ($W = W_2$). It is assumed that the aircraft flight includes only a steady-level portion. In other words, variables, such as the takeoff, climb, and descent, are not considered at this moment:

$$R = \int_0^R dX = -\int_{W_1}^{W_2} \frac{\eta_P (L/D)}{C} \frac{dW}{W} \tag{6.70}$$

Equation 6.70 is a general equation for range for a prop-driven aircraft. It is interesting to note from Equation 6.70, that range is apparently independent of aircraft speed. However, the SFC (C), prop efficiency (η_P), and lift-to-drag ratio (L/D) are all functions of aircraft speed. Thus, the range is indirectly a strong function of aircraft velocity. Recall that these parameters are not independent of one another. Moreover, Equation 6.70 indicates that in order to increase range, one must decrease aircraft weight and SFC, and increase prop efficiency and lift-to-drag ratio. For simplicity, we assume that SFC and prop efficiency are constant throughout the flight. In addition, the ratio L/D is equal to C_L/C_D in a steady-level flight. Hence,

$$R = -\frac{\eta_P}{C} \int_{W_1}^{W_2} \frac{C_L}{C_D} \frac{dW}{W} \tag{6.71}$$

To mathematically solve the integration of Equation 6.71, we need to specify the flight condition. As discussed in Section 5.4.2, the following three options may be considered to continuously decrease the lift during cruise (see Figure 5.14):

1. Decreasing flight speed (constant-altitude, constant-lift-coefficient flight)
2. Increasing altitude (constant-airspeed, constant-lift-coefficient flight)
3. Decreasing angle of attack (constant-altitude, constant-airspeed flight)

Since the only variable besides aircraft weight in the integration of Equation 6.71 is the lift coefficient (C_L), these three programs may be classified into two groups: (1) constant-lift-coefficient cruising flight (Programs 1 and 2) and (2) reduced lift coefficient cruising flight (program 3). The mathematical calculations of the range for these two groups are different; so they are presented separately.

6.4.2.1 Constant-Lift-Coefficient Cruising Flight

In a cruising flight when the lift coefficient is kept constant, there are two options: (1) reduce the airspeed and (2) increase the cruising altitude. For both of these programs, the mathematical solution is developed in the same way.

If we consider the first flight condition (1), where the aircraft angle of attack (i.e., lift coefficient) is held constant, the drag coefficient (C_D) will be constant as well. Then, the ratio C_L/C_D can be taken out of the integration. Hence, the solution of the integration (Equation 6.71) will be as

$$R = -\frac{\eta_P}{C} \frac{C_L}{C_D} \left[\ln W_2 - \ln W_1 \right] = -\frac{\eta_P}{C} \frac{L}{D} \ln\left(\frac{W_2}{W_1}\right) = \frac{\eta_P}{C} \frac{L}{D} \ln\left(\frac{W_1}{W_2}\right) \tag{6.72}$$

Since the weight of the aircraft at the end of flight is equal to the initial weight minus the fuel weight,

$$W_2 = W_1 - W_f \tag{6.73}$$

Therefore, Equation 6.72 can be reformatted in terms of fuel weight as

$$R_{1,2} = \frac{\eta_P (L/D)}{C} \ln\left(\frac{1}{1-(W_f/W_1)}\right) = \frac{\eta_P (L/D)}{C} \ln\left(\frac{1}{1-G}\right) \tag{6.74}$$

This is referred to as the *Breguet* range equation for a prop aircraft (similar to Equation 5.78 that is derived for a jet aircraft). The subscript "1, 2" indicates that this range equation is for flight Programs 1 and 2. Equation 6.74 is similar to the range equation for jet aircraft. The only difference is that airspeed has not directly appeared in the equation. The parameter G is the fuel-weight ratio, that is, the ratio between fuel weight (W_f) and aircraft weight at the beginning of the flight (W_1):

$$G = \frac{W_f}{W_1} \tag{6.75}$$

In Equation 6.74, all parameters except C are without units. Since the unit of range is in terms of distance (such as m, km, ft, and nm), the unit of C must be converted into the reciprocal of distance (such as 1/m, 1/km, 1/ft, and 1/nm). Recall that the unit of C is initially "lb/(h·hp)" or "N/(h·kW)" or "kg/J", or "μg/J".

In practice, to keep the lift coefficient constant as the weight of the aircraft decreases, Equation 6.6 reveals that the pilot has two options: (1) the air density (ρ) must be decreased and (2) the airspeed (V) must be decreased. In the first option, the air density (ρ) must decrease in a manner so as to keep the ratio of the lift to weight constant (i.e., 1). The only way that this can be done is to increase the altitude in an appropriate manner. Consequently, the aircraft will be in a continuous climb (i.e., *cruise-climb*), which appears to violate the level-flight condition of a zero flight path angle. It has been demonstrated in Section 5.4.2 that the cruise-climb flight path angle is sufficiently small so as to justify the use of the level-flight equations and solutions for cruise-climb. In the second option, the thrust should be decreased along the flight path by reducing the throttle. More details of cruise-climb and throttle reduction process are provided in Chapter 5.

Equation 6.74 illustrates that the range for a prop-driven aircraft is a function of prop efficiency, fuel-weight fraction, and lift-to-drag ratio, as well as an inverse function of the SFC. To increase the range, one must increase prop efficiency, fuel-weight fraction, and lift-to-drag ratio, and decrease the SFC. In the first flight program, when the initial velocity (V_1) is given, the final speed (V_2) is calculated using Equation 5.72 as derived in Chapter 5. In the second flight program, when the initial altitude (ρ_1) is given, the final altitude (ρ_2) is calculated using Equation 5.81 as derived in Chapter 5.

6.4.2.2 Non-Constant-Lift-Coefficient Cruising Flight

In a cruising flight when the lift coefficient is decreased along the flight path, both the airspeed and the cruising altitude are kept constant. The pilot will gradually push the stick/wheel to reduce the angle of attack. This will cause the lift coefficient to be

decreased to keep the lift equal to aircraft weight. To solve the integration (Equation 6.71) in this flight condition, we initially eliminate weight from the denominator and lift from the numerator:

$$R_3 = -\frac{\eta_P}{C}\int_{W_1}^{W_2}\frac{dW}{D} \tag{6.76}$$

The variations of drag with respect to aircraft weight are nonlinear. As derived in Chapter 5 (Equation 5.35), the drag is a function of aircraft weight:

$$D = \frac{1}{2}\rho V^2 S C_{D_o} + \frac{2KW^2}{\rho V^2 S} \tag{6.77}$$

Plugging Equation 6.77 into Equation 6.76 yields

$$R_3 = -\frac{\eta_P}{C}\int_{W_1}^{W_2}\frac{dW}{(1/2)\rho V^2 S C_{D_o} + \left(2KW^2/\rho V^2 S\right)} \tag{6.78}$$

or

$$R_3 = -\frac{\eta_P}{C\left(2K/\rho V^2 S\right)}\int_{W_1}^{W_2}\frac{dW}{\left(\rho V^2 S\right)^2 C_{D_o}/4K + W^2} \tag{6.79}$$

Using a mathematical reference [69], the solution of the integration with a similar form is determined:

$$\int \frac{dx}{a^2 + x^2} = \frac{1}{a}\tan^{-1}\left(\frac{x}{a}\right) \tag{6.80}$$

where

$$a = \frac{1}{2}\rho V^2 S\left(\frac{C_{D_o}}{K}\right)^{1/2} \tag{6.81}$$

Therefore, the solution for the integration is

$$R_3 = \frac{\eta_P}{C\left(2K/\rho V^2 S\right)}\frac{1}{(1/2)\rho V^2 S\left(C_{D_o}/K\right)^{1/2}}\left[\tan^{-1}\left(\frac{W}{(1/2)\rho V^2 S\left(C_{D_o}/K\right)^{1/2}}\right)\right]_{W_1}^{W_2} \tag{6.82}$$

Since the maximum lift-to-drag ratio is related to $\sqrt{KC_{D_o}}$, as in Equation 6.9 $\left(\sqrt{KC_{D_o}} = \frac{1}{2(C_L/C_D)_{\max}}\right)$, the equation will be reduced to

$$R_3 = \frac{2\eta_P (L/D)_{\max}}{C}\left[\tan^{-1}\left(\frac{2W_1}{\rho V^2 S\sqrt{C_{D_o}/K}}\right) - \tan^{-1}\left(\frac{2W_2}{\rho V^2 S\sqrt{C_{D_o}/K}}\right)\right] \tag{6.83}$$

As derived in Equation 6.10, the term $\sqrt{C_{D_o}/K}$ is equal to the minimum drag lift coefficient, $C_{L_{\min D}}$:

$$R_3 = \frac{2\eta_P (L/D)_{\max}}{C}\left[\tan^{-1}\left(\frac{2W_1}{\rho V^2 S C_{L_{\min D}}}\right) - \tan^{-1}\left(\frac{2W_2}{\rho V^2 S C_{L_{\min D}}}\right)\right] \tag{6.84}$$

The bracketed term represents the difference between two angles (in radian). Equation 6.83 is valid for any given constant altitude and any given constant velocity, as long as the altitude and the velocity are permissible (i.e., within the flight envelope of the aircraft). In this flight program, the initial lift coefficient is

$$C_{L_1} = \frac{2W_1}{\rho V^2 S} \tag{6.85}$$

The final lift coefficient is readily obtained as

$$C_{L_2} = \frac{2W_2}{\rho V^2 S} \tag{6.86}$$

where W_2 is the final weight at the end of cruise. Inserting the relationship between initial weight, final weight, and fuel weight ($W_2 = W_1(1-G)$) into Equation 6.84, we obtain

$$R_3 = \frac{2\eta_P (L/D)_{\max}}{C}\left[\tan^{-1}\left(\frac{2W_1}{\rho V^2 S C_{L_{\min D}}}\right) - \tan^{-1}\left(\frac{2W_1(1-G)}{\rho V^2 S C_{L_{\min D}}}\right)\right] \tag{6.87}$$

From the theoretical point of view, all three flight programs are realizable, but in practice, only the third case is acceptable and approved for GA aircraft by the FAA. This case is hard to follow because the pilot must constantly decrease the angle of attack, through the deflection of the elevator. However, for an aircraft equipped with an autopilot, this is an easy task. This case is the safest flight program among the three possible programs. Furthermore, we have two range equations for prop aircraft compared with three range equations for jet aircraft (refer to Section 5.4).

Example 6.5

A GA aircraft with a mass of 2,000 kg has a piston-prop engine with a maximum power of 373 kW. Other characteristics of this aircraft are as follows:

$$S = 20\,\text{m}^2, C_{D_o} = 0.023, K = 0.04, m_f = 300\,\text{kg}, C = 0.5\,\text{lb/h/hp}\,(84.5\,\mu\text{g/J}),$$
$$\eta_P = 0.8, C_{L_{\max}} = 1.8.$$

a. Determine the range of this aircraft, if it begins to cruise with a speed of 150 knots at an altitude of 7,000 m. In this flight program, the lift coefficient is kept constant, but altitude is gradually increased.
b. Determine the range of this aircraft if it cruises at a constant speed of 150 knots and at a constant altitude of 7,000 m. In this flight program, the lift coefficient is gradually decreased.

Solution

a. Range, if aircraft begins to cruise with a speed of 150 knots at an altitude of 7,000 m and a constant lift coefficient (cruise-climb):

At the altitude of 7,000 m, the air density is 0.59 kg/m^3. The lift coefficient for this flight is

$$C_L = \frac{2mg}{\rho SV^2} = \frac{2\times 2{,}000\times 9.81}{0.59\times 20\times(150\times 0.514)^2} = 0.56 \tag{6.85}$$

The drag coefficient is

$$C_D = C_{D_o} + KC_L^2 = 0.023 + 0.04\times 0.56^2 = 0.035 \tag{3.12}$$

The lift-to-drag ratio is

$$\left(\frac{L}{D}\right) = \frac{C_L}{C_D} = \frac{0.56}{0.035} = 15.74 \tag{5.13}$$

We need to convert the unit of SFC to 1/km. One horsepower is equivalent to 550 lb·ft/s, one knot is 6,076 ft/hr, one nm is 1.852 km, and one hour is 3,600 s.

$$C = 0.5\,\text{lb/h/hp} = 0.5\,\text{lb/}(\text{h}\cdot\text{hp}) = 0.5\times\frac{6{,}076}{3{,}600\times 550\times 1.852} = 0.000828\,\text{km}^{-1}$$

The ratio between fuel weight and aircraft weight is

$$G = \frac{m_f}{m_{\text{TO}}} = \frac{300}{2{,}000} = 0.15 \tag{6.75}$$

Thus, the range is

$$R = \frac{\eta_P\left(\frac{L}{D}\right)}{C}\ln\left(\frac{1}{1-G}\right) = \frac{0.8\times 15.74}{0.000828}\ln\left(\frac{1}{1-0.15}\right) = 2{,}470.2\,\text{km} \tag{6.74}$$

If we assume that SFC is constant, the distance of 2,470.2 km is the range for this flight condition. Although in practice, SFC is a function of altitude, and thus, the range would be slightly different.

b. Range with a constant speed of 150 knots at constant altitude of 7,000 m

$$\left(\frac{L}{D}\right)_{\max} = \frac{1}{2\sqrt{KC_{D_o}}} = \frac{1}{2\sqrt{0.04\times 0.025}} = 15.8 \tag{6.9}$$

$$R_3 = \frac{2\eta_P (L/D)_{\max}}{C}\left[\tan^{-1}\left(\frac{2W_1}{\rho V^2 S\sqrt{C_{D_o}/K}}\right) - \tan^{-1}\left(\frac{2W_2}{\rho V^2 S\sqrt{C_{D_o}/K}}\right)\right] \quad (6.83)$$

$$R_3 = \frac{2\times 0.8\times 15.74}{0.000828}\left[\begin{array}{l}\tan^{-1}\left(\dfrac{2\times 2{,}000\times 9.81}{0.59\times(150\times 0.541)^2\times\sqrt{0.023/0.04}}\right)\\ -\tan^{-1}\left(\dfrac{2\times(2{,}000-300)\times 9.81}{0.59\times(150\times 0.541)^2\times\sqrt{0.023/0.04}}\right)\end{array}\right]$$

$$= 1{,}575\,\text{km}$$

c. Comparison of both ranges

$$\%\,\text{Dif} = \frac{2{,}470.2 - 1{,}575}{2{,}470.2} = 36.2$$

It is noticed that the range for the cruise-climb is about 36.2% longer than the range for a constant-altitude flight.

6.4.3 Maximum Range Calculation

Equations 6.74 and 6.83 illustrate that the range for a prop-driven aircraft is a function of prop efficiency, fuel-weight fraction, and lift-to-drag ratio, as well as an inverse function of the SFC. We assume for a given aircraft that prop efficiency, fuel-weight fraction, and the SFC are constant. Now, the question is that, on what flight condition (i.e., altitude, velocity, and lift coefficient) the maximum range is obtained. As presented in the previous section, there are two techniques to determine the range: (1) constant-lift-coefficient cruising flight (Programs 1 and 2), and (2) non-constant-lift-coefficient cruising flight (program 3). These two cases are investigated separately.

6.4.3.1 Constant-Lift-Coefficient Cruising Flight

For two flight programs with a constant lift coefficient, that is, (1) decreasing the flight speed (constant-altitude, constant-lift-coefficient flight) and (2) increasing the altitude (constant-airspeed, constant-lift-coefficient flight), we derived Equation 6.74. To maximize range ($R_{\max}$), we can employ two techniques. The first one is to set the differential equation of 6.58 equal to zero and solve for parameters such as velocity and altitude. The second technique is to differentiate Equation 6.74 with respect to velocity and set to zero.

Using this technique, one can conclude that, if SFC and prop efficiency are assumed to be constant, the maximum range is achieved when the aircraft is cruising with a speed corresponding to the maximum lift-to-drag ratio. Figure 6.7 demonstrates the variations of range with respect to velocity for the aircraft introduced in Example 6.5. As noticed, there is one velocity that delivers the maximum range speed. This velocity will be derived in the next section.

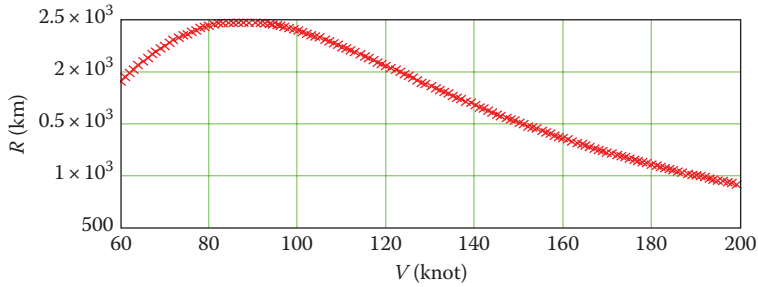

FIGURE 6.7 Variations of range with respect to velocity.

Hence, for the first case (where lift coefficient $[C_L]$ is held constant) the equation for the maximum range for Programs 1 and 2 will be obtained as follows:

$$R_{\max_{1,2}} = \frac{\eta_P (L/D)_{\max}}{C} \ln\left(\frac{1}{1-G}\right) \tag{6.88}$$

This equation is not directly a function of altitude. However, the velocity corresponding to the maximum lift-to-drag ratio is a function of altitude. Thus, to maximize the range, the pilot may fly at any altitude, but should fly with the corresponding velocity. In the first flight program, when the initial velocity (V_1) is given, the final speed (V_2) is calculated using Equation 5.72 as derived in Chapter 5.

In Equation 6.88, all parameters except C are without unit. Since the unit of range is in terms of distance (such as m, km, ft, and nm), the unit of C must be converted into the reciprocal of distance (such as 1/m, 1/km, 1/ft, and 1/nm). Recall that the unit of C is initially "lb/(h·hp)" or "N/(h·W)".

In the second flight program, when the initial altitude (ρ_1) is given, the final altitude (ρ_2) is calculated using Equation 5.83. Thus, the density ratio at the end of the cruise-climb flight (σ_2) can be expressed in terms of both the initial density ratio ($\sigma = \rho/\rho_o$) and the fuel fraction; that is,

$$\sigma_2 = \sigma_1 (1-G) \tag{5.83}$$

where σ_1 is the air density ratio at the beginning of the cruise.

6.4.3.2 Non-Constant-Lift-Coefficient Cruising Flight

For the third flight programs where the angle of attack is decreased throughout the flight (constant-altitude, constant-airspeed flight), we derived Equation 6.83 for the regular range. For a given aircraft, this equation is only a function of altitude and velocity; both are inside the bracketed term that represents the difference between two angles. To maximize the range for this flight operation, one must maximize the difference between the two angles.

Figure 6.8 demonstrates the variations of range as a function of velocity and three altitudes (sea level, 5,000 m, and 11,000 m) for the aircraft introduced in Example 6.5 when flying according to the third flight program. This trend represents the typical

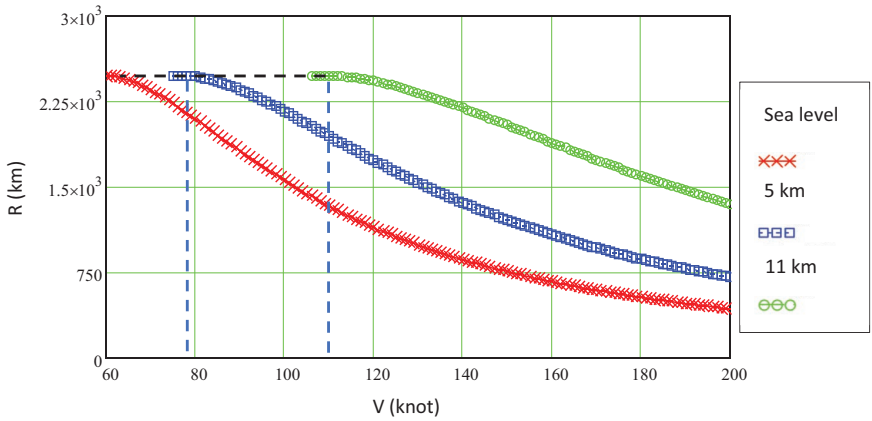

FIGURE 6.8 Variations of range as a function of velocity and altitude.

variations [66] for every prop-driven aircraft. The starting point of every graph is the lowest permissible speed, which is the stall speed at that specific altitude. The stall speeds at altitudes of sea level, 5,000 m, and 11,000 m are 58, 74.7, and 106.2 knots, respectively. All three flights have the same maximum range of 2,478 km.

It is interesting to see that the altitude (air density, ρ) does not affect the maximum range. However, for each flight, the maximum range occurs at a specific velocity, which is the lowest permissible speed. Hence, the maximum range will be achieved at every altitude, but when flying at the lowest permissible speed ($V_{\min}$). Therefore, the expression for the maximum range for the third flight program will be as follows:

$$R_{\max_3} = \frac{2\eta_P (L/D)_{\max}}{C}\left[\tan^{-1}\left(\frac{2W_1}{\rho V_{\min}^2 S\sqrt{C_{D_o}/K}}\right) - \tan^{-1}\left(\frac{2W_2}{\rho V_{\min}^2 S\sqrt{C_{D_o}/K}}\right)\right] \quad (6.89)$$

The term $\sqrt{C_{D_o}/K}$ is equal to the minimum drag lift coefficient, $C_{L_{\min D}}$ (Equation 6.48). Using the relationship between initial weight, final weight, and fuel weight ($W_2 = W_1(1-G)$, Equation 6.73), we obtain

$$R_{\max_3} = \frac{2\eta_P (L/D)_{\max}}{C}\left[\tan^{-1}\left(\frac{2W_1}{\rho V_{\min}^2 S C_{L_{\min D}}}\right) - \tan^{-1}\left(\frac{2W_1(1-G)}{\rho V_{\min}^2 S C_{L_{\min D}}}\right)\right] \quad (6.90)$$

where ρ stands for air density at any given altitude, and $V_{\min}$ stands for the lowest permissible true airspeed at that altitude. If the minimum velocity is assumed to be equal to the stall speed, Equation 6.90 may be expressed as

$$R_{\max_3} = \frac{2\eta_P (L/D)_{\max}}{C}\left[\tan^{-1}\left(\frac{C_{L_{\max}}}{C_{L_{\min D}}}\right) - \tan^{-1}\left(\frac{C_{L_{\max}}(1-G)}{C_{L_{\min D}}}\right)\right] \quad (6.91)$$

It should be emphasized that this relationship (Equation 6.91) is based on the assumption that the prop efficiency and SFC do not vary with velocity. In effect, the prop

efficiency and SFC are functions of velocity, so the interested reader should modify the equation accordingly. The aforementioned point about the units of range and C is also applicable here.

6.4.4 Maximum Range Speed

As addressed in the preceding section, among three flight programs in a range mission, the maximum range in program 2 (constant-airspeed, constant-lift-coefficient flight) is achieved only when flying at a unique constant velocity. Furthermore, in the first flight program (constant-altitude, constant-lift-coefficient flight), the maximum range is achieved only when the flight begins at a unique velocity. The maximum range for both flight programs is determined using Equation 6.86.

Although airspeed does not directly appear in Equations 6.86, on a closer scrutiny, one can determine the airspeed an aircraft must fly to maximize the aircraft range. In this equation, the lift-to-drag ratio is found on the numerator; hence, any particular speed that corresponds to this particular lift-to-drag ratio will deliver a particular speed. So, to achieve the maximum range, one must fly with a speed that yields the maximum lift-to-drag ratio. By referring to Equation 6.47 and Section 6.3.2, one can conclude that the maximum range speed ($V_{\max_R}$) is the same as the maximum lift-to-drag ratio velocity which is equal to the minimum drag speed ($V_{\min_D}$). The reason is that for a prop-driven aircraft, the minimum drag speed is equivalent to the maximum lift-to-drag speed. Thus, for a prop-driven aircraft, and for the first and second flight programs, the maximum range velocity is

$$V_{\max_{R1}} = V_{\max_{R2}} = V_{\min_D} \tag{6.92}$$

or

$$V_{\max_{R1}} = V_{\max_{R2}} = \sqrt{\frac{2mg}{\rho S\sqrt{C_{D_o}/K}}} \tag{6.93}$$

$$C_{L_{\max_R}} = \sqrt{C_{D_o}/K} \tag{6.94}$$

It is evident that flying with such speed requires the pilot to keep this speed constant throughout the flight.

Please note that due to speed stability (as in Section 5.3.3), it is recommended that pilots fly at a speed about 5%–10% greater than the minimum drag speed. However, this yields about 2% less range than the theoretical value. Recall in the first flight program (constant-altitude, constant-lift-coefficient flight), when the initial velocity (V_1) is given, the final speed (V_2) is calculated using Equation 5.72 as derived in Chapter 5.

For a prop-driven aircraft at which the maximum range speed is theoretically less than the stall speed, a safe maximum range speed is selected to be approximately 10%–20% higher than the stall speed:

$$V_{\max_R} = kV_s \tag{6.95}$$

where

$$1.1 < k < 1.2 \tag{6.96}$$

The maximum range in the third flight program is determined using Equation 6.91. For a given aircraft, this equation is only a function of altitude and velocity, both of which are inside the bracketed term that represents the difference between two angles. To maximize the range for this flight operation, one must maximize the difference between the two angles. Hence, the maximum range will be achieved at every altitude, but when flying at the lowest permissible speed ($V_{\min}$). In the third flight program, $V_{\min}$ is the lowest permissible true airspeed at that altitude.

$$V_{\max_{R3}} = V_{\min} = kV_s \tag{6.97}$$

where

$$1.1 < k < 1.2 \tag{6.98}$$

Safety issues should be considered while selecting the value for k.

Example 6.6

A GA utility aircraft with a mass of 3,500 kg has a turboprop engine with a maximum power of 750 hp (559.3 kW). Other characteristics of this aircraft are as follows:

$$S = 28\,\text{m}^2, C_{D_o} = 0.025, K = 0.051, m_f = 700\,\text{kg}, \eta_P = 0.75, C_{L_{\max}} = 1.8,$$
$$C = 0.5\,\text{lb/h/hp}\,(84.5\,\mu\text{g/J})$$

a. Determine the maximum range of this aircraft, if flying with a constant velocity and constant lift coefficient at a starting altitude of 15,000 ft (4,572 m).
b. What is the corresponding airspeed to this range?
c. Calculate the flight duration.
d. How much engine power is needed for this flight operation at the beginning of the flight?
e. Repeat b, c, and d at sea level.

Solution

The air density at 4,572 m from Appendix A is 0.768 kg/m^3.

a. Maximum range
The second flight program involves constant velocity and constant lift coefficient:

$$\left(\frac{L}{D}\right)_{\max} = \frac{1}{2\sqrt{KC_{D_o}}} = \frac{1}{2\sqrt{0.051 \times 0.025}} = 14 \tag{6.9}$$

We need to convert the unit of SFC to 1/km. One horsepower is equivalent to 550 lb·ft/s, 1 knot is 6,076 ft/hr, 1 nm is 1.852 km, and 1 h is 3,600 s.

$$C = 0.5\,\text{lb}/(\text{h}\cdot\text{hp}) = 0.5\times\frac{6{,}076}{3{,}600\times550\times1.852} = 0.000828\,\text{km}^{-1}$$

The ratio between fuel weight and aircraft weight is

$$G = \frac{m_f}{m_{\text{TO}}} = \frac{700}{3{,}500} = 0.2$$

Since the altitude and lift coefficient are kept constant, this flight is in the category of the second flight program (i.e., cruise-climb). Hence, the maximum range is

$$R_{\max_2} = \frac{\eta_P\left(\frac{L}{D}\right)_{\max}}{C}\ln\left(\frac{1}{1-G}\right) = \frac{0.75\times14}{0.000828}\ln\left(\frac{1}{1-0.2}\right) = 2{,}828.3\,\text{km} \quad (6.88)$$

If we assume that SFC is constant, the range of 2,829 km is the maximum range. Although in practice, SFC is a function of altitude, and thus, the maximum range could be a little bit different.

b. Maximum range speed

$$V_{\max_{R2}} = \sqrt{\frac{2mg}{\rho S\sqrt{C_{D_o}/K}}} = \sqrt{\frac{2\times3{,}500\times9.81}{0.768\times28\times\sqrt{0.025/0.051}}} = 67.53\,\text{m/s} = 131.2\,\text{knot} \quad (6.93)$$

while

$$V_s = \sqrt{\frac{2mg}{\rho SC_{L_{\max}}}} = \sqrt{\frac{2\times3{,}500\times9.81}{0.768\times28\times1.8}} = 42.1\,\text{m/s} = 81.9\,\text{knot} \quad (2.27)$$

Since the maximum range speed is greater than the stall speed, the calculation in part a is valid.

c. Flight duration

$$t = \frac{\text{Distance}}{\text{Speed}} = \frac{R_{\max}}{V_{\max_R}} = \frac{2{,}828.6\times1{,}000}{67.53\times3{,}600} = 41{,}888\,\text{s} = 11.64\,\text{h}$$

d. Engine power at the beginning of the flight

$$C_{L_{\max_R}} = \sqrt{\frac{C_{D_o}}{K}} = \sqrt{\frac{0.025}{0.051}} = 0.7 \quad (6.94)$$

$$C_D = C_{D_o} + KC_L^2 = 0.025 + \left[0.051\times0.7^2\right] = 0.05 \quad (3.12)$$

$$D = \frac{1}{2}\rho V^2 SC_D = \frac{1}{2}\times0.786\times67.53^2\times28\times0.05 = 2{,}451\,\text{N} \quad (3.1)$$

$$T = D = 2{,}451\,\text{N} \tag{6.5}$$

$$T = \frac{P\eta_P}{V} \Rightarrow P = \frac{T \cdot V}{\eta_P} = \frac{2{,}451 \times 67.53}{0.75} = 220{,}696\,\text{W} = 220.7\,\text{kW} = 296\,\text{hp} \tag{6.7}$$

e. Sea level

$$V_{\max_R} = \sqrt{\frac{2mg}{\rho S\sqrt{C_{D_o}/K}}} = \sqrt{\frac{2 \times 3{,}500 \times 9.81}{1.225 \times 28 \times \sqrt{0.025/0.051}}} \tag{6.93}$$

$$= 53.46\,\text{m/s} = 103.9\,\text{knot}$$

$$t = \frac{R_{\max}}{V_{\max_R}} = \frac{2{,}828.6 \times 1{,}000}{53.46 \times 3{,}600} = 14.7\,\text{h}$$

$$T = D = \frac{1}{2}\rho V^2 S C_D = \frac{1}{2} \times 1.225 \times (53.46)^2 \times 28 \times 0.05 = 2{,}451\,\text{N} \tag{6.5}$$

Same thrust!

$$P = \frac{T \cdot V}{\eta_P} = \frac{2{,}451 \times 53.46}{0.75} = 174{,}736\,\text{W} = 174.7\,\text{kW} = 234.3\,\text{hp} \tag{6.7}$$

By comparing the results, we obtain the following conclusions:

- The flight duration at sea level is about 20.8% longer than the flight duration at 15,000 ft. However, the airspeed at sea level is about 20.8% slower than the airspeed at 15,000 ft.
- To achieve maximum range at sea level, the required power is about 31.2% of the maximum engine power. However, to achieve maximum range at 15,000 ft, the required power is about 39.5% of the maximum engine power.

Case Study - Example 6.7

The single-engine prop-driven trainer aircraft Pilatus PC-9 is required to fly a distance of 2,000 km at 20,000 ft (6,096 m) with two airspeeds: cruise speed (556 km/h or 300 knots) and maximum range speed. If the SFC is 0.5 lb/h/hp or 84.5 μg/J, how much fuel is needed for each flight operation? Assume that for both cases, the airspeed and angle of attack are kept constant throughout the flight, but the altitude is increased. The features of this aircraft are given in Example 6.4.

Solution

a. Flight with maximum range speed

The second flight program involves constant airspeed and angle of attack, so

$$R_{\max_2} = \frac{\eta_P (L/D)_{\max}}{C} \ln\left(\frac{1}{1-G}\right) \tag{6.88}$$

$$\left(\frac{L}{D}\right)_{\max} = \frac{1}{2\sqrt{KC_{D_o}}} = \frac{1}{2\sqrt{0.06\times 0.02}} = 14.4 \tag{6.9}$$

We need to convert the unit of SFC to 1/km. One horsepower is equivalent to 550 lb·ft/s, 1 knot is 6,076 ft/hr, 1 nm is 1.852 km, and 1 h is 3,600 s.

$$C = 0.5\ lb/(h\cdot hp) = 0.5\times\frac{6{,}076}{3{,}600\times 550\times 1.852} = 0.000828\ km^{-1}$$

$$2{,}000 = \frac{0.8\times 14.4}{0.000828}\ln\left(\frac{1}{1-G}\right) \Rightarrow \ln\left(\frac{1}{1-G}\right) = 0.143 \Rightarrow G = 0.134 \tag{6.88}$$

$$G = \frac{W_f}{W_1} = \frac{m_f}{m_1} \Rightarrow m_f = 0.134\times 3{,}200 = 427.8\,\text{kg} \tag{6.75}$$

b. Flight with cruise speed

At 20,000 ft (6,096 m), from Appendix A, the air density is 0.653 kg/m^3.

$$R_2 = \frac{\eta_P (L/D)}{C}\ln\left(\frac{1}{1-G}\right) \tag{6.74}$$

$$C_L = \frac{2mg}{\rho V^2 S} = \frac{2\times 3{,}200\times 9.81}{0.653\times(300\times 0.514)^2\times 16.29} = 0.248 \tag{6.6}$$

$$C_D = C_{D_o} + KC_L^2 = 0.02 + \left[0.06\times 0.248^2\right] = 0.024 \tag{3.12}$$

$$\frac{L}{D} = \frac{C_L}{C_D} = \frac{0.248}{0.024} = 10.46$$

$$2{,}000 = \frac{0.8\times 10.46}{0.000828}\ln\left(\frac{1}{1-G}\right) \Rightarrow G = 0.18 \tag{6.74}$$

$$G = \frac{W_f}{W_1} = \frac{m_f}{m_1} \Rightarrow m_f = 0.18\times 3{,}200 = 574.8\,\text{kg} \tag{6.75}$$

This result indicates that the flight with cruise speed requires 25.6% more fuel. Please note that we ignored the effect of the change in altitude in the final results.

6.4.5 Comparison and Conclusion

The maximum range in the first and second flight programs (see Figure 5.14) is determined using Equation 6.86, while the maximum range in the third flight program is determined using Equation 6.91. Equations 6.86 and 6.91 yield two different values. It is interesting to note that the maximum ranges of two flight scenarios are very much different. The first one is based on a reduction in airspeed or an increase in altitude as the aircraft weight decreases, while the second one is based on a reduction in the angle of attack. If we divide these two equations, we have

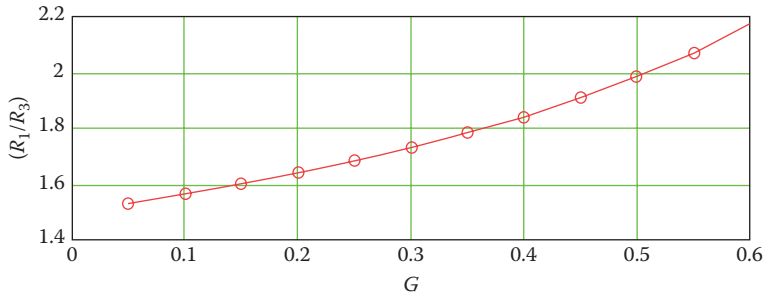

FIGURE 6.9 A graphical representation for Equation 6.99.

$$\frac{R_{\max_{1,2}}}{R_{\max_3}} = \frac{\ln\left(\dfrac{1}{1-G}\right)}{2\left[\tan^{-1}\left(\dfrac{C_{L_{\max}}}{C_{L_{\min_D}}}\right) - \tan^{-1}\left(\dfrac{C_{L_{\max}}(1-G)}{C_{L_{\min_D}}}\right)\right]} \tag{6.99}$$

This equation very well reflects the point that the difference between two ranges depends on the difference between their fuel-weight ratios (G). Figure 6.9 is a graphical representation for Equation 6.99. With greater fuel-weight ratio, a flight with constant angle of attack will have a much longer range compared with a flight with constant speed and constant altitude. There is a large difference between range performances as shown by the two equations. For instance, if an aircraft has a 30% fuel-weight ratio (i.e., $G=0.3$) and a flight with constant angle of attack, Programs 1 and 2 (including cruise-climb flight) have about 73% more range compared with a constant-speed and constant-altitude flight program 3.

However, unlike a jet aircraft, both flight Programs 1 and 2 yield the same maximum range for a prop-driven aircraft. Hence, there is no improvement in range with cruise-climb over the first flight program. Thus, even if aviation regulations may allow the increase in altitude [36] throughout the flight (step-climb), the increase in range is not considerable. Thus, there is no real advantage or need for a prop-driven aircraft to fly cruise-climb in a range mission. In fact, the maximum range of all these three flight programs is independent of the altitude. But at each given altitude, a particular velocity must be maintained to keep the equilibrium state of the flight.

So, the best practical scenario for gaining the maximum range for a prop-driven aircraft is a flight with constant altitude and constant lift coefficient, but with reduced speed (see Figure 6.10). The flight speed begins with the minimum drag at the initial weight and ends with the minimum drag at the final weight. According to Equation 5.97, no altitude is recommended to maximize the range. However, as the higher altitude is selected, the minimum drag velocity is increased. Thus, a higher altitude yields a shorter time. Therefore, the *highest possible altitude* (close to the absolute ceiling) is recommended for a range mission.

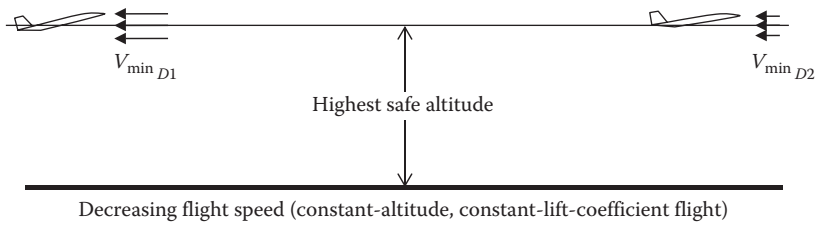

FIGURE 6.10 Best range flight program.

Due to fuel consumption, the pilot needs to maintain equilibrium by using one (or more) of the following three techniques: (1) reduction of airspeed, (2) reduction of air density through increasing altitude, and (3) reduction of lift coefficient.

The reduction of speed is applied by decreasing the throttle setting. The reduction of lift coefficient is applied by decreasing the aircraft angle of attack (via pushing the stick). The reduction of speed is the technique that was employed by Voyager aircraft in its very long trip. The Voyager had a speed of 120 knots at the beginning of flight when fuel tanks were full. But at the end of flight, when the fuel tanks were almost empty, it had a speed of about 110 knots. The second technique is the cruise-climb flight that is not allowed for most aircraft by FAA regulations.

It is interesting to note that both cases of flight operations (a and b) yield the same range, but the cruise-climb has a shorter flight time. Thus, the third flight program offers the lowest range and is not recommended for a range mission. The single-engine light aircraft Cessna 172 (Figure 3.17) has a range of 485 nm [79] when flying at 8,000 ft, while having a range of 750 nm when flying at 10,000 ft. For both cases, the aircraft carries 50 gallons of fuel, with 45 min of reserve fuel, and employs 75% of the engine power.

In the third flight program, the initial lift coefficient is:

$$C_{L_1} = \frac{2W_1}{\rho_1 V_1^2 S} \tag{6.100}$$

The final lift coefficient is:

$$C_{L_2} = \frac{2W_1}{\rho_2 V_2^2 S} \tag{6.101}$$

Equations 6.100 and 6.101 reveal the relationship between lift coefficient and altitude (air density) and airspeed for initial and final flight conditions. Table 6.3 presents a summary of range equations with corresponding flight variables.

6.5 ENDURANCE

Another significant aircraft performance and design parameter for a prop-driven aircraft is endurance. Endurance (E) is the length of time that an aircraft can remain airborne for a given expenditure of fuel and for a specified set of flight condition. For more details, refer to Section 5.5. In this section, the technique to determine

TABLE 6.3
Summary of Range Equations

Flight Program	Range		Flight Variable						
			Speed		Altitude		Lift Coefficient		Weight
	Type	Equation	Initial	Final	Initial	Final	Initial	Final	Final
1.	Regular	6.74	Given	5.72	Given	Same	6.98	Same	6.73
	Maximum	6.88	6.93	5.72	[a]	Same	6.98	Same	6.73
2.	Regular	6.74	Given	Same	Given	5.176	6.98	Same	6.73
	Maximum	6.88	6.93	Same	[a]	5.176	6.98	Same	6.73
3.	Regular	6.87	Given	Same	Given	Same	6.98	6.99	6.73
	Maximum	6.90	6.95	Same	[a]	Same	6.85	6.99	6.73

[a] The flight at any altitude (with appropriate velocity and lift coefficient) yields the same maximum range. However, the highest altitude yields the shortest flight time.

the regular endurance of a given flight condition for a prop-driven aircraft will be addressed. In addition, the technique to calculate the maximum endurance (E_{max}) and its corresponding speed (V_{max_E}) will be presented.

6.5.1 Regular Endurance

To calculate the endurance, it is assumed that the aircraft is in a steady-level flight for the entire duration of flight. For an aircraft with the turboprop or piston-prop engine, the specific endurance is defined as

$$\text{SE} = -\frac{dt}{dW} \tag{6.102}$$

The minus sign is used to account for a decrease in fuel weight (i.e., fuel consumption along the flight path) during the flight mission. By employing the definition (Equation 6.65) of SFC (C) and fuel flow rate (Q), we obtain the following equation:

$$\frac{dt}{-dW} = \frac{1}{CP} \tag{6.103}$$

The engine thrust is a function of engine power, propeller efficiency, and aircraft speed:

$$T = \frac{P\eta_P}{V} \tag{6.7}$$

In a steady-level flight, the lift is assumed to be equal to weight, and thrust is equal to drag (Equations 6.5 and 6.6). When Equation 6.7 is inserted into Equation 6.103, T (i.e., thrust) is replaced with a D (i.e., drag). Furthermore, both numerator and denominator are multiplied with an L (i.e., lift), and then L in denominator is replaced with a W (i.e., weight):

$$dt = \frac{-dW}{CP} = -\frac{\eta_P dW}{CTV} = -\frac{\eta_P dW}{CTV}\frac{L}{L} = -\frac{\eta_P dW}{CDV}\frac{L}{W} \tag{6.104}$$

or

$$dt = -\frac{\eta_P (L/D)}{CV}\frac{dW}{W} \tag{6.105}$$

This equation indicates that five parameters are effective on endurance: prop efficiency, airspeed, SFC, lift-to-drag ratio, and fuel weight. However, these parameters are not independent of one another. To increase endurance, one must increase prop efficiency; decrease aircraft speed, SFC, and aircraft weight; and increase lift-to-drag ratio. Recall that the lift-to-drag ratio is a function of speed.

To derive an equation for endurance, we now integrate the specific endurance for the entire time of flight. The endurance is obtained by integrating Equation 6.105 between $t = 0$, where the fuel tanks are full ($W = W_1$), and $t = E$, where the fuel tanks are empty ($W = W_2$). Conditions at the start of cruise will be identified by subscript 1 and at the end of cruise by the subscript 2:

$$E = \int dt = -\int_{W_1}^{W_2} \frac{\eta_P (L/D)}{CV}\frac{dW}{W} \tag{6.106}$$

where W_1 and W_2 are, respectively, the aircraft weight at the beginning and at the end of flight. Equation 6.106 is a general equation for endurance for a prop-driven aircraft. Since the fuel is consumed during flight, the aircraft weight is constantly decreased during the flight. To maintain the steady-level flight, we have to decrease the lift as well. Considering the lift equation, it has three independent parameters: velocity (V), altitude or its corresponding air density (ρ), and angle of attack (α), or its associated lift coefficient (C_L). Of the many possible solutions, only three will be examined: in each case, two flight parameters will be held constant throughout the flight, and only one parameter will be decreased. Three options of interest (see Figure 5.14) are as follows:

1. Decreasing flight speed (constant-altitude, constant-lift-coefficient flight)
2. Increasing altitude (constant-airspeed, constant-lift-coefficient flight)
3. Decreasing angle of attack (constant-altitude, constant-airspeed flight)

For each flight program, the integral equation will be set up based on the general equation (Equation 6.106) and then will be solved to find a closed-form solution for the endurance equation.

Based on the safety regulations and practical considerations, the first option is recommended for the majority of aircraft. Now, we consider the individual case of endurance for prop-driven aircraft.

6.5.1.1 Flight Program 1: Constant-Altitude, Constant-Lift-Coefficient Flight

In this flight program, the velocity is decreased as the weight is decreased. Noting that in a steady-level flight, $L/D = C_L/C_D$, so the endurance integration (Equation 6.106) for this flight operation is expressed as:

$$E_1 = -\frac{\eta_P}{C}\frac{C_L}{C_D}\int_{W_1}^{W_2}\frac{1}{V}\frac{dW}{W} \tag{6.107}$$

We need to convert any non-constant parameter (other than weight) in terms of constant parameters. In Equation 6.107, the only variable is velocity, which in a steady-level flight (Equation 6.6) is

$$V = \sqrt{\frac{2W}{\rho S C_L}} \tag{6.108}$$

Substituting Equation 6.108 into Equation 6.107, we obtain

$$E_1 = -\frac{\eta_P}{C}\frac{C_L}{C_D}\int_{W_1}^{W_2}\sqrt{\frac{\rho S C_L}{2W}}\frac{dW}{W} = \frac{\eta_P}{C}\sqrt{\frac{\rho S}{2}}\frac{C_L^{3/2}}{C_D}\int_{W_2}^{W_1}\frac{dW}{W^{3/2}} \tag{6.109}$$

The solution to this integration is

$$E_1 = \frac{\eta_P}{C}\sqrt{2\rho S}\frac{C_L^{3/2}}{C_D}\left[\frac{1}{\sqrt{W_2}} - \frac{1}{\sqrt{W_1}}\right] \tag{6.110}$$

where the lift coefficient is calculated from Equation 6.85. As we derived in Section 5.4, this leads to the fact that the velocity at the end of flight is reduced to a new value determined by Equation 5.72 or 5.129.

6.5.1.2 Flight Program 2: Constant-Airspeed, Constant-Lift-Coefficient Flight

In this flight program, the altitude is increased as the aircraft weight is decreased (i.e., cruise-climb). By inspection, we notice that the closed-form solution to the integral equation (Equation 6.106) for this flight option results in the following solution:

$$E_2 = \frac{\eta_P (L/D)}{CV}\ln\left(\frac{1}{1-G}\right) \tag{6.111}$$

where G is the fuel fraction (W_f/W_1). The altitude at the end of cruise-climb flight (h_2) can be determined by calculating the density ratio at the end of the cruise-climb flight (σ_2) from Equation 5.83, that is,

$$\sigma_2 = \sigma_1(1-G) \tag{5.83}$$

where σ_1 is the air density ratio at the beginning of the cruise. Then, one can utilize Appendix A or B to determine the final altitude.

6.5.1.3 Flight Program 3: Constant-Altitude, Constant-Airspeed Flight

To find a closed-form solution to the integral equation (Equation 6.106) for this flight option, we use the same technique as we did in Section 5.5.2.3. Hence, the details of derivation will not be discussed here. Since the lift is equal to the weight during cruise, the L from the numerator and W from the denominator of Equation 6.106 are eliminated. Thus, the endurance equation for this flight program can be simplified as

$$E = -\frac{\eta_P}{CV}\int_{W_1}^{W_2}\frac{dW}{D} \tag{6.112}$$

By inserting drag (Equation 5.35) and using the integration model (Equations 5.137 and 5.138), the closed-form solution will be

$$E_3 = \frac{\eta_P}{V}\frac{2(L/D)_{\max}}{C}\left[\tan^{-1}\left(\frac{2W_1}{\rho V^2 S\sqrt{C_{D_o}/K}}\right)-\tan^{-1}\left(\frac{2W_2}{\rho V^2 S\sqrt{C_{D_o}/K}}\right)\right] \tag{6.113}$$

In Equation 6.48, the term $\sqrt{C_{D_o}/K}$ is equal to the minimum drag lift coefficient, $C_{L_{\min D}}$. Thus,

$$E_3 = \frac{\eta_P}{V}\frac{2(L/D)_{\max}}{C}\left[\tan^{-1}\left(\frac{2W_1}{\rho V^2 S C_{L_{\min D}}}\right)-\tan^{-1}\left(\frac{2W_2}{\rho V^2 S C_{L_{\min D}}}\right)\right] \tag{6.114}$$

In this flight program, the initial lift coefficient and the final lift coefficient are readily obtained by Equations 6.100 and 6.101, respectively. Inserting the relationship between initial weight, final weight, and fuel weight ($W_2 = W_1(1-G)$) into Equation 6.113 and converting the difference between the tangent of two angles, we may reformat Equation 6.114 into

$$E_3 = \frac{2\eta_P (L/D)_{\max}}{CV}\tan^{-1}\left[\frac{G(L/D)_1}{2(L/D)_{\max}\left[1-KC_{L_1}G(L/D)_1\right]}\right] \tag{6.115}$$

where subscript 1 refers to the beginning of the flight. This case is more convenient in short endurance flight operations. The pilot will push the elevator to gradually reduce the aircraft angle of attack.

Note that, in Equations 6.110, 6.111, 6.113, and 6.115, the unit of C and V must be compatible. For instance, if the unit of V is m/s, the unit of C must be 1/s; in this case, the unit of endurance would be the second. Similarly, when the unit of V is knot, the unit of C must be 1/h. In this case, the unit of endurance would be the hour. Be careful not to use the unit of lb/h/hp for C in this equation.

6.5.2 Maximum Endurance Speed for Prop-Driven Aircraft

Among three flight programs to keep the equilibrium in a steady-level flight, two programs have a constant velocity (2 and 3) throughout the entire flight. We would like to find the velocity to maximize the endurance for a prop-driven aircraft. In this process, we assume that C, η_P, and G are constant.

6.5.2.1 Flight Program 1: Constant-Altitude, Constant-Lift-Coefficient Flight

The maximum endurance speed for prop-driven aircraft for this flight program is the same as flight program 2, as will be presented. This is indirectly evident by inspecting Equation 6.110. The interested reader is encouraged to speculate the case and prove it for himself/herself.

6.5.2.2 Flight Program 2: Constant-Airspeed, Constant-Lift-Coefficient Flight

For the case of a constant-airspeed, constant-lift-coefficient flight (flight program 2), we need to maximize the ratio $(L/D)/V$. By inspecting Equation 6.111, one can conclude that the maximum endurance for prop-driven aircraft is achieved when the aircraft is flying at the minimum power speed:

$$V_{\max_E} = V_{P_{\min}} \tag{6.116}$$

By using Equations 6.20, 6.22, and 6.23, one can obtain:

$$V_{\max_E} = V_{\min_P} = \sqrt{\frac{2mg}{\rho S\sqrt{3C_{D_o}/K}}} \tag{6.117}$$

$$C_{L_{\max_E}} = C_{L_{\min_P}} = \sqrt{\frac{3C_{D_o}}{K}} \tag{6.118}$$

Thus, the endurance of a prop-driven aircraft will be maximized when ratio of $C_L^{3/2}/C_D$ has its maximum value. Therefore,

$$(L/D)_{\max_E} = 0.866(L/D)_{\max} \tag{6.119}$$

For a prop-driven aircraft in which the maximum endurance speed is theoretically less than the stall speed, a safe maximum endurance speed is selected to be about 10%–20% higher than the stall speed:

$$V_{\max_E} = kV_s \tag{6.120}$$

where

$$1.1 < k < 1.2 \tag{6.121}$$

The minimum power that yields the maximum endurance (first flight program) is

$$P_{\min} = T_{\min_P} \cdot V_{\min_P} \tag{6.122}$$

Using Equations 5.11 and 6.119, one can obtain the following equation:

$$P_{\max_E} = P_{\min} = \frac{WV_{\max_E}}{0.866(L/D)_{\max}} \tag{6.123}$$

Note that a cruising flight is not feasible when the engine power is lower than this power. It is beneficial to compare this expression for minimum power to Equation 6.46 that we derived earlier.

6.5.2.3 Flight Program 3: Constant-Altitude, Constant-Airspeed Flight

For the case of a constant-altitude, constant-airspeed flight (flight program 3), we need to maximize the value inside the bracketed term that represents the difference between two angles in Equation 6.114. However, for each flight, the maximum endurance occurs at a specific velocity, which is the lowest permissible speed. Hence, the maximum endurance will be achieved at every altitude, but when flying at the lowest permissible speed ($V_{\min}$). In the third flight program, $V_{\min}$ is the lowest permissible true airspeed at that altitude:

$$V_{\max_{E3}} = V_{\min} = kV_s \tag{6.120}$$

where

$$1.1 < k < 1.2 \tag{6.121}$$

Safety issues should be considered when selecting a value for k. It should be emphasized that this relationship (Equation 6.120) is based on the assumption that the prop efficiency and SFC do not vary with velocity. In effect, the prop efficiency and SFC are functions of velocity, so the interested reader should modify the equation accordingly.

6.5.3 Maximum Endurance

Now we are able to derive a relationship for maximum endurance by employing the materials covered in Sections 6.5.1 and 6.5.2. Recall that we have three choices in a long-duration flight to compensate a reduction in aircraft weight and keep the equilibrium. They are (1) constant-altitude, constant-lift-coefficient flight; (2) constant-airspeed, constant-lift-coefficient flight; and (3) constant-altitude, constant-airspeed flight. In this section, the technique to determine the maximum endurance for a prop-driven aircraft is presented. Table 6.4 illustrates the maximum endurance for several prop-driven aircraft.

6.5.3.1 Flight Program 1: Constant-Altitude, Constant-Lift-Coefficient Flight

For a flight program where the altitude and lift coefficient are held constant and speed is decreased, an expression for the maximum endurance will be readily obtained

TABLE 6.4
Maximum Endurance for Several Prop-Driven Aircraft

No.	Aircraft	Engine	Type	m_{TO} (kg)	P (kW)	Fuel (L)	E_{max} (h, min)
1.	ENAEA Avion liviano	Piston-prop	GA	600	62	80	3, 32′
2.	Cessna 172	Piston-prop	Single engine GA	1,111	120	212	5
3.	Enstrom F-28	Piston-prop	Helicopter	1,179	168	151	3, 30′
4.	Aerotec	Piston-prop	Trainer	960	150	140	4
5.	Enaer T-36	Piston-prop	Acrobatic	1,338	224	291	5, 30′
6.	Harbin SH-5	Turboprop	Bomber	45,000	4 × 2,350	20,000	15
7.	Aviones	Piston-prop	Agriculture	1,499	224	204	2, 36′
8.	Epsilon	Piston-prop	Trainer	1,250	224	210	3, 45′
9.	Valmet L-70	Piston-prop	Trainer	1,040	150	170	6, 12′
10.	Rutan Model 76 Voyager	Piston-prop	Record breaker	5,148	75 + 97	4,060	235
11.	Lockheed C-130J Hercules	Turboprop	Transport	70,305	4 × 3,423	25,552	10
12.	Pilatus PC-9	Turboprop	Trainer	3,200	857	535	2, 20′
13	Breguet 1150 Atlantic	Turboprop	Air patrol	46,200	2 × 1,193	23,120	18
14	Reaper	Turboprop	Hunter UAV	4,760	671	2,200	14
15	ATR-72	Turboprop	Regional airliner	23,000	2 × 1,845	6,400	10
16	De Havilland Dash 8	Turboprop	Regional airliner	15,600	2 × 1,864	3,160	11
17	AeroVironment RQ-11 Raven	Electric	Small UAV	1.9	0.4	Battery	1

from Equation 6.110. Assuming η_P, C, and G are constant, the endurance in this flight program is only a function of altitude (ρ) and velocity (V). To maximize the endurance, one must fly at the lowest altitude or the highest air density (i.e., sea level) and fly at the velocity that maximizes the ratio $C_L^{3/2}/C_D$. Thus, the maximum endurance will be obtained from the following expression:

$$E_{1_{\max}} = \frac{\eta_P}{C}\sqrt{2\rho_{SL}S}\left(\frac{C_L^{3/2}}{C_D}\right)_{\max}\left[\frac{1}{\sqrt{W_2}} - \frac{1}{\sqrt{W_1}}\right] \tag{6.124}$$

As we derived earlier, the velocity to maximize the ratio $C_L^{3/2}/C_D$ is the minimum power velocity (Equation 6.117). The ratio $\left(C_L^{3/2}/C_D\right)_{\max}$ is (Equation 6.41) only a function of zero-lift drag coefficient and induced drag factor:

$$\left(\frac{C_L^{3/2}}{C_D}\right)_{\max} = \frac{0.57}{K^{3/4}C_{D_o}^{1/4}} \tag{6.125}$$

Thus, the velocity at the beginning and at the end of flight will be

$$V_{\max_{E1}} = \sqrt{\frac{2W_1}{\rho S\sqrt{3C_{D_o}/K}}} \tag{6.126}$$

$$V_{\max_{E2}} = \sqrt{\frac{2W_2}{\rho S\sqrt{3C_{D_o}/K}}} \tag{6.127}$$

The lift coefficient throughout the flight will be constant and is determined from Equation 6.118. The higher the flight altitude, the lower the endurance. Moreover, the higher the airspeed, the lower the endurance.

6.5.3.2 Flight Program 2: Constant-Airspeed, Constant-Lift-Coefficient Flight

For a flight program where speed and lift coefficient are held constant, an expression for the maximum endurance will be readily obtained from Equation 6.111. Assuming η_P, C, and G to be constant, the endurance in this flight program is only a function of lift-to-drag ratio (L/D) and velocity (V), but independent of altitude. However, lift-to-drag ratio is a function of airspeed. Therefore, to maximize the endurance, one must fly at a velocity that maximizes the ratio $(L/D)/V$. Thus, the maximum endurance will be obtained from the following expression:

$$E_{2_{\max}} = \frac{\eta_P}{C}\left(\frac{(L/D)}{V}\right)_{\max} \ln\left(\frac{1}{1-G}\right) \tag{6.128}$$

For a typical aircraft, the ratio $(L/D)/V$ is maximized, when it is cruising with a speed equal to minimum power speed (Equation 6.117). As we derived earlier (Equation 6.119), the minimum power lift-to-drag ratio is 86.6% of the maximum lift-to-drag ratio. Thus,

$$\left(\frac{(L/D)}{V}\right)_{\max} = \frac{(L/D)_{\min_P}}{V_{\min_P}} = \frac{0.866(L/D)_{\max}}{V_{\min_P}} \tag{6.129}$$

Hence, the maximum endurance will be

$$E_{2_{\max}} = \frac{0.866\eta_P(L/D)_{\max}}{CV_{\min_P}} \ln\left(\frac{1}{1-G}\right) \tag{6.130}$$

where lift-to-drag ratio is 86.6% of the maximum lift-to-drag ratio. In this flight operation, the altitude is increased gradually, that is, *cruise-climb*. The altitude at the end of cruise-climb flight (h_2) can be determined by calculating the density ratio at the end of the cruise-climb flight (σ_2) from Equation 5.83. Then, one can utilize Appendix A or B to determine the final altitude. The lift coefficient is constant throughout the flight and is determined by Equation 6.118. In this flight program, flight at any altitude will yield the same maximum endurance.

6.5.3.3 Flight Program 3: Constant-Altitude, Constant-Airspeed Flight

For flight program where altitude and airspeed are held constant, but the angle of attack is gradually decreased, an expression for the maximum endurance will be readily obtained from Equation 6.113, or 6.114, or 6.115. Assuming η_P, C, and G are

constant, the endurance in this flight program is only a function of lift-to-drag ratio (L/D), velocity (V), and altitude (ρ).

However, lift coefficient and the lift-to-drag ratio is a function of airspeed and altitude. Therefore, to maximize the endurance, one must fly at a velocity that minimizes the required power (i.e., $V_{\max_E} = V_{\min_P}$) and at the lowest altitude (i.e., sea level). Thus, the maximum endurance will be obtained from the following expression:

$$E_{3_{\max}} = \frac{\eta_P}{V_{\min_P}} \frac{2(L/D)_{\max}}{C} \left[\tan^{-1}\left(\frac{2W_1}{\rho_{SL} V_{\min_P}^2 S\sqrt{C_{D_o}/K}} \right) - \tan^{-1}\left(\frac{2W_2}{\rho_{SL} V_{\min_P}^2 S\sqrt{C_{D_o}/K}} \right) \right] \tag{6.131}$$

or

$$E_{3_{\max}} = \frac{2\eta_P (L/D)_{\max}}{C V_{\min_P}} \tan^{-1}\left(\frac{G(L/D)_{\min_P}}{2(L/D)_{\max}\left[1 - KC_{L_{\min_P}} G(L/D)_{\min_P}\right]} \right) \tag{6.132}$$

The initial lift coefficient is the minimum power lift coefficient:

$$C_{L_1} = C_{L_{\min_P}} = \sqrt{\frac{3C_{D_o}}{K}} \tag{6.133}$$

Inserting the expressions for minimum power lift-to-drag ratio $(L/D)_{\min_P}$ and the minimum power lift coefficient from Equations 6.118 and 6.119 into Equation 6.132, we obtain

$$E_{3_{\max}} = \frac{2\eta_P (L/D)_{\max}}{C V_{\min_P}} \tan^{-1}\left(\frac{0.866(L/D)_{\max} G}{2(L/D)_{\max}\left[1 - K\sqrt{3C_{D_o}/K}\, G\left(0.866 \frac{1}{2\sqrt{KD_{D_o}}}\right)\right]} \right) \tag{6.134}$$

which is reduced to

$$E_{3_{\max}} = \frac{2\eta_P (L/D)_{\max}}{C V_{\min_P}} \tan^{-1}\left(\frac{0.433G}{1 - 0.75G} \right) \tag{6.135}$$

Although this equation is not evidently a function of altitude, Equation 6.131 implies that for a prop-driven aircraft, the maximum endurance is achieved when cruising at the lowest altitude (i.e., sea level). The final lift coefficient is obtained from

$$C_{L_2} = \frac{2W_2}{\rho_{SL} V_{\min_P}^2 S} \tag{6.136}$$

Please note that in endurance equations (6.124, 6.130, 6.131, and 6.135), the unit of SFC must be 1/distance (e.g., 1/m, 1/nm, 1/km, or 1/ft). Please also note the unit of the ratio inside parentheses in Equation 6.58 is radian. The maximum endurance equations (6.124, 6.131, and 6.135) indicate that *if a pilot is looking for maximizing the endurance, he or she must fly at the lowest altitude (i.e., sea level).*

Example 6.8

Consider the aircraft in Example 6.6. Determine the maximum endurance of this aircraft for two altitudes: sea level and 15,000 ft (4,572 m) altitude.

Solution

From Problem 6.6, we have $m = 3{,}500$ kg, $S = 28\,\text{m}^2$, $C_{D_o} = 0.025$, $K = 0.051$, $m_f = 700$ kg, $C = 0.5$ lb/h/hp (or 84.5 μg/J), $\eta_P = 0.75$, $C_{L_{\max}} = 1.8$, $(L/D)_{\max} = 14$.

a. Sea level

The maximum endurance speed is

$$V_{\max_E} = \sqrt{\frac{2mg}{\rho_o S\sqrt{3C_{D_o}/K}}} = \sqrt{\frac{2\times 3{,}500\times 9.81}{1.225\times 28\times\sqrt{(3\times 0.025)/0.051}}} = 40.6\,\text{m/s} = 79\,\text{knot} \tag{6.117}$$

The stall speed is

$$V_s = \sqrt{\frac{2mg}{\rho_o S C_{L_{\max}}}} = \sqrt{\frac{2\times 3{,}500\times 9.81}{1.225\times 28\times 1.8}} = 33.3\,\text{m/s} = 64.8\,\text{knot} \tag{2.27}$$

Since the maximum endurance speed is greater than the stall speed, the calculations can be based on the derived equations.

We need to convert the unit of SFC to 1/m. One horsepower is equivalent to 550 lb·ft/s, 1 knot is 6,076 ft/hr, 1 nm is 1.852 km, and 1 h is 3,600 s

$$C = 0.5\ \text{lb/(h}\cdot\text{hp)} = 0.5\times\frac{6{,}076}{3{,}600\times 550\times 1.852} = 0.000828\,\text{km}^{-1} = 8.28\times 10^{-7}\,\text{m}^{-1}$$

$$\left(\frac{C_L^{3/2}}{C_D}\right)_{\max} = \frac{0.57}{K^{3/4}C_{D_o}^{1/4}} = \frac{0.57}{0.051^{3/4}(0.025)^{1/4}} = 13.36 \tag{6.125}$$

$$E_{1_{\max}} = \frac{\eta_P}{C}\sqrt{2\rho_{SL}S}\left(\frac{C_L^{3/2}}{C_D}\right)_{\max}\left[\frac{1}{\sqrt{W_2}} - \frac{1}{\sqrt{W_1}}\right] \tag{6.124}$$

$$E_{1_{\max}} = \frac{0.75}{8.28\times 10^{-7}}\sqrt{2\times 1.225\times 28}\times 13.36\left[\frac{1}{\sqrt{27{,}459}} - \frac{1}{\sqrt{34{,}323}}\right]$$

$$= 63{,}810\,\text{s} = 17.72\,\text{h}$$

$$E_{2_{\max}} = \frac{0.866\eta_P \left(\frac{L}{D}\right)_{\max}}{CV_{\max_E}} \ln\left(\frac{1}{1-G}\right) \tag{6.130}$$

$$= \frac{0.866 \times 0.75 \times 14}{8.28 \times 10^{-7} \times 40.6} \ln\left(\frac{1}{1-0.2}\right) = 60,297\,\text{s} = 16.75\,\text{h}$$

$$E_{3_{\max}} = \frac{2\eta_P (L/D)_{\max}}{CV_{\max_E}} \tan^{-1}\left(\frac{0.433G}{1-0.75G}\right)$$

$$= \frac{2 \times 0.75 \times 14}{8.28 \times 10^{-7} \times 46.92} \tan^{-1}\left(\frac{0.433 \times 0.2}{1-0.75 \times 0.2}\right) \tag{6.132}$$

$$= 17.6\,\text{h}$$

b. 15,000 ft (4,572 m) altitude

The air density at 4,572 m is 0.768 kg/m^3. The maximum endurance speed at 4,572 m altitude is

$$V_{\max_E} = \sqrt{\frac{2mg}{\rho S\sqrt{3C_{D_o}/K}}} = \sqrt{\frac{2 \times 3,500 \times 9.81}{0.768 \times 21 \times \sqrt{3 \times 0.025/0.051}}} \tag{6.117}$$

$$= 51.3\,\text{m/s} = 99.74\,\text{knot}$$

By repeating the calculations in section "a" for 15,000 ft (4,572 m), we will obtain the following results:

$$E_{1_{\max}} = 14\,\text{h}$$
$$E_{2_{\max}} = 13.3\,\text{h}$$
$$E_{3_{\max}} = 13.93\,\text{h}$$

It is noticed that the maximum endurance is reduced by about 21% at 150,000 ft (4,572 m). For this aircraft, the maximum endurance will be gained when flying with constant altitude and constant angle of attack (program 1).

6.5.4 Comparison and Conclusion

The maximum endurance for a prop-driven aircraft in three flight programs is determined through Equations 6.124, 6.130, and 6.135. It is interesting to note that the maximum endurances of three flight scenarios are very much different, particularly at greater fuel-weight ratios. In general, the first flight program (constant-altitude, constant-lift-coefficient flight) yields the highest maximum endurance. If we divide these three equations, we have

$$\frac{E_{\max_1}}{R_{\max_2}} = \frac{\dfrac{\eta_P}{C}\sqrt{2\rho_{SL}S}\left(\dfrac{C_L^{3/2}}{C_D}\right)_{\max}\left[\dfrac{1}{\sqrt{W_2}} - \dfrac{1}{\sqrt{W_1}}\right]}{\dfrac{0.866\eta_P (L/D)_{\max}}{CV_{\min_P}} \ln\left(\dfrac{1}{1-G}\right)} \tag{6.137}$$

$$\frac{E_{\max_1}}{R_{\max_3}} = \frac{\dfrac{\eta_P}{C}\sqrt{2\rho_{SL}S}\left(\dfrac{C_L^{3/2}}{C_D}\right)_{\max}\left[\dfrac{1}{\sqrt{W_2}}-\dfrac{1}{\sqrt{W_1}}\right]}{\dfrac{2\eta_P(L/D)_{\max}}{CV_{\min_P}}\tan^{-1}\left(\dfrac{0.433G}{1-0.75G}\right)} \tag{6.138}$$

Equations 6.137 and 6.138 reflect the difference between three endurances depending on the difference between their fuel-weight ratio (G). Figure 6.11 is a graphical representation for Equations 6.137 and 6.138.

The higher the fuel-weight ratio, the longer the aircraft endurance of a flight program 1 as compared with a flight of constant speed (flight programs 2 and 3). There is a considerable difference between endurance performances shown by three equations. For instance, if an aircraft has a 50% fuel-weight ratio (i.e., $G=0.5$), the program 1 (i.e., a constant altitude, constant-lift-coefficient flight) will have about 20% more endurance compared with flight programs 2 and about 8% more endurance compared with flight programs 3. It is emphasized that the maximum endurances of all three flight programs are dependent on altitude and they have their absolute maximum endurance at sea level. Table 6.5 presents a summary of range equations with corresponding flight variables.

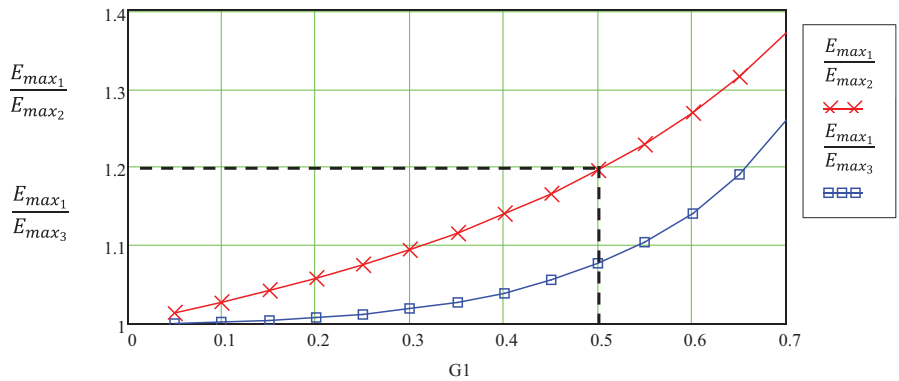

FIGURE 6.11 A graphical representation for Equations 6.137 and 6.138.

TABLE 6.5
Summary of Endurance Equations

Flight Program	Endurance		Flight Variable						
			Speed		Altitude		Lift Coefficient		Weight
	Type	Equation	Initial	Final	Initial	Final	Initial	Final	Final
1.	Regular	6.110	Given	Same	Given	Same	6.85	Same	6.73
	Maximum	6.124	6.126	6.127	Sea level	Same	6.85	Same	6.73
2.	Regular	6.111	Given	Same	Given	Given	6.85	Same	6.73
	Maximum	6.130	6.117	Same	Sea level	5.136	6.85	Same	6.73
3.	Regular	6.115	Given	Same	Given	Same	6.85	6.86	6.73
	Maximum	6.135	6.117	Same	Sea level	Same	6.133	6.136	6.73

6.6 CEILING

6.6.1 Definition

A very important criterion for aircraft performance is the ceiling. Ceiling is defined as the highest altitude at which an aircraft can safely have a straight-line steady sustained flight. Another definition is the highest altitude that an aircraft can reach by its own engine and have a sustained flight. The higher the ceiling, the better the performance. For more descriptions, please refer to Section 5.6. The primary reason for having the ceiling is the lack of sufficient air density at high altitudes to be consumed by prop-driven engine for combustion. So, the engine power is reduced with altitude.

On the other hand, as the air density is decreased, the drag force is decreased as well. At low altitudes, the available power is greater than the required power. However, the rate of reduction of available engine power is higher than the rate of reduction of required power. The variations of available engine power and aircraft required power are depicted by two curves in Figure 6.12. Thus, these two curves have an intersection that is the altitude for ceiling. As an aircraft flies higher and higher, the amount of available air decreases, so the available power reduces as well. As a result, at one particular altitude, the maximum available power is barely enough for an aircraft to maintain its level flight. This is the very ceiling.

In Chapter 5, we defined five types of ceilings: (1) absolute ceiling, (2) service ceiling, (3) cruise ceiling, (4) combat ceiling, and (5) maximum operating altitude. The definitions and features of these ceilings are addressed in Chapter 5, so they will not be repeated here. However, the definition of maximum operating altitude for a GA aircraft is slightly different than that for prop-driven aircraft. Most prop-driven aircraft are classified under Part 23 of the Federal Aviation Regulations (FARs). Based on the FARs, Part 23 [6], Section 1527, the maximum operating altitude is defined as follows: (1) The maximum altitude up to which operation is

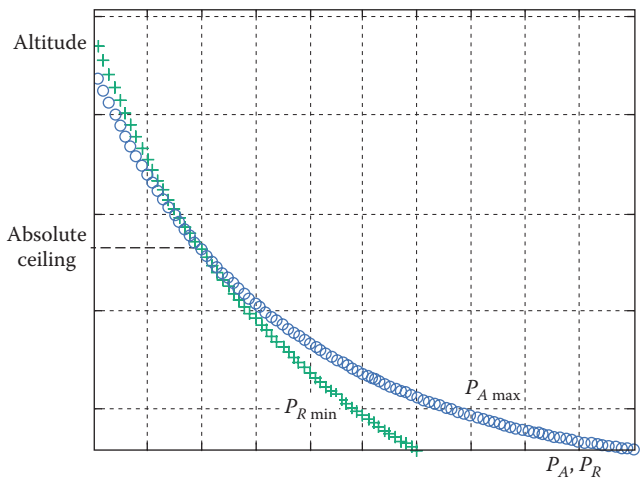

FIGURE 6.12 Variations of engine power and aircraft required power versus altitude.

TABLE 6.6
Ceiling of Several Prop-Driven Aircraft

No.	Aircraft	Type	Engine	Power (hp)	Mass (kg)	Service Ceiling (ft)
1.	Reims-Cessna F406 Caravan II	Utility	Turboprop	2 × 500	4,246	30,000
2.	DR 400 Dauphin	Trainer	Piston-prop	112	1,050	12,000
3.	Embraer/FMA CBA-123	Transport	Turboprop	2 × 1,300	7,800	41,000
4.	Harbin Y-12	Transport	Turboprop	2 × 500	5,300	22,960
5.	Shaanxi Y-8	Transport	Turboprop	4 × 1,100	61,000	34,120
6.	Socata TB30 Epsilon	Trainer	Piston-prop	300	1,250	23,000
7.	Breguet Br.1150 Atlantic	Maritime patrol	Turboprop	2 × 6,100	45,000	30,000
8.	PiaggioP180 Avanti	Transport	Turboprop	2 × 800	4,767	41,000
9.	Cessna 0-1E Bird Dog	Patrol	Piston-prop	213	1,090	18,500
10.	Lockheed C-130H Hercules	Transport	Turboprop	4 × 4,508	79,380	30,000
11.	Lockheed P-3C Orion	Reconnaissance	Turboprop	4 × 4,910	64,410	28,300
12.	General Atomics MQ-9 Reaper	Hunter UAV	Turboprop	900	4,760	50,000
13.	De Havilland Dash 8	Regional airliner	Turboprop	2 × 2,500	15,600	27,000
14.	Tupolev Tu-126	Reconnaissance	Turboprop	4 × 14,795	170,000	33,000
15.	GrummanS-2E Tracker	Military	Piston-prop	2 × 1,525	13,222	21,000
16.	Beech C-12C Huron	Transport	Turboprop	2 × 850	5,670	35,000
17.	Beech-150 Musketeer	Trainer	Piston-prop	150	1,020	11,080
18.	Short Skyvan 3M	Transport	Turboprop	2 × 715	6,577	21,000
19.	ATR-72	Regional airliner	Turboprop	2 × 2,475	23,000	25,000
20.	Silver Eagle	Ultralight	Piston-prop	23	251	12,000

allowed, as limited by flight, structural, powerplant, functional or equipment characteristics, must be established. (2) A maximum operating altitude limitation of not more than 25,000 ft must be established for pressurized airplanes unless compliance with Section 23.775(e) is shown.

In general, the ceiling of a jet aircraft is higher than the ceiling of a propeller-driven aircraft. Table 6.6 shows the ceiling of several prop-driven aircraft. The maximum ceiling for aircraft with piston-prop engine is about 25,000 ft, and the maximum ceiling for aircraft with turboprop engine is about 40,000 ft.

6.6.2 Absolute Ceiling for Aircraft with Piston-Prop Engine

In this section, the technique to calculate the absolute ceiling of an aircraft with a piston-prop engine is presented. In a straight-level steady flight, the thrust is equal to drag:

$$T = D \tag{6.5}$$

In addition, the required power (P_R) is equal to the available power (P_A), which is supplied by the engine:

$$P_R = P_A \tag{6.139}$$

The required power is defined as aircraft drag multiplied by airspeed:

$$P_R = D \cdot V \tag{6.140}$$

The available power is equal to the engine shaft power multiplied by the propeller efficiency:

$$P_A = \eta_P \cdot P \tag{6.141}$$

The available engine power is a function of air density as defined in Chapter 4 (Equation 4.14):

$$P_{\max} = P_{\max_{SL}} \left(\frac{\rho}{\rho_o} \right)^{1.2} \tag{6.142}$$

At the absolute ceiling, aircraft must fly with the lowest required power (i.e., the minimum power airspeed) and provide the highest available power:

$$P_{R_{\min}} = P_{A_{\max}} \tag{6.143}$$

or

$$D_{\min_P} \cdot V_{\min_P} = \eta_P \cdot P_{\max} \tag{6.144}$$

As derived in Section 6.3, the true minimum power airspeed is

$$V_{\min_{P_T}} = \sqrt{\frac{2mg}{\rho S \sqrt{3C_{D_o}/K}}} \tag{6.20}$$

On the other hand, the equivalent minimum power airspeed is

$$V_{\min_{P_E}} = \sqrt{\frac{2mg}{\rho_o S \sqrt{3C_{D_o}/K}}} \tag{6.145}$$

Subscript E denotes equivalent airspeed and subscript T denotes true airspeed. Furthermore, the aircraft drag is a function of air density:

$$D = \frac{1}{2} \rho V^2 S C_D \tag{3.1}$$

As discussed in Section 6.3, an aircraft requires the minimum power if it is cruising with the minimum power speed, so

$$D_{\min_P} = \frac{1}{2} \rho V_{\min_{P_T}}^2 S C_{D_{\min_P}} = \frac{1}{2} \rho_o V_{\min_{P_E}}^2 S C_{D_{\min_P}} \tag{6.146}$$

where

$$C_{D_{\min P}} = 4C_{D_o} \tag{6.25}$$

Now we substitute Equations 6.25, 6.146, and 6.142 into Equation 6.144. Since air density (ρ) in this equation is at the ceiling, we use ρ_{ac} instead:

$$\eta_P P_{\max_{SL}} \left(\frac{\rho_{ac}}{\rho_o}\right)^{1.2} = \frac{1}{2}\rho_o V_{\min P_E}^2 S\left(4C_{D_o}\right) V_{\min P_T} \tag{6.147}$$

The true airspeed (V_T) and the equivalent airspeed (V_E) have the following relationship in terms of air density:

$$\frac{V_E}{V_T} = \sqrt{\frac{\rho}{\rho_o}} \tag{2.25}$$

So, Equation 6.147 is reformatted as

$$\eta_P P_{\max_{SL}} \left(\frac{\rho_{ac}}{\rho_o}\right)^{1.2} = \frac{1}{2}\rho_o V_{\min P_E}^2 S\left(4C_{D_o}\right) \frac{V_{\min P_E}}{\sqrt{\rho_{ac}/\rho_o}} \tag{6.148}$$

or

$$\left(\rho_{ac}\right)^{1.2} \rho_{ac}^{0.5} = \frac{\rho_o^{1.2}\rho_o\rho_o^{0.5} V_{\min P_E}^2 S\left(4C_{D_o}\right)}{2\eta_P P_{\max_{SL}}} \tag{6.149}$$

By solving this nonlinear equation for air density at the absolute ceiling (ρ_{ac}), we will have the following solution:

$$\rho_{ac} = \left(\frac{2\rho_o^{2.7} V_{\min P_E}^3 S C_{D_o}}{\eta_P P_{\max_{SL}}}\right)^{1/1.7} \tag{6.150}$$

This equation is employed to determine the absolute ceiling for an aircraft with a piston-prop engine. Note that, the subscript *E* denotes equivalent airspeed. When the air density (ρ_{ac}) is determined from Equation 6.150, refer to the atmospheric table (such as Appendix A or B) to find its corresponding altitude, which is the absolute ceiling. Please note that the minimum power speed must be greater than the stall speed; otherwise, use $k{\cdot}V_s$ (Equation 6.28).

6.6.3 Absolute Ceiling for Aircraft with Turboprop Engine

In this section, the technique to calculate the absolute ceiling of an aircraft with a turboprop engine is presented. At the absolute ceiling, aircraft must fly with the lowest required power (i.e., the minimum power airspeed) and provide the highest available power. The general technique is similar to the technique for an aircraft with

a piston-prop engine. The main difference is on the variations of turboprop engine power with altitude:

$$P = P_o\left(\frac{\rho}{\rho_o}\right)^{0.9} \quad \text{(troposphere)} \tag{4.27}$$

$$P = P_{11}\left(\frac{\rho}{\rho_{11}}\right) \quad \text{(stratosphere)} \tag{4.28}$$

By substituting these two equations into Equation 6.144, we can derive two expressions for the absolute ceiling. We have two cases: (1) absolute ceiling is assumed to be within the first layer and (2) absolute ceiling is assumed to be within the second layer. We address each case separately.

1. **Absolute ceiling is assumed to be within the first (troposphere) layer.**
   By substituting Equations 4.27, 6.25, and 6.146 into Equation 6.144, one can obtain

$$\eta_P P_{\max_{SL}}\left(\frac{\rho_{ac}}{\rho_o}\right)^{0.9} = \frac{1}{2}\rho_o V_{\min_{P_E}}^2 S\left(4C_{D_o}\right)\frac{V_{\min_{P_E}}}{\sqrt{\rho_{ac}/\rho_o}} \tag{6.151}$$

   or

$$\left(\rho_{ac}\right)^{0.9}\left(\rho_{ac}\right)^{0.5} = \frac{\rho_o^{0.9}\rho_o^{0.5}\rho_o V_{\min_{P_E}}^3 S\left(4C_{D_o}\right)}{2\eta_P P_{\max_{SL}}} \tag{6.152}$$

   After a few algebraic steps, we will have the following result:

$$\rho_{ac} = \left[\frac{2\rho_o^{2.4} V_{\min_{P_E}}^3 S C_{D_o}}{\eta_P P_{\max SL}}\right]^{1/1.4} \tag{6.153}$$

   This is used to determine the absolute ceiling for an aircraft with turboprop engine. When the air density (ρ_{ac}) is determined from Equation 6.153, refer to the atmospheric table (such as Appendix A or B) to find its corresponding altitude, which is the absolute ceiling.

2. **Absolute ceiling is assumed to be within the second (stratosphere) layer.**
   By substituting Equations 4.28, 6.25, and 6.146 into Equation 6.144, one will obtain

$$\eta_P P_{\max_{SL}}\left(\frac{\rho_{ac}}{\rho_o}\right)^{0.9}\left(\frac{\rho}{\rho_{11}}\right) = \frac{1}{2}\rho_o V_{\min_{P_E}}^2 S\left(4C_{D_o}\right)\frac{V_{\min_{P_E}}}{\sqrt{\rho_{ac}/\rho_o}} \tag{6.154}$$

   or

$$\left(\rho_{ac}\right)^{0.9}\rho_{ac}\left(\rho_{ac}\right)^{0.5} = \frac{\rho_o^{0.9}\rho_o^{0.5}\rho_o\,\rho_{11} V_{\min_{P_E}}^3 S\left(4C_{D_o}\right)}{2\eta_P P_{\max_{SL}}} \tag{6.155}$$

After a few algebraic steps, we will obtain the following expression:

$$\rho_{ac} = \left[\frac{2\rho_o^{2.4}\rho_{11} V_{\min P_E}^3 S C_{D_o}}{\eta_P P_{\max_{SL}}} \right]^{1/2.4} \tag{6.156}$$

This equation is employed to determine the absolute ceiling for an aircraft with turboprop engine. When the air density (ρ_{ac}) is determined from Equation 6.156, refer to the atmospheric table (such as Appendix A or B) to find its corresponding altitude, which is the absolute ceiling.

Equations 6.153 and 6.156 yield the absolute ceiling for a turboprop aircraft. In the practical application, it is recommended to initially assume that absolute ceiling is located within the first layer and employ Equation 6.153. If the result of the calculations disagrees with this assumption, that is, if the absolute ceiling is within the second layer, then use Equation 6.156. Please note that the minimum power speed must be greater than the stall speed; otherwise, use $k{\cdot}V_s$ (Equation 6.28).

Example 6.9

Consider a prop-driven aircraft with the following features:

$$m = 4,500\,\text{kg}, S = 42\,\text{m}^2, P_{\max_{SL}} = 671.1\,\text{kW}, C_{D_o} = 0.024, K = 0.06, \eta_P = 0.7, C_{L_{\max}} = 1.8.$$

Determine the absolute ceiling for this aircraft.

a. Assume the aircraft has a piston engine.
b. Assume the aircraft has a turboprop engine.

Solution

a. Piston-prop engine

$$V_{\min_{P_E}} = \sqrt{\frac{2mg}{\rho_o S\sqrt{3C_{D_o}/K}}} = \sqrt{\frac{2\times 4,500\times 9.81}{1.225\times 42\times\sqrt{(3\times 0.024)/0.06}}} \tag{6.145}$$

$$= 39.6\,\text{m/s} = 76.9\,\text{knot}$$

The stall speed is

$$V_{S_E} = \sqrt{\frac{2mg}{\rho_o S C_{L_{\max}}}} = \sqrt{\frac{2\times 4,500\times 9.81}{1.225\times 42\times 1.8}} = 30.9\,\text{m/s} = 60\,\text{knot} \tag{2.27}$$

The minimum power speed is greater than the stall speed.

$$\rho_{ac} = \left[\frac{2\rho_o^{2.7} V_{\min_{P_E}}^3 S C_{D_o}}{\eta_P P_{\max_{SL}}} \right]^{1/1.7} = \left[\frac{2\times 1.225^{2.7}\times 39.6^3\times 42\times 0.024}{0.7\times 671.1\times 1,000} \right]^{1/1.7} = 0.633\,\text{kg/m}^3 \tag{6.150}$$

Based on Appendix A, the corresponding altitude to this air density is 6,370 m or 20,900 ft. Thus, the absolute ceiling of this aircraft with a piston-prop engine is 20,900 ft.

b. Turboprop engine

We initially assume that absolute ceiling is within the first layer, so we use Equation 6.153:

$$\rho_{ac} = \left[\frac{2\rho_o^{2.4} V_{\min_{PE}}^3 S C_{D_o}}{\eta_P P_{\max_{SL}}}\right]^{1/1.4} = \left[\frac{2\times 1.225^{2.4}\times 39.57^3\times 42\times 0.024}{0.7\times 671.1\times 1{,}000}\right]^{1/1.4} = 0.55\,\text{kg/m}^3 \tag{6.153}$$

According to Appendix A, the corresponding altitude to this air density is 7,590 m, or 24,900 ft. Thus, the absolute ceiling of this aircraft with turboprop-driven engine is 24,900 ft. Since our guess is correct, no further calculation is required. As we expected, the absolute ceiling of this aircraft with a turboprop engine is higher than that with a piston-prop engine.

6.7 CRUISE PERFORMANCE

As shown in Figure 5.11, the major phase of the mission of a transport aircraft is cruise, which is also the longest phase. For a transport aircraft, the cruise phase of flight consumes the majority of fuel. Due to this reason, transport aircraft are usually designed for an optimum performance at their cruise speed, which frequently means the longest range. The cost of flight for a transport aircraft can be minimized by optimizing the cruising flight. A number of wing parameters such as airfoil section and setting angle are determined primarily based on the cruise performance [71]. Compared with other phases of flight, the cruise is historically the safest phase of a flight. In this section, the analysis of two topics, namely, cruise speed, and cruise altitude, will be addressed.

6.7.1 Cruise Speed

An aircraft is not usually flying with the maximum speed for a long time. The primary reason is the engine life and cost of maintenance. Two engine-rated powers often published by the engine manufacturers are: (1) maximum power, and (2) cruise power. The maximum engine power is usually employed for takeoff operation which usually takes about less than a minute. The cruise engine power is a rated power that is specific for cruise speed. This power is allowed to be employed for a long time. For instance, the turboprop engine Alison 225 generates 420 hp for takeoff and 369 hp for cruising flight. Thus, engine manufacturers do not recommend utilizing the maximum engine power for a long time; instead, they recommend employing a partial engine power for a long time such as cruising flight.

The cruising speed is always less than the maximum speed. The single-engine light aircraft Cessna 172 (Figure 3.17) with a 160 hp piston engine [79] has a cruise speed of 122 knots when flying at 8,000 ft with 75% of the engine power while having a maximum speed of 125 knots at sea level. Table 6.7 presents [9] the cruise performance of Cessna 172 (Figure 3.17) at standard flight conditions for two flight

TABLE 6.7
Cruise Performance of Cessna 172 at ISA Flight Conditions

Altitude (ft)	Shaft Rotational Speed (rpm)	Percent of Engine Power	Speed (knot)
8,000	2,650	75	122
	2,600	71	120
	2,500	64	114
	2,400	58	109
	2,300	52	103
	2,200	47	97
12,000	2,600	64	118
	2,500	58	113
	2,400	53	107
	2,300	48	101
	2,200	44	95

altitudes. The single-seat sport-plane CAP 232 [9] has a maximum level speed of 189 knot, while its maximum cruising speed at 75% power is 174 knot, and the economy cruise speed is 145 knots. It is interesting to note that this aircraft has a never exceeded the speed of 219 knots and a stall speed of 56 knots.

The aircraft speed for a long cruising flight when a percentage of the engine power (see Figure 6.3) is employed is called the cruise speed (V_C). The cruising speed is a function of various parameters such as aircraft weight, flight altitude, flight duration, distance, fuel cost, and atmospheric conditions. The cruising altitude is also a function of several parameters, including the FARs and international flight laws. As a rule of thumb for a light aircraft, the following limitations usually apply:

$$0.7\,V_{\max} < V_C < 0.9\,V_{\max} \tag{6.157}$$

There are two methods to determine the cruise speed: (1) Based on engine performance charts, and (2) Based on range mission. These two methods will be discussed separately.

6.7.1.1 Based on Engine Performance Chart

When the aircraft engine manufacturer provides the data for utilizing engine for a long-duration cruise (e.g., Table 6.7), the technique that was developed in Section 6.3 is employed to determine the cruise speed. Based on Equations 6.62 and 6.63, we can have the following equations to obtain the aircraft cruise speed:

$$nP_{\max_{SL}}\eta_P\left(\frac{\rho}{\rho_o}\right)^{0.9} = \frac{1}{2}\rho V_C^3 S C_{D_o} + \frac{2K(mg)^2}{\rho V_C S} \quad \text{(turboprop)} \tag{6.158}$$

$$nP_{\max_{SL}}\eta_P\left(\frac{\rho}{\rho_o}\right)^{1.2} = \frac{1}{2}\rho V_C^3 S C_{D_o} + \frac{2K(mg)^2}{\rho V_C S} \quad \text{(piston prop)} \tag{6.159}$$

where n is a number between 0.5 and 0.9 that determines what percentage of the maximum engine power is recommended to be used in a cruising (i.e., long) flight. The recommended values for n for various flight conditions (i.e., percent of throttle setting) should be extracted from engine charts. Hence, $nP_{\max}$ is the rated engine power for cruising flight. Table 6.1 provides cruising speeds for several prop-driven aircraft. Typically, most piston-prop aircraft use about 75% of their maximum engine power in a cruising flight. In transport aircraft, cruising speed is one of the primary considerations in sizing the engine.

Case Study - Example 6.10

The aircraft in Example 6.4 (PC-9) is recommended to employ only 75% of its maximum engine power for a cruising flight at 20,000 ft (6,096 m) altitude. Determine the aircraft's cruising speed.

Solution

From Example 6.4:

$$m_{\text{TO}} = 3{,}200\,\text{kg}, S = 16.29\,\text{m}^2, P_{\max_{\text{SL}}} = 857.5\,\text{kW}, C_{D_o} = 0.02, K = 0.06, \eta_P = 0.8.$$

At 6,096 m, from Appendix A, the air density is 0.653 kg/m^3. Since the aircraft has a turboprop engine, we use

$$nP_{\max_{\text{SL}}}\,\eta_P\left(\frac{\rho}{\rho_o}\right)^{0.9} = \frac{1}{2}\rho V_C^3 S C_{D_o} + \frac{2K(mg)^2}{\rho V_C S}$$

$$\Rightarrow 0.75\times 857.5\times 1{,}000\times 0.8\times\left(\frac{0.653}{1.225}\right)^{0.9} = 0.5\times 0.653\times V_C^3\times 16.29\times 0.02 + \frac{2\times 0.06\times(3{,}200\times 9.81)^2}{0.653\times V_C\times 16.29} \tag{6.158}$$

$$\Rightarrow 292{,}100 = 0.106V_C^3 + \frac{11{,}109{,}341}{V_C}$$

The only acceptable solution for this algebraic equation is 124; thus,

$$V_C = 124\,\text{m/s} = 240.9\,\text{knot}.$$

This cruising speed is 85% of the maximum speed (282 knot). It is observed that although only 75% of maximum engine power is used, the cruising speed is 85% of the maximum speed.

6.7.1.2 Based on Range Mission

When the engine performance charts for the optimum performance (best range) are not provided, the theoretical value of the cruise speed is determined by using the lift coefficient for the maximum range and the cruising altitude. In a constant-altitude

cruise, the lift is equal to weight, particularly when the aircraft is cruising for the purpose of maximizing range:

$$W = L_{\max_R} = \frac{1}{2}\rho_C V_C^2 S C_{L_{\max_R}} \tag{6.160}$$

When the cruise altitude is known, we can thus, obtain the cruise velocity based on the velocity to maximize the range (see Equation 6.93):

$$V_C = \sqrt{\frac{2W}{\rho_C S C_{L_{\max_R}}}} \tag{6.161}$$

where the cruise lift coefficient (C_{L_C}) is determined by Equation 6.94:

$$C_{L_C} = C_{L_{\max_R}} = \sqrt{\frac{C_{D_o}}{K}} \tag{6.162}$$

Typical values of the cruise lift coefficient for a majority of prop-driven aircraft vary from 0.2 to 0.5. These cruise lift coefficients correspond to the aircraft angle of attacks of about 2°–5°. Most prop-driven aircraft (e.g., Lockheed C-130 Hercules; Figure 8.3) have about 4°–5° of angle of attack at the beginning of cruise, while about 2°–3° of angle of attack at the end of cruising flight.

The cruising velocities of prop-driven aircraft typically vary from 150 to 350 knots. The light utility aircraft Cessna 208 Caravan with a turboprop engine [9] has a cruising speed of 175 knots at 10,000 ft. The medium transport aircraft Lockheed Super Hercules C-130J (Figure 8.3) with four turboprop engines [9] has an economic cruising velocity of 339 knots, while the maximum cruising speed is 355 knots at 25,000 ft.

Equation 6.161 suggests that the cruise speed increases with altitude (via ρ_C) and declines with aircraft weight. In addition, the value of aircraft cruise speed depends on the inverse of the wing area (indeed, its square root); as the wing area is decreased, the cruise velocity is increased. Furthermore, the aircraft cruise speed is a direct function of the square root of the wing loading (W/S). The following section provides a technique to determine the cruise altitude.

6.7.2 Cruise Altitude

Another important parameter affecting the cruising performance is the cruise altitude, which is the level portion of aircraft travel where the flight is most fuel-efficient. The cost of flight at various altitudes depends on the speed. To optimize the cruise performance, a prop-driven aircraft must be flown with a specific cruising speed at each altitude. The cruising altitudes of different aircraft are not the same. This altitude is a function of several parameters such as aircraft weight, aviation regulations, and the distance to the destination. In fact, other than practical factors (such as traffic and safety regulations), the cost of flight is the main factor to determine the cruise altitude. The calculation of the cruise altitude is a challenging problem [71] and should take into account a number of parameters simultaneously.

Figure 6.13 shows the range (in statute mile) for the light aircraft Piper PA-28 Cherokee Arrow (with a maximum takeoff weight of 2,650 lb and various throttle settings) versus altitude. The examination of Figure 6.13 shows that the range increases linearly with altitude, and also with increasing engine power. When 75% of the engine power is employed, the range is 740 miles at 7,000 ft altitude, while the range is 800 miles when 55% of the engine power is utilized. A major reason for this difference is the reduction in SFC with rated power. The aircraft is burning 10.15 gallons of fuel per hour (GPH) when 75% of the engine power [57] is employed in a cruising flight. However, with a 65% rated power, the value is 9.16 GPH, and for a 55% rated power, the value is only 8 GPH.

Typical cruise altitude for medium transport aircraft is about 25,000–30,000 ft, and the typical cruise altitude for light GA aircraft is about 15,000–25,000 ft. The service ceiling of the six-seat utility aircraft Beech Bonanza 36 with a piston engine is 18,500 ft. The service ceiling of the light utility aircraft Cessna 208 Caravan with a turboprop engine is 22,800 ft. The medium transport aircraft Lockheed Super Hercules C-130J (Figure 8.3) with four turboprop engines [78] has a cruising altitude of 28,000 ft, while the service ceiling with a mass of 66,680 kg is 30,560 ft. The average cruise altitude for a helicopter to fly at ranges is around 12,000 ft to 15,000 ft. However, the highest recorded helicopter flight occurred in 1972 as 40,820 ft.

Fundamental principles to determine the cruise altitude for a prop-driven aircraft are very similar to that for a jet aircraft. For more details, refer to Section 5.7.2.

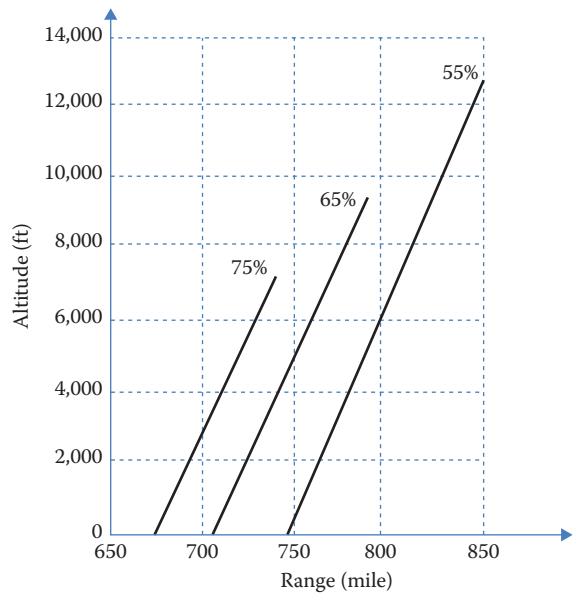

FIGURE 6.13 Range for the Cherokee Arrow versus altitude.

6.8 SUMMARY AND COMPARISON

At the end of this chapter, it is convenient to summarize the materials and also compare various speeds for jet and prop-driven aircraft. The similarities between some performance parameters for prop-driven aircraft and jet aircraft is very beneficial. Two important speeds are the minimum drag speed and the minimum power speed. Table 6.8 compares the similarities between lift coefficient, drag coefficient, and speed for three important lift-to-drag ratios. They are useful when it comes to practical applications. Table 6.8 also provides equation numbers for various flight parameters. Furthermore, Table 6.9 compares speeds for three performance parameters: range, endurance, and ceiling. In fact, these two tables present a comparison between several performance parameters for jet and prop-driven aircraft.

Table 6.10 provides typical values for a number of parameters for a fixed-wing aircraft.

TABLE 6.8
Comparison between Various Parameters for Jet and Prop-Driven Aircraft

No.	C_L and C_D	C_L	C_D	C_{D_o}	Speed	Corresponding Speed	V
1.	$\left(\frac{C_L}{C_D}\right)_{\max}$ (5.28)	$\sqrt{\frac{C_{D_o}}{K}}$ (6.10) (5.44)	$2C_{D_o}$ (6.10) (5.44)	KC_L^2 (5.47) (6.11)	$\sqrt{\frac{2W}{\rho S\sqrt{C_{D_o}/K}}}$ (5.23), (6.47)	Minimum drag speed	$V_{(L/D)_{\max}}$
2.	$\left(\frac{C_L^{3/2}}{C_D}\right)_{\max}$	$\sqrt{\frac{3C_{D_o}}{K}}$ (6.22)	$4C_{D_o}$ (6.25)	$\frac{1}{3}KC_L^2$ (6.24)	$\sqrt{\frac{2W}{\rho S\sqrt{3C_{D_o}/K}}}$ (6.20)	Minimum power speed	$0.76V_{(L/D)_{\max}}$
3.	$\left(\frac{C_L^{1/2}}{C_D}\right)_{\max}$	$\sqrt{\frac{C_{D_o}}{3K}}$ (5.104)	$\frac{4}{3}C_{D_o}$ (5.106)	$3KC_L^2$ (5.106)	$\sqrt{\frac{2W}{\rho S\sqrt{C_{D_o}/3K}}}$ (5.104)	Maximum range speed for jet aircraft	$1.32V_{(L/D)_{\max}}$

TABLE 6.9
Summary of Speeds for Various Flight Missions

	Maximum Range	Maximum Endurance	Absolute Ceiling
Prop Aircraft	$V_{\min_D}$	$V_{\min_P}$	$V_{\min_P}$
Jet Aircraft	$V_{\left(C_L^{1/2}/C_D\right)_{\max}}$	$V_{\min_D}$	$V_{\min_D}$

TABLE 6.10
Typical Values for a Number of Parameters for a Fixed-Wing Aircraft

No	Parameter	Typical Values	Name
1	C_{D_o}	0.02–0.03	Zero-lift drag coefficient – retractable landing gear
2	C_{D_o}	0.03–0.045	Zero-lift drag coefficient – fixed landing gear
3	AR	5–30	Aspect ratio
4	C_{L_C}	0.2–0.5	Cruise lift coefficient
5	$C_{L_{max}}$	1.5–2.8	Maximum lift coefficient
6	e	0.6–0.9	Oswald efficiency factor
7	η_P	0.6–0.8	Propeller efficiency
8	$(C_L/C_D)_{\max}$	6–10	Maximum lift-to-drag ratio – fixed landing gear
9	$(C_L/C_D)_{\max}$	8–30	Maximum lift-to-drag ratio – retractable landing gear

PROBLEMS

In all problems, assume a sea-level ISA condition, unless otherwise stated.

6.1 An aircraft with a prop-driven 100 hp engine is flying at a speed of 120 knots. If the propeller generates 200 lb of thrust, determine the prop efficiency.

6.2 The aircraft in Problem 6.1 has a mass of 1,000 kg, a wing area of 15 m^2, and an induced drag factor of 0.057. What is the maximum lift-to-drag ratio of this aircraft?

6.3 Calculate minimum drag speed, minimum power speed, maximum range speed, and maximum endurance speed for the aircraft in Problem 6.2. Assume aircraft maximum lift coefficient is 1.5.

6.4 A piston-prop aircraft has the following characteristics:

$$m_{\text{TO}} = 1{,}500\,\text{kg}, S = 16\,\text{m}^2, K = 0.065, C_{D_o} = 0.025, P = 223.7\,\text{kW},$$

$$\eta_P = 0.82, C_{L_{\max}} = 1.7, m_f = 300\,\text{kg}, C = 0.54\,\text{lb/h/hp}\,(91.2\,\mu\text{g/J}).$$

Plot the variations of maximum speed versus altitude. At what altitude, will the maximum speed reach its absolute maximum value?

6.5 The aircraft in Problem 6.4 is cruising at 75% of the maximum engine power at 10,000 ft. What is the aircraft's cruising speed?

6.6 Determine the absolute ceiling of the aircraft in Problem 6.4.

6.7 The pilot for the aircraft in problem 5.4 is 200 kg. The pilot is going to increase absolute ceiling of the aircraft by carrying less fuel, that is, weight reduction. What is the absolute ceiling, when the fuel tank gets empty when reaching that altitude?

6.8 The SFC of the engine for the aircraft in Problem 6.4 is 0.54 lb/h/hp (91.2 μg/J). The pilot decides to fly 500 km. How much fuel must be carried? Assume constant altitude and constant lift-coefficient.

6.9 How long the aircraft in Problem 6.4 can stay in the air (i.e., find the maximum endurance)? Assume 15,000 ft (4,572 m).

6.10 An aircraft with two turboprop engines has the following characteristics:

$$m_{TO} = 3{,}500\,\text{kg},\ S = 20\,\text{m}^2,\ K = 0.057, C_{D_o} = 0.025, P = 2 \times 447\,\text{kW},$$

$$\eta_P = 0.86,\ C_{L_{max}} = 1.8, C_{L_{max}} = 1.8,\ C = 0.6\,\text{lb/h/hp}(101.4\,\mu\text{g/J}),\quad m_f = 800\,\text{kg}.$$

Will this aircraft be able to fly at a speed of 280 knots at 25,000 ft (7,620 m)? What about at sea level?

6.11 Will the aircraft in Problem 6.10 be able to fly over the Himalayas, which has a height of 8,880 m?

6.12 The aircraft in Problem 6.10 is carrying one-half of the total fuel. What is its maximum range?

6.13 The aircraft in Problem 6.10 is flying with 80% of maximum engine power at 15,000 ft (4,572 m) to a city that is located at 2,600 km distance. When the aircraft is going to land, the pilot receives a message that the runway (sea level altitude) is busy and he or she must wait for a period. How long this aircraft can safely fly around (with a constant velocity)? Assume that fuel tanks were full at the beginning of the flight.

6.14 One of the engines of the aircraft in Problem 6.10 is inoperative. What is the absolute ceiling of this aircraft in this condition?

6.15 The aircraft in Problem 6.10 is planning to fly at its maximum speed at 5,000 ft (1,524 m). What is the range for this flight operation?

6.16 Determine the maximum range of the aircraft in Problem 6.10 at the following flight conditions:

a. Constant lift coefficient
b. Constant speed and constant altitude

6.17 The aircraft in Problem 6.10 needs to have a 30% increase in its absolute ceiling. What must be the new engine power for this requirement?

6.18 The aircraft in Problem 6.10 has a mission to fly around the globe at the equator by aerial refueling. Assume no wind and sea level. How many times must it refuel to finish this mission? Earth's radius is 6,371 km.

6.19 A military cargo aircraft with four turboprop engines has the following characteristics:

$$m_{TO} = 80{,}000\,\text{kg},\ S = 160\,\text{m}^2,\ K = 0.05,\ C_{D_o} = 0.03,\ P = 13{,}420\,\text{kW},$$

$$\eta_P = 0.86, C_{L_{max}} = 2.1,\ C = 0.75\,\text{lb/h/hp}(126.7\,\mu\text{g/J}),\ m_f = 25{,}000\,\text{kg}.$$

The aircraft is required to carry extra packages, each of which has a mass of 100 kg. How many of these packages can be carried to travel 2,000 km; as equivalent to fuel saved?

6.20 A aircraft designer is in the process of selecting a piston-prop engine for a racer aircraft that has the following characteristics:

$$m_{TO} = 1{,}800\,\text{kg},\ S = 12\,\text{m}^2,\ K = 0.055,$$

$$C_{D_o} = 0.021,\ \eta_P = 0.86,\ C_{L_{max}} = 2.1.$$

The aircraft is required to fly at a maximum speed of 500 knots. What is the required engine power?

6.21 A human-powered prop aircraft has the following characteristics:

$$m_{TO} = 95\,\text{kg},\ S = 93\,\text{m}^2,\ e = 0.95, C_{D_o} = 0.019,$$

$$\eta_P = 0.96,\ C_{L_{max}} = 1.4,\ b = 30\,\text{m}.$$

It is estimated that the pilot is capable of providing 0.5 hp of human power for 10 min.

a. What is the maximum lift-to-drag ratio?
b. Determine the minimum drag speed and minimum power speed.
c. Calculate the maximum speed of this aircraft.
d. What is the absolute ceiling of this aircraft?
e. What is the maximum range of this aircraft?

6.22 An ultralight aircraft with a piston-prop engine has the following characteristics:

$$m_{TO} = 110\,\text{kg},\ S = 10\,\text{m}^2,\ K = 0.02,\ C_{D_o} = 0.015,\ P = 3.73\,\text{kW},$$

$$\eta_P = 0.8, C_{L_{max}} = 1.6, C = 0.6\,\text{lb/h/hp}\,(101.4\,\mu\text{g/J}),\ m_f = 10\,\text{kg}.$$

Calculate the maximum speed.

6.23 Calculate the maximum range for the aircraft in Problem 6.22.

6.24 Calculate the maximum endurance for the aircraft in Problem 6.22.

6.25 Calculate the absolute ceiling for the aircraft in Problem 6.22.

6.26 Calculate the maximum speed for the aircraft in Problem 6.19.

6.27 Calculate the absolute ceiling for the aircraft in Problem 6.19.

6.28 A sedan car has the following features:

$$m = 800\,\text{kg},\ C_{D_o} = 0.05,\ P = 90\,\text{kW}.$$

This car is required to be converted to a car-aircraft that is able to fly at a speed of 200 km/h at sea level.

a. What is the required wing area to realize this requirement? Assume $K = 0.04$, $V_s = 40$ knot, $\eta_P = 0.7$, $C_{L_{max}} = 1.5$; and adding wing and tail does not increase the aircraft weight.
b. What is the absolute ceiling of such car-aircraft?

6.29 For the following piston-prop-driven aircraft,

$$S = 53\,\text{m}^2,\ m_{TO} = 5{,}000\,\text{kg},\ C_{D_o} = 0.038,\ b = 18\,\text{m},\ e = 0.86,$$

$$C = 0.64\,\text{lb/h/hp}\,(108.1\,\mu\text{g/J}),\ \eta_P = 0.83,\ C_{L_{max}} = 1.5, m_f = 1{,}300\,\text{kg}.$$

a. Determine the maximum range if the beginning altitude is 15,000 ft. Assume constant-lift coefficient.
b. Determine the maximum range speed.
c. Determine the duration to travel this range.

6.30 A regional transport aircraft with two turboprop engines has the absolute ceiling of 34,000 ft. What is the aircraft maximum speed at 12,000 ft?

$$W_{TO} = 18{,}000\,\text{lb},\ S = 342\,\text{ft}^2,\ C_{D_o} = 0.028,$$

$$\text{AR} = 9.3,\ \eta_P = 0.84,\ e = 0.86,\ C_{L_{max}} = 1.9.$$

6.31 Determine the maximum endurance for a GA aircraft with a turboprop engine and the following features:

$$S = 280\,\text{ft}^2,\ W_{\text{TO}} = 8{,}500\,\text{lb},\ K = 0.07, C_{D_o} = 0.025,\ \eta_P = 0.76,$$

$$W_f = 1{,}400\,\text{lb}, C_{L_{\max}} = 1.7,\ \text{SFC} = 0.67\,\text{lbf/hr/hp},\ P_{\max} = 800\,\text{hp}.$$

Assume the pilot will hold both airspeed and altitude constant throughout the flight operation.

6.32 An amphibian aircraft with two turboprop engines, each generating 210 hp, has the following features:

$$W = 3{,}900\,\text{lb},\ S = 270\,\text{ft}^2,\ b = 42\,\text{ft},\ e = 0.85,$$

$$C_{D_o} = 0.034,\ C_{L_{\max}} = 1.3,\ \eta_P = 0.73.$$

Calculate the absolute ceiling.

6.33 The following turboprop transport aircraft that has a fuel capacity of 17,300 kg and an SFC of 0.66 lb/h/hp (111.5 μg/J). Determine the maximum endurance (in hour) of this aircraft if it flies with a constant airspeed and constant angle of attack. Assume that the aircraft begins its flight at 25,000 ft (7,620 m) altitude.

$$S = 253\,\text{m}^2,\ m_{\text{TO}} = 69{,}200\,\text{kg},\ C_{L_{\max}} = 2.3,$$

$$K = 0.06,\ C_{D_o} = 0.022,\ \eta_P = 0.76.$$

6.34 Consider the aircraft in Problem 6.33. The aircraft is at 12,000 ft altitude with a speed of 160 KTAS. Determine the range
   a. If the pilot holds the altitude and speed constant throughout the flight
   b. If the pilot holds the lift coefficient and speed constant throughout the flight
   c. If the pilot holds the lift coefficient and altitude constant throughout the flight

6.35 Consider the aircraft in Problem 6.33. The aircraft is at 18,000 ft altitude with a speed of 110 KTAS. Determine the endurance
   a. If the pilot holds the altitude and speed constant throughout the flight
   b. If the pilot holds the lift coefficient and speed constant throughout the flight
   c. If the pilot holds the lift coefficient and altitude constant throughout the flight

6.36 A piston-prop-driven ultralight aircraft has a maximum takeoff mass of 300 kg, a wing area of 16 m^2, and a wing span of 10 m. Assume the aircraft has the following characteristics: $C_{D_o} = 0.03,\ e = 0.82,\ \eta_P = 0.7,\ C_{L_{\max}} = 1.6.$

Determine the minimum power velocity and the minimum power that the engine needs to generate at sea level so that the aircraft is airborne for a steady-level flight at 4,000 m.

6.37 A four turboprop engine-driven cargo aircraft has a maximum takeoff weight of 150,000 lb, a wing area of 1,800 ft^2, and a wing span of 130 ft. Assume the aircraft has the following characteristics:

$$C_{D_o} = 0.027,\ e = 0.82, \eta_P = 0.8,\ C_{L_{\max}} = 2.2.$$

Determine the minimum power velocity and the minimum power that the engines need to generate at sea level in order for the aircraft to be airborne for a steady-level flight at 25,000 ft.

6.38 A GA aircraft with a mass of 2,200 kg has a piston-prop engine with a maximum power of 447.4 kW. Other characteristics of this aircraft are as follows:

$$S = 23\,\text{m}^2,\ C_{D_o} = 0.026,\ K = 0.05,\ m_f = 400\,\text{kg},$$

$$C = 0.6\,\text{lb/h/hp}(101.4\,\mu\text{g/J}),\ \eta_P = 0.72,\ C_{L_{\max}} = 1.7.$$

a. Determine the range of this aircraft if it begins to cruise with a speed of 150 knots at an altitude of 6,000 m. In this flight program, the lift coefficient is kept constant. Ignore the reserve fuel, and assume the fuel in tanks is fully consumed.
b. Determine the range of this aircraft if it is cruising at a constant speed of 150 knots and at a constant altitude of 6,000 m. Assume the fuel in tanks is completely consumed. Ignore the reserve fuel, and assume the fuel in tanks is completely consumed.

6.39 A GA aircraft with a mass of 3,000 kg has a turboprop engine with a maximum power of 1,100 hp. Other characteristics of this aircraft are as follows:

$$S = 17\,\text{m}^2,\ C_{D_o} = 0.022,\ K = 0.045,\ m_f = 550\,\text{kg},$$

$$C = 0.62\,\text{lb/h/hp}(104.7\,\mu\text{g/J}),\ \eta_P = 0.74,\ C_{L_{\max}} = 2.1.$$

a. Determine the range of this aircraft if it begins to cruise with a speed of 300 knots (555.6 km/h) at an altitude of 6,000 m. In this flight program, the lift coefficient is kept constant. Ignore the reserve fuel, and assume the fuel in tanks is completely consumed.
b. Determine the range of this aircraft if it is cruising with a constant speed of 300 knots (555.6 km/h) at a constant altitude of 6,000 m. Assume the fuel in tanks is completely consumed. Ignore the reserve fuel, and assume the fuel in tanks is completely consumed.

6.40 A firefighting amphibian aircraft is equipped with two turboprop engines and has the following characteristics:

$$m_{\text{TO}} = 17{,}000\,\text{kg},\ S = 100\,\text{m}^2,\ P_{\max} = 2\times 1{,}500\,\text{kW},$$

$$C_{D_o} = 0.03,\ K = 0.04,\ \eta_P = 0.73$$

The aircraft is recommended to employ only 60% of its maximum engine power for a cruising flight at 15,000 ft altitude. Determine the aircraft cruising speed.

6.41 A GA aircraft is equipped with a piston-prop engine and has the following characteristics:

$$m_{\text{TO}} = 1{,}200\,\text{kg},\ S = 16\,\text{m}^2,\ P_{\max} = 120\,\text{kW},\ C_{D_o} = 0.035,\ K = 0.04,\ \eta_P = 0.72$$

The aircraft is recommended to employ only 70% of its maximum engine power for a cruising flight at 10,000 ft (3,050 m) altitude. Determine the aircraft cruising speed.

6.42 A military cargo aircraft with four turboprop engines has the following characteristics:

$$W_{\mathrm{TO}} = 18{,}000\ lb, S = 1{,}700\ ft^2, K = 0.05, C_{D_o} = 0.028,$$

$$P = 16{,}000\ hp, \eta_P = 0.84.$$

The aircraft is recommended to employ only 75% of its maximum engine power for a cruising flight at 35,000 ft altitude. Determine the aircraft cruising speed.

7 Climb and Descent

7.1 INTRODUCTION

A regular flight of every conventional aircraft includes a climb and a descent. Chapters 5 and 6 have dealt with a steady-level flight of a jet and propeller-driven airplane, respectively. In this chapter, we change our focus to an airplane in a steady, accelerated, and unaccelerated climbing flight.

Climb and descent are two other parameters in aircraft performance evaluation, although the climb is much more significant. Climb normally follows takeoff, and descent is necessary prior to landing (see Figure 5.11). Climb is the gain of altitude compared to a reference level (usually sea level or sometimes initial airport altitude), but descent is the loss of altitude. In climb, aircraft potential energy (PE) is increased, but in descent, the same PE is consumed. Climb needs a source of energy, that is, primarily the engine, but descent often does not need any source, since the aircraft weight is the major force for descent. The gravitational force from the earth pulls the aircraft toward its center. When an aircraft gains altitude without consuming energy or without employing engine power (e.g., from rising warm air), it is referred to as *soaring*.

There are several climb parameters for climb performance evaluation, such as rate of climb (ROC), time to climb, and climb angle. An aircraft with the highest ROC, the lowest time to climb, and the highest climb angle possesses a higher performance. Among these three criteria, the ROC is usually the most important one. In general, among various manned aircraft, fighter aircraft have the highest ROC. Among various unmanned aircraft, the anti-aircraft missile has the highest ROC. The ROC is crucial in the following two aspects: (1) operational point of view and (2) safety point of view. For both reasons, an aircraft designer tries to deliver an aircraft with the highest possible ROC. In climb analysis, we focus mainly on three major parameters:

1. Maximum ROC (fastest climb)
2. Maximum climb angle (steepest climb)
3. Minimum cost climb (most-economical climb)

There are several instances in a flight mission where the climb plays a very crucial role. Imagine that you are flying with an airplane and you suddenly encounter a major obstacle ahead – a tall building, a hill, or even a mountain. The ability of your airplane to climb up and pass over such obstacles depends critically on its climbing characteristics. Or imagine that you encounter a bad weather or turbulence at some altitude and you want to get rid of it by climbing quickly to a higher altitude. How fast you can do this depends on the climbing features of your aircraft. In cities that are located between mountains, the pilot of an aircraft needs to take extra caution to take off and climb safely as well as to descend and land safely.

DOI: 10.1201/9781003279068-7

Or imagine that you are a military fighter pilot and you scramble to take off and intercept a target at some prescribed altitude. You need to reach that target as fast as possible; how soon you can do so depends on the climbing characteristics of your fighter. In the same fighter, if you feel that an enemy missile is following and targeting you, one way to escape from such a missile is to climb to a higher altitude just by fast climbing. As a safety issue, if you lose an engine for a multiengine aircraft during a takeoff operation, the aircraft must still be able to climb safely to prevent hitting surrounding buildings.

For these and other reasons, the climb performance of an airplane is an essential part of the overall performance scenario. In some cases, the ROC is important, but in other cases, the climb angle is more crucial. Climb performance is the subject of this chapter.

Based on the statistics, the ROC of light airplanes is about 1,000–2,000 feet per minute (fpm), transport aircraft about 3,000–8,000 fpm, and fighter aircraft about 30,000–60,000 fpm. Gliders' ROC is zero (in fact, negative), as is expected. The exception is when a glider encounters a warm stream of air that is rising upward. In this circumstance, gliders will climb to higher altitudes.

The maximum ROC is basically at sea level and is decreased with altitude. At four altitudes, the ROC has a defined magnitude.

1. At absolute ceiling, the maximum ROC is zero.
2. At service ceiling, the maximum ROC is 100 fpm (0.5 m/s).
3. At cruise ceiling, the maximum ROC is 300 fpm (1.5 m/s).
4. At combat ceiling, the maximum ROC is 500 fpm (2.5 m/s).

These four altitudes (ceilings) are different, but they are unique for any given aircraft. The following sections develop some of the terminology and basic performance fundamentals of climb and descent. In this chapter, we first present the basic fundamentals of climbing flight. Then, governing equations of climb are derived. The techniques to determine several aspects of climbing flight such as the maximum ROC, the maximum climb angle, and the time to climb are discussed. Then, you will be introduced to descending flight as it is very similar to climb in many ways. The final section of this chapter is about gliding flight that is a descent without power.

7.2 BASIC FUNDAMENTALS

By definition, an aircraft in flight has an airspeed in the direction of the flight path. Consider an orthogonal three-axis coordinate system, where x is along the horizontal, z is perpendicular to x and upward, and y is perpendicular to the xz plane. Based on this assumption, the airspeed has three components in three axes: (1) horizontal component of forward speed (x-direction), (2) side component or side speed (y-direction), and (3) vertical component or upward speed (z-direction). ROC is the vertical component of aircraft airspeed. ROC depends on two parameters: aircraft airspeed (V) and climb angle (γ).

In climb analysis, three angles are influential: (1) aircraft angle of attack (α), (2) pitch angle (θ), and (3) climb angle (γ). The aircraft angle of attack is defined as the

angle between the aircraft flight path and a reference line (usually the fuselage centerline). The climb angle, γ, is defined as the angle between the instantaneous flight path direction (the direction of the relative wind, V) and the horizontal. The pitch angle is the sum of the angle of attack and the climb angle.

$$\theta = \gamma + \alpha \tag{7.1}$$

Figure 7.1 clarifies these three definitions. The aircraft angle of attack (α) and pitch angle (γ) is mostly controlled by an elevator via a stick. The climb angle (θ) is mainly controlled by thrust force. However, these three angles interact with each other simultaneously.

The maximum angle of attack of most aircraft is frequently <15°, but the maximum climb angle is often around 10°–30°. Keep in mind that γ is neither the angle of attack of the airplane (α) nor the pitch angle (θ) – a misconception frequently held initially by students new to this subject. The angle of attack is, as usual, the angle between a reference line (in aircraft) and the relative wind.

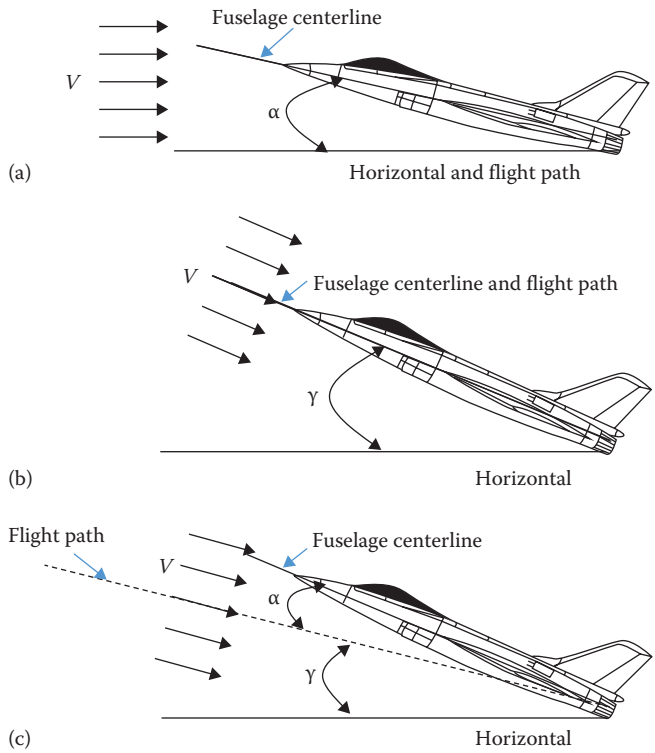

FIGURE 7.1 Climb angle and angle of attack. (a) The aircraft in cruise; (b) the aircraft in climb with zero angle of attack; and (c) the aircraft in climb with an angle of attack.

The reference line to measure the angle of attack is different for various aircraft components. For wing angle of attack (α_w), the reference line is the mean geometric chord of the wing. For horizontal tail angle of attack (α_{ht}), the reference line is the mean geometric chord of the horizontal tail. For fuselage angle of attack (α_f), the reference line is fuselage centerline. Finally, for airplane angle of attack (α_a), the reference line is a straight line passing through the fuselage centerline (or along fuselage floor).

The most important climb parameter is the ROC, which we denote as ROC. The ROC is the rate of change of altitude per unit time

$$\text{ROC} = \frac{dh}{dt} = \dot{h} \tag{7.2}$$

where h is the altitude and t is the time. For instance, if an aircraft is increasing 100 m of altitude in each 5 s, the ROC will be 100/5 = 20 m/s or 1,200 m/min or 3,936 fpm.

Now, consider Figure 7.2 that illustrates the forces on an airplane in a steady-state constant speed climb (i.e., weight [W], lift [L], drag [D], and thrust [T]). The aircraft engine often has a setting angle, i_T (often about 2°–5°).

The aircraft in Figure 7.2 is climbing with a constant acceleration (a). Based on Newton's second law, we can write the equilibrium of the forces in the direction of flight as

$$T\cos(i_T + \alpha) - D - W\sin(\gamma) = ma = m\frac{dV}{dt} \tag{7.3}$$

If we ignore the engine setting angle in our calculations, the thrust will act parallel to the flight path direction. In general, this is not quite true, but in conventional aircraft, the effects of an inclination of the thrust vector are small enough to be neglected. Furthermore, for simplicity, we may assume that the thrust line is in the direction of flight (ignoring the effect of angle of attack on engine thrust). For more simplicity,

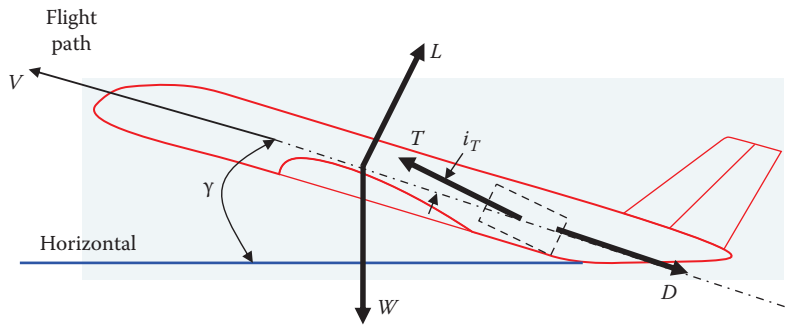

FIGURE 7.2 Forces on an aircraft in climb.

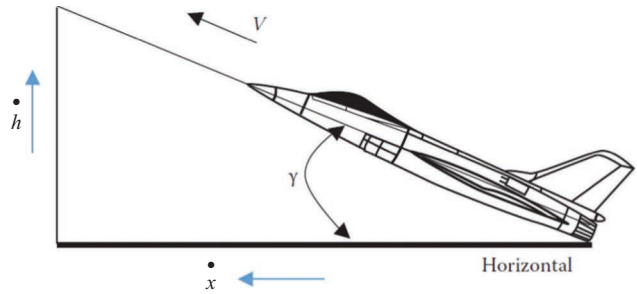

FIGURE 7.3 Aircraft speed and ROC.

we assume that all forces are passing through the aircraft center of gravity and the aircraft angle of attack is zero. Based on these simplifying assumptions, we have

$$T - D - mg\sin(\gamma) = m\frac{dV}{dt} \tag{7.4}$$

In Figure 7.3, the aircraft airspeed vector V is resolved into its horizontal and vertical components ($\dot{x}$ and $\dot{h}$), respectively. The variable $\dot{x}$ is the velocity component along the horizontal (i.e., dx/dt). In particular, the vertical component $\dot{h}$ is, by definition, the ROC of the airplane. Hence, the relationship between forward speed (V) and the ROC is:

$$V\sin(\gamma) = \frac{dh}{dt} = \dot{h} \tag{7.5}$$

Multiplying both sides by V, and substituting Equation 7.5 into 7.4, yields

$$TV - DV - mg\dot{h} = mV\frac{dV}{dt} \tag{7.6}$$

or

$$(T - D)V = \frac{d}{dt}\left[mgh + \frac{1}{2}mV^2\right] \tag{7.7}$$

The terms in Equation 7.7 are meaningful. On the right-hand side, mgh is the aircraft PE; $\frac{1}{2}mV^2$ is the aircraft kinetic energy (KE), and their summation is the total energy of the aircraft. On the left-hand side, $T - D$ is the aircraft excess force and $(T - D)V$ is called the aircraft excess power (P_{Ex}). Based on Equation 7.7, the excess power of an aircraft in climb is equal to the rate of change of aircraft energy in unit time. In other words, a climb results in a change in the total energy of the aircraft. This includes

both PE and KE. If the aircraft is climbing with a constant airspeed, the excess power is equivalent to the rate of change of PE (i.e., gaining height).

Thus, the climbing performance of an aircraft can be viewed as an energy exchange between the powerplant and the KE and PE of an aircraft. If the aircraft is in a steady level flight and the power is increased to exceed the amount needed for sustained level flight, then more work is being done on the aircraft than is required to overcome the drag. As a result, the KE or PE, or both, will increase, although there is no angle between the fuselage centerline and the horizontal. Which one increases depends on how the aircraft is being controlled.

The product of engine thrust (T) and the aircraft airspeed (V) for a level flight is referred to as *available power* (P_A). Similarly, the product of aircraft aerodynamic drag (D) and the aircraft airspeed for a level flight is called the *required power* (P_R). Thus, the excess power (P_{Ex}) is

$$P_{Ex} = (T - D)V = TV - DV = P_A - P_R \tag{7.8}$$

The concepts of "the available power" and "the required power" are valid for both jet and propeller-driven aircraft. Figure 7.4 demonstrates the variations of the available power and the required power with airspeed. As the excess power is increased, the ROC is increased too. Referring to Figure 7.4, it is noticed that the excess power has a limit (maximum), which indicates that the ROC has also a limit in any aircraft. Recall from the discussion in Chapter 4 that the engine power is decreased with altitude. So, the ROC also declines with altitude. The ROC becomes zero at an altitude called the *absolute ceiling* since there is no excess power. At that altitude, an aircraft can barely hold its altitude and is just able to cruise.

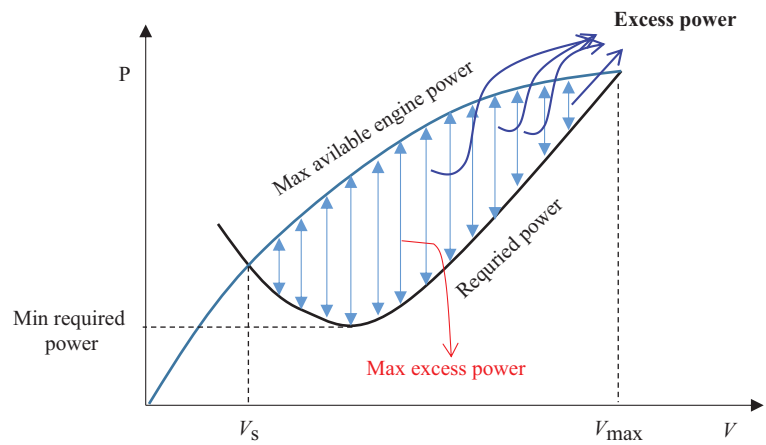

FIGURE 7.4 Variations of power with speed.

In general, two parameters can be controlled in climb: aircraft speed and altitude. In other words, there are two solutions/techniques for a climbing flight:

1. Consumption of excess energy of the engine that is not needed for a cruising flight
2. Consumption of KE of aircraft, which means the speed reduction

The first solution is a typical approach in a climb, where, as long as the engine has excess power, the aircraft will climb. In contrast, the second method implies that there is no excess power, but the airspeed and altitude are exchanged. In this technique, the KE is converted into PE. It implies, to gain height, one must lose speed. Gliders (sailplanes) and kites are able to use warm airstream energy to climb. This is an exception and we do not consider this case as an option for other aircraft.

A climbing flight can be either accelerated or unaccelerated. The first part of most climb operations is often an accelerated one up to a certain altitude. The second part follows afterward, and it is when the aircraft reaches its optimum climbing condition. In this part, the climb is unaccelerated. In this chapter, the unaccelerated climb is primarily addressed.

Figure 7.5 illustrates the climb strategy and variations of ROC [10] for the transport aircraft McDonnell Douglas DC-10-10 with altitude for two aircraft takeoff weights (240,000 and 440,000 lb). The aircraft is equipped with three GE CF6-8D high bypass ratio turbofan engines, with each generating 185 kN of thrust. After takeoff, the aircraft initially climbs while accelerating until it reaches the airspeed of 250 knots. Then, its instructed plan is to climb at 250 knots (EAS) up to 10,000 ft, then to climb at 340 knots (EAS) up to 27,880 ft, and then continue to climb at $M = 0.85$ up to the cruising altitude. The fourth climb segment has a much smaller climb angle compared with the other climb segments.

7.3 GOVERNING EQUATIONS OF CLIMB

Consider a climbing aircraft as shown in Figure 7.2 in a two-dimensional plane. In this case, the x-axis is considered to be along the flight path and the z-axis to be perpendicular to the x-axis. For a steady (unaccelerated) climb with a constant speed, V, the governing equations of motion for two axes are representing the equilibrium of forces:

$$T\cos(i_T + \alpha) - D - W\sin(\gamma) = 0 \tag{7.9}$$

$$L + T\sin(i_T + \alpha) - W\cos(\gamma) = 0 \tag{7.10}$$

We assume the aircraft as a point mass, and the thrust line coincides with the flight path (i.e., $i_T = 0$). The aircraft angle of attack is also assumed to be negligible (i.e., $\alpha = 0$). By these simplifying assumptions, Equation 7.9 will be

$$T - D - W\sin(\gamma) = 0 \tag{7.11}$$

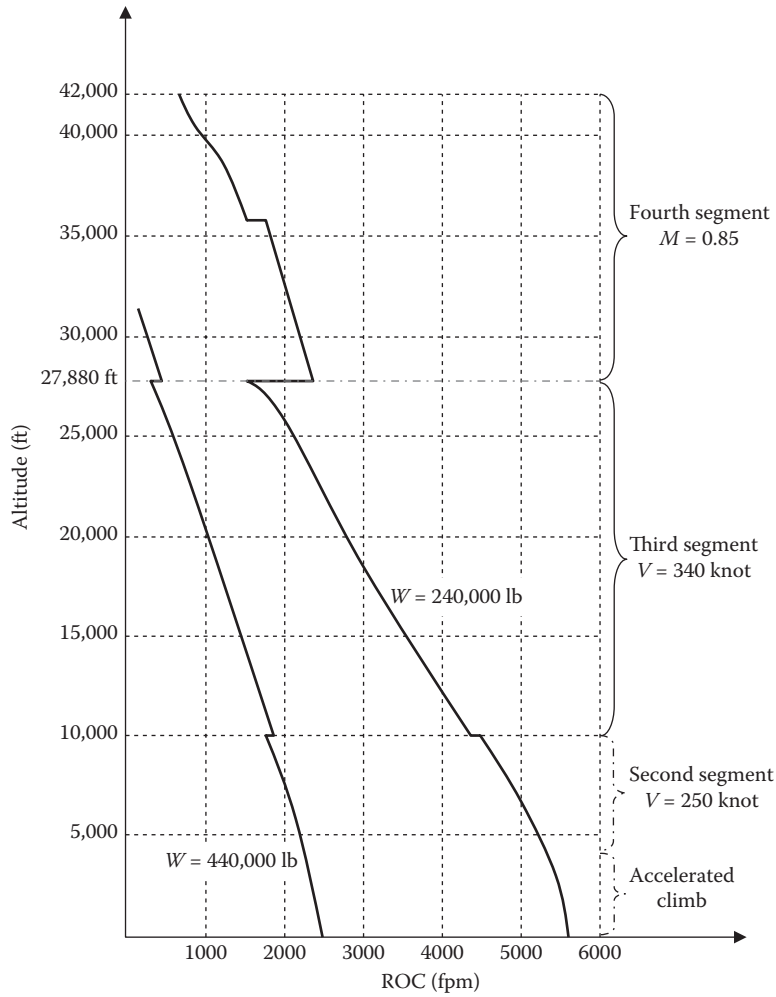

FIGURE 7.5 Variations of ROC of transport aircraft DC-10-10 versus altitude.

This represents the equilibrium of forces in the *x*-direction. Thus, the angle of climb may be calculated from the following equation:

$$\sin(\gamma) = \frac{T - D}{W} \tag{7.12}$$

In the *z*-direction, the equilibrium of forces with the simplifying assumptions will result in:

$$L - W\cos(\gamma) = 0 \tag{7.13}$$

A few results can be derived from Equations 7.12 and 7.13. From Equation 7.12, we see that the climb angle is a function of engine thrust, drag, and reciprocal of the aircraft weight. To increase the climb angle, one must increase the engine thrust and decrease the aircraft drag and weight. The heavier the aircraft, the lower the climb angle would be. The more aerodynamic the aircraft (which means less drag), the higher the climb angle would be. As the engine generates more thrust, the aircraft can climb with a higher climb angle.

The maximum possible climb angle, 90° (i.e., vertical climb), is realizable only when the numerator of Equation 7.12 (i.e., $T-D$) is greater than its denominator (i.e., weight). Moreover, the faster the aircraft flies, the lower the climb angle will be. This is because as the airspeed is increased, so does the aircraft drag. Therefore, a lighter aircraft has a better climb performance than a heavier aircraft.

Furthermore, from Equation 7.13, it can be concluded that, during a climbing flight, the lift is always less than the aircraft weight. This implies that the main part of climb capability is based on engine thrust. An aircraft with an engine with a greater thrust will have a higher climb performance than an aircraft with a lower engine thrust.

Simultaneous solution of Equations 7.11 and 7.13 enables us to analyze the climbing flight. Depending on the type of the problem (either analysis or design), we can solve for two unknown variables, for instance, the climb angle and airspeed for the purpose of aircraft performance analysis and the engine thrust and lift for an aircraft design. In the following sections, various solution approaches for various cases will be presented.

An aircraft in a climbing flight has the following three velocities:

1. Aircraft speed or airspeed, V, that is the aircraft speed relative to the air along flight path.
2. The horizontal component of the airspeed or the aircraft speed parallel to the horizontal, V_H. If there is no wind, this speed is equal to aircraft ground speed. This speed is very important in navigation and is equal to

$$V_H = \dot{x} = V\cos(\gamma) \tag{7.14}$$

3. The vertical component of the airspeed, or the aircraft speed perpendicular to the horizontal, V_V. This is – by definition – the ROC.

$$V_V = \dot{h} = \text{ROC} = V\sin(\gamma) \tag{7.15}$$

These three velocities demonstrate a triangle as sketched in Figure 7.3. These speeds are very significant in climbing flight analysis. If we multiply both sides of Equation 7.12 by the airspeed (V), we will obtain

$$V\sin(\gamma) = \frac{(T-D)V}{W} \tag{7.16}$$

The left-hand side of this equation looks familiar. Earlier in this chapter, we defined the required power and the available power. Using those terms, we can write

$$V\sin(\gamma) = \frac{TV - DV}{W} = \frac{P_A - P_R}{W} \tag{7.17}$$

The left-hand side of Equation 7.17 is, by definition, ROC (see Equation 7.5) of the aircraft

$$\text{ROC} = V\sin(\gamma) \tag{7.18}$$

It is evident that the ROC depends directly on excess power (see Figure 7.4) in combination with the inverse of the aircraft weight. The higher the thrust, the lower the drag; the lower the weight, the higher will be the climb performance – all of which make common sense even without the benefit of these equations.

Recall from Chapter 4 that both power (in propeller-driven engines) and thrust (in jet engines) decline with altitude. Referring to Equation 7.17, this results in the reduction of excess power, and consequently, a reduction of the ROC.

It is beneficial to emphasize that for a steady climbing flight, lift is less than weight (see Equation 7.13). This is because, for climbing flight, part of the weight of the airplane is supported by the thrust, and hence less lift is needed than that for a level flight. In turn, this has an impact on drag: less lift means less drag due to lift. For a given velocity V, the drag in a climbing flight is less than that for a level flight. For example, an aircraft in a climbing flight with 45° of climb angle needs to produce a lift in the amount of 86.6% of its weight (i.e., cos (30) = 0.866).

Example 7.1

A business jet aircraft with a mass of 12,700 kg and two turbofan engines each generating a thrust of 23.7 kN is climbing with an airspeed of 250 knots (463 km/h). If aircraft drag is 12,000 N, determine the ROC and climb angle. In addition, how high the aircraft will fly in 2 min? Ignore the variations of the aircraft weight, drag, and engine thrust during this period.

Solution

The aircraft ROC is

$$\text{ROC} = \frac{(T-D)V}{W} = \frac{(2\times 23{,}700 - 12{,}000)\times(500\times 0.5144)}{12{,}700\times 9.81} = 36.55\,\text{m/s} \tag{7.16}$$

The climb angle is

$$\text{ROC} = V\sin(\gamma) \Rightarrow \gamma = \sin^{-1}\left(\frac{\text{ROC}}{V}\right) = \sin^{-1}\left(\frac{36.55}{250\times 0.5144}\right)$$
$$\Rightarrow \gamma = 0.288\,\text{rad} = 16.5^\circ \tag{7.18}$$

$$\text{ROC} = \frac{dh}{dt} \Rightarrow h = \text{ROC} \cdot t = 36.55 \times 2 \times 60 = 4{,}386.7\,\text{m} = 14{,}392\,\text{ft} \qquad (7.5)$$

So, the aircraft will climb 4,387 m or 14,392 ft in 2 min.

Two important parameters in climb analysis are climb angle (γ) and ROC. In our analysis, we are looking to see at what flight conditions, these parameters are at their maximum values. So, we are looking to determine the maximum rate of climb ($\text{ROC}_{\max}$) and maximum climb angle ($\gamma_{\max}$). By knowing these two parameters, we can judge the climb performance of an aircraft. Hence, the two important climb performance criteria are

1. Fastest climb: when an aircraft ROC is at its maximum value
2. Steepest climb: when the climb angle is maximum

Both of these parameters are crucial in the climb performance analysis. The steepest climb is a significant factor in flight safety (e.g., during takeoff operation). The fastest climb is primarily important in aircraft maneuverability (e.g., fighter maneuverability when facing with an enemy fighter). In the next two sections, the analytical solutions to determine both maximum ROC and maximum climb angle for jet and propeller-driven aircraft will be introduced.

Any aircraft has the maximum ROC and the maximum climb angle at sea level. Both maximum ROC and maximum climb angle become zero at absolute ceiling. In Chapters 5 and 6, the analytical approach to determine absolute ceiling for both jet and propeller-driven aircraft is presented.

Example 7.2

Aircraft A is climbing with a speed of 200 knots and climb angle of 15°. Aircraft B is climbing with a speed of 100 knots (lower velocity) and a climb angle of 30° (higher angle).

a. Determine which aircraft has the highest ROC.
b. Determine the time to climb to 10,000 ft altitude of aircraft A and B. Ignore the variations of engine thrust with altitude.

Solution

The ROC

$$\text{ROC}_A = V\sin(\gamma) \Rightarrow (200 \times 0.5144) \times \sin(15) = 26.63\,\text{m/s} = 5{,}242\,\text{fpm} \qquad (7.18)$$

$$\text{ROC}_B = V\sin(\gamma) \Rightarrow (100 \times 0.5144) \times \sin(30) = 25.72\,\text{m/s} = 5{,}063.4\,\text{fpm} \qquad (7.18)$$

Thus, the ROC of aircraft A is higher than the ROC of aircraft B.

Time to climb

$$\text{ROC} = \frac{dh}{dt} \Rightarrow t = \frac{h}{\text{ROC}_A} \Rightarrow t_A = \frac{10{,}000}{5{,}242} = 1.9\,\text{min} \qquad (7.2)$$

$$t_B = \frac{10{,}000}{5{,}063.4} = 1.97\,\text{min} \tag{7.2}$$

Example 7.3

Aircraft A is climbing with a speed of 180 knots and ROC of 2,600 fpm. Aircraft B is climbing with a speed of 150 knots and ROC of 3,000 fpm. Which aircraft has the highest climb angle?

Solution

The climb angle is obtained by using the following equation:

$$\begin{aligned} \text{ROC} = V\sin(\gamma) \Rightarrow \gamma_A &= \sin^{-1}\left(\frac{\text{ROC}}{V}\right) \\ &= \sin^{-1}\left(\frac{2{,}600}{180\times 0.5144\times 196.85}\right) \Rightarrow \gamma_A = 8.2^\circ \end{aligned} \tag{7.18}$$

$$\text{ROC} = V\sin(\gamma) \Rightarrow \gamma_B = \sin^{-1}\left(\frac{3{,}000}{150\times 0.5144\times 196.85}\right) \Rightarrow \gamma_B = 11.4^\circ \tag{7.18}$$

Thus, the climb angle of aircraft B is higher than the climb angle of aircraft A.

Currently, the highest ROC and the highest climb angle belong to fighter aircraft. These aircraft are able to climb with 90° of climb angle (e.g., single-seat fighter aircraft General Dynamics [now Lockheed Martin] F-16 Fighting Falcon, Figure 7.6) and an ROC of about 60,000 fpm. So, other than helicopters, several fighter aircraft are able to climb vertically. This means that their engine thrusts are greater than their aircraft weights.

FIGURE 7.6 A Lockheed F-16CJ Fighting Falcon in a climbing flight. (Courtesy of Steve Dreier.)

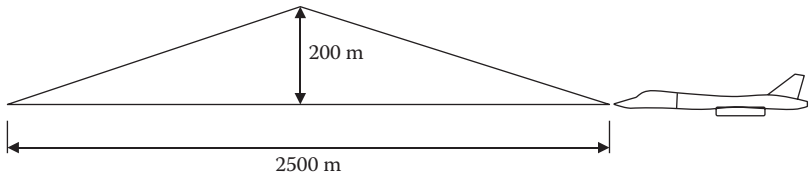

FIGURE 7.7 Aircraft in Example 7.4.

Example 7.4

Aircraft A and B in Example 7.3 are just facing a mountain with a height of 200 m and a diameter of 2,500 m. Which aircraft can safely fly over this mountain and survive?

Solution

Based on geometry of the mountain (sketched in Figure 7.7), the slope of the mountain is

$$\gamma = \tan^{-1}\left(\frac{200}{2{,}500/2}\right) = 9.1^\circ$$

The aircraft must have at least a climb angle higher than 9.1° to fly safely over the mountain.

Any aircraft that has a climb angle lower than this number will hit the mountain and crash. Since $\gamma_B > 9.1^\circ$ and $\gamma_A < 9.1^\circ$, aircraft B will safely fly over the mountain, but aircraft A will hit and crash into the mountain.

7.4 FASTEST CLIMB

The most important climb parameter in fighter aircraft is the fastest climb. The fastest climb is when an aircraft is climbing with the ROC_{max} condition. Fastest climb is synonymous with a climb at the maximum rate and is of much greater interest to us than the steepest climb. Fastest climb requires the minimum time to climb to a specified altitude, which is of high importance to air traffic control and must keep the air space clear of traffic. The fastest climb often requires the smallest amount of fuel and thus will result in more available fuel for cruising flight. This flight condition has a specific climb speed and a specific climb angle.

The altitude where the maximum ROC is zero is the highest altitude achievable in a steady-level flight. In Chapter 5, we defined the absolute ceiling as the altitude where $ROC_{max} = 0$. A more useful quantity is the service ceiling, conventionally defined as the altitude where $ROC_{max} = 100$ ft/min. The service ceiling represents the practical upper limit for a steady-level flight.

In Figure 7.8, the maximum ROC (on the abscissa) is plotted versus altitude (on the ordinate); for many conventional airplanes, this variation is almost (but not precisely) linear. The absolute, service, and cruise ceilings are also depicted in Figure 7.8, which illustrates a graphical technique for finding these ceilings.

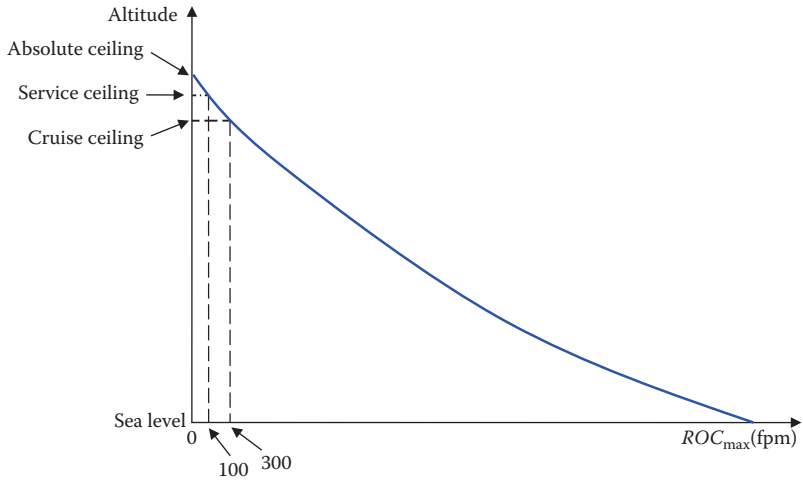

FIGURE 7.8 Typical variations of the maximum ROC versus altitude.

A temporary or instantaneous climb does not have a performance value. For instance, consider a general aviation (GA) aircraft that is not able to climb vertically. If the aircraft pilot suddenly decides to increase the aircraft climb angle to 90°, this is possible for a very short time, since the initial energy of the aircraft lets the pilot do so. But this flight situation cannot be sustained because the aircraft speed will decrease very rapidly and goes to zero.

Hence, the pilot has to return to normal cruising flight; otherwise, the aircraft will definitely go into a descending situation (such as a spin) that may be uncontrollable. Three parameters affecting the fastest climb are (1) engine power (for propeller-driven aircraft) or engine thrust (for jet aircraft), (2) aircraft speed, and (3) climb angle.

In this section, an analytical approach to determine the maximum ROC for both jet and propeller-driven aircraft is presented. In Section 7.5, we will discuss the influence of climb angle on climbing flight. Section 7.4.1 is devoted to the analysis of the fastest climb for jet aircraft, while Section 7.4.2 is devoted to the analysis of the fastest climb for propeller-driven aircraft.

7.4.1 Jet Aircraft

Based on Equation 7.18, the fastest climb or the ROC_{max} is when an aircraft climbs with a speed for maximum rate of climb $\left(V_{ROC_{max}}\right)$ and employs the climb angle that submits the maximum rate of climb $\left(\gamma_{ROC_{max}}\right)$:

$$ROC_{max} = V_{ROC_{max}} \sin\left(\gamma_{ROC_{max}}\right) \tag{7.19}$$

Now, we need to determine two parameters: (1) $V_{ROC_{max}}$, and (2) $\left(\gamma_{ROC_{max}}\right)$. These two variables are independent of each other and their calculation techniques are presented in Sections 7.4.1.1 and 7.4.1.2, respectively.

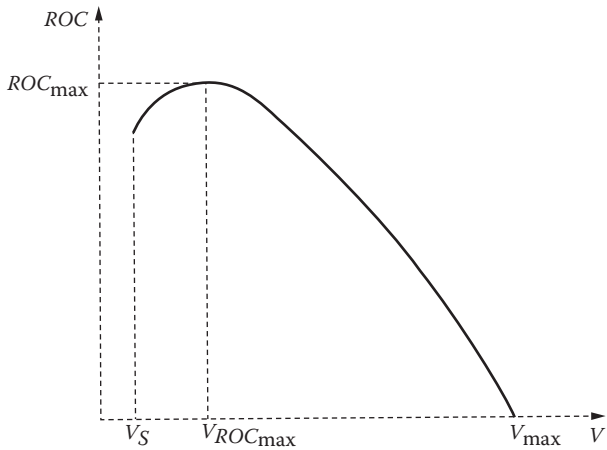

FIGURE 7.9 Effect of the aircraft speed on the ROC.

7.4.1.1 Calculation of Speed for Maximum ROC

As the engine thrust is increased, the climb gets faster (and also steeper). This is evident from Equations 7.12 and 7.18. As we increase the aircraft velocity, the ROC will initially increase up to a maximum value and then decreases. If the pilot decides to increase the ROC further, (s)he must reduce the climb angle, which results in a decrease in ROC (see Figure 7.9). This will continue until the aircraft reaches it maximum speed. At this condition, a climb is no longer possible and the ROC will be zero.

As defined in Section 7.3 (combining Equations 7.16 and 7.18), the ROC is

$$\mathrm{ROC} = \frac{TV - DV}{W} \tag{7.20}$$

This expression indicates that the ROC is proportional to the excess power per unit weight (see Figure 7.4). To maximize the ROC, the numerator must be maximized, while the denominator (aircraft weight) is minimized:

$$\mathrm{ROC}_{\max} = \frac{(TV - DV)_{\max}}{W_{\min}} \tag{7.21}$$

For simplicity, we assume that the engine thrust is constant with aircraft speed. The ROC can be maximized by setting its first derivative with respect to the true airspeed equal to zero; that is,

$$\frac{d}{dV}\mathrm{ROC} = \frac{d}{dV}\left[\frac{(TV - DV)}{W}\right] = 0 \tag{7.22}$$

Carrying out this differentiation, when the aircraft weight is assumed constant, produces the condition for the fastest climb of a jet aircraft

$$T - D - V\frac{dD}{dV} = 0 \tag{7.23}$$

In Section 5.3.1, for a level flight, we had the following equation for drag force:

$$D = C_{D_o}\frac{1}{2}\rho V^2 S + \frac{2KW^2}{\rho V^2 S} \tag{5.35}$$

Since the climb angle is frequently small, we can also use this expression for the drag force in a climbing flight. The differentiation of this drag with respect to velocity is

$$\frac{dD}{dV} = C_{D_o}\rho VS + \frac{1}{3}\frac{2KW^2}{\rho S}\frac{1}{V^3} \tag{7.24}$$

Substituting Equations 5.35 and 7.24 into Equation 7.23 and reformatting, we will obtain

$$T - C_{D_o}\frac{1}{2}\rho V^2 S + \frac{2K(W)^2}{\rho V^2 S} - V\left[C_{D_o}\rho VS + \frac{1}{3}\frac{2K(W)^2}{\rho S}\frac{1}{V^3}\right] = 0 \tag{7.25}$$

or

$$T - C_{D_o}\frac{3}{2}\rho V^2 S + \frac{2K(W)^2}{\rho V^2 S} - \left[\frac{2}{3}\frac{K(W)^2}{\rho S}\frac{1}{V^3}\right] = 0 \tag{7.26}$$

which simplifies to

$$T - C_{D_o}\frac{3}{2}\rho V^2 S + \frac{4K(W)^2}{3\rho V^2 S} = 0 \tag{7.27}$$

Dividing this equation by $2/\left(3\rho C_{D_o} S\right)$ results in

$$V^2 - \frac{2T}{3\rho C_{D_o} S} - \frac{4K(W)^2}{3\rho^2 V^2 C_{D_o} S^2} = 0. \tag{7.28}$$

We can further simplify this equation by recalling from Chapter 5 that maximum lift-to-drag ratio is

$$\left(\frac{L}{D}\right)_{\max} = \frac{1}{2\sqrt{KC_{D_o}}} \tag{5.24}$$

Hence,

$$V^4 - \frac{2T}{3\rho C_{D_o} S} V^2 - \frac{1}{3}\left[\frac{W}{\rho V C_{D_o} S\left(L/D\right)_{\max}}\right]^2 = 0 \tag{7.29}$$

Equation 7.29 is a quadratic equation in terms of V^2. Solving for an acceptable solution (a reasonable airspeed) yields the following expression:

$$V_{\mathrm{ROC}_{\max}} = \sqrt{\frac{T}{3\rho C_{D_o} S}\left[1 + \sqrt{1 + \frac{3}{\left[\left(\frac{L}{D}\right)_{\max}\frac{T}{W}\right]^2}}\right]} \tag{7.30}$$

This equation yields the airspeed to deliver the maximum ROC. Any solution that yields a negative speed or any complex number is neglected, since it is not a realistic option. In addition, any velocity lower than the stall speed is not acceptable. In pilot terminology, V_y refers to the velocity at which $\mathrm{ROC}_{\max}$ occurs, while V_x refers to the velocity at which maximum climb angle occurs.

It is noticed that the speed for maximum climb rate is strongly dependent on the engine thrust that for a given throttle setting decreases with altitude. To increase the $\mathrm{ROC}_{\max}$ (through $V_{\mathrm{ROC}_{\max}}$), one must increase the engine thrust. This speed is also a function of the altitude (ρ) and the wing area, zero-lift drag coefficient, and the maximum lift–drag ratio.

At the absolute ceiling for a given throttle setting, the thrust-to-weight ratio is equal to the reciprocal of the maximum lift-to-drag ratio, so that the term inside the bracket at the ceiling is equal to three (i.e., $1+2$). Since the *T/W* ratio has its largest magnitude at sea level, the sea-level magnitude of the term in the bracket will approach a magnitude of 2 for large values of the product of $(L/D)_{\max}$ and *T/W*. Consequently, the term in the bracket will take a magnitude between 2 and 3.

Equation 7.29 is a mathematical expression. It may not always submit a reasonable solution. If the solution is a speed that is less than the stall speed (V_s), we have to resort to a safe speed. The reason is that a safe and continuous climb for a conventional aircraft with a speed less than the stall speed is impossible. So, in this case, the speed for $\mathrm{ROC}_{\max}$ must be higher than the stall speed

$$V_{\mathrm{ROC}_{\max}} = kV_s \tag{7.31}$$

where *k* is a factor between 1.1 and 1.3. For civil aircraft, the parameter *k* is between 1.2 and 1.3, but for military aircraft, *k* is between 1.05 and 1.15. The exact magnitude of *k* depends on several factors such as mission of the aircraft and airworthiness regulations. The $\mathrm{ROC}_{\max}$ is obtained by substituting $V_{\mathrm{ROC}_{\max}}$ from Equation 7.29 into Equation 7.19.

7.4.1.2 Calculation of Climb Angle for Maximum ROC

The maximum ROC (Equation 7.19) has two variables, one of which was calculated in Section 7.4.1.1 (Equation 7.30). The technique to determine the second parameter $\left(\gamma_{ROC_{max}}\right)$ is described in this section. The governing equations of motion of an aircraft in a climb that is delivering ROC_{max} are obtained from original governing equations of motion of a regular climbing flight (Equations 7.11 and 7.13). We only need to replace general climb angle (γ) with climb angle for the maximum ROC $\left(\gamma_{ROC_{max}}\right)$ and the general airspeed with the speed for maximum ROC (i.e., $V_{ROC_{max}}$)

$$T - D - W\sin\left(\gamma_{ROC_{max}}\right) = 0 \tag{7.32}$$

$$L - W\cos\left(\gamma_{ROC_{max}}\right) = 0 \tag{7.33}$$

where lift (L) and drag (D) are obtained in a similar manner to any other flight conditions (Equations 2.4 and 2.5). We also need to replace general airspeed (V) and lift coefficient (C_L) for those of the maximum ROC $\left(V_{ROC_{max}}\right)$

$$L = \frac{1}{2}\rho V_{ROC_{max}}^2 S C_{L_{ROC_{max}}} \tag{7.34}$$

$$D = \frac{1}{2}\rho V_{ROC_{max}}^2 S C_{D_{ROC_{max}}} \tag{7.35}$$

Lift coefficient and drag coefficient are related through parabolic drag polar (Equation 3.12):

$$C_{D_{ROC_{max}}} = C_{D_o} + K C_{L_{ROC_{max}}}^2 \tag{7.36}$$

Equations 7.32–7.36 are five simultaneous nonlinear algebraic equations. To find $\gamma_{ROC_{max}}$, we need to solve these five equations simultaneously. The five unknown variables are climb angle for the maximum ROC $\left(\gamma_{ROC_{max}}\right)$, drag ($D$), lift ($L$), lift coefficient ($C_L$), and drag coefficient (C_D). The first unknown is the one we are looking for and the other four unknowns are intermediate variables. One way to solve for unknowns is to employ a numerical analysis technique.

However, there is another easier and direct way to find a closed-form solution for the angle corresponding to the maximum ROC, $\gamma_{ROC_{max}}$. Solving Equation 7.31 for $\gamma_{ROC_{max}}$ yields

$$\gamma_{ROC_{max}} = \sin^{-1}\left[\frac{T - D_{ROC_{max}}}{W}\right] \tag{7.37}$$

Substituting Equations 7.33–7.36 into this equation, and after some algebraic manipulation (the details are left to the interested reader), we will obtain the following expression:

$$\gamma_{\mathrm{ROC}_{\max}} = \sin^{-1}\left[\frac{T}{W} - \frac{\rho V_{\mathrm{ROC}_{\max}}^2 S C_{D_o}}{2W} - \frac{2KW}{\rho S V_{\mathrm{ROC}_{\max}}^2}\right] \tag{7.38}$$

An elaborate expression of Equation 7.38 is obtained by factoring the weight (W). This operation results in the following formula for the angle corresponding to the maximum ROC:

$$\gamma_{\mathrm{ROC}_{\max}} = -\sin^{-1}\left[\frac{0.25}{KW}\left(\sqrt{-8K\rho TSV_{\mathrm{ROC}_{\max}}^2 + \rho^2 S^2 V_{\mathrm{ROC}_{\max}}^4 \left(1 + 4KC_{D_o}\right)} - \rho S V_{\mathrm{ROC}_{\max}}^2\right)\right] \tag{7.39}$$

This climb angle $\left(\gamma_{\mathrm{ROC}_{\max}}\right)$ will be substituted along with the speed for $\mathrm{ROC}_{\max}$ (Equation 7.30) into Equation 7.19 to determine $\mathrm{ROC}_{\max}$ for jet aircraft.

If there are no flight constraints or limitations, the fastest climb of a jet aircraft will obviously occur when the maximum thrust is used. Examination of the fastest climb relationships (including Equations 7.32 and 7.39) shows that a jet aircraft with a high ROC is characterized by one or more of the following: a large engine thrust (T), a large wing area (S), a low weight (W), a large maximum lift-to-drag ratio, $(L/D)_{\max}$, and a small zero-lift drag coefficient. The absolute $\mathrm{ROC}_{\max}$ occurs at the sea level and decreases with altitude, going to zero at the absolute ceiling.

Figure 7.10 shows the calculated $\mathrm{ROC}_{\max}$ for a large twin-engine jet transport aircraft with a maximum takeoff mass of 200,000 kg. From this figure, the absolute ceiling for this aircraft is estimated to be 38,000 ft. The curves of Figure 7.10 were prepared for two flight conditions: (1) all (both) engines operating and (2) one engine operating. The calculations were repeated using only one engine to estimate engine-out performance. Observe that losing an engine more than halves the ROC since the ROC is proportional to the difference between the thrust and drag – not the thrust alone.

From Equations 7.19, 7.21, and 7.35, we can derive a few important conclusions. To improve the climb performance for a jet aircraft to increase the maximum climb rate, one must

1. Increase engine thrust
2. Reduce aircraft weight
3. Reduce wing area
4. Reduce wing aspect ratio
5. Reduce aircraft zero-lift drag coefficient

These are the factors that can be changed in the aircraft design process. For design and optimization analyses, these factors are the most critical ones.

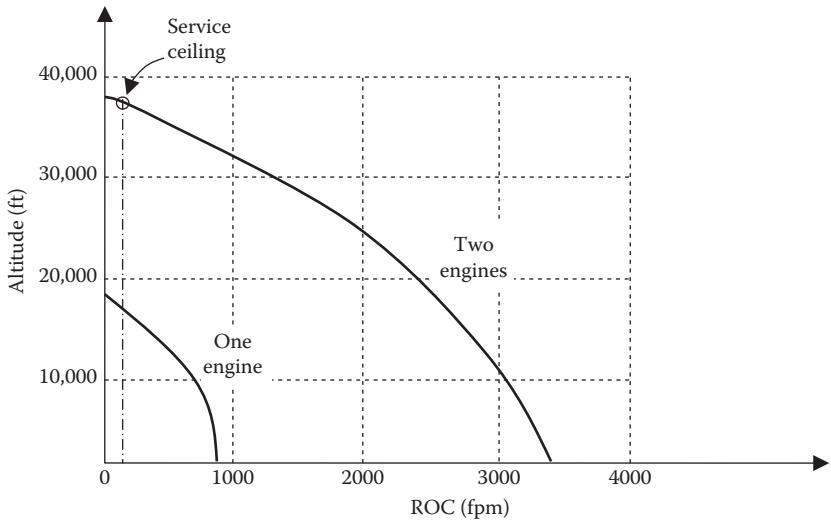

FIGURE 7.10 Maximum rate of climb for a twin-engine large transport jet aircraft.

Case Study - Example 7.5

The fighter jet aircraft McDonnell Douglas (now Boeing) F/A-18 (Figure 8.10a) with two turbofan engines has the following features:

$$m_{\text{TO}} = 23{,}500\,\text{kg},\ S = 38\,\text{m}^2,\ b = 12.3\,\text{m},\ e = 0.9,\ C_{L_{\max}} = 2.4,$$
$$T = 2 \times 79.2\,\text{kN}\left(\text{with afterburner}\right)$$

Assume that the clean zero-lift drag coefficient of this fighter is 0.015. Determine the maximum ROC if the aircraft flies with a mass of 16,000 kg.

Solution

We first need to calculate a few parameters:

$$\text{AR} = \frac{b^2}{S} = \frac{12.3^2}{38} = 3.98 \tag{3.9}$$

$$K = \frac{1}{\pi e\,\text{AR}} = \frac{1}{3.14 \times 0.9 \times 3.98} = 0.089 \tag{3.8}$$

$$\left(\frac{C_L}{C_D}\right)_{\max} = \frac{1}{2\sqrt{KC_{D_o}}} = \frac{1}{2\sqrt{0.089 \times 0.015}} = 13.7 \tag{5.24}$$

The speed for ROC_{max} is

$$V_{ROC_{max}} = \sqrt{\frac{T}{3\rho C_{D_o} S}\left[1+\sqrt{1+\frac{3}{\left[\left(\frac{L}{D}\right)_{max}\frac{T}{W}\right]^2}}\right]}$$

$$= \sqrt{\frac{2\times 79{,}200}{3\times 1.225\times 0.015\times 38}\left[1+\sqrt{1+\frac{3}{\left[13.7\times\frac{2\times 79{,}200}{16{,}000\times 9.81}\right]^2}}\right]} \quad (7.30)$$

$$= 389.6\,\text{m/s}$$

We need to compare this speed with the stall speed at the current weight

$$V_s = \sqrt{\frac{2mg}{\rho S C_{L_{max}}}} = \sqrt{\frac{2\times 16{,}000\times 9.81}{1.225\times 38\times 2.4}} = 53\,\text{m/s} \quad (2.49)$$

The ROC_{max} speed is higher than the stall speed so that it is acceptable.

Calculation of the climb angle:

$$\gamma_{ROC_{max}}$$

$$= -\sin^{-1}\left[\frac{0.25}{KW}\left(\sqrt{-8K\rho TSV_{ROC_{max}}^2+\rho^2 S^2 V_{ROC_{max}}^4\left(1+4KC_{D_o}\right)}-\rho SV_{ROC_{max}}^2\right)\right] \quad (7.39)$$

Substitution

$$\frac{0.25}{KW} = \frac{0.25}{0.089\times 156{,}906} = 0.000018\,\text{N}^{-1}$$

$$8K\rho TSV_{ROC_{max}}^2 = 8\times 0.089\times 1.225\times 158{,}400\times 38(389.6)^2 = 7.95\times 10^{11}\,\text{N}^2$$

$$\rho^2 S^2 V_{ROC_{max}}^4 = (1.225)^2(38)^2(389.6)^4 = 5\times 10^{13}\,\text{N}^2$$

$$4KC_{D_o} = 4\times 0.089\times 0.015 = 0.0053$$

$$\rho SV_{ROC_{max}}^2 = (1.225)(38)(389.6)^2 = 7.07\times 10^6\,\text{N}$$

$$\gamma_{ROC_{max}} = -sin^{-1}\left[0.000018\times\left(\sqrt{-7.95\times 10^{11}+5\times 10^{13}\times(1+0.0053)}-7.07\times 10^6\right)\right] = 42.3^\circ$$

The maximum ROC:

$$ROC_{max} = V_{ROC_{max}}\sin\left(\gamma_{ROC_{max}}\right)$$
$$= 389.6\times\sin(42.3) \Rightarrow ROC_{max} = 262.4\,\text{m/s} = 51{,}658\,\text{fpm} \quad (7.19)$$

This is very close to the published data.

Case Study - Example 7.6

Consider the business jet aircraft Hawker 800 (with twin turbofan engines) with a mass of 12,700 kg and a maximum engine thrust of 2×23.7 kN. Assume the pilot is utilizing the maximum thrust in a climbing flight and the following characteristics:

$$S = 34.75\,\text{m}^2, \quad C_{D_o} = 0.02, \quad K = 0.05$$

a. Plot the variations of ROC with respect to airspeed for various altitudes up to 10,000 m.
b. Plot the variations of climb angle corresponding to ROC_{max} versus altitude.

Include the variations of the engine thrust during this period. Ignore the reduction of aircraft weight as it climbs.

Solution

a. The main governing equation for ROC versus airspeed is Equation 7.17. We mainly need to vary airspeed and altitude to determine the corresponding ROC. For this purpose, a MATLAB® file is written to repeat the calculations. Figure 7.11 illustrates the results. The variations of engine thrust are modeled with Equation 4.19.

   The figure shows the results for 11 altitudes from sea level to 10,000 m. It is observed that each altitude has a unique maximum ROC, and it is happening at a unique airspeed. For instance, the maximum ROC at sea level is 9,328 ft/min (47.4 m/s) at a velocity of 379 knots (702 km/h), while the maximum ROC at 10,000 m is 2,400 ft/min (12.2 m/s) at a velocity of 402 knots (702 km/h).

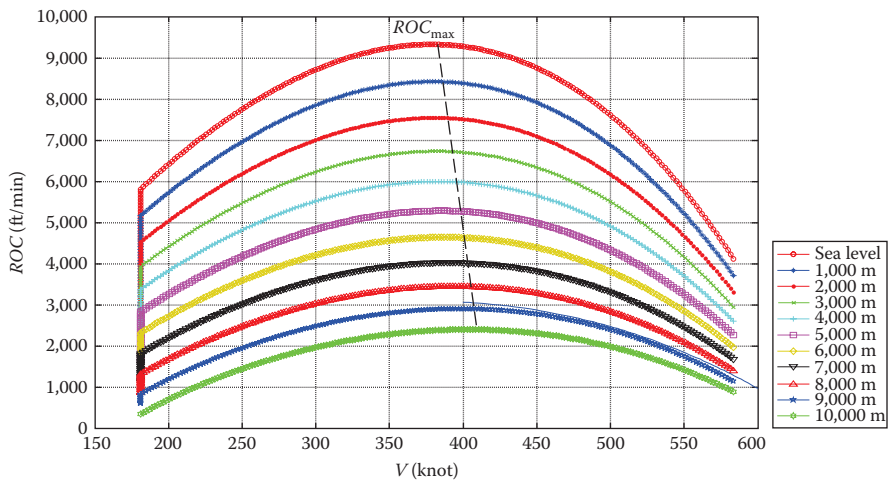

FIGURE 7.11 Theoretical ROC for a business jet aircraft Hawker 800.

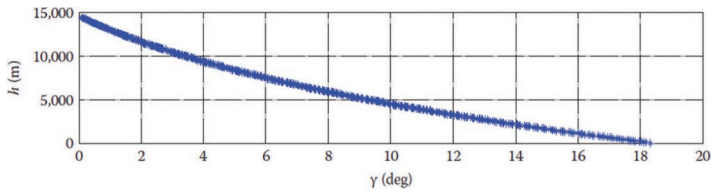

FIGURE 7.12 Variations of the climb angle corresponding the maximum rate of climb versus altitude.

b. This part is very similar to Example 7.5, whereas the governing equation is 7.39. This time, we vary altitude, and the MATLAB code will carry out the calculations and plot the result (See Figure 7.12).

7.4.2 Propeller-Driven Aircraft

The basic fundamentals and general techniques to calculate the ROC_{max} for propeller-driven aircraft (with either turboprop or piston-prop engine) are very similar to those described and developed for jet aircraft. Similar to the technique for jet aircraft, the ROC_{max} for propeller-driven aircraft will be obtained from

$$ROC_{max} = V_{ROC_{max}} \sin\left(\gamma_{ROC_{max}}\right) \tag{7.19}$$

But the technique to determine the maximum ROC velocity $\left(V_{ROC_{max}}\right)$ and the climb angle for maximum ROC $\left(\gamma_{ROC_{max}}\right)$ is different from those for jet aircraft. These two parameters ($V_{ROC_{max}}$ and $\gamma_{ROC_{max}}$) are determined separately, and their calculation techniques are presented in Sections 7.4.2.1 and 7.4.2.2, respectively.

7.4.2.1 Airspeed for Maximum ROC

In propeller-driven aircraft, the engine thrust is a function of power, propeller efficiency, and airspeed (see Equation 4.2). Thus, the available power (i.e., TV) is

$$TV = P\eta_P \tag{7.40}$$

The substitution of this equation into Equation 7.20 yields

$$ROC = \frac{P\eta_P - DV}{W} \tag{7.41}$$

By inspection of this equation, we can conclude that the maximum ROC for a propeller aircraft, assuming the weight is constant, is achieved when the available power is maximized, and the required power (DV) is minimized

$$ROC_{max} = \frac{\left(P\eta_P\right)_{max} - (DV)_{min}}{W} \tag{7.42}$$

Hence, to maximize the ROC, we need to do the following:

1. Maximize available engine power
2. Maximize propeller efficiency
3. Minimize the product of aircraft drag (D) and airspeed (V)

The combination of items 1, 2, and 3 implies that the excess power must be maximized:

$$\mathrm{ROC}_{\max} = \frac{(P_{\mathrm{Ex}})_{\max}}{W} \tag{7.43}$$

If the propeller efficiency can be kept constant at its highest magnitude (e.g., using a variable pitch-prop), the maximization of excess power occurs when the aircraft flies with the minimum power speed $\left(V_{\min_P}\right)$. Therefore,

$$V_{\mathrm{ROC}_{\max}} = V_{\min_P} \tag{7.44}$$

Hence, the aircraft speed for $\mathrm{ROC}_{\max}$ for a variable-pitch propeller-driven aircraft (using Equation 6.20) is

$$V_{\mathrm{ROC}_{\max}} = \sqrt{\frac{2mg}{\rho S\sqrt{\frac{3C_{D_o}}{K}}}} \quad (\text{variable-pitch prop}) \tag{7.45}$$

However, if a fixed-pitch propeller is employed, we need to determine speed that minimized the excess power. We know that the maximum power and minimum DV occur at very different speeds. We do not have a mathematical equation that models the variations of prop efficiency as a function of speed for all aircraft.

It is mathematically hard to calculate such speed, but climbing at a higher speed than the minimum power speed will increase the prop efficiency and increases the maximum available power (See Figure 7.4). Hence, a higher airspeed (See Figure 4.35) will yield a better fastest-climb performance. The $\mathrm{ROC}_{\max}$ speed is experimentally found to be about 50% greater than minimum power speed.

$$V_{\mathrm{ROC}_{\max}} = kV_{\min_P} = k\sqrt{\frac{2mg}{\rho S\sqrt{\frac{3C_{D_o}}{K}}}} \quad (\text{fixed-pitch prop}) \tag{7.46}$$

where k is experimentally determined to be between 1.3 and 1.4.

For the Cessna 172 (from the POH and the FAA), the $V_{\min_D} = 65\,\text{knot}, V_{\min_P} = 49\,\text{knot}$ while $V_{\mathrm{ROC}_{\max}} = 73\,\text{knot}$. In pilot terminology, V_x refers to the velocity at which maximum climb angle occurs (best angle-of-climb speed), while V_y refers to the velocity at which $\mathrm{ROC}_{\max}$ occurs (best rate-of-climb speed). Figure 7.13 demonstrates the typical variations of ROC and climb angle for a typical piston-prop as a function of airspeed.

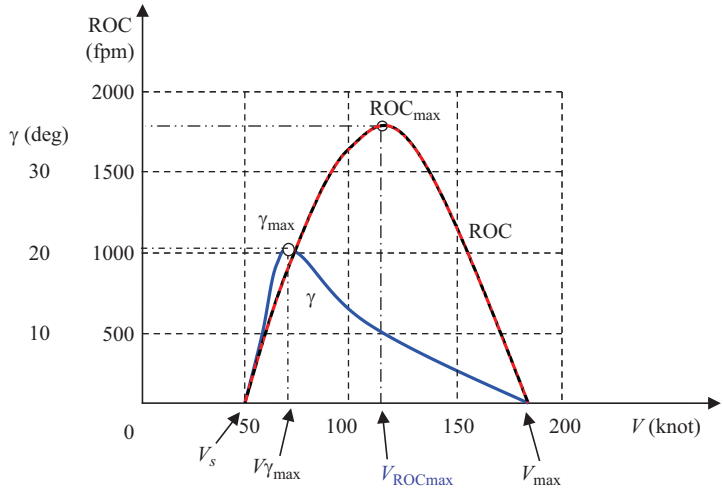

FIGURE 7.13 Variations of ROC and climb angle for a piston-prop aircraft with respect to airspeed.

By comparing the airspeed corresponding to the minimum power (Equation 7.45), and the airspeed corresponding to the minimum drag (Equation 5.38), one can conclude that, $V_{\mathrm{ROC}_{\max}} > V_{\min_{\mathbf{D}}}$.

The curves of Figure 7.13 show that, for a given wing loading, the magnitude of the ROC is very sensitive to deviations from the minimum power airspeed. Climbing with any airspeed other than the minimum power airspeed will result in a lower climb rate other than the maximum ROC. In other words, a climb at a higher airspeed than the minimum power airspeed significantly penalizes the fastest climb performance.

7.4.2.2 Climb Angle for Maximum ROC

The method to calculate climb angle for maximum ROC $\left(\gamma_{\mathrm{ROC}_{\max}}\right)$ for propeller-driven aircraft is similar to the method for jet aircraft. The main difference is that instead of five simultaneous algebraic equations, we have to simultaneously solve six algebraic equations. The sixth equation is the relationship between engine power and engine thrust through propeller efficiency. The equations are

$$T - D - W\sin\left(\gamma_{\mathrm{ROC}_{\max}}\right) = 0 \tag{7.47}$$

$$L - W\cos\left(\gamma_{\mathrm{ROC}_{\max}}\right) = 0 \tag{7.48}$$

$$L = \frac{1}{2}\rho V_{\mathrm{ROC}_{\max}}^2 S C_L \tag{7.49}$$

$$D = \frac{1}{2}\rho V_{\mathrm{ROC}_{\max}}^2 S C_D \tag{7.50}$$

$$C_D = C_{D_o} + KC_L^2 \tag{7.51}$$

$$T = \frac{P\eta_P}{V_{\mathrm{ROC}_{\max}}} \tag{7.52}$$

Equations 7.47–7.52 are six simultaneous nonlinear algebraic equations. To find $\gamma_{\mathrm{ROC}_{\max}}$, we need to solve these six equations simultaneously. The six unknown variables are climb angle for maximum ROC $\left(\gamma_{\mathrm{ROC}_{\max}}\right)$, thrust ($T$), drag ($D$), lift ($L$), lift coefficient ($C_L$), and drag coefficient (C_D). The first unknown variable is the one we are mainly interested about, and the other five are intermediate unknown variables.

If you are a practicing engineer, you have to use an engineering software package such as MATLAB, or MathCad to simultaneously solve these equations. If you are a student, and using a calculator, you have to use a numerical analysis technique or a trial-and-error technique. The best starting point is to assume a reasonable number for the climb angle $\left(\gamma_{\mathrm{ROC}_{\max}}\right)$ such as 10°.

However, there is another easier and direct way to find a closed-form solution for the angle corresponding to the maximum ROC, $\gamma_{\mathrm{ROC}_{\max}}$. Solving Equation 7.44 for $\gamma_{\mathrm{ROC}_{\max}}$ yields

$$\gamma_{\mathrm{ROC}_{\max}} = \sin^{-1}\left[\frac{T - D_{\mathrm{ROC}_{\max}}}{W}\right] \tag{7.53}$$

Substituting Equations 7.48–7.52 into this equation, and after some algebraic manipulation (the details are left to the reader as a practice), we will obtain the following expression:

$$\gamma_{\mathrm{ROC}_{\max}} = \sin^{-1}\left[\frac{P\eta_P}{V_{\mathrm{ROC}_{\max}} W} - \frac{\rho V_{\mathrm{ROC}_{\max}}^2 SC_{D_o}}{2W} - \frac{2KW}{\rho S V_{\mathrm{ROC}_{\max}}^2}\right] \tag{7.54}$$

An elaborate expression of Equation 7.54 is obtained by factoring the weight (W). This operation results in the following formula for the angle corresponding to the maximum ROC:

$$\gamma_{\mathrm{ROC}_{\max}} = -\sin^{-1}\left[\frac{0.25}{KW}\left(\sqrt{16K^2W^2 + \rho^2 S^2 V_{\mathrm{ROC}_{\max}}^4 \left(1 + 4KC_{D_o}\right) - 8PKS\rho\eta_P V_{\mathrm{ROC}_{\max}}} - \rho S V_{\mathrm{ROC}_{\max}}^2\right)\right] \tag{7.55}$$

This climb angle $\left(\gamma_{\mathrm{ROC}_{\max}}\right)$ will be substituted along with the speed for $\mathrm{ROC}_{\max}$ (Equation 7.45) into Equation 7.19 to determine the $\mathrm{ROC}_{\max}$ for propeller-driven aircraft. Table 7.1 shows [9] the $\mathrm{ROC}_{\max}$ for several jet and propeller-driven aircraft (with the maximum takeoff weight) at sea level.

TABLE 7.1
Maximum Rate of Climb for Several Jet and Propeller-Driven Aircraft

No.	Aircraft	Manufacturer	Type	Engine	*P* (kW) or *T* (kN)	m_{TO} (kg)	*ROC* (fpm)
1.	Dauphin	Robin	Trainer	Piston	134	1,100	600
2.	CL-215T	Canadair	Amphibian	Piston	2×1,566	19,731	1,000
3.	Epsilon	Aerospatiale	Military trainer	Piston	224	1,250	1,850
4.	B-1 Lancer	Rockwell	Bomber	Turbofan	4×77.4 kN	216,364	5,678
5.	Silver Eagle	Mitchell wing	Ultralight	Piston	17	251	640
6.	F406	Rimes/Cessna	Utility	Turboprop	2×373	4,246	1,850
7.	CBA-123	Embraer	Transport	Turboprop	2×970	7,800	2,900
8.	Super King Air B200	Beech	Transport	Turboprop	2×634	5,670	740
9.	Quantum	Pegasus	Ultralight trike	Piston	60	409	980
10.	TBM 700	Socata/Mooney	Business	Turboprop	522	2,672	2,303
11.	P180 Avanti	Piaggio	Transport	Turboprop	2×597	4,767	3,650
12.	Rafale	Dassault	Fighter	Turbofan	2×50 kN	24,500	60,000
13.	Alphajet	Dassault/Dornier	Trainer	Turbofan	2×14.1 kN	8,000	11,220
14.	Mirage 2000	Dassault	Fighter interceptor	Turbofan	95.1 kN	17,000	56,000
15.	Euro-fighter	BAE, Airbus, Alenia	Fighter	Turbofan	2×90 kN	23,500	62,000
16.	B 747-400	Boeing	Transport	Turbofan	4×252 kN	362,875	2,350
17.	F/A-18	McDonnell Douglas	Fighter	Turbofan	2×71.2 kN	25,400	59,945
18.	Skyhawk	McDonnell	Fighter Bomber	Turbojet	50 kN	4,581	8,000
19.	Microjet 200B	Microjet	Trainer	Turbojet	2×1.3 kN	1,300	1,705
20	V-22 Osprey	Bell Boeing	VTOL	Turboprop	2×4,586	21,546	4,000

From Equations 7.19 and 7.53, we can derive a few important conclusions. To improve the climb performance for a propeller-driven aircraft to increase the maximum climb rate, one must

a. Increase engine power
b. Reduce aircraft weight
c. Increase wing area
d. Increase wing aspect ratio
e. Reduce aircraft zero-lift drag coefficient

These factors can be changed in the aircraft design process. For design and optimization analyses, these factors are the most critical ones.

Case Study - Example 7.7

Consider the GA aircraft Cessna 172 (Figure 3.17) with a maximum takeoff mass of 1,110 kg, and a piston engine [79] with a maximum power of 120 kW – with a fixed-pitch prop. The characteristics of the aircraft are as follows:

$$S = 16.2\,\text{m}^2,\ \text{AR} = 7.32,\ C_{D_o} = 0.032,\ e = 8, \eta_P = 0.6,\ V_s = 51\,\text{knot}$$

a. Determine the ROC_{max} at sea level.
b. Determine the aircraft service ceiling.

Solution

At sea level, the air density is 1.225 kg/m^3. We first need to calculate *K*:

$$K = \frac{1}{\pi e\,\text{AR}} = \frac{1}{3.14 \times 0.8 \times 7.32} = 0.054 \tag{3.8}$$

The speed for ROC_{max} with a fixed-pitch prop is (a value of 1.35 is selected for *k*)

$$V_{\text{ROC}_{\text{max}}} = k\sqrt{\frac{2mg}{\rho S\sqrt{\frac{3C_{D_o}}{K}}}} = 1.35 \times \sqrt{\frac{2 \times 1{,}110 \times 9.81}{1.225 \times 16.2 \times \sqrt{\frac{3 \times 0.032}{0.054}}}} \tag{7.45}$$

$$= 37.6\,\text{m/s} = 73.2\,\text{knot}$$

The airspeed for the ROC_{max} is greater than the stall speed, so it is acceptable.

$$\gamma_{\text{ROC}_{\text{max}}} = -\sin^{-1}\left[\frac{0.25}{KW}\left(\sqrt{16K^2W^2 + \rho^2 S^2 V_{\text{ROC}_{\text{max}}}^4\left(1 + 4KC_{D_o}\right) - 8PKS\rho\eta_P V_{\text{ROC}_{\text{max}}}} - \rho S V_{\text{ROC}_{\text{max}}}^2\right)\right] \tag{7.55}$$

After the substitution, we will obtain:

$$\gamma_{\text{ROC}_{\text{max}}} = 0.097\,\text{rad} = 5.58°$$

The ROC_{max} for this propeller-driven aircraft is

$$\text{ROC}_{\text{max}} = V_{\text{ROC}_{\text{max}}} \sin\left(\gamma_{\text{ROC}_{\text{max}}}\right) = 37.6 \times \sin(5.58) = 3.66\,\text{m/s} = 721\,\text{fpm} \tag{7.19}$$

The published magnitude [9] for the ROC_{max} is 721 fpm (The same!).

To determine the service ceiling, we repeat the aforementioned calculations for various altitudes to obtain the altitude at which the ROC_{max} is 100 fpm. Using a computer code, the plot in Figure 7.14 is produced that illustrates the variations of ROC_{max} versus altitude. From the plot of Figure 7.14, the altitude for service ceiling is 13,900 fpm. The published magnitude [9] for the service ceiling is 13,500 ft.

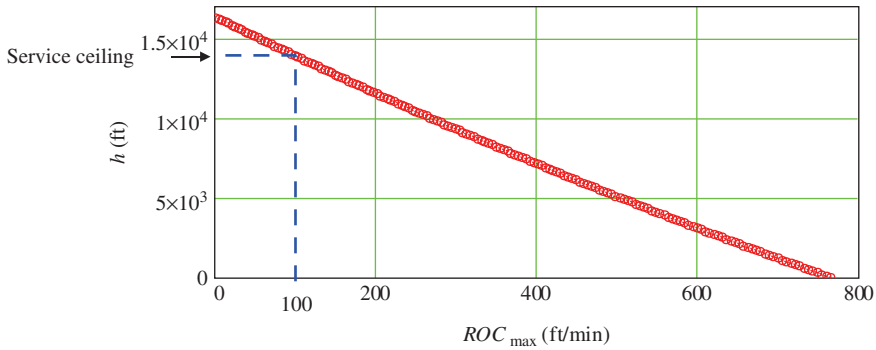

FIGURE 7.14 Variations of maximum rate of climb versus altitude for Cessna 172.

7.5 STEEPEST CLIMB

The flight path of a climbing aircraft has always an angle with the horizontal. This angle has a maximum magnitude, which is unique for every aircraft at any flight condition (e.g., aircraft weight, altitude). The maximum angle of climb is achieved only under special circumstances (e.g., a specific airspeed). In this section, we will introduce the flight conditions that result in a climb with a maximum climb angle. We also present a technique that enables the reader to calculate this angle for any aircraft. A climbing flight with the maximum climb angle is referred to as the *steepest climb.*

In a takeoff operation, it is of utmost interest in clearing obstacles, such as mountains, trees, and buildings at the end of the runway. The steepest climb is another important aircraft performance evaluation factor by which the upper limit for the climb angle is established.

For some aircraft, the fastest climb is more critical than the steepest climb, but in others, the steepest climb is more important than the fastest climb. The performance requirements usually drive the fastest climb, while the airworthiness requirements (particularly in transport aircraft) often influence the steepest climb. The maximum climb angle is a function of several parameters such as engine power (in propeller-driven aircraft), engine thrust (in jet aircraft), aircraft speed, and aircraft weight, aircraft center of gravity, altitude, and elevator control power (i.e., elevator area, maximum elevator deflection, and tail arm).

Figure 7.15 shows the typical variations of climb angle with: panel (a) engine power/thrust and panel (b) aircraft weight. To increase the climb angle, the pilot must increase engine power (in propeller-driven aircraft) or engine thrust (in jet aircraft). The highest climb angle will be obtained when the engine thrust or the engine power is at maximum and the aircraft weight is at minimum.

Another factor affecting the steepest climb is the airspeed. The aircraft speed does not have a direct linear effect on the maximum climb angle. The aircraft speed must be varied to a specified magnitude for the steepest climb. For a given aircraft, the pilot can maximize either the ROC (i.e., fastest climb) or the climb angle (i.e., steepest climb). These two climb performance objectives occur at different flight conditions. Figure 7.16 illustrates the typical relationship between the ROC and

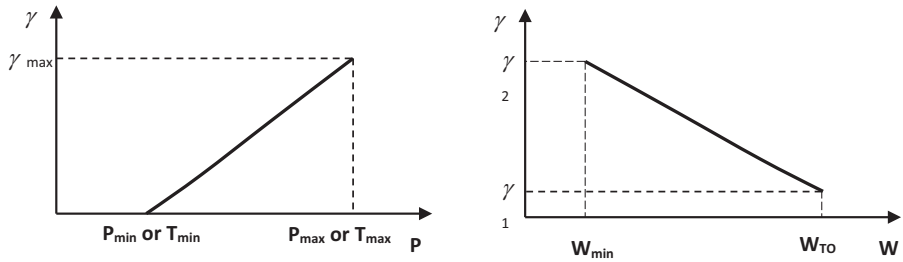

FIGURE 7.15 Variations of the climb angle with engine power/thrust and aircraft weight. (a) Variations with engine power/thrust and (b) variations with aircraft weight.

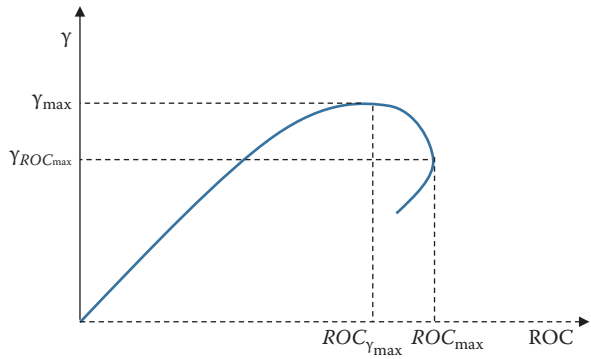

FIGURE 7.16 Typical relationship between ROC and climb angle.

climb angle, for a given engine throttle, an aircraft weight, and an altitude. As the pilot varies the angle of attack, the airspeed, climb angle, and ROC will vary.

Consider an aircraft in a climbing flight where the pilot employs its maximum available thrust. As the pilot increases the angle of attack, the climb angle will also increase. This trend will continue up to a fixed point, where the climb angle begins to decrease. Therefore, at one angle, steepest climb happens, while at another climb angle, fastest climb occurs. Figure 7.17 shows typical variations of the maximum climb angle versus altitude. This figure implies that the maximum climb angle declines with altitude too. For both types of aircraft (jet and propeller-driven), the maximum climb angle depends on altitude, such that at absolute ceiling, it becomes zero.

The maximum climb angle for majority of aircraft is about 15°–20°. However, fighter aircraft has much higher climb angle, such that a few fighters (such as General Dynamics [now Lockheed Martin] F-16 Fighting Falcon (Figure 7.6), Mikoyan MiG-29 (Figure 3.20), and McDonnell Douglas [now Boeing] AV-8B Harrier II) have 90° for the maximum climb angle. In other words, these jet fighters can climb vertically (Harrier II can also land vertically). The navy version of advanced fighter Lockheed Martin *F-35* Lightning II (Figure 5.5) has such capability too. Figure 7.16 illustrates a Lockheed F-16CJ Fighting Falcon with a turbofan engine in a climbing flight with

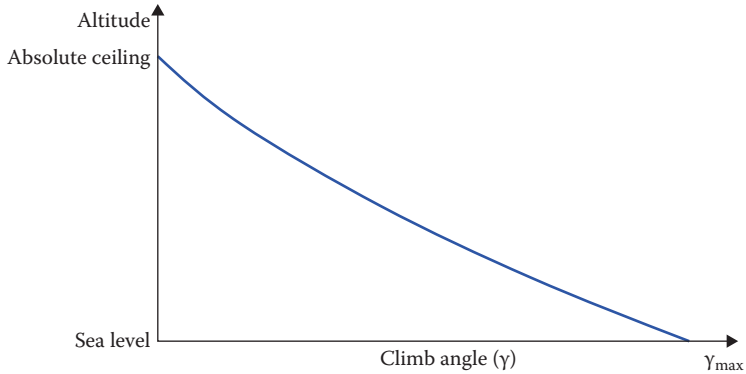

FIGURE 7.17 Variations of climb angle versus altitude.

(a) (b)

FIGURE 7.18 Two transport aircraft in climbing flight. (a) Embraer 190LR; (b) Boeing 777. (Courtesy of Jan Seler.)

a climb angle of nearly 90°. Figure 7.18 shows a transport aircraft Boeing 777 and *Embraer 190LR* (both with two turbofan engines) in a climbing flight.

The general equation of climb (Equation 7.14) is used to investigate the steepest climb. Equation 7.14 is reproduced in the following form:

$$\gamma = \sin^{-1}\left(\frac{T-D}{W}\right) \tag{7.56}$$

Mathematically, to increase the climb angle in this equation, the numerator must be increased, while the denominator is decreased. Thus, for a given aircraft weight (W_{min}), to maximize the climb angle (γ_{max}), one needs to maximize the thrust (T_{max}), while at the same time to minimize the drag (D_{min}). This is equivalent to maximizing the thrust-to-weight ratio.

$$\gamma_{max} = \sin^{-1}\left(\frac{T_{max}-D_{min}}{W_{min}}\right) \tag{7.57}$$

Engine thrust depends on the altitude and throttle and drag depend on the altitude, aircraft speed, and aircraft configuration. Furthermore, using Equation 7.11, we can write

$$\gamma = \cos^{-1}\left(\frac{L}{W}\right) \tag{7.58}$$

or

$$\gamma_{\max} = \cos^{-1}\left(\frac{L_{\max}}{W_{\min}}\right) \tag{7.59}$$

This implies that we have to increase the lift to maximize climb angle (i.e., maximizing the lift-to-weight ratio). This point is obvious for a rotary-wing aircraft. However, for a fixed-wing aircraft, in Chapter 9, this ratio is given a name and its significance will be presented. Two criteria of Equations (7.57) and (7.59) are not linearly related, since they are nonlinear functions of speed. For precise analysis, we have to consider the type of engine and dig more. Then, the ROC for the steepest climb is

$$\mathrm{ROC}_{\gamma_{\max}} = V_{\gamma_{\max}} \sin\left(\gamma_{\max}\right) \tag{7.60}$$

This equation has two unknowns: (1) speed for the steepest climb $\left(V_{\gamma_{\max}}\right)$ and (2) maximum climb angle ($\gamma_{\max}$). We will discuss these parameters for jet and propeller-driven aircraft separately in Sections 7.5.1 and 7.5.2. The technique covered in this section provides acceptable accuracy for a conventional aircraft. For high-performance aircraft, such as interceptor aircraft, special considerations should be given to include acceleration along the flight path.

7.5.1 Jet Aircraft

Maximum climb angle for a jet aircraft is directly determined by employing Equation 7.57. In flight operation, the pilot has to employ the maximum thrust and, at the same time, fly with a speed that produces the minimum drag. Thus, the speed for maximum climb angle $\left(V_{\gamma_{\max}}\right)$ is the minimum drag speed as introduced in Chapter 5 (Equation 5.38). So,

$$V_{\gamma_{\max}} = V_{\min_D} = \left(\frac{2mg}{\rho S}\right)^{1/2}\left(\frac{K}{C_{D_o}}\right)^{1/4} \tag{7.61}$$

Hence, the minimum drag is obtained as

$$D_{\min} = \frac{1}{2}\rho S C_{D_{\min D}}\left(V_{\min_D}\right)^2 \tag{7.62}$$

where the drag coefficient for minimum drag is rewritten for convenience from Chapter 5 (Equation 5.43)

$$C_{D_{\min D}} = 2C_{D_o} \tag{5.47}$$

Substituting the minimum drag (Equation 7.62) into Equation 7.57 yields the maximum climb angle for a jet aircraft.

$$\gamma_{\max} = \sin^{-1}\left(\frac{1}{W}\left[T_{\max} - \frac{1}{2}\rho S\left(2C_{D_o}\right)\left(\frac{2W}{\rho S\sqrt{\frac{C_{D_o}}{K}}}\right)\right]\right)$$

or

$$\gamma_{\max} = \sin^{-1}\left(\frac{T_{\max}}{W} - 2\sqrt{KC_{D_o}}\right) \tag{7.63}$$

Then, by substituting the maximum climb angle (Equation 7.63) and the steepest climb speed $\left(V_{\gamma_{\max}}\right)$ into Equation 7.61, we are able to analyze the steepest climb for a jet aircraft. Thus, the ROC that corresponds to the maximum climb angle is determined by

$$\mathrm{ROC}_{\gamma_{\max}} = \sqrt{\frac{2W}{\rho S\sqrt{\frac{C_{D_o}}{K}}}}\left[\frac{T_{\max}}{W} - 2\sqrt{KC_{D_o}}\right] \tag{7.64}$$

This equation can be used only if the theoretical airspeed for the steepest climb (Equation 7.61) is greater than the stall speed; otherwise, use Equation 7.57. Note from Equation 7.63 that $\gamma_{\max}$ does not depend on wing loading, but from Equation 7.61, $V_{\gamma_{\max}}$ varies directly as $(W/S)^{1/2}$. Hence, everything else being equal, for a flight at $\gamma_{\max}$, the ROC is higher for higher wing loadings. Also, the effect of altitude is clearly seen from these results. Since $(L/D)_{\max}$ does not depend on altitude, then from Equation 7.57, $\gamma_{\max}$ decreases with altitude because T decreases with altitude.

However, from Equation 7.61, $V_{\gamma_{\max}}$ increases with altitude. These are competing effects in determining $\mathrm{ROC}_{\gamma_{\max}}$ from Equation 7.60. However, the altitude effect on $\gamma_{\max}$ usually dominates, and $\mathrm{ROC}_{\gamma_{\max}}$ usually decreases with increasing altitude.

Equation 7.61 is a mathematical formula. It may not always submit a reasonable magnitude. For any given airplane, it is theoretically possible for $V_{\gamma_{\max}}$ to be found out to be less than the stall speed. For such a case, it is not possible for that airplane to achieve the theoretical maximum climb angle. If the solution is a speed that is less than the stall speed (V_s), we have to resort to a safe speed. Therefore, in this case, the speed for maximum climb angle must be slightly higher than the stall speed

$$V_{\gamma_{\max}} = kV_s \tag{7.65}$$

where k is a number between 1.1 and 1.3. For civil aircraft, the parameter k is between 1.2 and 1.3, but for fighter aircraft, k is between 1.05 and 1.15. The exact k depends on several factors such as mission of the aircraft, and military and airworthiness regulations.

From Equation 7.63, we can derive a few important conclusions. To improve the climb performance for a jet aircraft to increase the maximum climb angle, one must

1. Increase engine thrust
2. Reduce aircraft weight
3. Reduce wing area
4. Reduce wing aspect ratio
5. Reduce aircraft zero-lift drag coefficient

These are the factors that can be changed in the aircraft design process. For design and optimization analyses, these factors are the most critical ones.

Case Study - Example 7.8

The fighter aircraft McDonnell F-4C Phantom has two turbojet engines each generating 75.6 kN of thrust. Other characteristics of this fighter are:

$$m = 24{,}765\,\text{kg},\ S = 49.24\,\text{m}^2,\ C_{D_0} = 0.029,\ b = 11.7\,\text{m},\ e = 0.7,\ C_{L_{\max}} = 2.2.$$

Assume C_{D_o} is constant at all altitudes. Analyze the steepest climb for this aircraft (i.e., determine maximum climb angle) at sea level and at 30,000 ft (9,144 m) altitude. Then, calculate the corresponding ROC at both altitudes.

Solution

First, we need to calculate K and $C_{D_{\min D}}$

$$\text{AR} = \frac{b^2}{S} = \frac{11.7^2}{49.24} = 2.78 \tag{3.9}$$

$$K = \frac{1}{\pi e\,\text{AR}} = \frac{1}{3.14 \times 0.7 \times 2.78} = 0.164 \tag{3.8}$$

$$C_{D_{\min D}} = 2C_{D_o} = 2 \times 0.029 = 0.058 \tag{5.43}$$

- Sea level

  The speed for the steepest climb is

$$V_{\gamma_{\max}} = \left(\frac{2mg}{\rho S}\right)^{1/2}\left(\frac{K}{C_{D_o}}\right)^{1/4} = \left(\frac{2 \times 24{,}765 \times 9.81}{1.225 \times 49.24}\right)^{1/2}\left(\frac{0.164}{0.029}\right)^{1/4} = 138.49\,\text{m/s} \tag{7.61}$$

We need to compare this speed with the stall speed:

$$V_s = \sqrt{\frac{2mg}{\rho S C_{L_{\max}}}} = \sqrt{\frac{2\times 24{,}765\times 9.81}{1.225\times 49.24\times 2.2}} = 60.5\,\text{m/s} \tag{2.27}$$

The maximum climb angle speed is higher than the stall speed, so it is acceptable. Then, minimum drag at this flight condition is

$$D_{\min} = \frac{1}{2}\rho S C_{D_{\min_D}} \left(V_{\min_D}\right)^2 = \frac{1}{2}\times 1.225\times 49.24\times 0.058\times (138.49)^2 = 33{,}549.7\,\text{N} \tag{7.62}$$

Hence, the maximum climb angle is

$$\gamma_{\max} = \sin^{-1}\left(\frac{T_{\max} - D_{\min}}{W_{\min}}\right) = \sin^{-1}\left(\frac{2\times 75.6\times 1{,}000 - 33{,}549.7}{24{,}765\times 9.81}\right) = 28.96^\circ \tag{7.57}$$

Therefore, the ROC for the steepest climb will be

$$\begin{aligned} \text{ROC}_{\gamma_{\max}} &= V_{\gamma_{\max}} \sin\left(\gamma_{\max}\right) = 138.49\times \sin(28.96) \\ &= 67.05\,\text{m/s} = 13{,}196\,\text{fpm} \end{aligned} \tag{7.60}$$

- 30,000 ft altitude (9,144 m)

  Based on Appendix B, the air density at 30,000 ft is 0.00089 slug/ft^3, which is equivalent to 0.4586 kg/m^3. Then, the speed for the steepest climb is

$$V_{\gamma_{\max}} = \left(\frac{2mg}{\rho S}\right)^{1/2}\left(\frac{K}{C_{D_o}}\right)^{1/4} = \left(\frac{2\times 24{,}765\times 9.81}{0.4586\times 49.24}\right)^{1/2}\left(\frac{0.164}{0.029}\right)^{1/4} = 226.34\,\text{m/s} \tag{7.61}$$

We need to compare this speed with the stall speed:

$$V_s = \sqrt{\frac{2mg}{\rho S C_{L_{\max}}}} = \sqrt{\frac{2\times 24{,}765\times 9.81}{0.4586\times 49.24\times 2.2}} = 98.96\,\text{m/s} \tag{2.27}$$

The maximum climb angle speed is higher than the stall speed, which is acceptable.

Then, minimum drag at this flight condition is

$$\begin{aligned} D_{\min} &= \frac{1}{2}\rho S C_{D_{\min_D}} \left(V_{\min_D}\right)^2 \\ &= \frac{1}{2}\times 0.4586\times 49.24\times 0.058\times (138.49)^2 = 24{,}038.3\,\text{N} \end{aligned} \tag{7.62}$$

At 30,000 ft (first layer), the engine thrust is decreased as

$$T = T_O\left(\frac{\rho}{\rho_o}\right)^{0.9} = 2\times 75.6\times 1{,}000\times\left(\frac{0.4586}{1.225}\right)^{0.9} = 62{,}448.2\,\text{N} \tag{4.16}$$

Hence, the maximum climb angle is

$$\gamma_{\max} = \sin^{-1}\left(\frac{T_{\max} - D_{\min}}{W_{\min}}\right) = \sin^{-1}\left(\frac{62{,}448.2 - 24{,}038.3}{24{,}765 \times 9.81}\right) = 6.83^{\circ} \tag{7.57}$$

Therefore, the ROC for the steepest climb will be

$$\begin{aligned} \mathrm{ROC}_{\gamma_{\max}} &= V_{\gamma_{\max}} \sin\left(\gamma_{\max}\right) = 226.34 \times \sin(6.83) \\ &= 26.92\,\mathrm{m/s} = 5{,}297.3\,\mathrm{fpm} \end{aligned} \tag{7.60}$$

It is observed that the aircraft's steepest climb at high altitude is significantly reduced.

7.5.2 Propeller-Driven Aircraft

In the case of a propeller-driven aircraft, we begin calculation of the maximum climb angle with the relationship between climb angle and engine thrust. From Equation 7.56, we had

$$\gamma = \sin^{-1}\left(\frac{T - D}{W}\right) \tag{7.56}$$

We know that the engine thrust is a function of engine power, propeller efficiency, and aircraft speed. It is evident from the discussion in Section 7.4 that maximum climb angle is obtained when we use maximum engine power ($P_{\max}$). Using Equation 4.2 and assuming the propeller efficiency to be constant, we can write

$$T_{\gamma_{\max}} = \frac{P_{\max}\eta_P}{V_{\gamma_{\max}}} \tag{7.66}$$

In addition, the climb angle is a function of aircraft speed. Thus, we need to find out the proper aircraft speed for the maximum climb angle $\left(V_{\gamma_{\max}}\right)$. To maximize climb angle, we need to maximize the *excess thrust* (i.e., the difference between the available thrust and the thrust required to cruise with a given airspeed) and minimize the aircraft weight. This implies that we need to increase thrust, while at the same time decreasing the drag. Engine thrust depends on the altitude and aircraft speed, and drag depends on the altitude, aircraft speed, and aircraft configuration. By substituting Equation 7.66 into Equation 7.56, the maximum climb angle is obtained

$$\gamma_{\max} = \sin^{-1}\left[\frac{\left(\left(P_{\max}\eta_P / V_{\gamma_{\max}}\right) - D\right)_{\max}}{W_{\min}}\right] \tag{7.67}$$

Here, there are two unknowns: γ_{max} and $V_{\gamma_{max}}$; we will determine them separately in Sections 7.5.2.1 and 7.5.2.2. When we calculated these parameters, the ROC that corresponds to the maximum climb angle is given by

$$\mathrm{ROC}_{\gamma_{max}} = V_{\gamma_{max}} \sin\left(\gamma_{max}\right) \tag{7.60}$$

This equation is similar to the equation we presented for a jet aircraft.

7.5.2.1 Calculation of Aircraft Speed for Maximum Climb Angle

In a steady climb, the equilibrium of forces in the z direction is

$$L - W\cos\left(\gamma\right) = 0 \tag{7.13}$$

where the lift is

$$L = \frac{1}{2}\rho V^2 S C_L \tag{2.4}$$

Substituting the lift equation into Equation 7.13 yields

$$C_L = \frac{2W\cos\left(\gamma\right)}{\rho V^2 S} \tag{7.68}$$

Furthermore, the equilibrium of forces in the forward (x-axis) direction is

$$T - D - W\sin\left(\gamma\right) = 0 \tag{7.11}$$

where the drag is

$$D = \frac{1}{2}\rho V^2 S C_D \tag{2.5}$$

By using drag polar equation (3.12), it will expand to

$$D = \frac{1}{2}\rho V^2 S\left(C_{D_o} + KC_L^2\right) \tag{7.69}$$

Substituting the lift coefficient (Equation 7.68) into this equation yields

$$D = \frac{1}{2}\rho V^2 S\left(C_{D_o} + K\left(\frac{2W\cos\left(\gamma\right)}{\rho V^2 S}\right)^2\right) \tag{7.70}$$

Substituting this drag and the engine thrust (Equation 4.2) into Equation 7.56, and after a few algebraic steps (the details are left to the interested reader), we obtain

$$\sin(\gamma) = \frac{\frac{P\eta_P}{V} - \frac{1}{2}\rho V^2 S C_{D_o}}{W} - \frac{2WK\left(\cos(\gamma)\right)^2}{\rho V^2 S} \tag{7.71}$$

This is a nonlinear algebraic equation in terms of climb angle (γ) and does not have a closed-form solution. We need to make an assumption to simplify the equation without losing the desired accuracy. The assumption we make is to assume $\cos(\gamma) = 1$ in the drag expression only; this is a reasonable assumption. This assumption leads to remarkably accurate results for climb performance for climb angles up to 45°. This assumption is particularly reasonable because the normal climb angles of conventional aircraft are usually less than 30°. The assumption simplifies Equation 7.71 to

$$\sin(\gamma) = \frac{\frac{P\eta_P}{V} - \frac{1}{2}\rho V^2 S C_{D_o}}{W} - \frac{2WK}{\rho V^2 S} \tag{7.72}$$

The maximum climb angle is obtained by differentiation of this equation with respect to aircraft speed and setting it equal to zero:

$$\frac{d\left(\sin(\gamma)\right)}{dV} = \frac{-\left(P\eta_P/V^2\right) - \rho V S C_{D_o}}{W} + \frac{4WK}{\rho V^3 S} = 0 \tag{7.73}$$

Expanding this equation (the details are left to the reader as a practice), we obtain the following:

$$V_{\gamma_{\max}}^4 = \frac{P\eta_P}{\rho S C_{D_o}} V_{\gamma_{\max}} - \frac{4W^2K}{\rho^2 C_{D_o} S^2} = 0 \tag{7.74}$$

There is no analytical solution to this nonlinear equation. If you have a powerful software, solve the equation directly. However, it can be shown that for a typical propeller-driven airplane, the magnitude of the last two terms in Equation 7.74 is much larger than the magnitude of the first term. Hence, a reasonable approximation can be obtained by dropping the first term $\left(V_{\gamma_{\max}}^4\right)$ in Equation 7.74 to obtain the speed for maximum climb angle for a propeller-driven airplane. This assumption yields the following result:

$$V_{\gamma_{\max}} = \frac{4W^2K}{\rho \eta_P P_{\max} S} \tag{7.75}$$

Note: As we discussed earlier, it is theoretically possible for $V_{\gamma_{\max}}$ to be less than the stall speed. For such a case, it is not possible for the airplane to achieve the

theoretical maximum climb angle. If the solution is a speed that is less than the stall speed (V_s), we have to resort to a safe speed. So, in this case, the speed for maximum climb angle must be higher than the stall speed

$$V_{\gamma_{\max}} = kV_s \tag{7.65}$$

where k is a number between 1.1 and 1.3. For civil aircraft, the parameter k is between 1.2 and 1.3, but for military aircraft, k is between 1.1 and 1.2. The exact k depends on several factors such as mission of the aircraft, and military and airworthiness regulations.

It is clear – as the name implies – that, the maximum climb angle is *always* greater than the climb angle for maximum ROC

$$\gamma_{\max} > \gamma_{\mathrm{ROC}_{\max}} \tag{7.76}$$

This is evident by contemplating the meaning of the word "maximum".

7.5.2.2 Calculation of Maximum Climb Angle

To calculate the maximum climb angle for a propeller-driven aircraft, we need to insert the speed for maximum climb angle $\left(V_{\gamma_{\max}}\right)$ from Equation 7.75 into Equation 7.72. Thus,

$$\gamma_{\max} = \sin^{-1}\left[\frac{P\eta_P}{WV_{\gamma_{\max}}} - \frac{1}{2W}\rho V_{\gamma_{\max}}^2 SC_{D_o} - \frac{2KW}{\rho V_{\gamma_{\max}}^2 S}\right] \tag{7.77}$$

From Equation 7.77, we can derive a few important conclusions. To improve the climb performance for a propeller-driven aircraft to increase the maximum climb angle, one must

1. Increase engine power
2. Reduce aircraft weight
3. Increase wing area
4. Increase wing aspect ratio
5. Reduce aircraft zero-lift drag coefficient

These are the factors that can be varied in the aircraft design process. For design and optimization analyses, these factors are the most critical ones. The relationships among the airspeeds for level flight and two climb programs (fastest and steepest) are sketched in Figure 7.19. It can be seen that the speeds for steepest climb, fastest climb, maximum speed, and minimum drag speed are all very close and converge at the absolute ceiling.

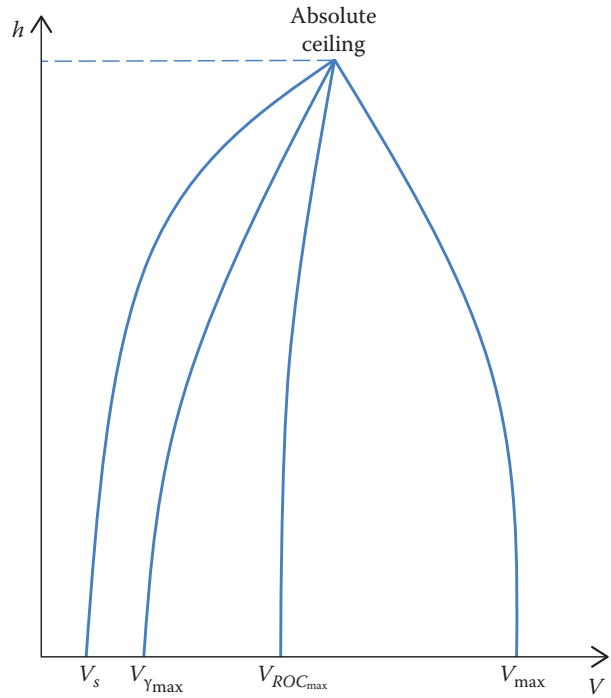

FIGURE 7.19 Relationships between level flight and climb airspeeds with altitude.

Example 7.9

Calculate the maximum climb angle at 12,000 ft (3,658 m) and its associated ROC for a utility aircraft which has two turboprop engines and the following characteristics:

$$m = 6{,}000\,\text{kg},\ S = 30\,\text{m}^2,\ P = 2\times 671.1\,\text{kW},\ b = 16\,\text{m},$$

$$C_{L_{max}} = 1.8,\ \eta_P = 0.85,\ C_{D_o} = 0.024,\ e = 0.87.$$

Solution

First, we need to calculate K and engine power at altitude:

$$\text{AR} = \frac{b^2}{S} = \frac{16^2}{30} = 8.53 \tag{3.9}$$

$$K = \frac{1}{\pi e\,\text{AR}} = \frac{1}{3.14\times 0.87\times 8.53} = 0.043 \tag{3.8}$$

Based on Appendix B, the air density at 12,000 ft (3,658 m) is 0.001648 slug/ft^3, which is equivalent to 0.849 kg/m^3. At 12,000 ft (first layer), the available power for this turboprop engine is decreased as

$$P = P_o\left(\frac{\rho}{\rho_o}\right)^1 = 2\times 671.1\times\left(\frac{0.849}{1.225}\right) = 930.212\,\text{kW} \tag{4.27}$$

Then, the speed for the steepest climb is

$$V_{\gamma_{\max}} = \frac{4W^2K}{P_{\max}\rho\eta_P S} = \frac{4\times(6{,}000\times 9.81)^2\times 0.043}{930{,}212\times 0.849\times 0.85\times 30} = 29.47\,\text{m/s} \tag{7.75}$$

We need to compare this speed with the stall speed:

$$V_s = \sqrt{\frac{2mg}{\rho S C_{L_{\max}}}} = \sqrt{\frac{2\times 6{,}000\times 9.81}{0.849\times 30\times 1.8}} = 50.65\,\text{m/s} \tag{2.49}$$

The airspeed for the maximum climb angle is less than the stall speed, so it is not acceptable. An acceptable airspeed is determined as (k is assumed to be 1.2)

$$V_{\gamma_{\max}} = kV_s = 1.2\times 50.65 = 60.78\,\text{m/s} \tag{7.65}$$

Hence, the maximum climb angle is

$$\begin{aligned}\gamma_{\max} &= \sin^{-1}\left(\frac{P\eta_P}{VW} - \frac{1}{2W}\rho V^2 S C_{D_o} - \frac{2WK}{\rho V^2 S}\right)\\ &= \sin^{-1}\left[\frac{2\times 930{,}212\times 0.85}{60.78\times 6{,}000\times 9.81} - \frac{1}{2\times 6{,}000\times 9.81}\right.\\ &\qquad \left.\times 0.849\times(60.78)^2\times 30\times 0.024 - \frac{2\times 6{,}000\times 9.81\times 0.043}{0.849\times(60.78)^2\times 30}\right]\\ &= 8.53^\circ\end{aligned} \tag{7.72}$$

Therefore, the ROC for the steepest climb will be:

$$\begin{aligned}\text{ROC}_{\gamma_{\max}} &= V_{\gamma_{\max}}\sin(\gamma_{\max}) = 60.78\times\sin(8.53)\\ &= 9.013\,\text{m/s} = 1{,}774.2\,\text{fpm}\end{aligned} \tag{7.60}$$

7.6 INTERIM SUMMARY

In this section, the climb performance is summarized (see Table 7.2); and the equation numbers for two cases of (1) fastest climb and (2) steepest climb for two types of aircraft (a) jet and (b) propeller-driven are presented.

TABLE 7.2
Climb Performance Equation Numbers

No.	Climb Program	What Is Maximized?	Climb Angle		Airspeed		Rate of Climb	
			Jet	Propeller-Driven	Jet	Propeller-Driven	Jet	Propeller-Driven
1.	Fastest climb	Rate of climb	7.38 or 7.39	7.54 or 7.55	7.30	7.45	7.19	7.19
2.	Steepest climb	Climb angle	7.63	7.77	7.61	7.75	7.60 or 7.64	7.60

7.7 GRAPHICAL ANALYSIS

A very beneficial approach in the analysis of the climb performance is to use a graphical technique. In this approach, a plot (also known as hodograph diagram [56]) is constructed, which is the variations of the vertical component of airspeed (V_V) versus horizontal component of airspeed (V_H). The ordinate is V_V, which also is the ROC, while the abscissa is the horizontal component of velocity; V_H, as depicted in Figure 7.20. Figure 7.3 illustrates the geometric relation among forward airspeed, V, horizontal speed, vertical speed, and climb angle (γ):

$$V_H = V \cdot \cos(\gamma) \tag{7.14}$$

$$V_V = V \cdot \sin(\gamma) \tag{7.15}$$

These relations are also shown in this plot. By employing this graph, one can simultaneously determine the ROC_{max} and the maximum climb angle.

In this plot, three points (1, 2, and 3) are of significant interest, each representing an important feature in a climbing flight. Consider an arbitrary point on curve, which is denoted by point 1 in Figure 7.20. Draw a line from the origin to this point. Geometrically, the length of the line is airspeed, V, and the angle it makes with the horizontal axis is the corresponding climb angle (γ) at that velocity. Point 2 (the highest point) in Figure 7.20 represents the maximum ROC; the length of the line from the origin to point 2 is the aircraft airspeed at the maximum ROC, which is denoted by $V_{ROC_{max}}$, and the angle it makes with the horizontal axis is the climb angle for maximum ROC or $\gamma_{ROC_{max}}$.

A line drawn through the origin and tangent to the hodograph curve locates point 3 in Figure 7.20. The angle of this line relative to the horizontal defines the maximum climb angle, γ_{max}. The length of the line from the origin to the tangent point (point 3) is the velocity at the maximum climb angle.

In addition, through this graph, one can graphically compare the steepest climb with the fastest climb. The graph highlights that the ROC_{max} does not correspond to the maximum climb angle. Recall that the maximum climb angle γ_{max} is important

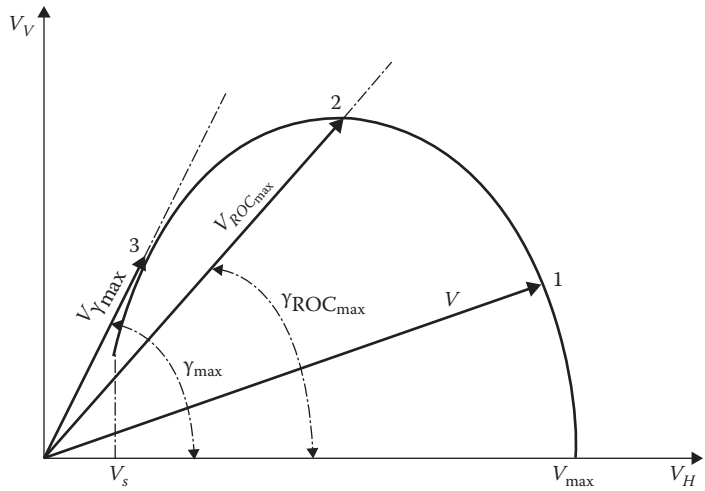

FIGURE 7.20 Diagram for climb performance analysis.

when the pilot needs to clear an obstacle while covering the minimum horizontal distance along the ground. The ROC_{max} is important when the pilot desires to achieve a certain altitude in a minimum amount of time. Note that V is almost smallest at γ_{max}, and it increases as γ is made smaller. This is why ROC_{max} does not occur at γ_{max}. Furthermore, since $ROC = V\sin(\gamma)$, from point 3 to point 2, the increase in V exceeds the decrease in sin (γ), leading to an increase in $V\sin(\gamma)$.

To sketch the hodograph, one needs to plot the variations of the vertical component of the airspeed (V_H) with respect to the horizontal component of the airspeed (V_V). The horizontal and vertical components (V_H and V_V) of the airspeed are determined through Equations 7.14 and 7.15, respectively. In this process, one needs to select an airspeed that ranges from the stall speed to the maximum speed. Then, calculate the corresponding climb angle (γ) to each airspeed. The expression for climb angle as a function of airspeed for a jet aircraft is derived by inserting lift and drag Equations 2.4 and 2.5 into Equations 7.11 and 7.13. This will yield

$$\gamma = \sin^{-1}\left[\frac{T}{W} - \frac{1}{2W}\rho V^2 S C_{D_o} - \frac{2KW\left(\cos(\gamma)^2\right)}{\rho S V^2}\right] \tag{7.78}$$

Similarly, for a propeller-driven aircraft, using Equation 7.40, Equation 7.78 is changed as

$$\gamma = \sin^{-1}\left[\frac{P\eta_P}{VW} - \frac{1}{2W}\rho V^2 S C_{D_o} - \frac{2KW\left(\cos(\gamma)^2\right)}{\rho V^2 S}\right] \tag{7.79}$$

Note that the climb angle (γ) appears on both sides of Equations 7.78 and 7.79. These two equations are highly nonlinear, and there are no closed-form solutions. For typical climb angles, we can set $\cos(\gamma) = 1$ without losing accuracy. Thus, Equations 7.78 and 7.79 are simplified to

$$\gamma = \sin^{-1}\left[\frac{T}{W} - \frac{1}{2W}\rho V^2 S C_{D_o} - \frac{2KW}{\rho V^2 S}\right] \quad (\text{jet aircraft}) \tag{7.80}$$

$$\gamma = \sin^{-1}\left[\frac{P\eta_P}{VW} - \frac{1}{2W}\rho V^2 S C_{D_o} - \frac{2KW}{\rho V^2 S}\right] \quad (\text{propeller-driven aircraft}) \tag{7.81}$$

For a given aircraft weight (e.g., maximum takeoff weight), a given maximum engine thrust, and a given altitude, Equation 7.80 demonstrates the nonlinear relation between climb angle and airspeed for a jet aircraft. Similarly, for a given maximum takeoff weight, a given maximum engine power, and a given altitude, Equation 7.81 demonstrates the nonlinear relationship between the climb angle and airspeed for a propeller-driven aircraft. Equations 7.80 and 7.81 each have only one acceptable solution for each set of given data and provide the exact solutions for the climb performance analysis. If more than one solution satisfies Equation 7.80 (or 7.81), pick the lowest positive value. The angle should be between 0° and 90°.

The procedure to construct the hodograph diagram (as in Figure 7.20) is as follows:

1. Select an airspeed (begin with the stall speed).
2. Calculate the climb angle corresponding to this airspeed from Equation 7.80 (for a jet aircraft) or Equation 7.81 (for a propeller-driven aircraft).
3. Determine horizontal velocity (V_H) from Equation 7.14 ($V \cdot \cos(\gamma)$).
4. Determine vertical velocity (V_V) from Equation 7.15 ($V \cdot \sin(\gamma)$).
5. Select a new airspeed (you may increase the previous one by 1 knot).
6. This process is continued until the maximum speed is reached, which in theory means a zero climb angle and a zero V_V.
7. Plot of V_H (from step 3) versus V_V (from step 4).
8. Identify the highest point in the plot (as point 2 in Figure 7.20). This point represents the fastest climb.
9. Identify the point in the plot with the highest slope when a line is drawn to it from the origin (as point 3 in Figure 7.20). This point represents the steepest climb.

In this process, each plot is based on a given aircraft weight (e.g., maximum takeoff weight), a given engine thrust (e.g., maximum thrust), and a given altitude (e.g., sea level). An example using MATLAB programming to demonstrate the application of the technique is provided in Chapter 10.

7.8 MOST-ECONOMICAL CLIMB

In Sections 7.4 and 7.5, two interesting climb operations, the fastest climb and the steepest climb, are introduced. The third climb program of interest is the most-economical climb, the climb that uses the smallest amount of fuel. This flight program is the most interesting program to airliners and transport aircraft, since it requires the lowest fuel cost. In 2022, the fuel price was about US$4.8 per US gallon. To gain altitude, fuel must be consumed, and so the aircraft's weight is decreased. In Chapter 4, for the definition of specific fuel consumption (C) for a jet aircraft, we had

$$\frac{dW}{dt} = -CT \tag{7.82}$$

The negative sign is an indication of the fuel weight reduction with time. Combining Equations 7.2 and 7.17, the ROC can be obtained as

$$\frac{dh}{dt} = \frac{TV - DV}{W} \tag{7.83}$$

Dividing Equation 7.82 by Equation 7.83 (and canceling dt), the fuel-weight-altitude exchange ratio is obtained as

$$\frac{dW}{dh} = \frac{-CTW}{TV - DV} \tag{7.84}$$

or

$$\frac{dh}{dW} = \frac{TV - DV}{-CTW} \tag{7.85}$$

For an ideal jet engine (turbofan or turbojet), we assume that the thrust is independent of the airspeed and that the specific fuel consumption is constant. The negative sign represents the weight reduction during a climb operation. Recall the numerator is the excess power. This expression represents the fuel flow rate per unit of excess power per unit of aircraft weight. For most-economical climb, we wish to maximize this parameter as

$$\left(\frac{dh}{dW}\right)_{\max} = \frac{(TV - DV)_{\max}}{(-CTW)_{\min}} \tag{7.86}$$

Comparing this result with Equation 7.21, we note that there is a strong similarity between the fastest climb and the most-economical climb. In both cases, we need to maximize the excess power. Thus, with our assumptions and approximations, the *fastest climb is almost the most-economical climb.* In reality, the airspeed for most-economical climb is slightly lower than that for the fastest climb, since the engine

thrust and specific fuel consumption vary with speed. However, the airspeed for most-economical climb is much closer to the fastest-climb airspeed than to the steepest climb airspeed.

Since the aircraft is climbing, and the air density is gradually decreasing, the airspeed for most-economical climb is decreased too. Accordingly, the ROC is gradually decreasing. Therefore, the climb angle must be varied to meet the requirement for the most-economical climb. Due to this point, no equation for climb angle, climb speed, and climb rate is derived here.

7.9 TIME TO CLIMB AND FUEL TO CLIMB

In the climb analysis, there are other parameters of interest such as "time to climb" and "fuel to climb". Time to climb is another climb performance analysis criterion. For a transport aircraft, the time to climb is an economical issue, while for a fighter aircraft in a fight mission, it means win or lose.

The ROC, by definition, is the vertical component of the aircraft's velocity, which is simply the time rate of change of altitude *dh/dt*. Hence

$$\dot{h} = \frac{dh}{dt} = \mathrm{ROC} = V\sin(\gamma) \tag{7.87}$$

Thus, the time dt required to gain the small height dh at a given instantaneous altitude is

$$dt = \frac{dh}{\mathrm{ROC}} = \frac{dh}{V\sin(\gamma)} \tag{7.88}$$

Since the aircraft can consume a considerable amount of fuel during the climb to a high altitude, the effect of the weight change (reduction) must be accounted for. Thus, we cannot simply linearize this equation and divide altitude by a constant maximum ROC. In Equation 7.88, both V and γ are functions of altitude. The time to climb from one altitude h_1 to another h_2 is obtained by integrating Equation 7.88 between the two altitudes

$$t = \int_{h_1}^{h_2} \frac{dh}{\mathrm{ROC}} = \int_{h_1}^{h_2} \frac{dh}{V\sin(\gamma)} \tag{7.89}$$

When the time to climb is considered from sea level, h_1 is assumed to be zero. Hence, the time to climb from sea level to any given altitude h is

$$t = \int_{0}^{h} \frac{dh}{V\sin(\gamma)} = \int_{0}^{h} \frac{dh}{\mathrm{ROC}} \tag{7.90}$$

If in Equation 7.90 the ROC_{max} is used at each altitude, then it becomes the minimum time (t_{min}) to climb to altitude; h, which corresponds to the fastest climb:

$$t_{\min} = \int_0^h \frac{dh}{\mathrm{ROC}_{\max}} = \int_0^h \frac{dh}{V_{\mathrm{ROC}_{\max}} \sin\left(\gamma_{\mathrm{ROC}_{\max}}\right)} \tag{7.91}$$

It is often hard to integrate this equation to find time to climb since both $V_{ROC_{max}}$ and $\gamma_{ROC_{max}}$ are nonlinear functions of altitude. In the preliminary analysis, it is recommended that rather than attempting to integrate Equation 7.91, the average values are used to determine the increment of time for a specific altitude interval. This is an approximate technique and yields inaccurate results since we use a linearized equation for each altitude interval.

Furthermore, such a calculation improves the approximation and allows the inclusion of thrust reduction due to the altitude change. In the spanwise calculation, an estimate for the fuel used in the climb can also be evaluated. Using such a method, the integration is converted to the following algebraic sum expression:

$$t_{\min} = \sum_{i=0}^{n} \frac{\Delta h}{V_{\mathrm{ROC}_{\max_i}} \sin\left(\gamma_{\mathrm{ROC}_{\max_i}}\right)} = \sum_{i=0}^{n} \frac{\Delta h}{\mathrm{ROC}_{\max_i}} \tag{7.92}$$

The sum of the steps yields the total time to a desired altitude. For this purpose, the total altitude needs to be divided into n number of small heights. Takeoff and climb segment of the flight represents only 8%–15% of the total time [80] of a medium- (e.g., Boeing 737–800) to long-range (e.g., Boeing 777-200 and Boeing 747-400) flight. The transport aircraft Embraer E190 with a maximum takeoff mass of 51,800 kg takes 16 min to climb to 35,000 ft cruising altitude.

The fuel mass to climb (m_f) is the amount of fuel that is consumed by aircraft engine to reach a desired altitude. Employing Equation 7.82, and the time to climb introduced earlier, the following expression is derived for the fuel to climb:

$$m_f = \sum_{i=0}^{n} \frac{C_i T_i}{g} \Delta t \tag{7.93}$$

where C is the specific fuel consumption, and T is the maximum engine thrust at altitude. The distance to climb (X) is the amount of horizontal distance (or ground distance, if the wind is ignored) that is covered by aircraft to reach a desired altitude. The ground distance in a climb may be calculated in a similar manner by employing Equation 7.14.

$$X = \sum_{i=0}^{n} V_i \cos\left(\gamma_i\right) \Delta t \tag{7.94}$$

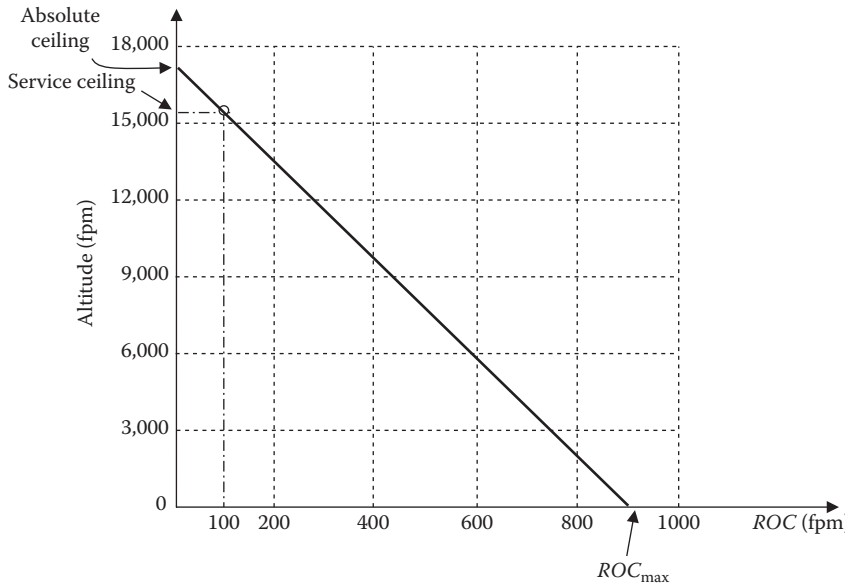

FIGURE 7.21 Maximum rate of climb for the Cherokee Arrow versus altitude.

Figure 7.21 shows [57] the ROC_{max} for the light aircraft Piper PA-28 Cherokee Arrow (with a maximum takeoff weight of 2,650 lb and full throttle) versus altitude. Examination of this figure shows that the maximum ROC varies almost linearly with altitude. Based on this approximation, we can write

$$\text{ROC}_{\text{max}} = \text{ROC}_{\text{max}_{\text{SL}}} + kh \tag{7.95}$$

where h is a desired altitude, $\text{ROC}_{\text{max}_{\text{SL}}}$ is the ROC_{max} at the sea level, and k is the slope of the line. To find k, we apply this equation for absolute ceiling. At the absolute ceiling, the ROC_{max} is zero, and so

$$\text{ROC}_{\text{max}_{\text{ac}}} = 0 = \text{ROC}_{\text{max}_{\text{SL}}} + kh_{\text{ac}} \tag{7.96}$$

Thus, the slope k is obtained as

$$k = \frac{-\text{ROC}_{\text{max}_{\text{SL}}}}{h_{\text{ac}}} \tag{7.97}$$

Inserting k from Equation 7.97 into Equation 7.95 yields

$$\text{ROC}_{\text{max}} = \text{ROC}_{\text{max}_{\text{SL}}} + \frac{-\text{ROC}_{\text{max}_{\text{SL}}}}{h_{\text{ac}}} h = \text{ROC}_{\text{max}_{\text{SL}}} \left(1 - \frac{h}{h_{\text{ac}}}\right) \tag{7.98}$$

where h is a desired altitude, and h_{ac} is the absolute ceiling. Substituting Equation 7.98 into Equation 7.91, and solving the integration, we obtain

$$t_{min} = \frac{h_{ac}}{ROC_{max_{SL}}} \ln\left(\frac{1}{1-\left(h/h_{ac}\right)}\right) \tag{7.99}$$

Note that the reference for this equation is the sea level. Equation 7.99 can be generalized for the shortest time to climb from an altitude, h_1, to another altitude, h_2

$$t_{min} = \frac{h_{ac}}{ROC_{max_1}} \ln\left(\frac{1}{1-\left(h_2/h_{ac}\right)}\right) \tag{7.100}$$

where ROC_{max_1} is the maximum ROC at altitude h_1. The time to climb is a nonlinear function of altitude; the higher the altitude, the longer is the time. However, due to the logarithmic nature of the formula, the latter part of the climb takes much longer than the first part.

In general, once the flaps are retracted, the pilot should accelerate to maximum ROC speed. From a fuel consumption perspective, a full-thrust takeoff and a full-thrust climb profile offer [80] the most fuel economy for an unrestricted climb. However, from an aircraft cost perspective, this must be balanced with engine degradation and time between overhauls, as well as guidance from the engine manufacturer.

Figure 7.22 demonstrates time to climb to the absolute ceiling for the jet aircraft Cessna Citation III with a service ceiling of 51,000 ft and an ROC_{max} of 3,700 ft/min. It is interesting to see that it takes about 43 min to climb to its service ceiling, while it takes longer (about 50 min) to climb from service ceiling to the absolute ceiling.

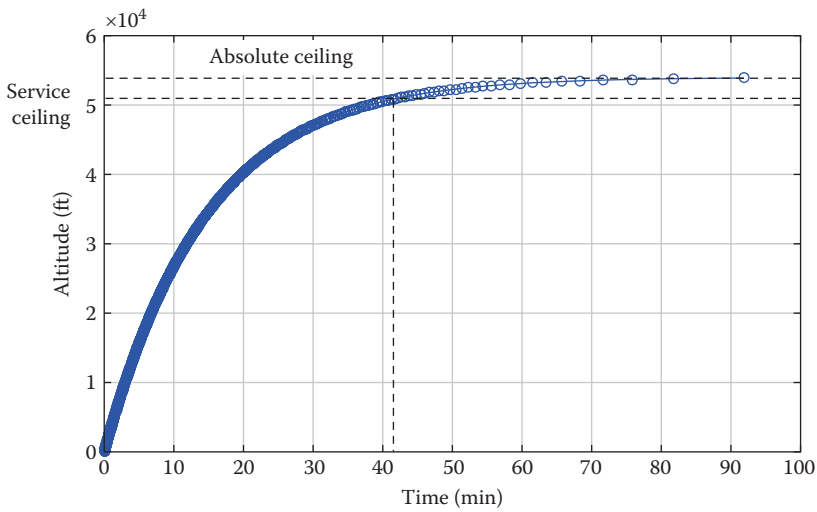

FIGURE 7.22 Time to climb for the jet aircraft Cessna Citation III.

TABLE 7.3
Typical Velocity and Altitude for a Boeing 777 in a Climbing Flight

No.	Speed in knot (km/h)	Altitude (km)	Distance from Airport (km)	Time Elapsed (min)	Remark
1.	154 (285.2)	0	0	0	Rotation
2.	205 (380)	2,130	24	3.5	
3.	250 (463)	3,000	29	5	
4.	389 (720)	3,600	38	6	
5.	397 (735)	4,000	44	7	
6.	420 (778)	4,960	57	9	
7.	440 (815)	5,700	72	11	
8.	458 (848)	6,400	84	13	
9.	474 (878)	8,000	120	18	
10.	480 (889)	10,000	258	30	
11.	**495 (917)**	**11,000**	**450**	**41**	**Cruise altitude**

The bold values indicate the cruising flight parameters.

In the first section of the figure, the variation of time with altitude is almost linear. However, in the latter part, the slope is gradually decreasing logarithmically. The asymptote indicates that the aircraft has reached the absolute ceiling. Table 7.3 illustrates (from the author's experience) the altitude, velocity, and timing for a Boeing 777 (Figure 7.18) climbing flight. Another Boeing aircraft, the B-717, climbs very well, passing 10,000 ft in 4 min after brake release, with a climb speed of 289 KIAS.

Case Study - Example 7.10

The ROC_{max} of the transport aircraft Boeing 747-400 (Figure 8.10b), with four turbofan engines each generating 252 kN of thrust, at sea level is 2,350 ft/min (11.94 m/s), and its service ceiling is 43,000 ft (13,110 m). Assuming the absolute ceiling is 46,000 ft (14,020 m), what is the minimum time to climb the service ceiling?

Solution

$$t_{\min} = \frac{h_{ac}}{ROC_{max_{SL}}} \ln\left(\frac{1}{1-\left(h/h_{ac}\right)}\right) = \frac{46{,}000}{2{,}350} \ln\left(\frac{1}{1-\left(43{,}000/46{,}000\right)}\right) = 53.4\,\text{min} \qquad (7.99)$$

It takes about 53 min to climb to the altitude of 43,000 ft.

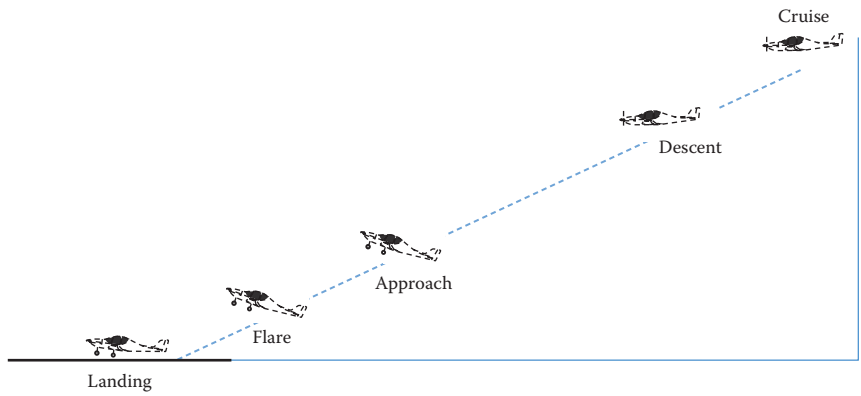

FIGURE 7.23 Flight phases from cruise to landing.

7.10 DESCENT

Descending flight is another flight operation that must be evaluated for aircraft performance analysis. It is not as important as climbing flight, but there are a few instances that an aircraft must perform well; otherwise, aircraft may end up having a crash. Descending flight is the major flight operation prior to landing (see Figure 7.23) for a conventional aircraft. It is the lowest-cost flight operation. A descent during air travel is any portion of the flight where an aircraft decreases the altitude and is the opposite to an ascent or a climb. Descents are an essential component of an approach to landing. Large transport aircraft in a long-range flight begins to descend (from cruise ceiling) when the aircraft has about 150–250 km to the destination airport. This is equivalent to about 20–30 min of a long-range flight.

A normal descent after a cruising flight and prior to the landing will be decelerating; that is, the aircraft speed should be gradually decreased from cruising velocity to the approach speed. Other intentional descents might be to avoid traffic, poor flight conditions (turbulence, icing condition, and bad weather), clouds (particularly under visual flight rule), to see something lower, to enter warmer air, or to take advantage of wind direction of a different altitude, particularly with balloons.

Another situation that may require an aircraft descent is during emergencies, such as a sudden decompression forcing an emergency descent to below 10,000 ft, which is the maximum safe altitude for an unpressurized aircraft. Involuntarily descent might occur from a decrease in engine power (i.e., all engine inoperative), a decrease in lift (e.g., wing icing), an increase in drag, or flying in an air mass moving downward, such as a terrain-induced downdraft, near a thunderstorm (see Chapter 1), in a downburst or microburst. Rapid descents are due to dramatic changes in the cabin air pressure – even pressurized aircraft – and can result in discomfort in the middle ear.

Normally, descents take place at a constant angle of descent (about 3°–5° for most aircraft). The pilot controls the angle of descent by varying engine power/thrust, which is about 10%–30% of the total power/thrust, and pitch attitude (lowering the nose) to keep the airspeed constant. In extreme cases, an emergency descent is demanded. An emergency descent (due to cases such as an uncontrollable fire and

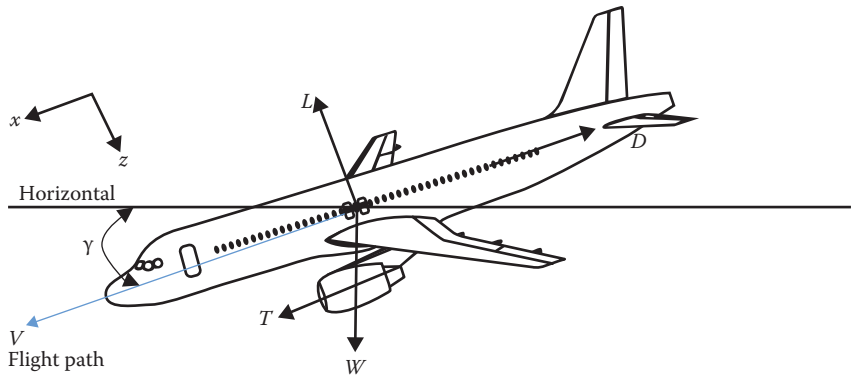

FIGURE 7.24 Contributing forces in a descending flight.

a sudden loss of cabin pressure) is a maneuver for descending as rapidly as possible to a lower altitude or to the ground for an emergency landing. Unpowered descent (such as engine failure) is steeper than a powered descent but flown in a similar way as a glider. If the nose is too high for the chosen power, the airspeed will decrease until eventually the aircraft stalls. Typical descend angle for large transport aircraft ranges from 1° to 3°; and rarely descend [36] at angles >10°. It is interesting to note that the Space Shuttle (Figure 4.26) has a space descent of 21°, while having an air descent angle of 3°.

Whenever the vertical forces (lift plus vertical component of engine thrust) are less than aircraft weight, aircraft will lose height and will descend. Descent can be simply viewed as a negative climb. If the engine is turned off during a descending flight, this flight operation is called *gliding flight*. An extreme case is when the descent angle is 90° and this flight program is referred to as *dive*. The *diving* is a beautiful part of a maneuvering flight usually carried out by an acrobatic aircraft. Due to the downward direction of a *dive*, the flight is often accelerating.

Figure 7.24 demonstrates the contributing forces (weight, W; lift, L; drag, D; and thrust, T) in a descending flight (constant speed). In an unaccelerated descending flight, equilibrium of forces in x and z directions are

$$\sum F_z = 0 \Rightarrow L - W\cos(\gamma) = 0 \tag{7.101}$$

$$\sum F_x = 0 \Rightarrow D - T - W\sin(\gamma) = 0 \tag{7.102}$$

In a descending flight, the drag is greater than thrust, and lift is smaller than weight. If the aircraft speed is kept constant, KE is not changed. Instead, PE is decreased in the form of losing height. Using Equation 7.101, we can write

$$\gamma = \cos^{-1}\left(\frac{L}{W}\right) \tag{7.103}$$

Hence, the rate of change of altitude depends on the lift-to-weight ratio. As we reduce the engine thrust, the rate of altitude reduction is increased too. The rate of descent (ROD) is defined as

$$\text{ROD} = V\sin(\gamma) \tag{7.104}$$

where V is the aircraft airspeed and γ represents the descent angle. For a typical decelerated descend, we need to include the deceleration (a) in the governing equations. Based on Newton's second law, in a decelerated descend, the governing equations in x and z directions are

$$\sum F_z = ma_z \Rightarrow L - W\cos(\gamma) = ma_z \tag{7.105}$$

$$\sum F_x = ma_x \Rightarrow T + W\sin(\gamma) - D = ma_x \tag{7.106}$$

where a_x is the deceleration along the x-axis and a_z is the deceleration along the z-axis. The deceleration in x direction is a function of final and initial airspeeds and is obtained from

$$a_x = \frac{V_2^2 - V_1^2}{2X} \tag{7.107}$$

where X is the total distance traveled along x-axis, V_2 is the final speed, and V_1 is the initial speed. Table 7.4 illustrates (from personal experience) the altitude, velocity, and flap deflection for a Boeing 777 (Figure 7.18) in a descending flight (from cruise to the landing).

Case Study - Example 7.11

The jet aircraft Cessna 560 with a maximum thrust of 13.55 kN and a mass of 7,000 kg is required to descend with a 5° of descent angle and maintaining a constant speed.

a. If the desired velocity is 250 knots (463 km/h), what percentage of the engine thrust is required for this flight operation?
b. Assume air density is constant at 1.1 kg/m^3. What must be the aircraft angle of attack? Assume $\alpha_o = 0$.
c. Determine the ROD.

$$S = 31.83\,\text{m}^2,\ C_{D_o} = 0.02,\ a = 5.21/\text{rad},\ K = 0.05$$

TABLE 7.4
Typical Velocity and Flap Deflection for a Boeing 777 in a Descent

No.	Speed (knot)	Altitude (ft)	Distance from Airport (mile)	Flap Deflection (°)	Descent Rate (fpm)	Spoiler
1.	485	36,000	164	0	0	Not used
2.	428	20,000	112	0	2,500	Not used
3.	351	15,000	87	0	2,500	Deflected
4.	286	10,000	69	0	2,500	Deployed
5.	245	6,000	33	0	1,500	Deployed
6.	214	4,000	23	5	1,500	Deployed
7.	183	3,000	13	10	1,500	Deployed
8.	156	1,500	6	15–20	1,500	Deployed
9.	152	500	1.8, Final approach	30–40	1,000	Deployed
10.	148	0	Touchdown	30–40	0	Deployed

Solution

a. Percentage of the engine thrust
The lift is

$$L - W\cos(\gamma) = 0 \Rightarrow L = W\cos(\gamma) = 7{,}000 \times 9.81 \times \cos(5) = 68{,}409\,\text{N} \quad (7.101)$$

The lift coefficient

$$L = \frac{1}{2}\rho V^2 S C_L \Rightarrow C_L = \frac{L}{(1/2)\rho V^2 S} = \frac{68{,}409}{0.5 \times 1.1 \times (250 \times 0.5144)^2 \times 31.83} = 0.236 \quad (2.4)$$

$$C_D = C_{D_o} + KC_L^2 = 0.02 + 0.05 \times 0.236^2 = 0.0228 \quad (3.12)$$

$$D = \frac{1}{2}\rho V^2 S C_D = 0.5 \times 1.1 \times (250 \times 0.5144)^2 \times 31.83 \times 0.0228 = 6{,}601\,\text{N} \quad (2.5)$$

$$D - T - W\sin(\gamma) = 0 \Rightarrow T = D - W\sin(\gamma)$$
$$T = 6{,}601 - 7{,}000 \times 9.81 \times \sin(5) = 6{,}601 - 5{,}985 = 616\,\text{N} \quad (7.102)$$

The ratio between the required thrust and available thrust is

$$\frac{616}{13{,}550} = 0.045$$

Thus, the pilot needs to employ only 4.5% of the engine thrust for this descending flight operation.

b. Aircraft angle of attack

$$a = C_{L_\alpha} = \frac{dC_L}{d\alpha} = \frac{C_L}{\alpha} \Rightarrow \alpha = \frac{C_L}{C_{L_\alpha}} \tag{2.10}$$

$$\alpha = \frac{0.236}{5.2} = 0.04538\,\text{rad} = 2.6^\circ$$

c. Rate of descent

$$\text{ROD} = V\sin(\gamma) = 250 \times 0.5144 \times \sin(5) = 11.208\,\text{m/s} = 2{,}208\,\text{ft/min} \tag{7.104}$$

Case Study - Example 7.12

The transport aircraft Boeing 777-200 (Figure 7.18b) with a takeoff mass of 200,000 kg and two turbofan engines each generating a sea-level thrust of 342 kN is required to descend from 12,000 ft (3,658 m) to 11,000 ft (3,353 m). In this descending flight, the airspeed should be decreased from 195 to 185 m/s when a 10-mile (16.093 km) horizontal distance is covered (See Figure 7.25). Determine what percentage of the engine thrust should be employed at the beginning of this descent. Assume that the deceleration in the *z*-axis (See Figure 7.24) is zero. Other characteristics of the aircraft are given as

$$S = 427.8\,\text{m}^2,\ b = 60.9\,\text{m},\ C_{D_o} = 0.02,\ e = 0.87.$$

Solution

At 12,000 ft, the air density is 0.001648 slug/ft^3 or 0.849 kg/m^3. The altitude reduction is 1,000 ft or 305 m. The total distance traveled along the flight path (*x*-axis) is

$$X = \sqrt{h^2 + D^2} = \sqrt{(305)^2 + (16{,}093)^2} = 16{,}096.3\,\text{m}$$

The deceleration along *x*-axis is

$$a_x = \frac{V_2^2 - V_1^2}{2X} = \frac{185^2 - 195^2}{2 \times 16{,}096.3} = -0.118\,\text{m/s}^2 \tag{7.107}$$

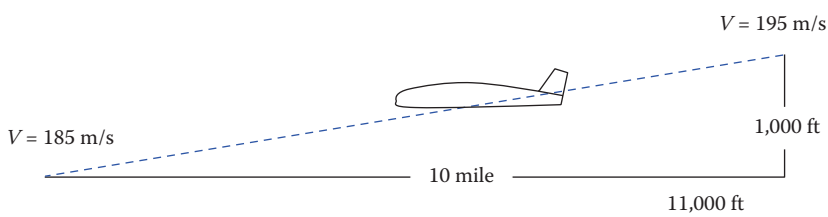

FIGURE 7.25 Descending flight of the aircraft in Example 7.12 (figure is not to scale).

From Figure 7.25, the descent angle is

$$\gamma = \tan^{-1}\left(\frac{305}{16{,}093}\right) = 0.019\,\text{rad} = 1.085°$$

We first need to calculate a few parameters

$$\text{AR} = \frac{b^2}{S} = \frac{60.9^2}{427.8} = 8.67 \tag{3.9}$$

$$K = \frac{1}{\pi e\,\text{AR}} = \frac{1}{3.14 \times 0.87 \times 8.67} = 0.042 \tag{3.8}$$

In z direction

$$L - W\cos(\gamma) = ma_z \tag{7.105}$$

Since $a_z = 0$, the lift is

$$L - W\cos(\gamma) = 0 \Rightarrow L = W\cos(\gamma) = 200{,}000 \times 9.81 \times \cos(1.085) = 1{,}960{,}978\,\text{N}$$

The lift coefficient

$$L = \frac{1}{2}\rho V^2 S C_L \Rightarrow C_L = \frac{L}{0.5\rho V^2 S} = \frac{1{,}960{,}978}{0.5 \times 0.849 \times (195)^2 \times 427.8} = 0.284 \tag{2.4}$$

At the beginning of the descent, drag is

$$C_D = C_{D_o} + KC_L^2 = 0.02 + 0.042 \times 0.284^2 = 0.0234 \tag{3.12}$$

$$D = \frac{1}{2}\rho V^2 S C_D = 0.5 \times 0.849 \times (195)^2 \times 427.8 \times 0.0234 = 161{,}664\,\text{N} \tag{2.5}$$

The required thrust for this descent is

$$T + W\sin(\gamma) - D = ma_x \Rightarrow T = D - W\sin(\gamma) + ma_x \tag{7.106}$$

$$T_{\text{req}} = 161{,}664 - 200{,}000 \times 9.81 \times \sin(1.085) + 200{,}000 \times (-0.118) = 100{,}916\,\text{N}$$

However, the available thrust at 12,000 ft (troposphere) is

$$T_{\text{av}} = T_O\left(\frac{\rho}{\rho_o}\right)^1 = 2 \times 342{,}000\left(\frac{0.849}{1.225}\right) = 474{,}025\,\text{N} \tag{4.24}$$

The ratio between the required thrust and available thrust is

$$\frac{T_{\text{req}}}{T_{\text{av}}} = \frac{100{,}916}{474{,}025} = 0.213$$

Thus, the pilot needs to employ only 21.3% of the engine thrust for this descending flight operation.

7.11 GLIDING FLIGHT

Gliding is the most important recreational activity and competitive flight sport in which pilots fly unpowered aircraft such as kites, hang gliders, gliders, or sailplanes. A powered heavier-than-air craft may also experience gliding flight when all engines are inoperative during a flight or when the aircraft runs out of fuel. A glide is a basic maneuver in which the aircraft loses altitude in a controlled descent with little or no engine power. The forward motion is maintained by aircraft weight pulling the airplane along an inclined path. The glide rate is controlled by balancing the forces of weight, lift, and drag.

The glide operation is usually performed relatively close to the ground, and so for a pilot, the accuracy of the execution and the formation of proper technique and habits are of special importance. Three most common methods of takeoff for gliders are: (1) towed by another powered aircraft, (2) winch (for gliders/sailplanes), and (3) self-launching (for motor gliders). The first method requires assistance from another aircraft, which needs to take off simultaneously.

After launch or assisted takeoff, a glider pilot searches for a local rising air to gain height. If conditions are ready enough, an experienced pilot can fly many hours before returning to the home airfield and occasionally flight over 100 km are made. A powered aircraft is expected to glide when the engine is running out of fuel as long as possible. The light aircraft Piper PA-28 Cherokee Arrow (with a maximum takeoff weight of 2,650 lb, when propeller is *wind milling*) can glide for a horizontal distance of 22 miles [57] if the starting altitude is 14,000 ft. However, when the aircraft begins the glide at the height of 8,000 ft, the horizontal distance would be 12.5 miles.

In a gliding flight, the flying skill of the pilot and the weather conditions are very critical for a safe landing. When there is no certified airfield for landing in the nearby area, the pilot has to land in the closest flat surface (this may be a farm or just a highway). This section deals with the concept of glide and the parameters affecting this flight program.

When a glider is in rising hot air, the aircraft will soar and gain PE (i.e., will climb without consumption of energy!). This flight operation is similar to the climbing flight of a hot air balloon. However, when the air is calm and has the same temperature as the surrounding, a glider aircraft should lose PE to gain KE. Because the application of control surfaces is somewhat different in glides than in powered descents, gliding maneuvers require the perfection of a technique somewhat different from that required for ordinary power-on maneuvers [81].

The lack of engine thrust will allow an aircraft only to glide/descend. For such case, only three forces will contribute to its performance: (1) weight, (2) lift, and (3) drag. The force diagram for an unpowered aircraft in a gliding flight is shown in Figure 7.26. For an accelerated glide, where γ is the glide angle (the flight path angle), the application of Newton's second law yields

$$L - W\cos\gamma = ma_x \tag{7.108}$$

$$D - W\sin\gamma = ma_z \tag{7.109}$$

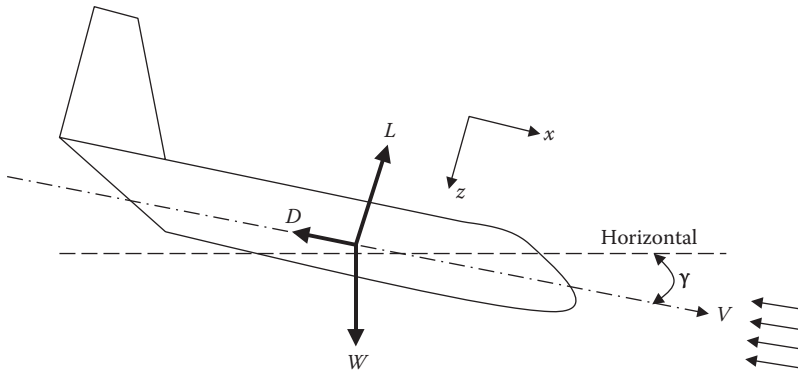

FIGURE 7.26 The force diagram for an unpowered aircraft in a gliding flight.

where a_x is the acceleration in the flight path axis, and a_z is the acceleration in the z-axis. The extreme case is a free-falling (dive) where there is no lift, and the glide angle is 90°:

$$D - W = ma_x \tag{7.110}$$

For a steady unaccelerated glide,

$$L - W\cos\gamma = 0 \tag{7.111}$$

$$D - W\sin\gamma = 0 \tag{7.112}$$

The equilibrium glide angle is obtained by dividing Equation 7.111 by Equation 7.112:

$$\frac{\sin\gamma}{\cos\gamma} = \frac{D}{L} = \frac{C_D}{C_L} \tag{7.113}$$

or

$$\tan(\gamma) = \frac{D}{L} = \frac{1}{L/D} \tag{7.114}$$

Thus, the glide angle is

$$\gamma = \tan^{-1}\left[\frac{1}{(L/D)}\right] \tag{7.115}$$

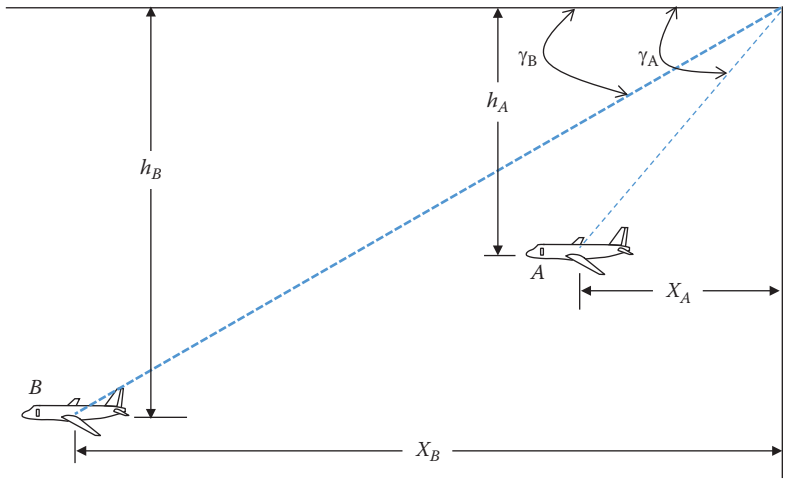

FIGURE 7.27 Two scenarios for a gliding flight operation.

This equation demonstrates that the glide angle is strictly a function of the lift-to-drag ratio; the higher the *L/D*, the shallower is the glide angle. Hence, the glide angle does not depend on the aircraft weight or flight altitude. Two major gliding flight programs are

1. Glide with maximum ground distance
2. Glide with maximum flight time (minimum sink rate)

We will discuss both cases separately in Sections 7.11.1 and 7.11.2. These two flight operation approaches are illustrated in Figure 7.27. This figure compares two aircraft (A and B) at different gliding flight programs for the same duration of time. Both aircraft have flown for 1 min, but aircraft A has lost smaller height, whereas aircraft B has covered more horizontal distance. Aircraft A has used the first flight operation, but aircraft B has followed the second flight approach.

7.11.1 Gliding Flight with Maximum Ground Distance

The glide with a maximum ground distance (range) occurs when an aircraft flies with the minimum glide angle (γ_{min}). At this situation, the maximum ground distant (i.e., maximum range) is covered. This glide operation is suitable for a powered aircraft with all engines inoperative. Pilots must maximize their horizontal distance, to find an appropriate place to land safely. An interesting parameter in this flight operation is the glide ratio, that is, the horizontal distance covered with each unit of lost altitude. The higher the glide ratio, the longer the horizontal distance covered with losing each unit of altitude. This ratio is about 10–15 for majority of modern aircraft, but for gliders, the ratio is about 30–40.

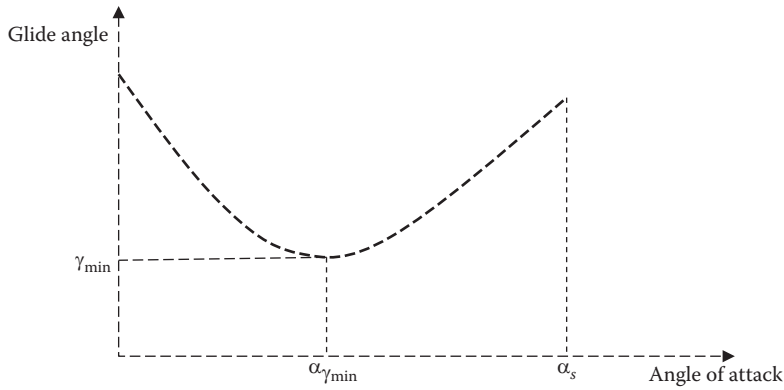

FIGURE 7.28 Relationship between the angle of attack and the glide angle.

From Equation 7.114, it can be readily concluded that, the smallest glide angle (i.e., γ_{min}) occurs when the denominator is maximized. Hence, the aircraft is at a flight condition where the lift-to-drag ratio is maximum, that is, $(L/D)_{max}$

$$\gamma_{min} = \tan^{-1}\frac{1}{(L/D)_{max}} \tag{7.116}$$

As an example, an aircraft with a maximum lift-to-drag ratio of 19 must glide with a glide angle of 3° (tan(3) = 1/19). To glide with a specific glide angle, a pilot must adjust aircraft angle of attack (α) at a specific value by deflecting aircraft elevator (see Figure 7.28). Only one specific angle of attack will provide the minimum glide angle. Recall from Chapter 5 that the maximum lift-to-drag ratio is

$$\left(\frac{L}{D}\right)_{max} = \frac{1}{2\sqrt{KC_{D_o}}} \tag{5.24}$$

So,

$$\gamma_{min} = \tan^{-1}\left(2\sqrt{KC_{D_o}}\right) \tag{7.117}$$

Recall from Chapter 3 that the induced drag correction factor (K) is inversely proportional to the wing aspect ratio:

$$K = \frac{1}{\pi e\,\mathrm{AR}} \tag{3.8}$$

Therefore, to minimize the glide angle, one must decrease the induced drag correction factor (K), which implies that the wing aspect ratio (AR) must be increased. Structurally, the wing AR and the wing span have some limits. In practice, the

highest AR belongs to gliders with the magnitude of about 25–40. The GlobalFlyer, a long-range aircraft for record attempt with a mass of 10,024 kg and a wing AR of 32.6 has a glide ratio of 37.

From Equation 7.116, we see that the glide angle is only a function of lift-to-drag ratio, and the minimum glide angle is achieved when the aircraft glides (flies) at an airspeed that yields the maximum *L/D* or the minimum drag (i.e., $V_{D_{\min}}$). In Chapter 5, we derived such velocity as defined in Equation 5.38. Thus,

$$V_{\gamma_{\min}} = V_{D_{\min}} = \sqrt{\frac{2mg\cos\left(\gamma_{\min}\right)}{\rho S\sqrt{C_{D_o}/K}}} \tag{7.118}$$

where $\gamma_{\min}$ is determined via Equation 7.117. Recall that this speed is not the aircraft horizontal speed; it is the equilibrium glide airspeed (in the direction of flight path).

Caution: As we discussed before, it is possible for $V_{\gamma_{\min}}$ to be theoretically less than the stall speed. For such a case, it is not possible for that airplane to achieve the theoretical minimum descent angle. If the solution is a speed that is less than the stall speed (V_s), we have to resort to a safe speed. So, in this case, the speed for minimum glide angle must be slightly higher than the stall speed

$$V_{\gamma_{\min}} = kV_s \tag{7.119}$$

where k is a number between 1.1 and 1.3. For civil aircraft, the parameter k is between 1.2 and 1.3, but for military aircraft, k is between 1.1 and 1.2. The exact k depends on several factors such as mission of the aircraft and airworthiness regulations. By using Equation 7.104, the rate of sink (ROS) for minimum glide angle is obtained as

$$\text{ROS}_{\gamma_{\min}} = V_{\gamma_{\min}}\sin\left(\gamma_{\min}\right) \tag{7.120}$$

where the aircraft velocity $\left(V_{\gamma_{\min}}\right)$ is given by Equation 7.118. The maximum horizontal distance covered in a gliding unpowered flight is

$$d_{\max} = \frac{\Delta h}{\tan\left(\gamma_{\min}\right)} \tag{7.121}$$

where Δh is the height that is lost during glide operation. For most hang gliders, the glide ratio is about 20:1 (travel forward 20 m while only losing 1 m of altitude), speed range is 35–130 km/h, and the best glide is at 50–60 km/h.

7.11.2 Gliding Flight with Maximum Flight Time

In a climbing flight, we are usually willing to climb as fast as possible, while in a gliding flight, the goal is to descend as slowly and as long as possible. The gliding flight with maximum flight time (endurance) occurs when an aircraft is flying with

the minimum sink rate. The ROD or ROS is the vertical component (V_z) of gliding velocity (V) of the aircraft. For unpowered glide, it is analogous to ROC for powered flight. As indicated in Figure 7.22, and the same as what we had in Section 7.8, the ROS is

$$\text{ROS} = V_z = V\sin(\gamma) \tag{7.122}$$

Although the ROS is a positive number, it is in a downward direction. Multiplying both sides of Equation 7.112 by aircraft gliding velocity (V), we have

$$DV - W\sin(\gamma)V = 0 \Rightarrow DV = WV_z \tag{7.123}$$

or

$$V_z = \frac{DV}{W} = \frac{(1/2)\rho V^3 S C_D}{W} \tag{7.124}$$

We wish to minimize the ROS (or V_z) of the aircraft; which is mathematically performed by minimizing the numerator of Equation 7.124. The only parameter that we can control is the aircraft velocity (V). By definition, the DV is the power required for a steady-level flight. Hence, the minimum sink rate occurs at the glide velocity for the minimum required power. From Chapter 6, the velocity for minimum power (Equation 6.20) is

$$V_{\text{ROS}_{\min}} = V_{\min_P} = \sqrt{\frac{2mg}{\rho S\sqrt{3C_{D_o}/K}}} \tag{7.125}$$

Note that this velocity is initially derived for a level flight. However, here, this velocity is the gliding velocity (not level). This is correct since the theoretical goal is to minimize the required power, but the practical objective is to minimize the sink rate. These two goals are consistent. This is the reason why "cos (γ)" is not used in the numerator of Equation 7.125.

Caution: As we discussed earlier, it is possible for $V_{\text{ROS}_{\min}}$ to be theoretically less than the stall speed. For such a case, it is not possible for that airplane to achieve the theoretical minimum sink rate. If the solution is a speed that is less than the stall speed (V_s), we have to resort to a safe speed. Thus, in this case, the speed for the minimum sink rate must be higher than the stall speed

$$V_{\text{ROS}_{\min}} = kV_s \tag{7.126}$$

where k is a number between 1.1 and 1.3. For a civil aircraft, the parameter k is between 1.2 and 1.3, but for a military aircraft, k is between 1.1 and 1.2. The exact value of k depends on several factors such as the aircraft mission and airworthiness regulations.

To find the minimum sink rate, we will develop a relationship that relates the sink rate and flight variables. Then, we will differentiate it with respect to one variable (e.g., glide angle, γ). By substituting V from Equations 7.111 and 2.4 into Equation 7.122, we have

$$\mathrm{ROS} = V\sin(\gamma) = \sqrt{\frac{2mg\cos(\gamma)}{\rho S C_L}}\sin(\gamma) \tag{7.127}$$

Substituting sin(γ) from Equation 7.113 into this equation, we can obtain

$$\mathrm{ROS} = \sqrt{\frac{2mg}{\rho S C_L}}\cos(\gamma)\frac{C_D}{C_L} = \sqrt{\frac{2mg}{\rho S C_L}}\sqrt{\cos(\gamma)^2\frac{C_D^2}{C_L^2}} \tag{7.128}$$

or

$$\mathrm{ROS} = \sqrt{\frac{2mg\cos^2(\gamma)}{\rho S\left(C_L^3/C_D^2\right)}} \tag{7.129}$$

To determine the maximum ROS, we need to differentiate Equation 7.129 with respect to the glide angle (i.e., $d\,\mathrm{ROS}/d\,\gamma$). Differentiation of this nonlinear equation with respect to glide angle is a difficult task. An easier way is to assume that γ is small enough to be neglected, or $\cos^2(\gamma) \approx 1$ (as it is true enough). Then, we will show that $\mathrm{ROS}_{\min}$ occurs at $\left(C_L^3/C_D^2\right)_{\max}$. In Chapter 6, we showed that when an aircraft is flying with the minimum power speed, the parameter $\left(C_L^3/C_D^2\right)$ will be maximized (Equations 6.20 and 6.41). The glide velocity for the minimum sink rate is less than that for minimum glide angle since the aircraft angle for the minimum sink rate is more than that for minimum glide angle. Thus, the minimum ROS is:

$$\mathrm{ROS}_{\min} = \sqrt{\frac{2W}{\rho S\left(C_L^3/C_D^2\right)_{\max}}} = \sqrt{\frac{2W}{\rho S\left[\left(C_L^{3/2}/C_D\right)_{\max}\right]^2}} \tag{7.130}$$

This equation shows that the sink rate decreases with decreasing altitude (i.e., increasing air density) and increases as the square root of the wing loading (W/S). Note that, $\left(C_L^3/C_D^2\right)_{\max} = \left[\left(C_L^{3/2}/C_D\right)_{\max}\right]^2$.

The aircraft velocity for the minimum ROS (corresponding to the maximum $\left(C_L^3/C_D^2\right)$) is less than that for minimum glide angle (corresponding to the maximum (C_L/C_D)). As we proved in Equation 6.41, we have

$$\left(\frac{C_L^{3/2}}{C_D}\right)_{\max} = \frac{0.57}{K^{3/4}C_{D_o}^{1/4}} \tag{6.41}$$

Thus,

$$\mathrm{ROS}_{\min} = \sqrt{\frac{2W}{\rho S\left[\dfrac{0.57}{K^{3/4}C_{D_o}{}^{1/4}}\right]^2}} \tag{7.131}$$

The minimum sink rate is

$$\mathrm{ROS}_{\min} = V_{\mathrm{ROS}_{\min}} \sin\left(\gamma_{\mathrm{ROS}_{\min}}\right) \tag{7.132}$$

So, the glide angle for minimum sink rate is

$$\gamma_{\mathrm{ROS}_{\min}} = \sin^{-1}\left(\frac{\mathrm{ROS}_{\min}}{V_{\mathrm{ROS}_{\min}}}\right) \tag{7.133}$$

A graphical technique to analyze a gliding flight is to utilize a *hodograph*. The hodograph of a gliding flight (i.e., variations of vertical speed vs. horizontal speed) is sketched in Figure 7.29. Such a graph can graphically provide two significant results: (1) A line from origin tangent to the curve defines the minimum glide angle ($\gamma_{\min}$) and (2) the lowest point on the graph represents the minimum sink rate ($\mathrm{ROS}_{\min}$). These two points usually do not coincide, which indicates that the minimum ROS does not correspond to the minimum glide angle.

The aircraft maximum duration of such gliding flight from the altitude h is

$$t_{\max} = \frac{h}{\mathrm{ROS}_{\min}} \tag{7.134}$$

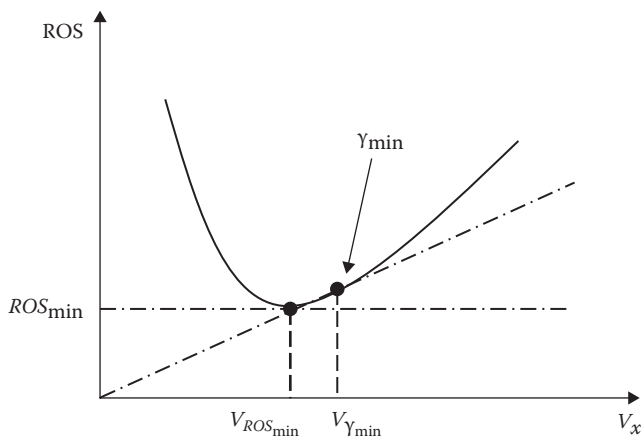

FIGURE 7.29 Hodograph for a gliding flight.

The aircraft will land after traveling a horizontal distance of

$$d_{t_{\max}} = \frac{h}{\tan\left(\gamma_{\mathrm{ROS}_{\min}}\right)} \tag{7.135}$$

Example 7.13

The pilot of a hang glider with a total mass of 120 kg and a wing area of 17 m^2 is going to glide from a height of 500 m to sea level. The aircraft has $C_{D_o} = 0.016$; $K = 0.09$, $C_{L_{\max}} = 1.2$.

a. What is the maximum flight time that the hang glider can be airborne?
b. If the goal is to be airborne as long as possible; what must be the glide angle?
c. How far (horizontal distance) will the aircraft glide from this point before touching the ground for this glide program?

Assume that the air density is constant throughout the flight at 1.225 kg/m^3.

Solution

a. Glide duration

To achieve the maximum flight time, the glider must fly with a speed that results in the minimum sink rate:

$$\left(\frac{L}{D}\right)^{3/2}_{\max} = \frac{1}{4}\left(\frac{3}{KC_{D_o}^{1/3}}\right)^{3/4} = \frac{1}{4}\left(\frac{3}{0.09\times(0.016)^{1/3}}\right)^{3/4} = 9.75 \tag{6.41}$$

$$\mathrm{ROS}_{\min} = \sqrt{\frac{2mg}{\rho S\left[\left(C_L^{3/2}/C_D\right)_{\max}\right]^2}} = \sqrt{\frac{2\times120\times9.81}{1.225\times17\times9.75^2}} = 1.09\,\mathrm{m/s} \tag{7.130}$$

An alternate way to determine $\mathrm{ROS}_{\min}$ is to use Equation 7.131 directly.

Both will yield the same result. In this case, the aircraft will fly for a maximum duration of

$$t_{\max} = \frac{h}{\mathrm{ROS}_{\min}} = \frac{500}{1.09} = 458.5\,\mathrm{s} \approx 7.6\,\mathrm{min} \tag{7.134}$$

b. Best glide angle

The aircraft speed for this flight is

$$V_{\mathrm{ROS}_{\min}} = \sqrt{\frac{2mg}{\rho S\sqrt{3C_{D_o}/K}}} = \sqrt{\frac{2\times120\times9.81}{1.225\times17\sqrt{(3\times0.016)/0.09}}} = 12.4\,\mathrm{m/s} \tag{7.125}$$

We need to check the flight safety by comparing this value with the stall speed

$$V_s = \sqrt{\frac{2mg}{\rho S C_{L_{\max}}}} = \sqrt{\frac{2\times 120\times 9.81}{1.225\times 17\times 1.2}} = 9.7\,\text{m/s} \tag{2.49}$$

The aircraft glide speed of 12.4 m/s is greater than the stall speed and is acceptable. This speed is used to determine the minimum glide angle:

$$\gamma_{\text{ROS}_{\min}} = \sin^{-1}\left(\frac{\text{ROS}_{\min}}{V_{\text{ROS}_{\min}}}\right) = \sin^{-1}\left(\frac{1.09}{12.4}\right) \tag{7.133}$$

This results in the best glide angle (γ) of

$$\gamma_{\text{ROS}_{\min}} = 0.088\,\text{rad} = 5.05^\circ$$

c. Ground distance

The aircraft will land after traveling a horizontal distance of

$$d_{t_{\max}} = \frac{h}{\tan\left(\gamma_{\text{ROS}_{\min}}\right)} = \frac{500}{\tan(5.05)} = 5{,}664\,\text{m} = 5.66\,\text{km} \tag{7.135}$$

Example 7.14

A sailplane with a total mass of 500 kg and a wing area of 18 m^2 is gliding from a height of 500 m to sea level. The aircraft has the following characteristics: $C_{D_o} = 0.014$, AR = 35, $e = 0.8$, $C_{L_{\max}} = 1.2$. Determine the minimum glide angle. Assume that the air density is constant throughout the flight at 1.225 kg/m^3.

Solution

The induced drag correction factor is

$$K = \frac{1}{\pi e\,\text{AR}} = \frac{1}{3.14\times 0.8\times 35} = 0.011 \tag{3.8}$$

The maximum lift-to-drag ratio is

$$\left(\frac{L}{D}\right)_{\max} = \frac{1}{2\sqrt{KC_{D_o}}} = \frac{1}{2\sqrt{0.011\times 0.014}} = 39.63 \tag{5.24}$$

So,

$$\gamma_{\min} = \tan^{-1}\frac{1}{\left(L/D\right)_{\max}} = \tan^{-1}\left[\frac{1}{39.63}\right] = 0.025\,\text{rad} = 1.44^\circ \tag{7.116}$$

The minimum glide angle is just 1.44°.

PROBLEMS

Note: The given data and the required parameters are at sea level, unless otherwise stated.

7.1 A jet trainer is climbing with a speed of 300 knots (555.6 km/h) and a climb angle of 12°. What is its ROC?

7.2 A light aircraft with a mass of 3,200 kg is climbing with 9° of climb angle. Determine how much lift this aircraft has produced.

7.3 The maximum engine power at sea level of a turboprop aircraft is 10,000 hp (745.7 kW), and its propeller efficiency is 0.9. Is the aircraft capable of climbing with a speed of 400 km/h at 10,000 ft altitude (3,048 m)? Assume $S = 100\,\text{m}^2$, $C_D = 0.04$.

7.4 The aircraft Skymaster (C-54) has four piston engines and the following characteristics:

$$m = 33{,}113\,\text{kg},\ S = 135.9\,\text{m}^2,\ P = 4 \times 1{,}081\,\text{kW},\ K = 0.042,$$

$$C_{L_{\max}} = 1.9,\ V_{\max} = 445\,\text{km/h},\ \eta_P = 0.85,\ C_{D_o} = 0.028.$$

a. Plot the variations of required power versus aircraft speed.
b. What is the maximum excess power?
c. At what aircraft speed, this maximum excess power occurs?

7.5 An aircraft is required to climb to 20,000 ft altitude. Determine which scenario results in a shorter time to climb:
a. Climb with a speed of 150 knots and climb angle of 13°.
b. Climb with a speed of 170 knots and climb angle of 11°.

7.6 The stealth bomber aircraft F-117 Night Hawk has a mass of 45,360 kg and two turbofan engines each rated at 111.7 kN of thrust. At a climbing flight condition, the aircraft is generating 423,000 N of lift. Calculate the climb angle and aircraft drag.

7.7 A jet aircraft is climbing with a rate of climb of 22,638 ft/min and a speed of 400 knots. Determine the horizontal speed of the aircraft.

7.8 The fighter aircraft Saab-37 (Viggen) with a turbofan engine has the following characteristics:

$$m = 20{,}500\,\text{kg},\ S = 52.2\,\text{m}^2,\ T = 115.5\,\text{kN},\ e = 0.8,$$

$$C_{L_{\max}} = 2.4,\ C_{D_o} = 0.022,\ b = 10.6\,\text{m}$$

Determine the maximum ROC for this aircraft at sea level.

7.9 The transport aircraft Beechcraft C-12 has two turboprop engines and the following characteristics:

$$m = 5{,}670\,\text{kg},\ S = 28.15\,\text{m}^2,\ P = 2 \times 634\,\text{kW},\ b = 16.161\,\text{m},$$

$$C_{L_{\max}} = 1.8,\ \eta_P = 0.83,\ C_{D_o} = 0.026,\ e = 0.86.$$

Calculate the velocity corresponding to the maximum ROC. Assume a variable-pitch propeller.

7.10 Calculate the maximum climb angle of the aircraft in Problem 7.8.

7.11 At what altitude the maximum climb angle of the aircraft in Problem 7.8 is 5°?

7.12 A jet aircraft is climbing with a speed of 300 knots and a climb angle of 12°. How long does it take to reach 30,000 ft altitude? Ignore the change in density throughout this flight.

7.13 The pilot of an agricultural aircraft (flying at sea level) suddenly realizes that there is a mountain in front of the aircraft at a distance of 1,000 m. The mountain has a height of 2,000 m and a base diameter of 8,000 m. The pilot decides to climb with the maximum ROC of 2,500 fpm (12.7 m/s) and a climb speed of 70 knots (129.6 km/h). Does this aircraft survive or crash into the mountain?

7.14 A fighter aircraft is flying at an altitude of 40,000 ft over an enemy land. The pilot realizes that a missile was just launched toward the aircraft. The missile has a speed of 2,000 knots and its absolute ceiling is 60,000 ft. If the absolute ceiling of the aircraft is 70,000 ft, what must be the ROC of the aircraft such that aircraft can escape from this missile? Assume both aircraft and missile have constant ROC.

7.15 The transport aircraft Lockheed 140B (Jet Star) with four turbojet engines has the following characteristics:

$$m = 19{,}051\,\text{kg},\ S = 50.4\,\text{m}^2,\ T = 4 \times 14.7\,\text{kN},\ b = 16.6\,\text{m},$$

$$C_{L_{\max}} = 2.3,\ C_{D_o} = 0.028,\ e = 0.77$$

Calculate the service ceiling of this aircraft.

7.16 Plot the variations of aircraft speed versus climb angle for the aircraft in Problem 7.15. From this plot, determine the maximum speed and maximum climb angle of the aircraft.

7.17 Determine the maximum ROC of the aircraft in Problem 7.15 at sea level when one engine is inoperative.

7.18 Plot the variations of aircraft maximum ROC versus altitude for the aircraft in Problem 7.4. Assume a variable-pitch propeller.

7.19 Plot the variations of aircraft maximum climb angle versus altitude for the aircraft in Problem 7.15.

7.20 The fighter aircraft MiG-25 with two turbojet engines has the following characteristics:

$$m = 35{,}000\,\text{kg},\ S = 56\,\text{m}^2,\ T = 2 \times 120.6\,\text{kN},\ b = 14\,\text{m},$$

$$C_{L_{\max}} = 1.8,\ C_{D_o} = 0.022,\ e = 0.8,\ C = 1\,\text{lb/h/lb}.$$

The aircraft is required to climb to 40,000 ft (12,190 m) altitude as fast as possible:

a. How long does this climb take?
b. How much fuel is consumed?
c. Determine the ground distance for this climb. You may assume a linear variation of speed for this section.

7.21 A kite with a mass of 110 kg is gliding while it is producing 1,075 N of lift.
   a. Determine the glide angle.
   b. Calculate aircraft drag at this flight.

7.22 The sailplane Honle H-101 has the following characteristics:

$$m = 280\,\text{kg},\ S = 8.58\,\text{m}^2,\ b = 13.3\,\text{m},\ \left(L/D\right)_{\max} = 34.5,$$

$$e = 0.85,\ C_{L_{\max}} = 1.6$$

   a. Calculate the aircraft zero-lift drag coefficient $\left(C_{D_o}\right)$.
   b. Determine the minimum glide angle.
   c. Calculate minimum ROS.
   d. How much height the aircraft will lose after 15 min if the aircraft is in flight condition of part c? Assume air density is constant at 1 kg/m^3.
   e. How much ground distance the aircraft will cover after 15 min if the aircraft is in flight condition of part b? Assume air density is constant at 0.8 kg/m^3.
   f. If the initial height is 10,000 ft (3,048 m) altitude, determine the maximum time that the aircraft can be airborne.

7.23 The Kite Polaris Super 16 has the following characteristics:

$$m = 116\,\text{kg},\ S = 15.8\,\text{m}^2,\ \text{AR} = 6.2,\ C_{L_{\max}} = 2.27,\ e = 0.75,\ C_{D_o} = 0.056$$

   a. Determine the maximum glide ratio.
   b. What is the minimum glide angle?
   c. Calculate the minimum drag speed.
   d. If the pilot desires to be airborne for 10 min, what must be the initial height to begin flight with?

7.24 A GA aircraft with two piston-prop engines has the following characteristics:

$$m = 1{,}270\,\text{kg},\ S = 12\,\text{m}^2,\ P = 2\times 112\,\text{kW},$$

$$\text{AR} = 7,\ C_{L_{\max}} = 1.8,\ C_{D_o} = 0.024,\ e = 0.84$$

When the aircraft is flying at 15,000 ft altitude, the pilot suddenly notices that the fuel tank is empty. If the closest airport is at 50 km distance, can this aircraft land safely on this airport?

7.25 A jet aircraft with a maximum thrust of 18.2 kN and a mass of 8,200 kg is required to descend with a 6° of descent angle. Assume: $S = 40\,\text{m}^2$, $C_{D_o} = 0.022$, $a = 5.1$ 1/rad, $K = 0.04$.
   a. If the desired velocity is 260 knots, what percentage of engine thrust is needed for this flight operation? Assume air density is constant at 1.2 kg/m^3.
   b. What must be the angle of attack?
   c. Determine the ROD.

7.26 A jet (turbofan engine) aircraft with a maximum engine thrust of 15 kN (at sea level) and a mass of 6,000 kg is descending with a velocity of 150 KTAS. Assume: $S = 45\,\text{m}^2$, $C_{D_o} = 0.018$, $K = 0.05$.

a. If the pilot is using only 10% of the engine thrust, determine the descent angle at 5,000 ft.

b. Determine the ROD.

7.27 Analyze the steepest climb (i.e., determine the maximum climb angle) of the aircraft in Problem 7.9 at 10,000 ft (3,048 m) altitude. Then, calculate the corresponding ROC.

7.28 Analyze the fastest climb (i.e., determine the maximum ROC) of the aircraft in Problem 7.9 at 10,000 ft (3,048 m) altitude. Then, calculate the corresponding climb angle. Assume a variable-pitch propeller.

7.29 The fastest climb performance of a jet aircraft with the following characteristics

$$T_{\max} = 20{,}000\,\text{lb},\ W = 80{,}000\,\text{lb},\ S = 800\,\text{ft}^2$$

is tabulated in Table 7.5. Plot the variations of aircraft speed, maximum rate of climb, and its associated climb angle with altitude.

Then, determine the service ceiling.

7.30 Consider the following twin turbojet engine aircraft:

$$m = 12{,}500\,\text{kg},\ S = 74\,\text{m}^2,\ C_{D_o} = 0.019,$$
$$K = 0.042,\ C_{L_{\max}} = 2.2,\ T_{\max_{SL}} = 2 \times 40{,}000\,\text{N}$$

a. Determine the maximum climb angle at 10,000 ft (3,048 m).

b. Determine the corresponding ROC.

TABLE 7.5
Fastest Climb Values of Jet Aircraft in Problem 7.29

h (1,000 ft)	*T/W*	*V* (fps)	$\text{ROC}_{\max}$ (fps)	γ (°)
0	0.25	698	106.7	8.8
5	0.216	702	89.7	7.35
10	0.184	708	74.0	6.00
15	0.157	717	61.3	5.7
20	0.133	728	47.2	3.72
25	0.112	743	35.3	2.72
30	0.0935	763	24.0	1.8
35	0.0775	790.4	13.4	0.97
40	0.0615	832.3	1.244	0.08
40.58	0.06	837.4	0	0

7.31 A fighter jet aircraft is climbing with a speed of 380 knots and a climb angle of 24° at 15,000 ft (4,572 m) with ISA + 20 conditions. What will be the cruising speed (in terms of the Mach number) if the pilot decides to cruise with the same thrust setting?

$$m_{\text{TO}} = 72{,}000\,\text{kg},\ S = 232\,\text{m}^2,\ C_{D_o} = 0.026,\ K = 0.035,\ C_{L_{\max}} = 2.3$$

7.32 A jet (turbofan engine) aircraft has a maximum climb angle of 21° at 12,000 ft. What is its maximum speed (in KTAS) at 18,000 ft? The aircraft has the following characteristics:

$$W = 12{,}300\,\text{lbf},\ S = 342\,\text{ft}^2,\ C_{D_o} = 0.022,\ e = 0.92,\ \text{AR} = 6.3,\ C_{L_{\max}} = 2.1$$

7.33 A cargo aircraft has four piston engines, each generating 2,350 hp at sea level. It has the following characteristics:

$$W_{\text{TO}} = 73{,}000\,\text{lbf},\ S = 1{,}464\,\text{ft}^2,\ \text{AR} = 7.5,$$

$$C_{L_{\max}} = 2.4,\ \eta_P = 0.85,\ C_{D_o} = 0.022,\ e = 0.83.$$

Determine the maximum climb angle (in degrees) at sea level.

7.34 Consider the business jet aircraft Gulfstream G-550 with a maximum take-off mass of 41,277 kg, a wing area of 105.63 m^2, a wing span of 27.69 m, and two turbofan engines each generating 68.4 N of thrust. Assume the following:

$$C_{D_o} = 0.02,\ e = 0.85,\ V_s = 85\,\text{knot}\,(157.4\,\text{km/h}),\ V_{\max} = 600\,\text{knot}\,(1{,}111\,\text{km/h})$$

Construct the hodograph for this aircraft for sea level. From the graph, determine the maximum ROC and the maximum climb angle.

7.35 The maximum ROC of the fighter aircraft Lockheed Martin F-16 Fighting Falcon (Figure 7.6) with a single afterburning turbofan engine) at sea level is 50,000 ft/min, and its service ceiling is 56,000 ft. Assuming the absolute ceiling is 60,000 ft, what is the minimum time to climb to the service ceiling?

7.36 The maximum ROC of the transport aircraft Boeing 737-300 (with two turbofan engines) at sea level is 1,800 ft/min, and its service ceiling is 37,000 ft. Assuming the absolute ceiling is 40,000 ft, what is the minimum time to climb to the service ceiling?

7.37 The pilot of a hang glider with a total mass of 140 kg and a wing area of 16 m^2 is going to glide from a height of 400 m to sea level. The aircraft has $C_{D_o} = 0.017$ and $K = 0.08$, $C_{L_{\max}} = 1.1$.

a. What is the maximum flight time that the hang glider can be airborne?
b. If the goal is to be airborne as long as possible; what must be the glide angle?
c. How far (horizontal distance) the aircraft will glide from this point before touching the ground for this glide program?
d. Assume that the air density is constant throughout the flight at 1.225 kg/m^3.

7.38 The pilot of a hang glider with a total mass of 110 kg and wing area of 14 m^2 is going to glide from a height of 300 m to sea level. The aircraft has $C_{D_o} = 0.019$ and $K = 0.07$, $C_{L_{max}} = 1.2$
   a. What is the maximum flight time that the hang glider can be airborne?
   b. If the goal is to be airborne as long as possible; what must be the glide angle?
   c. How far (horizontal distance) the aircraft will glide from this point before touching the ground for this glide program?
   d. Assume that the air density is constant throughout the flight at 1.225 kg/m^3.

7.39 Consider a sailplane with a total mass of 700 kg is going to glide from a height of 1,000 m to sea level. The aircraft has the following characteristics: $C_{D_o} = 0.015$ and AR = 40, $e = 0.85$, $C_{L_{max}} = 1.3$. Determine the minimum glide angle. Assume that the air density is constant throughout the flight.

7.40 Consider a sailplane with a total mass of 800 kg is going to glide from a height of 1,500 m to sea level. The aircraft has the following characteristics: $C_{D_o} = 0.016$, AR = 30, $e = 0.91$, $C_{L_{max}} = 1.4$. Determine the minimum glide angle. Assume that the air density is constant throughout the flight at 1.2 kg/m^3.

7.41 Calculate and plot the variations of horizontal distance versus altitude (up to 2,500 m) for the aircraft in Problem 7.38.

7.42 Calculate and plot the variations of minimum glide angle versus altitude (up to 4,000 m) for the aircraft in Problem 7.40. Assume $S = 8\ m^2$.

7.43 The transport aircraft Boeing 767-200 with a mass of 143,000 kg and two turbofan engines each generating a sea-level thrust of 222 kN is required to descend from 15,000 ft (4,572 m) to 14,000 ft (4,267 m). In this descending flight, the airspeed should be decreased from 200 to 190 m/s when a 15 km horizontal distance is covered. Assume that the deceleration in the z-axis (Figure 7.24) is zero. Other characteristics of the aircraft are given as

$$S = 283.3\,m^2,\ b = 47.6\,m,\ C_{D_o} = 0.019,\ e = 0.92$$

Determine what percentage of the engine thrust should be employed at the beginning of this descent.

7.44 The transport aircraft Boeing 737-100 with a mass of 40,000 kg and two turbofan engines each generating a sea-level thrust of 64 kN is required to descend from 20,000 ft (6,096 m) to 19,000 ft (5,791 m). In this descending flight, the airspeed should be decreased from 240 to 230 m/s when an 18 km horizontal distance is covered. Assume that the deceleration in the z-axis (Figure 7.24) is zero. Other characteristics of the aircraft are given as

$$S = 102.3\,m^2,\ b = 28.35\,m,\ C_{D_o} = 0.021,\ e = 0.9$$

Determine what percentage of the engine thrust should be employed at the beginning of this descent.

7.45 A large transport aircraft (Boeing 777-300ER) is descending with an initial velocity of 440 mph at an altitude of 18,000 ft. The ground distance to the landing airport is 100 miles, and the landing speed is 180 mph.

Determine: (a) descent angle, (b) duration of descent, (c) rate of descent, and (d) deceleration.

7.46 A large transport aircraft is descending with an initial velocity of 318 mph at an altitude of 8,200 ft. The ground distance to the landing airport is 40 miles, and the landing speed is 180 mph. Determine: (a) descent angle, (b) duration of descent, (c) rate of descent, and (d) deceleration.

7.47 A large transport aircraft is descending with an initial velocity of 234 mph at an altitude of 4,000 ft. The ground distance to the landing airport is 18 miles, and the landing speed is 180 mph. Determine: (a) descent angle, (b) duration of descent, (c) rate of descent, and (d) deceleration.

7.48 A light GA aircraft with a piston engine that generates 160 hp at sea level has the following characteristics:

$$W_{TO} = 2{,}450\,\text{lbf},\ S = 174\,\text{ft}^2,\ \text{AR} = 7.3,$$

$$C_{L_{max}} = 1.8,\ \eta_P = 0.73,\ C_{D_o} = 0.035,\ e = 0.81.$$

Determine the maximum ROC at sea level. Assume a fixed-pitch propeller.

7.49 Determine the maximum climb angle for the aircraft given in Problem 7.48.

7.50 A regional airliner with two turboprop engines – each generating 1,800 hp at sea level – has the following characteristics:

$$W_{TO} = 29{,}000\,\text{lbf},\ S = 450\,\text{ft}^2,\ \text{AR} = 9,$$

$$C_{L_{max}} = 2.1,\ \eta_P = 0.78,\ C_{D_o} = 0.021,\ e = 0.85.$$

Determine the maximum ROC at sea level.

7.51 Determine the maximum climb angle for the aircraft given in Problem 7.50. Assume a variable-pitch propeller.

7.52. The following plot (Figure 7.30) illustrates the variations of airspeed and altitude as a function of time for a transport aircraft from takeoff to cruise altitude:

Determine: (a) average climb angle, (b) average acceleration, and (c) average ROC. Assume the aircraft travels a ground distance of 40 miles to reach the cruise altitude.

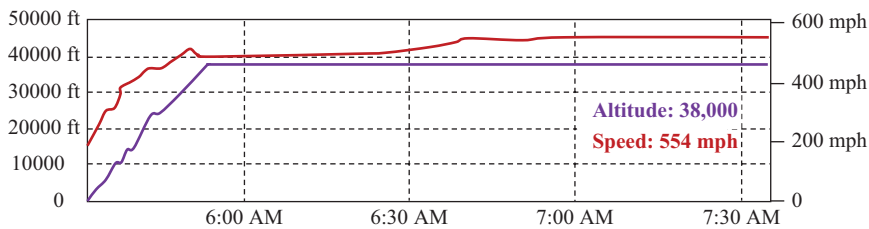

FIGURE 7.30 Variations of speed and altitude as a function of time.

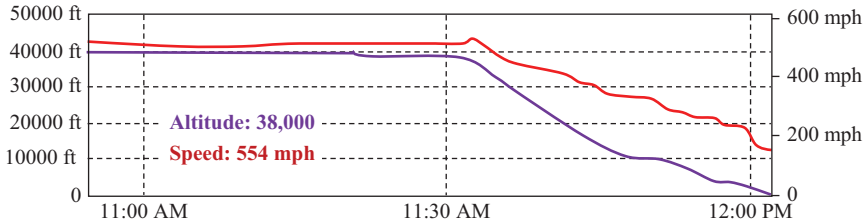

FIGURE 7.31 Variations of speed and altitude as a function of time.

7.53 The following plot (Figure 7.31) illustrates the variations of airspeed and altitude as a function of time for a transport aircraft from cruise altitude to landing:

Determine: (a) average descent angle, (b) average deceleration, and (c) average rate of descent. Assume the aircraft is at a ground distance of 120 miles from airport before begins descending.

7.54 The fighter aircraft Lockheed P-38 Lightning has four piston engines, each generating 1,425 hp at sea level. It has the following characteristics:

$$W_{TO} = 21{,}600\,\text{lbf},\ S = 327.5\,\text{ft}^2,\ \text{AR} = 8.26,\ C_{L_{max}} = 1.8,$$

$$C_{D_o} = 0.027,\ e = 0.84.$$

$$\eta_P = 0.6$$

Determine the maximum ROC at sea level. (Note: It has been measured to be 3,715 fpm).

7.55 A long endurance unmanned aircraft with a mass of 4,100 kg is equipped with a turboprop engine. The UAV – which is climbing with an airspeed of 95 knots – is producing 6,200 N of drag. In this flight condition, the engine is generating 730 kW of shaft power, while the propeller efficiency is 74%. Determine the ROC.

8 Takeoff and Landing

8.1 INTRODUCTION

In order for any conventional aircraft to become airborne, it must first take off from the ground or sea. In contrast, in order for an aircraft to return to airport or base, it must finally land on a proper airfield. Takeoff and landing that are assumed to be two significant phases of flight are two criteria for aircraft performance analysis. These two flight phases are inherently of accelerated motion, as the aircraft speed at the beginning of takeoff and at the end of landing is zero (Figure 8.1). The acceleration at takeoff is positive, while at landing it is negative. The pilot must increase the aircraft speed during takeoff and must decrease the aircraft speed while landing.

An aircraft usually employs its maximum engine power or thrust during takeoff, whereas the engine is normally idle or at low power/thrust during landing. Takeoff varies the aircraft status from being on a runway to airborne, while landing brings the aircraft from an airborne status to the ground. The takeoff and landing phases have technically opposite features, but compared to other flight phases (e.g., cruise and climb), they have several common characteristics, which are as follows:

1. The aircraft motions in both takeoff and landing must be accelerated (positive or negative), but in other flight phases, it could be without acceleration.
2. The aircraft angle of attack in both takeoff and landing experiences a large variation (more than 10°), but in other flight phases, it has a small variation.
3. Landing gear has a vital role in both takeoff and landing, but it is assumed a dead weight in other phases of flight.
4. Several hazards threaten these two flight phases, including stall, hitting an obstacle, and crash, while these rarely happen at other flight phases.

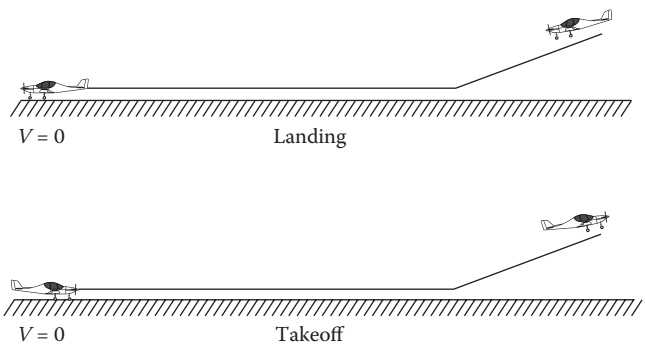

FIGURE 8.1 Landing and takeoff.

DOI: 10.1201/9781003279068-8

Therefore, the takeoff and landing operations are more prone to flight hazards than other flight programs (e.g., cruise or climb).

5. The airspeed at takeoff and landing is very low (close to stall speed), so high-lift devices are employed during these flight phases.
6. Two of the significant factors in determining the cost for building a runway (consequently airport) are takeoff and landing performance, such as takeoff speed, landing speed, and ground roll.
7. The type of runway surface (e.g., concrete, asphalt, and soft ground) is important only at takeoff and landing, not at other flight phases.
8. The aircraft usually has its maximum weight at takeoff, whereas it has often the lowest weight at landing.
9. Automatic control, in the past three decades, has been proved to be working, safe, reliable, and practical; employing autopilot is currently widespread for large transport aircraft. Though this phenomenon has been tested for takeoff and landing, it is still not reliable enough to be adopted by airlines. This is due to the critical significance of human life and cannot be traded with other factors. It is predicted that human pilot will control the aircraft during takeoff and landing for long run, and there is no reliable option other than human control in the near future.

The aircraft primary takeoff performance is often determined by the required runway. The shorter the runway, the better the aircraft's takeoff performance. In aircraft carriers, other techniques and devices such as catapult and arresting gear are provided to make takeoff and landing feasible and to make takeoff run and landing run shorter. An aircraft that could take off and land in a runway with a length of less than 500 ft is called short takeoff and landing (STOL) aircraft. The aircraft that is able to take off and land vertically are referred to as vertical takeoff and landing (VTOL). These two groups of aircraft are referred to as V/STOL aircraft. Most fighters are of V/STOL type. V-22 Osprey, Harrier AV-8B, and Bell XV-15 are examples of VTOL aircraft.

From the airworthiness point of view, it is recommended to design an aircraft with STOL run requirements. Airworthiness standards such as Federal Aviation Regulations (FAR) and European Aviation Safety Agency (EASA) regulate flight phases and require aircraft to have takeoff run and landing run within specific magnitudes. Despite careful design and skilled pilots' precautions, the largest portion of aircraft crash in the world happens during these two flight phases. Whenever landing conditions are not satisfactory (e.g., bad weather, busy air traffic, unexpected appearance of hazards on the runway, and mechanical failure), the pilot has to discontinue the approach and choose another viable approach under more favorable conditions (i.e., go-around).

This chapter is devoted to takeoff and landing performance analyses. It describes takeoff and landing procedures in detail and introduces parameters influencing takeoff and landing performance. Then the governing equations of motion for takeoff and landing are derived and, finally, the technique to measure and determine aircraft performance during takeoff and landing is presented. As there are several similarities between takeoff and landing, the materials that are covered in takeoff will not be

repeated in landing. The principles, governing equations, terminology, and a number of examples for takeoff and landing are presented.

8.2 TAKEOFF PRINCIPLES

Takeoff can be construed as a flight maneuver during which an aircraft is accelerated from stop and after rolling on the runway for a short period of time (a couple of [10–60] seconds), it becomes airborne and initiates climb. As Figure 8.2 illustrates, this flight phase has three stages: (1) ground roll or ground run, (2) transition or rotation, and (3) airborne.

After taxiing, the pilot brings the aircraft to the beginning of the runway and waits for control tower permission. At this stage, the engine is idle and the brakes hold the aircraft from moving forward. Soon after the pilot receives permission to take off, he/she pushes the engine throttle to the end position and then, releases the brakes. This generates the maximum permissible (see Section 4.7.1 for flat-rated engine) engine thrust and the aircraft begins to accelerate. The primary job of the pilot at this point is to maneuver the aircraft on the runway and to avoid any deviation (maintain a straight path). This operation continues until the aircraft reaches a specific speed, called the rotation (or transition) speed. At this time, the pilot must pull the stick (or yoke) to deflect the elevator to an up position. When the elevator is deflected up, the tail will produce a negative tail lift and consequently generate a positive pitching moment around the main gear. This pitching moment will rotate the aircraft around the main gear, so the nose will be lifted up.

As the nose is pitching up, the aircraft (and wing) angle of attack is increased. The pilot is careful not to reach the stall angle for safety. An increase in the angle of attack will cause an increase in the lift coefficient, and thus, more lift force is generated. The second part of the takeoff operation takes only a few (1–5) seconds for most aircraft types. At this stage, only the main gear is in contact with the ground and is rolling, so the nose gear will be in the air. This part of takeoff is referred to as *transition or rotation*, since it is the stage between ground rolling and airborne. During rotation, the pilot must be careful not to allow the aircraft to exceed the stall angle of attack, which is often around 15° for most aircraft. Although the fuselage is rotating around the main gear, the motion path is still along the runway, so the pilot must not allow the aircraft to divert from its straight path.

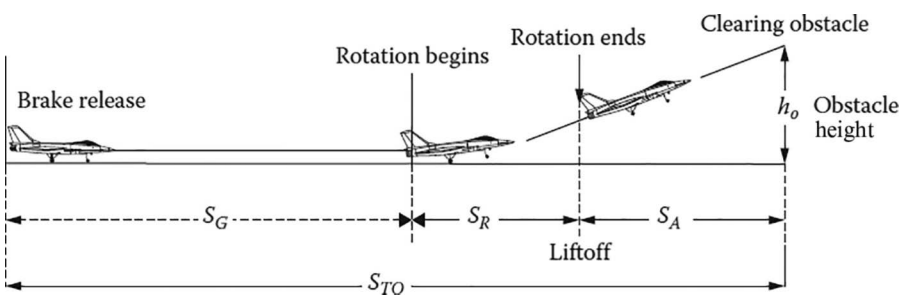

FIGURE 8.2 Three major stages of the takeoff operation.

As soon as the lift plus the vertical component of thrust is more than the aircraft weight, the aircraft will start to lift off. The speed at the time of liftoff is called *liftoff speed*, which is slightly greater than the stall speed. From this point onward, the aircraft will gradually climb from the ground. Although the third part of takeoff is similar to a climb, and there is no contact between the aircraft and the ground at this stage, it is still considered as part of the takeoff operation until it passes from an imaginary obstacle height. Therefore, the runway under the flight path is assumed to be part of takeoff run. The FAA airworthiness standards define this obstacle height as 50 ft for civil transport aircraft and 35 ft for fighters. Table 8.1 illustrates the variations of several parameters such as lift coefficient, aircraft speed, angle of attack, pitch angle, and climb angle at these three stages of takeoff.

Takeoff and landing are considered as two of the most dangerous phases of flight since the control of aircraft close to the ground is not an easy task if a mishap occurs. Some possibilities of mishaps [82] are inoperative engine(s), landing gear failure, tire flatting, hitting obstacles, cross wind effect, bird strike, tail strike, and rear fuselage contact with the ground. According to statistics, a significant number of aircraft crashes happen during takeoff and landing. For these reasons, pilots are trained to make decision when encountering such mishaps.

In addition, airworthiness regulations emphasize more safety aspects during takeoff and landing rather than cruise or climb. For example, if a multiengine aircraft loses one engine, the asymmetric thrust will force the aircraft to yaw around aircraft center of gravity. During this time, the pilot must quickly decide to weather to continue the flight and control unwanted yaw or abort the takeoff. One of the factors influencing the pilot's decision is the time of mishap: whether it is during ground roll or after liftoff.

Takeoff is considered complete when the aircraft has reached a safe maneuvering altitude, or an en-route climb has been established. From the transport aircraft pilot's point of view, takeoff is technically assumed to be the flight operation between brake release and a safe height of 1,500 ft above the terrain is reached. Therefore, even after clearing the obstacle, the pilot must follow the takeoff flight path until the aircraft reaches this altitude. Figure 8.3 illustrates a Lockheed Martin C-130J Hercules, a transport aircraft, at takeoff and landing.

In this section, important speeds (Figure 8.4) and their features that are vital for takeoff analysis are introduced. When an aircraft takes off from standstill, the following speeds will be passed before transiting to a climb stage:

1. *Stationary speed* ($V=0$): This is the aircraft speed relative to the ground at the beginning of the runway. At this speed, the pilot is ready for brake release and takeoff upon receiving permission from the control tower.
2. *Minimum control speed* (V_{mc}): This is the minimum speed at which a multiengine aircraft can be controlled in yaw and continue a straight path down the runway, if one or more engines fail during takeoff. This means if an aircraft experiences inoperative engine(s) during takeoff, it cannot be directionally controlled if the aircraft's speed is less than V_{mc}. In such a situation, the only option is to shut down all other engines and stop the aircraft. If the

TABLE 8.1
Details of a Takeoff Operation for a Conventional Aircraft with a Nose Gear (Tricycle) Configuration

No.	Stage	Lift (L) Plus Vertical Component of the Thrust		Lift Coefficient (C_L)		Speed (V)		Fuselage Angle of Attack		Pitch Angle (θ)		Contact between Gear and Ground	
		Start	End	Start	End	Start	End	Start	End	Start	End	Start	End
1.	Ground roll	0	$<W$	a	a	0	1.1 Vs	0	0	0	0	All gears have contact	All gears have contact
2.	Transition	$<W$	$=W$	a	b	1.1 Vs	1.2 Vs	0	d	0	d	All gears have contact	Only main gear has contact
3.	Airborne	$=W$	$>W$	b	c	1.2 Vs	1.3 Vs	d	d	d	e	Only main gear has contact	No contact

Notes: (1) Flap angle is constant during takeoff; (2) Elevator will be deflected up at the beginning of rotation; (3) $a = C_{LC} + \Delta C_{L_{flap}}$; (4) $b = C_{L_{max}} / (k_1)^2$, $k_1 = 1.1 - 1.2$; (5) $c = C_{L_{max}} / (k_2)^2$, $k_2 = 1.2 - 1.3$; (6) $d = 0 \le \alpha \le (\alpha_s - 1)$; $0 \le \theta \le (\alpha_s - 1)$; (7) $e = 0 \le \theta \le \gamma_{max}$.

(a)

(b)

FIGURE 8.3 Lockheed Martin C-130J Hercules during (a) takeoff and (b) landing. (Courtesy of Steve Dreier.)

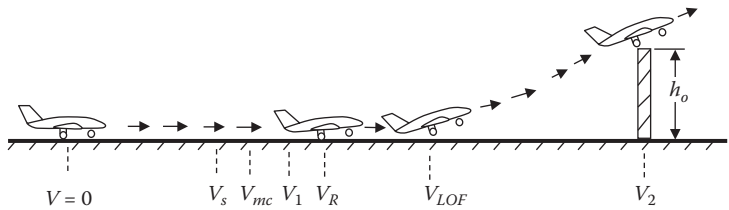

FIGURE 8.4 Reference speeds during takeoff operation.

speed is higher than V_{mc}, the aircraft can maintain a straight flight and safely continue its takeoff and liftoff from the ground, since the directional control is possible through the directional control surface (i.e., rudder).

In the case where One or more Engines are Inoperative (OEI), a directional moment that is generated through an asymmetric (Figure 8.5) thrust is

$$N_{\text{asym}} = \sum T_i \cdot Y_{T_i} \tag{8.1}$$

where T_i is the thrust of ith operative engine, and Y_{T_i} is the distance between ith engine thrust and the aircraft center of gravity in the y direction. This moment can be nullified or balanced only via an aerodynamic yawing moment. In a directionally trimmed aircraft, the sum of the yawing moments (N) about the aircraft center of gravity is zero:

$$\sum N_{\text{cg}} = 0 \tag{8.2}$$

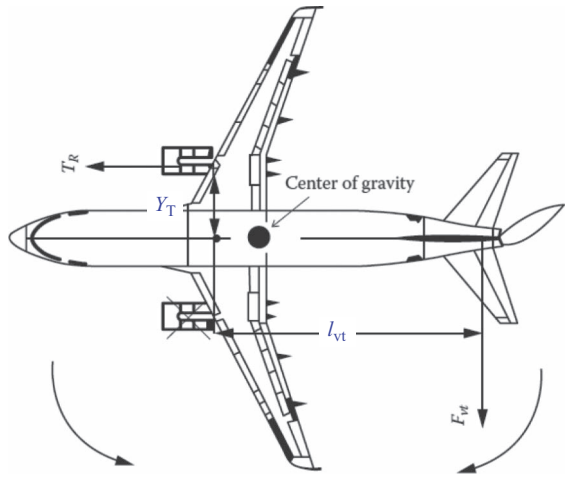

FIGURE 8.5 Vertical tail yawing moment for directional control in an asymmetric thrust situation.

The aerodynamic yawing moment is the product of a vertical tail lift (i.e., side force) and its distance to the aircraft's center of gravity (as the moment arm, l_{vt}). The vertical tail lift, F_{vt} (side force), as an aerodynamic force can be calculated using the following equation:

$$F_{vt} = \frac{1}{2}\rho V^2 S_{vt} C_{L_{vt}} \tag{8.3}$$

where S_{vt} is the vertical tail planform area (including rudder), and $C_{L_{vt}}$ is the vertical tail lift coefficient. This equation demonstrates that the vertical tail side force is a function of aircraft speed, vertical tail area, air density at the runway elevation, and vertical tail lift coefficient.

In an aircraft with a fixed configuration at a specific elevation, the only variable is aircraft speed. Indeed, the maximum vertical lift coefficient is obtained by maximum rudder deflection, the typical value of which is about 0.9–1.6. When other operating engines generate their maximum thrusts during takeoff, the asymmetric thrust moment is known. A directional trim is achieved when the vertical tail lift can produce the yawing moment (N_{vt}) equal to the thrust asymmetric moment (N_{asym}):

$$N_{vt} = F_{vt} \cdot l_{vt} \tag{8.4}$$

where l_{vt} is the distance between the vertical tail aerodynamic center to the aircraft center of gravity. Inserting Equations 8.1, 8.3, and 8.4 into directional trim equation (Equation 8.2) allows us to obtain the minimum control speed. Therefore, the minimum control speed will be determined by

$$V_{mc} = \sqrt{\frac{2\sum T_i \cdot Y_{T_i}}{\rho S_{vt} C_{L_{vt}} l_{vt}}} \tag{8.5}$$

If the aircraft speed is less than V_{mc}, while OEI, and if the pilot is not shutting down other engine(s), the aircraft will not be directionally controllable. Therefore, the aircraft will deviate out of the runway, hit an obstacle, and be damaged. This speed, V_{mc}, should not exceed stall speed, V_s; otherwise, the aircraft is considered to have a major design problem and a significant safety issue. Such aircraft will not receive an FAA certificate and must be redesigned.

Example 8.1

A transport aircraft has twin turbofan engines, each generating 170 kN of thrust. The distance between each engine thrust line and aircraft center of gravity is 12 m, and the distance between the vertical tail aerodynamic center and the aircraft center of gravity (l_{vt}) is 42 m. If the maximum lift coefficient of the vertical tail is 0.9 and the vertical tail area is 40 m^2, determine the minimum control speed of this aircraft at sea level.

Solution

When one engine (say the left one) is not operating, the right engine will produce an undesirable yawing moment that needs to be nullified. This is an equilibrium requirement, so the undesirable yawing moment of the asymmetric thrust (Tl_T) must be opposed by the yawing moment of the vertical tail:

$$\sum N_{cg} = 0 \Rightarrow T_{left} l_T = L_{vt} l_{vt} \tag{8.2}$$

$$L_{vt} = \frac{T_{left} l_T}{l_{vt}} = \frac{170 \times 1{,}000 \times 12}{42} \Rightarrow L_{vt} = 48{,}571.4\,\text{N}$$

The minimum control speed can be determined from the following vertical tail lift equation:

$$\begin{aligned} L_{vt} &= \frac{1}{2}\rho V_{mc}^2 S_{vt} C_{L_{max_{vt}}} \\ \Rightarrow V_{mc} &= \sqrt{\frac{2L_{vt}}{\rho S_{vt} C_{L_{max_{vt}}}}} = \sqrt{\frac{2 \times 48{,}571.4}{1.225 \times 40 \times 0.9}} \Rightarrow V_{mc} = 46.93\,\text{m/s} = 91.24\,\text{knot} \end{aligned} \tag{8.3}$$

3. *Stall speed* (V_s): As described in Chapter 2, the stall speed is the minimum speed at which the aircraft-level flight can be maintained. If the airspeed is less than stall speed, aircraft lift will not be sufficient to hold the aircraft airborne. At this speed, the wing stalls and produces its maximum lift coefficient. The aircraft must have the speed above V_s before it is capable of lifting off the ground. At this speed, the aircraft is not stable and is prone to a couple of undesired/unpleasant incidences such as spin. A stall may lead to a deep stall and crash. Therefore, pilots are advised to keep a safe buffer above stall speed.

For incidence, according to the NTSB's report [26], the reason for the Gulfstream G650 test aircraft crash shortly after takeoff is that, when AOA reached 11.2° during the accident takeoff, the AOA exceeded the stall AOA for the combination of flap setting, Mach number, and roll angle present at the time, resulting in a loss of roll control.

4. *Engine failure speed* (V_{EF}): This is a critical speed that relates to engine failure and the aircraft stopping before the end of the runway. The calculation of runway length for airport builders is based on aircraft engine failure at the most critical conditions during takeoff. This phenomenon has been heavily regulated by FAR. If one or more engines fail during takeoff, there are two options for a pilot: to stop the aircraft or to continue taking off. One of the parameters that affects the pilot's decision is aircraft speed. If engine failure happens prior to this critical speed, the pilot can shut down all engines and stop the aircraft using brakes and other means, since enough runway is available. But, if the failure happens after the V_{EF}, the pilot is allowed to continue the takeoff operation, since not enough runway would be available.
5. *Decision speed* (V_d or V_1): The decision speed is usually slightly greater than the critical engine failure speed since it takes 1 or 2 s for the pilot to notice the engine failure. During this period, aircraft speed will increase from V_{EF} to V_d. At this speed, the pilot will decide whether to abort flight, or to continue takeoff. If the pilot notices engine failure after V_1, the pilot should not stop the aircraft since the runway is not long enough to allow for a safe stop. However, when the aircraft has accelerated beyond this speed, the takeoff must be continued even if the critical engine fails until V_1 a takeoff must be rejected.

Figure 8.6 illustrates the typical relationship among V_1, V_{EF}, and a safe stop. The best runway length is the length at which aircraft safety is guaranteed if V_1 and V_{LO} are equal. The speed V_1 must be set by the aircraft

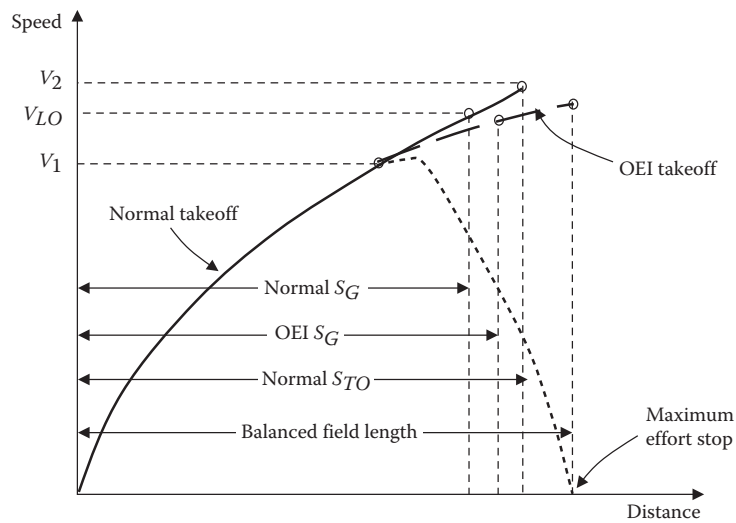

FIGURE 8.6 Decision speed and balanced field length.

designer; however, V_1 must not be less than V_{EF}, plus the speed increment gained during the interval required by the pilot to take appropriate action in terms of applying the retardation means. The balanced field length [82] is the shortest runway on which a balanced field takeoff (with safety regulations) can be performed. It is a condition where the required *accelerate-stop* distance is equal to the required takeoff distance.

6. *Rotation speed* (V_R): The rotation speed is the speed at which the pilot pulls the stick or yoke to initiate the rotation about the main gear. At this time, the elevator will be deflected up, so the aircraft's nose and nose gear will be lifted up too, due to the pitching moment produced by the horizontal tail. This is the beginning of a transition between ground roll and being airborne; thus, this speed is sometimes referred to as the transition speed. The speed V_R must be greater than V_1 and $>1.05\ V_{mc}$.
7. *Liftoff speed* (V_{LO}): The speed at the end of the rotation stage is called liftoff speed; this is when the aircraft will begin to be airborne. At this speed, the main gear will be separated from the runway; thus, the aircraft will lift off the ground.
8. *Minimum safety* speed (V_2): The speed at which climbing is possible and safe, even when one engine is inoperative, is referred to as the minimum safety speed. The takeoff climb speed V_2 is the demonstrated airspeed at the obstacle height (35 or 50 ft). The minimum safety speed must be $>1.1V_{mc}$ and may not be $<1.2V_s$ for twin-engine and three-engine prop-driven aircraft or for turbofan/turbojet aircraft without provision for reducing the stall speed with the most critical engine being inoperative. The speed V_2 must be selected by the aircraft designer to provide the climb gradient required by FAR 23.121 or 25.121, but may not be $<V_R$ plus the speed increment attained before reaching the obstacle height.

The actual sequence of speeds is more complicated than introduced in this section. The reader can refer to FAR 23.53 and FAR 25.107 [6] for further information on these takeoff speeds. Most of these speeds are selected during the aircraft design phase and will influence the pilot's operation during takeoff. The pilot must be familiar with all these speeds to react properly during various situations and weather conditions. Operationally, the runway length must be such that the aircraft can be safely operated under four scenarios: (1) accelerate—stop with All Engines Operative (AEO), (2) accelerate—stop with OEI, (3) accelerate—go with OEI, and (4) accelerate—go with AEO. The following summarizes a few important requirements [6] set by FAR.

$$\begin{aligned} V_{mc} \le V_1 \ge V_R \\ V_R \ge 1.05 V_{mc} \\ V_{LO} \ge 1.1 V_s \\ V_2 \ge 1.2 V_s \end{aligned} \tag{8.6}$$

Several of these velocity requirements are translated into takeoff rotation requirements. This criterion also dictates the most forward location of the aircraft's center of gravity (cg).

For the Boeing 747 at a gross weight of 550,000 lb; V_1, V_R, and V_2 at a flap deflection of 20 degrees are 111, 124, and 143 knot respectively.

There are various performance requirements for a takeoff operation. One of the requirements is about takeoff rotation. For an aircraft with a tricycle landing gear, and at the forward position of the cg, the aircraft must be able to rotate about the main gear (and lift the nose), when aircraft has attained 80% of its liftoff speed. For a transport aircraft, the initial angular acceleration about the main gear (rotation point) should have a value of 6–8 deg/s^2 [21]. Then an average angular velocity (i.e., pitch rate) of 2–3 deg/s should be maintained such that the takeoff rotation process does not take more than 3–4 s. Upon liftoff, the aircraft should be flying [81] at approximately the pitch attitude that will allow it to accelerate to $V_{\mathrm{ROC}_{\max}}$.

8.3 TAKEOFF PERFORMANCE ANALYSIS

The most important parameter in takeoff performance analysis is the "takeoff run" (S_{TO}). In this section, a technique to evaluate the takeoff run is presented. There are a couple of techniques to analyze takeoff performance and solve for the takeoff run. The principles and formulations in all the available techniques are the same, but the approach to solve the equations or integrating them is different.

The takeoff run is divided into three segments (Figure 8.2): (1) ground roll (S_G), (2) rotation or transition section (S_R), and (3) airborne (initial climb) section (S_A). Each section will be dealt with separately. The takeoff run (S_{TO}) will be the summation of these three sections:

$$S_{\mathrm{TO}} = S_G + S_R + S_A \tag{8.7}$$

In general, at most airports, the runway is usually about 30% longer than the highest takeoff run needed for the largest aircraft. The reason is the safety issue and to provide extra runway to bring the aircraft to rest, if the pilot decides to abort the takeoff. The summation of the first two sections (i.e., ground roll and rotation section) is about 80% of the takeoff run. Although in the third section (i.e., airborne section), there is no contact between aircraft landing gear and runway, it is considered as part of the takeoff run. The reason is airworthiness since the height between the aircraft and the ground is too small for this part of the runway to be used for any other purpose.

8.3.1 Ground Segment

Consider the aircraft in Figure 8.7 is accelerating on a runway. There are five active forces that are applied simultaneously: (1) Engine thrust (T), (2) Aircraft drag (D), (3) Aircraft lift (L), (4) Aircraft weight (W), and (5) The friction force between landing gear wheels and the runway (F_f).

The variations of these forces are illustrated as a function of airspeed in Figure 8.7. Both drag and lift forces gradually increase as the aircraft gains speed. However, the engine thrust slightly decreases for both prop-driven and jet engines. But the rate of changes is not similar for the two engine types. The rate of reduction is a function of various aspects of aircraft configuration and propeller type. The features of various engines are described in Chapter 4. Furthermore, the friction force will be gradually decreasing to zero at liftoff.

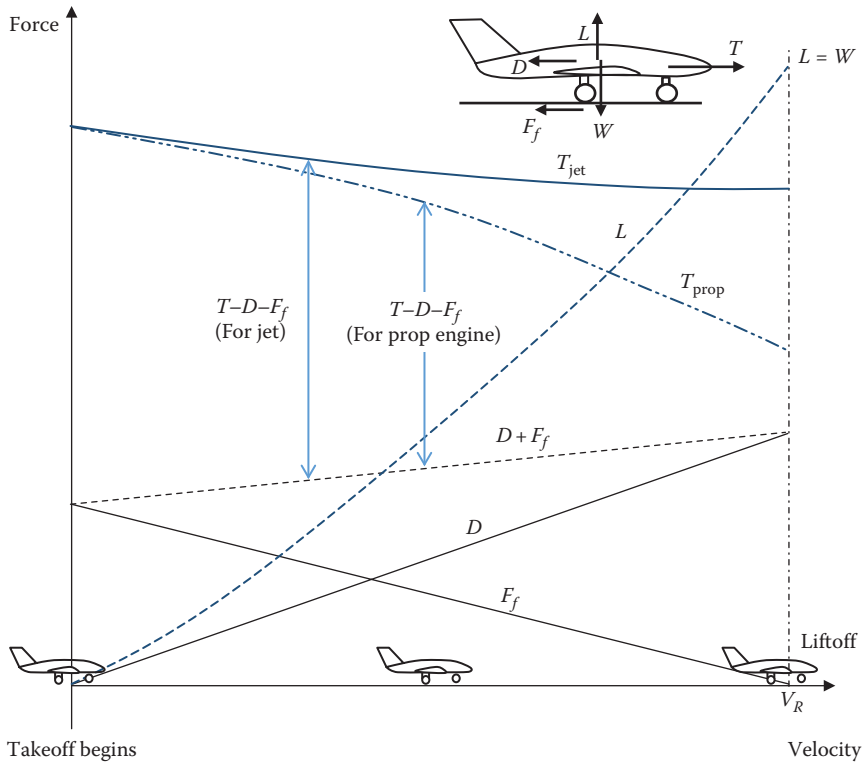

FIGURE 8.7 Force variations during a takeoff operation.

The friction force is proportional to the normal component N to the surface:

$$F_f = \mu N \tag{8.8}$$

where μ is a constant called the static rolling (hint: not sliding) friction coefficient. Table 8.2 illustrates the friction coefficient [83] between landing gear rolling wheels and various types of runway surfaces. At any given instant, the point of a rolling wheel in contact with the ground has no relative motion with respect to the ground (i.e., no sliding). However, there is some friction to the wheels' rolling for two reasons: (1) Each wheel has an axle/bearing (usually lubricated) that has a minor friction. (2) The wheel deforms (a small flat area), so the contact will take place over a certain area rather than a point.

This area is a function of the aircraft weight, tire internal pressure, and air temperature. As the aircraft weight is increased, this area (and friction) is increased, whereas if the internal tire pressure is increased, this area (and friction) is decreased. This is referred to as the rolling friction/resistance. Due to the complex nature of this friction and parameters involved, the exact values for the rolling coefficient have not been clearly deduced. The range of values for the surface of a runway is due to the

TABLE 8.2
Rolling Ground Friction Coefficient for Various Runway Surfaces

No.	Surface	Friction Coefficient (μ)	
		Takeoff (Brakes-Off)	Landing (Brakes-On)
1.	Dry concrete/asphalt	0.03–0.05	0.04–0.06
2.	Wet concrete/asphalt	0.04–0.06	0.05–0.07
3.	Dry short grass	0.05–0.06	0.06–0.07
4.	Wet short grass	0.07–0.08	0.08–0.09
5.	Long dry grass	0.08–0.12	0.09–0.14
6.	Soft ground	0.1–0.3	0.13–0.4
7.	Firm and dry dirt	0.06–0.1	0.08–0.14
8.	Metal on ground	0.4–0.7	0.5–0.7

quality of the surface and its age. The quality of a new asphalt runway is much better than that for an older asphalt runway, as it has a lower friction coefficient.

Table 8.2 introduces two friction coefficient values for each surface: brakes-on and brakes-off. During a takeoff operation, the brakes are not used (brakes-off), but during a landing operation, brakes are employed (brakes-on) to reduce the landing run. In addition, the last row in Table 8.2 is the friction between the aircraft body and the ground. This is for a landing case where the landing gear fails to extend and the aircraft has to land on its belly. In general, a wet surface (on a rainy day) causes more friction compared to a dry surface; therefore, the ground roll is about 10%–30% longer when the runway is wet. The typical acceleration during a takeoff is about 2–5 m/s^2 (0.2–0.5 *g*'s). For an aircraft with a tricycle landing gear, the acceleration creates an additional normal force on the nose gear, while reducing the normal force on the main gear.

Based on Newton's second law, the summation of all these forces provides the change in aircraft linear momentum:

$$\sum F = \frac{d}{dt}(mV) = m\frac{d}{dt}(V) + V\frac{d}{dt}(m) \tag{8.9}$$

A regular takeoff usually takes from a couple of seconds to about a minute and consumes <1% of the aircraft's total fuel weight. Consequently, the change in aircraft weight during a takeoff operation is <1%; thus, we can ignore the change in aircraft weight and assume that the aircraft mass is constant ($dm/dt = 0$) during takeoff. Therefore, we can simplify Equation 8.9 as

$$\sum F = m\frac{d}{dt}(V) \tag{8.10}$$

This equation can be applied in two directions: horizontal and normal. The ground roll is measured along the runway or in the horizontal direction. This implies that in the horizontal (x) direction, the summation of three horizontal forces is equal to aircraft mass multiplied by the rate of change of aircraft speed:

$$T - D - \mu N = m\frac{dV}{dt} \tag{8.11}$$

Although the engine thrust can be assumed to be constant (in fact, at its maximum value), two other forces (drag and normal force) vary significantly and are functions of aircraft speed, as shown in Figure 8.8. Therefore, these equations cannot be solved for acceleration in their current algebraic form. Equation 8.11 needs to be expanded such that it is a function of only one variable (e.g., velocity or acceleration). Acceleration is defined as the rate of change of velocity with time:

$$a = \frac{dV}{dt} \tag{8.12}$$

Thus, from Equations 8.11 and 8.12, the instantaneous acceleration is

$$a = \frac{T - D - \mu N}{m} \tag{8.13}$$

Velocity (or airspeed) is defined as the rate of change of displacement with time:

$$V = \frac{dS}{dt} \tag{8.14}$$

Expanding Equation 8.12 and replacing *dS/dt* with *V* (Equation 8.14), we obtain

$$a = \frac{dV}{dt} = \frac{dV}{dS}\frac{dS}{dt} = \frac{dV}{dS}V$$

or

$$dS = \frac{V}{a}dV \tag{8.15}$$

The ground roll or ground run (S_G) is determined by integrating both sides:

$$S_G = \int \frac{V}{a}dV \tag{8.16}$$

Substituting the acceleration from Equation 8.13 into Equation 8.16, we obtain:

$$S_G = \int \frac{mV}{T - \mu N - D}dV \tag{8.17}$$

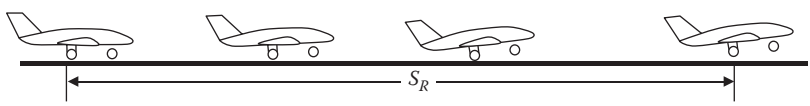

FIGURE 8.8 Rotation (transition) section.

where T is engine thrust, and μ is the coefficient of friction. The normal force is the algebraic sum of the aircraft weight and aircraft lift:

$$N = W - L \tag{8.18}$$

where the lift force is a function of aircraft speed:

$$L = L_{\text{TO}} = \frac{1}{2}\rho V^2 S C_{L_{\text{TO}}} \tag{8.19}$$

where the takeoff lift coefficient ($C_{L_{\text{TO}}}$) is a function of the cruise lift coefficient and the flap deflection as:

$$C_{L_{\text{TO}}} = C_{L_C} + \Delta C_{L_{\text{flapTO}}} \tag{8.20}$$

The technique to determine the additional lift coefficient due to flap ($\Delta C_{L_{\text{flapTO}}}$) is presented in Chapter 3. The equation for takeoff drag, from Equation 3.1, is

$$D = D_{\text{TO}} = \frac{1}{2}\rho V^2 S C_{D_{\text{TO}}} \tag{8.21}$$

where the takeoff drag coefficient, $C_{D_{\text{TO}}}$ (from Equation 3.12) is:

$$C_{D_{\text{TO}}} = C_{D_{o\text{TO}}} + K C_{L_{\text{TO}}}^2 \tag{8.22}$$

The logic behind Equation 8.20 is described here. The aircraft during ground roll is often at a level condition, so the wing/fuselage angle of attack is similar to the wing/fuselage cruise angle of attack. On the other hand, the high-lift device (e.g., flap) is deflected to increase the lift. Thus, the summation of these two coefficients gives the takeoff lift coefficient. The parameter C_{LC} (the cruise lift coefficient), from Equation 5.8, is a function of cruising speed (V_C) and cruising altitude (ρ_c):

$$C_{L_C} = \frac{2mg}{\rho_c V_C^2 S} \tag{8.23}$$

The parameter $\Delta C_{L_{\text{flapTO}}}$ is the extra lift coefficient added to the wing when the flap is deflected during takeoff. Various types of flaps and their features are described in Chapter 3. This parameter depends on not only the flap configuration but also its deflection. The flap deflection depends on atmospheric condition (e.g., temperature), plus payload weight. For initial calculations, you may assume the following values for the extra lift coefficient due to flap deflection $\left(\Delta C_{L_{\text{flapTO}}}\right)$: $0.3 - 0.5$ for GA aircraft, $0.4-0.7$ for large transport aircraft, and $0.4–0.6$ for fighter aircraft.

The technique to determine aircraft zero-lift drag coefficient for takeoff configuration, $C_{D_{o\text{TO}}}$, is discussed in Chapter 3. In general, $C_{D_{o\text{TO}}} = C_{D_{o\text{clean}}} + \Delta C_{D_{o\text{TO}}}$ (see Equation 3.62). The $\Delta C_{D_{o\text{TO}}}$ for a general aviation aircraft is about 0.005–0.01, for a small transport aircraft (e.g., business jet) about $0.014-0.018$, and for a large transport aircraft about 0.02–0.03. The general aviation aircraft Cessna 172 (Figure 3.17)

has a $\Delta C_{D_{\sigma TO}}$ of 0.006, the large transport aircraft Boeing 747 (Figure 8.10b [later in the chapter]) with a zero flap deflection has a of $\Delta C_{D_{\sigma TO}}$ 0.028, and the single-seat fighter aircraft Lockheed Martin F-22 Raptor (Figure 5.10) has a $\Delta C_{D_{\sigma TO}}$ of 0.014.

To accurately determine the lift and drag coefficients for takeoff configuration in the proximity of the ground, including the ground effect. In general, the proximity of an aircraft to ground during takeoff and landing will slightly increase the lift coefficient and reduce the drag coefficient. The proximity of the ground will straighten the flow streamlines (on the bottom surface of the wing) and reduce the effect of the wing camber. The influence of the ground on the flow around wing and tail is a function of the distance between aircraft and ground and the size of the wing. This effect is considerable when the vertical distance between the wing and the ground (h) is less than the wing's semispan ($b/2$). In such a condition, the upwash and downwash at the wing and the downwash at the horizontal tail will be affected. In addition, the ground effect will reduce the wing tip effect, which increases the effective wing aspect ratio. Reference [84] is recommended for ground effect analysis.

By applying these forces (Equations 8.18, 8.19, and 8.21) into Equation 8.17, and assuming the engine thrust is constant over the course of takeoff, we can solve for S_G. This integration is performed from zero to rotation speed (V_R):

$$S_G = \int_0^{V_R} \frac{mV}{T - \mu mg - 0.5\rho V^2 S\left(C_{D_{TO}} - \mu C_{L_{TO}}\right)} dV \tag{8.24}$$

This integration can be directly solved using a mathematical or engineering software package; however, there is a convenient solution. This integration can be modeled as follows:

$$S_G = \int_0^{V_R} \frac{V}{A + BV^2} dV \tag{8.25}$$

where

$$A = \frac{T}{m} - \mu g \tag{8.26}$$

$$B = \frac{-\rho S}{2m}\left(C_{D_{TO}} - \mu C_{L_{TO}}\right) \tag{8.27}$$

The solution for the integration of Equation (8.25) from standard mathematical handbooks [69] is obtained as:

$$S_G = \frac{1}{2B} \ln\left(V^2 + \frac{A}{B}\right) \tag{8.28}$$

where V is from 0 to V_R. When the limits are applied, and the term inside "ln" is simplified, the following is obtained:

$$S_G = \left[\frac{1}{2B}\ln\left(V^2 + \frac{A}{B}\right)\right]_0^{V_R} = \frac{1}{2B}\ln\left[\frac{A}{B}\right] - \frac{1}{2B}\ln\left[V_R^2 + \frac{A}{B}\right] = \frac{1}{2B}\ln\left[\frac{A/B}{V_R^2 + (A/B)}\right]$$

$$= \frac{1}{2B}\ln\left[\frac{A/B}{\left(BV_R^2 + A\right)/B}\right] = \frac{1}{2B}\ln\left[\frac{A + BV_R^2}{A}\right]$$

or

$$S_G = \frac{-1}{2B}\ln\left[\frac{A}{A + BV_R^2}\right] \tag{8.29}$$

When A and B are substituted from Equations 8.26 and 8.27, we have

$$S_G = \frac{-1}{2\left(-\rho S/2m\right)\left(C_{D_{TO}} - \mu C_{L_{TO}}\right)}\ln\left[\frac{(T/m) - \mu g}{(T/m) - \mu g + \left(-\rho S/2m\right)\left(C_{D_{TO}} - \mu C_{L_{TO}}\right)V_R^2}\right] \tag{8.30}$$

However, it is assumed that the rotation speed is slightly greater than the stall speed.

$$V_R = k_{LO}V_s \tag{8.31}$$

where $k_{LO} = 1.1–1.3$. But,

$$V_R^2 = k_{LO}^2 V_s^2 = k_{LO}^2 \frac{2mg}{\rho S C_{L_{max}}}$$

With this substitution and after canceling similar variables from the numerator and denominators, the final result would be

$$S_G = \frac{m}{\rho S\left(C_{D_{TO}} - \mu C_{L_{TO}}\right)}\ln\left[\frac{\left(T/mg\right) - \mu}{\left(T/mg\right) - \mu - \dfrac{k_{LO}^2\left(C_{D_{TO}} - \mu C_{L_{TO}}\right)}{C_{L_{max}}}}\right] \tag{8.32}$$

Either of Equation 8.24 or 8.32 may be utilized to determine the ground roll; both yield the same results. In Equation 8.24, one must integrate, while Equation 8.32 is an algebraic equation and can be solved readily. In both equations, all variables including engine thrust should be known. In practice, the engine thrust is a function of aircraft speed; thus, as the aircraft accelerates, the engine thrust varies. To have a precise answer, we must know the relationship between engine thrust and aircraft speed. This might be obtained from the engine manufacturer. For example, the following empirical relationship [36] with aircraft speed is applicable for turbofan engine thrust of a Boeing 747 (Figure 8.10a [later in the chapter]):

$$T = 46{,}100 - 56.7V + 0.0467V^2 \tag{8.33}$$

where T is in lb, and V is in ft/s. From Equation 8.33, we understand that the engine thrust is reduced more than 23% during takeoff from zero velocity to the liftoff speed (139 knots or 236 ft/s).

If the accurate relationship between engine thrust and airspeed is not known for a given aircraft, we have to resort to estimation. In a jet engine, the takeoff thrust can be assumed as 85%–95% of $T_{\max}$. But, in a prop-driven aircraft, where propeller efficiency is a function of aircraft speed, the takeoff engine thrust (T_{TO}) is estimated from the following equations:

$$T_{TO} = \frac{0.5P_{\max}}{V_R} \quad \left(\text{fixed-pitch propeller}\right) \tag{8.34}$$

$$T_{TO} = \frac{0.6P_{\max}}{V_R} \quad \left(\text{variable-pitch propeller}\right) \tag{8.35}$$

Equations 8.34 and 8.35 demonstrate that the average propeller efficiencies are 0.5 and 0.6 for fixed-pitch and variable-pitch propeller, respectively. This thrust estimation works for most aero-engines. A better thrust model might be found in the manufacturer's engine charts.

From Equation 8.32, we can draw the following conclusions:

1. The ground roll decreases with an increase in engine thrust (T), and engine power (P).
2. The ground roll decreases with an increase in the maximum lift coefficient $\left(C_{L_{\max}}\right)$.
3. The ground roll decreases with an increase in the wing area (S).
4. The ground roll decreases with an increase in prop efficiency (η_P).
5. The ground roll increases with an increase in altitude (i.e., decreasing air density; ρ).

In some cases, for a given aircraft with a given constant thrust, we need to determine how much extra thrust is required to satisfy a new given (i.e., shorter) ground roll. For instance, an aircraft with a specific amount of thrust is desired to take off in a runway shorter than its rated takeoff run. One way to achieve this objective is to use auxiliary rocket engine to boost the thrust. This technique is referred to as jet-assisted takeoff or JATO. This is a system for helping overloaded aircraft to take off by providing additional thrust in the form of small rockets, as has been employed by C-130 cargo plane (Figure 8.3), and LC-130 Skibird in Antarctica.

In case the takeoff ground roll (S_G) is given, but the required engine thrust (T) has to be determined, Equation 8.32 should be reformatted accordingly. After a few steps, the following relationship will be developed. The derivation is left to the reader as a homework problem.

$$T_{\mathrm{TO}} = W\left[\frac{\mu - \left(\mu + \dfrac{C_{D_{\mathrm{TO}}} - \mu C_{L_{\mathrm{TO}}}}{C_{L_{\mathrm{TO}}}}\right)\left[\exp\left(\dfrac{S_G \rho S\left(C_{D_{\mathrm{TO}}} - \mu C_{L_{\mathrm{TO}}}\right)}{m}\right)\right]}{1 - \left[\exp\left(\dfrac{S_G \rho S\left(C_{D_{\mathrm{TO}}} - \mu C_{L_{\mathrm{TO}}}\right)}{m}\right)\right]}\right] \tag{8.36}$$

where T_{TO} is the total engine thrust required to satisfy a given ground roll requirement.

Example 8.2

A transport aircraft with a takeoff mass of 150,000 kg (weight of 330,693 lb) has a wing area of 280 m^2 (3,014 ft^2) The aircraft cruising speed at 25,000 ft (7,620 m) is 525 knots, and the relation between engine thrust (in lbf) and airspeed (in fps) is as follows:

$$T = 0.1V^2 - 90V + 9{,}200.$$

Other characteristics of the aircraft are given:

$K = 0.05$, $C_{D_{o\mathrm{TO}}} = 0.055$, $\Delta C_{Lf} = 0$ (i.e., no flap deflection during takeoff), $V_s = 105$ knots, $V_R = 1.3\ V_s$. Determine the ground roll if the runway is dry concrete.

Solution

At 7,620 m, the air density is 0.55 kg/m^3. The cruising lift coefficient is

$$C_{L_C} = \frac{2mg}{\rho V_C^2 S} = \frac{2 \times 150{,}000 \times 9.81}{0.55 \times (525 \times 0.5144)^2 \times 280} = 0.262 \tag{8.23}$$

The takeoff lift and drag coefficients are

$$C_{L_{\mathrm{TO}}} = C_{L_C} + \Delta C_{L_{\mathrm{flap}}} = 0.262 + 0 = 0.262 \tag{8.20}$$

$$C_{D_{\mathrm{TO}}} = C_{D_{o\mathrm{TO}}} + KC_{L_{\mathrm{TO}}}^2 = 0.055 + 0.05 \times (0.262)^2 = 0.0584 \tag{8.22}$$

The ground roll is determined through the integration method directly:

$$S_G = \int_0^{V_R} \frac{mV}{T - \mu mg - 0.5\rho V^2 S\left(C_{D_{\mathrm{TO}}} - \mu C_{L_{\mathrm{TO}}}\right)} dV \tag{8.24}$$

Since the relation between engine thrust and airspeed is given in British units, other parameters should be converted to the British unit system. From Table 8.2, the friction coefficient for a concrete surface is 0.02. We proceed as follows:

$$C_{D_{\mathrm{TO}}} - \mu C_{L_{\mathrm{TO}}} = 0.0584 - (0.02 \times 0.262) = 0.05316$$

$$V_R = 1.3V_s = 1.3 \times 105 \times 1.688 = 230.2\,\text{ft/s}.$$

1 kg is equal to 0.0683 slug, and 1 m^2 is equal to 0.0929 ft^2. Thus,

$$\mu mg = 0.02 \times 150{,}000 \times 0.0683 \times 32.2 = 6{,}600\,\text{lb},$$

$$\frac{1}{2}\rho S V^2 = \frac{1}{2} \times 0.002378 \times (280 \times 0.0929) V^2 = 0.0309 V^2.$$

Now we can substitute all values and terms in the integration as follows:

$$S_G = \int_0^{230.2} \frac{150{,}000 \times 0.0683 V}{\left(0.1V^2 - 90V + 92{,}000\right) - 6{,}600 - 0.0309V^2(0.05316)} dV \qquad (8.24)$$

Solving the integration directly yields the following result:

$$S_G = 3{,}707\,\text{ft}.$$

Case Study - Example 8.3

A twin turbofan engine business aircraft – similar to Gulfstream G-650- with a take-off mass of 45,000 kg and a wing area of 120 m^2 has the following characteristics:

$b = 30$ m, $C_{D_{o_{fTO}}} = 0.004$, $C_{D_{o_{LG}}} = 0.007$, $\Delta C_{L_{flap}} = 0.6$; e = 0.86; V_c = 488 knots (at 25,000 ft or 7,620 m); $C_{D_o} = 0.019$.

Determine the total engine thrust required for a takeoff ground roll of 1,100 m at sea level for a runway with a friction coefficient of 0.04.

Solution

We first need to calculate a few parameters:

$$\text{AR} = \frac{b^2}{S} = \frac{30^2}{120} = 7.5 \qquad (3.9)$$

$$K = \frac{1}{\pi e\,\text{AR}} = \frac{1}{3.14 \times 0.86 \times 7.5} = 0.049 \qquad (3.8)$$

At 7,620 m, the air density is 0.55 kg/m^3. The cruising lift coefficient is as follows:

$$C_{L_C} = \frac{2mg}{\rho V_C^2 S} = \frac{2 \times 45{,}000 \times 9.81}{0.55 \times (488 \times 0.5144)^2 \times 120} = 0.212 \qquad (8.23)$$

The takeoff lift and drag coefficients are as follows:

$$C_{L_{\mathrm{TO}}} = C_{L_C} + \Delta C_{L_{\mathrm{flap}}} = 0.212 + 0.8 = 1.012 \tag{8.20}$$

$$C_{D_{o\mathrm{TO}}} = C_{D_{o\mathrm{clean}}} + C_{D_{o\mathrm{flap\text{-}TO}}} + C_{D_{o\mathrm{LG}}} = 0.019 + 0.004 + 0.007 = 0.03 \tag{3.62}$$

$$C_{D_{\mathrm{TO}}} = C_{D_{o\mathrm{TO}}} + KC_{L_{\mathrm{TO}}}^2 = 0.03 + 0.049 \times (1.012)^2 = 0.081 \tag{8.22}$$

The total engine thrust required is determined directly:

$$T_{\mathrm{TO}} = W\left[\frac{\mu - \left(\mu + \dfrac{C_{D_{\mathrm{TO}}} - \mu C_{L_{\mathrm{TO}}}}{C_{L_{\mathrm{TO}}}}\right)\left[\exp\left(\dfrac{S_G \rho S\left(C_{D_{\mathrm{TO}}} - \mu C_{L_{\mathrm{TO}}}\right)}{m}\right)\right]}{1 - \left[\exp\left(\dfrac{S_G \rho S\left(C_{D_{\mathrm{TO}}} - \mu C_{L_{\mathrm{TO}}}\right)}{m}\right)\right]}\right] \tag{8.36}$$

$$T_{\mathrm{TO}} = 45{,}000 \times 9.81\left[\frac{0.04 - \left(0.04 + \dfrac{0.081 - 0.04 \times 1.012}{1.012}\right)\left[\exp\left(\dfrac{1{,}100 \times 1.225 \times 120(0.081 - 0.04 \times 1.012)}{45{,}000}\right)\right]}{1 - \left[\exp\left(\dfrac{1{,}100 \times 1.225 \times 120(0.081 - 0.04 \times 1.012)}{45{,}000}\right)\right]}\right]$$

$$T_{\mathrm{TO}} = 147{,}930\,\mathrm{N} = 147.9\,\mathrm{kN}$$

Thus, each turbofan engine is required to generate 73.96 kN of thrust to satisfy the ground roll of 1,100 m. It is interesting to note that each turbofan of the Gulfstream G-650 generates 71.6 kN of thrust.

8.3.2 Rotation Segment

The second segment of a takeoff operation is referred to as the transition or rotation. The rotation section is a transition state from ground roll to airborne (Figure 8.8). At the beginning of the rotation section, all wheels have contact with the ground, but at the end, no wheel has contact with the ground. This segment ends with the liftoff. For an aircraft with a tricycle landing gear, the aircraft rotates about the main gear during this section. The aircraft angle of attack is gradually increased up to close to the stall angle.

Since the aircraft angle of attack is increased during this period, the aircraft lift is also increased significantly. Ideally, the airplane should be smoothly lifted off (or rotated by pulling stick/yoke which deflects the elevator up) to an attitude that will result in a high angle-of-attack. Many transport aircraft are prone to tail strikes during takeoff and landing. The rotation has to be performed gently and at a recommended pitch rate. Usually, more than 10° nose up is not recommended.

The rotation section is not easy to analyze since the aircraft undergoes transformation from the ground phase to the airborne phase while accelerating. To perform a precise analysis, we need to know more about aircraft center of gravity, elevator control power, and landing gear geometry. Since this section is short (compared with the total takeoff run), and its speed is nearly constant, the simplest way to approach this section is to assume a linear relationship between aircraft speed and the distance covered in this section. In other words, we assume that the aircraft experiences a constant speed. In a linear motion, the distance covered is equal to the speed of motion multiplied by the duration of motion. Therefore, the rotation distance (S_R or S_T) is

$$S_R = T_R \cdot V_R \tag{8.37}$$

where T_R is the duration of rotation and is estimated from Table 8.3 for various types of aircraft, and V_R is the rotation speed at the beginning of rotation.

Rotation speed has different values for various aircraft. A typical value is $1.1V_s$, where V_s is the aircraft stall speed. Typical stall speed for various aircraft types is given in Chapter 2. A more detailed description of the transition segment of the takeoff and a fully solved example are presented in Chapter 10.

8.3.3 Airborne Segment

The third segment of the takeoff run is the airborne section (or sometimes called initial climb). The liftoff speed at the beginning of airborne section is represented by V_{LO} and at the end of it by V_2. This section is in fact an accelerated climb (see Figure 8.9) and it lasts for a few seconds up to less than a minute. During this phase, the aircraft clears an obstacle height (h_o) while accelerating, and the velocity is increased from V_{LO} to V_2. The horizontal distance covered during the airborne segment is represented by S_A.

TABLE 8.3
Transition Time for Various Aircraft

No.	Aircraft Type	T_R (s)
1.	Highly maneuverable (e.g., fighter)	0.5–1
2.	Acrobatic	1–2
3.	General aviation – normal, utility	1–4
4.	Transport	3–6

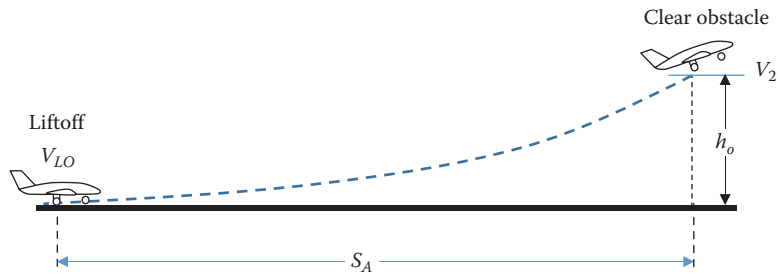

FIGURE 8.9 Airborne section.

Although there is no more friction force (no contact between landing gear and the ground), the airplane will accelerate less rapidly after liftoff (the airspeed is increased only <10% during this segment). This is due to the fact that the aircraft (1) is climbing, and (2) has much more drag. The aircraft has no contact with the runway during this section, but it is assumed to be an important part of the takeoff operation. The aircraft is clearing an imaginary obstacle at the end of the airborne section. Figure 8.9 illustrates the accelerated nature of the initial climb.

The obstacle height (h_o) is determined by airworthiness standards. Based on FAA regulations [6], obstacle height is 35 ft for a transport aircraft and 50 ft for a GA aircraft. Furthermore, military aircraft are required by MIL-STD [85] to clear a 50 ft obstacle during takeoff. It is recommended that the landing gear and flaps remain in the takeoff position until obstacles are cleared and even until the best climb rate speed has been established. Figure 8.10 shows a fighter aircraft (McDonnell Douglas EF-18A Hornet) and a transport aircraft (Boeing 747) in the takeoff operation. Both aircraft have a high angle of attack.

The takeoff performance of a Boeing 737 and a Boeing 747-100 are demonstrated in Figure 8.11. In Figure 8.11a, the variations of angle of attack and speed as a function of time for a Boeing 737- for rotation and airborne – is illustrated. In Figure 8.11b, the variations of altitude as a function of time for a Boeing 747-100 after lift off – are shown, where the interval between each time step is different.

The principle of work-energy states that the change in aircraft energy is equal to the work done on the aircraft by engine thrust and other forces:

$$\text{Work} = \Delta E_K + \Delta E_P \tag{8.38}$$

The aircraft at the end of the airborne section has more kinetic energy (E_K) and more potential energy (E_P). The change in kinetic energy of the aircraft with a mass of m during this section is equal to

$$\Delta E_K = \frac{1}{2} m\left(V_2^2 - V_{\text{LO}}^2\right) \tag{8.39}$$

Since the aircraft gains height (h_o) during the airborne section, its potential energy is also increased:

$$\Delta E_P = mgh_o \tag{8.40}$$

(a)

(b)

FIGURE 8.10 A fighter and a transport aircraft in takeoff flight. (a) A McDonnell Douglas EF-18A Hornet at takeoff. (Courtesy of Maurice Kockro.) (b) A Boeing 747, transport aircraft at takeoff. (Courtesy of Gustavo Corujo.)

Figure 8.12 depicts the forces applied during airborne segment of the takeoff. If the average climb angle is assumed to be γ, the accelerated climb governing equation from Newton's second law is:

$$T - D - mg\sin\gamma = ma \tag{8.41}$$

where the acceleration is a function of the initial and final velocities:

$$a = \frac{V_2^2 - V_{LO}^2}{2S_A'} \tag{8.42}$$

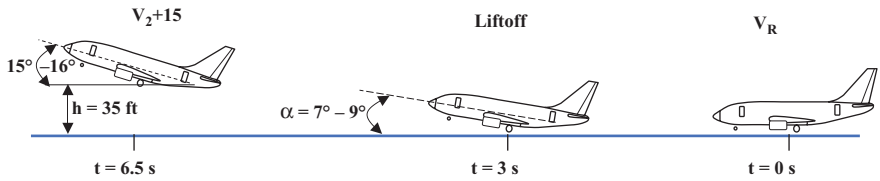

(a)

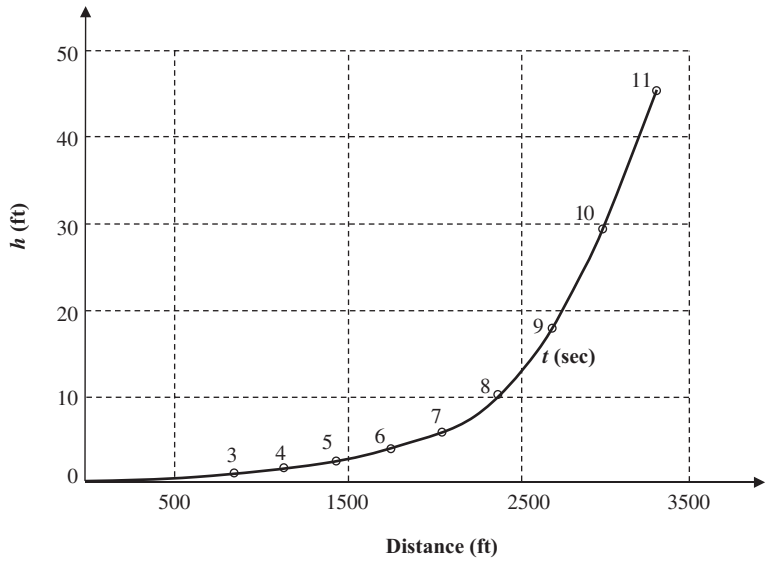

(b)

FIGURE 8.11 Takeoff performance of a Boeing 737 and a Boeing 747. (a) Rotation plus airborne segments for a Boeing 737, (b) takeoff performance of a Boeing 747-100 after liftoff.

where S'_A is the distance covered along the flight path. Figure 8.12 also shows the relationship between parameters S'_A and S_A. From the triangle, the Pythagorean equation yields

$$\left(S'_A\right)^2 = S_A^2 + h_o^2 \tag{8.43}$$

The climb angle (γ) is very small: about 2° for a transport aircraft and 8° for a normal GA aircraft. In addition, for the average climb angle, γ (Figure 8.12), we can write

$$\sin(\gamma) = \frac{h_o}{S'_A} \tag{8.44}$$

The initial velocity (V_{LO}) and final velocity (V_2) in the takeoff airborne segment are a function of the stall speed:

$$V_{\text{LO}} = k_{\text{LO}} V_s \tag{8.45}$$

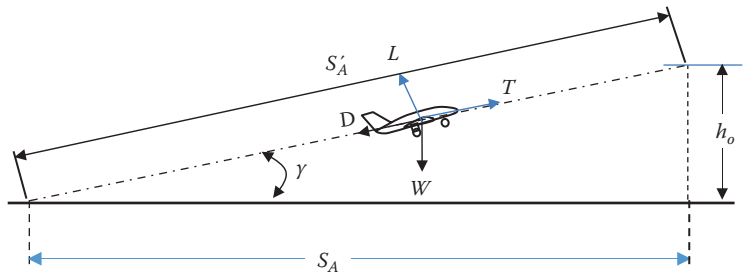

FIGURE 8.12 Forces during climb and relationship between parameters $S'A$ and S_A.

$$V_2 = k_2 V_s \tag{8.46}$$

where the factors k_{LO} and k_2 are regulated by FAR. Typical magnitudes are as follows:

$$k_{\text{LO}} = 1.1 - 1.2 \tag{8.47}$$

$$k_2 = 1.2 - 1.3 \tag{8.48}$$

For a fighter and an acrobat aircraft, it is recommended to use a value of 1.1 for k_{LO} and a value of 1.2 for k_2. For any other type of aircraft (e.g., GA and transport), use a value of 1.2 for k_{LO} and a value of 1.3 for k_2.

When "sin(γ)" from Equation 8.44, and the acceleration a from Equation 8.42 are inserted into Equation 8.41, we obtain

$$T - D - mg\frac{h_o}{S_A'} = m\frac{V_2^2 - V_{\text{LO}}^2}{2S_A'} \tag{8.49}$$

This equation has only one unknown, S_A'. Solving Equation 8.49 for this unknown yields

$$S_A' = \frac{mg}{T - D}\left[\frac{V_2^2 - V_{\text{LO}}^2}{2g} + h_o\right] \tag{8.50}$$

The thrust (T) and drag (D) are functions of airspeed (V), and the climb angle and mass are functions of time. Thus, the right-hand side of the equation is a function of time and velocity. Solving this equation and an accurate analysis of the airborne segment requires a computer code based on numerical methods. A fully solved example in Example 10.3, Chapter 10 illustrates the application of numerical methods to analyze takeoff airborne.

There is a less complex technique that yields a fairly accurate result. Without compromising on accuracy, we may assume the mass and climb angle are constant and use the average thrust and drag. Thus,

$$S'_A = \frac{mg}{T_{\text{ab}} - D_{\text{ab}}}\left[\frac{V_2^2 - V_{\text{LO}}^2}{2g} + h_o\right] \tag{8.51}$$

where the expression $T_{\text{ab}} - D_{\text{ab}}$ stands for the airborne (ab) average thrust minus the average drag of the aircraft during the airborne section. Employing the work–energy relationship gives the same results.

When the parameter S'_A is determined from Equation 8.51, use Equation 8.43 to calculate the airborne section of the takeoff run, S_A:

$$S_A = \sqrt{\left(S'_A\right)^2 + h_o^2} \tag{8.52}$$

The average speed during the airborne section is

$$V_{\text{ab}} = k_{\text{ab}} V_s \tag{8.53}$$

where the factor k_{ab} is

$$k_{\text{ab}} = \frac{k_{\text{LO}} + k_2}{2} \tag{8.54}$$

Therefore, the average aircraft drag during the airborne (ab) section is estimated as follows:

$$D_{\text{ab}} = \frac{1}{2}\rho S C_{D_A}\left(k_{\text{ab}} V_s\right)^2 \tag{8.55}$$

where the drag coefficient C_{D_A} is

$$C_{D_A} = C_{D_{o\text{TO}}} + K C_{L_A}^2 \tag{8.56}$$

The lift coefficient during the airborne segment is a function of the maximum lift coefficient:

$$C_{L_A} = \frac{C_{L_{\max}}}{k_{\text{ab}}^2} \tag{8.57}$$

The average engine thrust is estimated as follows:

$$T_{\text{ab}} = 0.9\, T_{\max} \tag{8.58}$$

$$T_{\text{ab}} = \frac{\eta_{\text{ab}} P_{\max}}{k_{\text{ab}} V_s} \tag{8.59}$$

where Equation 8.58 gives the estimation of average engine thrust during takeoff for an aircraft with a turbofan or a turbojet engine. Equation 8.59 is the estimation of

average engine thrust during takeoff for an aircraft with a turboprop or piston prop engine. If the propeller is fixed pitch, the coefficient η_{ab} is 0.6, but if it were a variable pitch, the coefficient η_{ab} would be 0.8.

Finally, when all three sections of the takeoff run (i.e., S_G, S_R, and S_A) are determined, it is readily calculated from their summation (Equation 8.7). Table 8.4 illustrates takeoff run for several jet and prop-driven aircraft. Figure 8.10b shows the

TABLE 8.4
Takeoff Run for Several Jet and Prop-Driven Aircraft

(a) Prop-Driven Aircraft

No.	Aircraft	Manufacturer	Type	Engine	P (kW)	m_{TO} (kg)	S_{TO} (m)
1.	CL-215T	Canadair	Amphibian	Piston prop	2×1,566	19,731	811
2.	F406/Caravan II	Raymz/Cessna	Utility	Turboprop	2×373	4,246	803
3.	Dauphin	Robin	Trainer	Piston prop	83.5	1,050	535
4.	Dakota	Piper	Light GA	Piston prop	175	1,361	371
5.	Beech Bonanza	Beech craft	Utility	Piston prop	212	1,633	383
6.	Silver Eagle	Silver	Ultralight	Piston prop	17	251	69
7.	CBA-123	Embraer/Fama	Transport	Turboprop	2×970	7,800	1,010
8.	Harbin Y-12	Harbin	Transport	Turboprop	2×373	5,300	425
9.	Shaanxi Y-8	Shaanxi	Transport	Turboprop	4×820	61,000	1,230
10.	Epsilon	Aerospatiale	Military trainer	Piston prop	224	1,250	640
11.	Atlantique 20	Dassault	Patrol	Turboprop	2×4,549	45,000	1,840
12.	P180 Avanti	Piaggio	Transport	Turboprop	2×596	4,767	736
13.	C-130 Hercules	Lockheed	Transport	Turboprop	4×3,362	79,380	1,573
14.	EMB-312 Tucano	Embraer	Trainer	Turboprop	560	2,550	380
15.	PC-9	Pilatus	Trainer	Turboprop	708	3,200	391
16.	Saab 340	Saab	Regional airliner	Turboprop	2×1,394	13,154	1,285
17.	V-22 Osprey	Bell Boeing	Tiltrotor VTOL	Turboprop/ turboshaft	2×4,586	21,546	0

(b) Jet Aircraft

No.	Aircraft	Manufacturer	Type	Engine	T (kN)	m_{TO} (kg)	S_{TO} (m)
1.	Citation 700	Cessna	Business jet	Turbofan	2×34	11,900	980
2.	Microjet 200	Microjet	Trainer	Turbojet	2×1.3	1,300	1,180
3.	Saab 35 Draken	Saab	Fighter	Turbofan	56.9	16,000	650
4.	Alpha Jet	Dassault/Dornier	Trainer	Turbofan	2×14.12	8,000	370
5.	AV-8B Harrier II	McDonnell	VTOL fighter	Turbofan	94.2	13,500	0
6.	C-5 Galaxy	Lockheed	Military cargo	Turbofan	4×191.2	379,657	2,530
7.	Boeing 747-400	Boeing	Transport	Turbofan	4×285	394,625	3,323
8.	A320neo	Airbus	Transport	Turbofan	2×120.6	79,000	1,951
9.	Global 7500	Bombardier	Business jet	Turbofan	2×84.2	52,096	1,768
10.	F/A-18E/F	Boeing	Fighter	Turbofan	2×49	23,540	1,580
11.	B 777-300ER	Boeing	Transport	Turbofan	2×513	351,535	3,201
12.	A-330-300	Airbus	Transport	Turbofan	2×316	242,000	2,607

aircraft Boeing 747 during takeoff. The takeoff run of this large transport aircraft is 3,333 m (2.07 miles).

Case Study - Example 8.4

The trainer aircraft Embraer EMB 312 Tucano has a turboprop engine with a variable pitch propeller and a takeoff mass of 2,550 kg. The aircraft cruise speed at 10,000 ft (3,048 m) is 172 knots (318 km/h). Other aircraft features are as follows:

$$S = 19.4\,\text{m}^2,\ P_{\max} = 560\,\text{kW},\ V_s = 67\,\text{knot}\,(124\,\text{km/h}),\ C_{D_{o_C}} = 0.021,\ C_{D_{o_{f\text{TO}}}} = 0.004,$$

$$C_{D_{o_{\text{LG}}}} = 0.007,\ b = 11.14\,\text{m},\ e = 0.86,\ \Delta C_{L_{\text{flapTO}}} = 0.4.$$

Calculate the takeoff run (S_{TO}) for this aircraft at sea level, if it is taking off from a dry asphalt runway.

Solution

We will determine three sections separately, and then they will be added. From Appendix B, the air density at 3,048 m is 0.904 kg/m³. From Table 8.2, the runway friction coefficient is 0.04.

a. Ground roll
To find ground roll, we proceed as follows:

$$C_{L_C} = \frac{2mg}{\rho S V_C^2} = \frac{2\times 2{,}550\times 9.81}{0.904\times 19.4\times(172\times 0.5144)^2} = 0.364 \tag{8.23}$$

$$C_{L_{\text{TO}}} = C_{L_C} + \Delta C_{L_{\text{flapTO}}} = 0.364 + 0.4 = 0.764 \tag{8.20}$$

$$C_{D_{o_{\text{TO}}}} = C_{D_{o_C}} + C_{D_{o_{f\text{TO}}}} + C_{D_{o_{\text{LG}}}} = 0.021 + 0.004 + 0.007 = 0.032 \tag{3.62}$$

$$\text{AR} = \frac{b^2}{S} = \frac{11.14^2}{19.4} = 6.4 \tag{3.9}$$

$$K = \frac{1}{\pi e\,\text{AR}} = \frac{1}{3.14\times 0.86\times 6.4} = 0.058 \tag{3.8}$$

$$C_{D_{TO}} = C_{D_{o_{TO}}} + KC_{L_{TO}}^2 = 0.032 + 0.058\times 0.764^2 = 0.066 \tag{8.22}$$

We assume, VR = 1.1 Vs, V2 = 1.3Vs, and Vab = 1.5Vs. From Equation 8.47, a value of 1.1 is selected for kLO. Since the propeller has a variable pitch, its average efficiency during ground roll is 0.6, so

$$T = \frac{0.6P_{\max}}{V_R} = \frac{0.6 \times 560 \times 1{,}000}{1.1 \times 67 \times 0.5144} = 8{,}851\,\text{N} \tag{8.35}$$

$$\frac{T}{mg} = \frac{8{,}851}{2{,}550 \times 9.81} = 0.354$$

$$C_{D_{\text{TO}}} - \mu C_{L_{\text{TO}}} = 0.066 - (0.04 \times 0.764) = 0.035$$

$$C_{L_{\max}} = \frac{2mg}{\rho S V_s^2} = \frac{2 \times 2{,}550 \times 9.81}{1.225 \times 19.4 \times (67 \times 0.5144)^2} = 1.77 \tag{2.26}$$

$$S_G = \frac{m}{\rho S\left(C_{D_{\text{TO}}} - \mu C_{L_{\text{TO}}}\right)} \ln\left[\frac{(T/mg) - \mu}{(T/mg) - \mu - \dfrac{k_{\text{LO}}^2\left(C_{D_{\text{TO}}} - \mu C_{L_{\text{TO}}}\right)}{C_{L_{\max}}}}\right] \tag{8.32}$$

$$S_G = \frac{2{,}550}{1.225 \times 19.4 \times 0.035} \ln\left[\frac{0.354 - 0.04}{0.354 - 0.04 - \dfrac{(1.1)^2 \times 0.035}{1.77}}\right] = 242.9\,\text{m}$$

b. Rotation or Transition run:
According to Table 8.3, the rotation time for this type of aircraft is between 1 and 4 s. Due to the type of the aircraft (trainer), we consider 1 s.

$$S_R = T_R V_R = 1 \times 1.1 \times 67 \times 0.5144 = 37.9\,\text{m}. \tag{8.37}$$

c. Airborne section:

$$S'_A = \frac{mg}{T_{\text{ab}} - D_{\text{ab}}}\left[\frac{V_2^2 - V_{\text{LO}}^2}{2g} + h_o\right] \tag{8.50}$$

Since the propeller is variable pitch, its efficiency during airborne segment is 0.8. The airborne thrust and drag (T_{ab}, D_{ab}) should be determined first.

$$T_{\text{ab}} = \frac{\eta_{\text{ab}} P_{\max}}{k_{\text{ab}} V_s} = \left[\frac{0.8 \times 560 \times 1{,}000}{1.25 \times 67 \times 0.5144}\right] = 10{,}385\,\text{N} \tag{8.59}$$

$$C_{L_A} = \frac{C_{L_{\max}}}{k_{\text{ab}}^2} = \frac{1.77}{1.25^2} = 1.134 \tag{8.57}$$

$$C_{D_a} = C_{D_{\sigma TO}} + KC_{L_A}^2 = 0.032 + 0.058 \times 1.134^2 = 0.106 \tag{8.56}$$

$$D_{ab} = \frac{1}{2}\rho S C_{D_A} (1.25\ V_2)^2 \tag{8.55}$$

$$D_{ab} = \frac{1}{2} \times 1.225 \times 19.4 \times 0.106 \times (1.25 \times 67 \times 0.5144)^2 = 2{,}346\,\text{N} \tag{8.55}$$

$$S'_A = \frac{2{,}550 \times 9.81}{10{,}385 - 2{,}346} \times \left[\frac{(1.3 \times 67 \times 0.5144)^2 - (1.2 \times 67 \times 0.5144)^2}{2 \times 9.81} + 15.24 \right] = 94.5\,\text{m} \tag{8.50}$$

where the obstacle height is 50 ft or 15.24 m for this GA aircraft.

$$S_A = \sqrt{(S'_A)^2 - h_o^2} = \sqrt{94.5^2 - 15.24^2} = 93.3\,\text{m} \tag{8.50}$$

d. Total takeoff run:

$$S_{TO} = S_G + S_R + S_A = 242.9 + 37.9 + 93.3 = 374.1\,\text{m} \tag{8.7}$$

According to published data [9], the takeoff run of the aircraft Tucano is 380 m.

8.4 LANDING

8.4.1 Landing Segments

Landing is the last phase of a regular flight, which brings the aircraft from airborne to ground status. After a descent from a cruise altitude, landing will be the last flight operation. A landing operation begins with an approach, then flare (round out), then rotation, and is finished with braking, and a stop.

Landing operation is similar to takeoff operation in many aspects, but has several critical differences, as follows:

1. Landing is the last stage of a regular flight, but takeoff is the first stage.
2. Takeoff is going from land or sea (runway) to airborne, but landing is changing the status from airborne to the ground or sea (runway).
3. In a takeoff operation, the maximum engine thrust is utilized, but in a landing operation, the least amount of thrust (even zero) is needed.
4. Takeoff without using engine (or outside help) is impossible, but landing without engine is quite possible.
5. Aircraft weight is usually much less in landing than in takeoff, since fuel is consumed during flight.
6. One of the important forces during landing is the brake force, but this force is never used during a takeoff. The brake force is sometimes reinforced with

other means such as parachute, engine thrust reversal, hook and string, and spoiler. These factors will reduce the landing run.

7. In general, the landing distance is shorter than the takeoff distance. The main reason is that the aircraft landing weight is less (about 20%–30%) than the takeoff weight.

Similar to takeoff, the most important parameter for the evaluation of landing performance is the length of the landing run. The shorter the landing run, the more desirable is the landing performance. The landing run is measured from the approach point at an imaginary obstacle (35 or 50 ft [11 or 15 m]) to a full stop. Aircraft speed at the beginning of landing operation is often the same as that at the end of takeoff operation. The maximum aircraft angle of attack during landing is often 2°–4° less than the maximum aircraft angle of attack during takeoff (e.g., 10°–15°).

To compensate for this angle of attack reduction, a higher flap deflection is employed. In most cases, flap deflection during landing is between 30° and 60°, while during takeoff it is between 5° and 30°. For instance, the transport aircraft Boeing 727 with a regular payload has the following angle of attack and flap deflection during various flight operations:

- Cruise aircraft angle of attack: 3°
- Takeoff aircraft angle of attack: 10°
- Landing aircraft angle of attack: 6°
- Takeoff flap deflection: 15°
- Landing flap deflection: 30°

Similar to takeoff, landing is also an accelerated operation, but its acceleration, unlike takeoff, is negative (in fact, deceleration). Aircraft speed during landing gradually decreases, while the angle of attack increases first, and then decreases. This variation makes the motion nonlinear, which complicates the landing analysis. The airspeed during approach is decreased by increasing the angle of attack, but the airspeed during ground roll is decreased by applying brakes. The angle of attack is increased during flare by pulling the stick/yoke, which causes the elevator to deflect up.

Landing operation is potentially the most hazardous part of a flight; this is confirmed by statistical reports. Typical reasons for this danger are crosswind landing, failure of landing gear for extension, flight traffic, and bad weather. For these reasons, some aircraft may have to abort landing at the planned airport and change their destinations. The pilot must reduce aircraft speed during landing as much as possible to ensure safe landing and reduce the possibilities of a mishap. A low speed during touchdown leads to fewer casualties and fewer consequences, should a crash happens during landing.

One of the effective parameters influencing the landing run is the brake force, while it is ineffective during takeoff operation. Because of these reasons, the relationship between landing run and takeoff run is not the same for every aircraft. Landing run for a VTOL aircraft (e.g., helicopter) is zero. In majority of aircraft, the landing run is shorter than the takeoff run. It is predicted that with advancements in new technologies, this relation will be reversed.

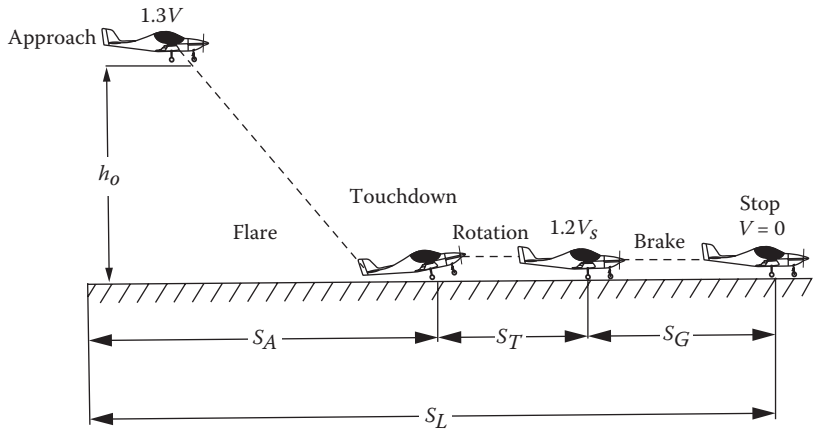

FIGURE 8.13 Landing run segments.

As Figure 8.13 demonstrates, the landing run is divided [82] into three segments: (1) Approach and flare, (2) Rotation, and (3) Brake.

The flight stage prior to a landing operation is usually descent, which has a low angle of attack (about 3°). The first segment of a landing operation is referred to as "approach" and the aircraft is prepared for landing. This segment starts from an obstacle height and ends with a touchdown.

The flare is the last part of an approach and brings the fuselage nose up such that the aircraft has a high angle of attack. At this moment, the aircraft speed is about $1.3V_s$. During this period, along with speed reduction, the height between aircraft and runway is also gradually reduced until the main gear touches down. This phase of landing is completely airborne. The ground distance covered during the approach is called approach run (S_A).

The roundout (i.e., flare) is a slow, smooth transition from a normal approach attitude to a landing attitude, gradually rounding out the flight path to one that is within a few centimeters above the runway. When the airplane approaches within about 3–6 m above the ground, the flare should be started and continue until the airplane touches down on the ground, since engine power/thrust is normally reduced to zero during the roundout. During a flare, elevator up should be gradually employed to slowly increase the angle of attack. This will cause the fuselage nose to gradually rise toward the desired landing pitch attitude.

The approach speed is a velocity close to the stall speed. For instance, the approach speed for jet airliner Airbus A-300-600 is 135 knots [9], while the touchdown velocity of the transport aircraft Boeing 777-300 (Figure 7.18) is 148 knots. The approach speed for jet fighter Dassault Mirage 2000 is 140 knots, while its landing speed is 125 knots. Furthermore, the approach speed for the business tri-jet aircraft Dassault Falcon 50 with a maximum takeoff mass of 18,000 kg, with eight passengers, and IFR reserve fuel is 107 knots.

The second phase of the landing run involves the distance (S_T) that aircraft is in rotation or transition from airborne to ground rolling. During this phase, aircraft is

rotated such that the angle of attack is reduced from its maximum value to about zero. The transition segment (for an aircraft with a tricycle landing gear) begins with a touchdown of the main gear and ends with the contact of the nose gear with the ground. When all wheels are in contact with the ground, the last phase of the landing operation begins. In the third segment (S_G), brakes and other means of speed reduction are active until the aircraft reaches a very low speed and is ready to taxi. During this phase, the aircraft rolls on the ground and prepares to stop.

The primary parameter to evaluate a landing operation is the landing run (S_L), which is the horizontal distance covered from approach to a full stop. The shorter the landing run, the better the landing performance. A typical landing run for a GA aircraft is about 150–1,000 m, while for a large transport aircraft it is about 1,500–3,500 m. The landing run for a fighter aircraft ranges from 100 to 1,000 m. A minimal takeoff run is possible only with the help of a catapult system.

The light aircraft Piper PA-28 Cherokee Arrow (with a maximum takeoff weight of 2,650 lb and 40° flap, and maximum braking) requires a ground roll of 760 ft [57] for landing. However, the aircraft requires a distance of 1,350 ft from an obstacle height of 50 ft. A related term to the landing distance is the *landing field length*, which is calculated by multiplying the actual distance required for landing by a safety factor of 1.667. For example, the landing field length for Boeing 757-200 (Figure 5.8) at maximum landing weight is ~1,550 m.

The landing distance is primarily influenced by brake, while the takeoff distance is mainly influenced by engine thrust. The landing distance for most jet aircraft is usually (about 10%–30%) shorter than the takeoff distance. One example is the business jet Gulfstream G-550 with a takeoff distance of 1,800 m, but a landing distance of 880 m. However, for a prop-driven aircraft, the engine power and brake effectiveness are very crucial. Thus, for an aircraft with a powerful engine and very effective brake, the landing distance is about 10%–30% shorter than the takeoff distance.

One example is Cessna 172 Skyhawk (Figure 3.17) with a takeoff distance of 497 m, but a landing distance of 407 m. However, for the aircraft Beech King Air 250, the takeoff distance is 643 m, while the landing distance is longer, 867 m. For many aircraft, the takeoff and landing distances are almost the same. For instance, the Piaggio P-180 Avanti [86] with twin turboprop engines and a maximum takeoff mass of 5,239 kg has a takeoff distance of 869 m, and a landing distance of 872 m. Table 8.5 provides landing distances (here, the length of runway after touchdown) for several aircraft.

8.4.2 Landing Calculations

This section is devoted to developing a technique to analyze the landing performance and a method to determine the landing run. The landing run (S_L) is the horizontal distance covered from obstacle height to a full stop. This distance is divided into three segments, which are treated separately. The total length of landing run (S_L) is the summation of three main sections:

$$S_L = S_A + S_T + S_G \tag{8.60}$$

TABLE 8.5
Landing Distance for Several Aircraft

No.	Aircraft	Type	Engine	Takeoff Mass (kg)	S (m^2)	S_L (m)
1.	Boeing 737-800	Airliner	Turbofan	79,015	125	1,634
2.	Boeing 777-300	Airliner	Turbofan	299,370	427.8	1,630
3.	Boeing 747-300	Airliner	Turbofan	377,840	511	1,942
4.	Gulfstream G550	Business jet	Turbofan	41,300	105.6	880
5.	Beechjet 400	Business jet	Turbofan	7,303	22.43	832
6.	Pilatus PC-9	Trainer	Turboprop	3,200	16.29	700
7.	Piaggio P180 Avanti	Transport	Turboprop	5,239	16	872
8.	Lockheed C-130 Hercules	Transport	Turboprop	58,967	162.1	777
9.	General Dynamics F-16 Fighting Falcon	Fighter	Turbofan	16,055	27.88	810
10.	Cessna Skyhawk	GA	Piston	1,157	16.2	407
11.	Piper Cherokee PA-28	GA	Piston	975	15.1	361
12.	Beech King Air 250	Business jet	Turboprop	5,670	28.8	876
13.	Bombardier Global 7500	Business jet	Turbofan	52,096	116.5	768

where S_A is the airborne (approach) segment, S_T is the transition segment, and S_G is the ground roll. In general, the technique to analyze the airborne section of landing is very similar to the method employed to calculate the airborne phase of takeoff run. The airborne segment S_A is measured from an obstacle height (h_o) up to touchdown. The transition section of landing run (S_T) is also determined in a similar manner by calculating the transition section of the takeoff run. But in the calculation of ground roll (S_G), we must consider the new force of brake and any other resisting forces.

8.4.2.1 Approach Section

The approach is essentially a decelerated descent; velocity is decreased while height is lost. During an approach (as in a glide), three forces are functioning: (1) lift, (2) drag, and (3) weight. Figure 8.14 illustrates the forces during the approach and the approach angle (γ).

We first determine the distance flown along the flight path S'_A, and then calculate the horizontal component of that distance (i.e., S_A). Figure 8.14 also depicts the relationship between parameters S'_A and S_A. Similar to the technique we employed in takeoff analysis, one can use Newton's second law and the decelerated descent governing equations (or the work–energy relationship) to develop the following equation:

$$S'_A = \frac{m_L g}{-D_{\text{ab}}}\left[\frac{V_{\text{TD}}^2 - V_2^2}{2g} + h_o\right] \tag{8.61}$$

where D_{ab} stands for the airborne (ab) average drag of the aircraft during approach. The aircraft mass at landing is denoted by m_L. In theory, the landing mass is equal to the takeoff mass (m_{TO}) minus fuel mass (m_f).

$$m_L = m_{\text{TO}} - m_f \tag{8.62}$$

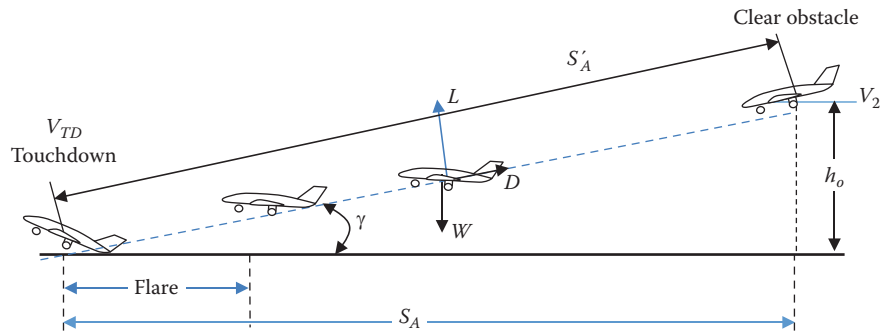

FIGURE 8.14 Approach flight path and the applied forces.

However, in an aborted takeoff, the landing mass is very close to the takeoff mass. The initial velocity (V_2) and final velocity (V_{TD}) in the approach are a function of stall speed:

$$V_2 = k_2 V_s \tag{8.63}$$

$$V_{TD} = V_L = k_{TD} V_s \tag{8.64}$$

where the factors k_{LO} and k_2 are regulated by FAR. Typical values are:

$$k_{TD} = 1.1 - 1.2 \tag{8.65}$$

$$k_2 = 1.2 - 1.3 \tag{8.66}$$

For a fighter and an acrobat aircraft, it is recommended to use a value of 1.1 for k_{TD} and a value of 1.2 for k_2. For any other types of aircraft (e.g., GA and transport), use a value of 1.2 for k_{TD} and a value of 1.3 for k_2. Therefore, the average aircraft drag during the airborne (ab) segment is estimated as follows:

$$D_{ab} = \frac{1}{2}\rho S C_{D_A} \left(k_{ab} V_s\right)^2 \tag{8.67}$$

where the drag coefficient during approach C_{D_A}, as developed in Chapter 3, is

$$C_{D_A} = C_{D_{oL}} + K C_{L_A}^2 \tag{8.68}$$

where $C_{D_{oL}}$ is the zero-lift landing drag coefficient. $C_{D_{oL}}$ is often greater than $C_{D_{oTO}}$ due to the application of greater flap deflection. Furthermore, during landing, other means such as spoiler is employed to increase aircraft drag. In the case of a large aircraft, a parachute behind fuselage may be used to create drag. For instance, a

39-foot-diameter braking parachute was used to slow down the space shuttle (Figure 4.26) during landing. This tool relieved stress on the brakes and tires and reduced the landing run as much as 2,000 ft. The technique to determine $C_{D_{o_L}}$ is presented in Chapter 3.

The lift coefficient during airborne segment C_{L_A} is a function of the maximum lift coefficient:

$$C_{L_A} = \frac{C_{L_{\max}}}{k_{\text{ab}}^2} \tag{8.69}$$

The average speed during the airborne section is

$$V_{\text{ab}} = k_{\text{ab}} V_s \tag{8.70}$$

where the factor k_{ab} is

$$k_{\text{ab}} = \frac{k_{\text{TD}} + k_2}{2} \tag{8.71}$$

From the geometry of triangle in Figure 8.15, we can derive the relation between the obstacle height (h_o) and the airborne distance (S_A) of the landing run:

$$S_A = \sqrt{(S'_A)^2 - h_o^2} \tag{8.72}$$

where the parameter S'_A is determined from Equation 8.61. The approach flight of a Canadair CC-144B Challenger, a business jet, is depicted in Figure 8.15.

8.4.2.2 Transition

The second segment of a landing operation is referred to as the transition (or rotation), which starts with a touchdown. The rotation section is a transition state from airborne to ground roll (Figure 8.16). An aircraft with a tricycle landing gear rotates about the main gear during this segment. At the beginning of the rotation segment, only the main gear is in contact with the ground, but at the end, all wheels are in contact with the ground. Since the aircraft angle of attack is decreased during this

FIGURE 8.15 Approach flight of a Canadair CC-144B Challenger. (Courtesy of Gustavo Corujo.)

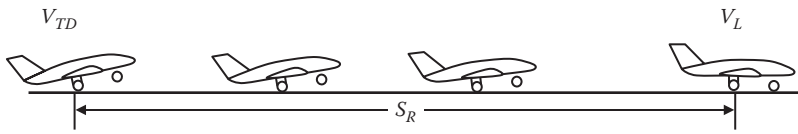

FIGURE 8.16 Rotation (transition) section.

period, the aircraft lift is also decreased significantly. Ideally, the airplane should be smoothly rotated to a level attitude by pushing stick/yoke (elevator down).

The rotation segment is too complex to analyze since the aircraft is in a transformation phase—from airborne phase to ground phase—while decelerating. To perform an accurate analysis, we need to know more about the aircraft center of gravity, elevator control power, and landing gear geometry. Since this segment is short (compared with the total landing run), and aircraft speed is *almost* constant, the simplest way to mathematically model this segment is to assume a linear relationship between aircraft speed and the distance covered in this segment. Thus, we assume that the aircraft experiences a constant speed. In a linear motion, the distance covered is equal to the speed of motion multiplied by the duration of motion. Thus, the rotation distance (S_R or S_T) simply is

$$S_R = T_R V_{\text{TD}} \tag{8.73}$$

where T_R is the duration of rotation and is estimated from Table 8.3 for various types of aircraft, and V_{TD} is the touchdown speed at the beginning of rotation. The touchdown speed has different values for various aircraft. A typical value is 1.1–1.3V_s, where V_s is the aircraft stall speed.

8.4.2.3 Ground Roll

In a ground roll, five forces (See Figure 8.17) are functioning: (1) aircraft weight, (2) drag, (3) lift, (4) brake force, and (5) friction force. Other forces such as reverse thrust can be added. Figure 8.18 also illustrates variations of forces acting on an aircraft during landing. The lift and drag are gradually decreasing due to the reduction of airspeed. Furthermore, the friction and brake force are increasing due to the reduction of normal force (in fact lift).

Based on Newton's second law, the summation of all forces generates a deceleration on the aircraft:

$$\sum F = m\frac{d}{dt}(V) \Rightarrow -T_{\text{rev}} - D - F_f - F_B - F_S = ma \tag{8.74}$$

where acceleration, a has a negative value (hence, deceleration), F_f stands for the friction force, F_B is the brake force, F_S is the sum of all other resisting forces, and D is aircraft drag.

The friction force is proportional to the normal component, N of the reaction of the surface. The proportionality coefficient is static rolling friction coefficient (μ). Table 8.2 provides the friction coefficient between landing gear rolling wheels

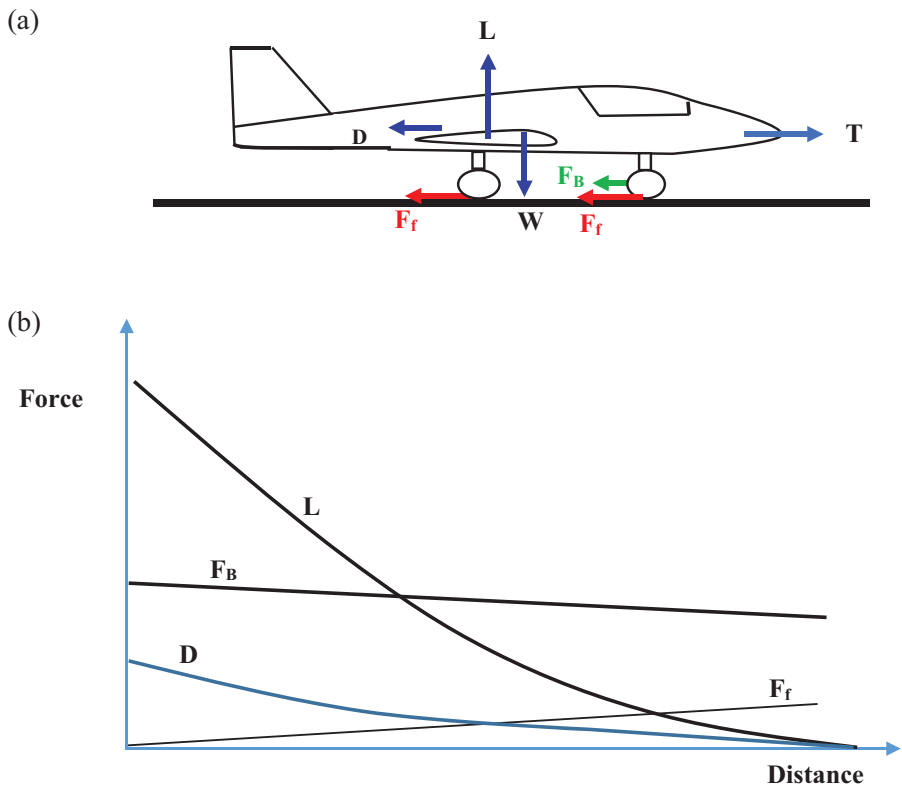

FIGURE 8.17 Variations of forces acting on an aircraft during landing: (a) active forces during ground roll and (b) variations of forces during ground roll.

and various types of runway surfaces. This table introduces two friction coefficient values for each surface: brakes-on and brakes-off. During a takeoff operation, the brakes are not used (brakes-off), but during a landing operation, they are employed (brakes-on) to reduce the landing run. Make sure to use the values for brake-on.

The friction force is proportional to the normal component, N of the reaction of the surface:

$$F_f = \mu N_L \tag{8.75}$$

The normal force is the algebraic sum of the aircraft weight and lift:

$$N_L = W_L - L_L \tag{8.76}$$

where the lift force during landing is a function of aircraft speed:

$$L = L_L = \frac{1}{2}\rho V^2 S C_{L_L} \tag{8.77}$$

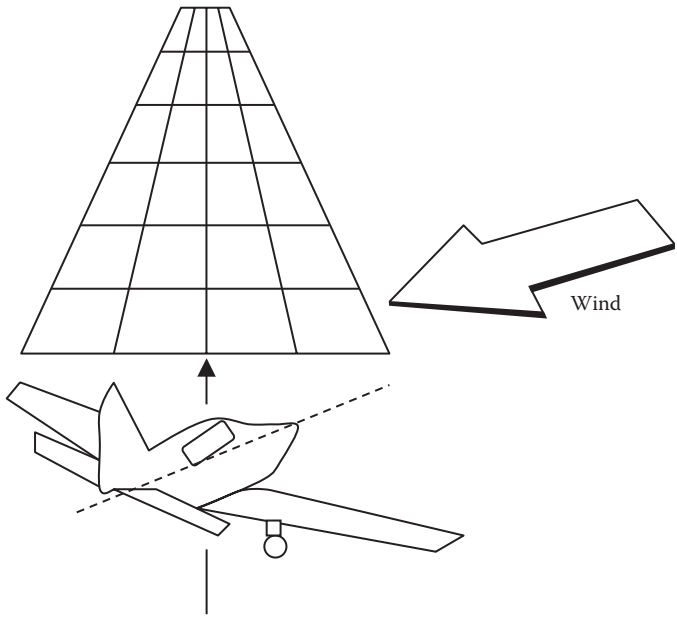

FIGURE 8.18 Crosswind and crabbing during landing.

where the landing lift coefficient is

$$C_{L_L} = C_{L_C} + \Delta C_{L_{\text{flap}L}} \tag{8.78}$$

The parameter $\Delta C_{L_{\text{flap}L}}$ is the additional lift coefficient added to the wing when flap is deflected during landing. The technique to determine the additional flap lift coefficient is presented in Chapter 3. The parameter W_L is the aircraft landing weight. In theory, the landing weight (Equation 8.62) is equal to the takeoff weight (W_{TO}) minus fuel weight (W_f). The landing drag from Chapter 3 is

$$D = D_L = \frac{1}{2}\rho V^2 S C_{D_L} \tag{8.79}$$

where the landing drag coefficient is

$$C_{D_L} = C_{D_{o_L}} + K C_{L_L}^2 \tag{8.80}$$

Various types of flaps and their features are described in Chapter 3. This parameter depends on not only flap type, but also flap deflection. Note that the flap deflection during landing is frequently greater than that for takeoff. The flap deflection and additional lift coefficient due to flap deflection $\left(\Delta C_{L_{\text{flap}L}}\right)$ depend on atmospheric conditions (e.g., temperature) plus payload weight. For initial calculations, you may assume the following values: 0.6–0.9 for a GA aircraft, 0.8–1.2 for a large transport aircraft, and 0.3–0.9 for a fighter aircraft.

The technique to determine the aircraft zero-lift drag coefficient for landing configuration $C_{D_{oL}}$ was introduced in Chapter 3. In general, $C_{D_{oL}}$ for a general aviation aircraft is about 0.035–0.055, and for a jet transport aircraft about 0.03–0.045. The fighter aircraft General Dynamics (now Lockheed Martin) F-16 Fighting Falcon (Figure 7.6) has a $C_{D_{oL}}$ of 0.032.

The brake force is a function of the brake mechanism, brake shoe size and materials, and aircraft speed. The brake force may be loosely construed as a friction force to be a function of aircraft weight as

$$F_B = \mu_B W_L \tag{8.81}$$

where W_L is the aircraft landing weight, and μ_B is the brake coefficient. A typical value for μ_B is 0.1–0.5. A typical value for deceleration (a) during a landing ground roll is about -3 to $-6\,\text{m/s}^2$. For an aircraft with a tricycle landing gear, the deceleration creates an additional normal force on the main gear, but reduces the normal force on the nose gear. In general, a wet surface causes more friction compared to a dry surface. However, a wet surface is slippery. Thus, the landing ground roll is about 10%–20% longer when the runway is wet.

In addition, the reverse thrust is a function of the mechanism to reverse the thrust as well as the airspeed. The reverse thrust is about 20%–50% of the maximum engine thrust. It can reduce the landing ground roll up to about 50%.

The engine thrust is always zero during ground roll, except when it is used as a resisting force (i.e., thrust reversal; T_{rev}). Most large transport aircraft are equipped with a mechanism to reverse the thrust during landing. With the same technique we developed in Section 8.3 for takeoff, we can write the following equations for landing:

$$S_G = \int_{V_L}^{0} \frac{-mV}{D + \mu N + F_B + T_{\text{rev}}} dV = \int_{0}^{V_L} \frac{mV}{D + \mu N + F_B + T_{\text{rev}}} dV \tag{8.82}$$

After substitution of the required terms, and a few algebraic steps, we obtain

$$S_G = \int_{0}^{V_L} \frac{mV}{\mu mg + F_B + 0.5\rho V^2 S\left(C_{D_L} - \mu C_{L_L}\right) + T_{\text{rev}}} dV \tag{8.83}$$

This integration may be solved directly or a closed-form solution may be derived. If you need to be more accurate to determine lift and drag coefficients for landing configuration, include the ground effect to determine lift and drag coefficients in the proximity of the ground. In general, the close proximity of an aircraft to ground during takeoff and landing will increase lift coefficient and reduce drag coefficient. The proximity of the ground will straighten the flow streamlines and reduce the effect of the wing camber. The influence of the ground on the flow around wing and tail is a function of the distance between the aircraft and the ground and the geometry of the wing.

This effect is considerable when the vertical distance between the wing and the ground (height, h) is less than the wing semispan ($b/2$). In such a condition, the upwash and downwash at the wing and downwash at the horizontal tail will be affected. In addition, the ground effect will reduce the wing tip effect, so the effective wing aspect ratio is increased. Reference [84] is recommended for ground effect analysis.

Example 8.5

A jet transport aircraft with a takeoff mass of 80,000 kg has a wing area of 125 m^2. The aircraft's cruising speed at 25,000 ft (7,620 m) is 570 knots (1,055 km/h), and the brake friction coefficient is 0.2. Other characteristics of the aircraft are given:

$$K = 0.05, C_{D_{oL}} = 0.07, \Delta C_{Lf} = 0.9, V_s = 110 knot, m_f = 16{,}000\ kg, V_L = 1.2V_s$$

Reverse thrust is not employed. Determine the landing ground roll, if the runway is dry concrete.

Solution

At 7,620 m, the air density is 0.55 kg/m^3. The cruising lift coefficient is

$$C_{L_C} = \frac{2mg}{\rho V_C^2 S} = \frac{2 \times 80{,}000 \times 9.81}{0.55 \times (570 \times 0.5144)^2 \times 125} = 0.265 \tag{8.23}$$

The landing lift and drag coefficients are

$$C_{L_L} = C_{L_C} + \Delta C_{L_{\text{flap}}} = 0.265 + 0.9 = 1.165 \tag{8.78}$$

$$C_{D_L} = C_{D_{oL}} + KC_{L_L}^2 = 0.07 + 0.05 \times (0.265)^2 = 0.138 \tag{8.80}$$

The ground roll is determined through the integration method directly.

$$S_G = \int_0^{V_L} \frac{mV}{\mu mg + F_B + (1/2)\rho V^2 S(C_{D_L} - \mu C_{L_L}) + T_{\text{rev}}} dV \tag{8.83}$$

Landing mass is

$$m_L = m_{\text{TO}} - m_f = 80{,}000 - 16{,}000 = 64{,}000\,\text{kg} \tag{8.62}$$

The brake force is

$$F_B = \mu_B W_L = 0.2 \times 64{,}000 \times 9.81 = 125{,}525\,\text{N} \tag{8.81}$$

Velocity at the beginning of ground roll is

$$V_L = 1.2V_s = 1.2 \times 110 \times 0.5144 = 67.91 \ m/s \tag{8.64}$$

From Table 8.2, the friction coefficient for a concrete surface in a landing condition (i.e., brakes-on) is 0.04. We proceed as follows:

$$C_{D_L} - \mu C_{L_L} = 0.138 - (0.04 \times 1.165) = 0.091$$

$$\mu mg = 0.04 \times 64,000 \times 9.81 = 25,105 \text{ N}$$

$$\frac{1}{2}\rho S = \frac{1}{2} \times 1.225 \times 125 = 76.6 \text{ kg/m}$$

Now we can substitute all terms in the integration as

$$S_G = \int_0^{67.91} \frac{64,000 V}{25,105 + 125,525 + 76.6 \times 0.091 V^2 + 0} dV \tag{8.83}$$

Solving the integration directly yields the following result:

$$S_G = 887.7 \ m$$

To analyze the landing operation and to see the relation between landing performance (i.e., landing run) and various aircraft parameters such as aircraft weight, brake force, aand flap deflection, we need to symbolically solve the integration (8.83). Similar to the technique to treat the takeoff ground roll problem, we can develop a closed-form solution for the integration of Equation 8.83 to find S_G. This integration can be modeled as:

$$S_G = \int_0^{V_L} \frac{V}{A + BV^2} dV \tag{8.84}$$

where

$$A = \frac{1}{m}(T_{\text{rev}} + F_B) + \mu g \tag{8.85}$$

$$B = \frac{\rho S}{2m}(C_{D_L} - \mu C_{L_L}) \tag{8.86}$$

The solution for the integration of Equation 8.84 from standard mathematical handbooks [69] is obtained as:

$$S_G = \frac{1}{2B}\ln\left[\frac{A + BV_L^2}{A}\right] \tag{8.87}$$

where A and B are substituted from Equations 8.85 and 8.86. With this substitution and after some algebraic manipulation (the details are left to the reader as a practice), the final result is:

$$S_G = \frac{m}{\rho S\left(C_{D_L} - \mu C_{L_L}\right)}\ln\left[\frac{(1/m)\left(T_{\text{rev}} + F_B\right) + \mu g + \left(\rho S/2m\right)\left(C_{D_L} - \mu C_{L_L}\right)V_L^2}{(1/m)\left(T_{\text{rev}} + F_B\right) + \mu g}\right] \tag{8.88}$$

The landing speed is assumed to be $k_L V_s$, therefore

$$S_G = \frac{-m}{\rho S\left(C_{D_L} - \mu C_{L_L}\right)}\ln\left[\frac{(1/W)\left(T_{\text{rev}} + F_B\right) + \mu}{(1/W)\left(T_{\text{rev}} + F_B\right) + \mu + \left(k_L^2/C_{L_{\max}}\right)\left(C_{D_L} - \mu C_{L_L}\right)}\right] \tag{8.89}$$

A typical value for k_L is 1.1–1.3. From Equation 8.89, we can draw the following conclusions:

1. The ground roll decreases with an increase in the maximum lift coefficient $\left(C_{L_{\max}}\right)$.
2. The ground roll decreases with an increase in reverse thrust (T_{rev}).
3. The ground roll decreases with an increase in aircraft drag (C_D), such as using a spoiler, and parachute.
4. The ground roll decreases with an increase in brake force (F_B).
5. The ground roll decreases with an increase in the wing area (S).
6. The ground roll increases with an increase in touchdown velocity (V_{TD}).
7. The ground roll increases with an increase in altitude (i.e., decreasing air density, ρ).

When all required elements of Equation 8.60 are substituted, the total landing run (S_L) will be determined.

Case Study - Example 8.6

Determine the landing ground roll for the trainer aircraft Embraer EMB 312 Tucano whose features are given in Example 8.4.

$$\mu = 0.04, C_{Do_{\text{flap}_L}} = 0.009, \Delta C_{L_{\text{flap}_L}} = 0.8; \mu_B = 0.3, k_L = 1.3, C_{L_{\max}} = 1.77.$$

This aircraft has no reverse thrust (i.e., $T_{\text{rev}} = 0$), and assume that 20% of the aircraft mass is decreased due to fuel consumption.

Solution

From Table 8.2, when brake is applied, the friction coefficient (μ) for a dry asphalt runway is 0.05. From Example 8.4, we have

$$C_{Lc} = 0.364, K = 0.058, C_{D_{oc}} = 0.021, C_{D_{oLG}} = 0.007.$$

The landing lift and drag coefficients are

$$C_{L_L} = C_{Lc} + \Delta C_{L_{\text{flap}L}} = 0.364 + 0.8 = 1.164 \tag{8.78}$$

$$C_{D_{oL}} = C_{D_{oC}} + C_{D_{oflL}} + C_{D_{oLG}} = 0.021 + 0.009 + 0.007 = 0.037 \tag{3.68}$$

$$C_{D_L} = C_{D_{oL}} + KC_{L_L}^2 = 0.037 + 0.058 \times (1.164)^2 = 0.115. \tag{8.80}$$

and

$$C_{D_L} - \mu C_{L_L} = 0.115 - 0.05 \times 1.164 = 0.057$$

In this example, the ground roll is determined through the algebraic equation (closed-form solution). The landing mass is

$$m_L = m_{\text{TO}} - m_f = 2{,}550 - 0.2 \times 2{,}550 = 2{,}040\,\text{kg} \tag{8.62}$$

The brake force is

$$F_B = \mu_B W_L = 0.3 \times 2{,}040 \times 9.81 = 6{,}002\,\text{N} \tag{8.81}$$

$$S_G = \frac{-m}{\rho S\left(C_{D_L} - \mu C_{L_L}\right)} \ln\left[\frac{(1/W)\left(T_{\text{rev}} + F_B\right) + \mu}{(1/W)\left(T_{\text{rev}} + F_B\right) + \mu + \left(k_L^2 / C_{L_{\max}}\right)\left(C_{D_L} - \mu C_{L_L}\right)}\right] \tag{8.89}$$

$$S_G = \frac{2{,}040}{1.225 \times 19.4(0.057)} \ln\left[\frac{(1/20{,}005)(0 + 6{,}002) + 0.05}{(1/20{,}005)(0 + 6{,}002) + 0.05 + \left(1.3^2/1.77\right)(0.057)}\right]$$

$$= 217.4\,\text{m} \tag{8.89}$$

Note that to calculate the landing velocity, we used the landing weight, but with the same $C_{L_{\max}}$.

8.5 EFFECT OF WIND AND SLOPE ON TAKEOFF AND LANDING

Takeoff and landing were introduced as two accelerated/ground flight operations. Our preliminary performance analysis assumed that the aircraft is flying through a stationary atmosphere, and the runway has no slope. In other words, there is no wind in the atmosphere, and the runway is not on an uphill or a downhill. However, two parameters of wind and runway slope have significant effects on takeoff and landing performance. The pilot must also react to these two natural phenomena carefully. These two parameters are divided into five different influencing variables:

1. Head wind
2. Tail wind

3. Crosswind
4. Positive slope
5. Negative slope

The influence of these five variables on takeoff and landing performances is different. In this section, takeoff and landing analysis techniques, when one of these variables is present will be examined. Recall from Chapter 2 that the aerodynamic features (lift and drag) of the aircraft depend on the velocity of the air relative to the aircraft, that is, airspeed. Thus, the aerodynamics of an aircraft in the air is not a function of wind; it is a function of airspeed. In addition to airspeed, however, takeoff and landing performance is a function of ground speed. Hence, a headwind will increase lift and drag during takeoff and landing; but it will decrease takeoff run and landing run.

For this reason, airport designers and pilots employ the effect of wind in a positive way such that it improves takeoff and landing performance. For instance, airport designers select a runway location and direction that is opposite to the direction of the prevailing wind. For example, if the prevailing wind is west–east, the runway will be built in the east–west direction.

If the wind direction is not constant throughout the year, at least two runways that cross each other are built. Similarly, if the prevailing wind is southwest to northeast, the same technique is employed. San Francisco International Airport has four runways to minimize aircraft waiting period and takeoff run by utilizing an optimal takeoff direction.

Furthermore, pilots often select their takeoff and landing directions such that they experience headwind. For the purpose of safety, takeoff and landing directions are always the same. This policy will prevent collisions of airplanes traveling in opposite directions. However, in reality, in many runways or landing areas, landings must be made while the wind is blowing across, rather than parallel to, the landing direction.

A crosswind also influences takeoff and landing significantly. We can consider two components for a crosswind: headwind or tailwind and a wind that is perpendicular to the aircraft flight path (i.e., runway). We just studied the effect of tailwind and headwind, but a wind perpendicular to the runway will force the aircraft to move out of the runway (see Figure 8.18). This is very dangerous and must be avoided. One of the popular techniques to save aircraft direction in the case of crosswind is *crabbing*.

As the name implies, crabbing comes from the motion technique of a crab; that is, the direction of aircraft nose is not in the direction of the runway (intended flight path). The result of crabbing is to move in the direction of the runway, since the right triangle rule dictates that the summation of two perpendicular vectors is in the direction of the third leg (i.e., hypotenuse) of the right triangle. The fundamentals of the five items discussed are similar, so we cover only two cases of headwind and positive slope. The reader should be able to derive conclusions for the other cases from the techniques introduced here.

It should be pointed out that, if the headwind speed is considerable compared with the liftoff speed, it is not safe to take off. The reason is that right after liftoff, the airspeed will suddenly decrease to a new value: the airspeed on ground minus wind speed. This may bring the aircraft to a stall speed, or even less than that. Thus, the

calculations in this section are applicable only if the relationship between headwind speed (V_{hw}) and liftoff speed satisfies the following inequality:

$$V_{hw} \leq (k_R - 1)V_{LO} \tag{8.90}$$

For instance, when the liftoff speed (in the presence of headwind) is 20% greater than the stall speed, and the wind speed is 20% of the stall speed, the aircraft airspeed right after liftoff will be equal to the stall speed:

$$V_{LO} = 1.2\ V_s - 0.2V_s = V_s \tag{8.91}$$

This liftoff is not safe, although the calculation predicts that the aircraft will have a shorter takeoff run.

8.5.1 Effect of Headwind on Takeoff

So far, we have assumed that ground speed and airspeed are equal. In reality, this assumption is unrealistic and usually there is a wind. Wind strongly affects takeoff and landing performance (i.e., distance). In general, headwind will reduce takeoff and landing distances (including ground roll). Conversely, tailwind will increase takeoff and landing distances (including ground roll).

When an aircraft is moving on the ground (i.e., runway), and there is a headwind or a tailwind, the aircraft velocity relative to the air (i.e., airspeed) is different from that relative to the ground. We denote the aircraft velocity relative to the ground as the ground speed V_g. The relationship between airspeed and ground speed is discussed in Chapter 2, and is not repeated here. Hence, we can write

$$V = V_g + V_{hw} \tag{8.92}$$

$$V = V_g - V_{tw} \tag{8.93}$$

where V_{hw} and V_{tw} are, respectively, headwind velocity and tailwind velocity. It is clear that the airspeed at the beginning of the runway (when the aircraft is stationary) is the same as headwind or tailwind. Since the lift and drag are functions of airspeed, headwind will increase lift and drag during ground roll, while tailwind will decrease both lift and drag during ground roll. In addition, since the rolling friction is a function of lift through the normal force, headwind will decrease the rolling friction, and, conversely, tailwind will increase the friction.

Now, consider an aircraft during takeoff operation that experiences headwind as illustrated in Figure 8.19. As explained earlier, the takeoff run during this flight situation is shorter than a takeoff run without a headwind. We can modify Equations 8.24 and 8.30 to determine the takeoff ground run in the presence of headwind $\left(S_{G_{hw}}\right)$ by defining new speeds for the integration. The airspeed at the beginning of the ground segment is equal to wind speed (V_w). On the other hand, the airspeed at the end of the

ground segment is equal to rotation speed plus wind speed ($V_R + V_w$). Hence, we can express the integration as

$$S_{G_{\text{hw}}} = \int_{V_W}^{V_R+V_W} \frac{m(V - V_w)}{T - \mu mg - (1/2)\rho V^2 S\left(C_{D_{\text{TO}}} - \mu C_{L_{\text{TO}}}\right)} dV \tag{8.94}$$

In the transition segment ($S_{T_{\text{hw}}}$), the rotation (ground) speed is not affected by the wind speed. So

$$S_{T_{\text{hw}}} = V_R T_R \tag{8.95}$$

where V_R denotes the transition or rotation speed, and T_R is the rotation time (from Table 8.3). By referring to Figure 8.19, the airborne segment (distance from the end of the rotation process until the obstacle is cleared) is

$$S_{A_{\text{hw}}} = S_A \frac{(V_{\text{LO}} - V_{\text{hw}})}{V_{\text{LO}}} \tag{8.96}$$

Therefore, the total takeoff distance, when headwind is blowing, is determined from the summation of three segments:

$$S_{\text{TO}_{\text{hw}}} = S_{G_{\text{hw}}} + S_{T_{\text{hw}}} + S_{A_{\text{hw}}} \tag{8.97}$$

Please note that the subscript hw refers to headwind. When there is tailwind, Equations 8.94–8.97 are also utilized, while the value for V_{hw} is negative. Therefore, headwind will reduce the takeoff distance, while tailwind will increase the takeoff distance.

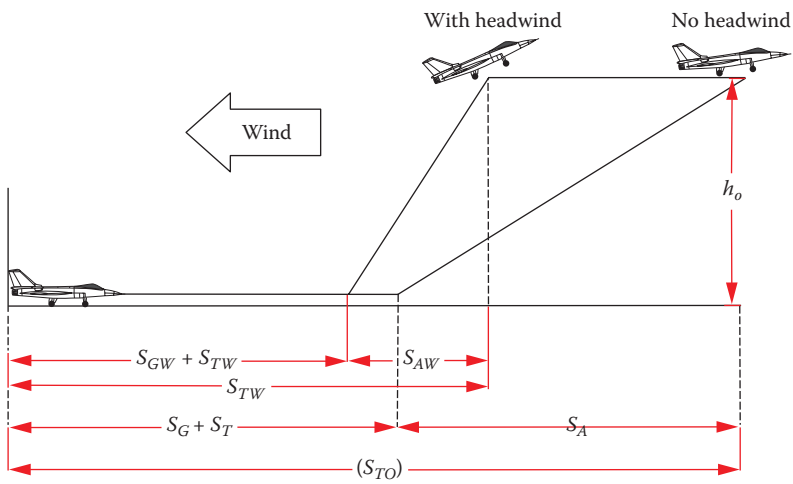

FIGURE 8.19 An aircraft during takeoff when headwind is blowing.

Similarly, the same logic can be applied to landing performance analysis. The landing ground roll in the presence of a head wind is governed by the modifying Equation 8.83 and changing the integration limits. This will result in the following integration:

$$S_G = \int_{V_{hw}}^{V_R+V_{hw}} \frac{m(V-V_w)}{\mu mg + F_B + (1/2)\rho V^2 S(C_{D_L} - \mu C_{L_L}) + T_{rev}} dV \tag{8.98}$$

This equation implies that the headwind will reduce the landing distance, while the tailwind will increase the landing distance.

8.5.2 Effect of Slope on Takeoff

Many cities, and, consequently, airports are located on mountainous or non-flat grounds. Thus, their runways have a positive or negative slope. When the runway has a positive slope, the aircraft has to climb during takeoff and landing operations. A runway slope functions similarly to a climb/descent angle. To improve takeoff performance, it is recommended to take off in the downhill direction, but land in the uphill direction. This technique will reduce takeoff and landing distances.

In a sloped runway, a component of aircraft weight will contribute to the acceleration. In a runway with a positive slope (uphill), the component of weight along the runway will reduce aircraft acceleration, so it makes the runway longer (Figure 8.20).

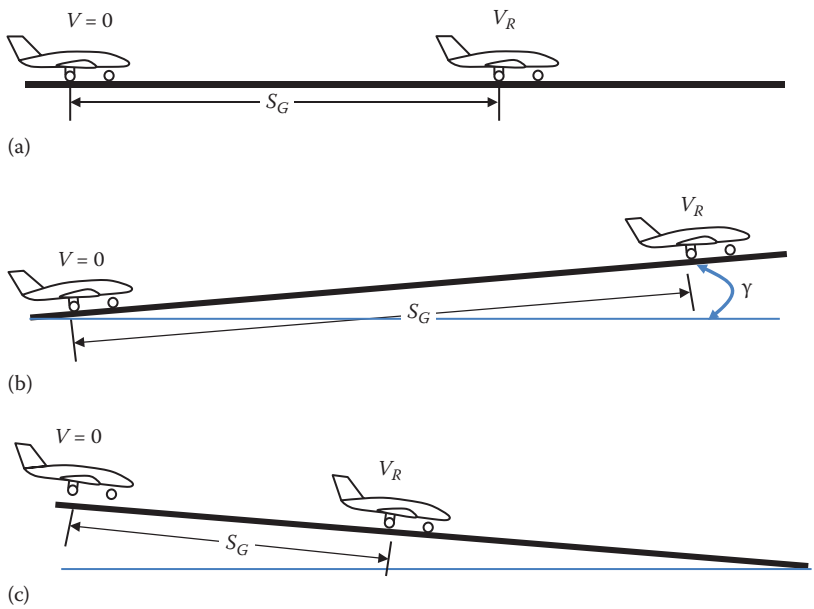

FIGURE 8.20 Effect of slope of takeoff ground roll: (a) flat runway, (b) positive slope (longer ground roll), and (c) negative slope (shorter ground roll).

On the contrary, in a runway with a negative slope (downhill), the component of weight along the runway will increase aircraft acceleration, so it makes the runway shorter.

The slope angle (γ) can be directly applied to the takeoff governing equations by adding the term "W sin(γ)". Here, we examine only the equations for the takeoff ground segment (S_{G_s}). Referring to Figure 8.21, and using Newton's second law, the following equation can be derived for this accelerated motion (with a positive slope of γ):

$$T - D - W\sin\gamma - \mu\left(W\cos\gamma - L\right) = ma \tag{8.99}$$

In contrast, when there is a negative slope (downhill), the sum of the forces along the runway is equal to aircraft mass multiplied by the acceleration:

$$T - D + W\sin\gamma - \mu\left(W\cos\gamma - L\right) = ma \tag{8.100}$$

After a few algebraic steps, similar to what has been performed in Section 8.2, we can develop the following expressions:

$$S_{G_s} = \int_0^{V_R} \frac{mV}{T - mg\sin\gamma - \mu mg\cos\gamma - (1/2)\rho V^2 S\left(C_{D_{TO}} - \mu C_{L_{TO}}\right)} dV \quad \text{(positive slope)} \tag{8.101}$$

$$S_{G_s} = \int_0^{V_R} \frac{mV}{T + mg\sin\gamma - \mu mg\cos\gamma - (1/2)\rho V^2 S\left(C_{D_{TO}} - \mu C_{L_{TO}}\right)} dV \quad \text{(negative slope)} \tag{8.102}$$

Equation 8.101 is used (with "$-mg$ sin(γ)") when there is a positive slope (uphill), while Equation 8.102 is utilized (with "$+mg$ sin(γ)") when there is a negative slope

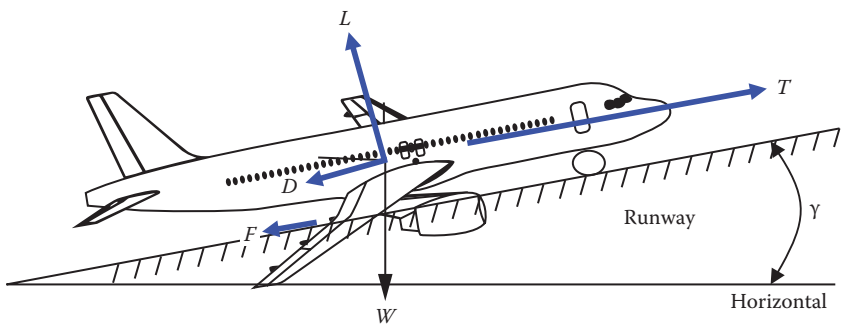

FIGURE 8.21 A runway with a positive slope.

(downhill). Solution of this integration yields the ground run for a runway when it has a positive/negative slope.

Case Study - Example 8.7

A jet transport aircraft similar to Boeing 737 with a takeoff mass of 50,000 kg has a wing area of 120 m^2. Other characteristics of the aircraft are as follows:

$$T_{\max} = 130\,\text{kN}, C_{L_C} = 0.2; K = 0.04, C_{D_{o\text{TO}}} = 0.05,$$

$$\Delta C_{L_{\text{flap}}} = 0.3, V_s = 110\,\text{knot}\,(203.7\,\text{km/h}), V_R = 1.2V_s.$$

Determine the takeoff ground roll for a dry concrete runway in these three cases:

a. Runway is flat with no slope.
b. Runway has a positive slope (uphill) of 5°.
c. Runway has a negative slope (downhill) of 5°.

Solution

The takeoff lift and drag coefficients are

$$C_{L_{\text{TO}}} = C_{L_C} + \Delta C_{L_{\text{flap}}} = 0.2 + 0.3 = 0.5 \tag{8.20}$$

$$C_{D_{\text{TO}}} = C_{D_{o\text{TO}}} + KC_{L_{\text{TO}}}^2 = 0.05 + 0.04 \times (0.5)^2 = 0.06 \tag{8.22}$$

a. *No slope:*
The ground roll is determined through the integration

$$S_G = \int_0^{V_R} \frac{mV}{T - \mu mg - (1/2)\rho V^2 S\left(C_{D_{\text{TO}}} - \mu C_{L_{\text{TO}}}\right)} dV \tag{8.24}$$

From Table 8.2, the friction coefficient for a concrete surface is 0.04. We proceed as follows:

$$C_{D_{\text{TO}}} - \mu C_{L_{\text{TO}}} = 0.06 - (0.04 \times 0.5) = 0.04,$$

$$V_R = 1.2V_s = 1.2 \times 110 \times 0.5144 = 67.91\,\text{m/s},$$

$$\mu mg = 0.04 \times 50{,}000 \times 9.81 = 19{,}613\,\text{N}.$$

$$\frac{1}{2}\rho S = \frac{1}{2} \times 1.225 \times 120 = 73.53\,\text{kg/m},$$

$$T = 0.9T_{\max} = 0.9 \times 130{,}000 = 117{,}000\,\text{N}.$$

Now we can substitute all terms in the integration as

$$S_G = \int_0^{67.91} \frac{50{,}000 V dV}{117{,}000 - 19{,}613 - 73.53V^2(0.04)} \tag{8.24}$$

Solving the integration directly yields the following result:

$$S_G = 1{,}275\,\text{m}$$

b. Positive *slope (uphill):*
The ground roll in the presence of a positive slope (uphill) is determined through the integration:

$$S_{G_s} = \int_0^{V_R} \frac{mV}{T - mg\sin\gamma - \mu mg\cos\gamma - (1/2)\rho V^2 S\left(C_{D_{\text{TO}}} - \mu C_{L_{\text{TO}}}\right)} dV \tag{8.101}$$

or

$$S_G = \int_0^{67.91} \frac{50{,}000 V dV}{117{,}000 - 50{,}000 \times 9.81 \times \sin(5) - 19{,}613\cos(5) - 73.53V^2(0.04)} \tag{8.101}$$

Solving the integration directly yields the following result:

$$S_G = 2{,}421\,\text{m}$$

c. Negative *slope (downhill):*
The ground roll in the presence of a negative slope (downhill) is determined through the integration

$$S_{G_s} = \int_0^{V_R} \frac{mV}{T + mg\sin\gamma - \mu mg\cos\gamma - (1/2)\rho V^2 S\left(C_{D_{\text{TO}}} - \mu C_{L_{\text{TO}}}\right)} dV \tag{8.102}$$

or

$$S_G = \int_0^{67.91} \frac{50{,}000 V dV}{117{,}000 + 50{,}000 \times 9.81 \times \sin(5) - 19{,}613\cos(5) - 73.53V^2(0.04)}$$

Solving the integration directly yields the following result:

$$S_G = 865\,\text{m}.$$

It is interesting to note that a positive slope of 5° will cause a 90% increase in the ground roll, while a negative slope of 5° will cause a 32% decrease in the ground roll.

8.6 LAUNCH

In general, there are multiple techniques for launching an unmanned aerial vehicle (UAV), including conventional takeoff and employing a mechanical ramp launcher. In this section, only the performance of a UAV, when catapulted via a ramp launcher is presented. For an UAV without landing gear, the takeoff will be conducted via a launch operation with the application of a ramp launcher.

The launch process is basically a linear accelerated motion, where the UAV is accelerating along the ramp until a safe launch speed is achieved. The UAV is frequently pushed forward by an external force added to the UAV engine thrust. The external force is provided by the launcher via a specific mechanism. The UAV engine must be at its maximum power/thrust since the UAV must continue the flight after being launched.

Figure 8.22 shows the launch forces and parameters for a UAV launch operation on a launcher with a launch angle of θ. The launch angle is often close to the UAV maximum climb angle. The applied force, F is the sum of an external force and the engine thrust. The *x*-axis is selected to be along the UAV motion path, and the *z*-axis is perpendicular to the *x*-axis. Thus, the UAV weight has two components, $W\cos(\theta)$ along the *z*-axis, and $W\sin(\theta)$ along the *x*-axis (indeed, opposite to the *x*-axis).

From Newton's second law (Equation 2.15), along the launcher ramp, the sum of the forces along the *x*-axis creates the acceleration:

$$\sum F_x = ma \tag{8.103}$$

where *m* denotes the UAV mass and "*a*" represents the linear acceleration. Three main forces are active during a launch operation: (1) Applied force (*F*), (2) UAV weigh (*W*), and friction force (F_f) between UAV cart and the launcher rails. However, if you would need to be more accurate, include UAV lift (*L*) and drag (*D*) forces. However, due to low speed, both aerodynamic forces may be neglected. The UAV-Ramp friction force (F_f) is:

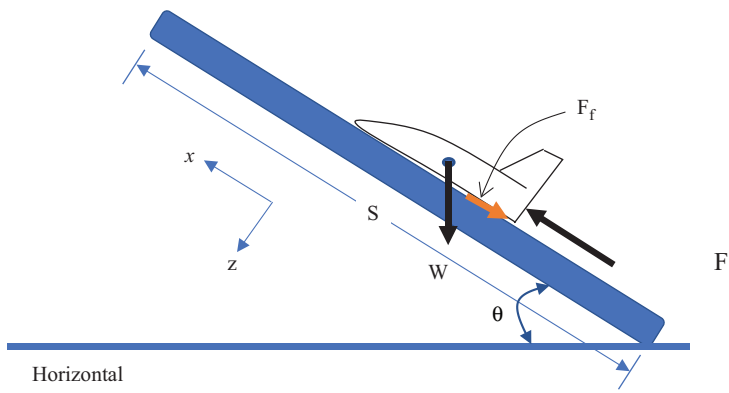

FIGURE 8.22 Launch forces and parameters during a launch.

$$F_f = \mu N = \mu(W - L_{\text{TO}}) \tag{8.104}$$

where μ is the friction coefficient between UAV legs (or cart) and the rails, and N denotes the normal force on the rail. Typical values for friction coefficient between two metallic surfaces range from 0.1 to 0.2. Ignoring the UAV lift, the normal force is the component of the UAV weight perpendicular to the rails:

$$N = W\cos(\theta) \tag{8.105}$$

From theory of dynamics, when a moving object with an initial velocity of V_1 accelerates to a new velocity of V_2, the distance (S) covered is governed by the following equation:

$$V_2^2 - V_1^2 = 2aS \tag{8.106}$$

Here, for a launcher, the distance S is the launcher stroke. The initial velocity at launch is often zero ($V_1 = 0$). The launch force must be strong enough so that the UAV at the end of launch achieves a velocity which is at least 10% greater than the UAV stall speed.

PROBLEMS

Note: Assume ISA flight conditions, unless otherwise stated.

8.1 A transport aircraft that stands at the beginning of a runway moves at a constant acceleration. If the speed reaches 94 knots (174 km/h) after traveling 1,700 m, what is the aircraft acceleration in terms of g?

8.2 Calculate the friction force of an aircraft with a mass of 120,000 kg on a dry concrete runway at the beginning of runway for a takeoff.

8.3 The utility aircraft Falcon with two turbofan engines has the following characteristics:

$$m_{\text{TO}} = 8{,}755\,\text{kg},\ S = 24.1\,\text{m}^2,\ T = 2\times 14.4\,\text{kN},$$

$$\Delta C_{L_{f\text{TO}}} = 0.8,\ C_{D_{o\text{TO}}} = 0.044,\ C_{L_{\max}} = 2.2,\ K = 0.052.$$

The aircraft cruising speed at 25,000 ft (7,620 m) is 492 knots (911 km/h). Determine the ground roll if the runway is dry asphalt and the airport is located at 3,000 ft altitude.

8.4 Solve Problem 8.3 under ISA + 15 flight condition.

8.5 Solve Problem 8.3 under ISA − 15 flight condition.

8.6 Assume the runway in Problem 8.3 has a positive slope of 3°. Determine the takeoff ground roll.

8.7 Assume the runway in Problem 8.3 has a negative slope of 3°. Determine the ground roll.

8.8 Consider the aircraft in Problem 8.3. Assume there is tailwind with a speed of 15 knots. Calculate the takeoff ground run.

8.9 Consider the aircraft in Problem 8.3. Assume there is headwind with a speed of 15 knots. Calculate the takeoff run.

8.10 Consider the aircraft in Problem 8.3. Assume there is headwind with a speed of 15 knots and the runway in Problem 8.3 has a positive slope of 3°. Calculate the takeoff ground run.

8.11 Consider the aircraft in Problem 8.3. Assume there is tailwind with a speed of 15 knots and the runway in Problem 8.3 has a negative slope of 3°. Calculate the takeoff run.

8.12 A navy fighter aircraft with two turbofan engines has a cruising speed of Mach 2.4 at 15,000 ft (4,572 m) and the following characteristics:

$$m_{\text{TO}} = 33{,}724\,\text{kg},\ S = 52.5\,\text{m}^2,\ T = 2 \times 93\,\text{kN},$$

$$\Delta C_{L_{f\text{TO}}} = 1.1,\ C_{D_{o\text{TO}}} = 0.038,\ C_{L_{\max}} = 2.4,\ \text{AR} = 7.3,\ e = 0.76.$$

To rotate the aircraft for takeoff, the pilot deflects elevators as soon as the airspeed is $1.1V_s$. How long did the aircraft have to travel before this speed was reached? Assume dry concrete runway.

8.13 A transport aircraft with two piston prop engines (with variable-pitch propellers) has a cruising speed of 260 knots (481.5 km/h) at 20,000 ft (6,096 m) and the following characteristics:

$$m_{\text{TO}} = 29{,}000\,\text{kg},\ S = 135\,\text{m}^2,\ P = 2 \times 1{,}864\,\text{kW},$$

$$\Delta C_{L_{f\text{TO}}} = 0.6,\ C_{D_{o\text{TO}}} = 0.053,\ C_{L_{\max}} = 1.8,\ K = 0.048,\ \eta_P = 0.7.$$

Determine the takeoff ground roll if the runway is on short grass but the airport is located at 1,500 m altitude.

8.14 A light aircraft with two turboprop engines (fixed-pitch propeller) has a cruising speed of 400 knots (741 km/h) at 20,000 ft (6,096 m) and the following characteristics:

$$m_{\text{TO}} = 4{,}400\,\text{kg},\ S = 26\,\text{m}^2,\ P = 2 \times 1{,}019\,\text{kW},\ \Delta C_{L_{fL}} = 0.7,\ C_{D_{oL}} = 0.06,$$

$$V_s = 55\,\text{knot}\,(101.9\,\text{km/h}),\ K = 0.053,\ \eta_P = 0.65,\ m_L = 0.8\,m_{\text{TO}}.$$

The aircraft must be able to land on a runway (dry concrete) with a length of 600 m. How much must be the brake force if the aircraft is touching down with a speed of 1.3 multiplied by stall speed?

8.15 Consider the aircraft in Problem 8.3. The aircraft is in a one-engine-inoperative situation, while it has traveled 400 m from the beginning of the runway.

a. Determine the aircraft speed at this moment.
b. How long has passed at this moment?
c. If the total length of the runway is 2,500 m, will this aircraft be able to finish the takeoff operation safely? If so, how long will the takeoff run be?
d. If the pilot decides to abort the takeoff, how long will the aircraft travel on the runway? Assume the brake friction coefficient is 0.3.

8.16 A business jet aircraft cruising speed at 25,000 ft (7,620 m) is 500 knots (926 km/h), and the relation between engine thrust (in lb) and airspeed (in fps) is as follows:

$$T = 0.1V^2 - 90V + 9{,}200.$$

Other characteristics are as follows:

$$m_{\mathrm{TO}} = 7{,}000\,\mathrm{kg},\ S = 20\,\mathrm{m}^2,\ T = 2 \times 12\,\mathrm{kN},\ \Delta C_{L_{f\mathrm{TO}}} = 0.4,$$

$$C_{D_{o\mathrm{TO}}} = 0.05,\ C_{L_{\max}} = 2,\ K = 0.045.$$

Determine the takeoff ground roll if the runway is wet concrete.

8.17 Consider the aircraft in Problem 8.3. Plot the variations of lift, drag, and speed as a function of the runway length (just for the ground roll part; i.e., 976 m).

8.18 Determine the takeoff transition segment of the aircraft in Problem 8.3.

8.19 Determine the takeoff airborne segment of the aircraft in Problem 8.3.

8.20 Consider the aircraft in Problem 8.13. There are several trees with a height of 10 m at a distance of 3,200 m in front of the runway. One day, the aircraft lost one engine, just at the liftoff on dry asphalt. Can this aircraft take off and safely clear these trees in this situation?

8.21 Determine the minimum controllable speed of the aircraft in Problem 8.14 if each engine is located at 5 m from fuselage centerline, and the vertical tail maximum lift coefficient is 1.2, and its aerodynamic center is located 14 m behind aircraft center of gravity. The vertical tail planform area is ¼ of wing reference area.

8.22 You are required to design a braking system via cable to land a fighter on a navy ship. The requirement is to stop the fighter in a 300 m runway when the fighter touches down on the deck with a speed of 180 knots (333.3 km/h). Determine the force (i.e., acceleration) that is applied to the pilot in terms of *g*.

8.23 Derive a closed-form solution for the integration in Equation 8.82.

8.24 Derive an equation for the minimum control speed for a prop-driven aircraft (similar to Equation 8.5).

8.25 A jet aircraft with two turbofan engines has the following features:

$$m_{\mathrm{TO}} = 14{,}500\,\mathrm{kg},\ S = 92\,\mathrm{m}^2,\ b = 34\,\mathrm{m},\ C_{L_{\max}} = 1.7,\ e = 0.85,$$

$$C_{D_{\mathrm{oclean}}} = 0.019,\ C_{D_{o\mathrm{LG}}} = 0.01,\ C_{D_{o\mathrm{flap}}} = 0.007,\ \Delta C_{L_{\mathrm{flap}}} = 0.4.$$

The aircraft cruise speed at 32,000 ft (9,753 m) is 280 KTAS (518.5 km/h). Determine the sea-level maximum engine thrust if the ground roll on a dry concrete runway at 6,000 ft (1,829 m) altitude is 1,200 m.

8.26 Determine the airborne segment of the takeoff distance of the following commercial jet (turbofan engine) transport aircraft. The airport is located at an altitude of 6,000 ft ISA condition.

$$S = 175\,\text{ft}^2,\ W_{\text{TO}} = 4{,}3001\text{b},\ C_{L_{\max}} = 1.8,$$

$$C_{D_{o\text{TO}}} = 0.035,\ K = 0.07,\ T_{\max} = 1{,}2601\text{bf}.$$

8.27 Determine the airborne segment of the takeoff distance of the following GA piston engine prop-driven (fixed pitch) aircraft. The airport is located at an altitude of 3,000 ft (914.4 m) ISA condition. Assume the runway is dry asphalt.

$$S = 20\,\text{m}^2,\ m_{\text{TO}} = 3{,}000\,\text{kg},\ P_{\max} = 522\,\text{kW},\ V_s = 70\,\text{knot},$$

$$C_{D_{\text{oc}}} = 0.023,\ C_{D_{o\text{TO}}} = 0.003,\ C_{D_{o\text{LG}}} = 0.006,\ \text{AR} = 9,\ e = 0.8.$$

8.28 A jet trainer aircraft has the following features:

$$C_{L_{\max}} = 1.9,\ m_{\text{TO}} = 4{,}240\,\text{kg},\ S = 32\,\text{m}^2,\ C_{D_{o\text{clean}}} = 0.03,\ C_{D_{o\text{LG}}} = 0.01,$$

$$C_{D_{o\text{flap}}} = 0.007,\ (L/D)_{\max} = 9.4,\ \Delta C_{D_{o\text{fTO}}} = 0.4,\ T_{\max\,\text{SL}} = 9{,}300\,\text{N}.$$

How much is the takeoff ground roll on a dry concrete runway that is located at the elevation of 4,000 ft (1,219 m) ISA condition? The aircraft cruising speed at 22,000 ft (6,705 m) is 170 knots (315 km/h).

8.29 Consider the aircraft in Problem 8.3 is in a situation where the ground roll is required to be 20% shorter. Determine how much the aircraft mass should be reduced to fulfill this requirement.

8.30 Start with Equation 8.32 and derive Equation 8.36 (i.e., the total engine thrust required to satisfy a given ground roll requirement, T_{TO}).

8.31 Begin with Equation 8.30 and derive the equation for ground roll (i.e., Equation 8.32).

8.32 Begin with Equation 8.98 and derive a closed-form solution for the integral equation for ground roll when headwind is present (Hint: Use the general mathematical solution in Equation 8.28).

8.33 Determine the landing ground roll for a jet transport aircraft similar to Airbus A-300 for a dry concrete runway. Other aircraft features are as follows:

$$m_{\text{TO}} = 160{,}000\,\text{kg};\ V_C = 1{,}019\,\text{km/h}\left(\text{at}\,10{,}670\,\text{m}\right),\ S = 260\,\text{m}^2,$$

$$C_{D_{o_{fL}}} = 0.01,\ \Delta C_{L_{fL}} = 1.2,\ \mu_B = 0.35,\ k_L = 1.3,\ C_{L_{\max}} = 2.1,\ K = 0.04,$$

$$C_{D_{oC}} = 0.018,\ C_{D_{o\text{LG}}} = 0.007,\ T_{\max} = 2 \times 250\,\text{kN}.$$

This aircraft has a reverse thrust equivalent to 20% of the maximum thrust, and assume up to landing 30% of the aircraft mass is decreased due to fuel consumption. The airport is at sea level with standard conditions.

8.34 Determine the landing ground roll for the aircraft in Problem 8.33. The airport is located at 8,000 ft (2,438 m) altitude with ISA + 20 flight condition.

8.35 Determine the landing ground roll for a light piston prop GA aircraft with the following features:

$$C_{L_{\max}} = 1.9, m_{\text{TO}} = 1{,}000\,\text{kg}, S = 10\,\text{m}^2, C_{D_{o\text{clean}}} = 0.025,$$

$$C_{D_{o\text{LG}}} = 0.007, C_{D_{o\text{flap}}} = 0.005, \text{AR} = 8, \Delta C_{L_{fL}} = 0.6,$$

$$C_{L_C} = 0.3, e = 0.8; \mu = 0.037, \mu_B = 0.35, k_L = 1.2.$$

This aircraft has no reverse thrust (i.e., $T_{\text{rev}} = 0$), and assume up to landing 20% of the aircraft mass is decreased due to fuel consumption.

8.36 Determine the landing ground roll for the aircraft in Problem 8.35. The airport is located at 3,000 ft (914 m) altitude with ISA − 15 flight condition.

8.37 A jet transport aircraft similar to Airbus 340-300 (Figure 1.8b) with a takeoff mass of 277,000 kg has a wing area of 360 m^2. Other characteristics of the aircraft are as follows:

$$T_{\max} = 4 \times 100\,\text{kN}, C_{L_C} = 0.3; K = 0.032, C_{D_{o\text{TO}}} = 0.03,$$

$$\Delta C_{L_f} = 0.4, V_S = 110\,\text{knot}\,(203.7\,\text{km/h}), V_R = 1.2V_s.$$

Determine the takeoff ground roll for a dry concrete runway for three cases:

a. Runway is flat with no slope.
b. Runway has a positive slope (uphill) of 3°.
c. Runway has a negative slope (downhill) of 3°.

8.38 The aircraft in Problem 8.37 utilizes two rocket engines (in addition to its installed engines) for an emergency takeoff, each generating 40 kN of thrust. Calculate the ground roll for this situation; the runway is flat with no slope.

8.39 A twin turbofan engine business aircraft with a takeoff mass of 30,000 kg and a wing area of 100 m^2 has the following characteristics:

$$b = 25\,\text{m}, C_{D_{of\_\text{TO}}} = 0.003, C_{D_{o\text{LG}}} = 0.008, \Delta C_{L_f} = 0.8, e = 0.9,$$

$$C_{L_C} = 0.24, C_{D_o} = 0.022.$$

Determine the total engine thrust required for a takeoff ground roll of 2,000 m at sea level for a runway with a friction coefficient of 0.05.

8.40 A jet aircraft with a takeoff mass of 10,000 kg and a stall speed of 80 knots (148.2 km/h) has the following characteristics:

$$\text{AR} = 12, C_{D_{o_{f\text{TO}}}} = 0.004, C_{D_{o\text{LG}}} = 0.007, \Delta C_{L_f} = 0.6, e = 0.86,$$

$$C_{L_{\max}} = 1.8, C_{D_o} = 0.019, V_c = 904\,\text{km/h}\left(\text{at } 7{,}600\,\text{m}\right).$$

Determine the total engine thrust required for a takeoff ground roll of 1,200 m at sea level for a runway with a friction coefficient of 0.04.

8.41 A small UAV with a mass of 120 kg is launched on a rail launcher with a length of 4.2 m. The speed at the end of launch (i.e., launch velocity) is 10 m/s. Ignore friction and drag.

a. Determine the UAV acceleration during launch.
b. Calculate the launch time.
c. What force is applied to the UAV during the launch?

8.42 A business aircraft with two turbofan engines has the following features:

$m_{TO} = 14{,}000\,\text{kg}$, $S = 90\,\text{m}^2$, $b = 35\,\text{m}$, $C_{Lmax} = 2.1$, $e = 0.85$,

$C_{Doclean} = 0.018$, $C_{DoLG} = 0.012$, $C_{Doflap} = 0.006$, $\Delta C_{Lflap} = 0.6$

The aircraft cruise speed at 32,000 ft is 320 KTAS. The ground roll on a dry concrete runway at 6,000 ft altitude is 1,200 m. Determine the sea level maximum engine thrust.

9 Turn Performance and Flight Maneuvers

9.1 INTRODUCTION

In Chapters 5–8, major flight operations, including takeoff, climb, cruise, descend, and landing, were presented. In addition, basic performance parameters, such as range, endurance, rate of climb, takeoff run, and ceiling, were discussed. These are the primary operations during a typical flight, but there are other flight operations such as turn and maneuver that are crucial to the aircraft performance. The maneuver power is a very significant criterion in the aircraft performance evaluation; thus, this chapter is devoted to various maneuvers and non-simple flight operations. This chapter presents techniques to analyze the performance of an aircraft in maneuvering flights using both prop-driven and jet engine(s).

Of primary interest in the analysis of aircraft performance is the determination of the aircraft maneuverability. Without doubt, missiles and fighters are the most maneuverable aircraft due to their specific missions in aerial attacks/fights. A fighter can survive a fighting area and return to its base safely if it has higher maneuver power (highest performance). Thus, the world market is witnessing new fighters (such as Lockheed Martin F-35 Lightning (Figure 5.5) each year with new capabilities. Each new fighter is often claimed to have particular/unique features, and no other aircraft is able to defeat it. Each year, various countries show their new achievements in fighter technologies and amaze their rivals.

Maneuver, in literature, means every non-simple motion. In aeronautics, maneuver refers to a transfer from a level, constant-speed, constant-altitude, and straight-line flight to an accelerated flight, which involves at least one turn/rotation. In other words, any flight operation that includes at least one rotation around one of its three body axes (x, y, or z) is called a maneuver. Figure 9.1 illustrates the aircraft axis system and three body axes.

These axes are perpendicular to each other (i.e., orthogonal), and their origin is the aircraft center of gravity (cg). The rotation about the x-axis (fuselage centerline) is referred to as "roll"; the rotation about the y-axis (wing imaginary centerline) is referred to as "pitch"; and the rotation about the z-axis (perpendicular to x–y plane) is referred to as "yaw". In this chapter, we select the body-fixed (or simply body) orthogonal axis system, which implies the axes are fixed on the aircraft body. Furthermore, the aircraft axes (and relevant plane) will rotate with the rotation of the aircraft body.

A flight maneuver consists of at least one rotation (roll, pitch, or yaw). These rotations are created by using control surfaces; the conventional ones are ailerons, elevator, and rudder. These control surfaces are similar to flaps and are located at the trailing edge of the wing, horizontal tail, and vertical tail, respectively (see Figure 9.1).

DOI: 10.1201/9781003279068-9

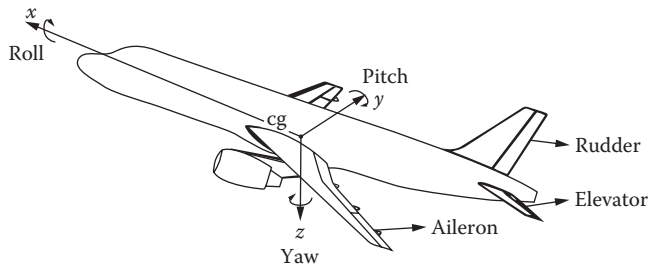

FIGURE 9.1 Aircraft axis system and aircraft control surfaces.

Most flight maneuvers have a combination of angular rotations. Figure 9.2 illustrates an attractive maneuver show that is performed by two groups of aircraft: (a) British Aerospace Hawk and (b) Mikoyan-Gurevich MiG-29.

In principle, the evaluation of maneuver power of an aircraft is based on the aircraft rotational acceleration/speed around its axes. The more powerful the engine and the easier to control an aircraft, the higher the aircraft performance will be in a maneuver. Besides engine power/thrust, the only way for an aircraft to escape from a surface-to-air or air-to-air missile is by having a very high rotational speed (higher than that of the missile) such as roll. In the case of a fighter, when it is chased by an enemy missile, if the fighter is capable of turning faster than the missile, it can survive, and then it will be able to shoot the missile down.

In general, aircraft are divided into the following four major categories:

1. Normal or non-maneuverable
2. Utility or semi-maneuverable
3. Maneuverable or aerobatic or acrobatic
4. Highly maneuverable

Standards, such as Federal Aviation Regulations Part 23, FAR 23 [87], describe the features of the first three categories. Military Standards such as MIL-STD define the requirements of highly maneuverable aircraft (e.g., fighters). With the advent of advanced technology, the maneuvering capabilities of highly maneuverable aircraft are constantly progressing. If two bodily and mentally similar fighter pilots are supposed to compete, the pilot whose aircraft is more maneuverable will win. In the aforementioned four categories, the following are the three main differences:

1. acceleration/speed of rotation about the axis
2. engine power/thrust
3. strength of the aircraft structure

In the aircraft maneuver analysis, these three parameters will be taken into account. Some basic maneuvers [81] are: (1) steep turns, (2) steep spiral, (3) chandelle, (4) lazy eight, (5) spin, (6) dive, and (7) inverted flight.

(a)

(b)

FIGURE 9.2 A spectacular maneuver was shown by a group of aircraft. (a) Four acrobatic British Aerospace Hawk aircraft. (Courtesy of Steve Dreier.) (b) Four Mikoyan-Gurevich MiG-29 jet fighters. (Courtesy of Georgi Petkov.)

The simplest and the most basic maneuver is the level turn. A turning flight can be horizontal (i.e., level), vertical, or with a slope. In any turn, the aircraft is flying around an imaginary center with a circular path and a radius of R. If the turn radius is constant, the turn is referred to as a coordinated turn. A coordinated turn is initially initiated with a roll that creates a bank angle. In a turning performance analysis, flight parameters such as turn radius, bank angle, turn rate, load factor (this will be defined later), and aircraft forward velocity are determined.

In this chapter, flight parameters that influence the turn and maneuver are defined and a number of flight maneuvers are described. The governing equations for a turning flight and various maneuvers will be derived. Since turn is a primary constituent of most maneuvers, the turn performance will be presented with more details. Another important section of this chapter is to introduce maneuverability and the calculation of aircraft performance in maneuvering flight, namely, fastest turn and tightest turn.

The jet aircraft and prop-driven aircraft are discussed separately. Furthermore, two important vertical maneuvers (pull-up and push-over) are described, and their equations of motion are derived. The maximum loads on an aircraft's structure generally occur when the aircraft is undergoing some form of acceleration, such as in maneuvers. During a maneuver, the forces that are applied to both the aircraft structure and the pilot are introduced. The calculation of the load factor and its significance will be presented. The last section of this chapter is devoted to how to plot the flight envelope (*V-n* diagram) which is very crucial to aircraft structural design.

9.2 FUNDAMENTALS OF TURNING FLIGHT

The turn with a low bank angle (i.e., shallow turn) is considered as the simplest flight maneuver. The bank angle is defined as the angle between the body *xy* plane and the horizontal (i.e., from the front view). In a turn, the aircraft will fly through all or part of a circle. The circle or loop could be horizontal, vertical, or at an angle relative to the horizontal. In this section, we begin our analysis with the simplest case; that is, the horizontal (i.e., level) turn. In order for an aircraft to have a coordinated turn, that is, to maintain a constant radius, it is necessary to have the following two rotations: (1) rotation about the *x*-axis (roll) and (2) rotation about the *z*-axis (yaw).

In this situation, one half of the wing (say the right side) moves down and the other half of the wing (say the left side) moves up, and thus, the aircraft begins to turn around an imaginary center. On the other hand, in order for an aircraft to maintain the altitude, the third rotation is also needed, that is, rotation about the *y*-axis (pitch). This will compensate the loss of lift through an increase in the aircraft angle of attack (α). The detail and reasons for these three rotations will be explained later in this chapter. A turn is made by banking the wings in the direction of the desired turn. A turn is considered more efficient when it yields a higher turn rate and a lower turn radius.

9.2.1 Governing Equations

In a level turn, the following six forces are present: (1) lift (L), (2) weight (W), (3) thrust (T), (4) centrifugal force (F_C), (5) drag (D), and (6) aerodynamic side force (F_y). An aircraft in a level-turning flight is depicted in Figure 9.3. When the turn radius and turn rate are constant, the turn is referred to as a *coordinated turn*. Thus, a coordinated turn features no slip and no skid. Thus, the aircraft is traveling in a circular path with a constant radius (R) and a constant airspeed (V). In order for a turn to be coordinated, the aircraft should rotate about the *x*-axis (roll) to produce a bank angle; ϕ. Consequently, the lift force has the following two components:

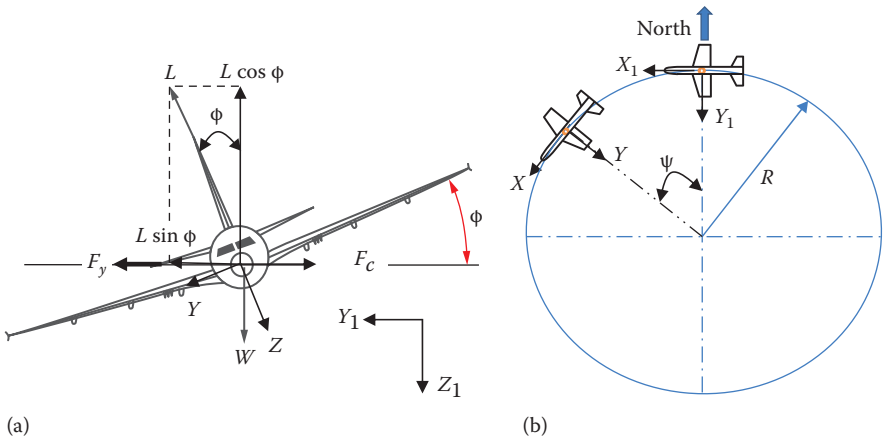

FIGURE 9.3 An aircraft in a level turning flight: (a) front and (b) top view.

(1) horizontal component (L sin ϕ) and (2) vertical component (L cos ϕ). When the aircraft banks, and there is no side force, the horizontal component of the lift force should balance the centrifugal force.

The yaw angle (Ψ) is usually determined by comparing the new instantaneous direction with the initial (or reference) direction. It is customary that the yaw angle orientation is compared with the north direction; so, the north is the reference direction. In this case, the yaw angle is called heading. The material in this section is about a coordinated steady-state level turn. The aircraft is flying with an angle of attack, α (not shown in the figure).

Since the aircraft has a constant airspeed and a constant radius, the applied and resultant forces are in equilibrium. Thus, in a level-coordinated turn, the sum of the forces along each three axis is zero. Thus, we can write the following equations:

$$\sum F_x = 0 \Rightarrow T\cos\alpha = D \tag{9.1}$$

$$\sum F_y = 0 \Rightarrow L\sin\phi - F_c = 0 \tag{9.2}$$

$$\sum F_z = 0 \Rightarrow L\cos\phi = W \tag{9.3}$$

This set of three equations are the governing equations of motion and illustrate the necessary conditions for a level steady-state turn. Any object, including an aircraft, in a rotational motion (e.g., turn) has a radial acceleration that is referred to as

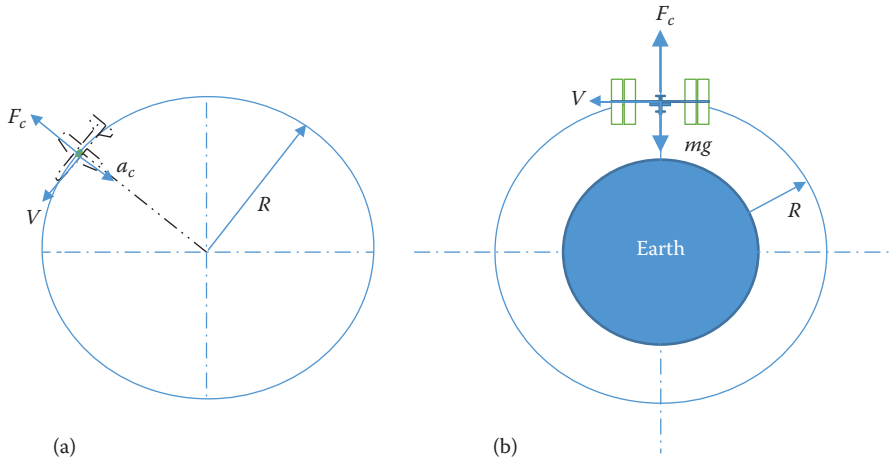

FIGURE 9.4 The centripetal acceleration and the centrifugal force. (a) An aircraft is a turn (top view) and (b) International space station.

centripetal acceleration (a_c). This acceleration is toward the center of turn (i.e., the circle). The centripetal acceleration is equal[1] to

$$a_c = \frac{V^2}{R} \tag{9.4}$$

Thus, the resultant force (F_c) is equal to the mass multiplied by the centripetal acceleration:

$$F_c = ma_c = m\frac{V^2}{R} \tag{9.5}$$

This force, which is a kind of inertial force, is referred to as the centrifugal force. Based on Newton's first law, for any acceleration, an inertial force in the opposite direction is created. Hence, for a centripetal acceleration, a centrifugal force is created (see Figure 9.4a). In some physics textbooks, this force is mistakenly referred to as the centripetal force. "Centripetal force" is not the correct term, since, as it will be proved, the direction of this force must be outward to provide the equilibrium and maintain a constant radius.

Another example is a spacecraft flight around the Earth in space. The International Space Station (ISS) is a spacecraft that is turning around the Earth without losing its height, simply by employing centrifugal force. The ISS centrifugal force is created due to its mass, velocity, and radius of rotation. An ISS astronaut is enjoying

[1] The proof can be found in most Physics textbooks.

weightlessness because his/her weight is balanced by his/her centrifugal force. Thus, for the ISS and each astronaut, the balance of forces along the radial direction yields

$$mg = m\frac{V^2}{R} \tag{9.6}$$

where m is the mass of the ISS or an astronaut, V is the linear velocity of the ISS or an astronaut, and R is the radius of rotation (i.e., height from the Earth center). Note that Figure 9.4b is not to scale, due to a need to demonstrate the large radius R and the small ISS in one figure. Now, we return to a level-coordinated turn. When the centrifugal force from Equation 9.5 is substituted in Equation 9.2, we will have the following interesting result:

$$L\sin\phi = m\frac{V^2}{R} \tag{9.7}$$

This equation is a physical statement to prove that the radial centrifugal force is balanced by the lift component L sin ϕ. As long as the combination of the velocity V, radius R, mass m, and bank angle ϕ satisfies Equation 9.7, the turn is coordinated, and there will be no skidding and slipping.

Furthermore, as Figure 9.3 illustrates, an aircraft in a level flight must always (as in a level turn) generate a vertical force equal to the aircraft weight to maintain the altitude. In fact, this vertical force is simply the vertical component of the lift in the z-axis (i.e., L cos ϕ). This demonstrates that, in a turn, the total lift force (L) must always be greater than the aircraft weight.

9.2.2 Load Factor and Bank Angle

The ratio between the lift and the aircraft weight (W) is an important parameter in the turn performance analysis. It is called the load factor and is shown by the symbol n:

$$n = \frac{L}{W} \tag{9.8}$$

The load factor, indeed, is a normalized acceleration. In addition, any centripetal acceleration can be normalized with respect to the gravitational acceleration, g. Hence, the load factor is usually stated in terms of g. It is customary, especially by the pilot community, to use the unit of g for the load factor (n), that is, g-load. The parameter g is the gravity constant, that is, 9.81 m/s^2 or 32.17 ft/s^2. For instance, when the lift is twice the aircraft weight (i.e., $n = 2$), the turn is said to be a 2-g turn. Recall that the mass of any given object is constant, but its weight is a function of gravity (g).

In a cruising flight, lift is equal to weight ($n = 1$). But, when the load factor is >1, as in a turning flight, the airspeed will be less than that of a cruising flight. So, if a pilot decides to turn while maintaining speed and altitude, he/she must increase the

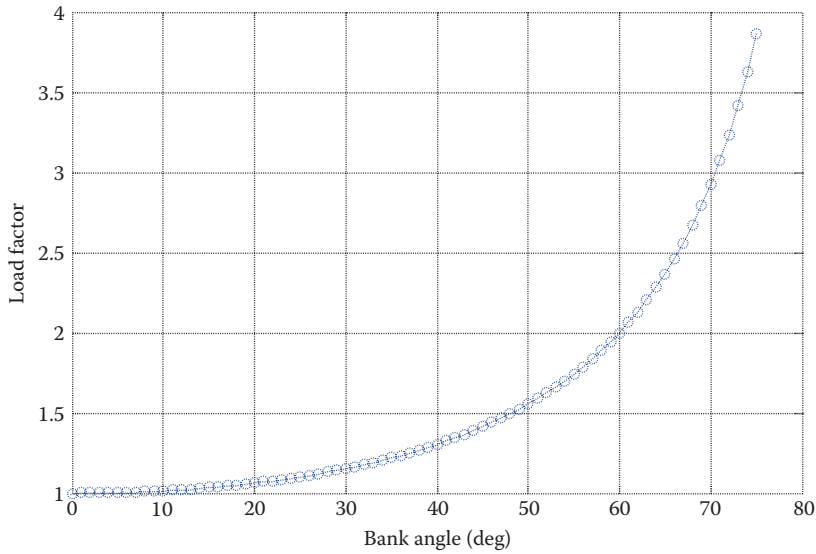

FIGURE 9.5 The variations of load factor versus aircraft bank angle.

engine thrust by deflecting the engine throttle. Inserting the value of n from Equation 9.8 into Equation 9.3, the load factor will be equal to

$$n = \frac{1}{\cos\phi} \tag{9.9}$$

Hence, the load factor – in a level turn - is only a function of the bank angle. This means that as the aircraft bank angle (ϕ) increases, the load factor (n) will increase as well. For instance, the load factor in a level turn with a 60° bank angle is equal to two (i.e., cos (60°) = 2), which implies that the lift must be twice the aircraft weight. This is particularly very important in an aircraft structural design, since the structure must sustain this much load. Figure 9.5 is the graphical demonstration of Equation 9.9. As Figure 9.5 demonstrates, the increase in the load factor in cases where the bank angle is >60° will be rapid. Only acrobatic (and highly maneuverable) aircraft are allowed to have a bank angle above 60°. In a visual flight, any turn with a bank angle >45° is referred to as the *steep turn*. Figure 9.26b illustrates a Dassault Rafale C in a very high bank angle turn (close to 90°).

Since the load factor in a level turn is only a function of the bank angle, the maximum permissible load factor is equivalent to the maximum permissible bank angle:

$$n_{max} = \frac{1}{\cos(\phi_{max})} \tag{9.10}$$

The maximum allowable load factor is limited by the aircraft structural strength or human tolerance. When the load factor in an aircraft is 1, it indicates that the

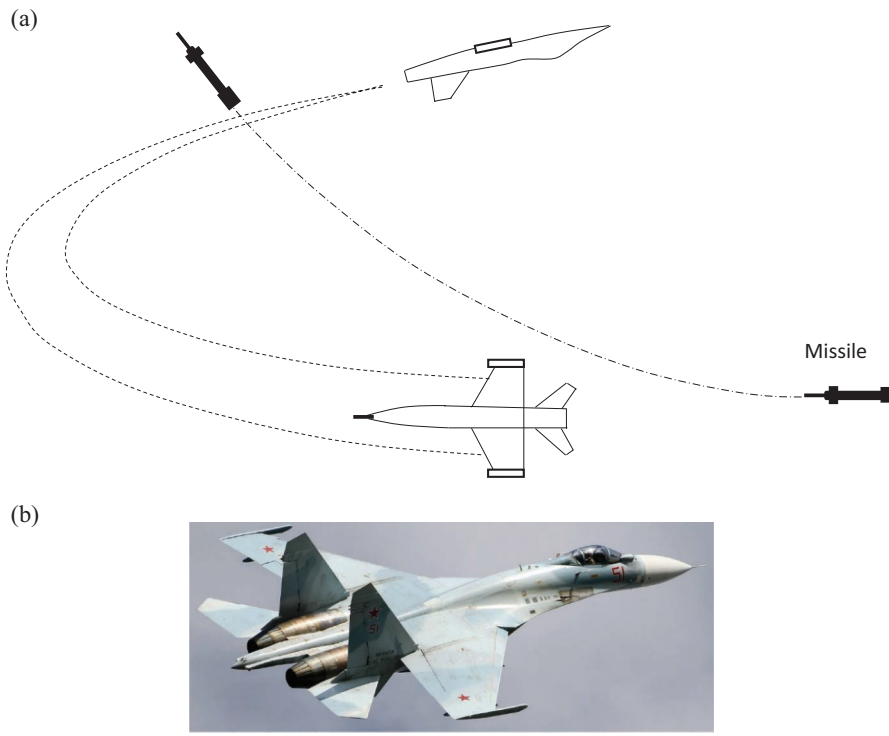

FIGURE 9.6 Defeating a missile through a very steep turn and a cobra maneuver. (a) Evading an air-to-air missile and (b) Sukhoi Su-27. (Courtesy of Weimeng.)

structure and also human onboard are carrying 1 *g*-load. In other words, its weight equals its mass times 1 *g* ($W = m$ (1 *g*)). If, for instance, the load factor is 3, it indicates that the aircraft structure must sustain a load that is equivalent to three times its weight. In any turning flight, the structure and the human onboard will have to carry a centripetal acceleration that may be expressed as a factor of *g* and may be presented as an applied load.

In the case of a human, this load is harmful and it particularly disturbs the blood system and brain. The human body, particularly the blood circulation system, is created in such a way that a human is comfortable in the environment of 1 *g*. Any other environment, including a zero-*g* (weightlessness) case, is harmful to the human body, especially in a long term. The blood circulation is affected by the number of *g*'s (load factor).

For other flight operations, similar expressions can be drawn. In some instances, especially for missiles, this load factor may increase as high as 30. Hence, the structure must carry this huge load safely. The aircraft structure must be strong enough to carry other loads including acceleration load such that the aircraft is able to perform its mission safely. As Figure 9.6 illustrates, a low-load factor fighter may end up getting targeted by a high-load factor missile. Defeating a missile requires a very steep turn, which generates a very high *g*-load. Figure 9.6b illustrates a Sukhoi Su-27, a twin-engine supermaneuverable aircraft, which is capable of performing a

TABLE 9.1
Maximum Allowable Load Factor for Various Types of Aircraft

No.	Aircraft Type	Maximum Positive Load Factor	Maximum Negative Load Factor
1.	Normal (non-acrobatic)	2.5–3.8	−1 to −1.5
2.	Utility (semi-acrobatic)	4.4	−1.8
3.	Acrobatic	6	−3
4.	Homebuilt	5	−2
5.	Transport	2.5–3.8	−1 to −2
6.	Bomber	2–4	−1 to −2
7.	Highly maneuverable	7–12	−3 to −6
8.	Missiles	15–30	−15 to −30

cobra maneuver. This fighter aircraft has a takeoff mass of 30,450 kg, a wing area of 62 m^2, and two turbofan engines, with a maximum speed of Mach 2.35.

If the *g*-load is more than the allowable design value, the structure will lose its integrity and may disintegrate during the flight. The load factor is usually positive, but in some instances, including pull-down, inverted flight, and when encountering a gust, it may become negative. In general, the absolute value of the maximum negative load factor must not exceed 0.4 times the maximum positive load factor. Past experiences forced Federal Aviation Administration to regulate the load factor on aircraft. Table 9.1 shows typical values for the load factor for various types of aircraft.

Equation 9.4 ($a_c = V^2/R$) implies that as the airspeed increases in a steady-state turn, the *g*-load will increase as well. It also implies that as the turn radius decreases, the load factor is increased. Both cases result in an increase in the centripetal acceleration and the centrifugal force.

At this moment, we can develop several meaningful relationships to analyze a turn. We begin with a few introductory equations and continue with the calculation of rate of turn (ω), turn radius (*R*), and stall speed in a turn. By inserting Equation 5.8 into Equations 9.8 and 9.9, one can derive the required lift coefficient in a level turning flight:

$$C_L = \frac{2nW}{\rho V^2 S} = \frac{2W}{\rho V^2 S \cos(\phi)} \tag{9.11}$$

This equation implies that as the bank angle (ϕ) increases, the lift coefficient must be increased. Furthermore, since the lift coefficient is directly a function of angle of attack (α), as the bank angle (ϕ) increases, the pilot must increase the angle of attack. This is obtained by deflecting the elevator upward. Moreover, we had the following lift equation from Chapter 2:

$$L = \frac{1}{2}\rho V_s^2 S C_{L_{\max}} \tag{2.26}$$

When we substitute this lift into Equations 9.8 and 9.9, we can derive a particular relationship for the stall speed in a level turn (V_{s_t}) as:

$$V_{s_t} = \sqrt{\frac{2mg}{\rho S C_{L_{\max}} \cos(\phi)}} = \sqrt{\frac{2nmg}{\rho S C_{L_{\max}}}} \tag{9.12}$$

Equation 9.12 clearly shows the inverse relation between the stall speed and bank angle $\sqrt{1/\cos(\phi)}$. This means that, when a pilot banks to turn, the load factor (n) is increased, and the stall speed is increased as well. If the pilot is not careful, it may pass the aircraft current airspeed (i.e., the airspeed may fall below stall speed). This equation shows that an aircraft may stall in a turn at any speed even at high speeds.

This is a safety warning for pilots since they must increase the aircraft speed in a level turn to avoid the stall in a turning flight. As an example, the stall speed in a level turn with a 45° bank angle is about 20% more than that for a level cruising flight. This is particularly crucial in the cases of takeoff and landing, since in some instances, the pilot must turn to clear an obstacle while taking off or landing. In these cases, the pilot must pay extra attention to the aircraft speed and make sure that the speed is above the stall speed for turning flight (V_{s_t}), which is greater than the regular stall speed (V_s). Hence, Equation 9.12 can be expressed as

$$V_{s_t} = V_s \sqrt{n} \tag{9.13}$$

where V_{s_t} and V_s are stall speeds for level turning flight and cruising flight, respectively.

9.2.3 Turn Radius

The load factor is a tool to measure applied load to the aircraft structure, the pilot, the crew, and the passengers. In a cruising flight, in which lift is equal to weight, the load factor is 1. This means that the structure must carry the aircraft weight safely, and the pilot, the crew, and the passengers must sustain a load that is equal to their weight (as usual). Now, consider, for instance, an aircraft in a level turn with a bank angle of 45°. In this case, the load factor (based on Equation 9.9) is 1.41, which leads to 41% more load on the aircraft structure and also on the human onboard. Moreover, each human onboard will have to carry 41% of his/her weight (not aircraft weight).

Dividing Equation 9.2 by 9.3 yields

$$\frac{L\sin\phi}{L\cos\phi} = \frac{F_c}{W} \tag{9.14}$$

Referring to the definition of the centrifugal force (Equation 9.5), we can obtain

$$\tan\phi = \frac{mV^2}{RW} = \frac{V^2}{gR} = \frac{a_c}{g} \tag{9.15}$$

Then,

$$a_c = g\tan\phi \tag{9.16}$$

Two accelerations (g and a_c) can be added as two vectors. Thus, the overall acceleration over the structure and human onboard is

$$a = \sqrt{g^2 + a_c^2} = \sqrt{g^2 + \left(g\tan(\phi)\right)^2} = g\sqrt{1+\tan(\phi)^2} \tag{9.17}$$

As an example, in a level turn with a bank angle of 45°, the total acceleration will be

$$a = g\sqrt{1+\tan(45)^2} = 1.41g$$

which implies that the pilot (and any human onboard) will have to sustain a 41% more g-load on his/her body. When the total acceleration (from Equation 9.17) is equal to 0, the flight operation may be classified as a case for *weightlessness*. This topic will be further investigated later in this chapter.

Inserting the equivalent of "cos ϕ" from Equation 9.9 ($\cos\phi = 1/n$) into the following trigonometric identity

$$\cos^2\phi + \sin^2\phi = 1 \tag{9.18}$$

we obtain:

$$\left(\frac{1}{n}\right)^2 + \sin^2\phi = 1 \tag{9.19}$$

Then, the following expression can be derived:

$$\begin{aligned}\sin\phi &= \sqrt{1-\frac{1}{n^2}} = \sqrt{\frac{n^2}{n^2}-\frac{1}{n^2}} = \frac{1}{n}\sqrt{n^2-1} \\ &= \cos\phi\sqrt{n^2-1} \Rightarrow \tan\phi = \sqrt{n^2-1}\end{aligned} \tag{9.20}$$

This equation again indicates that the load factor in a level turn is only a function of the bank angle. By substituting Equation 9.20 into Equation 9.15, the turn radius is expressed as

$$R = \frac{V^2}{g\sqrt{n^2-1}} \tag{9.21}$$

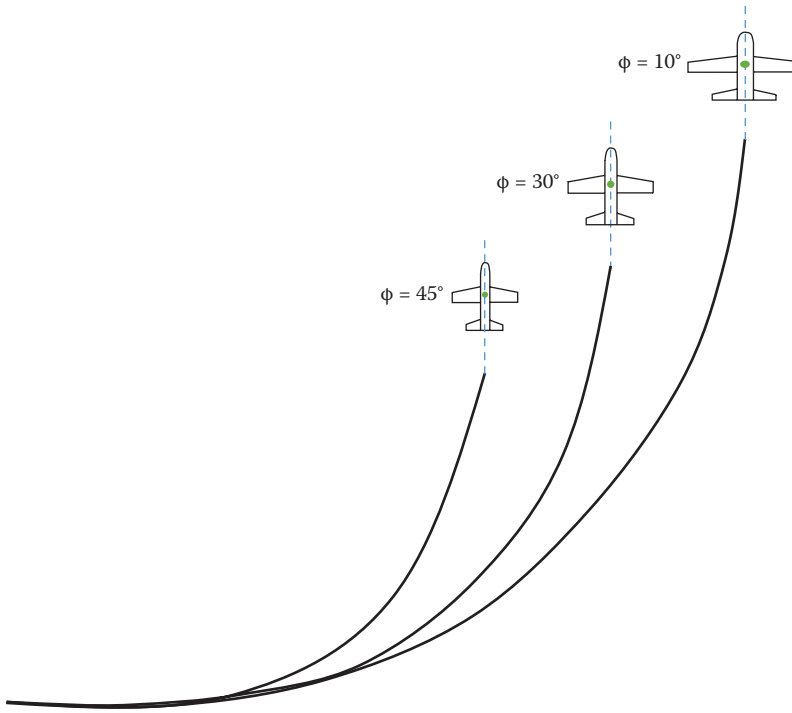

FIGURE 9.7 Level turn with a constant airspeed, varying bank angle.

Plugging tan ϕ from Equation 9.20 into Equation 9.21 yields

$$R = \frac{V^2}{g \tan \phi} \tag{9.22}$$

Mathematically, the minimum turn radius can be achieved when (1) the highest possible bank angle, and (2) the lowest possible airspeed are employed:

$$R = \frac{V_{\min}^2}{g \tan \phi_{\max}} \tag{9.23}$$

The highest possible bank angle and the lowest possible airspeed are functions of the engine maximum thrust/power, the aircraft structural strength, and the bodily strength of the human onboard. This will be further investigated in the next section.

This equation demonstrates that the turn radius depends only on aircraft airspeed and the bank angle (i.e., load factor). When the airspeed is kept constant (Figure 9.7), a larger bank angle will result in a smaller turn radius. In contrast, when the bank angle is kept constant, as the airspeed is increased, the turn radius is increased (Figure 9.8).

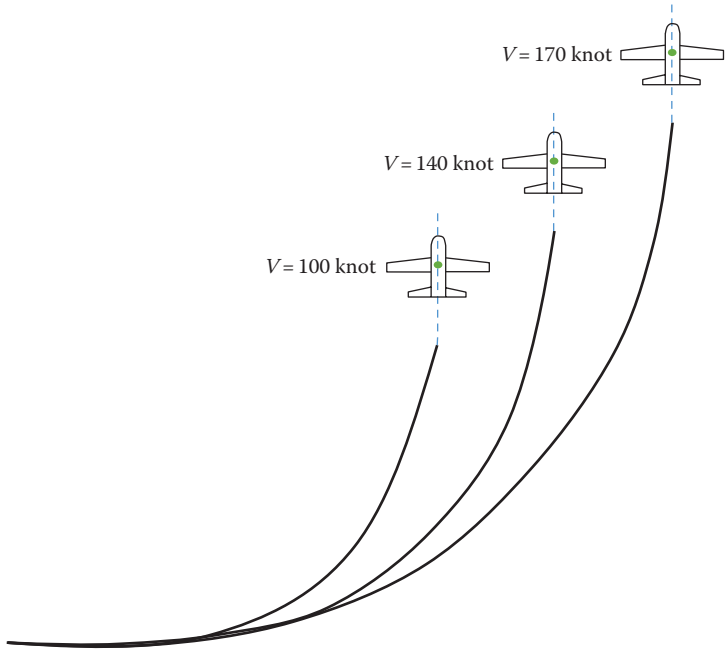

FIGURE 9.8 Level turn with a constant bank angle, varying airspeed.

To obtain the smallest possible turn radius, the pilot must decrease the aircraft speed to the lowest possible (i.e., the aircraft stall speed in the turn (V_{s_t})), and the highest possible load factor ($n_{\max}$). A higher load factor requires a stronger aircraft structure and also a stronger human body onboard. Equation 9.23 demonstrates that if a fighter pilot desires the tightest turn (i.e., turn with the smallest turn radius), he/she must employ the highest load factor. It will be proved later that, based on Equation 9.1, the maximum engine thrust is required to achieve the tightest turn.

9.2.4 Turn Rate

Another interesting turn parameter is the time elapsed to complete a turn. A 360° circle has a circumference of $2\pi R$. So, the time for a complete turn is equal to

$$t_{\text{circle}} = \frac{2\pi R}{V} \tag{9.24}$$

Furthermore, the angular value of a complete circle is 2π radian. Hence, the time required for a turn to change the heading in the amount of ω radian is equal to

$$t = \frac{2\pi R}{V}\frac{\psi}{2\pi} = \frac{R\psi}{V} \tag{9.25}$$

This equation implies that to reduce the time of a turn, one must increase the airspeed and decrease the turn radius. By inserting Equation 9.22 into Equation 9.25, the following expression is obtained:

$$t = \frac{V\psi}{g\tan(\phi)} \tag{9.26}$$

This equation implies that to reduce the time of a turn, one must increase the bank angle. Another interesting parameter in the turn performance analysis is the turn rate (ω) or angular velocity $(\dot{\psi})$. To obtain an expression for the turn rate, we begin with a basic definition. The turn rate is the amount of heading angle (ψ) that is traveled in a given time:

$$\omega = \dot{\psi} = \frac{d\psi}{dt} \tag{9.27}$$

The unit of turn rate is radians per second (rad/s) or degrees per second (deg/s). Now, return to Figure 9.3 and recall from dynamics, that the angular velocity is related to turn rate and turn speed (V) as

$$V = R\omega \tag{9.28}$$

By replacing R from Equation 9.22 with Equation 9.28, we obtain

$$V = \frac{V^2}{g\sqrt{n^2-1}}\omega$$

or

$$\omega = \frac{g\sqrt{n^2-1}}{V} \tag{9.29}$$

Since $\tan\phi = \sqrt{n^2-1}$ (Equation 9.20), Equation 9.29 can be written as

$$\omega = \frac{g\tan\phi}{V} \tag{9.30}$$

Equations 9.29 and 9.30 demonstrate that the turn rate depends only on the airspeed and the bank angle (i.e., load factor). Thus, to increase the turn rate, one must increase the bank angle and decrease the airspeed.

An increase in the load factor reflects an increase in the bank angle since the load factor is inversely proportional to the bank angle. Graphical representations of Equations 9.22 and 9.30 are illustrated in Figures 9.7 and 9.8, respectively. When the airspeed is kept constant, a larger bank angle (greater load factor) will result in a greater turn rate (Figure 9.7). In contrast, when the bank angle is held constant (n = constant), as the airspeed is increased, the turn rate is decreased (Figure 9.8).

The maximum turn rate can be mathematically achieved when (1) the highest possible bank angle and (2) the lowest possible airspeed are employed:

$$\omega_{max} = \frac{g \tan \phi_{max}}{V_{min}} \tag{9.31}$$

The highest possible bank angle and the lowest possible airspeed are functions of the engine maximum thrust/power, the aircraft structural strength, and the bodily strength of the human onboard. This will be further analyzed in the next section.

A standard turn rate [82,88] is defined as a 3 deg/s turn, which completes a 360° circle in 2 min. This is known as a 2-min turn, or 180 deg/min turn rate, which is mainly adopted by transport aircraft. Fast aircraft (e.g., fighters or acrobatic aircraft), or aircraft on certain precision approaches, use a half-standard rate (1.5 deg/s). For civil transport aircraft, ICAO mandates that all turns should be made "at a bank angle of 25° or at a rate of 3 deg/s, whichever requires the lesser bank [89].

For instance, for a standard turn rate, or rate one turn (3 deg/s) and velocity of 170 knots, the bank angle should be 25°, Equation 9.30 yields:

$$\phi = \tan^{-1}\left(\frac{V\omega}{g}\right) = \tan^{-1}\left[\frac{170 \times 0.514 \times \frac{3}{57.3}}{9.81}\right] = 0.437 \text{ rad} = 25° \tag{9.32}$$

The equations that have been derived so far are used for the preliminary analysis of an aircraft in turning flight. Note, if the airspeed (V) is in meter per second (m/s), and the gravity constant (g) is in meter per second squared (m/s^2), the unit of turn rate (ω) will be in radian per second (rad/s). The importance and the calculation of the maximum load factor will be presented in Section 9.5.1.

In an ideal case, the x–z plane is geometrically the plane of symmetry for an aircraft. Thus, the left side must mirror the right side (front view or top view). Although an aircraft is symmetric in the xy plane (top view), but during a turn, a sideslip angle (β) is often created (either positive or negative). The sideslip angle is defined as the angle between the body x-axis and the relative wind (from the top view). This will create a side force that consequently generates a slip/skid.

When an aircraft is slipping (into the turn) or skidding (out of the turn), the pilot must deflect the rudder to coordinate the turn. During a slipping turn, the radius of the turn decreases, while during a skidding turn, the radius of the turn increases. In a slip, the aircraft is yawing toward the outside of the turning flight path (negative sideslip angle). Furthermore, in a skid, the aircraft is yawing toward the inside of the turning flight path (positive sideslip angle). To fix both cases, the rudder should be deflected to adjust the sideslip angle, such that the side force is zero.

However, the throttle, elevator, and aileron are also employed to maintain the speed, altitude, and bank angle, respectively. During a coordinated turn, the typical value for a rudder deflection is about 0° to ±4°, while the typical value for the aileron is about 0° to ±2°. However, the required aileron deflections to roll the aircraft to the desired bank angle have much higher values (in the order of ±10° to ±20°). The "±"

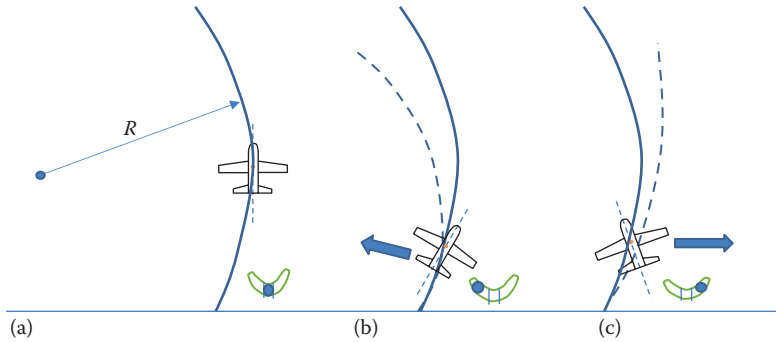

FIGURE 9.9 (a) Coordinated, (b) slipping, and (c) skidding turns (top view, left turn).

is used because the turn could be to the left (negative bank angle) or right (positive bank angle).

A pilot does not need to calculate the amount of required values for the deflections of rudder/aileron to maintain the coordination during a turn. Every modern aircraft has a turn coordinator (see Figure 9.9), which is an instrument consisting of a rate gyro to indicate the rate of yaw, and a curved glass inclinometer to indicate the relationship between gravity and centripetal acceleration. There is a ball inside the inclinometer that can move left/right. If the ball is at the center, it indicates that the turn is coordinated. However, if the ball is away from the center, the turn is not coordinated, and the side force is not zero.

In a left turn, the ball on the left side of the inclinometer indicates that the aircraft is slipping. However, the ball on the right side of the inclinometer implies that the aircraft is skidding. In contrast, in a right turn, the ball on the right side of the inclinometer indicates that the aircraft is slipping. However, the ball on the left side of the inclinometer indicates that the aircraft is skidding. In terms of the force equation, when the forces along the y-axis are not balanced, the resultant force will be either positive or negative. If the resultant force is positive, the aircraft will slip into the turn:

$$L\sin\phi - F_c + F_y > 0 \ \ (\text{slipping turn}, a_y > 0) \tag{9.33}$$

However, if the resultant force is negative, the aircraft will skid out of the turn:

$$L\sin\phi - F_c + F_y < 0 \ \ (\text{skidding turn}, a_y < 0) \tag{9.34}$$

It is reminded that the positive y-axis is to the right-hand side of the pilot. In general, when the ball is outside of the turn, the aircraft is skidding, while, when the ball is inside of the turn, the aircraft is slipping. The job of the pilot in all cases is just to "step on the ball", which means that he/she needs to press the rudder on the side where the ball is placed until the ball returns to the center. This causes the aircraft nose to move toward the flight path to help the turn stay coordinated.

Recall that the goal of "step on the ball" is not to make the sideslip angle to be zero; rather, the objective is to make the side force to get equal to zero. The side force can be zero with a non-zero sideslip angle. Thus, the rudder is not used to bring the nose back in line with the relative wind. The rudder deflection changes (i.e., corrects) the nose angle such that the side force is zero. This is a common mistake in the pilot community.

Example 9.1

Consider a very light aircraft (VLA) with a mass of 750 kg and an airspeed of 100 knots.

a. If the maximum permissible load factor is 3.8, what is the equivalent maximum bank angle?
b. Determine the corresponding turn radius for a coordinated turn with such a bank angle.
c. If the aircraft is turning coordinately with a radius of 300 m and a bank angle of 30°, calculate the airspeed and load factor.

Solution

a. Bank angle:

$$n = \frac{1}{\cos\phi} = 3.8 \Rightarrow \phi = 75^\circ \tag{9.9}$$

b. Turn radius:

$$R = \frac{V^2}{g\sqrt{n^2-1}} = \frac{(100\times 0.5144)^2}{9.8\times\sqrt{3.8^2-1}} \Rightarrow R = 72\,\text{m} \tag{9.21}$$

c. Load factor and airspeed:

$$n = \frac{1}{\cos\phi} = \frac{1}{\cos(30)} \Rightarrow n = 1.154 \tag{9.9}$$

$$R = \frac{V^2}{g\sqrt{n^2-1}} \Rightarrow V = \sqrt{Rg\sqrt{n^2-1}} = \sqrt{300\times 9.81\times\sqrt{1.154^2-1}} \Rightarrow V = 41.2\,\text{m/s} \tag{9.21}$$

Example 9.2

Determine the stall speed of a utility aircraft with a mass of 4,500 kg, a wing area of 19.5 m^2, and the maximum lift coefficient of 2.5. Perform this analysis at the sea level for the following two flight conditions:

a. Cruising flight.
b. Turning flight with a 30° bank angle.

Solution

At sea level, the air density is 1.225 kg/m^3.

a. Cruising flight

$$V_s = \sqrt{\frac{2mg}{\rho S C_{L_{\max}}}} = \sqrt{\frac{2\times 4{,}500\times 9.81}{1.225\times 19.5\times 2.5}} = 74.7\,\text{knot} \tag{2.27}$$

b. Turning flight with a 30° bank angle

$$V_{s_t} = \sqrt{\frac{2mg}{\rho S C_{L_{\max}} \cos(\phi)}} = \sqrt{\frac{2\times 4{,}500\times 9.81}{1.225\times 19.5\times 2.5\times \cos(30)}}$$
$$\Rightarrow V_s = 41.32\,\text{m/s} = 80\,\text{knot} \tag{9.12}$$

This example indicates that the stall speed in a turning flight is higher than that for a cruising flight. This is a general conclusion for any type of aircraft at any altitude.

Example 9.3

The aircraft introduced in Example 9.2 is cruising at the sea level with a speed of 250 knots. Assume that the lift curve slope (C_{L_α}) of the aircraft is 0.1 1/deg and $\alpha_o = 0$.

a. Determine the aircraft angle of attack for this flight condition.
b. If the pilot decides to turn with a 45° of bank angle while maintaining the same airspeed, what is the aircraft angle of attack?

Solution

At the sea level, the air density is 1.225 kg/m^3.

a. Aircraft angle of attack:

$$C_L = \frac{2W}{\rho V^2 S} = \frac{2\times 4{,}500\times 9.81}{1.225\times(250\times 0.5144)^2\times 19.5} \Rightarrow C_L = 0.22 \tag{5.8}$$

$$C_{L_\alpha} = \frac{C_L}{\alpha} \Rightarrow \alpha = \frac{C_L}{C_{L_\alpha}} = \frac{0.22}{0.1} = 2.2° \tag{2.10}$$

b. New aircraft angle of attack

$$C_L = \frac{2W}{\rho V^2 S\cos(\phi)} = \frac{2\times 4{,}500\times 9.81}{1.225\times(250\times 0.5144)^2\times 19.5\times\cos(45)} \Rightarrow C_L = 0.31 \tag{9.11}$$

$$C_{L_\alpha} = \frac{C_L}{\alpha} \Rightarrow \alpha = \frac{C_L}{C_{L_\alpha}} = \frac{0.31}{0.1} = 3.1° \tag{2.10}$$

The result of this example is a general conclusion; that is, an aircraft requires a greater angle of attack in a level turn compared with a cruising flight.

9.3 LEVEL TURN PERFORMANCE: JET AIRCRAFT

This section and Section 9.4 are devoted to the analysis of the turn performance for both jet and prop-driven aircraft. They cover the aircraft requirements to perform a level turn with a desired turn radius and turn rate. The type of aircraft engine will influence the aircraft turn performance in various aspects. Aircraft engines are divided into several groups, two of which are jet (e.g., turbofan and turbojet) and prop-driven (e.g., turboprop, piston-prop, and electric). This section presents the turn performance for a jet aircraft, while Section 9.4 presents the turn performance for a prop-driven aircraft. Two main unknown parameters to perform a level turn are engine thrust and engine power.

According to Equation 9.8, the load factor is defined as the ratio between the total lift and aircraft weight. Essentially, there are two types of maximum load factors: (1) maximum possible load factor (producible by the engine thrust/power) and (2) maximum allowable load factor (tolerable by the aircraft structure). It is crucial for the reader to identify the difference. Almost always, these two load factors are not equal for an aircraft. At any given velocity, the maximum possible load factor for a sustained level turn is constrained by the maximum engine thrust/power. In contrast, at any given velocity, the maximum allowable load factor for a sustained level turn is constrained by the maximum structural strength.

For a fighter aircraft, the maximum producible load factor by the engine thrust is often greater than the maximum tolerable load factor by the aircraft structure. However, for general aviation (GA) aircraft, the maximum producible load factor by the engine is often less than the maximum tolerable load factor by the aircraft structure. Thus, a fighter pilot should be careful not to set the aircraft in a turning flight, so that the maximum producible load factor is not generated. Therefore, when an expression illustrates the relation between the load factor and engine thrust, this is a producible load factor. However, the load factor in the *V-n* diagram (which will be introduced in Section 9.7) is the tolerable (allowable) load factor.

In Sections 9.5 and 9.6, it is shown that the maximum turn rate and the minimum turn radius require the maximum load factor. This section is devoted to the turn performance analysis for an aircraft with a jet engine (e.g., turbofan and turbojet). We first begin with rewriting equations that we derived in the previous section and also in Chapter 5, and then we develop new expressions that govern a level turn. In this section, four important parameters are described: (1) maximum producible load factor, (2) corner velocity, (3) maximum of the maximum load factor, and (4) airspeed that corresponds to the maximum of the maximum load factor. Then, the technique to determine them is presented: A few design and operational interesting points are also described.

9.3.1 Maximum Producible Load Factor

Returning to the fundamentals of a level coordinated turn, we notice that as the bank angle is increased, the magnitude of the lift (L) should be increased as well. For a given velocity, and a given bank angle (i.e., n), the lift coefficient must be increased accordingly

$$C_L = \frac{2nW}{\rho V^2 S} \tag{9.11}$$

As L increases, the drag due to lift will be increased:

$$D = \frac{1}{2}\rho V^2 S C_D = \frac{1}{2}\rho V^2 S\left(C_{D_o} + KC_L^2\right) \tag{9.35}$$

To maintain a sustained level turn, the engine thrust should also be increased (compared with its corresponding value at the cruising flight). If the effect of the aircraft angle of attack on the thrust component is neglected, the thrust equals the drag, that is, $T = D$. Thus,

$$T = D = \frac{1}{2}\rho V^2 S\left(C_{D_o} + K\left(\frac{2nW}{\rho V^2 S}\right)^2\right) \tag{9.36}$$

Solving this equation (the details are left to the reader) for the load factor, n yields

$$n = \sqrt{\frac{\rho V^2 S}{2KW^2}\left(T - \frac{1}{2}\rho V^2 S C_{D_o}\right)} \tag{9.37}$$

This equation provides the load factor as a function of a given set of velocity, engine thrust, altitude, aircraft weight, and aerodynamics features (i.e., K and C_{D_o}). The maximum value of n (i.e., maximum possible or producible) is obtained by employing the maximum thrust, having the lowest weight, and flying at the lowest altitude

$$n_{\max} = \sqrt{\frac{\rho_o V^2 S}{2KW_{\min}^2}\left(T_{\max} - \frac{1}{2}\rho_o V^2 S C_{D_o}\right)} \tag{9.38}$$

Provided that the sufficient magnitude of engine thrust is available for every velocity (from stall speed to maximum speed), the maximum load factor is a nonlinear function of velocity. A typical plot for the variations of producible maximum load factor as a function of airspeed for a business jet with a mass 16,000 kg, a maximum thrust of 60 kN, and a wing area of 50 m^2 is shown in Figure 9.10.

This plot often has an inflection point (Point A), which represents the maximum of the maximum load factor. This point corresponds to the velocity at which the highest bank angle can be employed in a sustained level turn. Another interesting location in this plot is point D which represents the maximum velocity. At this flight condition, the aircraft load factor is 1 and the aircraft is not able to turn. The third

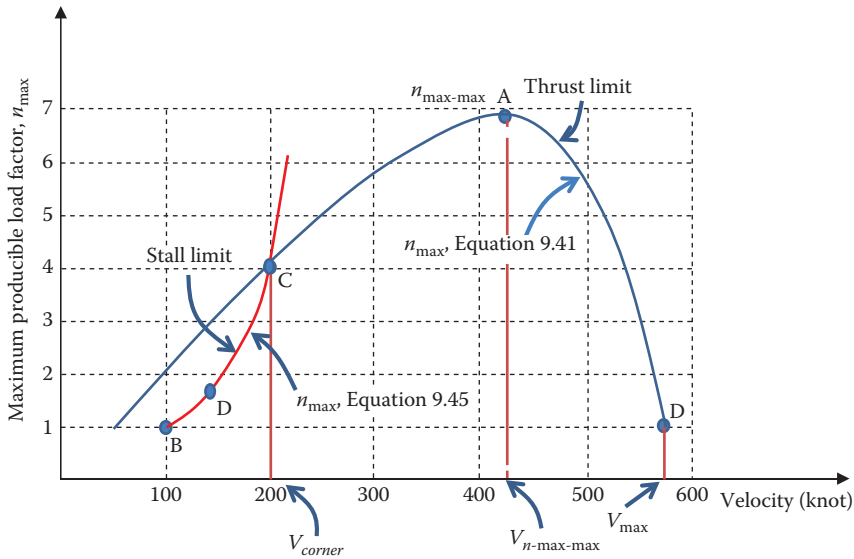

FIGURE 9.10 Variations of the maximum load factor versus airspeed in a level turn.

important location of the plot is point B which corresponds to the stall speed and has a load factor of 1. The fourth point (i.e., C) represents the corner velocity and is presented in the next section.

From Equation 9.10, we conclude that, at any speed,

$$\phi_{max} = \cos^{-1}\left(\frac{1}{n_{max}}\right) \tag{9.39}$$

This is the maximum achievable bank angle at any given speed. An aircraft is unable to employ any bank angle beyond the one, which is determined by Equation 9.39. This maximum achievable bank angle sets a fixed limit to the fastest turn and tightest turn, that is, aircraft maneuverability. If the pilot does not increase the engine thrust when entering a turn, by banking the aircraft, the aircraft speed will be reduced, while its stall speed (V_{s_t}) will be increased. This point will be further investigated in the next section.

9.3.2 Corner Velocity

From Equation 9.12, as the load factor (or bank angle) is increased, the stall speed is increased too in a level turn. Hence, the value of n cannot be such that the airspeed is below the turn stall speed. Any value of n at which the aircraft encounters the stall speed is not allowable. Thus, the maximum lift coefficient sets a definite limit on the value of n that is associated with the design aspects of an aircraft. In order for an aircraft to be able to achieve such maximum load factor, it must be able to produce a sufficient lift.

The corner velocity (V^*) is defined as the airspeed below which $n_{\max}$ is governed by the maximum lift coefficient, rather than the maximum engine thrust. The maximum load factor is of either the maximum producible n or the maximum tolerable n. The lowest value of these two n defines the corner speed.

Inserting the $n_{\max}$ from Equation 9.38 into Equation 9.11, we have the following equation that shows how much lift coefficient needs to be provided for such turn:

$$C_{L_{n\max}} = \frac{2n_{\max}W}{\rho V^2 S} \tag{9.40}$$

Every aircraft has a maximum limit for the lift coefficient; that is, $C_{L_{\max}}$. The required lift coefficient for a level turn when using the maximum thrust $\left(C_{L_{n_{max}}}\right)$ should be equal or less than the aircraft maximum lift coefficient:

$$C_{L_{n\max}} \leq C_{L\max} \tag{9.41}$$

Otherwise, the desired turn with the maximum thrust at such a given velocity (often a low speed) is not feasible. In such conditions, the maximum possible load factor is reduced due to the stall limit, and so it is determined by the following expression:

$$n_{\max} = \frac{\rho V^2 S C_{L_{\max}}}{2W} \quad \left(\text{when } V < V^*\right) \tag{9.42}$$

The typical values for the aircraft maximum lift coefficient are from 1.5 to 2.5. The value of the maximum lift coefficient may be with or without high-lift devices (e.g., flap). In theory, we may use a $C_{L_{\max}}$ with high-lift device. However, from an operational point of view, it is recommended not to employ the high-lift device in a level turn.

A typical plot for the variations of the producible maximum load factor as a function of airspeed and maximum lift coefficient for a business jet is also shown in Figure 9.10. Setting right-hand sides of Equations 9.38 and 9.42 equal to one other, one may determine the airspeed below which the load factor is constrained by stall ($C_{L_{\max}}$) rather than the maximum engine thrust (point C in Figure 9.10):

$$\frac{\rho V^2 S C_{L_{\max}}}{2W} = \sqrt{\frac{\rho V^2 S}{2KW^2}\left(T_{\max} - \frac{1}{2}\rho V^2 S C_{D_o}\right)} \tag{9.43}$$

To make this applicable for a generalized flight condition, a general altitude (ρ) and a given weight (W) are utilized. The derivation is as follows. First, both sides are squared

$$\left(\frac{\rho V^2 S C_{L_{\max}}}{2W}\right)^2 = \frac{\rho V^2 S}{2KW^2}\left(T_{\max} - \frac{1}{2}\rho V^2 S C_{D_o}\right)$$

Then, similar terms are canceled out from both sides:

$$\rho V^2 S C_{L\max}^2 = \frac{2}{K}\left(T_{\max} - \frac{1}{2}\rho V^2 S C_{D_o}\right)$$

or

$$K\rho V^2 S C_{L\max}^2 = 2T_{\max} - \rho V^2 S C_{D_o} \Leftarrow \rho V^2 S\left(K C_{L\max}^2 + C_{D_o}\right) = 2T_{\max}$$

Hence, the velocity is obtained as

$$V^* = \left[\frac{2T_{\max}}{\rho S\left(K C_{L\max}^2 + C_{D_o}\right)}\right]^{\frac{1}{2}} \tag{9.44}$$

This airspeed is denoted by V^* and is referred to as the *corner velocity*. The corner airspeed is the lowest speed at which the maximum engine thrust may be used. The corner speed (point C in Figure 9.10) plays a significant role in aircraft maneuverability. Please note that below this airspeed, the maximum thrust is not employed.

Using Equation 9.42, the corresponding maximum load factor to the corner speed $\left(n_{\max_C}\right)$ is readily determined as

$$n_{\max_C} = \frac{\rho\left(V^*\right)^2 S C_{L_{\max}}}{2W} \tag{9.45}$$

Caution: In deriving Equation 9.44, it is assumed that the corresponding maximum load factor to the corner speed $\left(n_{\max_C}\right)$ is allowed. If the structure is unable to handle such load factor (i.e., the maximum allowable load factor is less than the maximum producible load factor), the corner speed is defined as

$$V^* = \left[\frac{2n_{\max}W}{\rho S C_{L_{\max}}}\right]^{\frac{1}{2}} \tag{9.46}$$

In this case, $n_{\max}$ is a given parameter and is not calculated. Referring to Equation 9.29, the maximum possible turn rate when an aircraft turns at the corner speed is

$$\omega_{\max_C} = \frac{g\sqrt{n_{\max_C}^2 - 1}}{V^*} \tag{9.47}$$

Referring to Equation 9.21, the minimum possible turn radius, when an aircraft turns at the corner speed is

$$R_{\min_C} = \frac{V^{*2}}{g\sqrt{n_{\max_C}^2 - 1}} \tag{9.48}$$

The maximum possible turn rate and the minimum possible turn radius are very crucial to the aircraft maneuverability.

As seen in Figure 9.10, between points C and B, there is a point D, which is interesting in some turning flight cases. At this point, the aircraft is employing the maximum lift coefficient, while utilizing a fraction of the maximum thrust. The aircraft is flying with a velocity that is slower than the corner speed. The turn rate at this point is frequently less than the maximum turn rate, and the turn radius is frequently more than the minimum turn radius.

9.3.3 Maximum of the Maximum Load Factor

To determine the maximum of the maximum load factor $\left(n_{\max_{\max}}\right)$ and its corresponding velocity, we need to differentiate $n_{\max}$ with respect to V in Equation 9.41, and then set the derivative equal to zero:

$$\frac{dn_{\max}}{dV} = \frac{d}{dV}\sqrt{\frac{\rho_o V^2 S}{2KW_{\min}^2}\left(T_{\max} - \frac{1}{2}\rho V^2 S C_{D_o}\right)} = 0 \tag{9.49}$$

Solving this equation results in the corresponding velocity to the maximum of the maximum load factor. Then, inserting such velocity back into Equation 9.38 yields the maximum of the maximum load factor. This mathematical operation is lengthy; instead, there is another shorter method to reach this objective. The technique is based on the fundamental definition of the load factor. Since in a level turn, the aircraft drag is equal to the engine thrust, we can manipulate the expression (Equation 9.8) as follows:

$$n = \frac{L}{W}\frac{T}{T} = \frac{L}{W}\frac{T}{D} = \left(\frac{T}{W}\right)\left(\frac{L}{D}\right) \tag{9.50}$$

This expression includes two important ratios, namely, thrust-to-weight ratio (T/W) and lift-to-drag ratio (L/D). Thus, the load factor is equivalent to the multiplication of the thrust-to-weight ratio and lift-to-drag ratio. Any change in these two ratios will result in variations of the load factor. If the engine thrust remains constant at its maximum value, the producible load factor will reach its absolute maximum value ($n_{\max_{\max}}$), when the aircraft has its maximum lift-to-drag ratio $(L/D)_{\max}$:

$$n_{\max_{\max}} = \left(\frac{T_{\max}}{W}\right)\left(\frac{L}{D}\right)_{\max} \tag{9.51}$$

This equation indicates that the absolute maximum (maximum of the maximum) possible load factor is corresponding to only one velocity (i.e., the velocity corresponding to the maximum L/D). The $n_{\max}$, in turn, corresponds to only one (absolute

maximum) bank angle (i.e., ϕ_{max}). In Chapter 5, the following expression for the aircraft maximum lift-to-drag ratio was developed:

$$\left(\frac{L}{D}\right)_{max} = \frac{1}{2\sqrt{KC_{D_o}}} \tag{5.28}$$

By substituting Equation 5.24 into Equation 9.51, the absolute maximum producible load factor will be as follows:

$$n_{max_{max}} = \frac{T_{max}}{2W\sqrt{KC_{D_o}}} \tag{9.52}$$

Based on this equation, there are two constraints on the maximum producible load factor: (1) maximum engine thrust, and (2) maximum lift-to-drag ratio. These two factors determine the maximum producible load factor. Thus, the highest achievable turn performance is a function of these two constraints. To improve the turn performance, the designer must select more powerful engine(s) and also increase the maximum lift-to-drag ratio.

It is again emphasized that the maximum tolerable load factor is not usually the same as the maximum allowable load factor. The propulsion and aerodynamics are two wings of flight dynamics that determine the maximum producible load factor, that is, the best turn performance. The aircraft structure is a tool to carry flight mission; this tool must be light and possesses high strength. Aircraft structure and human onboard dictate the maximum allowable load factor. The structural design limits of a given aircraft represent a practical materialistic constraint on the maximum allowable load factor.

In majority of the aircraft types, the maximum producible load factor is less than the maximum allowable load factor. But, in many fighters, where their engines are too powerful, such as General Dynamics (now Lockheed Martin) F-16 Fighting Falcon (Figure 7.6), the maximum producible load factor is more than the maximum allowable load factor. In these aircraft, the pilot must be careful not to generate more load factor than the aircraft structure can carry.

By substituting Equation 9.52 into Equation 9.39, the absolute maximum producible bank angle in a level turn is expressed as

$$\phi_{max_{max}} = \cos^{-1}\left(\frac{2W\sqrt{KC_{D_o}}}{T_{max}}\right) \tag{9.53}$$

Thus, bank angle and load factor will reach their maximum values, when the thrust-to-weight ratio (T/W) and lift-to-drag ratio (L/D) reach their maximum values. In Chapter 5, it is shown that at the absolute ceiling, the thrust-to-weight ratio (T/W) is equal to the inverse of maximum lift-to-drag ratio ($(L/D)_{max}$). Thus, the expression (9.52) states that the load factor at absolute ceiling is equal to 1. In other words, the maximum bank angle at absolute ceiling is 0. This is obvious since no aircraft is able to turn unless it loses the altitude.

Another safety conclusion from Equation 9.51 is drawn for fighter pilots. A fighter pilot must not increase the engine thrust such that the load factor is more than its allowable value. Otherwise, the structure will break, and the aircraft will suffer. Hence, we can conclude the following expression for the maximum available (avl) and maximum allowable thrust:

$$\left(\frac{T_{\max}}{W}\right)_{\text{avl}} = \frac{n_{\max_p}}{(L/D)_{\max}} \tag{9.54}$$

$$\left(\frac{T_{\max}}{W}\right)_{\text{allow}} < \frac{n_{\max_A}}{(L/D)_{\max}} \tag{9.55}$$

where $n_{\max_p}$ (i.e., $n_{\max_{\max}}$) is the maximum producible load factor, while $n_{\max_A}$ is the maximum allowable load factor. Therefore, the maximum allowable load factor is always equal or less than the maximum producible load factor.

$$1 < n_{\max_A} \leq n_{\max_p} \tag{9.56}$$

For instance, consider an aircraft whose maximum producible load factor is 12, but the maximum allowable load factor is 9. If the maximum lift-to-drag ratio is 10, the pilot is not permitted to increase the engine thrust beyond the value equivalent to 90% of the aircraft thrust-to-weight ratio (during a turn):

$$\frac{T_{\max}}{W} < \frac{9}{10} \Rightarrow \frac{T_{\max}}{W} < 90\%$$

This ratio implies that the pilot is not allowed to employ the maximum engine thrust in some specific flight conditions during a level turn. This point must be noticed in fighter aircraft design and fighter pilot training. In addition, since the engine thrust is reduced with altitude, Equation 9.52 demonstrates that the load factor and, consequently, the turn performance is reduced with altitude.

9.3.4 Airspeed That Corresponds to the Maximum of the Maximum Load Factor

Another parameter of interest in the level turn performance analysis is the airspeed that corresponds to the maximum of the maximum producible load factor (i.e., when the maximum thrust is utilized). For this purpose, we first determine the airspeed in a turning flight as a function of the engine thrust and bank angle. Referring to Equation 3.1 and the definition of dynamic pressure $\left(q = \frac{1}{2}\rho V^2\right)$, the drag and lift forces are

$$D = qSC_D \tag{9.57}$$

$$L = qSC_L \tag{9.58}$$

where the lift and drag coefficients (using Equations 3.11 and 9.14) in a level term are

$$C_D = C_{D_o} + KC_L^2 \tag{3.12}$$

$$C_L = \frac{nW}{qS} \tag{9.59}$$

Substituting Equations 3.11 and 9.59 into Equation 9.57, the drag equation can be readily expressed into the following form:

$$D = qSC_{D_o} + \frac{Kn^2W^2}{qS} \tag{9.60}$$

In a coordinated level turn, the horizontal component of the engine thrust and aircraft drag is equal:

$$T\cos\alpha = D \tag{9.1}$$

The angle of attack is usually very small, so the equation can be simplified to

$$T = D \tag{9.61}$$

By substituting this equation into Equation 9.60, we obtain

$$S^2C_{D_o}q^2 - TSq + Kn^2W^2 = 0 \tag{9.62}$$

If we assume that the unknown in this equation is the load factor (n), the solution for this quadratic is obtained:

$$n = \frac{S}{W}\sqrt{\frac{Tq}{KS} - \frac{C_{D_o}q^2}{K}} = \frac{Sq}{W}\sqrt{\frac{1}{K}\left(\frac{T}{Sq} - C_{D_o}\right)} \tag{9.63}$$

This equation is used when engine thrust and airspeed are known, and we are looking for the possible load factor. Equation 9.62 is a quadratic equation with respect to q (dynamic pressure), and the solution is obtained by using the quadratic formula:

$$q = \frac{T}{2SC_{D_o}}\left[1 \pm \sqrt{1 - \frac{4C_{D_o}Kn^2W^2}{T^2}}\right] \tag{9.64}$$

Referring to the definition of dynamic pressure, we obtain

$$\frac{1}{2}\rho V^2 = \frac{T}{2SC_{D_o}}\left[1 \pm \sqrt{1 - \frac{4C_{D_o}Kn^2W^2}{T^2}}\right] \tag{9.65}$$

Hence, the airspeed in a turning flight is determined as

$$V = \sqrt{\frac{T}{\rho SC_{D_o}}\left[1 \pm \sqrt{1 - \frac{4C_{D_o}Kn^2W^2}{T^2}}\right]} \tag{9.66}$$

A specific bank angle (i.e., load factor) and a specific engine thrust will result in a specific airspeed at any particular altitude. Equation 9.66 has two solutions, and usually both answers are acceptable. Although two solutions satisfy the quadratic Equation (9.62), we are not allowed to employ any combination of engine thrust and bank angle, since they are related. There is a minimum engine thrust for any given bank angle and altitude.

By inserting Equations 5.6 and 5.24 into this equation, we will have another meaningful expression:

$$V = \sqrt{\frac{T}{\rho SC_{D_o}}\left[1 \pm \sqrt{1 - \left(\frac{nW}{T(L/D)_{\max}}\right)^2}\right]} \tag{9.67}$$

The application of the maximum engine thrust ($T_{\max}$) will result in the maximum load factor ($n_{\max}$), that is:

$$V = \sqrt{\frac{T_{\max}}{\rho SC_{D_o}}\left[1 \pm \sqrt{1 - \left(\frac{4C_{D_o}Kn_{\max}^2W^2}{T_{\max}^2}\right)^2}\right]} \tag{9.68}$$

This algebraic equation has frequently two answers (V_1 and V_2), which leads to two lift coefficients (C_{L1} and C_{L2}). However, there is a flight condition in which the maximum load factor will reach its absolute maximum $\left(n_{\max_{\max}}\right)$. We are interested in airspeed that corresponds to this maximum of the maximum load factor:

$$V_{n_{\max}} = \sqrt{\frac{T_{\max}}{\rho SC_{D_o}}\left[1 \pm \sqrt{1 - \frac{4C_{D_o}Kn_{\max_{\max}}^2W^2}{T_{\max}^2}}\right]} \tag{9.69}$$

An expression for the maximum of the maximum load factor has already been derived in Equation 9.52. Inserting this expression yields

$$V_{n_{\max}} = \sqrt{\frac{T_{\max}}{\rho S C_{D_o}}\left[1 \pm \sqrt{1 - \frac{4C_{D_o}K\left(\frac{T_{\max}}{2W\sqrt{KC_{D_o}}}\right)^2 W^2}{T_{\max}^2}}\right]} \tag{9.70}$$

This is further simplified to

$$V_{n_{\max}} = \sqrt{\frac{T_{\max}}{\rho S C_{D_o}}\left[1 \pm \sqrt{1-1}\right]} \tag{9.71}$$

or

$$V_{n_{\max}} = \sqrt{\frac{T_{\max}}{\rho S C_{D_o}}} \tag{9.72}$$

This expression is quite interesting. The airspeed that corresponds to the maximum of the maximum load factor is only a function of four parameters: (1) altitude, (2) wing area, (3) zero-lift drag coefficient, and (4) maximum engine thrust. This velocity, which is illustrated in Figure 9.10 (Point A), is less than the maximum speed and more than the corner speed.

By using the equations developed in this section, a performance engineer must be able to plot charts and graphical relationships among thrust, airspeed, turn rate, turn radius, bank angle, and altitude for a specific aircraft. These charts help reduce the stress of pilots by reducing their loads, thus making a turning flight safer.

Case Study - Example 9.4

The single-engine General Dynamics (now Lockheed Martin) F-16 Fighting Falcon (Figure 7.6) fighter jet aircraft has the following [9] characteristics:

$$m = 12{,}000\,\text{kg},\ S = 27.87\,\text{m}^2,\ b = 9.96\,\text{m},\ T_{\max} = 127\,\text{kN}$$

Assume: $e = 0.85$, $C_{D_o} = 0.017$ (low subsonic), $C_{D_o} = 0.032$ (transonic), $C_{D_o} = 0.04$ (supersonic), $C_{L_{\max}} = 2$. Note, the given value for the mass is for the aircraft loaded mass, and the given value for engine thrust is for the thrust with an afterburner.

For the sea level, determine

a. Corresponding velocity to the maximum producible load factor
b. Maximum producible load factor
c. Maximum producible bank angle
d. Corner velocity
e. Turn rate, if the aircraft turns with the corner velocity
f. Turn radius, if the aircraft turns with the corner velocity

Solution

We first need to find a few parameters:

$$\text{AR} = \frac{b^2}{S} = \frac{9.96^2}{28.87} = 3.43 \tag{3.9}$$

$$K = \frac{1}{\pi e\,\text{AR}} = \frac{1}{3.14 \times 0.85 \times 3.43} = 0.109 \tag{3.8}$$

a. Corresponding velocity to the maximum producible load factor

We first assume that the velocity lies in the low subsonic regime. So, a C_{D_o} of 0.017 is used:

$$V_{n_{\max}} = \sqrt{\frac{T_{\max}}{\rho S C_{D_o}}} = \sqrt{\frac{127{,}000}{1.228 \times 28.87 \times 0.017}} = 459.6\,\text{m/s} \tag{9.71}$$

However, this magnitude is within is transonic speed region. Thus, the result is not valid, and we need to use another C_{D_o} that is compatible. In the next step, we assume that the velocity lies in the transonic regime. So, a C_{D_o} of 0.032 is used:

$$V_{n_{\max}} = \sqrt{\frac{T_{\max}}{\rho S C_{D_o}}} = \sqrt{\frac{127{,}000}{1.228 \times 28.87 \times 0.032}} = 335\,\text{m/s} \tag{9.71}$$

This is a transonic speed and is acceptable.

b. The maximum producible load factor

Since the corresponding velocity to the maximum producible load factor occurs at the transonic speed, we use C_{D_o} of 0.032

$$n_{\max_{\max}} = \frac{T_{\max}}{2W\sqrt{KC_{D_o}}} = \frac{127{,}000}{2 \times 12{,}000 \times 9.81\sqrt{0.109 \times 0.032}} = 9.14 \tag{9.52}$$

c. The maximum producible bank angle

$$\phi_{\max} = \cos^{-1}\left(\frac{1}{n_{\max_{\max}}}\right) = \cos^{-1}\left(\frac{1}{9.14}\right) = 83.7^\circ \tag{9.39}$$

d. Corner velocity

We again assume that the corner velocity lies in the low subsonic regime. So, a C_{D_o} of 0.017 is used.

$$V^* = \sqrt{\frac{2T_{\max}}{\rho_o S\left[KC_{L\max}^2 + C_{D_o}\right]}} = \sqrt{\frac{2 \times 127{,}000}{1.225 \times 28.87\left[0.109 \times 2^2 + 0.017\right]}} \tag{9.44}$$

$$V^* = 125.9\,\text{m/s} = 244.8\ \text{knot}$$

Our assumption is proved to be true.

e. Turn rate, if the aircraft turns with the corner velocity
The load factor, when the aircraft is turning with the corner velocity, is

$$n_{\max_C} = \frac{\rho_o \left(V^*\right) SC_{L_{\max}}}{2W} = \frac{1.225 \times 125.9^2 \times 28.87 \times 2}{2 \times 12{,}000 \times 9.81} = 4.76 \tag{9.48}$$

$$\omega_{\max_C} = \frac{g\sqrt{n_{\max_C}^2 - 1}}{V^*} = \frac{9.81 \times \sqrt{4.76^2 - 1}}{125.92} = 0.363 \text{ rad/s} = 20.8 \text{ deg/s} \tag{9.50}$$

f. Turn radius, if it turns with the corner velocity:

$$R_{\min_C} = \frac{V^{*2}}{g\sqrt{n_{\max_C}^2 - 1}} = \frac{125.92^2}{9.81 \times \sqrt{4.76^2 - 1}} = 347 \text{ m} \tag{9.51}$$

Example 9.5

A subsonic transport aircraft with a turbofan engine has the following characteristics:

$$m = 120{,}000 \text{ kg},\ S = 245 \text{ m}^2,\ T_{\max \text{SL}} = 300 \text{ kN},$$

$$K = 0.06,\ C_{D_o} = 0.02 \left(\text{low subsonic}\right)$$

The maximum lift coefficient of the aircraft without flap deflection is 1.8. The pilot decides to have a level turn by only using 110 kN of the engine thrust at a 30° bank angle.

a. Determine the airspeeds for this turning flight.
b. What airspeed yields a higher turn rate?
c. What airspeed yields a lower turn radius?

Perform these calculations for two altitudes: (1) sea level, and (2) 30,000 ft.

Solution

We first need to find a few parameters:

$$\left(\frac{L}{D}\right)_{\max} = \frac{1}{2\sqrt{KC_{D_o}}} = \frac{1}{2\sqrt{0.06 \times 0.02}} = 14.4 \tag{5.24}$$

$$n = \frac{1}{\cos\phi} = \frac{1}{\cos(30)} = 1.155 \tag{9.9}$$

1. AT THE SEA LEVEL ($\rho = 1.225$ kg/m)

a. Airspeeds

The quadratic Equation (9.62) has the following solutions for velocities:

$$V = \sqrt{\frac{T}{\rho S C_{D_o}}\left[1 \pm \sqrt{1-\left(\frac{nW}{T(L/D)_{\max}}\right)^2}\right]}$$
$$= \sqrt{\frac{110\times 1{,}000}{1.225\times 245\times 0.02}\times\left[1 \pm \sqrt{1-\frac{(1.155\times 120{,}000\times 9.8)^2}{(110\times 1{,}000\times 14.4)^2}}\right]} \quad (9.67)$$

This results in two answers:

$$V_1 = 166.7 \text{ m/s} \quad \text{and} \quad V_2 = 94 \text{ m/s}$$

We need to inspect and ensure that these airspeeds are greater than the stall speed at this turning flight:

$$V_{s_t} = \sqrt{\frac{2mg}{\rho S C_{L_{\max}} \cos(\phi)}} = \sqrt{\frac{2\times 120{,}000\times 9.81}{1.225\times 245\times 1.8\times \cos(30)}}$$
$$\Rightarrow V_{S_t} = 70.83 \text{ m/s} = 182.8 \text{ knot} \quad (9.12)$$

Both airspeeds (V_1 and V_2) are greater than the stall speed, so both values are acceptable.

b. Turn rate

$$\omega = \frac{g\sqrt{n^2-1}}{V} \quad (9.29)$$

$$\omega_1 = \frac{g\sqrt{n^2-1}}{V_1} = \frac{9.18\sqrt{1.155^2-1}}{166.7} = 0.034 \text{ rad/s} = 1.945 \text{ deg/s} \quad (9.29)$$

$$\omega_2 = \frac{g\sqrt{n^2-1}}{V_2} = \frac{9.18\sqrt{1.155^2-1}}{94} = 0.06 \text{ rad/s} = 3.45 \text{ deg/s} \quad (9.29)$$

Thus, a turn with a lower speed yields a higher turn rate.

c. Turn radius

$$V = R\omega \Rightarrow R = \frac{V}{\omega} \quad (9.28)$$

$$R_1 = \frac{V_1}{\omega_1} = \frac{166.7}{0.034} = 4{,}910.7 \text{ m} = 4.9 \text{ km} \quad (9.28)$$

$$R_2 = \frac{V_2}{\omega_2} = \frac{94}{0.06} = 1{,}562.6\,\text{m} = 1.5\,\text{km} \tag{9.28}$$

It is observed that the turn with the lower airspeed yields a lower turn radius. By comparing the results, we can conclude that at the sea level, it is recommended to turn with the lower speed (94 m/s or 182.8 knots), since it is more efficient.

2. AT 30,000 FT ($\rho = 0.458$ kg/m)

The maximum engine thrust at 30,000 ft is

$$T = T_o\left(\frac{\rho}{\rho_o}\right)^{0.9} = 300 \times \left(\frac{0.458}{1.225}\right)^{0.9} = 123.7\,\text{kN} \tag{4.21}$$

The aircraft engine is producing enough thrust (more than 110 kN).

a. Airspeed
Two new airspeeds at 30,000 ft altitude are

$$V = \sqrt{\frac{110 \times 1{,}000}{0.458 \times 245 \times 0.02} \times \left[1 \pm \sqrt{1 - \frac{(1.155 \times 120{,}000 \times 9.8)^2}{(110 \times 1{,}000 \times 14.4)^2}}\right]} \tag{9.67}$$

This results in two answers:

$$V_1 = 272.7\,\text{m/s} \quad \text{and} \quad V_2 = 153.8\,\text{m/s}$$

Again, we need to inspect and make sure that these speeds are greater than the stall speed at this turning flight and 30,000 ft altitude.

$$V_{S_t} = \sqrt{\frac{2mg}{\rho S C_{L_{\max}} \cos(\phi)}} = \sqrt{\frac{2 \times 120{,}000 \times 9.81}{0.458 \times 245 \times 1.8 \times \cos(30)}} \Rightarrow V_{S_t} = 116\,\text{m/s} = 225.5\,\text{knot} \tag{9.12}$$

Both airspeeds (V_1 and V_2) are greater than the stall speed, so both values are acceptable.

b. Turn rate
The turn rates for these airspeeds are

$$\omega_1 = \frac{g\sqrt{n^2 - 1}}{V_1} = \frac{9.18\sqrt{1.155^2 - 1}}{272.7} = 0.021\,\text{rad/s} = 1.19\,\text{deg/s} \tag{9.29}$$

$$\omega_2 = \frac{g\sqrt{n^2 - 1}}{V_2} = \frac{9.18\sqrt{1.155^2 - 1}}{153.8} = 0.037\,\text{rad/s} = 2.11\,\text{deg/s} \tag{9.29}$$

Thus, a turn with a lower speed yields the higher turn rate.

b. Turn radius

$$R_1 = \frac{V_1}{\omega_1} = \frac{272.7}{0.021} = 13{,}134\,\text{m} = 13.1\,\text{km} \tag{9.28}$$

$$R_2 = \frac{V_2}{\omega_2} = \frac{153.8}{0.037} = 4{,}179\,\text{m} = 4.2\,\text{km} \tag{9.28}$$

It is again observed that, at 30,000 ft altitude, the turn with the lower airspeed yields a lower turn radius. Note that at the sea level, the thrust is about 1/3 of the maximum available engine thrust, while at 30,000, the thrust is about 90% of the maximum available engine thrust. By comparing the results for the sea level and 30,000 ft, we can have a general conclusion applicable for every aircraft. At a high altitude, the turn performance will be reduced; that is, the turn rate is reduced, and the turn radius is increased.

Hence, an aircraft has a lower maneuvering capability at high altitudes. It is worth mentioning that at 30,000 ft, the first airspeed is in high subsonic region ($M = 0.8$). However, at such speeds, C_{D_o} is much higher. This point is neglected in this example. In reality, you need to use a higher value of C_{D_o} for high subsonic speeds.

Case Study - Example 9.6

Consider the twin-turbofan-engine supersonic, combat aircraft McDonnell Douglas (now Boeing) F/A-18 Hornet (Figure 8.10a) with the following [9] characteristics:

$$m = 16{,}770\,\text{kg},\ S = 38\,\text{m}^2,\ b = 12.3\,\text{m},\ T_{\max} = 2 \times 79.2\,\text{kN}$$

Assume the maximum allowable load factor is 10, and $\alpha_o = 0$; $C_{L_\alpha} = 5.1/\text{rad}$; $e = 0.83$, $C_{D_o} = 0.022$ (subsonic), $C_{D_o} = 0.032$ (transonic); $C_{D_o} = 0.042$ (supersonic). The given mass is the aircraft loaded mass and the engine thrust is with the afterburner.

The maximum lift coefficient of the aircraft without using flap is 1.4. Will this fighter be able to turn (coordinated level) at a bank angle of 75° and a 1,000 m of turn radius at 10,000 ft? If so, determine the time that it takes to have a 180° turn (i.e., a half circle).

Solution

To investigate the capability of the aircraft for this turn, we need to inspect the following four items:

1. Is the desired load factor less than the maximum allowable load factor?
2. Is the desired load factor less than the maximum producible load factor?
3. Is the turn airspeed more than the turn stall speed?
4. Does the aircraft generate a sufficient thrust for this turn?

We first need to find the following two parameters:

$$\mathrm{AR} = \frac{b^2}{S} = \frac{12.3^2}{38} = 3.98 \tag{3.9}$$

$$K = \frac{1}{\pi e\,\mathrm{AR}} = \frac{1}{3.14 \times 0.83 \times 3.98} = 0.096 \tag{3.8}$$

At 10,000 ft, the air relative density is 0.738 and the air density is 0.904 kg/m^3. The maximum engine thrust at 10,000 ft is

$$T = T_{\mathrm{SL}}\left(\frac{\rho}{\rho_o}\right)^1 = 2 \times 79.2 \times (0.738)^1 = 116.9\,\mathrm{kN} \tag{4.19}$$

1. Desired load factor is

$$n = \frac{1}{\cos\phi} = \frac{1}{\cos(75)} = 3.86 \tag{9.9}$$

   The desired load factor is less than the maximum allowable load factor (i.e., 10).
2. The maximum producible load factor is

$$n_{\mathrm{max}_{\mathrm{max}}} = \frac{T_{\mathrm{max}}}{2W\sqrt{KC_{D_o}}} = \frac{116.9}{2 \times 16,770 \times 9.81\sqrt{0.096 \times 0.022}} = 7.72 \tag{9.52}$$

   The desired load factor is less than the maximum producible load factor.
3. Turn airspeed

$$\begin{aligned} R &= \frac{V^2}{g\sqrt{n^2-1}} \Rightarrow V = \sqrt{Rg\sqrt{n^2-1}} \\ &= \sqrt{1,000 \times 9.81 \times \sqrt{3.86^2-1}} \Rightarrow V = 191.3\,\mathrm{m/s} \end{aligned} \tag{9.21}$$

   This is a subsonic velocity, so C_{D_o} of 0.022 is used in the calculation of drag.

   The stall speed for this turn is

$$\begin{aligned} V_{S_t} &= \sqrt{\frac{2mg}{\rho S C_{L_{\mathrm{max}}} \cos(\phi)}} \\ &= \sqrt{\frac{2 \times 16,770 \times 9.81}{0.738 \times 1.225 \times 38 \times 1.4 \times \cos(75)}} \Rightarrow V_{S_t} = 162.5\,\mathrm{m/s} \end{aligned} \tag{9.15}$$

   The turn airspeed (191.3 m/s) is greater than the stall speed for this turn (162.5 m/s).

4. Required engine thrust

$$D = \frac{1}{2}\rho V^2 S\left(C_{D_o} + K\left(\frac{2nW}{\rho V^2 S}\right)^2\right) \tag{9.36}$$

$$D = \frac{1}{2}\times 0.904 \times 191.3^2 \times 38\left(0.022 + 0.096\left(\frac{2\times 3.86\times 16{,}770\times 9.81}{0.904\times 191.3^2\times 38}\right)^2\right)$$

$$= 75{,}696\,\text{N} = 75.7\,\text{kN}$$

The lift coefficient

$$C_L = \frac{2nW}{\rho V^2 S} = \frac{2\times 3.86\times 16{,}770\times 9.81}{0.904\times 191.3^2\times 38} = 1.011 \tag{9.11}$$

The aircraft angle of attack

$$C_{L_\alpha} = \frac{dC_L}{d\alpha} \Rightarrow \alpha = \frac{C_L}{C_{L_\alpha}} = \frac{1.011}{5} = 0.202\,\text{rad} = 11.6^\circ \tag{2.10}$$

In a level coordinated turn, the horizontal component of the thrust is equal to the drag

$$T\cos\alpha = D \tag{9.1}$$

The horizontal component of the thrust is

$$T\cos\alpha = 116.9\times\cos(11.6) = 114.5\,\text{kN}$$

The horizontal component of the available engine thrust is more than the required thrust (114.5 > 75.7) for this maneuver.

All four requirements are met. Thus, the fighter aircraft F/A-18 is capable of performing such a maneuver.

The time to complete a half circle is

$$t_{180} = \frac{\pi R}{V} = \frac{3.14\times 1{,}000}{191.3} = 16.4\,\text{s} \tag{9.24}$$

9.4 LEVEL TURN PERFORMANCE: PROP-DRIVEN AIRCRAFT

In this section, we present technique to analyze the turn performance analysis of an aircraft with a prop-driven engine, which includes turboprop engine, piston-prop, and electric engines. Four important turn parameters are: (1) maximum producible load factor, (2) corner velocity, (3) maximum of the maximum load factor, and (4) airspeed that corresponds to the maximum of the maximum load factor. We first begin by rewriting equations that we derived in the previous section and also in Chapter 5, and then, we develop new expressions that govern a level turn. Multiple designs and interesting operational points are also discussed.

9.4.1 Maximum Producible Load Factor

In a level flight (including a level coordinated turn), the relationship between the engine power and aircraft thrust is as follows:

$$P = \frac{TV}{\eta_P} \tag{4.2}$$

Most definitions, concepts, and equations that are presented in Section 9.3 are applicable to prop-driven aircraft. But, because of the presence of the propeller, we need to define new terms and derive new equations.

In an equilibrium condition, as in a level turn, the engine thrust is equal to aircraft drag ($T = D$). Hence:

$$P = \frac{DV}{\eta_P} \tag{9.73}$$

As derived in Section 9.3 (Equation 9.60) and using the definition of the dynamic pressure, the drag for a level turning flight of a prop-driven aircraft can be formulated as

$$D = \frac{1}{2}\rho V^2 S C_{D_o} + \frac{2Kn^2W^2}{\rho V^2 S} \tag{9.74}$$

By substituting this Equation into Equation 9.73, an expression is derived that represents the required power for a level turn at a given airspeed and specific bank angle:

$$P = \frac{1}{2\eta_P}\rho V^3 S C_{D_o} + \frac{2Kn^2W^2}{\rho V S \eta_P} \tag{9.75}$$

This equation implies that in an unaccelerated level turn, the required power is equal to the available engine power. This equation can be solved to find the load factor

$$P\rho V S\eta_P - \frac{1}{2}\rho^2 V^4 S^2 C_{D_o} = 2Kn^2W^2$$

$$\frac{P\rho V S\eta_P}{2KW^2} - \frac{\rho^2 V^4 S^2 C_{D_o}}{4KW^2} = n^2 \Rightarrow n = \sqrt{\frac{P\rho V S\eta_P}{2KW^2} - \frac{\rho^2 V^4 S^2 C_{D_o}}{4KW^2}}$$

or

$$n = \frac{S}{W}\sqrt{\frac{\rho V P \eta_P}{2KS} - \frac{\rho^2 V^4 C_{D_o}}{4K}} \tag{9.76}$$

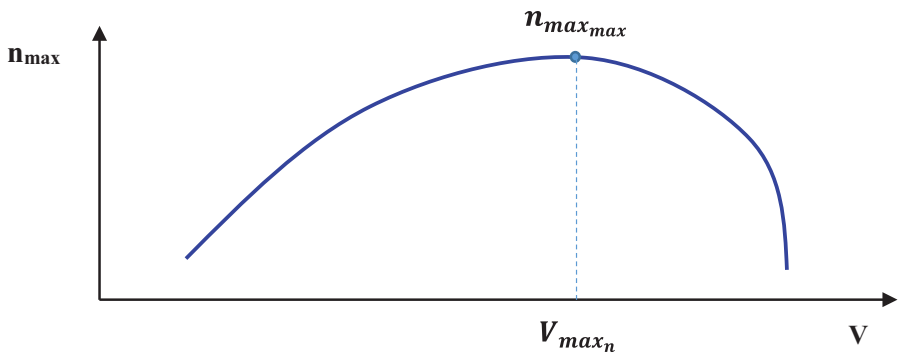

FIGURE 9.11 The variations of the maximum producible load factor versus airspeed.

This equation gives the producible load factor (then, bank angle) for a given velocity and engine power. The maximum value of n is obtained by employing the maximum engine power:

$$n_{\max} = \frac{S}{W}\sqrt{\frac{\rho V P_{\max}\eta_P}{2KS} - \frac{\rho^2 V^4 C_{D_o}}{4K}} \tag{9.77}$$

The maximum producible load factor is a nonlinear function of velocity. The value for $n_{\max}$ is dictated by the design parameters W/S, P, C_{D_o} and altitude (via ρ), and reaches an absolute maximum value at a velocity; this value of $n_{\max}$ represents the maximum of the maximum load factor. This point corresponds to the velocity at which the highest bank angle can be employed in a sustained level turn. Note that $n_{\max}$ attains a value of 1 at the maximum airspeed. Typical variations of $n_{\max}$ versus velocity as calculated from Equation 9.77 are illustrated in Figure 9.11.

9.4.2 Airspeed That Corresponds to the Maximum of the Maximum Load Factor

Equation 9.77 represents the maximum producible load factor as a nonlinear function of velocity. To determine the absolute maximum producible load factor in the case of a prop-driven aircraft, we differentiate Equation 9.80 with respect to airspeed (V) and set it equal to zero (i.e., the zero slope). For simplicity, it is assumed that the propeller efficiency is constant. The differentiation is applied:

$$\frac{dn_{\max}}{dV} = 0 \Rightarrow \frac{d}{dV}\left[\frac{\rho V P_{\max}\eta_P}{2KS} - \frac{\rho^2 V^4 C_{D_o}}{4K}\right]^{\frac{1}{2}} = 0 \tag{9.78}$$

From mathematics, $\frac{du^n}{dx} = n\frac{du}{dx}u^{n-1}$, where $n = 1/2$; hence, the differentiation yields

$$\frac{1}{2}\left[\frac{\rho P_{\max}\eta_P}{2KS} - \frac{4\rho^2 V^3 C_{D_o}}{4K}\right]\left[\frac{\rho V P_{\max}\eta_P}{2KS} - \frac{\rho^2 V^4 C_{D_o}}{4K}\right]^{\frac{1}{2}} = 0$$

The first term (i.e., 1/2) and the last term cannot be zero; hence, the second term must be zero.

$$\frac{\rho P_{\max}\eta_P}{2KS} - \frac{4\rho^2 V^3 C_{D_o}}{4K} = 0 \Rightarrow \frac{P_{\max}\eta_P}{2S} - \rho V^3 C_{D_o} = 0$$

which results in

$$V_{\max_n} = \left[\frac{P_{\max}\eta_P}{2\rho S C_{D_o}}\right]^{\frac{1}{3}} \tag{9.79}$$

The airspeed that corresponds to the absolute maximum producible load factor is directly a function of the maximum engine power and prop efficiency, and inversely a function of altitude, wing area, and zero-lift drag coefficient. This velocity should be greater than the turn stall speed. If the theoretical value is below the turn stall speed, assume the turn stall speed to be the acceptable value for $V_{\max_n}$.

9.4.3 Maximum of the Maximum Load Factor

We are interested to determine the aircraft absolute maximum producible load factor for a prop-driven aircraft. By substituting the airspeed from Equation 9.79 into Equation 9.78, the maximum producible load factor is obtained:

$$n_{\max} = \frac{S}{W}\sqrt{\frac{\rho\left[\frac{P_{\max}\ \eta_P}{2\rho S C_{D_o}}\right]^{\frac{1}{3}} P_{\max}\eta_P}{2KS} - \frac{\rho^2\left[\frac{P_{\max}\ \eta_P}{2\rho S C_{D_o}}\right]^{\frac{4}{3}} C_{D_o}}{4K}} \tag{9.80}$$

This may be simplified into the following short form. The derivation is left to the interested reader.

$$n_{\max_{\max}} = 0.687\left[\frac{\rho\eta_P^2 P_{\max}^2 S(L/D)_{\max}}{KW^3}\right]^{\frac{1}{3}} \tag{9.81}$$

where $(L/D)_{\max}$ is the lift-to-drag ratio (Equation 5.24). This equation allows the calculation of the absolute maximum producible load factor for a prop-driven aircraft. $n_{\max_{\max}}$ is directly a function of maximum engine power and prop efficiency, altitude, wing area, and inversely a function of aircraft weight, zero-lift drag coefficient, and

induced drag factor (K). Recall that in a jet aircraft (Section 9.3), the maximum producible load factor is a function of thrust-to-weight ratio and lift-to-drag ratio.

From Equation 9.39, we conclude that

$$\phi_{\max_{\max}} = \cos^{-1}\left(\frac{1}{n_{\max_{\max}}}\right) \tag{9.82}$$

This is the maximum achievable bank angle at any given speed. An aircraft is unable to employ any bank angle beyond the one that is determined by Equation 9.82. This maximum achievable bank angle sets a fixed limit to the fastest turn and tightest turn, that is, aircraft maneuverability.

9.4.4 Corner Velocity

The corner velocity (V^*) is the airspeed below which $n_{\max}$ is governed by the maximum lift coefficient, rather than the maximum engine power. As per Equation 9.12, as the load factor is increased, the stall speed is increased too, for a level turn. Hence, n cannot be such that the airspeed is below the turn stall speed. Any value of n in which the aircraft encounters the stall speed is not permissible/safe. Thus, the maximum lift coefficient sets a definite limit on the value of n, that is associated with the design aspects of an aircraft. The stall speed in a level turn for a prop-driven aircraft (from Equation 9.12) is determined similarly as in a jet aircraft:

$$V_{S_t} = \sqrt{\frac{2nmg}{\rho S C_{L_{\max}}}} \tag{9.83}$$

The required lift coefficient for a level turn when using the maximum thrust $\left(C_{L_{n_{\max}}}\right)$ should be equal or less than the aircraft maximum lift coefficient:

$$C_{L_{n_{\max}}} \leq C_{L_{\max}} \tag{9.84}$$

Otherwise, the desired turn with the maximum engine power at such a given velocity (often a low speed) is not feasible. In such conditions, the maximum possible load factor is reduced due to the stall limit; so, it is determined by the following expression:

$$n_{\max} = \frac{\rho V^2 S C_{L_{\max}}}{2W} \quad (\text{when } V < V^*) \tag{9.85}$$

Setting the right-hand sides of Equations 9.85 and 9.77 equal to each other, one may determine the airspeed below which the load factor is constrained by stall $\left(C_{L_{\max}}\right)$ rather than the maximum engine power (see Point C in Figure 9.10).

$$\frac{\rho V^2 S C_{L_{\max}}}{2W} = \frac{S}{W}\sqrt{\frac{\rho V P_{\max}\eta_P}{2KS} - \frac{\rho^2 V^4 C_{D_o}}{4K}} \tag{9.86}$$

The derivation will follow. First, an *S/W* is removed from both sides.

$$\frac{\rho V^2 C_{L_{\max}}}{2} = \sqrt{\frac{\rho V P_{\max} \eta_P}{2KS} - \frac{\rho^2 V^4 C_{D_o}}{4K}}$$

Then, both sides are squared.

$$\left(\frac{\rho V^2 C_{L_{\max}}}{2}\right)^2 = \frac{\rho V P_{\max} \eta_P}{2KS} - \frac{\rho^2 V^4 C_{D_o}}{4K}$$

All three terms are multiplied by $4KS$.

$$\rho^2 V^4 C_{L\max}^2 KS = 2\rho V P_{\max} \eta_P - \rho^2 V^4 C_{D_o} S$$

All three terms of the equation are divided by one V.

$$\rho V^3 C_{L_{\max}}^2 KS = 2P_{\max} \eta_P - \rho V^3 C_{D_o} S$$

A V^3 is factored out from two terms.

$$V^3 \left[\rho C_{L_{\max}}^2 KS + \rho C_{D_o} S\right] = 2P_{\max} \eta_P$$

Then, an expression for the corner speed in a level turn in terms of engine power is obtained.

$$V^* = \left[\frac{2P_{\max} \eta_P}{\rho S\left(C_{D_o} + KC_{L_{\max}}^2\right)}\right]^{\frac{1}{3}} \tag{9.87}$$

The corner airspeed is directly a function of the maximum engine power, but is inversely a function of the maximum lift coefficient.

The corner airspeed is the lowest airspeed at which the maximum engine power may be used. Furthermore, the corner speed is the largest possible stall speed in a level turn. It needs to be kept in mind that a level flight with a speed less than the stall speed is not possible. Moreover, the following two required conditions should be checked when using Equations 9.79, 9.80, and 9.87: (1) The flight speed should be above the turn stall speed; that is, the aircraft lift coefficient should be less than the maximum available lift coefficient, and (2) load factor is greater than unity. Any solution satisfying these two conditions is acceptable.

Using Equation 9.85, the corresponding maximum load factor to the corner speed $\left(n_{\max_C}\right)$ is readily determined as

$$n_{\max_C} = \frac{\rho\left(V^*\right)^2 S C_{L_{\max}}}{2W} \tag{9.88}$$

Caution: In deriving Equation 9.87, it is assumed that the corresponding maximum load factor to the corner speed $\left(n_{\max_C}\right)$ is allowed. If the structure is unable to handle such load factor (i.e., the maximum allowable load factor is less than the maximum producible load factor), the corner speed is defined as

$$V^* = \left[\frac{2n_{\max} W}{\rho S C_{L_{\max}}}\right]^{\frac{1}{2}} \tag{9.46}$$

In this case, $n_{\max}$ is a given design parameter and is not calculated. Referring to Equation 9.29, the maximum possible turn rate, when an aircraft turns at the corner speed is

$$\omega_{\max} = \frac{g\sqrt{n_{\max_C}^2 - 1}}{V^*} \tag{9.89}$$

Referring to Equation 9.21, the minimum possible turn radius, when an aircraft turns at the corner speed is

$$R_{\min} = \frac{V^{*2}}{g\sqrt{n_{\max_C}^2 - 1}} \tag{9.90}$$

The maximum possible turn rate and the minimum possible turn radius are very crucial to the aircraft maneuverability.

Case Study - Example 9.7

Consider the single-engine turboprop utility aircraft Cessna 208 Caravan with the following features:

$m_{\text{TO}} = 3{,}995\,\text{kg}, S = 25.9\,\text{m}^2, P = 647\,\text{kW}, b = 15.88\,\text{m}, V_s = 61\,\text{knot}, V_{\max} = 185\,\text{knot}.$

$\text{Assume}: C_{D_o} = 0.038, \eta_P = 0.85, e = 0.9.$

a. Determine the corner speed of the aircraft. Then, determine the corresponding load factor, turn rate, and turn radius.
b. What is the maximum producible load factor in a level turn? Then, determine its corresponding airspeed and bank angle.
c. Assume the aircraft is turning with an airspeed from corner speed to maximum speed. Plot the variations of load factor, bank angle, turn rate, and turn radius.

Assume sea level, constant prop efficiency, and constant zero-lift drag coefficient.

Solution

We first need to find two parameters:

$$\text{AR} = \frac{b^2}{S} = \frac{15.88^2}{25.9} = 9.74 \tag{3.9}$$

$$K = \frac{1}{\pi e \mathrm{AR}} = \frac{1}{3.14 \times 0.9 \times 9.74} = 0.036 \tag{3.8}$$

$$\left(\frac{L}{D}\right)_{\max} = \frac{1}{2\sqrt{KC_{D_o}}} = \frac{1}{2\sqrt{0.036 \times 0.038}} = 13.5 \tag{5.24}$$

a. Corner speed and its corresponding load factor, turn rate, and turn radius

$$C_{L_{\max}} = \frac{2mg}{\rho S V_s^2} = \frac{2 \times 3{,}995 \times 9.81}{1.225 \times 25.9 \times (61 \times 0.514)} = 2.51 \tag{2.27}$$

- Corner speed

$$V^* = \left[\frac{2P_{\max}\eta_P}{\rho S\left(C_{D_o} + KC_{L_{\max}}^2\right)}\right]^{\frac{1}{3}} = \left[\frac{2 \times 647{,}000 \times 0.85}{1.225 \times 25.9 \times \left(0.038 + 0.036 \times (2.51)^2\right)}\right]^{\frac{1}{3}} \tag{9.87}$$

$$= 50.7 \text{ m/s} = 98.5 \text{ knot}$$

- Corresponding load factor

$$n_{\max_C} = \frac{\rho\left(V^*\right)^2 SC_{L_{\max}}}{2W} = \frac{1.225 \times (50.7)^2 \times 25.9 \times 2.51}{2 \times 3995 \times 9.81} = 2.61 \tag{9.88}$$

- Corresponding turn rate

$$\omega_{\max} = \frac{g\sqrt{n_{\max_C}^2 - 1}}{V^*} = \frac{9.81\sqrt{2.61^2 - 1}}{50.7} = 0.466 \text{ rad/s} = 26.7 \text{ deg/s} \tag{9.89}$$

- Corresponding turn radius

$$R_{\min} = \frac{V^{*2}}{g\sqrt{n_{\max_C}^2 - 1}} = \frac{50.7^2}{9.81\sqrt{2.61^2 - 1}} = 108.7 \text{ m} \tag{9.90}$$

b. Maximum producible load and its corresponding airspeed and bank angle

$$n_{\max_{\max}} = 0.687\left[\frac{\rho\eta_P^2 P_{\max}^2 S(L/D)_{\max}}{KW^3}\right]^{\frac{1}{3}}$$

$$= 0.687\left[\frac{1.225 \times 0.85^2 \times 647{,}000^2 \times 25.9 \times 13.5}{0.036 \times (3{,}995 \times 9.81)^3}\right]^{\frac{1}{3}} = 2.68 \tag{9.81}$$

$$V_{\max_n} = \left[\frac{P_{\max}\eta_P}{2\rho SC_{D_o}}\right]^{\frac{1}{3}} = \left[\frac{647{,}000 \times 0.85}{2 \times 1.225 \times 25.9 \times 0.038}\right]^{\frac{1}{3}} = 61.3 \text{ m/s} = 119.3 \text{ knot} \tag{9.79}$$

$$\phi_{\max_{\max}} = \cos^{-1}\left(\frac{1}{n_{\max_{\max}}}\right) = \cos^{-1}\left(\frac{1}{2.68}\right) = 68.1^\circ \tag{9.82}$$

c. Plot (variations of load factor, bank angle, turn rate, and turn radius)

For each airspeed, first Equation 9.77 is used to determine its corresponding maximum load factor

$$n_{\max} = \frac{S}{W}\sqrt{\frac{\rho V P_{\max}\eta_P}{2KS} - \frac{\rho^2 V^4 C_{D_o}}{4K}} \tag{9.77}$$

Then, Equation 9.10 is utilized to determine its corresponding bank angle.

$$\phi_{\max} = \cos^{-1}\left(\frac{1}{n_{\max}}\right) \tag{9.10}$$

Then, Equations 9.29 and 9.21 are employed to determine its corresponding turn rate and turn radius.

$$\omega = \frac{g\sqrt{n_{\max}^2 - 1}}{V} \tag{9.29}$$

$$R = \frac{V^2}{g\sqrt{n_{\max}^2 - 1}} \tag{9.21}$$

Figure 9.12 and Table 9.2 demonstrate the variations of load factor, turn rate, bank angle, and turn radius versus airspeed. As expected, the maximum turn rate and minimum turn radius occur at a corner speed of 98.5 knots. Furthermore, at the maximum speed, the load factor is unity, the turn rate is zero, and the turn radius is infinity. The maximum achievable bank angle is 68.1°.

9.5 MANEUVERABILITY: JET AIRCRAFT

One of the important features of aircraft performance, particularly for fighters, acrobatic aircraft, and missiles, is the maneuvering capability [90]. In an aerial fight between two rival fighters, the winner is the one that has a higher maneuvering performance. In general, the term "maneuver" refers to any change in the flight path. A related topic in this context is the aircraft *agility* [91]. The overall concept of maneuverability for fighters/missiles (i.e., combat performance) is regarded as *agility*. The ability to turn with a speed of Mach 0.9 at 30,000 ft altitude, while pulling 5 g, is one of the significant characteristics of modern fighters. The *agility* is defined as the ability to maneuver rapidly along an arbitrary flight path.

The interested reader can refer to Reference [92] for more information on the history, definitions, and basic concepts in agility. Another related topic is the *supermaneuvrability* [93], which is defined as the "ability to fly in the post-stall regime", which is the domain of flight at high angles of attack (beyond stall angle).

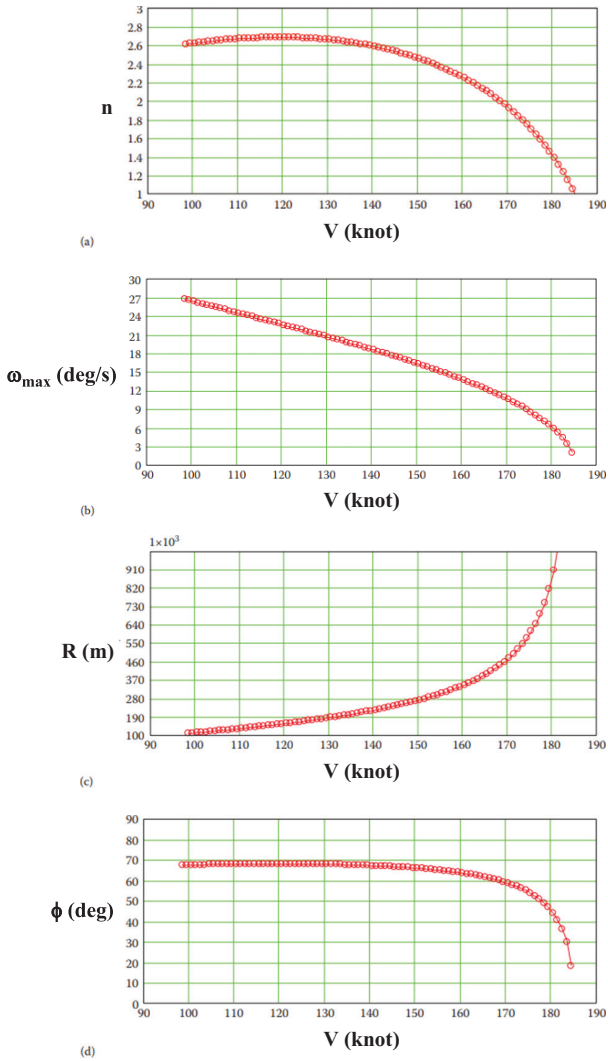

FIGURE 9.12 Variations of load factor, turn rate, bank angle, and turn radius versus airspeed for the aircraft in Example 9.7. (a) Variations of the maximum load factor with velocity. (b) Variations of turn rate with velocity. (c) Variations of turn radius with velocity. (d) Variations of bank angle with velocity.

Two criteria for the evaluation of maneuverability are: (1) fastest turn and (2) tightest turn. These two turns deal with the turn rate and turn radius, respectively. As the turn rate increases, the aircraft is assumed to be more maneuverable. In addition, as the turn radius decreases, the maneuverability increases. The minimum turn radius and maximum turn rate are important performance characteristics for an acrobat/fighter aircraft; they are much less important for a transport or normal GA aircraft.

TABLE 9.2
Turn Performance for the Aircraft in Example 9.7

No.	V (knot)	n_{max}	ϕ (deg)	ω (deg/s)	R (m)	Remarks
1.	98.5	2.61	67.47	26.73	108.6	Corner speed, max turn rate, max turn radius
2.	100	1.62	67.56	26.4	111.4	
3.	110	2.668	67.99	24.5	132	
4.	119.3	2.683	68.11	22.8	154.3	Max load factor, max bank angle
5.	120	2.682	68.1	22.6	156	
6.	130	2.66	67.92	20.7	185	
7.	140	2.591	67.23	18.6	221	
8.	150	2.464	66.05	16.4	269.6	
9.	160	2.26	63.7	13.8	340.9	
10.	170	1.944	59.04	10.7	467.8	
11.	180	1.428	45.5	6.18	857.6	
12.	185	1	0	0	∞	Max speed

When the turn radius is at its minimum value, the turn is referred to as the *tightest turn*. When the turn rate is at its maximum value, the turn is referred to as the *fastest turn*.

Since the representative of a jet engine is thrust (T), and the representative of a prop-driven engine is power (P), the maneuverability analyses of jet aircraft and prop-driven aircraft are presented separately. This section is arranged as follows: Section 9.5.1 is devoted to the fastest turn for jet aircraft, while the tightest turn for jet aircraft is discussed in Section 9.5.2. In contrast, Section 9.6.1 is devoted to analysis of the fastest turn for prop-driven aircraft, while the tightest turn for prop-driven aircraft is discussed in Section 9.6.2.

9.5.1 Fastest Turn: Jet Aircraft

When an aircraft is turning (level coordinated) with the maximum turn rate, the turn is referred to as the *fastest turn*. In fighters, a difference of about few seconds will result in winning a fight. The question in this section is to find out the requirements for the fastest turn. In other words, if a pilot decides to turn with the maximum turn rate, what are the bank angle, turn radius, and engine thrust? In this section, the expressions are derived to determine the maximum turn rate (ω) of a jet aircraft.

Mathematically, the maximum ω (optimum point) is obtained by differentiating Equation 9.29 with respect to airspeed (see Figure 9.13) and setting the derivative equal to zero ($d\omega/dV = 0$). The equation is repeated here for convenience:

$$\omega = \frac{g\sqrt{n^2 - 1}}{V} \tag{9.29}$$

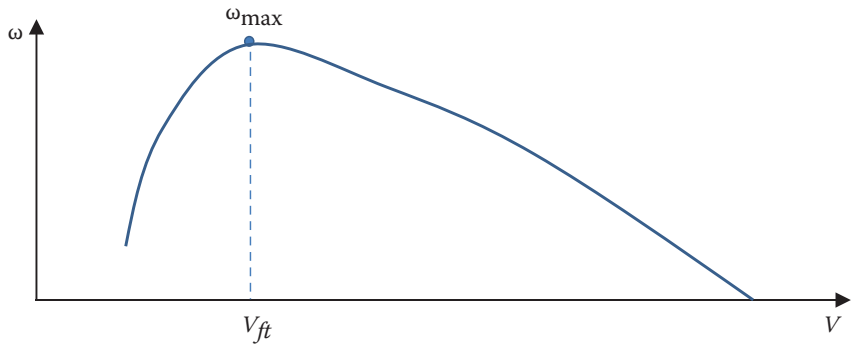

FIGURE 9.13 Variations of the turn rate versus airspeed.

Recall that, there are three limits for the maximum load factor: (1) engine thrust (i.e., maximum producible n), (2) stall (the maximum lift coefficient), and (3) structure (the maximum strength). The maximum ω does not necessarily correspond to $n_{\max}$ or minimum airspeed (V). We are looking for a set of values (n and V) that yield the maximum turn rate ($\omega_{\max}$). At first, we assume that any producible n is allowable and any corresponding velocity is allowed. Later on, we will inspect this condition.

The load factor is a function of engine thrust, aircraft weight, and speed, as shown in Equation 9.37:

$$n = \sqrt{\frac{\rho V^2 S}{2KW^2}\left(T - \frac{1}{2}\rho V^2 S C_{D_o}\right)} \tag{9.37}$$

By squaring both sides of this equation and inserting it into Equation 9.29, we obtain

$$\omega = \frac{g\sqrt{\dfrac{\rho V^2 S}{2KW^2} - \dfrac{\rho^2 V^4 S^2 C_{D_o}}{4KW^2} - 1}}{V}$$

Both numerator and denominator are functions of airspeed. Recall from mathematics, $\dfrac{d}{dx}\dfrac{u}{v} = \dfrac{(du/dx)v - (dv/dx)u}{v^2}$ and $\dfrac{d}{dx}u^k = k\dfrac{du}{dx}u^{k-1}$, where $k = 1/2$. Differentiating the ω with respect to airspeed results in

$$\frac{d\omega}{dV} = \frac{V\dfrac{\dfrac{1}{2}g\left[\dfrac{2\rho VST}{2KW^2} - \dfrac{4\rho^2 V^3 S^2 C_{D_o}}{4KW^2}\right]}{\sqrt{\dfrac{\rho V^2 ST}{2KW^2} - \dfrac{\rho^2 V^4 S^2 C_{D_o}}{4KW^2} - 1}} - g\sqrt{\frac{\rho V^2 ST}{2KW^2} - \frac{\rho^2 V^4 S^2 C_{D_o}}{4KW^2} - 1}}{V^2} = 0$$

The denominator cannot be zero. Thus, the numerator is set equal to zero:

$$V\frac{\frac{1}{2}\left[\frac{\rho VST}{KW^2}-\frac{\rho^2V^3S^2C_{D_o}}{KW^2}\right]}{\sqrt{\frac{\rho V^2ST}{2KW^2}-\frac{\rho^2V^4S^2C_{D_o}}{4KW^2}-1}}-\sqrt{\frac{\rho V^2ST}{2KW^2}-\frac{\rho^2V^4S^2C_{D_o}}{4KW^2}-1}=0$$

Multiplying both terms by the denominator of the first term yields

$$\frac{1}{2}V\left[\frac{\rho ST}{KW^2}-\frac{\rho^2V^3S^2C_{D_o}}{KW^2}\right]-\left[\frac{\rho V^2ST}{2KW^2}-\frac{\rho^2V^4S^2C_{D_o}}{4KW^2}-1\right]=0$$

or

$$\frac{\rho V^2ST}{2KW^2}-\frac{\rho^2V^4S^2C_{D_o}}{2KW^2}-\frac{\rho V^2ST}{2KW^2}-\frac{\rho^2V^4S^2C_{D_o}}{4KW^2}+1=0$$

By canceling the terms that contain T, we obtain

$$-\frac{\rho^2V^4S^2C_{D_o}}{2KW^2}+\frac{\rho^2V^4S^2C_{D_o}}{4KW^2}+1=0\Rightarrow\frac{\rho^2V^4S^2C_{D_o}}{2KW^2}\left(-1+\frac{1}{2}\right)+1=0$$

or

$$\frac{\rho^2V^4S^2C_{D_o}}{4KW^2}=1\Rightarrow V^4=\frac{4KW^2}{\rho^2V^4S^2C_{D_o}}\Rightarrow V^2=\frac{2W}{\rho S}\sqrt{\frac{K}{C_{D_o}}}$$

Hence, the expression for airspeed is

$$V_{\text{ft}}=V_{\omega_{\max}}=\sqrt{\frac{2W}{\rho S}\sqrt{\frac{K}{C_{D_o}}}}=\sqrt{\frac{2W}{\rho S\sqrt{C_{D_o}/K}}} \tag{9.91}$$

This equation yields the airspeed corresponding to the fastest turn. The subscript ft in this equation and other equations in this section stand for the *f*astest *t*urn. The theoretical fastest performance is rarely accessible since it requires an airspeed that is often less than the stall speed. When an aircraft is turning with a velocity less than the corner speed, V^* (from Equation 9.44), while employing the maximum engine thrust, the aircraft will encounter the stall. Hence, any theoretical value of V_{ft} from Equation 9.91 less than V^* is not valid. By comparing this equation with Equation 5.38, it can be concluded that the airspeed for the fastest turn for a jet aircraft is exactly the same as the minimum drag speed in a cruising flight:

$$V_{\text{ft}_{\text{jet}}}=V_{\min_D} \tag{9.92}$$

Note that, the value of V_{ft} from Equation 9.91 or 9.92 is valid only if it is equal to or greater than the corner speed ($V_{ft} \geq V^*$). Otherwise, assume $V_{ft} = V^*$. Referring to Equation 9.44, we obtain

$$V_{ft} = \sqrt{\frac{2T_{max}}{\rho S\left[KC_{L_{max}}^2 + C_{D_o}\right]}} \tag{9.93}$$

By comparing Equations 9.11 and 9.91, the following relationship can be derived:

$$C_{L_{ft}} = n_{ft}\sqrt{\frac{C_{D_o}}{K}} = n_{ft}C_{L_{(L/D)_{max}}} \tag{9.94}$$

where n_{ft} and $C_{L_{ft}}$, respectively, represent the load factor and lift coefficient for the fastest turn flight condition.

Equation 9.94 indicates that the required lift coefficient for the fastest turn is equal to n_{ft} multiplied by the lift coefficient for a maximum lift-to-drag flight condition. Another derivative of Equation 9.94 is as follows:

$$\left(\frac{L}{D}\right)_{ft} = \left(\frac{L}{D}\right)_{max}\left(\frac{2n_{ft}}{1+n_{ft}^2}\right) \tag{9.95}$$

Therefore, the lift-to-drag ratio in the fastest turn is less than the maximum lift-to-drag-ratio by a factor of $\frac{2n_{ft}}{1+n_{ft}^2}$. By substituting V_{ft} from Equation 9.91 into Equation 9.37, we can obtain an expression for the fastest turn load factor (n_{ft}):

$$n = \sqrt{\frac{\rho\left(\frac{2W}{\rho S}\sqrt{K/C_{D_o}}\right)S}{2KW^2}\left(T - \frac{1}{2}\rho\left(\frac{2W}{\rho S}\sqrt{K/C_{D_o}}\right)SC_{D_o}\right)}$$

This can be further simplified as

$$n = \sqrt{\frac{\sqrt{K/C_{D_o}}}{KW}\left(T - W\sqrt{\frac{K}{C_{D_o}}}C_{D_o}\right)}$$

$$= \sqrt{\frac{\sqrt{K/C_{D_o}}}{K}\left(\frac{T}{W} - \sqrt{\frac{K}{C_{D_o}}}C_{D_o}\right)} = \sqrt{\frac{\sqrt{K/C_{D_o}}}{K}\left(\frac{T}{W} - \sqrt{KC_{D_o}}\right)}$$

or

$$n_{ft} = \sqrt{\frac{T_{max}}{W\sqrt{KC_{D_o}}} - 1} \tag{9.96}$$

Equation 9.96 provides an expression for the load factor corresponding to the fastest turn in terms of maximum engine thrust, aircraft weight, and aerodynamic characteristics (i.e., K and C_{D_o}). By comparing n_{ft} and $n_{\max_{\max}}$ (Equation 9.52), one can conclude

$$n_{\text{ft}} = \sqrt{2n_{\max_{\max}} - 1} \tag{9.97}$$

Note that, the value of n_{ft} from this equation is valid only if V_{ft} is equal to or greater than the corner speed ($V_{\text{ft}} \geq V^*$). Otherwise, assume $n_{\text{ft}} = n_{\max_C}$. Referring to Equation 9.45, we get

$$n_{\text{ft}} = \frac{\rho\left(V^*\right)^2 SC_{L_{\max}}}{2W} \tag{9.98}$$

Referring to Equation 9.9, the bank angle corresponding to the fastest turn is

$$\phi_{\text{ft}} = \cos^{-1}\left(\frac{1}{n_{\text{ft}}}\right) \tag{9.99}$$

By definition, the turn rate for the fastest turn (ω_{ft}) is the same as the absolute maximum turn rate ($\omega_{\max}$). Using Equations 9.30 and 9.29, we obtain

$$\omega_{\text{ft}} = \frac{g\tan\left(\phi_{\text{ft}}\right)}{V_{\text{ft}}} = \frac{g\sqrt{n_{\text{ft}}^2 - 1}}{V_{\text{ft}}} \tag{9.100}$$

We can expand Equation 9.100 by inserting n_{ft} and V_{ft} from Equations 9.96 and 9.93 to develop a more general expression for the maximum turn rate:

$$\omega_{\text{ft}} = \frac{g\sqrt{\frac{T_{\max}}{W\sqrt{KC_{D_o}}} - 1 - 1}}{\sqrt{\frac{2W}{\rho S}\sqrt{\frac{K}{C_{D_o}}}}}$$

This can be further simplified to

$$\omega_{\max} = \omega_{\text{ft}} = g\sqrt{\frac{\rho S}{W}\left(\frac{T_{\max}}{KW} - \sqrt{\frac{C_{D_o}}{K}}\right)} \tag{9.101}$$

Note that, the value of ω_{ft} from this equation is valid only if V_{ft} is equal or greater than the corner speed ($V_{\text{ft}} \geq V^*$). Otherwise, assume $\omega_{\text{ft}} = \omega_{\max_C}$. Referring to Equation 9.47, we obtain

$$\omega_{\max} = \omega_{\text{ft}} = \frac{g\sqrt{n_{\max_C}^2 - 1}}{V^*} \tag{9.102}$$

TABLE 9.3
Summary of Equations for the Fastest Turn Parameters

No.	Fastest Turn Parameter	Symbol	If $V_{ft} \geq V^*$	If $V_{ft} < V^*$
1.	Airspeed corresponding to maximum turn rate	V_{ft}	9.91	9.93
2.	Load factor corresponding to maximum turn rate	n_{ft}	9.96	9.98
3.	Maximum turn rate	ω_{ft}	9.100 or 9.101	9.100 or 9.102
4.	Turn rate corresponding to maximum turn rate	R_{ft}	9.103	9.103 or 9.104
5.	Bank angle corresponding to maximum turn rate	ϕ_{ft}	9.99	9.99

From Equation 9.21, the turn radius corresponding to the fastest turn is

$$R_{ft} = \frac{V_{ft}^2}{g\sqrt{n_{ft}^2 - 1}} \tag{9.103}$$

If V_{ft} from Equation 9.91 is less than the corner speed ($V_{ft} < V^*$), referring to Equation 9.47, we obtain

$$R_{ft} = \frac{V^{*2}}{g\sqrt{n_{\max_C}^2 - 1}} \tag{9.104}$$

For majority of modern aircraft, unfortunately, the theoretical airspeed for fastest turn (V_{ft}) is less than the stall speed (V_s). In other words, their corresponding lift coefficient ($C_{L_{ft}}$) is higher than the maximum available lift coefficient ($C_{L_{max}}$).

Table 9.3 provides a summary of equations for the fastest turn parameters. As the table demonstrates, there are two sets of equations for each parameter: (1) one set for the case where $V_{ft} \geq V^*$, and (2) one set for the case where $V_{ft} < V^*$. Therefore, before you determine the maximum turn rate, you need to calculate the V_{ft} and corner speed (V^*) to compare. The value of V_{ft} is initially determined by Equation 9.91.

Now, we can draw a few conclusions to optimize a jet aircraft for the goal of improving the fastest turn performance; both on the operational side and on the design side. Equations 9.91–9.104 are clear indications of the roles of each aircraft parameter in aircraft maneuverability. We can have several interesting conclusions that help the designers to modify an aircraft to optimize the turn performance. To improve the fastest turn, one must

1. Increase engine thrust (T_{max}).
2. Reduce aircraft weight (W). A fighter usually has about 85% of its maximum takeoff weight in a fighting mission. This is when the stores are released and 50% of the fuel is consumed.
3. Increase wing area (S).
4. Decrease induced drag factor (K). This implies an increase in the wing aspect ratio (AR).
5. Reduce zero-lift drag coefficient (C_{D_o}) by increasing aerodynamic efficiency of the aircraft.

6. Fly at low altitude (to have a high ρ).
7. Increase the allowable load factor by strengthening the structure and by wearing g-suit by pilots.

It is interesting to note for a pilot that, for achieving the fastest turn, he/she should not increase both bank angle and airspeed, but the fastest turn is happening only at a specific bank angle and a specific airspeed.

As seen in Figure 9.10, between point C and point B, there is a point D, which is interesting in some turning flight cases. At this point, the aircraft is employing the maximum lift coefficient, while utilizing a fraction of the maximum thrust. The aircraft is flying with a velocity that is slower than the corner speed. The turn rate at this point is frequently less than the maximum turn rate. In some special cases, the turn rate at this point may be slightly greater compared with a turn when flown with the corner speed.

In current modern fighters, we notice all seven conditions except high AR and high wing area. The reason for low AR (of about 2–3) in modern fighters is the requirements such as roll control, structural consideration, low weight, and also aerodynamic considerations in supersonic flight. In addition, a high wing area is not practical; because an increase in the wing area will reduce the roll rate (i.e., roll control), control power, and maneuverability. Although a higher wing area leads to a higher turn rate, but, powerful engines and low zero-lift drag coefficient will compensate for this deficiency.

Equations 9.101 and 9.102 imply that, to have the fastest turn, the pilot must fly at a low altitude and also fly at a low speed. The aerial engagement usually begins at a speed of Mach 1.5–2 at a high altitude (50,000–60,000 ft). But a fighter pilot tries to reduce the airspeed and altitude to win the fight and target the enemy aircraft. The lowest limit of altitude for a fighter to execute a turn is the required height to recover (pull-up) from a dive safely in the maneuver.

Case Study - Example 9.8

Analyze the fastest turn performance for the fighter aircraft McDonnell Douglas (now Boeing) F/A-18 Hornet (Figure 8.10a) at sea level and 50,000 ft altitude (i.e., determine the maximum turn rate).

a. What are the load factor, bank angle, airspeed, and turn radius for this turn?
b. Determine the time required to cover a half circle (180°).

The characteristics of this aircraft are given in Example 9.6.

Solution

From Example 9.6, $m = 16{,}770\,\text{kg}$, $S = 38\,\text{m}^2$, $b = 12.3\,\text{m}$, $T_{\max} = 2 \times 79.2$ kN, $e = 0.83$, $C_{L_{\max}} = 1.4$, $C_{D_o} = 0.022$ (subsonic), $C_{D_o} = 0.032$ (transonic); $C_{D_o} = 0.042$ (supersonic), AR = 3.98, $K = 0.096$.

1. SEA LEVEL ($\rho = 1.225\,kg/m^3$)

We assume that the airspeed for the fastest turn is subsonic, so a C_{D_o} of 0.022 is used. If this assumption turns out to be false, it will be changed accordingly. We first need to compare the corner speed and the airspeed corresponding to the fastest turn:

$$V_{ft} = \sqrt{\frac{2W}{\rho S}}\sqrt{\frac{K}{C_{D_o}}} = \sqrt{\frac{2\times 16{,}770\times 9.81}{1.225\times 38}}\sqrt{\frac{0.096}{0.022}} \Rightarrow V_{ft} = 58.1\,m/s = 112.9\,knot \tag{9.91}$$

$$V^* = \sqrt{\frac{2T_{max}}{\rho_o S\left[KC_{L\max}^2 + C_{D_o}\right]}} \tag{9.87}$$

$$V^* = \sqrt{\frac{2\times 127{,}000}{1.225\times 28.87\left[0.109\times 1.4^2 + 0.022\right]}} \Rightarrow V^* = 179.7\,m/s = 349.3\,knot$$

since $V_{ft} < V^*$, from Equation 9.93, we consider $V_{ft} = V^* = 179.7$ m/s = 349.3 knot. According to Table 9.3, the equations in the fifth column are used.

Since the airspeed for fastest turn is subsonic, a C_{D_o} of 0.022 is kept.

- Load factor

$$n_{ft} = \frac{\rho\left(V^*\right)^2 SC_{L_{max}}}{2W} = \frac{1.225\times(179.7)^2\times 38\times 1.4}{2\times 16{,}770\times 9.81} = 6.4 \tag{9.98}$$

- Turn rate

$$\omega_{ft} = \frac{g\sqrt{n_{ft}^2 - 1}}{V_{ft}} = \frac{9.81\times\sqrt{6.4^2 - 1}}{179.7} = 0.345\,rad/s = 19.8\,deg/s \tag{9.100}$$

- Turn radius

$$R_{ft} = \frac{V_{ft}^2}{g\sqrt{n_{ft}^2 - 1}} = \frac{179.7^2}{9.81\times\sqrt{6.4^2 - 1}} = 521\,m \tag{9.103}$$

- Bank angle

$$\phi_{ft} = \cos^{-1}\left(\frac{1}{n_{ft}}\right) = \cos^{-1}\left(\frac{1}{6.4}\right) = 81^\circ \tag{9.99}$$

TABLE 9.4
A Comparison between Fastest Turn Performances of F/A-18 at Two Altitudes

Altitude	V (knot)	n	ϕ (deg)	ω (deg/s)	R (m)	t (s)
Sea level	349.3	6.4	81	19.8	521	9.1
50,000 ft	371	1.1	25.2	1.39	7,876	129.6

- Time required to cover a half circle

$$t = \frac{\pi R}{V} = \frac{3.14 \times 521}{179.1} = 9.1\,\text{s} \tag{9.24}$$

2. 15,000 ft

At an altitude of 50,000 ft, the air density ratio is 0.153 and the air density is 0.188 kg/m^3. The maximum engine thrust at this altitude is reduced to 24.2 kN (about an 85% reduction). The same calculations are repeated for this altitude. The results are shown in Table 9.4 for comparison.

It is observed that the fastest turn performance is extremely reduced at 50,000 ft altitude. Note that the C_{D_o} of the aircraft at 15,000 ft is slightly different from that for sea level. We intentionally ignored it for the sake of simplicity.

9.5.2 Tightest Turn: Jet Aircraft

Another important criterion for the evaluation of maneuverability of an aircraft is its ability to turn in the shortest possible radius. As this radius is shorter, the aircraft is considered to be more maneuverable. The turn with the shortest radius is referred to as the *tightest turn*. This is another aspect of level-turn performance analysis. In this section, the expressions are developed to determine the minimum turn radius for a jet aircraft.

We begin our analysis with Equation 9.21, which indicates that the turn radius is a function of airspeed and load factor:

$$R = \frac{V^2}{g\sqrt{n^2 - 1}} \tag{9.21}$$

Furthermore, the load factor is a function of airspeed as shown in Equation 9.37:

$$n = \sqrt{\frac{\rho V^2 S}{2KW^2}\left(T - \frac{1}{2}\rho V^2 S C_{D_o}\right)} \tag{9.37}$$

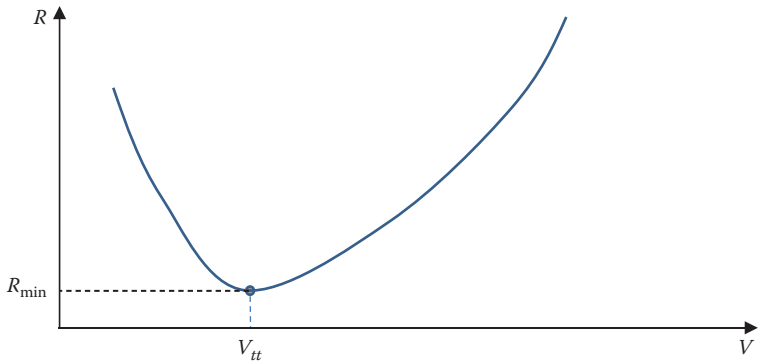

FIGURE 9.14 Variations of the turn radius versus airspeed.

Squaring both sides of this equation and plugging it into Equation 9.24 yields

$$R = \frac{V^2}{g\sqrt{\frac{\rho V^2 S}{2KW^2}\left(T - \frac{1}{2}\rho V^2 S C_{D_o}\right) - 1}} \tag{9.105}$$

Mathematically, the minimum radius (optimum point) is obtained by differentiating Equation 9.105 with respect to airspeed (see Figure 9.14) and set the derivative equal to zero:

$$\frac{dR}{dV} = \frac{d}{dV}\left(\frac{V^2}{g\sqrt{\frac{\rho V^2 S}{2KW^2}\left(T - \frac{1}{2}\rho V^2 S C_{D_o}\right) - 1}}\right) = 0 \tag{9.106}$$

Both numerator and denominator are functions of airspeed. Recall from mathematics that $\frac{d}{dx}\frac{u}{v} = \frac{(du/dx)v - (dv/dx)u}{v^2}$ and $\frac{d}{dx}v^k = k\frac{dv}{dx}v^{k-1}$, where $k = 1/2$. Differentiating the R with respect to airspeed results in

$$\frac{dR}{dV} = \frac{2Vg\sqrt{\frac{\rho V^2 ST}{2KW^2} - \frac{\rho^2 V^4 S^2 C_{D_o}}{4KW^2} - 1} - V^2 \frac{\frac{1}{2}g\left[\frac{2\rho VST}{2KW^2} - \frac{4\rho^2 V^3 S^2 C_{D_o}}{4KW^2}\right]}{\sqrt{\frac{\rho V^2 ST}{2KW^2} - \frac{\rho^2 V^4 S^2 C_{D_o}}{4KW^2} - 1}}}{g^2\left[\frac{\rho V^2 ST}{2KW^2} - \frac{\rho^2 V^4 S^2 C_{D_o}}{4KW^2} - 1\right]} = 0 \tag{9.107}$$

The denominator cannot be zero. Thus, the numerator is set equal to zero:

$$2Vg\sqrt{\frac{\rho V^2 ST}{2KW^2}-\frac{\rho^2 V^4 S^2 C_{D_o}}{4KW^2}-1}-V^2\frac{\frac{1}{2}g\left[\frac{\rho VST}{KW^2}-\frac{\rho^2 V^3 S^2 C_{D_o}}{KW^2}\right]}{\sqrt{\frac{\rho V^2 ST}{2KW^2}-\frac{\rho^2 V^4 S^2 C_{D_o}}{4KW^2}-1}}=0$$

Canceling one V from both terms and multiplying both terms by the denominator of the second term yield

$$2g\left[\frac{\rho V^2 ST}{2KW^2}-\frac{\rho^2 V^4 S^2 C_{D_o}}{4KW^2}-1\right]-V\left[\frac{1}{2}g\left[\frac{\rho VST}{KW^2}-\frac{\rho^2 V^3 S^2 C_{D_o}}{KW^2}-1\right]\right]=0$$

or

$$\frac{g\rho V^2 ST}{KW^2}-\frac{g\rho^2 V^4 S^2 C_{D_o}}{2KW^2}-2g-\frac{g\rho V^2 ST}{2KW^2}+\frac{g\rho^2 V^4 S^2 C_{D_o}}{2KW^2}=0$$

The second and the fifth terms are canceled out. Thus,

$$\frac{g\rho V^2 ST}{KW^2}-2g-\frac{g\rho V^2 ST}{2KW^2}=0\Rightarrow\left[\frac{g\rho V^2 ST}{KW^2}\right]\left(1-\frac{1}{2}\right)=2g\Rightarrow V^2=\frac{4KW^2}{\rho ST}$$

Hence, the expression for airspeed is obtained:

$$V_{\text{tt}}=V_{R_{\min}}=\sqrt{\frac{4KW^2}{\rho ST_{\max}}} \tag{9.108}$$

This equation gives the airspeed corresponding to the **t**ightest **t**urn (thus, the subscript tt). The theoretical tightest performance is rarely accessible since it requires an airspeed that is often less than the stall speed. When an aircraft is turning with a velocity less than the corner speed, V^* (from Equation 9.44), while employing the maximum engine thrust, the aircraft will encounter the stall. Hence, any theoretical value of V_{tt} from Equation 9.108 – if it is less than V^* - is not valid. Note that, the value of V_{ft} from Equation 9.108 is valid only if it is equal to or greater than the corner speed ($V_{\text{tt}}\geq V^*$). Otherwise, assume $V_{\text{tt}}=V^*$. Then, referring to Equation 9.44, we obtain

$$V_{\text{tt}}=\sqrt{\frac{2T_{\max}}{\rho S\left[KC_{L\max}^2+C_{D_o}\right]}} \tag{9.109}$$

Recall that $C_{L_{\max}}$ is the maximum lift coefficient during a level turn. Note that, the maximum lift coefficient of a fighter during an aerial fight is not the same as in a cruising flight because the full deflection of high-lift devices is not practical in such

a situation. Furthermore, the maximum lift coefficient at higher speeds is less than the maximum lift coefficient at lower speeds. Hence, the maximum lift coefficient for fighters that have a simple flap is just 1–1.2, and for fighters with an advanced flap, it is about 1.2–1.6.

By substituting V_{tt} from Equation 9.108 into Equation 9.37, we can obtain an expression for the tightest turn load factor (n_{tt}):

$$n_{tt} = \sqrt{\rho\frac{4KW^2}{\rho ST}\frac{S}{2KW^2}\left(T - \frac{1}{2}\rho\frac{4KW^2}{\rho ST}SC_{D_o}\right)}$$

$$= \sqrt{\frac{2}{T}\left(T - \frac{2KW^2C_{D_o}}{T}\right)} = \sqrt{2\left(1 - \frac{KW^2C_{D_o}}{T^2}\right)}$$

This can be further simplified as

$$n_{tt} = \sqrt{2 - \frac{4KC_{D_o}}{\left(T_{max}/W\right)^2}} \tag{9.110}$$

The magnitude of the second term on the right-hand side of this equation is much smaller than 2. An approximation to this equation is to drop that term:

$$n_{tt} \approx \sqrt{2} = 1.414 \tag{9.111}$$

The maximum theoretical value of load factor for the case of the tightest turn cannot exceed $\sqrt{2}$, which is 1.414. This conclusion, and the value of n_{tt} from this equation, is valid only if V_{tt} is equal to or greater than the corner speed ($V_{tt} \geq V^*$). Otherwise, assume $n_{tt} = n_{max_C}$. Then, referring to Equation 9.45, the accessible n_{tt} is given by

$$n_{tt} = \frac{\rho(V^*)^2 SC_{L_{max}}}{2W} \tag{9.112}$$

Referring to Equation 9.9, the bank angle corresponding to the tightest turn is

$$\phi_{tt} = \cos^{-1}\left(\frac{1}{n_{tt}}\right) \tag{9.113}$$

In case where the V_{tt} from Equation 9.108 is equal or greater than the corner speed ($V_{tt} \geq V^*$), the maximum theoretical value for the bank angle corresponding to the tightest turn will be

$$\phi_{tt} \approx \cos^{-1}\left(\frac{1}{1.414}\right) \approx 45° \tag{9.114}$$

By definition, the turn radius for the tightest turn (R_{tt}) is the same as the absolute minimum (shortest) turn radius (R_{min}). Using Equation 9.21, we obtain

$$R_{tt} = R_{min} = \frac{V_{tt}^2}{g\sqrt{n_{tt}^2 - 1}} \tag{9.115}$$

We can expand Equation 9.115 by inserting n_{tt} and V_{tt} from Equations 9.110 and 9.108 to develop a more general expression for the minimum turn radius:

$$R_{tt} = \frac{\dfrac{4KW^2}{\rho ST}}{g\sqrt{\left(\sqrt{2}\right)^2 - 1}}$$

which can be simplified to

$$R_{tt} = R_{min} = \frac{4Km^2}{g\rho ST_{max}} \tag{9.116}$$

The theoretical value of R_{tt} from this equation is valid, only if the V_{tt} from Equation 9.108 is equal or greater than the corner speed ($V_{tt} \geq V^*$). Otherwise, use Equation 9.115.

Now, we can draw a few conclusions to optimize a jet aircraft for the goal of improving the tightest turn performance and fastest turn performance, both on the operational side and on the design side. Equations 9.108–9.116 are clear indications of the role of each aircraft parameter on aircraft maneuverability. Equation 9.116 implies that to reduce the shortest radius, one must perform the following:

1. Increase the engine thrust (T).
2. Increase thrust-to-weight ratio (T/W).
3. Decrease aircraft weight (W).
4. Increase wing area (S).
5. Increase wing loading (W/S).
6. Decrease induced drag factor (K). This means that the AR and Oswald span efficiency factor (e) must be increased.
7. Increase $C_{L_{max}}$ by selecting powerful high-lift devices such as triple slotted flap.
8. Decrease stall speed (V_s).
9. Decrease zero-lift drag coefficient (C_{D_o}).

In addition, Equation 9.115 also implies that

10. The pilot must fly at a low speed.
11. The pilot must fly at a low altitude (high ρ).

In practice, the design parameters such as aircraft weight, engine thrust, wing span, wing AR, and wing area are governed by multiple requirements. Hence, the design is always a compromise. For instance, the wing loading is mainly dictated by landing/stall speed, rather than the fastest turn. Furthermore, the wing AR is more dictated by roll rate, rather than by the minimum turn radius. In addition, the thrust-to-weight ratio is mainly dictated by the maximum speed, rather than the turn performance requirements. Therefore, the combat region for a supersonic fighter is usually in the subsonic range.

Note that, the value of $R_{\min}$ from Equation 9.116 is valid only if V_{tt} is equal or greater than the corner speed ($V_{tt} \geq V^*$). Otherwise, assume $V_{tt} = V^*$. Then, referring to Equation 9.115, we obtain

$$R_{tt} = R_{\min} = \frac{V^{*2}}{g\sqrt{\left(\frac{\rho(V^*)^2 S C_{L_{\max}}}{2W}\right)^2 - 1}} \tag{9.117}$$

From Equations 9.29 and 9.30, the turn rate corresponding to the tightest turn is

$$\omega_{tt} = \frac{g\tan(\phi_{tt})}{V_{tt}} = \frac{g\sqrt{n_{tt}^2 - 1}}{V_{tt}} \tag{9.118}$$

For the majority of current aircraft, unfortunately, the theoretical airspeed for the tightest turn (V_{tt}) is less than the stall speed (V_s). In other words, their corresponding lift coefficient ($C_{L_{tt}}$) is higher than the maximum available lift coefficient ($C_{L_{\max}}$). Table 9.5 provides a summary of equations for the tightest turn parameters. As the table demonstrates, there are two sets of equations for each parameter: (1) one set for the case where $V_{tt} \geq V^*$, and (2) one set for the case where $V_{tt} < V^*$. Therefore, before you determine the minimum turn radius, you need to calculate the V_{tt} and corner speed (V^*) and compare them. The value of V_{tt} initially is determined by Equation 9.108.

If the theoretical magnitudes of airspeed for the tightest and fastest turn are less than the corner speed, both the tightest and fastest turns have a similar performance. The reason is that in both cases, the turn will be conducted with the corner speed and the same bank angle. Hence, both the fastest turn and tightest turn are usually

TABLE 9.5
Summary of Equations for the Tightest Turn Parameters

No.	Tightest Turn Parameter	Symbol	If $V_{tt} \geq V^*$	If $V_{tt} < V^*$
1.	Airspeed corresponding to minimum turn radius	V_{tt}	9.108	9.109
2.	Load factor corresponding to minimum turn radius	n_{tt}	9.110	9.112
3.	Turn rate corresponding to minimum turn radius	ω_{tt}	9.118	9.118
4.	Minimum turn radius	R_{tt}	9.115 or 9.116	9.115 or 9.116
5.	Bank angle corresponding to minimum turn radius	ϕ_{tt}	9.113	9.113

performed by using the maximum engine thrust and a speed close to stall speed. The theoretical airspeed for the tightest turn is usually less than the stall speed. In practice, there are two practical solutions to use theoretical airspeed:

1. By using modern high-lift devices such as triple-slotted flap, the maximum lift coefficient can be increased. However, this solution will increase aircraft zero-lift drag coefficient, so this solution is not practical.
2. Increase flight altitude, such that the required lift coefficient is equal to the maximum lift coefficient.

Therefore, the maximum lift coefficient is an important parameter for aircraft maneuverability. As this parameter is higher, that is, the stall speed is lower, the aircraft has a higher performance in maneuver.

As seen in Figure 9.10, between point C and point B, there is a point D, which is interesting in some turning flight cases. At this point, the aircraft employs the maximum lift coefficient, while utilizing a fraction of the maximum thrust. The aircraft is flying with a velocity that is slower than the corner speed. The turn radius at this point is frequently more than the minimum turn radius. In some special cases, the turn radius at this point may be slightly lower, compared with a turn when flown with the corner speed (Figure 9.10).

There are few advanced fighters [93] that are capable of flight with an angle of attack higher than the stall angle and fly beyond the stall (e.g., F-18/E, F-22, Su-33). This indicates that they are flying at an angle of attack that is much higher than the angle of attack corresponding to stall (*advent of supermaneuverability*). This operation is referred to as *super stall*. The Russian experimental single-seat supermaneuverable jet fighter Sukhoi Su-37 is an example. The Sukhoi Su-37 has two powerful turbofan engines [94], each generating 145 kN of thrust with afterburner. A flight with an angle of attack close to 40° is not imaginable, but with the help of very powerful jet engines, it has been practiced. So, we should not be concerned about the impracticality of some of our derived equations and their limited applications.

Another advanced fighter is the Lockheed Martin Joint Strike Fighter F-35 Lightning II (Figure 5.5) and it is a strike fighter plane [95,96] being procured in different versions for the Air Force, Marine Corps, and Navy. The F-35 program is the Department of Defense's largest weapon procurement program in terms of total estimated acquisition cost. This all-weather stealth multirole fighter, a fifth-generation strike fighter, was designed to replace the U.S. Air Force F-16s, Navy and Marine Corps F/A-18s, and Marine AV-8s. This fighter has a wing loading of 7,314 N/m^2 and a thrust-to-weight ratio of 0.87. The aerodynamic limits and structural limits reduce the maneuverability of an aircraft, and only the propulsion system and high-lift devices can expand these limits. Figure 9.15 illustrates nine acrobatic jet Aermacchi MB-339PAN aircraft in a flight maneuver that involves a fastest turn flight.

Figure 9.16 shows a typical relationship between the turn radius and airspeed during a turn. It demonstrates the impact of structural and aerodynamic limits on turn performance. The intersection between two limits is usually the corner speed or maneuvering speed. Figure 9.17 illustrates the variations of several airspeeds with altitude. It is observed that almost all of these speeds coincide at the absolute ceiling.

FIGURE 9.15 Nine acrobatic Aermacchi MB-339PAN aircraft in a turning flight maneuver. (Courtesy of Steve Dreier.)

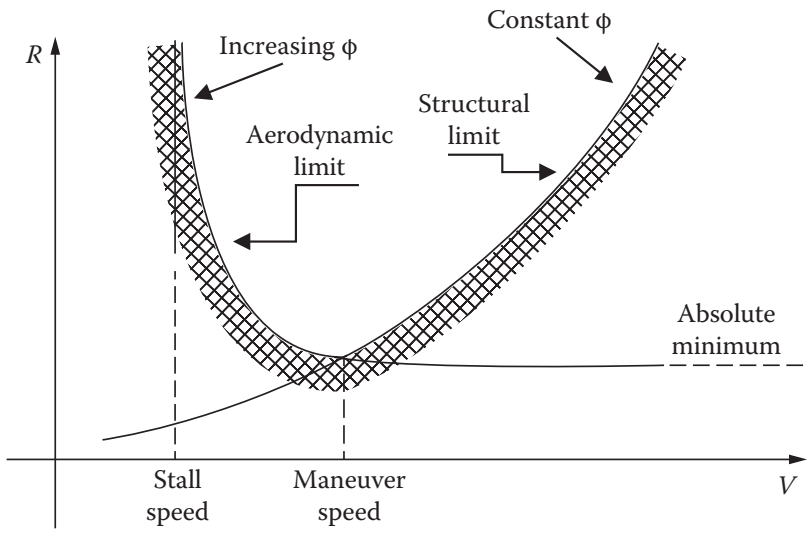

FIGURE 9.16 Typical aerodynamics and structural limit on turn performance.

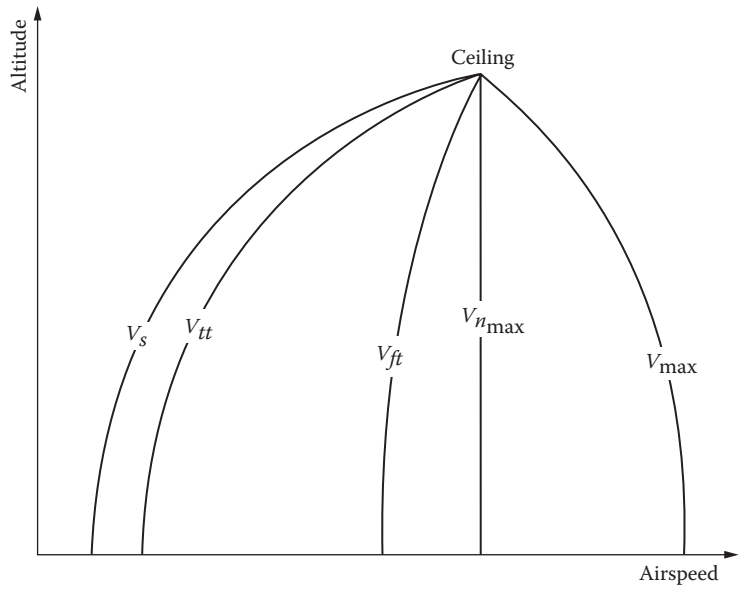

FIGURE 9.17 Variations of several airspeeds versus altitude.

Example 9.9

A jet fighter aircraft has the following characteristics:

$$m_{\text{TO}} = 25{,}000\ \text{kg},\ \ S = 40\,\text{m}^2,\ T_{\max} = 100\,\text{kN}, C_{D_o} = 0.014; b = 9\,\text{m}, C_{L_{\max}} = 1.3$$

$$\text{e} = 0.7;$$

Analyze the performance of the aircraft for the tightest turn at two flight conditions for sea level:

1. Theoretical solutions (i.e., application of the maximum engine thrust).
2. Turn with a speed that is 90% of the corner speed but having the maximum lift coefficient (i.e., point D in Figure 9.10).

Solution

We first need to find two parameters:

$$\text{AR} = \frac{b^2}{S} = \frac{9^2}{40} = 2.025 \tag{3.9}$$

$$K = \frac{1}{\pi e\,\text{AR}} = \frac{1}{3.14 \times 0.7 \times 2.025} = 0.225 \tag{3.8}$$

1. Application of the maximum engine thrust

$$V_{tt} = \sqrt{\frac{4KW^2}{\rho S T_{max}}} = \sqrt{\frac{4 \times 0.225 \times (25{,}000 \times 9.81)^2}{1.225 \times 40 \times 100{,}000}} = 104.97\,\text{m/s} = 204\,\text{knot} \quad (9.108)$$

$$V^* = \sqrt{\frac{2T_{max}}{\rho_o S\left[KC_{L_{max}}^2 + C_{D_o}\right]}} = \sqrt{\frac{2 \times 100{,}000}{1.225 \times 40\left[0.225 \times 1.3^2 + 0.014\right]}} = 101.8\,\text{m/s} = 198\,\text{knot} \quad (9.87)$$

V_{tt} is slightly greater than the corner speed ($V_{tt} \geq V^*$). So, we use the equations in the fourth column of Table 9.5.

$$n_{tt} = \sqrt{2 - \frac{4KC_{D_o}}{(T_{max}/W)^2}} = \sqrt{2 - \frac{4 \times 0.225 \times 0.014}{(100{,}000/25{,}000 \times 9.81)^2}} = 1.387 \quad (9.110)$$

$$\phi_{tt} = \cos^{-1}\left(\frac{1}{n_{tt}}\right) = \cos^{-1}\left(\frac{1}{1.387}\right) = 43.87° \quad (9.113)$$

$$R_{tt} = R_{min} = \frac{V_{tt}^2}{g\sqrt{n_{tt}^2 - 1}} = \frac{104.97^2}{9.81\sqrt{1.387^2 - 1}} = 1168.6\,\text{m} \quad (9.118)$$

Equation 9.116 yields the same value for the minimum radius.

2. Turn with a speed that is 90% of the corner speed but having the maximum lift coefficient.

   The new speed would be

$$V = 0.9V^* = 0.9 \times 101.8 = 91.66\,\text{m/s}$$

When $V < V^*$, but having the maximum lift coefficient, the load factor is

$$n = \frac{\rho V^2 S C_{L_{max}}}{2W} = \frac{1.225 \times 91.66^2 \times 40 \times 1.3}{2 \times 25{,}000 \times 9.81} = 1.091 \quad (9.42)$$

The bank angle would be

$$\phi = \cos^{-1}\left(\frac{1}{n}\right) = \cos^{-1}\left(\frac{1}{1.091}\right) = 23.6° \quad (9.9)$$

The turn radius would be

$$R = \frac{V^2}{g\sqrt{n^2 - 1}} = \frac{91.66^2}{9.81\sqrt{1.091^2 - 1}} = 1{,}958\,\text{m} \quad (9.21)$$

This turn radius is *40.3% longer* than the minimum turn radius. A reduction in the airspeed requires a reduction in the engine thrust.

$$T = D = \frac{1}{2}\rho V^2 S\left(C_{D_o} + KC_{L_{\max}}^2\right) \tag{9.35}$$

$$T = \frac{1}{2}\times 1.225 \times 91.66^2 \times 40 \times \left(0.014 + 0.225 \times 1.3^2\right) = 81{,}000N = 81\ kN$$

This thrust is 81% of the maximum engine thrust.

9.6 MANEUVERABILITY: PROP-DRIVEN AIRCRAFT

In this section, the maneuverability of propeller-driven aircraft is presented, which includes aircraft with engines such as turboprop, piston-prop, and electric engines. Two primary maneuverability criteria are (1) fastest turn and (2) tightest turn. These two cases are dealt separately. The fundamentals and concepts behind these two cases have been described in Section 9.5, so they are not repeated here. Recall that, in a prop-driven engine, the engine provides shaft power (P), but the propeller will convert it to an available thrust (T).

9.6.1 Fastest Turn: Prop-Driven Aircraft

In a prop-driven aircraft, similar to a jet aircraft, the fastest turn is a level turn in which the turn rate (ω) is the highest ($\omega_{\max}$). To find an expression for the maximum turn rate, we differentiate Equation 9.29 with respect to airspeed and set it equal to zero:

$$\omega = \frac{g\sqrt{n^2 - 1}}{V} \tag{9.29}$$

We are looking for a set of values (n and V) that yields the maximum turn rate ($\omega_{\max}$). At first, we assume any producible n is allowable and any corresponding velocity is allowed. Later on, we will inspect this condition. Furthermore, the load factor is a function of engine power, aircraft weight, and speed as:

$$n = \frac{S}{W}\sqrt{\frac{\rho V P \eta_P}{2KS} - \frac{\rho^2 V^4 C_{D_o}}{4K}} \tag{9.76}$$

By squaring both sides of this equation and plugging it into Equation 9.29, we obtain

$$\omega = \frac{g\sqrt{\frac{S^2}{W^2}\left(\frac{\rho V P \eta_P}{2KS} - \frac{\rho^2 V^4 C_{D_o}}{4K}\right) - 1}}{V} = \frac{g\sqrt{\left(\frac{\rho V P \eta_P S}{2KW^2} - \frac{\rho^2 S^2 V^4 C_{D_o}}{4KW^2}\right) - 1}}{V} \tag{9.119}$$

Both numerator and denominator are functions of airspeed. Recall from mathematics, $\frac{d}{dx}\frac{u}{v}=\frac{(du/dx)v-(dv/dx)u}{v^2}$ and $\frac{d}{dx}u^k=k\frac{du}{dx}u^{k-1}$, where $k=1/2$. Differentiating ω with respect to airspeed (see Figure 9.13) results in

$$\frac{d\omega}{dV}=\frac{V\dfrac{\frac{1}{2}g\left(\dfrac{\rho P\eta_P S}{2KW^2}-\dfrac{4\rho^2S^2V^3C_{D_o}}{4KW^2}\right)}{\sqrt{\left(\dfrac{\rho VP\eta_P S}{2KW^2}-\dfrac{\rho^2S^2V^4C_{D_o}}{4KW^2}\right)-1}}-g\sqrt{\left(\dfrac{\rho VP\eta_P S}{2KW^2}-\dfrac{\rho^2S^2V^4C_{D_o}}{4KW^2}\right)-1}}{V^2}=0 \tag{9.120}$$

The denominator cannot be zero. Thus, the numerator is set equal to zero:

$$V\frac{\frac{1}{2}g\left(\dfrac{\rho P\eta_P S}{2KW^2}-\dfrac{4\rho^2S^2V^3C_{D_o}}{4KW^2}\right)}{\sqrt{\left(\dfrac{\rho VP\eta_P S}{2KW^2}-\dfrac{\rho^2S^2V^4C_{D_o}}{4KW^2}\right)-1}}-g\sqrt{\left(\frac{\rho VP\eta_P S}{2KW^2}-\frac{\rho^2S^2V^4C_{D_o}}{4KW^2}\right)-1}=0$$

Multiplying both terms by the denominator of the first term and canceling out a g yields

$$V\frac{1}{2}\left(\frac{\rho P\eta_P S}{2KW^2}-\frac{\rho^2S^2V^3C_{D_o}}{KW^2}\right)-\left(\frac{\rho VP\eta_P S}{2KW^2}-\frac{\rho^2S^2V^4C_{D_o}}{4KW^2}-1\right)=0$$

or

$$\frac{V\rho P\eta_P S}{4KW^2}-\frac{\rho^2S^2V^4C_{D_o}}{2KW^2}-\frac{\rho VP\eta_P S}{2KW^2}+\frac{\rho^2S^2V^4C_{D_o}}{4KW^2}+1=0$$

$$\frac{V\rho P\eta_P S}{2KW^2}\left(-1+\frac{1}{2}\right)+\frac{\rho^2S^2V^4C_{D_o}}{2KW^2}\left(-1+\frac{1}{2}\right)+1=0\Rightarrow\frac{V\rho P\eta_P S}{4KW^2}+\frac{\rho^2S^2V^4C_{D_o}}{4KW^2}-1=0$$

This can be reformatted into the following expression:

$$V^4+\frac{P\eta_P V}{\rho SC_{D_o}}-\frac{4KW^2}{\rho^2S^2C_{D_o}}=0 \tag{9.121}$$

This is a nonlinear algebraic equation, and there is no analytical solution for this equation. To find a solution to this equation, we can show that, for a typical prop-driven aircraft, the magnitudes of the last two terms in Equation 9.121 are much

greater than the magnitude of the first term (V^4), and hence, a reasonable approximation can be obtained by dropping the first term (V^4). Hence,

$$\frac{P\eta_P V}{\rho S C_{D_o}} - \frac{4KW^2}{\rho^2 S^2 C_{D_o}} \approx 0 \tag{9.122}$$

This leads to an approximate solution for the fastest turn airspeed (V_{ft}) for a prop-driven aircraft:

$$V_{\text{ft}} = \frac{4KW^2}{\rho\eta_P \rho S} \tag{9.123}$$

This equation demonstrates the airspeed to maximize the turn rate for a prop-driven aircraft. Note that, Equation 9.123 delivers a theoretical solution (airspeed) that is usually less than the stall speed, so it is often impractical. The theoretical fastest performance is rarely accessible since it requires an airspeed that is often less than the stall speed. To overcome this problem, the best solution is to select a powerful high-lift device to increase the maximum lift coefficient. This in turn reduces the stall speed below the fastest turn airspeed. Thus, the maneuverability (fastest turn) of a prop-driven aircraft depends on the high-lift device (i.e., maximum lift coefficient).

When an aircraft is turning with a velocity less than the corner speed, V^* (from Equation 9.87), while employing the maximum engine power, it will encounter the stall. Hence, any theoretical value of V_{ft} from Equation 9.123 less than V^* is not acceptable. Note that, the value of V_{ft} from Equation 9.123 is valid, only if it is equal to or greater than the corner speed ($V_{\text{ft}} \geq V^*$). Otherwise, assume $V_{\text{ft}} = V^*$. Thus, referring to Equation 9.87, we obtain

$$V_{\text{ft}} = V^* = \left[\frac{2P_{\max}\eta_P}{\rho S\left(C_{D_o} + KC_{L_{\max}}^2\right)}\right]^{\frac{1}{3}} \tag{9.124}$$

By substituting Equation 9.123 into Equation 9.76, the load factor in the fastest turn (n_{ft}) is obtained:

$$n_{\text{ft}} = \frac{S}{W}\sqrt{\frac{\rho P\eta_P}{2KS}\left(\frac{4KW^2}{P\eta_P\rho S}\right) - \frac{\rho^2 C_{D_o}}{4K}\left(\frac{4KW^2}{P\eta_P\rho S}\right)^4} = \frac{S}{W}\sqrt{\frac{2W^2}{S^2} - \left(\frac{W}{S}\right)^2 \frac{4^3K^3W^6C_{D_o}}{P^4\eta_P{}^4\rho^2S^2}}$$

which can be simplified to

$$n_{\text{ft}} = \sqrt{2 - \frac{4^3K^3W^6C_{D_o}}{P^4\eta_P^4\rho^2S^2}} \tag{9.125}$$

The magnitude of the second term on the right-hand side of this equation is much smaller than 2. An approximation to this equation is to drop that term:

$$n_{\text{ft}} \approx \sqrt{2} = 1.414 \tag{9.126}$$

Please note that the value of n_{ft} from this equation is valid, only if V_{ft} is equal or greater than the corner speed ($V_{ft} \geq V^*$). Otherwise, assume $n_{ft} = n_{max_C}$. Then, referring to Equation 9.88, we obtain

$$n_{ft} = n_{max_C} = \frac{\rho\left(V^*\right)^2 S C_{L_{max}}}{2W} \tag{9.127}$$

Using Equation 9.9, the bank angle corresponding to the fastest turn can be written as

$$\phi_{ft} = \cos^{-1}\left(\frac{1}{n_{ft}}\right) \tag{9.128}$$

In case where the V_{ft} from Equation 9.123 is equal or greater than the corner speed ($V_{ft} \geq V^*$), the maximum theoretical value for the bank angle corresponding to the fastest turn will be

$$\phi_{ft} = \cos^{-1}\left(\frac{1}{1.414}\right) = 45° \tag{9.129}$$

From Equation 9.29, the turn rate that corresponds to the fastest turn (ω_{ft}) is a function of corresponding velocity and load factor:

$$\omega_{ft} = \frac{g\sqrt{n_{ft}^2 - 1}}{V_{ft}} \tag{9.130}$$

The maximum turn rate (ω_{max}) that yields the fastest turn will be obtained by inserting n_{ft} from Equation 9.126 and V_{ft} from Equation 9.123 into Equation 9.130:

$$\omega_{ft} = \frac{g\sqrt{\left(\sqrt{2}\right)^2 - 1}}{\frac{4KW^2}{P\eta_P \rho S}}$$

which can be simplified to

$$\omega_{max} = \omega_{ft} = \frac{gP\eta_P \rho S}{4KW^2} \tag{9.131}$$

From Equation 9.21, the turn radius corresponding to the fastest turn (R_{ft}) is obtained:

$$R_{ft} = \frac{V_{ft}^2}{g\sqrt{n_{ft}^2 - 1}} \tag{9.132}$$

TABLE 9.6
Summary of Equations for the Fastest Turn Parameters

No.	Fastest Turn Parameter	Symbol	If $V_{ft} \geq V^*$	If $V_{ft} < V^*$
1.	Airspeed corresponding to maximum turn rate	V_{ft}	9.126	9.127
2.	Load factor corresponding to maximum turn rate	n_{ft}	9.127	9.127
3.	Maximum turn rate	ω_{ft}	9.130	9.131
4.	Turn rate corresponding to maximum turn rate	R_{ft}	9.132	9.132
5.	Bank angle corresponding to maximum turn rate	ϕ_{ft}	9.131	9.132

Now, we can draw a few conclusions to optimize a prop-driven aircraft for the goal of improving the fastest turn performance, both on the operational side and on the design side. On the operational side, the fastest turn performance can be improved by increasing engine power, decreasing aircraft weight, increasing C_{D_o} (i.e., by deflecting flap), and decreasing altitude (i.e., to sea level). On the design side, the designer should increase the wing area, select a high-efficiency propeller, employ a powerful high-lift device, and also decrease the induced drag factor (K). This requires an increase in the wing AR or wing span.

Unfortunately, the theoretical airspeed for the fastest turn (V_{ft}) is usually less than the stall speed (V_s). In other words, their corresponding lift coefficients ($C_{L_{ft}}$) are higher than the maximum available lift coefficient ($C_{L_{max}}$). Table 9.6 provides a summary of equations for the fastest turn parameters. As the table demonstrates, there are two sets of equations for each parameter: (1) one set for the case where $V_{ft} \geq V^*$ and (2) one set for the case where $V_{ft} < V^*$. Therefore, before you determine the maximum turn rate, you need to calculate the V_{ft} and corner speed (V^*) and compare them. The value of V_{ft} is initially determined by Equation 9.123.

Example 9.10 examines the fastest turn performance of an aircraft with a prop-driven engine.

Case Study - Example 9.10

Consider the single-engine piston-prop acrobatic aircraft General Avia F 22 Pinguino with the following features:

$$m_{TO} = 900\,\text{kg}, \quad S = 10.82\,\text{m}^2, \quad P = 130\,\text{kW}, \quad b = 8.5, \quad V_s = 54\,\text{knot}$$

Assume: $C_{D_o} = 0.021$, $\eta_P = 0.8$, $e = 0.87$.

Evaluate the fastest turn performance of this acrobatic aircraft at sea level.

Solution

We first need to find three parameters: K, AR, and $C_{L_{\max}}$:

$$\text{AR} = \frac{b^2}{S} = \frac{8.5^2}{10.82} = 5.92 \tag{3.9}$$

$$K = \frac{1}{\pi e\,\text{AR}} = \frac{1}{3.14 \times 0.87 \times 5.92} = 0.06 \tag{3.8}$$

$$C_{L_{\max}} = \frac{2mg}{\rho S V_s^2} = \frac{2 \times 900 \times 9.81}{1.225 \times 10.82 \times (54 \times 0.514)^2} = 1.73 \tag{2.27}$$

We need to compare the corner speed and the airspeed corresponding to the fastest turn:

$$V_{\text{ft}} = \frac{4KW^2}{P\eta_P \rho S} = \frac{4 \times 0.06 \times (900 \times 9.81)^2}{130{,}000 \times 0.8 \times 1.225 \times 10.82} = 13.5\,\text{m/s} = 26.3\,\text{knot} \tag{9.123}$$

$$V^* = \left[\frac{2P_{\max}\eta_P}{\rho S\left(C_{D_o} + KC_{L_{\max}}^2\right)}\right]^{\frac{1}{3}} \tag{9.87}$$

$$V^* = \left[\frac{2 \times 130{,}000 \times 0.8}{1.225 \times 10.82 \times \left(0.021 + 0.06 \times (1.73)^2\right)}\right]^{\frac{1}{3}} \Rightarrow V^* = 42.9\,\text{m/s} = 83.3\,\text{knot}$$

Since $V_{\text{ft}} < V^*$, the theoretical value for the fastest is not practical. From Equation 9.127, we consider $V_{\text{ft}} = V^* = 42.9$ m/s = 83.3 knots. According to Table 9.6, the equations in the last column are used.

- **Load factor**

$$n_{\text{ft}} = n_{\max_C} = \frac{\rho\left(V^*\right)^2 SC_{L_{\max}}}{2W} = \frac{1.225 \times (42.9)^2 \times 10.82 \times 1.73}{2 \times 900 \times 9.81} = 2.38 \tag{9.127}$$

- Bank angle corresponding to the fastest turn

$$\phi_{\text{ft}} = \cos^{-1}\left(\frac{1}{n_{\text{ft}}}\right) = \cos^{-1}\left(\frac{1}{2.38}\right) = 65.2^\circ \tag{9.128}$$

- **The maximum turn rate**

$$\omega_{\text{ft}} = \frac{g\sqrt{n_{\text{ft}}^2 - 1}}{V_{\text{ft}}} = \frac{9.81 \times \sqrt{2.38^2 - 1}}{42.9} = 0.495 \text{ m/s} = 28.3 \text{ deg/s} \tag{9.130}$$

- **Turn radius**

$$R_{\text{ft}} = \frac{V_{\text{ft}}^2}{g\sqrt{n_{\text{ft}}^2 - 1}} = \frac{42.9^2}{9.81 \times \sqrt{2.38^2 - 1}} = 86.7 \text{ m} \tag{9.132}$$

- **Time required to cover a half circle**

$$t = \frac{\pi R}{V} = \frac{3.14 \times 86.7}{42.9} = 6.3 \text{ s} \tag{9.24}$$

9.6.2 Tightest Turn: Prop-Driven Aircraft

When an aircraft turns with the shortest possible radius, the turn is called the *tightest turn*. The tightest turn is another criterion for the evaluation of maneuverability of prop-driven aircraft. To determine the minimum turn radius, we need to differentiate the radius (Equation 9.21) with respect to airspeed and set it to zero:

$$R = \frac{V^2}{g\sqrt{n^2 - 1}} \tag{9.21}$$

We are looking for a set of values (n and V) that yields the minimum turn radius (R_{min}). At first, we assume any producible n is allowable and any corresponding velocity is allowed. Later on, we will inspect this condition. Furthermore, the load factor is a function of engine power, aircraft weight, and speed as given in Equation 9.76:

$$n = \frac{S}{W}\sqrt{\frac{\rho V P \eta_P}{2KS} - \frac{\rho^2 V^4 C_{D_o}}{4K}} \tag{9.76}$$

By squaring both sides of this equation, and plugging it into Equation 9.21, we obtain

$$R = \frac{V^2}{g\sqrt{\frac{S^2}{W^2}\left(\frac{\rho V P \eta_P}{2KS} - \frac{\rho^2 V^4 C_{D_o}}{4K}\right) - 1}} = \frac{V^2}{g\sqrt{\left(\frac{\rho V P \eta_P S}{2KW^2} - \frac{\rho^2 S^2 V^4 C_{D_o}}{4KW^2}\right) - 1}} \tag{9.133}$$

Mathematically, the minimum radius (optimum point) is obtained by differentiating Equation 9.133 with respect to airspeed (see Figure 9.14) and setting the derivative equal to zero:

$$\frac{dR}{dV} = \frac{d}{dV}\frac{V^2}{g\sqrt{\left(\frac{\rho VP\eta_P S}{2KW^2} - \frac{\rho^2 S^2 V^4 C_{D_o}}{4KW^2}\right) - 1}} = 0 \tag{9.134}$$

Both numerator and denominator are functions of airspeed. Recall from mathematics that $\frac{d}{dx}\frac{u}{v} = \frac{(du/dx)v - (dv/dx)u}{v^2}$ and, $\frac{d}{dx}v^k = k\frac{dv}{dx}v^{k-1}$ where $k = 1/2$. Differentiating R with respect to airspeed gives

$$\frac{dR}{dV} = \frac{2Vg\sqrt{\left(\frac{\rho VP\eta_P S}{2KW^2} - \frac{\rho^2 S^2 V^4 C_{D_o}}{4KW^2}\right) - 1} - V^2 \frac{\frac{1}{2}g\left[\frac{\rho P\eta_P S}{2KW^2} - \frac{4\rho^2 S^2 V^3 C_{D_o}}{4KW^2}\right]}{\sqrt{\left(\frac{\rho VP\eta_P S}{2KW^2} - \frac{\rho^2 S^2 V^4 C_{D_o}}{4KW^2}\right) - 1}}}{g^2\left[\frac{\rho VP\eta_P S}{2KW^2} - \frac{\rho^2 S^2 V^4 C_{D_o}}{4KW^2} - 1\right]} = 0 \tag{9.135}$$

The denominator cannot be zero. Thus, the numerator is set equal to zero:

$$2Vg\sqrt{\left(\frac{\rho VP\eta_P S}{2KW^2} - \frac{\rho^2 S^2 V^4 C_{D_o}}{4KW^2}\right) - 1} - V^2 \frac{\frac{1}{2}g\left[\frac{\rho P\eta_P S}{2KW^2} - \frac{4\rho^2 S^2 V^3 C_{D_o}}{4KW^2}\right]}{\sqrt{\left(\frac{\rho VP\eta_P S}{2KW^2} - \frac{\rho^2 S^2 V^4 C_{D_o}}{4KW^2}\right) - 1}} = 0$$

Multiplying both terms by the denominator of the second term and canceling out a "Vg" give

$$2\left[\left(\frac{\rho VP\eta_P S}{2KW^2} - \frac{\rho^2 S^2 V^4 C_{D_o}}{4KW^2}\right) - 1\right] - V\frac{1}{2}\left[\frac{\rho P\eta_P S}{2KW^2} - \frac{4\rho^2 S^2 V^3 C_{D_o}}{4KW^2}\right] = 0$$

or

$$\frac{\rho VP\eta_P S}{KW^2} - \frac{\rho^2 S^2 V^4 C_{D_o}}{2KW^2} - 2 - \frac{V\rho P\eta_P S}{4KW^2} + \frac{\rho^2 S^2 V^4 C_{D_o}}{2KW^2} = 0$$

The second and fifth terms are canceled out. Thus,

$$\frac{\rho VP\eta_P S}{KW^2} - 2 - \frac{V\rho P\eta_P S}{4KW^2} = 0 \Rightarrow \frac{\rho VP\eta_P S}{KW^2}\left(1 - \frac{1}{4}\right) = 2$$

Hence, the expression for airspeed is obtained as

$$V_{tt} = \frac{8KW^2}{3\rho P\eta_P S} \tag{9.136}$$

Please note that the subscript tt stands for the **t**ightest **t**urn. The theoretical tightest performance is rarely accessible since it requires an airspeed that is often less than the stall speed. When an aircraft is turning with a velocity less than the corner speed, V^* (from Equation 9.44), while employing the maximum engine power, the aircraft will encounter the stall. Hence, any theoretical value of V_{tt} from Equation 9.136 less than V^* is not valid. Note that, the value of V_{tt} from Equation 9.136 is valid, only if it is equal to or greater than the corner speed ($V_{tt} \geq V^*$). Otherwise, assume $V_{tt} = V^*$. Then, referring to Equation 9.87, we obtain

$$V_{tt} = V^* = \left[\frac{2P_{max}\eta_P}{\rho S\left(C_{D_o} + KC_{L\max}^2\right)}\right]^{\frac{1}{3}} \tag{9.137}$$

Recall that $C_{L_{max}}$ is the maximum lift coefficient during a level turn. The maximum lift coefficient when high-lift device is employed is much higher than that without high-lift device deflection. By substituting V_{tt} from Equation 9.136 into Equation 9.76, we can obtain an expression for the tightest turn load factor (n_{tt}):

$$n_{tt} = \frac{S}{W}\sqrt{\frac{\rho P\eta_P}{2KS}\frac{8KW^2}{3\rho P\eta_P S} - \frac{\rho^2 C_{D_o}}{4K}\left(\frac{8KW^2}{3\rho P\eta_P S}\right)^4}$$

which is reduced to

$$n_{tt} = \sqrt{\frac{4}{3} - \frac{12.6K^3W^6C_{D_o}}{S^2\rho^2P^4\eta_P^4}} \tag{9.138}$$

An approximation to this equation is to drop the second term on the right-hand side of the equation, since its magnitude is much smaller than 4/3. Thus,

$$n_{tt} \approx \sqrt{\frac{4}{3}} = 1.155 \tag{9.139}$$

Please note that the value of n_{tt} from this equation is valid, only if V_{tt} is equal to or greater than the corner speed ($V_{tt} \geq V^*$). Otherwise, assume $n_n = n_{\max_C}$. Then, referring to Equation 9.88, we obtain

$$n_{tt} = n_{\max_C} = \frac{\rho\left(V^*\right)^2 S C_{L_{\max}}}{2W} \tag{9.140}$$

Using Equation 9.9, the bank angle corresponding to the tightest turn can be written as

$$\phi_{tt} = \cos^{-1}\left(\frac{1}{n_{tt}}\right) \tag{9.141}$$

In case where V_{tt} from Equation 9.136 is equal to or greater than the corner speed ($V_{tt} \geq V^*$), the maximum theoretical value for the bank angle corresponding to the tightest turn will be 30°:

$$\phi_{tt} = \cos^{-1}\left(\frac{1}{1.155}\right) = 30° \tag{9.142}$$

By definition, the turn radius for the tightest turn (R_{tt}) is the same as the absolute minimum (shortest) turn radius ($R_{\min}$). Using Equation 9.21, we obtain

$$R_{tt} = R_{\min} = \frac{V_{tt}^2}{g\sqrt{n_{tt}^2 - 1}} \tag{9.143}$$

We can expand Equation 9.140 by inserting n_{tt} and V_{tt} from Equations 9.136 and 9.139 to develop a more general expression for the minimum (i.e., shortest) turn radius:

$$R_{tt} = \frac{\left(\frac{8KW^2}{3\rho P \eta_P S}\right)}{g\sqrt{1.155^2 - 1}}$$

which is reduced to

$$R_{tt} = R_{\min} = \frac{12.3}{g}\left[\frac{KW}{\rho P_{\max} \eta_P S}\right]^2 \tag{9.144}$$

The theoretical value of R_{tt} from this equation is valid only if V_{tt} from Equation 9.136 is equal or greater than the corner speed ($V_{tt} \geq V^*$). Otherwise, use Equation 9.143. Then, referring to Equation 9.140, we obtain

$$R_{tt} = R_{\min} = \frac{V^{*2}}{g\sqrt{\left(\frac{\rho\left(V^*\right)^2 S C_{L_{\max}}}{2W}\right)^2 - 1}} \tag{9.145}$$

Now, we can draw a few conclusions to optimize a prop-driven aircraft for the goal of improving the tightest turn performance, both on the operational side and on the design side. Equations 9.144 and 9.145 can be used to examine the role of each parameter on the minimum radius. To reduce the shortest radius, one must perform the following:

1. Increase the engine power (P).
2. Decrease aircraft weight (W).
3. Increase wing area (S).
4. Increase wing loading (W/S).
5. Decrease induced drag factor (K). This means that the AR and Oswald span efficiency factor (e) must be increased.
6. Increase $C_{L_{\max}}$ by selecting powerful high-lift devices such as double-slotted flap.
7. Decrease stall speed (V_s).
8. Decrease zero-lift drag coefficient (C_{D_o}).

In addition, Equation 9.144 also implies that

9. The pilot must fly at a low altitude (high ρ).
10. The pilot must fly at a low speed.

The aforementioned results may be grouped into two categories, namely, one for the pilot and one for the aircraft designer, to improve the tightest turn performance. Pilots must fly at a low altitude, employ the maximum engine power, and have a low weight by dropping non-necessary loads and stores. The higher the altitude, the lower will be the tightest turn performance.

To design a highly maneuverable aircraft, the designer must select a very powerful engine, use lightweight materials, increase wing area, and use a high-efficiency propeller. It is interesting to note that the parameter C_{D_o} does not explicitly appear in any of the aforementioned equations. Hence, it does not directly influence the tightest turn. However, if C_{D_o} is large, it will improve the turn performance with decreasing corner speed (as noted in Equation 9.137). Recall that when the flap is deflected, the aircraft C_{D_o} is increased.

From Equation 9.29, the turn rate that corresponds to the tightest turn (ω_{tt}) is a function of corresponding velocity and load factor:

$$\omega_{tt} = \frac{g\sqrt{n_{tt}^2 - 1}}{V_{tt}} \tag{9.146}$$

We can expand Equation 9.146 by inserting n_{tt} and V_{tt} from Equations 9.139 and 9.136 to develop a more general expression for the turn rate corresponding to the tightest turn:

$$\omega_{tt} = \frac{g\sqrt{1.155^2 - 1}}{\dfrac{8KW^2}{3\rho P \eta_P S}}$$

TABLE 9.7
Summary of Equations for the Tightest Turn Parameters

No.	Tightest Turn Parameter	Symbol	If $V_{tt} \geq V^*$	If $V_{tt} < V^*$
1.	Airspeed corresponding to minimum turn radius	V_{tt}	9.136	9.135
2.	Load factor corresponding to minimum turn radius	n_{tt}	9.141 or 9.142	9.140
3.	Turn rate corresponding to minimum turn radius	ω_{tt}	9.147	9.146
4.	Minimum turn radius	R_{tt}	9.144	9.145
5.	Bank angle corresponding to minimum turn radius	ϕ_{tt}	9.141	9.141

which is reduced to

$$\omega_{tt} = \frac{0.217\rho P \eta_P S}{K m^2 g} \tag{9.147}$$

The theoretical value of ω_{tt} from this equation is valid only if V_{tt} from Equation 9.136 is equal to or greater than the corner speed ($V_{tt} \geq V^*$). Otherwise, directly use Equation 9.146.

Table 9.7 provides a summary of equations for the tightest turn parameters. As the table demonstrates, there are two sets of equations for each parameter: (1) one set for the case where $V_{tt} \geq V^*$, and (2) one set for the case where $V_{tt} < V^*$. Therefore, before you determine the minimum turn radius, you need to calculate V_{tt} and corner speed (V^*) and compare them. The value of V_{tt} is initially determined by Equation 9.136.

Example 9.11

Consider a small radio or remotely controlled (RC) aircraft with the following characteristics:

$$m = 700\,\text{g}, \quad S = 0.2\,\text{m}^2, \quad b = 1\,\text{m}; \quad e = 0.8; \quad \eta_P = 0.7, \quad C_{D_o} = 0.03, \quad C_{L_{\max}} = 1.2$$

The airplane is employing a prop-driven electric motor where three cells of 2,100 mAh, 12 V Li-Po (lithium polymer) batteries provide electric energy for the motor. Evaluate the tightest turn performance of this aircraft at the sea level.

Solution

We first need to find two parameters, namely, AR and *K*:

$$\text{AR} = \frac{b^2}{S} = \frac{1^2}{0.2} = 5 \tag{3.9}$$

$$K = \frac{1}{\pi e \text{AR}} = \frac{1}{3.14 \times 0.8 \times 5} = 0.08 \tag{3.8}$$

Based on the description of the battery, a maximum current of 2.1 A (i.e., 2,100 mA) at 12 V is provided for 1 h (i.e., 3,600 s). Thus, the engine power from these batteries is

$$P_{\max} = IV = 2.1 \times 3 \times 12 = 75.6\,\text{W} \tag{4.35}$$

Airspeed corresponding to minimum turn radius

$$V_{\text{tt}} = \frac{8KW^2}{3\rho P \eta_P S} = \frac{8 \times 0.08 \times (0.7 \times 9.81)^2}{3 \times 1.225 \times 75.6 \times 0.7 \times 0.2} = 0.77\,\text{m/s} = 1.5\,\text{knot} \tag{9.136}$$

We need to compare the corner speed and the airspeed corresponding to the tightest turn:

$$V^* = \left[\frac{2P_{\max}\eta_P}{\rho S\left(C_{D_o} + KC_{L_{\max}}^2\right)}\right]^{\frac{1}{3}} = \left[\frac{2 \times 75.6 \times 0.7}{1.225 \times 0.2 \times \left(0.03 + 0.08 \times (1.2)^2\right)}\right]^{\frac{1}{3}}$$
$$\Rightarrow V^* = 14.4\,\text{m/s} = 28\,\text{knot} \tag{9.137}$$

Since $V_{\text{tt}} < V^*$, the theoretical value for the tightest is not practical. From Equation 9.137, we consider $V_{\text{tt}} = V^* = 14.4$ m/s. According to Table 9.7, the equations in the last column are used. The load factor is

$$n_{\text{tt}} = n_{\max_C} = \frac{\rho\left(V^*\right)^2 SC_{L_{\max}}}{2W} = \frac{1.225 \times (14.4)^2 \times 0.2 \times 1.2}{2 \times 0.7 \times 9.81} = 4.44 \tag{9.140}$$

The turn radius for the tightest turn (R_{tt}) is

$$R_{\text{tt}} = R_{\min} = \frac{V_{\text{tt}}^2}{g\sqrt{n_{\text{tt}}^2 - 1}} = \frac{14.4^2}{9.81\sqrt{4.44^2 - 1}} = 4.89\,\text{m} \tag{9.143}$$

9.7 VERTICAL MANEUVERS

In Sections 9.2–9.6, a group of flight operations were introduced that were based on the level turn. In a level turn, two rotations, namely, roll and yaw, are usually cooperating. There are another group of maneuvers that are not based on roll or yaw. However, they are based on another rotation, namely, pitch. The pull-up, pull-down (or push-over), dive, and pull-out from steep dive are four maneuvers that fall into this category. Dive is an extreme nose-down attitude (e.g., vertical), increasing both airspeed and descent rate. Based on Federal Aviation Regulations (FAR), the normal and utility aircraft are not allowed to perform these maneuvers. Only acrobatic or highly maneuverable aircraft are allowed to perform such maneuvers. Figure 3.20 illustrates Mikoyan MiG-29 supersonic fighter aircraft in a high-*g* pull-up maneuver.

In this section, the analysis of these two maneuvers is described. In the pull-up and push-over, the aircraft is traveling in the vertical plane (in fact, in a vertical loop

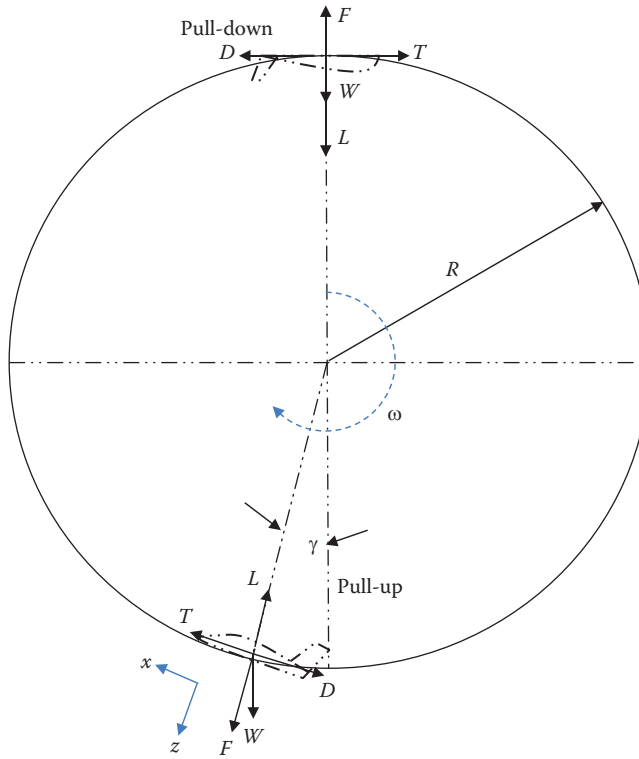

FIGURE 9.18 Pull-up and pull-down maneuvers.

with a radius of R). When the aircraft is on the lower half of the loop (or circle), the maneuver is called pull-up. In contrast, when the aircraft is on the upper half of the loop, the maneuver is called pull-down or push-over. In a pull-up, the lift is greater than the aircraft weight, but in a pull-down, the lift is less than weight. In fact, in pull-down, the aircraft is in an inverted flight situation (i.e., upside down). In both cases, the climb angle (γ) is constantly varying. In these two maneuvers, the turn rate is, in fact, the rate of change of climb angle. Thus, the turn rate is

$$\omega = \dot{\gamma} = \frac{d\gamma}{dt} \tag{9.148}$$

Figure 9.18 demonstrates forces that are applied on both pull-up and pull-down maneuvers. There is an important distinction between vertical maneuvers and a coordinated level turn. In a level coordinated turn, no force (other than human's weight) is felt by human onboard, while in a vertical maneuver, a centrifugal force (via a centripetal acceleration) is felt. In an extreme case, a high centripetal acceleration (also referred to as the g-load) may cause a human to pass out. Hence, a vertical maneuver is more limited by human strength, rather than by the strength of the

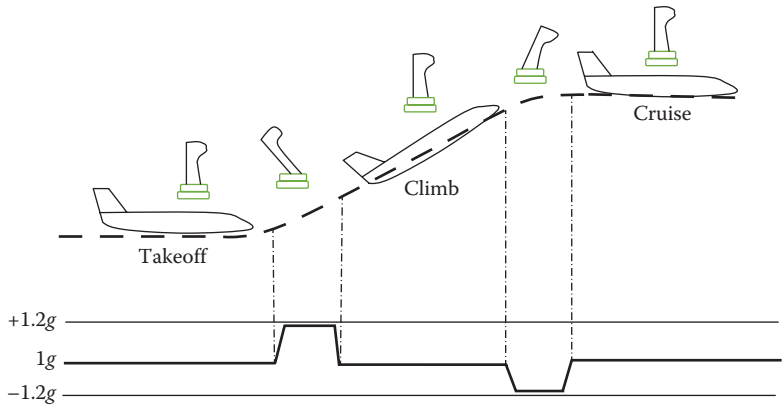

FIGURE 9.19 Variations of load factor with respect to the pitch rate for a transport aircraft.

aircraft structure. A very strong structure can handle a load factor of about 20–30, while a normal human is hardly capable of functioning under a load factor of more than about 6.

When n is higher than 1, the blood pressure will be increased and the blood will be moving away (i.e., upward/downward). This is referred to as the hydrostatic blood pressure effect [97]. In an extreme case, the blood will be pumped up in the brain by the g-load. Since this is harmful to the brain, the fighter pilots wear a specific suit called g-suit to limit the undesired blood circulation in the brain (upward motion). The strength of a human pilot can be artificially increased by wearing a g-suit to reduce the damaging effects of high internal blood pressure.

The higher the load factor, the greater the blood pressure in the brain area (including the eyes and ears regions). A high load factor may even cause the blood pressure to puncture the ear diaphragm and outer layer of the eye, and to lose consciousness. Thus, a load factor beyond 9 is very dangerous to eyes, ears, and brain, and should be avoided. The interested reader may refer to Reference [93] to study the current concepts on g-protection.

A very familiar example for the variations of load factor for a civil transport aircraft (Figure 9.19) is when the flight pitch angle (θ) is varied. During a phase change from a level flight (such as a takeoff) to a climbing flight, a rotation or vertical turn (similar to a pull-up) is necessary. At this period, the positive load factor is increased. In contrast, during a return from a climbing flight to a level flight (such as a cruise), another vertical turn (similar to a pull-down) is necessary. At this period, the negative load factor is increased. During both periods, the pilot will apply a force (pull/push) to stick/yoke to deflect the elevator.

9.7.1 Pull-Up and Pull-Out

Consider an aircraft in a pull-up maneuver (i.e., the aircraft in the lower half of the loop in Figure 9.18). The aircraft is turning vertically (pulling up) with a constant airspeed, V, inside a vertical loop (circle) with a radius, R. When the flight path is

a vertical circle, the governing equations of motion are based on the equilibrium of forces. Five forces are present in this flight maneuver: (1) weight (W), (2) lift (L), (3) thrust (T), (4) drag (D), and (5) centrifugal force ($F_C = mV^2/R$). The equilibrium of forces along x- and z-axes yields

$$\sum F_x = 0 \Rightarrow T = D \tag{9.149}$$

$$\sum F_z = 0 \Rightarrow L - W\cos\gamma = m\frac{V^2}{R} \tag{9.150}$$

For simplicity, we consider the aircraft is at the lowest point of the loop; that is, the climb angle (γ) is zero. Thus, Equation 9.150 is reduced to

$$L - W = m\frac{V^2}{R} \tag{9.151}$$

We are interested in the turn radius (R) and turn rate (ω) at the instant where the maneuver is initiated. An instantaneous maneuver is initiated by a sudden change in the lift and is achieved by a sudden increase in the angle of attack. This initiation causes the aircraft to begin to climb with a constant pitch rate. The instantaneous turn radius is obtained from Equation 9.151 as follows:

$$R = m\frac{V^2}{L-W} = \frac{W}{g}\frac{V^2}{L-W} = \frac{V^2}{g\left(\frac{L}{W}-1\right)} \tag{9.152}$$

We already have defined L/W as the load factor (n), so Equation 9.152 can be expressed as:

$$R = \frac{V^2}{g(n-1)} \tag{9.153}$$

The flight path of a pull-out from a dive (Figure 9.20) resembles the lower right quarter of the circle. An ideal pull-out of a dive is performed by gliding (i.e., zero thrust) at constant speed along a circular arc until the glide path is horizontal. Equations 9.151–9.153 may be utilized to analyze the aircraft motion in this quarter, particularly at the end of the quarter (i.e., when the path gets horizontal).

In the case of a pull-out (of a dive), the radius is limited by the dive speed and the maximum allowable load factor. The dive speed should not pass the never-exceeded speed (V_{NE}); otherwise, the structure will break (e.g., the tail may shear off). For instance, the never-exceeded speed of aircraft Mooney M20TN is 194 knots, while its maneuvering speed is 128 knots. With a given dive speed, the

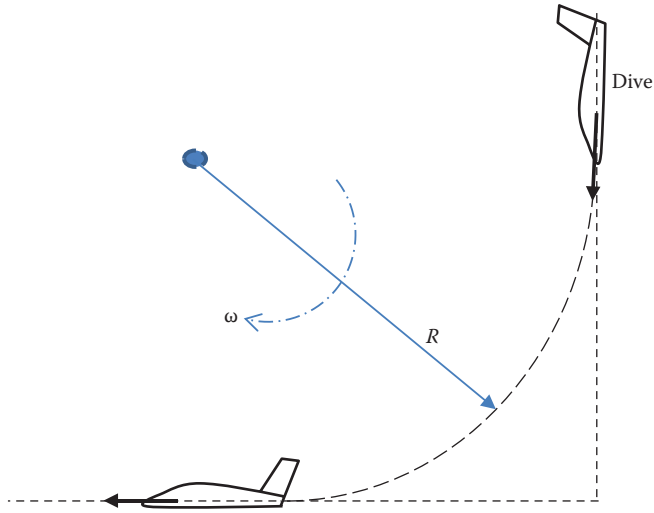

FIGURE 9.20 Pulling out from a dive.

minimum radius in a pull-out is determined when the pilot applies the maximum allowable load factor:

$$R_{\min} = \frac{V^2}{g(n_{\max} - 1)} \tag{9.154}$$

From Equation 9.153, the load factor in a pull-up and pull-out is obtained as follows:

$$n = \frac{V^2}{Rg} + 1 \tag{9.155}$$

Please note that this load factor is not a function of the bank angle, since the aircraft is not rolling. So, do not confuse the load factor in a pull-up (or pull-out) with the load factor in a level turn. They are not related.

The angular velocity is defined as the linear airspeed divided by the radius, so the instantaneous turn rate is obtained from Equation 9.153 as:

$$\omega = \frac{V}{R} = \frac{V}{\dfrac{V^2}{g(n-1)}} = \frac{g(n-1)}{V} \tag{9.156}$$

Equations 9.153–9.156 are employed to analyze a pull-up maneuver. These equations are valid only in the vicinity of the lowest point of a vertical loop. Therefore, they are not valid when the climb angle is more than 10°. To increase the maneuverability of an aircraft in a pull-up, the turn rate should be increased and the turn radius should be decreased. These objectives require a low speed and a high load factor.

The combination of these two requirements implies that the best pull-up will be achieved while flying with the stall speed, the maximum load factor, and with the corresponding engine thrust. If the instantaneous thrust is the maximum available thrust, the aircraft will not have the sufficient thrust necessary to sustain the speed for the entire pull-up. Hence, the speed will gradually decrease as the aircraft climbs. For a pull-up, the corner speed is defined as

$$V^* = \left[\frac{2n_{\max}W}{\rho S C_{L_{\max}}}\right]^{\frac{1}{2}} \tag{9.157}$$

where $n_{\max}$ is the maximum allowable load factor (i.e., tolerable by the aircraft structure). Referring to Equations 9.153 and 9.156, the minimum turn radius and the maximum turn rate in a pull-up can be obtained by

$$R_{\min} = \frac{V^{*2}}{g(n_{\max}-1)} \tag{9.158}$$

$$\omega_{\max} = \frac{g(n_{\max}-1)}{V^*} \tag{9.159}$$

Note that, the corner speed in a pull-up is different than that for a level turn. The instantaneous centripetal acceleration (from Equations 9.4 and 9.153) at the instant shown in Figure 9.20 is

$$a_c = \frac{V^2}{\frac{V^2}{g(n-1)}}$$

which is simplified to

$$a_c = g(n-1) \tag{9.160}$$

Since the direction of the centripetal acceleration is downward, the total acceleration is determined by adding gravity to it

$$a_{\text{tot}} = g(n-1) + g = ng \tag{9.161}$$

which implies that the human onboard must sustain a load factor that is n times the gravity. The human tolerance will apply a limit to the maximum allowable value of load factor, which consequently limits the pull-up maneuver. Therefore, a pull-out maneuver of a dive is primarily restricted by human factors (not by engine power/thrust).

Example 9.12

Consider an acrobatic aircraft with a mass of 1,500 kg diving with a velocity of 100 knots.

a. If the aircraft pulls out of the dive with a radius of 150 m, determine the load factor.
b. If the maximum allowable load factor is 6, determine the minimum radius for a pull-out of this dive.

Solution

a. Load factor

$$n = \frac{V^2}{Rg} + 1 = \frac{(100 \times 0.514)^2}{150 \times 9.81} + 1 \Rightarrow n = 2.8 \tag{9.155}$$

b. Minimum radius

$$R_{\min} = \frac{V^2}{g(n_{\max} - 1)} = \frac{(100 \times 0.514)^2}{9.81 \times (6 - 1)} = 54\,\text{m} \tag{9.154}$$

The minimum radius for this pull-out is 54 m.

9.7.2 Pull-Down

The analysis of a pull-down maneuver is fundamentally similar to the analysis of a pull-up. Consider the aircraft in the upper half of the loop (Figure 9.18). The aircraft is turning vertically (pulling down) at a constant airspeed, *V*, inside a vertical loop with a constant radius, *R*. When the flight path is a vertical circle, the governing equations of motion are based on the equilibrium of forces. Similar to the pull-up, the same five forces are present in this flight maneuver: (1) weight, (2) lift, (3) thrust, (4) drag, and (5) centrifugal force. It is interesting to note that the aircraft is upside down and the lift is downward in a pull-down maneuver:

$$\sum F_x = 0 \Rightarrow T = D \tag{9.162}$$

$$\sum F_z = 0 \Rightarrow L + W\cos\gamma = m\frac{V^2}{R} \tag{9.163}$$

For simplicity, we consider the aircraft is at the highest point of the loop; that is, γ is zero. Thus, Equation 9.163 is simplified as

$$L + W = m\frac{V^2}{R} \tag{9.164}$$

We are interested in the turn radius (R) and turn rate (ω) at this particular instant. The instantaneous turn radius is obtained from Equation 9.164 as follows:

$$R = m\frac{V^2}{L+W} = \frac{W}{g}\frac{V^2}{L+W} = \frac{V^2}{g\left(\frac{L}{W}+1\right)} = \frac{V^2}{g(n+1)} \tag{9.165}$$

Thus, the load factor in a pull-down is obtained from Equation 9.168 as follows:

$$n = \frac{V^2}{Rg} - 1 \tag{9.166}$$

The angular velocity is defined as linear speed divided by radius, so the instantaneous turn rate is obtained from Equation 9.165 as:

$$\omega = \frac{V}{R} = \frac{V}{\frac{V^2}{g(n+1)}} = \frac{g(n+1)}{V} \tag{9.167}$$

Equations 9.165–9.167 are employed to analyze a pull-down maneuver. By comparing Equations 9.155 and 9.166, we conclude that the load factor in a pull-up maneuver is higher than that for a pull-down maneuver. With the same radius and the same airspeed, the load factor of a pull-up and a pull-out is $2g$ greater than that for a pull-down:

$$n_{\text{pullup}} - n_{\text{pull-down}} = \left(\frac{V^2}{Rg}+1\right) - \left(\frac{V^2}{Rg}-1\right) = 2 \tag{9.168}$$

However, the reader can also imagine the hardship that an acrobatic pilot is experiencing in a pull-down maneuver, since he/she is sitting upside down! (i.e., aircraft is inverted; see Figure 9.18). This is not an easy task. Two beautiful pull-up and pull-down maneuvers by prop-driven aircraft (pull-up by two Mudry CAP-10B and pull-down by two Silence Twister) are demonstrated in Figure 9.21.

9.8 ZERO-GRAVITY FLIGHT

The primary source of gravity is the Earth. However, there are a couple of sources of artificial gravity such as turn (e.g., level turn, vertical turn). In any kind of rotation (such as in a turn), a type of acceleration called radial or centripetal acceleration is generated. This acceleration can function similarly to the Earth's gravity. The centripetal acceleration and gravitational constant (g) have the same unit (e.g., m/s^2). In a turn, the load factor (n) may be expressed as a factor of gravity.

The centripetal acceleration is a vector, sometimes added to gravity if they both are in the same direction. If they have opposite directions, they are subtracted from one another. Thus, as a vector, the centrifugal force is sometimes added to the weight

(a) (b)

FIGURE 9.21 (a) Mudry CAP-10B and (b) Silence Twister. (Courtesy of Kas van Zonneveld.)

and sometimes subtracted from it. In a vertical loop, the centrifugal force can cancel out the gravitational force at the top point of the loop. In this section, two cases are presented: (1) orbital flight and (2) free fall cruise.

9.8.1 Orbital Flight

A very famous case for weightlessness (i.e., zero-gravity) is the orbital flight by spacecraft. An ISS astronaut is enjoying weightlessness because his/her weight (downward) is balanced by his/her centrifugal force (outward); F_C. Under such conditions, weightlessness is created by having the right values for space flight velocity and radius and is experienced by anybody onboard (i.e., astronauts). Thus, for the ISS and each astronaut, the balance of forces along the radial direction, using Equation 9.6, yields

$$W = F_C \Rightarrow mg = m\frac{V^2}{R} \tag{9.169}$$

For the human onboard (in fact, for any object) with a given mass, m, this equation is reduced to

$$g = \frac{V^2}{R} \tag{9.170}$$

where m is the mass of the ISS or an astronaut, V is the linear orbital velocity of the ISS or an astronaut, and R is the radius of rotation, orbit (see Figure 9.4b).

The radius in this case is the distance between the spacecraft and the center of the Earth. Whenever the combination of velocity and radius satisfies Equation 9.170, weightlessness is felt. If there is no drag at that altitude, the spacecraft will stay in that altitude (i.e., orbit radius) forever.

Example 9.13

Determine the orbital velocity of a spacecraft at an altitude of 200 km from the Earth if weightlessness is desired. Assume the gravity is 9.81 m/s^2 at the height of 200 km and the Earth's radius is 6,371 km. Then, compare this velocity with the speed of sound at the sea level (i.e., 340 m/s).

Solution

$$g = \frac{V^2}{R} \Rightarrow 9.8 = \frac{V^2}{200{,}000 + 6{,}371{,}000} \tag{9.170}$$

The solution of this equation yields

$V = 8{,}025$ m/s $= 8.02$ km/s $= 28{,}889$ km/h

This orbital velocity is 23.6 times the speed of sound at sea level.

9.8.2 Free Fall Cruise

Section 9.8.1 presented a case for the weightlessness in the space for astronauts; this case is not feasible for an aircraft flying in the air. One practical case for the weightlessness (i.e., zero-gravity) in the air is a kind of cruising (in fact, descending) flight (see Figure 9.22), where the lift is set to be zero ($L = 0$). This flight maneuver is a practical way to experience *weightlessness/microgravity* without leaving the Earth. During such flight, and for a short period of time, scientists/engineers are provided the opportunity to test satellite components or predict problems with experiments destined for the ISS before they are shipped into orbit. It is interesting to note that, currently a private company runs a zero-gravity flight with an Airbus

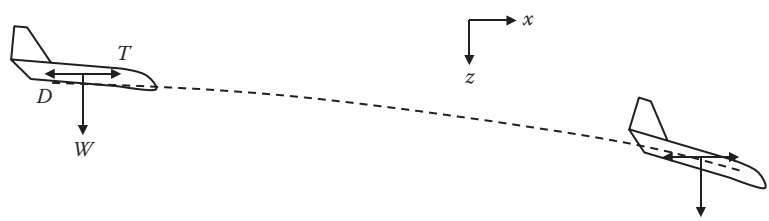

FIGURE 9.22 The free-fall cruising flight to generate weightlessness.

300 with a price tag of about $5,000. Each flight experience is about 20 s. In 2015, the European company Novespace resumed microgravity science flights aboard a new Zero-g Airbus A310. The flights make up one of the world's most demanding flight programs.

In this section, the governing equations of motion for such flight are derived. In a free-fall cruising flight, every movable object (including human onboard) inside the aircraft begins falling freely to the Earth; the contents act as if they are weightless. Since the acceleration in the z-direction is exactly the same as g, an inertial force will be produced in the opposite (upward) direction. This will cancel out the weight of each object. Recall that for any acceleration, there will be an inertial force in the opposite direction. This force is equal to the mass of each object times the motion acceleration.

The flight starts at a high altitude with a given cruising airspeed, V_o. In addition, the engine thrust is set to be equal to the aircraft drag. The forward direction is named as the x-axis, and the downward direction is named as the z-axis. Since the aircraft is under the influence of aircraft weight (W) in the z-direction, it will fall freely in the z-direction. Hence, in the z-direction, the flight will be accelerated under the influence of gravity, g

$$a_z = g \tag{9.171}$$

This relation implies that in the z-direction, the velocity (V_z) is a function of time ($V_z = g \cdot t$) and is exponentially increasing with height. The vertical velocity (V_z) during this accelerated motion is obtained as

$$V_{z_2}^2 - V_{z_1}^2 = 2g\Delta h \tag{9.172}$$

where Δh denotes the height lost in the z-direction, 1 and 2 refer to two arbitrary points. The goal is to keep the airspeed in the x-direction (V_x) always constant and equal to the initial velocity

$$V_x = V_o \tag{9.173}$$

Hence, the acceleration in the x-direction (a_x) is zero:

$$a_x = 0 \tag{9.174}$$

Furthermore, since the aircraft is accelerating in the z-direction, the aircraft velocity in the flight path direction is gradually increasing.

$$V = \sqrt{V_x^2 + V_z^2} \tag{9.175}$$

Since the forward velocity is constant, the horizontal distance traveled in the forward direction is

$$X = V_o t \tag{9.176}$$

The velocity in the z-direction as a function of distance traveled can be obtained from

$$V_z = \frac{gX}{V_o} \tag{9.177}$$

Since the downward velocity is changing due to gravity, the height lost in the z-direction is

$$\Delta h = \frac{1}{2} g t^2 \tag{9.178}$$

The instantaneous height is

$$h = h_o - \Delta h \tag{9.179}$$

When the time, t is calculated from Equation 9.176 and inserted into Equation 9.179, the aircraft height (h) as a function of distance traveled (X) is

$$h = h_o - \frac{1}{2} g \left(\frac{X}{V_o} \right)^2 \tag{9.180}$$

However, since the aircraft has an initial cruising velocity, V_o; the aircraft will descend with a large descent angle. Therefore, the flight path will be parabolic. The instantaneous flight path angle is

$$\gamma = \tan^{-1} \left(\frac{h}{X} \right) \tag{9.181}$$

To make the lift equal to zero, the pilot must set the stick/yoke (thus, elevator), such that the aircraft angle of attack (α) is equal to the aircraft zero-lift angle of attack (α_o):

$$\alpha = \alpha_o \tag{9.182}$$

A typical value for such angle of attack is about −1° to −2°. This will set the aircraft lift coefficient equal to zero:

$$C_L = 0 \tag{9.183}$$

The engine thrust is equal to the aircraft drag in the forward direction:

$$T = D_x = \frac{1}{2}\rho V_x^2 S C_D \tag{9.184}$$

Since the lift coefficient is equal to zero, the drag coefficient will be

$$C_D = C_{D_o} \tag{9.185}$$

Since the velocity in the forward direction is constant, the required engine thrust is

$$T = \frac{1}{2}\rho V_o^2 S C_{D_o} \tag{9.186}$$

This magnitude of the thrust during this flight is much less than that for the cruising flight. It should be clarified that as the aircraft is falling, the downward acceleration is gradually reduced due to the aircraft drag in the z-direction. Hence, in the beginning, there will be a complete *weightlessness*, while afterward, there will be a *microgravity*. For a human, weightlessness and microgravity seem to be almost the same. However, for the high-resolution instruments, the change in acceleration may be crucial. To have a complete weightlessness in the entire flight duration, a negative lift must be produced to cancel out the drag in the z-direction.

So far, the presence of the drag force in the z-direction has been ignored. If you would like to be more accurate, you need to include the aircraft drag in the z-direction (Figure 9.23), which affects the acceleration in the z-axis. According to Newton's second law, in the z-direction, the sum of the forces is equal to the mass times the acceleration:

$$W - D_z = ma_z \tag{9.187}$$

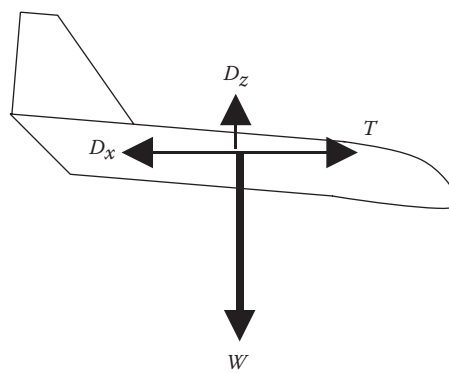

FIGURE 9.23 Forces on an aircraft during free fall cruising.

FIGURE 9.24 KC-135A Stratotanker. (Courtesy of Fabian Dirscherl.)

where m is the mass of the aircraft, and D_z is the drag force in the z-direction.

$$D_z = \frac{1}{2}\rho V_z^2 S_z C_{D_z} \tag{9.188}$$

where C_{D_z} denotes the aircraft drag coefficient in the z-direction, and S_z is the aircraft total planform area from down-view:

$$S_z = S_f + S + S_{\text{ht}} \tag{9.189}$$

where S_f represents the fuselage down-view projected area, and S_{ht} is the horizontal tail area.

The aircraft drag coefficient in the z-direction (C_{D_z}) is not easy to calculate. The wind tunnel tests may be employed to determine the value for C_{D_z}. For the preliminary analysis, a typical value of 0.5–0.7 (see Table 3.1) may be utilized. Thus, the real acceleration in the z-direction (microgravity) is

$$a_z = \frac{W - D_z}{m} \tag{9.190}$$

The engine thrust and air density are functions of altitude. The NASA Johnson Space Center used Boeing KC-135A Stratotanker (Figure 9.24) for weightlessness trials. Astronauts called the aircraft "The Vomit Comet", because the parabolic flight path that is used to make zero g's inspires *airsickness* in neophyte astronauts. Example 9.14 demonstrates the application of the governing equations to determine flight variables. An example in Chapter 10 shows the application of MATLAB® to plot the parabolic flight path for a zero-gravity flight.

Example 9.14

An Airbus 300 is employed in a zero-gravity flight. The flight started at 8,000 m with a velocity of 226.3 m/s (440 knots) and lasted about 20 s. Determine (1) horizontal distance traveled, (2) height lost, (3) vertical velocity, (4) average descent angle, and (5) total velocity, at the end of 20 s. Ignore the drag force in the z-direction.

Solution

1. Horizontal distance traveled

$$X = V_o t = 226.3 \times 20 = 4{,}527\,\text{m} = 4.53\,\text{km} \tag{9.176}$$

2. Height lost

$$\Delta h = \frac{1}{2} g t^2 = \frac{1}{2} \times 9.81 \times 20^2 = 1{,}961\,\text{m} = 1.96\,\text{km} \tag{9.178}$$

3. Vertical velocity

$$V_2 = \frac{gX}{V_o} = \frac{9.81 \times 4{,}527}{226.3} = 196.1\,\text{m/s} = 381.2\,\text{knot} \tag{9.177}$$

4. Average descent angle

$$\gamma = \tan^{-1}\left(\frac{h}{X}\right) = \tan^{-1}\left(\frac{1{,}961}{4{,}527}\right) = 23.4° \tag{9.181}$$

5. Total velocity

$$V = \sqrt{V_x^2 + V_z^2} = \sqrt{226.3^2 + 196.1^2} = 299.5\,\text{m/s} = 1{,}070\,\text{km/h} \tag{9.175}$$

9.9 *V-N* DIAGRAM

9.9.1 Flight Envelope

The flight regime of any aircraft usually includes all permissible combinations of speeds, altitudes, weights, centers of gravity, and configurations. This regime is primarily shaped by aerodynamics, propulsion, structure, and dynamics of aircraft. The borders of this flight regime are referred to as the *flight envelope* or maneuvering envelope. The safety of human onboard is guaranteed by aircraft designer and manufacturer, as long as the flight is within the boundaries of the published flight envelope. Pilots are always trained and warned through flight instruction manuals not to fly out of the flight envelope, since the aircraft is not stable, not controllable, or not structurally strong enough outside the boundaries of the flight envelope. A mishap or even a crash is expected, if an aircraft is flown outside the flight envelope.

The flight envelope has various types; each of which is usually the allowable variations of one flight/aircraft parameter versus another flight/aircraft parameter. These envelopes are calculated and plotted by flight dynamics engineers and employed by pilots and flight crews. For instance, the load masters of a cargo aircraft must

pay extra caution to the center of gravity location whenever they distribute various loads on the aircraft. There have been several crashes and mishaps that National Transportation Safety Board's report indicated that, load masters are responsible for them since they either deployed more loads than allowed or misplaced the payload (such that the aircraft cg has gone beyond the allowable range). Nose-heavy and tail-heavy flights are two flight concepts that pilots are familiar with, and are often experienced and are trained to deal with safely.

Pilots use several graphs and charts in conducting their flight operations. Four important envelopes are as follows:

1. Diagram of variations of aircraft lift coefficient versus Mach number ($C_L - M$)
2. Diagram of variations of airspeed versus altitude ($V - h$)
3. Diagram of variations of center of gravity versus aircraft weight ($X_{cg} - W$)
4. Diagram of variations of load factor versus airspeed (*V-n*)

One of the most important diagrams of the flight envelope is the *V-n* diagram. This envelope demonstrates the variations of the allowable load factor versus airspeed. In other words, it depicts the aircraft limit load factor as a function of airspeed. As it is presented in Section 9.3, the allowable load factor is different from the producible load factor. The allowable load factor is a function of the strength of the aircraft structure, while the producible load factor is a function of engine power/thrust and flight condition. In the case of an aircraft with a very powerful engine, while the structure is not strong enough, the allowable load factor, in a level/vertical turn, is less than the producible load factor. But, in the case of an aircraft with a regular engine, while the structure is very strong, the allowable load factor, in a level turn, is more than producible load factor.

One of the primary reasons that this diagram is highly important is that the maximum load factor that is extracted from this graph is a reference number in the aircraft structural design. If the maximum load factor is undercalculated, the aircraft cannot withstand the flight loads safely. For this reason, it is recommended that structural engineers recalculate and replot the *V-n* diagram on their own to ensure the safety issues.

In this section, details of the technique to plot the *V-n* diagram are introduced. Figure 9.25 shows a typical *V-n* diagram for a GA aircraft. This diagram is, in fact, a combination of two diagrams: (1) the *V-n* diagram without consideration of gust and (2) the *V-n* diagram with the effect of gust. In this section, we first have another look at the load factor and then present some new concepts on the load factor. Then, the phenomena of gust and gust load are described. At the end of this section, the technique to plot *V-n* diagram is completely described. This description is supported by a solved example.

9.9.2 Load Factor

There are several forces that are active during a flight operation such as aircraft weight, engine thrust, lift, and drag. The weight of an aircraft on the ground/air

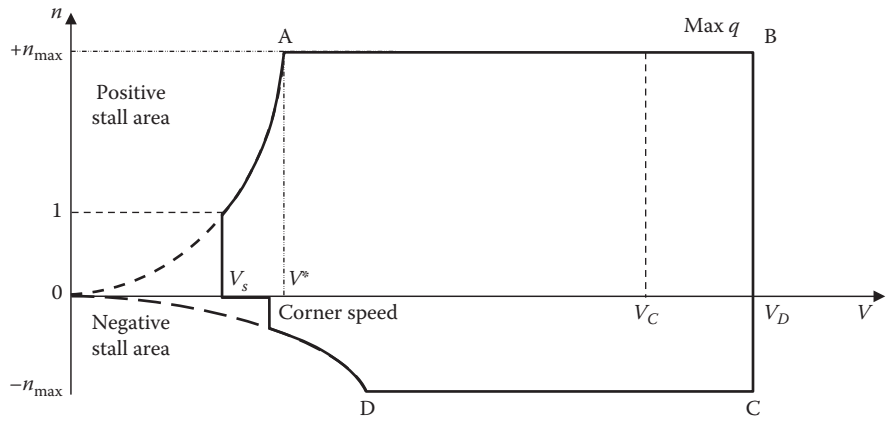

FIGURE 9.25 A typical *V-n* diagram for a GA aircraft.

is naturally produced by the gravity (i.e., mass times gravity). But, there are other sources of load to the aircraft during flight, such as the inertial forces (e.g., centrifugal force due to centripetal acceleration, a_c), gust loads, and landing load. The combination of these forces will apply load on the aircraft structure and on human onboard. Two forces of lift and centrifugal force may be compared with the aircraft weight and expressed with respect to weight. In some instances of flight such as turn and pull-up, the aircraft must generate a lift force such that, it is greater than the aircraft weight. During a cruising flight, the lift is equal to weight, while during a level turn, the lift is greater than the weight. Recall that we defined the load factor as the ratio between the lift and weight:

$$n = \frac{L}{W} \tag{9.8}$$

In principle, there are four types of load factors: (1) maximum producible load factor by the lift using the maximum engine thrust/power in a level turn, (2) maximum producible load factor by the centrifugal force in the extreme case of the pull-out of a dive, (3) maximum producible load factor in an undesired motion produced by the lift/inertial force due to a gust/turbulence, and (4) maximum allowable load factor (tolerable by the aircraft structure and the human onboard). As the load factor increases, the load on the aircraft structure (e.g., wing and tail) will be increased; thus, the structure should be stronger. In the aircraft structural design, the highest allowable load factor is considered. Furthermore, a pilot is not allowed to create a load factor, which is not safe for structure or is beyond his/her body physical strength.

To expand the concept of load factor, other loads/forces (including centrifugal force) are usually normalized through load factor and aircraft weight (i.e., n times mass times g, $n.m.g$). In other words, aircraft load is expressed as a factor of the

TABLE 9.8
Statistical Values of Load Factor for Several Aircraft

No.	Aircraft	Engine	m_{TO} (kg)	*P* or *T*	+*n*	−*n*
1.	Cirrus SR20	Piston	1,360	200 hp	3.8	−1.9
2.	Pegasus Quantum	Piston	409	80 hp	6	−3
3.	PITTS S-2A	Piston	680	200 hp	9	−4.5
4.	Sukhoi SU-26M	Piston	800	360 hp	11	−9
5.	Cessna 172—Normal	Piston	1,111	160 hp	3.8	−1.52
6.	Cessna 172—Utility	Piston	1,111	160 hp	4.4	−1.76
7.	Canadair CL-215	Turboprop	17,100	2×2,100 hp	3.25	−1
8.	Cessna 208	Turboprop	3,311	600 hp	3.8	−1.52
9.	Pilatus PC-12	Turboprop	4,500	1,200 hp	3.4	−1.36
10.	Eurofighter	Turbofan	17,000	2×90 kN	9	−3
11.	Jaguar	Turbofan	15,700	2×36 kN	8.6	—
12.	Mirage 2000	Turbofan	10,960	64.3 kN	13.5	—
13.	BAe Hawk 60	Turbofan	8,570	23.8 kN	8	−4
14.	Boeing Skyfox	Turbofan	7,365	2×16.5 kN	7.3	−3.5
15.	Cessna 650	Turbofan	9,979	2×16.2 kN	3	−1
16.	Rockwell X-31	Turbofan	7,228	71 kN	9	−4
17.	Lockheed Martin F-22 Raptor	Turbofan	27,216	2×156 kN	9	—
18.	Bell Boeing V-22 Osprey	Turboprop/ turboshaft	21,546	2×6,150 hp	3.3	−0.84

standard acceleration due to gravity ($g = 9.81\ \text{m/s}^2 = 32.17\ \text{ft/s}^2$). For instance, the load factor in a pull-up from Equation 9.155 can be written as a function of g and a_c:

$$n = \frac{a_c}{g} + 1 \tag{9.191}$$

where a_c is the centripetal acceleration (V^2/R). As this acceleration increases (i.e., airspeed increases or turn radius decreases), the load factor will increase as well. Hence, in a vertical turn (e.g., pull-up/pull-out), the load factor is only a function of centripetal acceleration. In contrast, in a level turn, the load factor is only a function of the bank angle. Table 9.8 demonstrates real values [9] of the maximum load factor for several jet and prop-driven aircraft.

9.9.3 Maneuver Diagram

The *V-n* diagram is basically an envelope that indicates the limits of load factor and speed for a safe flight. Here, the load factor is the maximum allowable n, not the maximum producible *n*. In this section, we assume that there is no gust during the flight, so its effect is neglected. This diagram is sometimes referred to as the *maneuver diagram*. Figure 9.25 demonstrates a typical plot of a *V-n* diagram with a

maximum load factor for positive limit and a maximum load factor for negative limit. It is usually composed of three lines plus two curves. The two curves on the left-hand side represent the aerodynamic limit on the load factor imposed by stall ($C_{L_{\max}}$). The two straight lines on the top and bottom represent the maximum positive and negative allowable load factors, respectively. The vertical line on the right represents the maximum allowable airspeed.

The expression for the top curve is extracted from the stall equation in a level turn:

$$V_{s_t} = \sqrt{\frac{2nmg}{\rho S C_{L_{\max}}}} \tag{9.12}$$

This equation can be solved for the maximum load factor for a given velocity; the V_{s_t} will be replaced with a V:

$$n = \frac{V^2 \rho S C_{L_{\max}}}{2mg} \tag{9.192}$$

The velocity for this section is between two limits. The lowest limit is the stall velocity (V_s) for a cruising flight. The upper limit is the velocity that yields a load factor, which is equal to the maximum positive load factor. The top curve is literally a plot of Equation 9.192. The region above this curve in the *V-n* diagram is the stall area. An aircraft is unable to have a sustained flight when the aircraft angle of attack is greater than the stall angle. Since no aircraft can fly continuously at a flight condition above this curve, this is one of the limits on the aircraft maneuverability.

Based on Equation 9.192, as the airspeed increases, the maximum load factor will increase proportionally to V^2. However, $n_{\max}$ cannot be allowed to increase indefinitely. It is constrained by the structural strength (structural limit load factor). The top horizontal line denotes the positive limit load factor in the *V-n* diagram.

The flight velocity corresponding to the intersection between the left top curve and top horizontal line (point A) is referred to as the *corner velocity* and designated as V^* (V-star). The corner velocity can be obtained by solving Equation 9.192 for velocity, yielding

$$V^* = \sqrt{\frac{2n_{\max}mg}{\rho S C_{L_{\max}}}} \tag{9.193}$$

where the value of $n_{\max}$ corresponds to point A. This speed sometimes is referred to as *maneuvering speed* (V_A). By comparing Equations 9.193 and 2.27, one can obtain the relation between the maneuvering speed and the normal stall speed:

$$V_A = \sqrt{n_{\max}} V_s \tag{9.194}$$

Point A is then called the *maneuver point*. At this point, both lift coefficient and load factor are simultaneously at their highest possible magnitudes. The corner velocity

is an interesting velocity for fighter pilots and acrobatic aircraft. At speeds less than V^*, the aircraft will not be structurally damaged due to the generation of load factor less than n_{max}. In contrast, at speeds greater than V^*, maneuverability decreases since the speed is too high. Thus, fighter pilots are recommended to select this speed for much of their maneuvering missions. For majority of the cases, and according to the discussions presented in Sections 9.5 and 9.6, this point simultaneously corresponds to the *tightest turn and fastest turn* of an aircraft. The GA aircraft Cessna 172 has a maneuvering speed of 97 knots, while its stall speed is 47 knots. Typical corner velocities of current modern fighters are around 250–350 KEAS.

The right-hand side of the *V-n* diagram, vertical line BC, is the highest speed limit. This speed is usually selected to be the *dive speed*. At flight speeds higher than this limit, the dynamic pressure (q) and flight loads are greater than the design limit for the aircraft. At speeds above dive speed, destructive phenomena such as flutter and aileron reversal may happen, which leads to structural damage, failure, or even disintegration. This speed limit (dive speed) is a redline speed for the aircraft and it should never be exceeded. Due to this reason, this velocity is also referred to as the never-exceeded speed (V_{NE}). The dive speed (V_D) is usually higher than the aircraft maximum speed (V_{max}). In addition, the aircraft maximum speed (V_{max}) is slightly greater than the aircraft cruising speed (V_C). From FAR Part 23, the following regulations have been reproduced for the relation between the dive speed and the cruising speed for GA aircraft:

$$V_D \geq 1.4V_C \quad \text{(normal aircraft)} \tag{9.195}$$

$$V_D \geq 1.5V_C \quad \text{(utility aircraft)} \tag{9.196}$$

$$V_D \geq 1.55V_C \quad \text{(acrobatic aircraft)} \tag{9.197}$$

The techniques to calculate the maximum and cruising speeds have been presented in Chapters 5 and 6. The bottom line of the *V-n* diagram, given by horizontal line CD, corresponds to the maximum negative limit load factor that is a structural limit when the aircraft is in a situation such as inverted flight (Figure 9.26a). The bottom left curve corresponds to the negative stall angle of attack. Since most wing airfoils have positive camber, their positive stall angles are often much higher than the absolute values of their negative stall angles. This curve defines the negative stall area. The absolute value for the typical negative maximum lift coefficient is about 50% of the positive maximum lift coefficient. Therefore, the typical stall speed for an inverted flight is about 40% greater than the stall speed for a normal flight. Example 9.15 demonstrates the details of plotting a *V-n* diagram for an aircraft.

9.9.4 Gust *V-n* Diagram

The atmosphere is a dynamic system that encompasses a variety of undesired phenomena. These phenomena include wind, turbulence, gust, wind shear, jet stream, mountain wave, and thermal flow. Since the gust in the atmosphere is a true story,

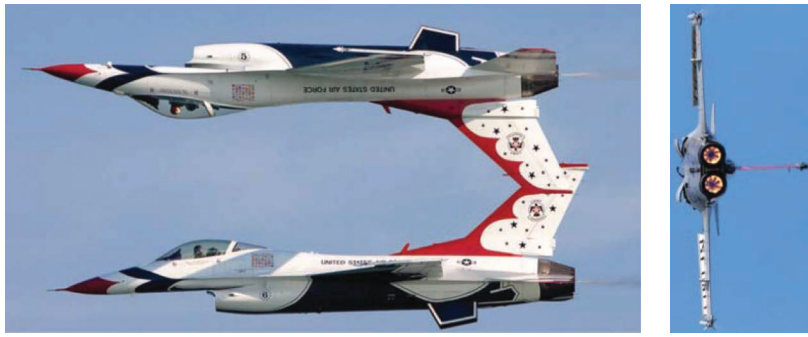

(a) (b)

FIGURE 9.26 Two flight maneuvers with a high load factor. (a) Lockheed F-16CM Fighting Falcon in an inverted flight. (b) Dassault Rafale C in a very high bank angle turn. (Courtesy of Fabrizio Capenti.)

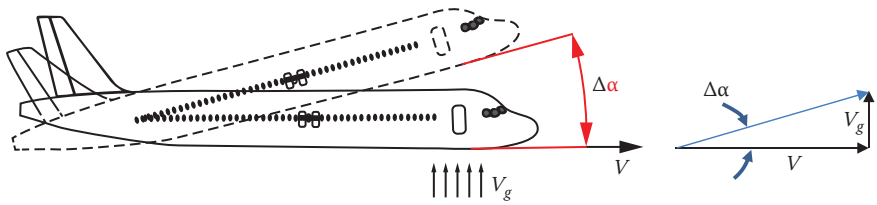

FIGURE 9.27 The geometry of an upward gust and induced angle of attack.

aircraft designers must predict the gust loads and add them to the aircraft regular load (i.e., maneuver load) to have a safe and reliable structure in the real flight operations. In this section, we concentrate to plot a *V-n* diagram, when only gust and turbulence loads are considered. This diagram is sometimes referred to as the gust envelope.

Gusts are not predictable but are usually expected to happen during a cruising flight. The loads experienced when an aircraft encounters a strong gust may not exceed the allowable load. Hence, we must pay attention to gust load when plotting *V-n* diagram. We need to know the gust velocity to determine the gust load. It is very hard to measure gust velocity, since it happens suddenly. The design requirements for gust velocities are often extracted from flight tests data. An airplane must be designed to withstand loads on each lifting surface (e.g., wing and tail) resulting from gusts.

A gust may hit an aircraft from any direction. The one that affects the load factor is an upward gust or a downward gust, which may lead to a pith up/down or a plunging motion. When an aircraft experiences a gust, the immediate effect is an increase or a decrease in the angle of attack. Figure 9.27 shows the geometry of an upward gust. Consider an upward gust with a velocity of V_g hits under the nose of an aircraft cruising with the velocity of V. This incidence can be modeled as an induced

angle of attack. The instantaneous change (increase) in the angle of attack ($\Delta\alpha$) is determined using

$$\Delta\alpha = \tan^{-1}\left(\frac{V_g}{V}\right) \tag{9.198}$$

Since the gust speed is much smaller than the aircraft speed, the corresponding angle is small (usually <15°). Hence, Equation 9.198 may be linearized as

$$\Delta\alpha \approx \left(\frac{V_g}{V}\right) \ (\text{in rad}) \tag{9.199}$$

Any sudden change (increase) in the angle of attack will produce a sudden change (increase) in the aircraft lift coefficient (ΔC_L). Referring to Equation 2.10, one can obtain

$$\Delta C_L = C_{L_\alpha}\Delta\alpha \tag{9.200}$$

This in turn will generate a sudden change (increase) in the lift (ΔL). Referring to Equation 2.4, we obtain

$$\Delta L = \frac{1}{2}\rho V^2 S\Delta C_L \tag{9.201}$$

Consequently, this change in the lift will create a change in the load factor. Recall the definition of the load factor (Equation 9.8):

$$\Delta n = \frac{\Delta L}{W} \tag{9.202}$$

Equation 9.202 indicates that a gust will change the load factor, and will generate a load called gust load.

There are various models for gust prepared by various researchers. Here, we use the FARs for the gust modeling. According to FAR 23 (Section 23.333), a GA aircraft must be able to withstand positive and negative gusts of 50 ft/s at the cruise velocity from the sea level up to 20,000 ft. From 20,000 to 50,000 ft, the gust velocity decreases linearly to 25 ft/s. Moreover, the aircraft must carry gust load during dive speed if the gust speed is 25 ft/s. In addition, a commuter aircraft must safely fly at maneuver speed when it encounters a gust with the velocity of 66 ft/s.

According to FAR 25, a transport aircraft must be able to withstand positive and negative gusts of 85 fps at the cruise velocity from the sea level up to 30,000 ft altitude. From 30,000 to 80,000 ft, the gust velocity decreases linearly to 30 ft/s. However, at the design speed for maximum gust intensity (V_B), the gust speed is equal to 1.32 times the values obtained from the cruising speed.

TABLE 9.9
Gust Speed for Constructing Gust-Induced Load

No.	Aircraft Type	Airspeed	Sea Level up to 20,000 ft	20,000–50,000 ft
1.	GA normal, utility, acrobatic	Cruise speed	50 ft/s	50 ft/s decreases linearly to 25 ft/s
		Dive speed	25 ft/s	25 ft/s decreases linearly to 12.5 ft/s
2.	Commuter	Design speed for maximum gust intensity	66 ft/s	66 ft/s decreases linearly to 38 ft/s
No.	**Aircraft Type**	**Airspeed**	**Sea Level up to 30,000 ft**	**30,000–80,000 ft**
3.	Transport	Cruise speed	85 ft/s	85 ft/s decreases linearly to 30 ft/s
		Design speed for maximum gust intensity	112 ft/s	112 ft/s decreases linearly to 40 ft/s

These data and regulations are employed to plot the gust *V-n* diagram (Gust envelope). A summary of these requirements [87, 98] is presented in Table 9.9. Design speed for maximum gust intensity, V_B, is a speed greater than the maneuvering speed and less than the cruise speed.

For modeling the "gust-induced load factor" as a function of gust speed and aircraft characteristics, the FAR 23 (Section 23.341) recommendation is employed. In the absence of a more rational analysis, the gust load factors are computed using the following equation:

$$n = 1 + \frac{k_g V_{gE} V_E a \rho S}{2W} \tag{9.203}$$

where W denotes the aircraft weight (in N), ρ is the air density (in kg/m^3), S is the wing area (in m^2), V_E is the aircraft equivalent airspeed (in m/s), V_{gE} is the gust equivalent speed (in m/s), and a is wing lift curve slope during the gust encounter (in 1/rad). In addition, the parameter k_g denotes the gust alleviation factor and is determined by the following expression:

$$k_g = \frac{0.88\mu_g}{5.3 + \mu_g} \tag{9.204}$$

and μ_g is called the aircraft mass ratio and is calculated using the following relationship:

$$\mu_g = \frac{2m}{\rho C a S} \tag{9.205}$$

where C is the wing mean geometric chord (in m), and m denotes the aircraft mass (in kg). Note that; although in FAR; the gust speeds are expressed in ft/s, the unit in

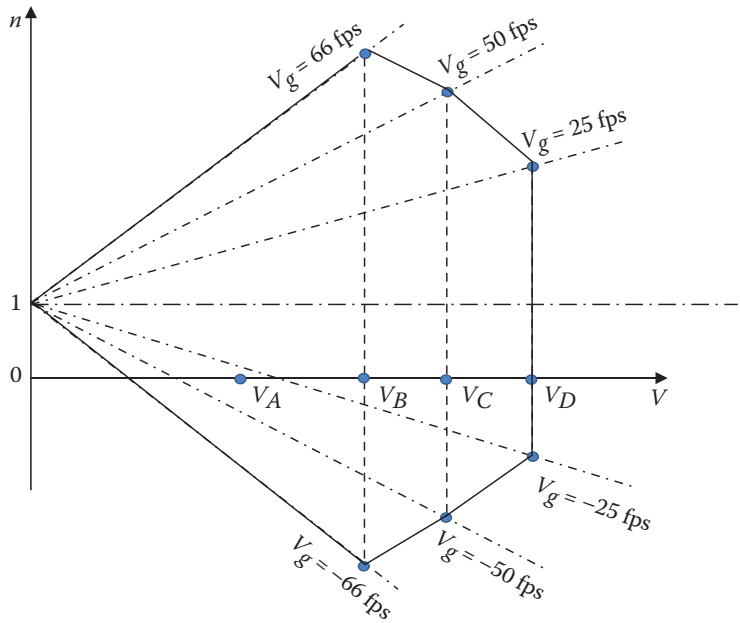

FIGURE 9.28 A typical gust *V-n* diagram (Gust envelope).

Equations 9.203–9.205 is in SI system (i.e., it is not in British units). The density of air in Equation 9.203 is the standard air density (1.225 kg/m^3), while the air density in Equation 9.205 is the air density at the flight altitude considered, which leads to higher gust load factors as flight altitude increases from sea level to 20,000 ft. Negative maneuvering load factors may be decreased between cruise speed and dive speed.

The gust *V-n* diagram is plotted using lines based on Equation 9.203 for various speeds (e.g., 25, 50, and 66 ft/s) and for both positive and negative load factors. Then, the intersections between these three lines with their respective velocities (e.g., design speed for maximum gust intensity (V_B), cruising speed (V_C), and dive speed (V_D)) must be marked. The gust *V-n* diagram (i.e., gust envelope) is plotted for several altitudes to determine the highest load factor. Figure 9.28 shows a typical gust *V-n* diagram. This diagram will be finally combined, with a special method, with the basic *V-n* diagram to obtain the final completed *V-n* diagram.

9.9.5 Flight Envelope: Combined *V-n* Diagram

The technique to plot a basic *V-n* diagram is introduced in Section 9.9.3. Moreover, in Section 9.9.4, the technique to plot the gust *V-n* diagram is presented. This section is about the technique to combine the basic *V-n* diagram with the gust *V-n* diagram to construct a *flight envelope*. The maximum combined load factor is usually higher than the individual load factor in each case.

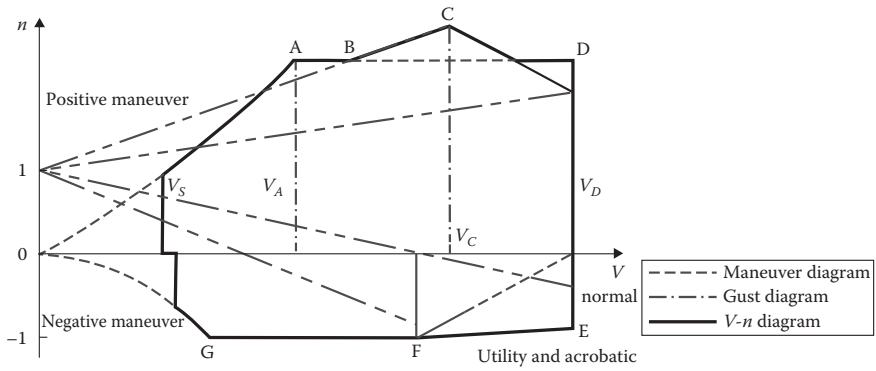

FIGURE 9.29 A typically combined *V-n* diagram (flight envelope) for an aircraft.

To construct the flight envelope, follow these steps:

1. Place both *V-n* diagrams (maneuver and gust) in one plot.
2. Identify and mark the intersection points or corner points for each individual diagram.
3. Identify and mark the intersection points between the lines of second diagram and the lines and curves of the first diagram.
4. Connect all outer intersection points with straight lines (except stall curves).
5. Check for sanity. Make sure that no intersection point or corner point is outside the envelope. Also, no point should be in the stall regions.

A typically combined *V-n* diagram for an aircraft is illustrated in Figure 9.29. In this example figure, the maximum load factor is determined from point C (intersection of the cruise speed with the 55 ft/s gust line). The *V-n* diagram (flight envelope) is unique for each aircraft, and pilots and flight crew members are required to fly and operate inside this flight envelope. From this diagram, one can observe that the maximum allowable load factor is higher than the one required by FAR requirements. This is an undesired influence of the gust on the structural design. The following example demonstrates details of the technique to plot the combined *V-n* diagram (flight envelope) for an acrobatic aircraft.

Example 9.15

Plot the flight envelope (combined *V-n* diagram) for the following GA acrobatic aircraft. Then, determine the maximum load factor.

$$m = 2{,}300\,\text{kg},\ S = 19.33\,\text{m}^2, C_{L_{\max}} = 2, -C_{L_{\max}} = -1.2, \text{AR} = 7, C_{L_\alpha} = a = 6.3\,1/\text{rad},$$

$$V_c = 310\,\text{KEAS or } 159.5\,\text{m/s (at } 10{,}000\,\text{ft}).$$

Solution

FAR does specify regulations/requirements for gust loads as well as a positive maximum load factor and a negative maximum load factor for acrobatic aircraft. We first need to calculate the AR and mean aerodynamic chord:

$$\mathrm{AR} = \frac{b^2}{S} \Rightarrow b = \sqrt{\mathrm{AR} \cdot S} = \sqrt{7 \times 19.33} \Rightarrow b = 11.63\,\mathrm{m} \tag{3.9}$$

For a rectangular wing, $S = b \cdot C$. Hence:

$$\bar{C} = \frac{S}{b} = \frac{19.33}{11.63} \Rightarrow \bar{C} = 1.66\,\mathrm{m}$$

The combined *V-n* diagram is plotted in three steps: (1) basic (maneuver) *V-n* diagram, (2) gust *V-n* diagram, and (3) combined *V-n* diagram.

1. BASIC *V-N* DIAGRAM

As discussed in Section 9.9.3, the general shape of the basic *V-n* diagram resembles Figure 9.30. We just need to determine the coordinates of points K, J, G, F, B, and A. The unit of velocity in the graph is selected to be in knot (KEAS).

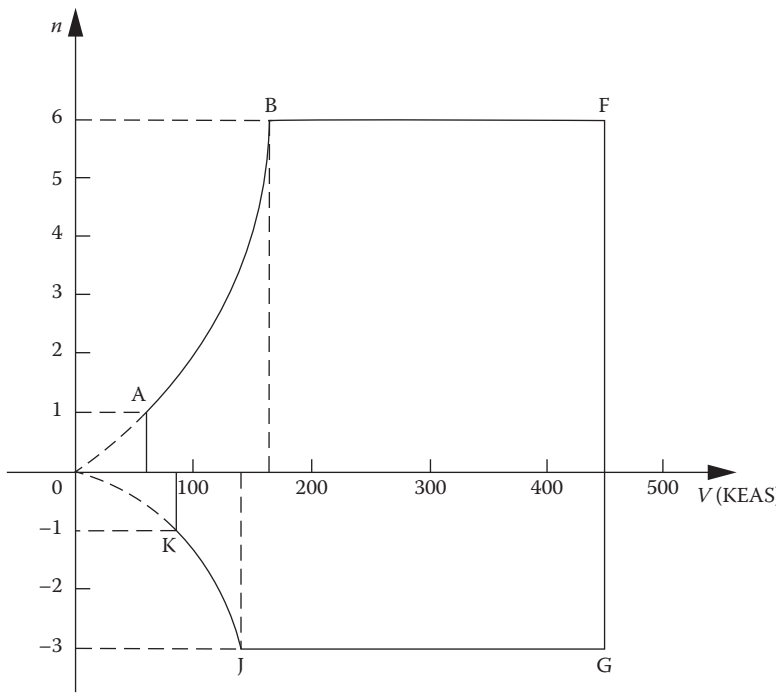

FIGURE 9.30 The basic *V-n* diagram for the acrobatic aircraft in example.

Since the aircraft is acrobatic, the maximum limit load factor, based on FAR 23, is as follows:

- (Positive) $n_{\max} = +6$,
- (Negative) $n_{\max} = -(0.5 \times 6) = -3$.

The dive speed of this aircraft from Equation 9.197 is

$$V_D = 1.55V_C = 1.55 \times 310 = 480.5 \text{ knot.} \tag{9.197}$$

Hence, the coordinates of points F and G are (6, 480.5) and (–3, 480.5). To determine coordinates of points A, B, J, K, we need to derive two equations regarding $C_{L_{\max}}$.

$$V_s = \sqrt{\frac{2mg}{\rho S C_{L_{\max}}}} = \sqrt{\frac{2 \times 2{,}300 \times 9.81}{1.225 \times 19.33 \times 2}} = 30.87 \text{ m/s} = 60 \text{ KEAS} \tag{2.27}$$

Thus, the coordinates of point A are (1, 60). The top stall curve or the load factor as a function of airspeed (in m/s) is

$$n = \frac{\rho V^2 S C_{L_{\max}}}{2W} = \frac{1.225 \times V^2 \times 19.33 \times 2}{2 \times 2{,}300 \times 9.81} = 0.100105V^2 \tag{9.192}$$

For point B, the load factor is given as 6, so the corresponding speed is determined by

$$6 = 0.100105\ V^2 \Rightarrow V = 75.6 \text{ m/s} = 147 \text{ KEAS}$$

Thus, the coordinates of point B are (6, 147). With the same technique, we can derive the equation for the lower stall curve

$$V_{sl} = \sqrt{\frac{-2mg}{\rho S\left(-C_{L_{\max}}\right)}} = \sqrt{\frac{-2 \times 2{,}300 \times 9.81}{1.225 \times 19.33 \times (-1.2)}} = 39.85 \text{ m/s} = 77.5 \text{ KEAS} \tag{2.27}$$

So, the coordinates of point K are (–1, 77.5). The lower stall curve or the load factor as a function of airspeed (in m/s) is

$$-n = \frac{\rho V^2 S\left(-C_{L_{\max}}\right)}{2W} = \frac{1.225 \times V^2 \times 19.33 \times (-1.2)}{2 \times 2{,}300 \times 9.81} = -0.00063V^2 \tag{9.192}$$

For point J, the load factor is given as –3; hence, the corresponding speed is determined as

$$-3 = -0.00063\ V^2 \Rightarrow V = 69 \text{ m/s} = 134.2 \text{ KEAS}$$

Thus far, we have collected the following coordinates:

O → (0, 0),
A → (1, 60),
B → (6, 147),
F → (6, 480.5),
G → (–3, 480.5),
J → (–3, 134.2),
K → (–1, 77.5).

By using these data, we can plot the basic *V-n* diagram as illustrated in Figure 9.30.

2. GUST *V-N* DIAGRAM

The variations of load factor as a function of airspeed (V) and gust speed (V_g) are given by

$$n = 1 + \frac{k_g V_{gE} V_E a \rho S}{2W} \tag{9.203}$$

Since the cruising speed is given for 10,000 ft, two flight conditions are considered for the maximum load factor. Then, we calculate n for both V_C and V_D.

A. Sea Level

The aircraft mass ratio is

$$\mu_g = \frac{2m}{\rho CaS} = \frac{2 \times 2,300}{1.225 \times 1.66 \times 6.3 \times 19.33} = 18.75 \tag{9.205}$$

Then, the gust alleviation factor is obtained as

$$k_g = \frac{0.88\mu_g}{5.3 + \mu_g} = \frac{0.88 \times 18.75}{5.3 + 18.75} = 0.684 \tag{9.204}$$

From Table 9.9, at sea level with the cruising speed, the gust velocity of ±50 ft/s (i.e., ±15.25 m/s) should be considered; thus, the load factor will be

$$n = 1 + \frac{0.684 \times (\pm 15.25) \times V \times 6.3 \times 1.225 \times 19.33}{2 \times 2,300 \times 9.81} \Rightarrow n = 1 \pm 0.03436V \tag{9.203}$$

Since the cruising speed (V_C) is 310 KEAS,

$$n = 1 + 0.03436V = 1 + 0.03436 \times 310 \times 0.5144 = 6.48 \ (\text{positive value})$$

$$n = 1 - 0.03436V = 1 - 0.03436 \times 310 \times 0.5144 = -4.48 \ (\text{negative value})$$

We perform similar calculations for the dive speed. When the aircraft is flying with dive speed (V_D), the gust speed should be ±25 ft/s (i.e., ±7.5 m/s). Hence, the load factor is

$$n = 1 + \frac{0.684 \times (\pm 7.5) \times V \times 6.3 \times 1.225 \times 19.33}{2 \times 2,300 \times 9.81} \Rightarrow n = 1 \pm 0.01688V \tag{9.203}$$

Since the dive speed (V_D) is 480.5 KEAS,

$$n = 1 + 0.01688V = 1 + 0.01688 \times 480.5 \times 0.5144 = 1 + 4.173 = 5.173 \ (\text{positive value})$$

$$n = 1 - 0.01688V = 1 - 0.01688 \times 480.5 \times 0.5144 = 1 - 4.173 = -3.173 \ (\text{negative value})$$

b. 10,000 ft Altitude

At 10,000 ft altitude, the air density is 0.9 kg/m³. Parameters μ_g and k_g are obtained:

$$\mu_g = \frac{2m}{\rho CaS} = \frac{2 \times 2{,}300}{0.9 \times 1.66 \times 6.3 \times 19.33} = 26.54 \tag{9.205}$$

$$k_g = \frac{0.88\mu_g}{5.3 + \mu_g} = \frac{0.88 \times 26.54}{5.3 + 26.54} = 0.733 \tag{9.204}$$

When the gust velocity is ±50 ft/s (i.e., ±15.25 m/s), the load factor will be

$$n = 1 + \frac{0.733 \times (\pm 15.25) \times V \times 6.3 \times 0.9 \times 19.33}{2 \times 2{,}300 \times 9.81} \Rightarrow n = 1 \pm 0.02715V \tag{9.203}$$

The cruising speed (V_C) is given as 310 KEAS; therefore,

$$n = 1 + 0.02715V = 1 + 0.02715 \times 310 \times 0.5144 = 5.26 \ (\text{positive value})$$

$$n = 1 - 0.02715V = 1 - 0.02715 \times 310 \times 0.5144 = -3.26 \ (\text{negative value})$$

When the aircraft is flying with the dive speed (V_D), the gust speed should be ±25 ft/s (i.e., ±7.5 m/s). Hence, the load factor is

$$n = 1 + \frac{0.733 \times (\pm 7.5) \times V \times 6.3 \times 0.9 \times 19.33}{2 \times 2{,}300 \times 9.81} \Rightarrow n = 1 \pm 0.01315V \tag{9.203}$$

The dive speed (V_D) is given as 480.5 KEAS; therefore,

$$n = 1 + 0.01315V = 1 + 0.01315 \times 480.5 \times 0.5144 = 1 + 3.25 = 4.25 \ (\text{positive value})$$

$$n = 1 - 0.01315V = 1 - 0.01315 \times 480.5 \times 0.5144 = 1 - 3.25 = -2.25 \ (\text{negative value})$$

By comparison between the results of Sections (a) and (b), we see that the maximum load factor at sea level is higher than the load factor at 10,000 ft (as we expected). Recall that, equivalent airspeeds are independent of altitude. Therefore, we conclude

$$+n_{\max} = 6.48$$
$$-n_{\max} = -4.48$$

Thus, the coordinates of points D and I are, respectively (6.48, 310) and (−4.48, 310). The gust *V-n* diagram is sketched in Figure 9.31.

3. COMBINED *V-N* DIAGRAM

Now, we have sufficient data to plot the combined *V-n* diagram. We first, place both diagrams (maneuver and gust) in one plot. Then, we identify and mark the intersection points or corner points for each individual diagram (points A, B, D, F, H, I, K in Figure 9.32). Now, we observe that the line BF and the gust line

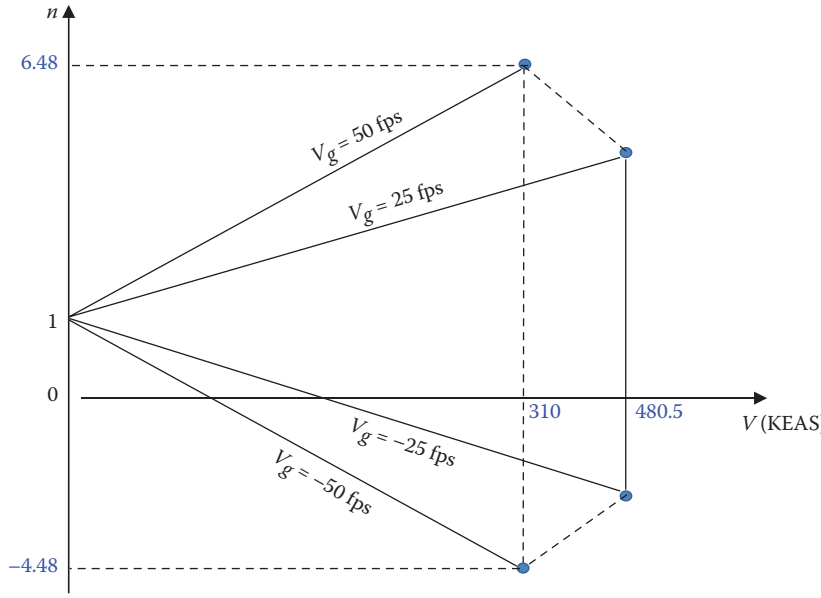

FIGURE 9.31 The gust *V-n* diagram.

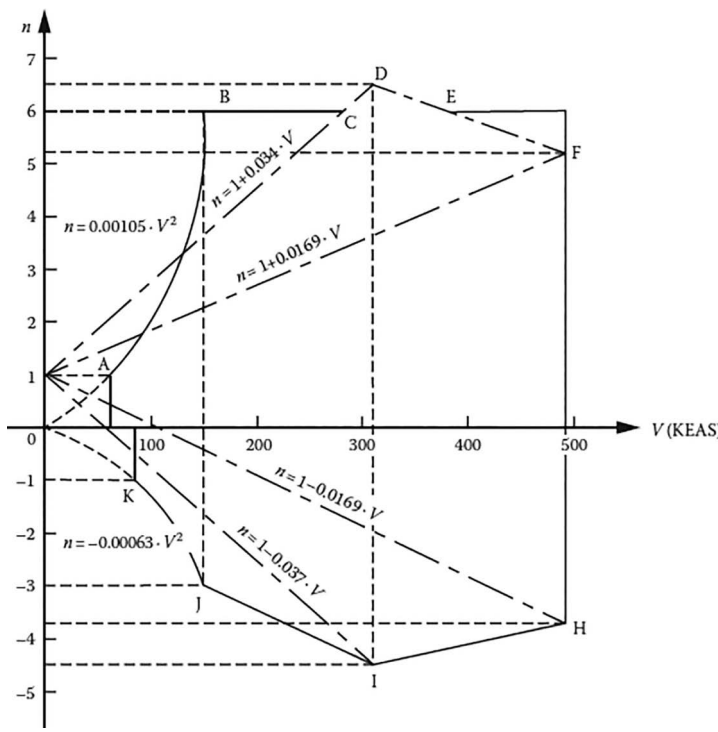

FIGURE 9.32 The combined (final) *V-n* diagram for the acrobatic aircraft.

($n = 1 + 0.03436V$) have an intersection. This is marked as point C. In addition, the line BF has an intersection with the line between two positive gust lines. This is marked as point E. The last step is to connect all outer intersection points with straight lines; the combined *V-n* diagram is created. As a check for sanity, we make sure that no intersection point or corner point is outside the plotted envelope. Also, no point is in the stall regions.

Figure 9.32 demonstrates the final *V-n* diagram that includes the gust effect. As a conclusion, we observe that the FAR requires that the maximum allowable load factor should be 6. However, due to the gust, this parameter is increased to 6.48.

PROBLEMS

Note: (1) Assume sea-level ISA conditions, unless otherwise stated. (2) A turn implies a level-coordinated turn unless otherwise stated. (3) The given m implies the maximum takeoff mass. (4) The given T or P implies the maximum sea level engine thrust or power.

9.1 A fighter aircraft with a mass of 25,000 kg is turning with a bank angle of 60°. The turn is level and coordinated.
   a. How much lift the aircraft is generating?
   b. What centrifugal force is applied on the aircraft?

9.2 If the aircraft in Problem 9.1 is turning with an airspeed of 300 knots, determine its turn radius.

9.3 Consider an acrobatic aircraft with the following characteristics:

$$m = 8{,}900\,\text{kg}, \quad S = 25\,\text{m}^2, \quad C_{L_{\max}} = 2.3.$$

   a. Determine the aircraft stall speed for the straight-level flight.
   b. Determine the aircraft stall speed for a level turning flight with a bank angle of 30°.

9.4 A jet transport aircraft with a mass of 180,000 kg is in a level turn. The aircraft has produced 2,038,970 N of lift.
   a. Calculate the load factor for this flight condition.
   b. What is the aircraft bank angle?

9.5 A utility aircraft is turning with a speed of 150 knots and a radius of 1,664 m.
   a. Determine the load factor for this flight condition.
   b. How long does it take for the aircraft to perform a complete 360° turn?

9.6 The maximum load factor of a fighter aircraft is 8. What is the aircraft speed for a level turn with a radius of 300 m when pulling this g-load?

9.7 The fighter jet aircraft F-100 (Super Saber) has a turbojet engine and the following characteristics:

$$m = 15{,}800\,\text{kg}, S = 35.8\,\text{m}^2, C_{L_{\max}} = 2.4,$$

$$T_{\text{SL}} = 75.4\,\text{kN}, \quad b = 11.82\,\text{m}, e = 0.82, C_{D_o} = 0.019.$$

Plot speed envelope (the allowable/reachable region of speed for altitudes; i.e., stall/maximum) up to 50,000 ft for this aircraft.

9.8 For the aircraft in Problem 9.7
   a. Determine the maximum producible load factor at sea level and 20,000 ft.
   b. Calculate the corner speed at sea level and 20,000 ft.

9.9 A prop-driven commuter aircraft has the following features:

$$m = 5{,}860\,\text{kg},\ S = 24.5\,\text{m}^2,\ C_{L_{\max}} = 2.2,\ -C_{L_{\max}} = -1.3,$$

$$n_{\max} = +5,\ \ -n_{\max} = -2.5,\ b = 11.6\,\text{m},\ C_{L_\alpha} = a = 4.3\,1/\text{rad}.$$

The aircraft cruising speed at sea level in terms of Mach number is 0.4.
   a. Plot the basic *V-n* diagram for this aircraft.
   b. Plot the gust *V-n* diagram for this aircraft.
   c. Plot the combined *V-n* diagram for this aircraft.
   d. What is the maximum allowable load factor?

9.10 Sketch an aircraft with a mass m, an engine thrust T in a climbing flight with a climb angle γ, while turning with a bank angle ϕ and an airspeed *V*. Illustrate three axes (*x*, *y*, and *z*) plus all forces. Then, derive the governing equations of motion (along *x*, *y*, and *z*) for this flight condition.

9.11 Sketch an aircraft in a vertical diving operation. Illustrate two axes (*x* and *z*) plus all forces. Derive the governing equations of motion (along *x* and *z*) for this flight condition.

9.12 Consider a jet aircraft with a mass *m*, a wing area *S*, and a maximum engine thrust *T* in a level turning flight with an airspeed *V* with a bank angle ϕ. Derive a general relationship for the maximum speed for this turning flight.

9.13 Consider a prop-driven aircraft with a mass *m*, a wing area *S*, and a maximum engine power *P* in a level turning flight with an airspeed *V* with a bank angle ϕ. Derive a general relationship for the maximum speed for this turning flight.

9.14 Consider the following aircraft diving with the engine idling (i.e., $T = 0$), and zero lift.

$$m = 200\,\text{kg}, S = 20\,\text{m}^2, C_{D_o} = 0.022.$$

Determine the maximum diving speed (terminal speed) at 15,000 ft.

9.15 Consider a light piston prop-driven aircraft with the following features:

$$m = 1{,}200\,\text{kg},\ S = 12.5\,\text{m}^2,\ C_{L_{\max}} = 1.7,$$

$$P = 149.1\,\text{kW},\ \ \eta_P = 0.8,\ \ C_{D_o} = 0.032,\ \ K = 0.062.$$

   a. Determine the maximum producible load factor at sea level.
   b. Calculate the corner speed at sea level.

9.16 The jet transport aircraft Tupolev TU-134 has two turbofan engines and the following characteristics:

$$m_{TO} = 47{,}000\,\text{kg}, S = 127.3\,\text{m}^2;$$

$$T_{\max_{SL}} = 2 \times 66.7\,\text{kN},\ b = 29\,\text{m};\ e = 0.88; C_{D_o} = 0.018.$$

What is the maximum allowable bank angle when one of the engines is inoperative?

9.17 The fighter aircraft Mikoyan MiG-29 (Figure 3.20) has two turbofan engines and the following characteristics:

$$m_{TO} = 18{,}480\,\text{kg},\ T_{SL} = 2 \times 81.4\,\text{kN};$$

$$S = 38\,\text{m}^2;\ C_{L_{\max}} = 2.3,\ C_{D_o} = 0.021,\ K = 0.11$$

What is the maximum producible load factor at 30,000 ft?

9.18 If the pilot of Mikoyan MiG-29 with the data given in Problem 9.17 decides to turn with a bank angle of 30° at 40,000 ft, and 60% of engine available thrust, what is the maximum speed for this turning flight?

9.19 The Mikoyan MiG-29 pilot is planning to have a complete turn in 120 s at 30,000 ft with the lowest possible speed. The aircraft data are given in Problem 9.17.

a. Determine the required airspeed and bank angle.
b. What is the turn radius?

9.20 Is the aircraft in Problem 9.17 able to turn with a bank angle of 75°, and an airspeed of 400 knots at 25,000 ft? If so, how long does it take to have a complete 360° turn?

9.21 The aircraft in Problem 9.16 is turning with a bank angle of 45° at a speed of 180 knots at 15,000 ft. If the aircraft lift curve slope is 4.5 1/rad, determine the aircraft angle of attack. Assume $\alpha_o = 0$.

9.22 The prop-driven aircraft in Problem 9.15 is turning with a speed of 130 knots and 90% of engine power at 5,000 ft. Calculate the maximum allowable bank angle for this flight condition.

9.23 What is the shortest turn radius for the prop-driven aircraft in Problem 9.15?

a. At sea level
b. At 10,000 ft

9.24 Determine the maximum turn rate for the prop-driven aircraft in Problem 9.15.

a. At sea level
b. At 15,000 ft

9.25 Determine the shortest turn radius for the jet aircraft in Problem 9.17.

a. At sea level
b. At 30,000 ft

9.26 Determine the maximum turn rate for the jet aircraft in Problem 9.17.

a. At sea level
b. At 30,000 ft

9.27 For the prop-driven commuter aircraft introduced in Problem 9.9, determine the corner speed 10,000 ft.

9.28 A GA normal aircraft has a turboprop engine and the following features:

$$P_{\max_{SL}} = 675\,\text{hp}, S = 280\,\text{ft}^2,\ W_{TO} = 8{,}000\,\text{lbf},$$

$$K = 0.07, C_{D_o} = 0.027,\ \eta_P = 0.84,\ V_s = 65\,\text{KEAS}.$$

a. Calculate the maximum turn rate at 5,000 ft altitude.
b. Calculate the associated turn radius.
c. Calculate the associated bank angle.

9.29 A jet (turbofan engine) aircraft is turning with a radius of 5,200 ft at a constant altitude of 10,000 ft.

$$W_{TO} = 70{,}000\,\text{lb}, S = 900\,\text{ft}^2, C_{D_o} = 0.021,$$

$$K = 0.04, T_{\max_{SL}} = 25{,}000\,\text{lbf}, n_{\max} = 4,\ C_{L_{\max}} = 1.8.$$

a. If the bank angle is 45°, find the aircraft speed.
b. How much thrust the engine must generate to have this sustained turning flight?
c. How long does it take to perform a 180° turn?
d. Determine the aircraft corner velocity.
e. Determine the aircraft minimum turn radius.

9.30 A fighter jet aircraft has the following characteristics:

$$m_{TO} = 10{,}000\,\text{kg}, S = 24\,\text{m}^2,\ b = 8\,\text{m}, T_{\max_{SL}} = 100\,\text{kN}, e = 0.8,\ C_{L_{\max}} = 1.7$$

$$C_{D_o} = 0.015\,(\text{low subsonic}), C_{D_o} = 0.03\,(\text{transonic}); C_{D_o} = 0.042\,(\text{supersonic}).$$

a. Determine the corresponding velocity to the maximum producible load factor.
b. Determine the maximum producible load factor.
c. Determine the maximum producible bank angle.

9.31 A jet transport aircraft has two turbofan engines and the following characteristics:

$$m_{TO} = 60{,}000\,\text{kg}, S = 150\,\text{m}^2;$$

$$T_{\max_{SL}} = 2 \times 80\,\text{kN}, b = 35\,\text{m}; e = 0.82; C_{D_o} = 0.02, C_{L_{\max}} = 2.6.$$

a. Determine the corner velocity.
b. Determine the turn rate if it turns with the corner velocity.
c. Determine the turn radius if it turns with the corner velocity.

9.32 A civil subsonic jet transport aircraft has the following characteristics:

$$m = 100{,}000\,\text{kg}, S = 220\,\text{m}^2, T_{\max_{SL}} = 260\,\text{kN}, K = 0.04,$$

$$C_{D_o} = 0.018\,(\text{low subsonic}), C_{L_{\max}} = 2.3.$$

The pilot decides to have a level turn by only using 50% of the engine thrust at a 45° bank angle.

a. Determine the airspeeds for this turning flight.
b. What airspeed yields a higher turn rate?
c. What airspeed yields a lower turn radius?

9.33 Consider a twin-turbofan-engine supersonic aircraft with the following characteristics:

$$m = 18{,}000\,\text{kg}, \quad S = 40\,\text{m}^2, \; b = 14\,\text{m}, \; T_{\max} = 2 \times 90\,\text{kN}.$$

Assume the maximum allowable load factor is 8 and $\alpha_o = 0$; $C_{L_\alpha} = 4.31/\text{rad}$; $e = 0.8$, $C_{D_o} = 0.018$ (subsonic), $C_{D_o} = 0.028$ (transonic); $C_{D_o} = 0.037$ (supersonic), $C_{L_{\max}} = 1.7$.

Is this fighter able to turn with a bank angle of 65°, and a 1,200 m of turn radius at 15,000 ft? If so, determine the time that it takes to have a 180° turn (a half circle).

9.34 Consider a single-engine piston-prop acrobatic aircraft with the following features:

$$m_{\text{TO}} = 1{,}200\,\text{kg}, \; S = 14\,\text{m}^2, P = 200\,\text{kW}, \; b = 10,$$

$$V_s = 60\,\text{knot (with flap)}, C_{D_o} = 0.023, \eta_P = 0.75, e = 0.8.$$

Evaluate the fastest turn performance (i.e., determine the maximum turn rate).

9.35 Consider a small remote-controlled (RC) aircraft with the following characteristics:

$$m = 1{,}000\,\text{g}, \quad S = 0.25\,\text{m}^2, \quad b = 1.3\,\text{m}; \quad e = 0.7;$$

$$\eta_P = 0.65, \quad C_{L_{\max}} = 1.4, \quad C_{D_o} = 0.033.$$

The airplane is employing a prop-driven electric motor where four cells of 2,000 mAh 12 V Li-Po batteries provide electric energy for the motor. Evaluate the tightest turn (i.e., determine the minimum turn radius).

9.36 Consider a small radio-controlled (RC) aircraft with the following characteristics:

$$m = 1.5\,\text{kg}, \quad S = 0.4\,\text{m}^2, \quad b = 1.6\,\text{m}; \quad e = 0.74;$$

$$\eta_P = 0.65, \quad C_{D_o} = 0.036, \quad C_{L_{\max}} = 1.2.$$

The airplane is employing a prop-driven electric motor where four cells of 2,000 mAh 12 V Li-Po batteries provide electric energy for the motor. Evaluate the tightest turn (i.e., determine the minimum turn radius).

9.37 Consider an acrobatic aircraft with a mass of 1,200 kg diving with a velocity of 130 knots.
   a. If the aircraft pulls out of the dive with a radius of 200 m, determine the load factor.
   b. If the maximum allowable load factor is 5, determine the minimum radius for a pull-out of this dive.

9.38 Consider an acrobatic aircraft with a mass of 2,000 kg is diving with a velocity of 150 knots.
   a. If the aircraft pulls out of the dive with a radius of 300 m, determine the load factor.
   b. If the maximum allowable load factor is 7, determine the minimum radius for a pull-out of this dive.

9.39 Determine the orbital velocity of a spacecraft at an altitude of 300 km from the Earth, if weightlessness is desired. Assume the gravity is 9.8 m/s^2 at the height of 300 km and the Earth's radius is 6,371 km. Then, compare this velocity with the speed of sound at sea level (i.e., 340 m/s).

9.40 Determine the orbital velocity of a spacecraft at geostationary altitude (i.e., 36,000 km from the Earth) if weightlessness is desired. Assume the gravity is 9.6 m/s^2 at that height and the Earth's radius is 6,371 km. Then, compare this velocity with the speed of sound at sea level (i.e., 340 m/s).

9.41 A jet transport aircraft is employed in a zero-gravity flight. The flight started at 10,000 m with a velocity of 400 knots and lasted 22 s. Determine (1) horizontal distance traveled, (2) height lost, (3) vertical velocity, (4) average descent angle, and (5) total velocity at the end of 22 s. Ignore the drag force in the z-direction.

9.42 An unmanned aircraft is employed in a zero-gravity flight. The flight started at 60,000 ft with a velocity of 400 knots and lasted 40 s. Determine (1) horizontal distance traveled, (2) height lost, (3) vertical velocity, (4) average descent angle, and (5) total velocity at the end of 40 s. Ignore the drag force in the z-direction.

9.43 Plot the flight envelope (combined *V-n* diagram) for the following GA normal aircraft. Then, determine the maximum load factor. Assume the maximum positive and negative limit maneuvering load factors to be +3.5 and −1.5, respectively.

$$m = 1{,}800\,\text{kg},\quad S = 14\,\text{m}^2,\quad C_{L_{\max}} = 1.8,\quad -C_{L_{\max}} = -0.9,\quad \text{AR} = 6,$$

$$C_{L_\alpha} = a = 4\ \ 1/\text{rad},\quad V_c = 280\,\text{KEAS or } 144\,\text{m/s (at } 20{,}000\,\text{ft)}$$

9.44 Plot the flight envelope (combined *V-n* diagram) for the following jet transport aircraft. Then, determine the maximum load factor. Assume the maximum positive and negative limit maneuvering load factors to be +3.8 and −2, respectively.

$$m = 100{,}000\,\text{kg},\ S = 200\,\text{m}^2,\ C_{L_{\max}} = 2.3,\ -C_{L_{\max}} = -1.2,\quad \text{AR} = 9,$$

$$C_{L_\alpha} = a = 5\,1/\text{rad},\ V_c = 500\,\text{KEAS or } 257.2\,\text{m/s (at } 35{,}000\,\text{ft}).$$

9.45 A Navy fighter aircraft with a weight of 60,000 lb is taking off with a speed of 150 knots from an aircraft carrier in only 2 s. Determine aircraft acceleration during takeoff in g's.

9.46 A Navy fighter aircraft with a weight of 55,000 lb is landing on an aircraft carrier with a landing distance of 320 ft and a landing speed of 160 knots. Determine aircraft deceleration during landing in g's.

10 Aircraft Performance Analysis Using Numerical Methods and MATLAB®

10.1 INTRODUCTION

Aircraft performance problems are grouped into two categories: (1) point performance and (2) mission performance. In the point performance problem, all aircraft parameters and flight conditions such as aircraft weight and altitude are fixed. In the mission performance, the time is a new parameter during which several aircraft parameters and flight conditions vary. The solution for point performance problems (e.g., the maximum speed) is often straightforward, usually involves a few equations, and often requires plugging numbers into one or more equations. However, the analyses of mission performance problems are tedious and complex.

There are complex performance cases and flight missions where the analysis requires a long and complex mathematical solution. A popular and powerful technique for such cases is the numerical method [99]. When the time step in numerical method is kept very short (e.g., 0.01 s), the accuracy of results will be reliable. For the complete coverage of theories behind each flight case, you need to refer to the relevant section in other chapters.

In this chapter, several aircraft performance cases (primarily mission performance problems) are analyzed using numerical methods; with mainly MATLAB® software package (i.e., MATLAB code). They include the following flight cases:

1. A MATLAB code to determine transition distance (S_T) for an aircraft during takeoff rotation
2. A MATLAB code to determine the altitude versus time for a free fall
3. A MATLAB code to calculate airborne section of an aircraft during takeoff
4. A MATLAB code to construct the hodograph
5. A MATLAB code for fastest climb analysis
6. A MATLAB code to determine the height versus time for an aircraft during a limb
7. A MATLAB code to plot the parabolic path and to analyze a zero-gravity flight
8. A MATLAB code to plot V-n diagram

MATLAB is a high-level language [100] and very powerful matrix-based programming language for performing mathematical and engineering calculations. MATLAB [101] has an extensive set of routines, predefined built-in math functions,

DOI: 10.1201/9781003279068-10

operators, and tools for solving problems and drawing graphical outputs. MATLAB provides a variety of toolboxes; a toolbox is a collection of special files called m-files. MATLAB is basically command-driven (e.g., *plot, log, for*, and *end*).

The author assumes that the reader is familiar with the basic fundamentals of programming with MATLAB and knows how to use MATLAB commands and write codes. Hence, no overview of MATLAB routines and background materials is provided. If this is the first time to use MATLAB, you may refer to the references such as [102,103]. In addition, MATLAB has an online help facility [104] that may be employed when a need arises.

10.2 TAKE-OFF ROTATION ANALYSIS USING NUMERICAL METHODS

10.2.1 Mission Analysis

Theory behind take-off rotation is presented in Chapter 8, so it is not repeated here. For convenience, an aircraft with a tricycle landing gear is considered. Recall that the rotation is around the point of contact between the main gear and the ground. Figure 10.1 illustrates the forces during take-off rotation.

Assumptions

1. The angular pitch acceleration remains constant during the rotation.
2. Aircraft weight and engine thrust remain constant during the rotation.

10.2.2 Governing Equations

Angular change (θ) in an accelerated rotation ($\ddot{\theta}$):

$$\theta_2 = \theta_1 + \omega_1 t + \frac{1}{2}\ddot{\theta}t^2 \tag{10.1}$$

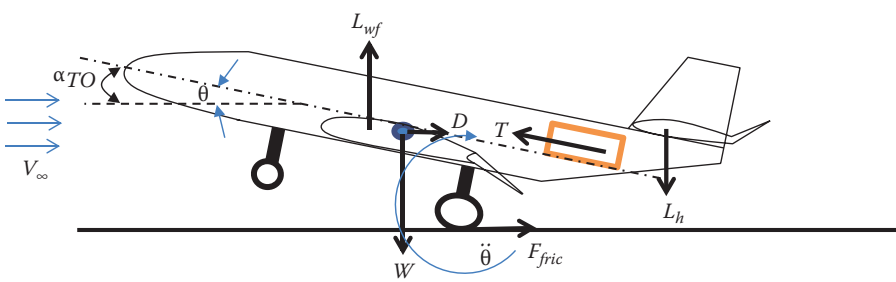

FIGURE 10.1 Forces during a take-off rotation.

Angular velocity (ω) in an accelerated rotation:

$$\omega_2 = \omega_1 + \ddot{\theta} t \tag{10.2}$$

$$\omega_2^2 - \omega_1^2 = 2\ddot{\theta}\theta \tag{10.3}$$

Take-off angle:

$$\alpha_{\mathrm{TO}} = \theta \tag{10.4}$$

Wing-fuselage lift coefficient:

$$C_{L_{\mathrm{wf}}} = C_{L_{\mathrm{wf}_o}} + C_{L_{\alpha_{\mathrm{wf}}}} \alpha_{\mathrm{TO}} \tag{10.5}$$

$$C_{L_{\mathrm{wf}}} = C_{L_C} + \Delta C_{L_f} + C_{L_\alpha} \alpha_{\mathrm{TO}} \tag{10.6}$$

Wing-fuselage lift:

$$L_{\mathrm{wf}} = \frac{1}{2} \rho V^2 S C_{L_{\mathrm{wf}}} \tag{10.7}$$

where it is assumed that

$$C_L = C_{L_{\mathrm{wf}}} \tag{10.8}$$

Drag coefficient:

$$C_D = C_{D_o} + K C_L^2 \tag{10.9}$$

Drag:

$$D = \frac{1}{2} \rho V^2 S C_D \tag{10.10}$$

Linear acceleration (*a*):

$$\sum F_x = m \frac{dV}{dt} \Rightarrow T \cos\left(i_T + \alpha_{\mathrm{TO}}\right) - D - \mu N = ma \tag{10.11}$$

Linear velocity (V) during an accelerated motion:

$$V_2^2 - V_1^2 = 2aS_T \tag{10.12}$$

Linear distance (x) during an accelerated motion:

$$x_2 = x_1 + V_1 t + \frac{1}{2}at^2 \tag{10.13}$$

Flap lift coefficient:

$$\Delta C_{L_f} = K_f \delta_f \tag{10.14}$$

Normal force to the ground (N):

$$N = W + L_h - L_{\text{wf}} - T\sin\left(i_T + \alpha_{\text{TO}}\right) \tag{10.15}$$

Horizontal tail lift:

$$L_h = \frac{1}{2}\rho V^2 S_h C_{L_{\alpha h}} \tag{10.16}$$

Tail lift coefficient:

$$C_{L_h} = C_{L_{ho}} + C_{L_{\alpha h}}\alpha_{\text{TO}} \tag{10.17}$$

Example 10.1

Consider a transport aircraft (similar to a Boeing 737) with a take-off mass of 50,000 kg, the engine thrust of 2×60 kN, and with the following characteristics:

$$S = 100\,\text{m}^2, S_h = 25\,\text{m}^2, K = 0.04, \mu = 0.04, C_{D_{o\text{TO}}} = 0.05, \ddot{\theta} = 1.8\,\text{deg/s}^2,$$

$$C_{L_c} = 0.3,\ \Delta C_{L_f} = 0.4,\ i_T = 5°, V_R = 120\,\text{knot}; C_{L_{\alpha_{\text{wf}}}} = 5.5\frac{1}{\text{rad}}; C_{L_{\alpha h}} = 4.5\frac{1}{\text{rad}}; C_{L_{ho}} = -1.2.$$

Determine the distance the aircraft travels (Figure 10.1) during take-off rotation (S_T) at sea level. Using a simulation program, plot the variations of (1) aircraft angle of attack, (2) distance traveled, (3) airspeed, (4) wing-fuselage lift, (5) drag, and (6) normal force as a function of time.

Solution

A MATLAB® code is written. A time step (Δt) of 0.01 s is selected. The simulation is continued until the normal force is zero, which means that the aircraft begins to lift off.

$$t_1 = 0 \Rightarrow \omega_1 = x_1 = \theta_1 = 0, V_1 = V_R,\ t_2 = t_1 + \Delta t$$

MATLAB CODE

```
clc
clear all

% Take-off rotation analysis

m=50000; % kg; aircraft take-off mass
S=100; % m^2; wing area
Sh=25; % m^2; tail area
g = 9.81; % m/s^2
T = 2*60000; % N; Engine Thrust
W_TO = m*g; % N; Take-off weight
K =0.04; % induced drag coef.
CDoTO=0.04; % Take-off drag coef.
mu=0.04; % friction coef.
theta_dd=1.8/57.3; % rad/s^2; take-off rotation pitch angular
acceleration
CLc=0.3; % cruise lift coef.
d_CLf=0.4; % additional flap lift coef.
CL_alfa= 5.5; %1/rad; aircraft lift curve slope;
CLah = 4.5; %1/rad; horizontal tail lift curve slope
CLho = -1.2; % initial horizontal tail lift coef.
dt=0.01; % time step
t_tot = 3.4; % sec
iT = 5/57.3; % rad engine setting angle
rho = 1.225; % kg/m^2; air density
theta(1) = 0; % pitch angle
d_theta(1)=0;
x(1)=0; % distance traveled
V(1)= 120*0.514; % m/s; rotation speed
w(1)=0; % angular velocity (rad/sec)
time1(1) = 0;
alpha(1) = 0; % angle of attack
CLwf(1)=CLc+d_CLf; % wing-fuselage lift coef.
CLh(1) = CLho; % initial horizontal tail lift coef.
Lwf(1) = 0.5*rho*V(1)^2*S*CLwf(1); % wing-fuselage lift
CD(1) = CDoTO+K*CLwf(1)^2; % drag coef.
D(1) = 0.5*rho*V(1)^2*S*CD(1); % drag
Lh(1) = 0.5*rho*V(1)^2*Sh*CLh(1); % horizontal tail lift
N(1) = W_TO-Lh(1)-Lwf(1)-T*sin(iT+alpha(1)); % normal force to
the ground
a(1) = (T*cos(iT+alpha(1))-D(1)-mu*N(1))/m; % linear acceleration
i=1;
```

```
for t = dt:dt:t_tot % sec
    theta(i+1)=theta(i)+w(i)*dt+0.5*theta_dd*dt^2;
    w(i+1)=w(i)+theta_dd*dt;
    d_theta(i+1)=theta(i+1)-theta(i);
    alpha(i+1)=theta(i+1);
    x(i+1)=x(i)+V(i)*dt+0.5*a(i)*dt^2;
    dx=x(i+1)-x(i);
    V(i+1)=sqrt(V(i)^2+2*a(i)*dx);
    CLwf(i+1)=CLc+d_CLf+CL_alfa*alpha(i+1);
    CD(i+1)=CDoTO+K*CLwf(i+1)^2;
    Lwf(i+1)=0.5*rho*V(i+1)^2*S*CLwf(i+1);
    D(i+1)  =0.5*rho*V(i+1)^2*S*CD(i+1);
    CLh(i+1)=CLho+CLah*alpha(i+1);
    Lh(i+1)=0.5*rho*V(i+1)^2*Sh*CLh(i+1);
    N(i+1)=W_TO-Lh(i+1)-Lwf(i+1)-T*sin(iT+alpha(i+1));
    a(i+1)=(T*cos(iT+alpha(i+1))-D(i+1)-mu*N(i+1))/m;
    time1(i+1)=t;
    i=i+1;
end

subplot(511)
plot(time1,alpha*57.3,'rO-'); grid
xlabel ('time (sec)')
ylabel ('alpha (deg)')

subplot(512)
plot(time1,x,'b*-'); grid
xlabel ('time (sec)')
ylabel ('S_T (m)')

subplot(513)
plot(time1,V/0.514,'gd-'); grid
xlabel ('time (sec)')
ylabel ('V (knot)')

subplot(514)
plot(time1,a,'r+'); grid
xlabel ('time (sec)')
ylabel ('a (m/s^2)')

subplot(515)
plot(time1,D,'c*-',time1,Lwf,'ks-',time1,N,'m*-'); grid
xlabel ('time (sec)')
ylabel ('D (N), Lwf (N), N (N)')
legend('D','Lwf','N')
```

RESULTS OF SIMULATION

When this MATLAB code is executed, five plots (Figure 10.2) that illustrate the variations of: (1) aircraft angle of attack, (2) distance traveled, (3) airspeed, (4) wing-fuselage lift, (5) drag, (6) normal force, and (7) acceleration with time are produced.

Based on the simulation results, the take-off rotation takes 3.4 s (Figure 10.2).

$$S_T = 220\,\text{m}, \alpha_{\text{TO}} = 10.4°, V_2 = 131.3\,\text{knot}.$$

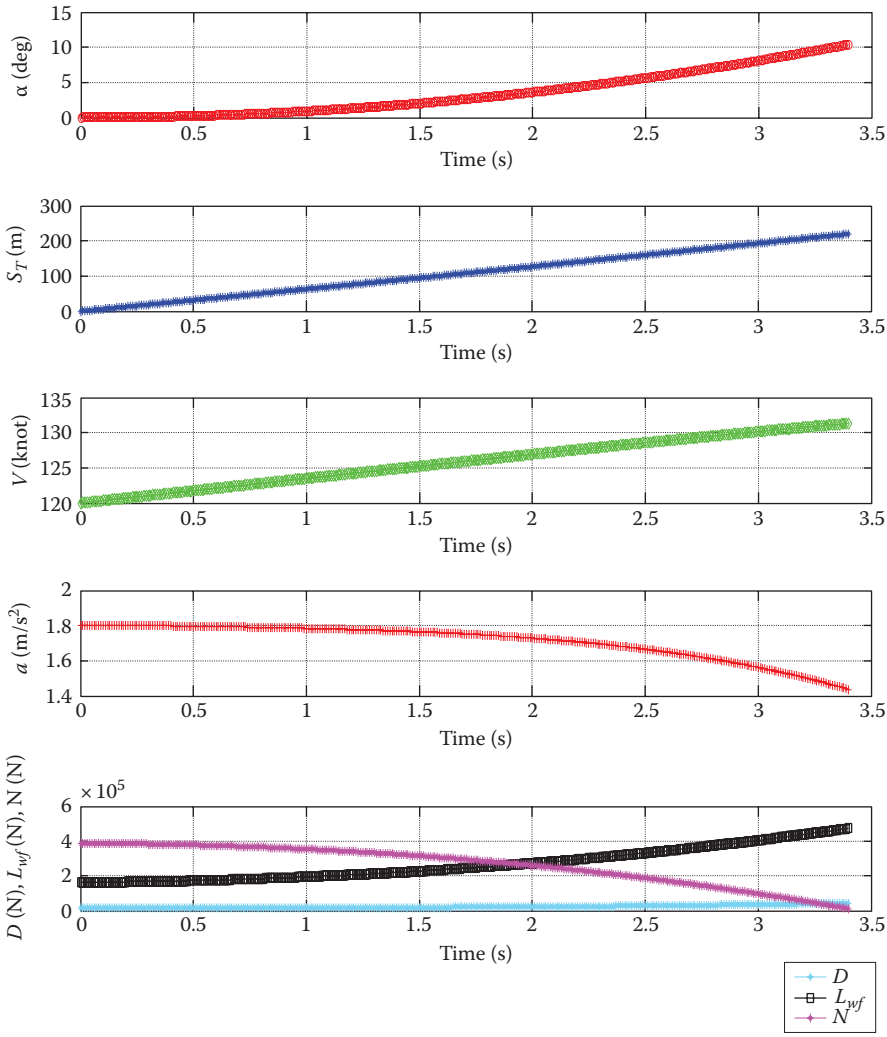

FIGURE 10.2 Variations of (1) aircraft angle of attack, (2) distance traveled, (3) airspeed, (4) wing-fuselage lift, (5) drag, (6) normal force, and (7) acceleration; as a function of time.

10.3 FREE FALL SIMULATION

10.3.1 Flight Analysis

In this section, the numerical analysis of a free fall is presented, where an object is falling under the force of its weight, while the drag is acting in the opposite direction. Whenever the drag is equal to the weight, the velocity is referred to as the *terminal velocity*. Theory behind drag and governing equations for a free fall are presented in Chapters 1–3, so they are not repeated here. Figure 10.3 illustrates the active forces in a free fall.

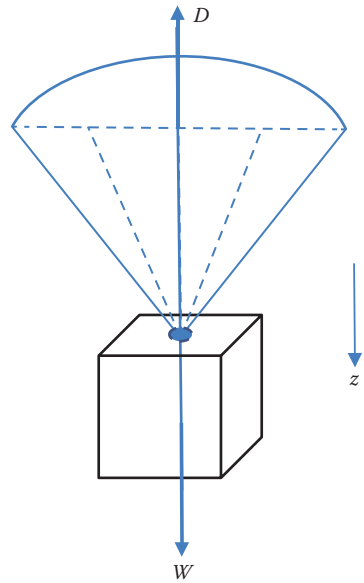

FIGURE 10.3 Forces in a free fall.

In this section, a MATLAB code is presented to determine the altitude versus time for a free fall of an object. In this motion, only two forces are involved: namely, weight (W) and drag (D). The weight is assumed to be constant, while the drag is a function of airspeed (V) and the air density (ρ).

10.3.2 Governing Equations

Height (h) difference during a free fall:

$$h_2 = h_1 + V_1 t + \frac{1}{2} a t^2 \tag{10.18}$$

$$\frac{1}{2} a t^2 + V_1 t - \Delta h = 0 \tag{10.19}$$

This is a quadratic equation that is a function of time (t), and the general solution to this equation is

$$t = \frac{-V_1 \pm \sqrt{V_1^2 - 4(0.5a)(-\Delta h)}}{2(0.5a)} \tag{10.20}$$

where only one solution (the positive one) is acceptable.

Linear velocity (V) during an accelerated motion:

$$V_2^2 - V_1^2 = 2ah \tag{10.21}$$

Linear acceleration (a) is z-direction:

$$\sum F_z = m\frac{dV}{dt} \Rightarrow W - D = ma \tag{10.22}$$

The weight of the object is

$$W = mg \tag{10.23}$$

Drag:

$$D = \frac{1}{2}\rho V^2 S C_D \tag{10.24}$$

The drag coefficient (C_D) is a function of the object external shape. In this equation, S is the reference area, which is assumed to be the projected area perpendicular to the motion path.

The air density (ρ) is a function of pressure and temperature (ideal-gas law or gas equation of state):

$$\rho = \frac{P}{RT} \tag{10.25}$$

where R, the gas constant for air, is 287.3 J/kg K.

The air temperature (T) has a linear variation in the first layer (troposphere) at ISA condition and is mathematically modeled by the following equation:

$$T_{\text{ISA}} = T_o - Lh \tag{10.26}$$

In the lower region of the second layer (stratosphere), the temperature will be constant as

$$T_{\text{ISA}} = -56°\text{C} \tag{10.27}$$

The temperature at a non-ISA condition is

$$T = T_{\text{ISA}} + \Delta T \tag{10.28}$$

where ΔT is the temperature difference between non-ISA and ISA conditions.

The pressure (P) is a nonlinear function of altitude and, in the first layer of atmosphere, can be related to the temperature as

$$P_{\text{ISA}} + P_o\left(\frac{T_{\text{ISA}}}{T_o}\right)^{5.256} \tag{10.29}$$

However, in the lower region of the second layer (stratosphere),

$$P_{\text{ISA}} = 0.2234 P_o \exp\left(\frac{11{,}000 - h}{6{,}342}\right) \tag{10.30}$$

The altitude (h) is in terms of meter in Equation 10.30.

Example 10.2

Consider a cargo box connected to a parachute is dropped from (a) 50 m, (b) 11,000 m ISA condition (Figure 10.3). The total mass of the cargo box plus the parachute is 100 kg, and the projected area of the parachute is 10 m^2. The drag coefficient of the box plus parachute is $C_D = 1.2$.

Determine:

1. The time that takes the box to reach the ground
2. The terminal velocity

In the end, plot the variations of height, velocity, and acceleration versus time.

Solution

A MATLAB code is written. A height-step (Δh) of 1 m is selected. The simulation is continued until the box hits the ground (i.e., $h = 0$).

```
% Free Fall analysis
clc
clear all
m=100; % kg; aircraft take-off mass
S=10; % m^2; wing area
g = 9.81; % m/s^2
W = m*g; % N; Take-off weight
CD=1.2; % drag coef.
dh=1; % m, height step
R1=287; % J/kg.K
L1=6.5/1000; % K/m lapse rate
h_tot = 50; % m, altitude
rho_o = 1.225; % kg/m^2; sea level air density
V(1)= 0; % m/s; rotation speed
To=(15+273); % K sea level temperature
Po=101325; % Pa, sea level pressure
T(1)=To-L1*h_tot;
P(1)=Po*(T(1)/To)^5.256;
rho(1)=P(1)/(R1*T(1));
D(1) = 0.5*rho(1)*V(1)^2*S*CD; % drag
```

```
a(1) = g; % linear acceleration
t(1)=0;
delta(1)=0;
H(1)=h_tot ;
T1(1)=0;
i=1;

for h = h_tot-1:-dh:0 % m
T(i+1)=To-L1*h;
P(i+1)=Po*(T(i+1)/To)^5.256;
rho(i+1)=P(i+1)/(R1*T(i+1));
V(i+1)=sqrt (  V(i)^2+2*a(i)* dh  );
D(i+1) = 0.5*rho(i+1)*V(i+1)^2*S*CD; % drag
a(i+1) = (W-D(i+1))/m; % linear acceleration
H(i+1)=h;
delta(i+1)=V(i+1)^2+4*0.5*a(i+1)*dh;
t(i+1)=(-V(i+1)+sqrt(delta(i+1)))/(a(i+1));
T1(i+1)=T1(i)+t(i+1);
i=i+1;
end

subplot(311)
plot(T1,V,'rO-'); grid
xlabel ('time (sec)')
ylabel ('Velocity (m/s)')

subplot(312)
plot(T1,H,'b*-'); grid
xlabel ('time (sec)')
ylabel ('H (m)')

subplot(313)
plot(T1,a,'gd-'); grid
xlabel ('time (sec)')
ylabel ('a (m/s^2)')
```

When this MATLAB code is executed, two groups of three plots (Figure 10.4) that illustrate the variations of height, velocity, and acceleration with time are produced.

As it is observed, the terminal velocity is a function of altitude, and decreases with altitude. However, the terminal velocity for a free fall from a height of 50 m from the ground is 11.55 m/s.

10.4 TAKE-OFF AIRBORNE SECTION ANALYSIS USING NUMERICAL METHODS

10.4.1 Mission Description

In this section, the numerical analysis of the airborne section (see Figure 10.5) for an aircraft during a take-off operation is presented. Theory behind take-off rotation is presented in Chapter 8, so it is not repeated here. The main objective is to determine the runway distance that the aircraft is traveling during the airborne section, that is, S_A. The forces and variables in the airborne section are depicted in Figure 10.6.

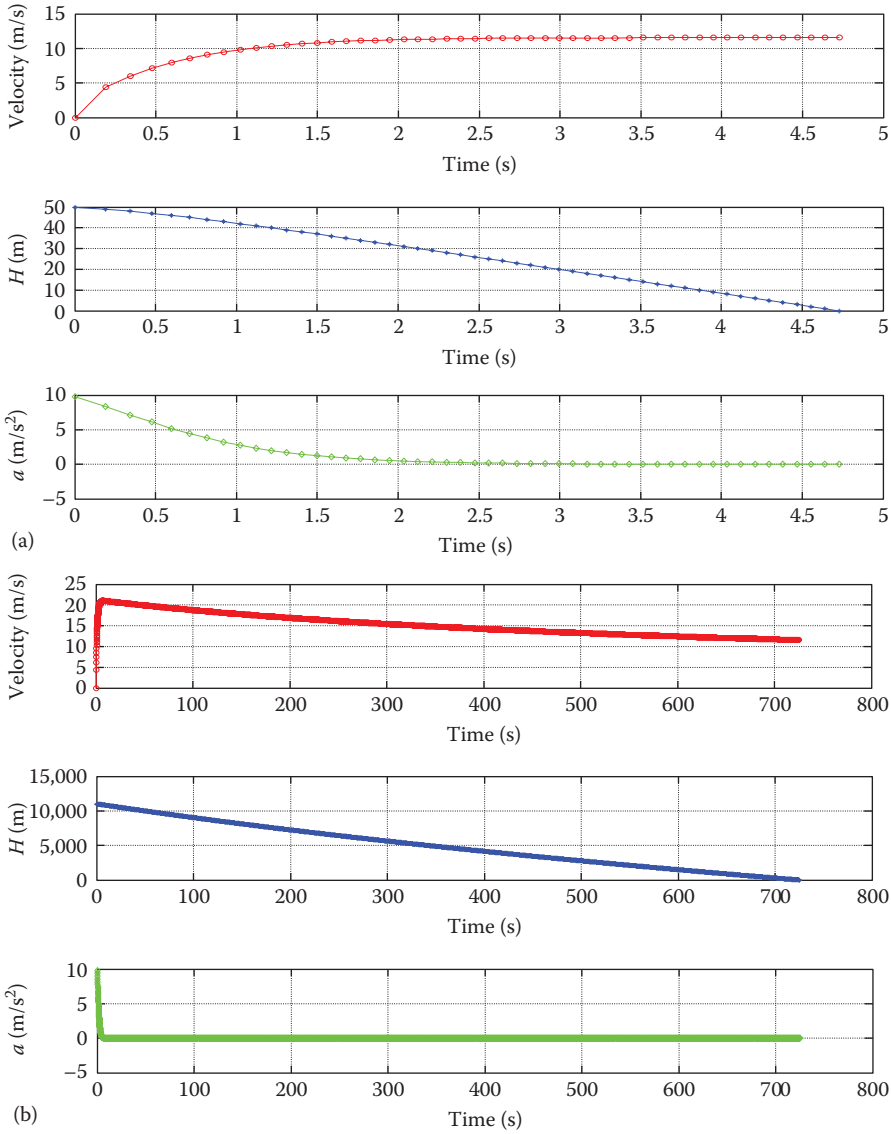

FIGURE 10.4 Variations of velocity, height, and acceleration versus time. (a) Altitude of 50 m and (b) altitude of 11,000 m.

Assumptions

1. Aircraft weight, engine thrust, and angle of attack remain constant during take-off airborne.
2. Landing gear is extended.
3. The engine setting angle is zero.

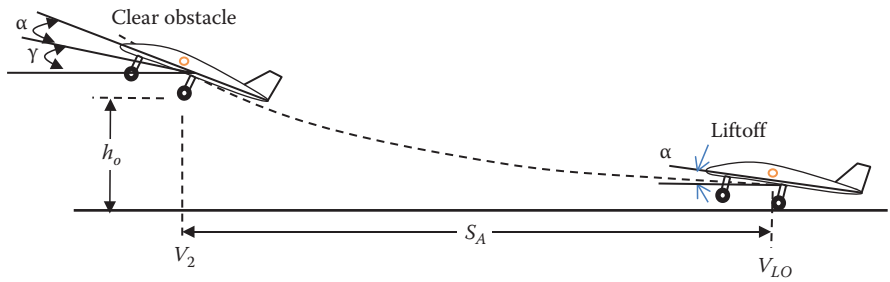

FIGURE 10.5 Airborne section.

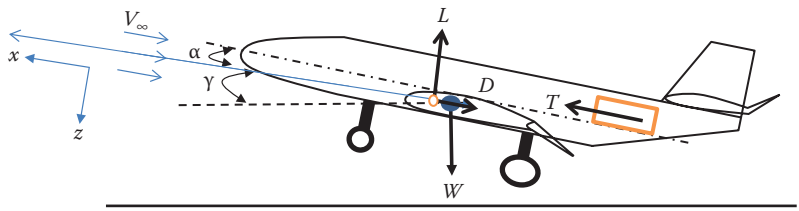

FIGURE 10.6 Forces during take-off airborne section.

10.4.2 Governing Equations

The third section of the take-off run is the airborne section. The speed at the beginning of the airborne section is the liftoff speed and is called V_{LO} and, at the end of it, it is called V_2. This section is in fact an accelerated climb and it usually takes several seconds.

The governing equations of motion along two axes are:

$$T\cos(\alpha) - D - W\sin(\gamma) = ma_x \quad (\text{along } x\text{-axis}) \tag{10.31}$$

$$L + T\sin(\alpha) - W\cos(\gamma) = ma_z \quad (\text{along } z\text{-axis}) \tag{10.32}$$

where γ is the instantaneous climb angle. In these equations, three unknown variables are the climb angle and the accelerations along x and z axes.

The acceleration in the direction of flight path a is

$$a_x = \frac{dV}{dt} \tag{10.33}$$

The linear velocity (V) during an accelerated motion in the direction of flight path is

$$V_2^2 - V_1^2 = 2a\Delta x \tag{10.34}$$

where d is the distance traveled during the climb in the direction of climb. The horizontal component of the airspeed, or the aircraft speed parallel to the horizontal, V_H, is equal to aircraft ground speed:

$$V_H = V\cos(\gamma) \tag{10.35}$$

The vertical component of the airspeed, or the aircraft speed perpendicular to the horizontal; V_V is also the rate of climb (ROC):

$$V_V = \dot{h} = V\sin(\gamma) \tag{10.36}$$

Linear distance (x) during an accelerated motion along x is

$$x_2 = x_1 + V_1 t + \frac{1}{2}a_x t^2 \tag{10.37}$$

The distance traveled in the direction of runway is

$$S = x\cos(\gamma) \tag{10.38}$$

Linear height (h) during an accelerated climb motion along z is

$$z_2 = z_1 + V_{1z} t + \frac{1}{2}a_z t^2 \tag{10.39}$$

The height gained is

$$H = z\cos(\gamma) \tag{10.40}$$

The average engine thrust during airborne (T_{ab}) is estimated as

$$T_{ab} = T_{max}\left(\text{Jet engine}\right) \tag{10.41}$$

$$T_{ab} = \frac{k_{ab}P_{max}}{V_R}\left(\text{Prop-driven engine}\right) \tag{10.42}$$

where k_{ab} is 0.5 for a fixed-pitch propeller, and 0.6 for a variable-pitch propeller.

Two aerodynamic forces are lift and drag.

Wing-fuselage lift:

$$L_{wf} = \frac{1}{2}\rho V^2 S C_{L_{wf}} \tag{10.43}$$

Drag:

$$D = \frac{1}{2}\rho V^2 S C_D \tag{10.44}$$

Wing-fuselage lift coefficient:

$$C_{L_{\text{wf}}} = C_{L_C} + \Delta C_{L_f} + C_{L_\alpha}\alpha_{\text{TO}} \tag{10.45}$$

where it is assumed that

$$C_L = C_{L_{\text{wf}}} \tag{10.46}$$

Drag coefficient:

$$C_D = C_{D_o} + KC_L^2 \tag{10.47}$$

Example 10.3

Problem statement: Consider a transport aircraft (similar to a Boeing 737) with a take-off mass of 50,000 kg, the engine thrust of 2×60 kN, and with the following characteristics:

$$S = 100\,\text{m}^2, K = 0.04, \mu = 0.04,\ C_{D_{o\text{TO}}} = 0.05, C_{L_c} = 0.3,$$
$$\Delta C_{L_f} = 0.4, \alpha_{\text{TO}} = 10°, V_s = 115\,\text{knot}; C_{L_{\alpha_{\text{wf}}}} = 5.5\,1/\text{rad}.$$

Determine the distance the aircraft travels during take-off airborne (S_A) at sea level. Using a simulation program, plot the variations of (1) aircraft climb angle, (2) distance traveled, (3) airspeed, and (4) height as a function of time.

Solution

A MATLAB code is written. A time step (Δt) of 0.01 s is selected. The simulation is continued until a 35 ft obstacle is cleared.

Unknowns: γ, V, x, h, a_x, a_z
Initial conditions: $\alpha_o = \alpha_{\text{TO}} = 10°$, $\gamma_o = 0$, $V_o = 1.2\ V_s$, $a_o = 0$, $x_o = 0$, $h_o = 0$

```
% Airborne section during a take-off

clc
clear all
```

```
m=50000; % kg; aircraft take-off mass
S=100; % m^2; wing area
g = 9.807; % m/s^2
T = 120000; % N; Engine Thrust
W = m*g; % N; Take-off weight
K =0.04; % induced drag coef.
Vs= 115; % knot stall speed
CDoTO=0.05; % Take-off drag coef.
CLc=0.3; % cruise lift coef.
d_CLf=0.4; % additional flap lift coef.
CL_alfa= 5.2; %1/rad; aircraft lift curve slope;
alpha = 10/57.3; %rad, Take-off angle
dt=0.1; % time step
t_tot = 5.8; % sec
rho = 1.225; % kg/m^2; air density
CL=CLc+d_CLf+CL_alfa*alpha; % wing-fuselage lift coef.
CD = CDoTO+K*CL^2; % drag coef.
x(1)=0; % distance traveled
V(1)= 1.2*Vs*0.5144; % m/s; Lift-off speed
Vz(1)=0; % m/s; speed normal to x-axis
time1(1) = 0;
gama(1) = 0; % climb angle
L(1) = 0.5*rho*V(1)^2*S*CL; % wing-fuselage lift
D(1) = 0.5*rho*V(1)^2*S*CD; % drag
a_x(1) = 0; % linear acceleration along x
a_z(1) = 0; % linear acceleration along z
z(1)=0;
S_A(1)=0;
H(1)=0;
i=1;

for t = 0:dt:t_tot % sec

    a_x(i+1)= (1/m)*(T*cos(alpha)-D(i)-W*sin(gama(i)));
    a_z(i+1)= (1/m)*(L(i)+T*sin(alpha)-W*cos(gama(i)));
    x(i+1)=V(i)*dt+0.5*a_x(i+1)*dt^2;
    S_A(i+1)=x(i+1)*cos(gama(i))+S_A(i);
    z(i+1)=Vz(i)*dt+0.5*a_z(i+1)*dt^2;
    H(i+1)=z(i+1)*cos(gama(i))+H(i);
    Vz(i+1)=z(i+1)/dt;
    gama(i+1)=asin(z(i+1)/x(i+1));
    V(i+1)=sqrt(V(i)^2+2*a_x(i+1)*x(i+1));
    L(i+1)= 0.5*rho*V(i+1)^2*S*CL;
    D(i+1)= 0.5*rho*V(i+1)^2*S*CD;
    time1(i+1)=t;
    i=i+1;
end

subplot(411)
plot(time1,gama*57.3,'rO-'); grid
xlabel ('time (sec)')
ylabel ('Climb angle (deg)')

subplot(412)
plot(time1,S_A,'b*-'); grid
xlabel ('time (sec)')
ylabel ('S_A (m)')
```

```
subplot(413)
plot(time1,V/0.514,'gd-'); grid
xlabel ('time (sec)')
ylabel ('V (knot)')

subplot(414)
plot(time1,H*3.28,'m*-'); grid
xlabel ('time (sec)')
ylabel ('h (ft)')
```

RESULTS

The results of the simulation show that the take-off airborne ground distance to clear 35 ft is 420 m (Figure 10.7).

When this MATLAB code is executed, four plots (Figure 10.7) that illustrate the variations of aircraft climb angle, distance traveled, airspeed, and height as a function of time are produced.

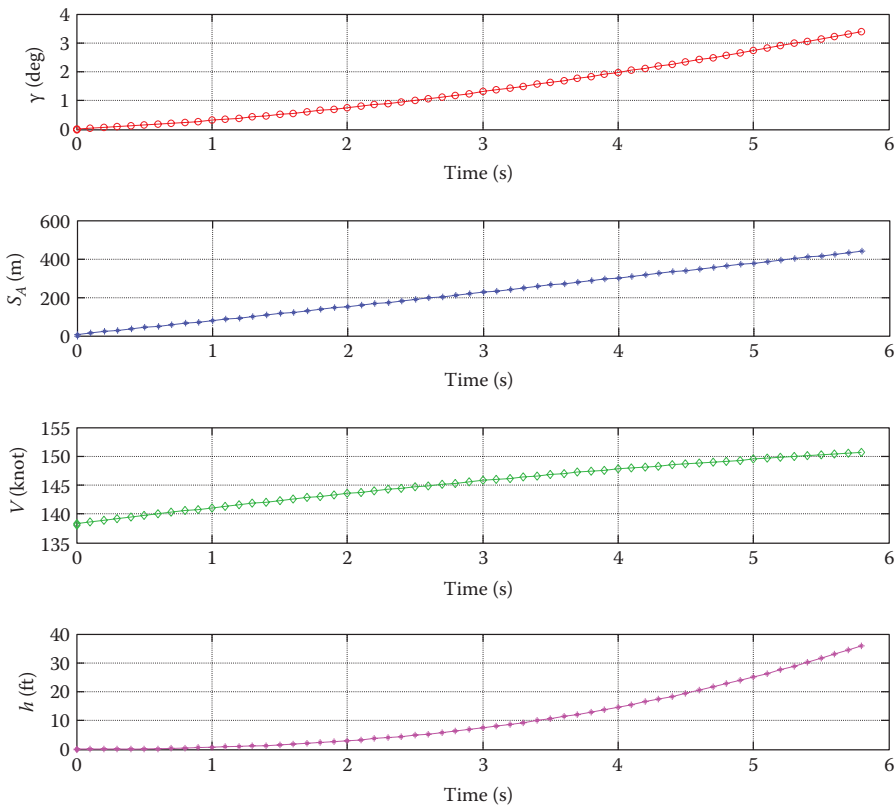

FIGURE 10.7 Variations of (1) Aircraft climb angle, (2) distance traveled, (3) airspeed, (4) height as a function of time.

10.5 CLIMB ANALYSIS USING NUMERICAL METHODS: CONSTRUCT THE HODOGRAPH

10.5.1 Review of Fundamentals

A very beneficial approach in analysis of the climb performance is using a graphical technique. In this approach, a plot (also known as hodograph diagram) is constructed, which is the variations of the vertical component of airspeed (V_V) versus the horizontal component of airspeed (V_H). The ordinate is V_V, which also is the rate of climb, while the abscissa is the horizontal component of velocity V_H, as depicted in Figure 7.20. Section 7.7 introduces the theory behind this topic. The geometric relation among forward airspeed, V, horizontal speed, vertical speed, and climb angle (γ) are

$$V_H = V\cos(\gamma) \tag{10.48}$$

$$V_V = V\sin(\gamma) \tag{10.49}$$

This relation is also shown in this plot. By employing this graph, one can simultaneously determine the maximum rate of climb and the maximum climb angle. The relation between climb angle and airspeed for a jet aircraft is derived as Equation 7.78. It is repeated here for convenience:

$$\sin(\gamma) = \frac{\left(\frac{T}{V}\right) - \left(\frac{1}{2}\right)\rho V^2 S C_{D_o}}{W} - \frac{2WK\left(\cos(\gamma)\right)^2}{\rho V^2 S} \tag{10.50}$$

This is a nonlinear algebraic equation in terms of climb angle (γ) and does not have a closed-form solution. We need to make an assumption to simplify the equation without losing the desired accuracy. The assumption we make is to assume $\cos(\gamma) = 0$ in the drag expression only; this is a reasonable assumption. The expressions for climb angle as a function of airspeed for jet and propeller-driven aircraft were derived in Sections 7.4 and 7.5 (as Equations 7.80 and 7.81). They are repeated here for convenience:

$$\gamma = \sin^{-1}\left[\frac{T}{W} - \frac{1}{2W}\rho V^2 S C_{D_o} - \frac{2KW}{\rho S V^2}\right] \left(\text{jet aircraft}\right) \tag{10.51}$$

$$\gamma = \sin^{-1}\left[\frac{P\eta_P}{VW} - \frac{1}{2W}\rho V^2 S C_{D_o} - \frac{2KW}{\rho V^2 S}\right] \left(\text{propeller-driven aircraft}\right) \tag{10.52}$$

To sketch the hodograph, one needs to plot the variations of the vertical component of the airspeed (V_H) with respect to the horizontal component of the airspeed (V_V). The horizontal and vertical components (V_H and V_V) of the airspeed are determined through Equations 10.48 and 10.49, respectively. In this process, one needs to select an airspeed that ranges from stall speed to the maximum speed. Then, calculate the corresponding climb angle (γ) to each airspeed. Through this graph, one can graphically compare the steepest climb with the fastest climb. The graph highlights that the maximum rate of climb does not correspond to the maximum climb angle.

The procedure to construct the hodograph diagram is as follows:

1. Select an airspeed (begin with the stall speed).
2. Calculate the climb angle corresponding to this airspeed from Equation 10.50 or 10.51 (for a jet aircraft), or Equation 10.52 (for a prop-driven aircraft).
3. Determine horizontal velocity (V_H) from Equation 10.48 ($V\cos(\gamma)$).
4. Determine vertical velocity (V_V) from Equation 10.49 ($V\sin(\gamma)$).
5. Select a new airspeed (you may increase the previous one by 1 knot).
6. This process is continued until the maximum speed is reached, which in theory means a zero climb angle and a zero V_V.
7. Plot values of V_H (from step 3) versus V_V (from step 4).

In this process, each plot is based on a given aircraft weight (e.g., maximum take-off weight), a given engine thrust (e.g., maximum thrust), and a given altitude (e.g., sea level).

Example 10.4

Consider the business jet aircraft Gulfstream G-550 with a maximum take-off mass of 41,277 kg, a wing area of 105.63 m^2, a wing span of 27.69 m, and two turbofan engines each generating 68.4 kN of thrust. Assume the following:

$$C_{D_o} = 0.022,\ e = 0.85,\ V_s = 85 \text{ knot}, V_{max} = 550 \text{ knot}$$

Construct the hodograph for this aircraft for sea level. From the graph, determine the maximum rate of climb and the maximum climb angle.

Solution

The aircraft weight (mg) is 404,789 N, and the stall speed is 43.73 m/s. We will start from 44 m/s. First, we need to calculate AR and *K*:

$$\text{AR} = \frac{b^2}{S} = \frac{27.69^2}{105.63} = 7.26 \tag{3.9}$$

$$K = \frac{1}{\pi e \,\text{AR}} = \frac{1}{3.14 \times 0.85 \times 7.26} = 0.052 \tag{3.8}$$

The climb angle is determined from the following formula:

$$\sin(\gamma) = \frac{\frac{T}{V} - \frac{1}{2}\rho V^2 S C_{D_o}}{W} - \frac{2WK(\cos(\gamma))^2}{\rho V^2 S} \tag{10.50}$$

Substitution of the given values yields

$$\sin(\gamma) = \frac{2\times 68{,}400}{404{,}789} - \frac{1}{2}1.225\times(44)^2\times 0.02\frac{105.63}{404{,}789} - \frac{2\times 0.052\times 404{,}789(\cos(\gamma))^2}{1.225\times(44)^2\times 105.63} \tag{10.51}$$

This is a nonlinear algebraic equation in terms of climb angle (γ); the solution is

$$\gamma = 0.171\,\text{rad} = 9.78°.$$

For other velocities, the following MATLAB code is written to do the calculations and plotting.

```
clc
clear all

m=41277; % kg
g=9.81; % m/s^2
W=m*g;
S=105.63; % m^2
b=27.69; % m
rho=1.225;
T=2*68400; %N
a=340; %m/s;
CDo = 0.02;
AR = b^2/S;
e1=0.85;
K=1/(3.14*e1*AR);
 j=1;

for V=49:1:320 % velocity in m/s

    for i = 1:0.1:60 % climb angle in deg
    gam = i/57.3;
    LHS=sin(gam);
    num=2*K*W*(cos(gam))^2;
    den=ro*S*V^2;
    RHS=(T/W)-(0.5*rho*S*CDo*(V^2)/W)-(num/den);

    if abs(LHS)-abs(RHS)<0.002
        if LHS > RHS
    gama (j) = gam*57.3;
    V1(j)=V;
    LS(j)=LHS;
```

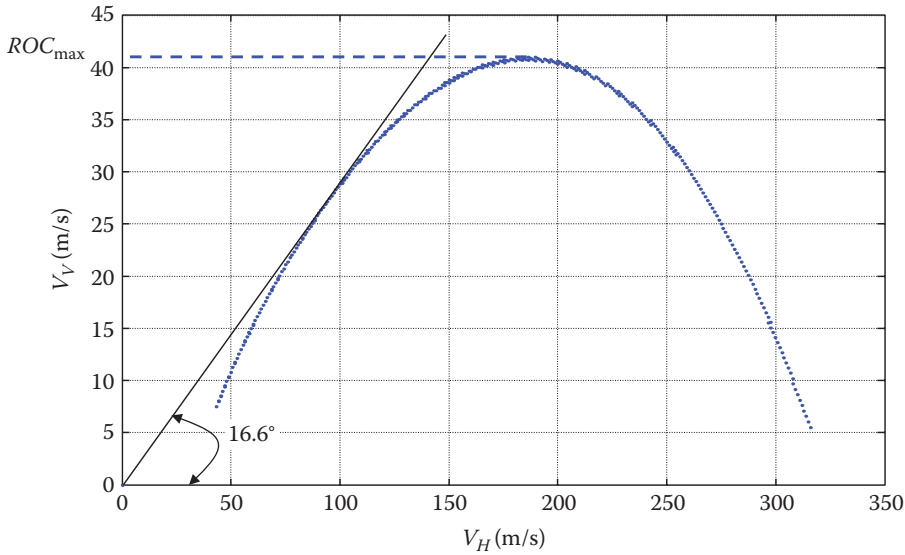

FIGURE 10.8 Hodograph for Gulfstream IV.

```
    RS(j)=RHS;
    VV(j)= V*sin(gam);
    VH(j)= V*cos(gam);
        end
    end
    j=j+1;
    end
end

plot(VH, VV,'b.'); grid
xlabel ('V_H (m/s)')
ylabel ('V_V (m/s)')
```

Figure 10.8; which is produced by this MATLAB code, illustrates the hodograph. The tangent line; dash line, and the angle of 16.6° are added to the plot later.

From Figure 10.8, the maximum rate of climb is identified to be 40.8 m/s or 8,031 ft/min. Furthermore, the maximum climb angle is determined to be 16.6° (i.e., $\tan^{-1}$ (26.2/88)). In practice, any point on the tangent indicates the maximum angle with respect to origin. Hence,

$$\text{ROC} = 8{,}031\,\text{ft/min}$$

$$\gamma_{\max} = 16.6°$$

Please note that in this example, we assumed a constant C_{D_o} for the aircraft. In practice, C_{D_o} is increased with airspeed, particularly at high subsonic velocities. For more accurate results, you need to use a more realistic model for drag polar.

10.6 FASTEST CLIMB ANALYSIS USING NUMERICAL METHODS

10.6.1 Fastest Climb Analysis

The fastest climb or the maximum rate of climb (ROC_{max}) occurs when an aircraft climbs with a speed for maximum rate of climb $\left(V_{ROC_{max}}\right)$ and employs the climb angle that submits the maximum rate of climb $\left(\gamma_{ROC_{max}}\right)$. Section 7.4 introduces the theory behind such flight.

The expression for climb angle as a function of airspeed for jet aircraft is derived in Section 7.4.1 (as Equation 7.19). It is repeated here for convenience:

$$ROC_{max} = V_{ROC_{max}} \sin\left(\gamma_{ROC_{max}}\right) \tag{10.53}$$

We need to determine two parameters: $V_{ROC_{max}}$ and $\gamma_{ROC_{max}}$. These two variables are independent of each other and their calculation techniques are presented in Sections 7.4.1.1 and 7.4.1.2, respectively. The expressions for airspeed and climb angle for a jet aircraft are derived in Section 7.4.1 (as Equations 7.30 and 7.38). They are repeated here for convenience:

$$V_{ROC_{max}} = \sqrt{\frac{T}{3\rho C_{D_o} S}\left[1+\sqrt{1+\frac{3}{\left[(L/D)_{max}(T/W)\right]^2}}\right]} \tag{10.54}$$

$$\gamma_{ROC_{max}} = \sin^{-1}\left[\frac{T}{W} - \frac{\rho V_{ROC_{max}}^2 S C_{D_o}}{2W} - \frac{2KW}{\rho S V_{ROC_{max}}^2}\right] \tag{10.55}$$

In addition, any velocity lower than the stall speed is not acceptable.

Example 10.5

Consider the business jet aircraft Gulfstream G-550 with a maximum take-off mass of 41,277 kg, a wing area of 105.63 m^2, a wing span of 27.69 m, and two turbofan engines each generating 68.4 N of thrust. Assume the following:

$$C_{D_o} = 0.02,\ e = 0.85,\ C_{L_{max}} = 2.6,\ V_{max} = 600 \text{ knot}.$$

Calculate and plot the maximum rate of climb versus altitude for Gulfstream IV. Then, identify the absolute ceiling from the graph.

Solution

The following MATLAB code is written. A height-step (Δh) of 100 m is selected.

```
clc
clear all
% Gulfstream G-550
```

```
m=41277; % kg
b=27.69; % m
g=9.81; % m/s^2
W=m*g; % weight in N
S=105.63; % m^2
ro=1.225; % kg/m^3
CLmax = 2.6;
Th_o=2*68400; % Thrust in N
AR = b^2/S;
e1=0.85;
K=1/(3.14*e1*AR);
CDo = 0.02;
dh=100; % m, height step
R1=287; % J/kg.K
L1=6.5/1000; % K/m lapse rate
h_tot = 13800; % m, altitude
ho=0;
rho_o = 1.225; % kg/m^2; sea level air density
To=(15+273); % K sea level temperature
Po=101325; % Pa, sea level pressure
T(1)=To-L1*ho;
P(1)=Po*(T(1)/To)^5.256;
rho(1)=P(1)/(R1*T(1));
Th(1) = Th_o*rho(1)/rho_o; % Thrust
LDmax=1/(2*sqrt(K*CDo));
A(1)=(Th_o/(3*S*rho_o*CDo));
V_ROC(1)=sqrt(A(1)*(1+sqrt(1+3/(LDmax^2*(Th_o/W)^2))));
Vs(1)=sqrt((2*W)/(rho_o*S*CLmax));

if V_ROC(1)< Vs(1)
    V_ROC(1)= 1.1* Vs(1)
end

H(1)=ho;
CL(1)=(2*W)/(rho_o*S*(V_ROC(1)^2));
CD(1)=CDo+K*CL(1)^2;
D(1)=0.5*rho_o*V_ROC(1)^2*S*CD(1);
gama(1)=asin((Th(1)-D(1))/W);
ROCmax(1)=V_ROC(1)*sin(gama(1));
ROC_fpm(1)=ROCmax(1)*196.85;

i=1;
for h = ho:dh:h_tot% altitude in meter
T(i+1)=To-L1*h;
P(i+1)=Po*(T(i+1)/To)^5.256;

if h>11000
    T(i+1)=-56+273; % K
    P(i+1)=0.2234*Po*exp((11000-h)/6342);
end

rho(i+1)=P(i+1)/(R1*T(i+1));
Th(i+1) = Th_o*rho(i+1)/rho_o; % Thrust

A(i+1)=(Th(i+1)/(3*S*rho(i+1)*CDo));
V_ROC(i+1)=sqrt(A(1)*(1+sqrt(1+3/(LDmax^2*(Th(i+1)/W)^2))));
```

```
if h==11000
    Th1=Th(i+1)
    A1=A(i+1)
    V1=V_ROC(i+1)
end

Vs(i+1)=sqrt((2*W)/(rho(i+1)*S*CLmax));

if V_ROC(i+1)< Vs(i+1)
   V_ROC(i+1)= 1.1* Vs(i+1);
end

CL(i+1)=(2*W)/(rho(i+1)*S*(V_ROC(i+1)^2));
CD(i+1)=CDo+K*CL(i+1)^2;
D(i+1)=0.5*rho(i+1)*V_ROC(i+1)^2*S*CD(i+1);
gama(i+1)=asin((Th(i+1)-D(i+1))/W);
ROCmax(i+1)=V_ROC(i+1)*sin(gama(i+1));
ROC_fpm(i+1)=ROCmax(i+1)*196.85;
H(i+1)=h;
i=i+1;
end

subplot 311
plot(ROC_fpm,H*3.281,'rO-'); grid
ylabel ('altitude (ft)')
xlabel ('ROC_max (ft/min)')

subplot 312
plot(V_ROC/0.514,H*3.281,'rO-'); grid
ylabel ('altitude (ft)')
xlabel ('Airspeed (knot)')

subplot 313
plot(gama*57.3,H*3.281,'rO-'); grid
ylabel ('altitude (ft)')
xlabel ('Climb angle (deg)')
```

When this MATLAB code is executed, three plots that illustrate the variations of the maximum rate of climb, corresponding velocity, and corresponding climb angle versus altitude are produced. Figure 10.9, which is produced by this MATLAB code, illustrates the results.

From the graph in Figure 10.9, we identify that the absolute ceiling is 13,800 m.

10.7 TIME TO CLIMB ANALYSIS USING NUMERICAL METHODS

10.7.1 Review of Fundamentals

The time to climb is a climb performance analysis criterion. For a transport aircraft, the time to climb is an economical issue, while for a fighter aircraft in a fight mission, it means win or loss. Section 7.9 introduces the theory behind such flight. The time to climb from one altitude, h_1 to another altitude, h_2 is obtained by integrating Equation 7.89 between the two altitudes:

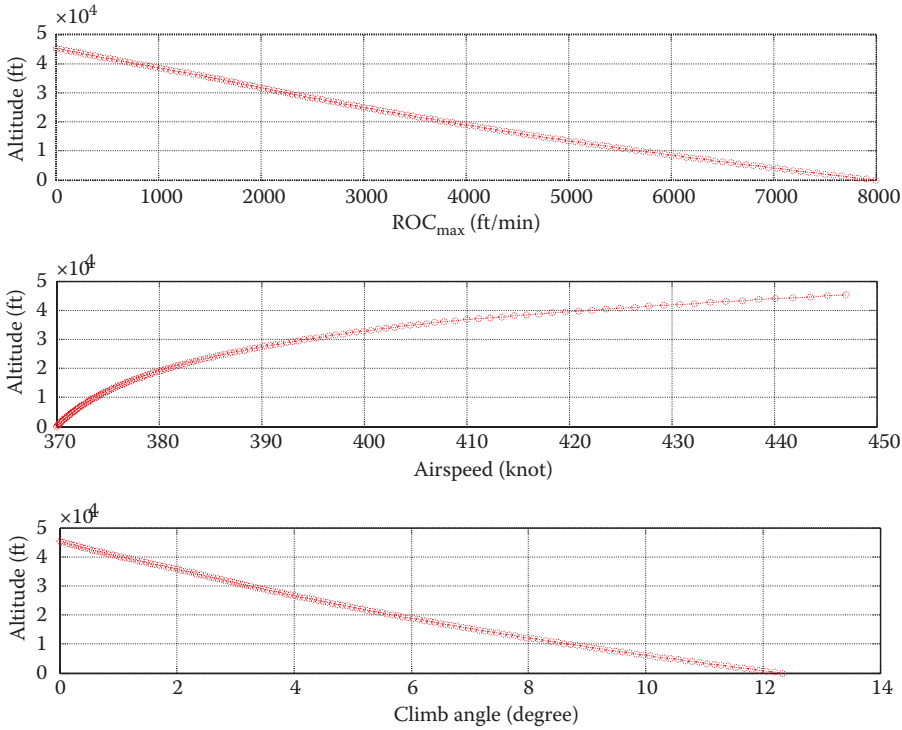

FIGURE 10.9 The variation of maximum rate of climb versus altitude for Gulfstream IV.

$$t = \int_{h_1}^{h_2} \frac{dh}{\text{ROC}} = \int_{h_1}^{h_2} \frac{dh}{V \sin(\gamma)} \tag{10.56}$$

When the time to climb is considered from sea level, h_1 is assumed to be zero. If the maximum rate of climb is used at each altitude, then it becomes the minimum time to climb to altitude h (see Equation 7.99):

$$t_{\min} = \frac{h_{ac}}{\text{ROC}_{\max_{SL}}} \ln\left(\frac{1}{1-(h/h_{ac})}\right) \tag{10.57}$$

Please note that the reference for this equation is the sea level

Example 10.6

Consider the business jet aircraft Cessna Citation III with an absolute ceiling of 54,000 ft and a maximum rate of climb of 3,700 ft/min. Plot the variations of altitude versus time, and then calculate the minimum time to climb to the absolute ceiling.

Solution

The following MATLAB code is written. A height-step (Δh) of 100 ft is selected.

```
% Climb analysis; Cessna Citation III

clc
clear all

h_ac = 54000; % ft
ROCmax = 3700; % ft/min
h1 = 54000; % ft
dh = 100; % ft
T(1) = 0;
i = 1;
h(1)=0;

for h = 0:dh:h1 % m
    i = i+1;
    T(i)=(h_ac/ROCmax)*log(1/(1-(h/h_ac)));
    h2(i) =h;

end

plot(T,h2,'bO-'); grid
xlabel ('Time (minute)')
ylabel ('Altitude (ft)')
```

Figure 10.10, which is produced by this MATLAB code, illustrates the results.

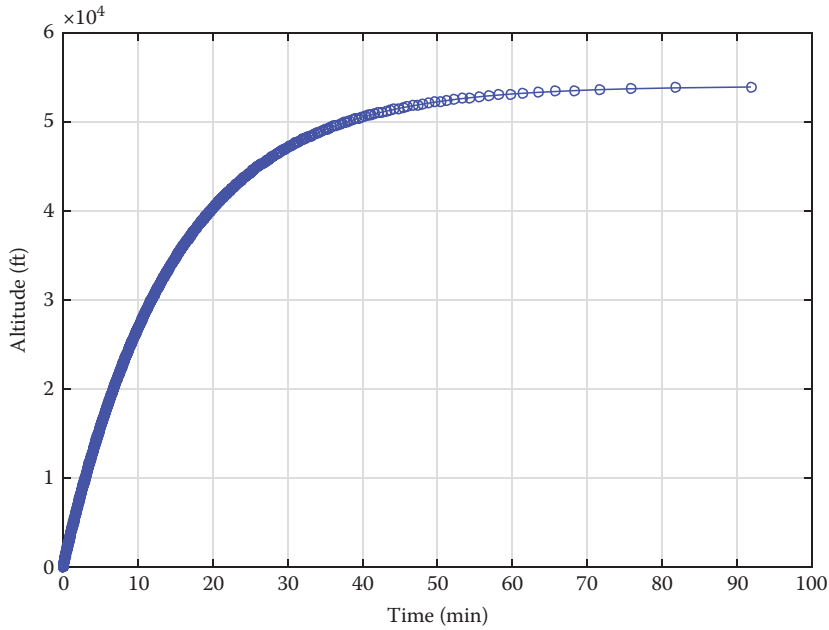

FIGURE 10.10 The variations of altitude versus time (climb history).

Figure 10.10 demonstrates time to climb to the absolute ceiling for the jet aircraft Cessna Citation III with an absolute ceiling of 54,000 ft and a maximum rate of climb of 3,700 ft/min. It is interesting to see that it takes about 43 min to climb to its service ceiling, while it takes longer (about 50 min) to climb from service ceiling to the absolute ceiling. In the first section of the figure, the variation of time with altitude is almost linear. However, in the latter part, the slope is gradually decreasing logarithmically. The asymptote indicates that the aircraft has reached the absolute ceiling.

10.8 PARABOLIC PATH FOR A ZERO-GRAVITY FLIGHT

10.8.1 Mission Analysis and Governing Equations

One practical case for the weightlessness (i.e., zero-gravity) in the air is a kind of cruising (in fact, descending) flight (see Figure 9.22) where the lift is set to be zero ($L=0$). This flight maneuver is a practical way to experience *weightlessness/microgravity* without leaving Earth. Section 9.8.2 introduces the theory behind such flight. In this section, an overview of the fundamentals is provided.

The flight starts at a high altitude with a given cruising airspeed, V_o. In addition, the engine thrust is set to be equal to the aircraft drag. The forward direction is named as the x-axis, and the downward direction is named as the z-axis. Since the aircraft is under the influence of aircraft weight (W) in the z-direction, it will fall freely in the z-direction. Hence, in the z-direction, the flight will be accelerated under the influence of gravity, g:

$$a_z = g \tag{10.58}$$

The vertical velocity (V_z) during this accelerated motion is governed by the following equation:

$$V_{z_2}^2 - V_{z_1}^2 = 2gh \tag{10.59}$$

Hence, the linear velocity in the z-direction is obtained by the following equation:

$$V_z = \sqrt{V_1^2 + 2g\Delta h} \tag{10.60}$$

The height lost in the z-direction is

$$\Delta h = \frac{1}{2} g t^2 + Vt \tag{10.61}$$

Since the aircraft has an initial cruising velocity, V, the aircraft will descend with a large descent angle (θ). Therefore, the flight path will be parabolic. The instantaneous flight path angle is

$$\gamma = \tan^{-1}\left(\frac{h}{X}\right) \tag{10.62}$$

The aircraft total velocity in the flight path direction is gradually increasing and is obtained by the following equation:

$$V = \sqrt{V_x^2 + V_z^2} \tag{10.63}$$

where V_x is the initial cruising velocity.

Example 10.7

A transport aircraft similar to an Airbus 300 is employed in a zero-gravity flight. The flight is started at 8,000 m with a velocity of 226 m/s and lasts about 24 s. Plot the variations of (1) height, (2) vertical velocity, (3) total velocity, and (4) descent angle as a function of time. Ignore the drag in the z-direction.

Solution

The following MATLAB code is written. A time step (Δt) of 0.1 s is selected.

```
Matlab m-file
clc
clear all

H(1) = 8000 % m; initial height
g = 9.81; % m/s^2
dt=0.1; % time step
t_tot = 24; % sec
x(1)=0; % distance traveled
V= 226; % m/s; rotation speed
Vt(1)=V;
Vz(1)=0;
h(1)=0;
gama(1) = 0;
time1(1) = 0;
i=1;

for t = dt:dt:t_tot % sec
x(i+1)=V*dt+x(i);
h(i+1)= 0.5*g*dt^2+Vz(i)*dt+h(i);
dh=h(i+1)-h(i);
H(i+1)=H(1)-h(i+1);
Vz(i+1)=sqrt(Vz(i)^2+(2*g*dh));
gama(i+1)=atan(h(i+1)/x(i+1))+gama(1);
Vt(i+1)= sqrt(Vz(i+1)^2+V^2);
time1(i+1)=t;
```

```
i=i+1;
end
subplot(411)
plot(time1,H,'rO'); grid
xlabel ('time (sec)')
ylabel ('altitude (m)')

subplot(412)
plot(time1,Vz,'rx'); grid
xlabel ('time (sec)')
ylabel ('vertical speed (m/s)')

subplot(413)
plot(time1,Vt,'rO-'); grid
xlabel ('time (sec)')
ylabel ('total speed (m/s)')

subplot(414)
plot(time1,gama*57.3,'r*'); grid
xlabel ('time (sec)')
ylabel ('desced angle (deg)')
```

PLOT AND RESULTS

Figure 10.11, which is produced by this MATLAB code, illustrates the results.

The figures demonstrate that the aircraft loses about 3,000 m during this zero-gravity flight. At the end of flight, the descent angle is about 28°, while the total velocity is about 330 m/s.

10.9 *V-N* DIAGRAM

10.9.1 Overview of *V-n* Diagram

One of the most important diagrams of the flight envelope is the *V-n* diagram. This envelope demonstrates the variations of the allowable load factor versus airspeed. Figure 9.25 shows a typical *V-n* diagram for a GA aircraft. This diagram is, in fact, a combination of two diagrams: (1) the *V-n* diagram without consideration of gust and (2) the *V-n* diagram with the effect of gust. In this section, we only consider the *V-n* diagram without gust. The diagram (i.e., envelope) has five sides; three top, right, and bottom sides are just represented each by a line. The top and bottom sides are representing the maximum positive and negative load factors (i.e., $+n_{\max}$ and $-n_{\max}$), and the values of n are given by the customer or FAA regulations.

The right-hand side of the *V-n* diagram is the highest speed limit and is usually selected to be the *dive speed* (for GA aircraft, see Equations 9.195–9.197). The left side of the envelope has often two halves and provides the aerodynamic limit (i.e., stall speed). The two halves are nonlinear functions of airspeed, and each is represented by a curve. Both curves are governed by the following Equation (9.192):

$$n = \frac{V^2 \rho S C_{L_{\max}}}{2mg} \tag{10.64}$$

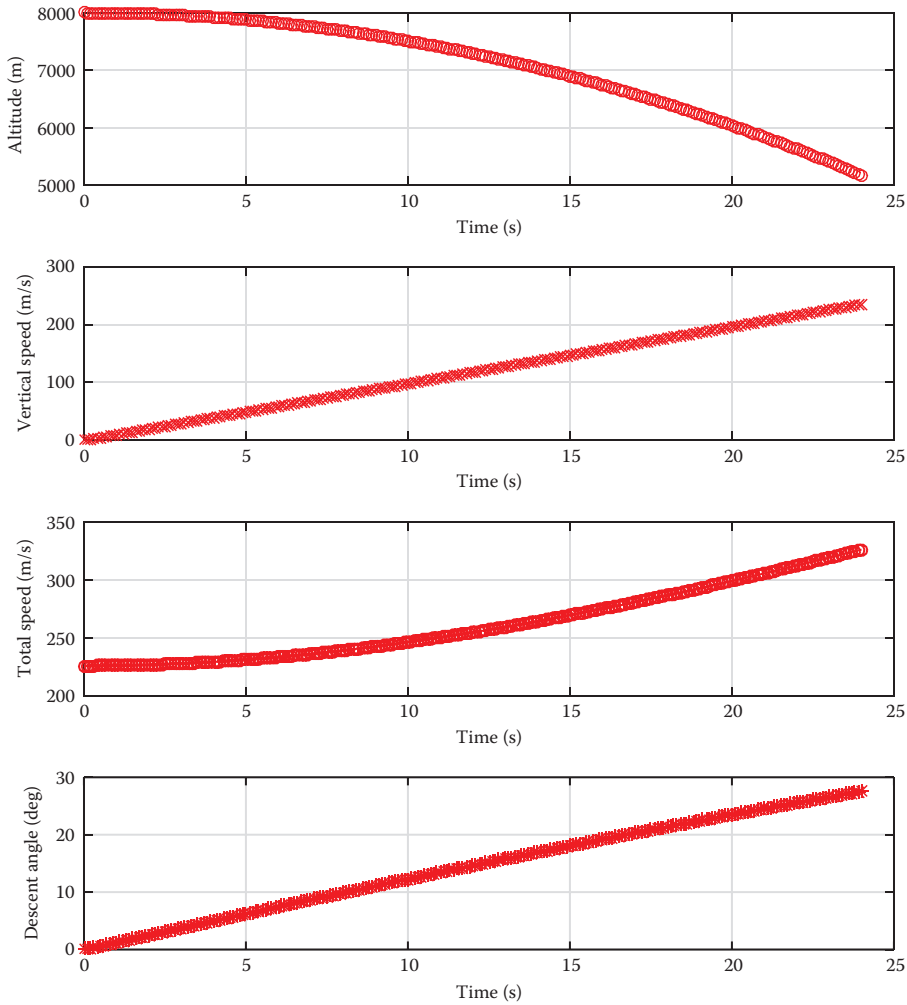

FIGURE 10.11 Variations of height, vertical velocity, total velocity, and descent angle as a function of time.

The values of the maximum positive and negative lift coefficient (i.e., $-C_{L_{\max}}$ and $+C_{L_{\max}}$) should be known from the aerodynamic characteristics of the aircraft.

Example 10.8

Consider a semi-acrobatic GA aircraft with a maximum take-off mass of 6,000 kg, a wing area of 25 m^2, and a dive speed of 360 m/s. Assume the following:

$$+C_{L_{\max}} = 1.8, -C_{L_{\max}} = -1.1,\ n_{\max} = +5,\ -n_{\max} = -2.2$$

Plot the *V-n* diagram for sea level altitude.

Solution:

The following MALTAB code is written.

```
clc
clear all
close all
S = 25; % wing area (m^2)
V_d=360; % dive speed (m/s)
m = 6000; % aircraft mass (kg)
CLmax_p = 1.8; % Maximum positive lift coefficient
CLmax_n = -1.1; % Maximum negative lift coefficient
n_max_p = 5; % Maximum positive load factor
n_max_n = -2.2; % Maximum negative load factor
g =  9.81; % gravity (m/s^2)
rho = 1.225; % air density (kg/m^3)

% Allocate space for arrays to define envelope
n_s_up  = zeros (1,V_d);
n_s_low  = zeros (1,V_d);
n_up  = zeros (1,V_d);
n_low  = zeros (1,V_d);
V1 = zeros (1,V_d);

% Set up arrays to correspond with the edges of the envelope
for V = 1: V_d  % airspeed
V1(V) = V;
n_s_up (V) = 0.5 *rho*V^2*S*CLmax_p/(m*g);
n_s_low (V) = 0.5 *rho*V^2*S*CLmax_n/(m*g);
n_up  (V) = n_max_p;
n_low  (V) = n_max_n;
end

% Plot the flight envelope - there is a little overlap
hold on
plot (V1(1:103), n_s_up (1:103), 'linewidth',3)
plot (V1(1:88), n_s_low (1:88), 'linewidth',3)
plot (V1(102:V_d), n_up (102:V_d), 'linewidth',3)
plot (V1(87:V_d), n_low (87:V_d), 'linewidth',3)
plot ([V_d V_d], [n_max_p, n_max_n], 'linewidth',3)
hold off
xlabel ('Airspeed (m/s)')
ylabel ('Load factor (n)')
title ('Flight envelope for a semi-acrobatic GA aircraft')
axis ([0 V_d+10 -3 5.5])
grid
```

RESULTS

When this MATLAB code is executed, the following plot (Figure 10.12) is produced.

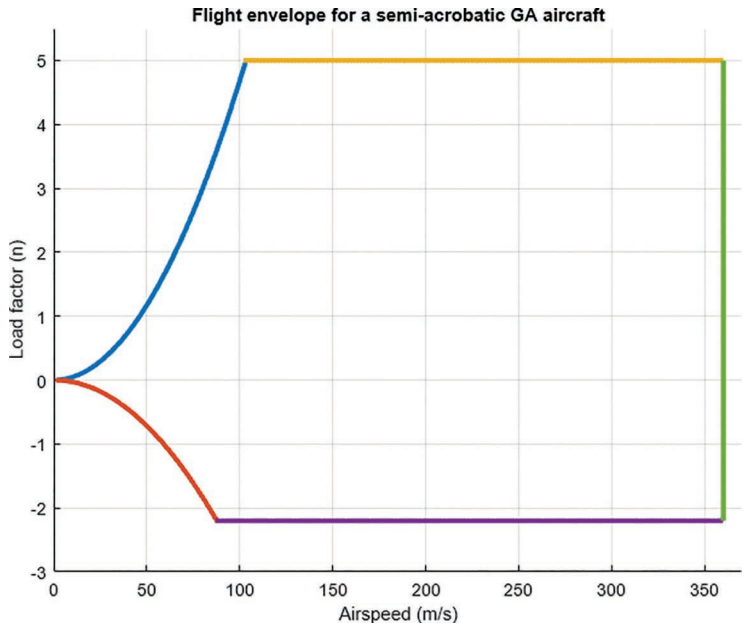

FIGURE 10.12 Flight envelope for a semi-acrobatic GA aircraft.

PROBLEMS

10.1 Consider a transport aircraft with a take-off mass of 40,000 kg, the engine thrust of 2 × 50 kN, and with the following characteristics:

$$S = 90\,\text{m}^2,\ S_h = 20\,\text{m}^2,\ K = 0.045,\ \mu = 0.035,\ C_{D_{\sigma\text{TO}}} = 0.055,$$

$$\ddot{\theta} = 1.6\,\text{deg}/\text{s}^2,\ C_{L_c} = 0.3,\ \Delta C_{L_f} = 0.5,\ i_T = 4°,\ V_R = 115\,\text{knot};$$

$$C_{L_{\alpha_{\text{wf}}}} = 5.2\ 1/\text{rad};\ C_{L_{\alpha_h}} = 4.7\ 1/\text{rad};\ C_{L_{h_o}} = -1.1.$$

Determine the distance the aircraft travels during take-off rotation (S_T) at sea level. Using a simulation program, plot the variations of (1) aircraft angle of attack, (2) distance traveled, (3) airspeed, (4) wing-fuselage lift, (5) drag, and (6) normal force as a function of time.

10.2 Consider a transport aircraft with a take-off mass of 250,000 kg, the engine thrust of 2 × 360 kN, and with the following characteristics:

$$S = 430\,\text{m}^2,\ S_h = 100\,\text{m}^2,\ K = 0.03,\ \mu = 0.03,\ C_{D_{\sigma\text{TO}}} = 0.04,$$

$$\ddot{\theta} = 2.2\,\text{deg}/\text{s}^2,\ C_{L_c} = 0.35,\ \Delta C_{L_f} = 0.5,\ i_T = 6°,\ V_R = 130\,\text{knot};$$

$$C_{L_{\alpha_{\text{wf}}}} = 5.11/\text{rad};\ C_{L_{\alpha_h}} = 4.2\ 1/\text{rad};\ C_{L_{h_o}} = -1.4$$

Determine the distance the aircraft travels during take-off rotation (S_T) at sea level. Using a simulation program, plot the variations of: (1) aircraft angle of attack, (2) distance traveled, (3) airspeed, (4) wing-fuselage lift, (5) drag, and (6) normal force as a function of time.

10.3 Consider a box connected to a parachute that is dropped from 5,000 m ISA condition. The total mass of the cargo box plus the parachute is 300 kg, and the projected area of the parachute is 20 m^2. The drag coefficient of the box plus parachute is $C_D = 1.4$.

Determine

1. The time that the box takes to reach the ground
2. The terminal velocity

In the end, plot the variations of height, velocity, and acceleration versus time.

10.4 Consider an airman who is jumping from an aircraft and opens his parachute at 2,000 m ISA + 20 condition. The total mass of the jumper plus the parachute is 120 kg, and the projected area of the parachute is 8 m^2. The drag coefficient of the man plus parachute is $C_D = 1.1$.

Determine

1. The time that the jumper takes to reach the ground
2. The terminal velocity

In the end, plot the variations of height, velocity, and acceleration versus time.

10.5 Consider a transport aircraft with a take-off mass of 70,000 kg, the engine thrust of 2 × 80 kN, and with the following characteristics:

$$S = 130\,m^2,\ K = 0.03,\ \mu = 0.05,\ C_{D_{\sigma TO}} = 0.06,\ C_{L_c} = 0.2,$$

$$\Delta C_{L_f} = 0.5,\ \alpha_{TO} = 10°,\ V_s = 120\,\text{knot};\ C_{L_{\alpha_{wf}}} = 5.21/\text{rad}.$$

Determine the distance the aircraft travels during take-off airborne (S_A) at sea level. Using a simulation program, plot the variations of: (1) aircraft climb angle, (2) distance traveled, (3) airspeed, and (4) height as a function of time. Select a time step of 0.01 s, and continue the simulation until a 35 ft obstacle is cleared.

10.6 Consider a jet transport aircraft with a take-off mass of 27,000 kg, the engine thrust of 2 × 60 kN, and with the following characteristics:

$$S = 70\,m^2,\ K = 0.033,\ \mu = 0.034,\ C_{D_{\sigma TO}} = 0.04,$$

$$C_{L_c} = 0.25,\ \Delta C_{L_f} = 0.6,\ \alpha_{TO} = 10°,\ V_s = 95\,\text{knot};\ C_{L_{\alpha_{wf}}} = 4.8\,1/\text{rad}.$$

Determine the distance the aircraft travels during take-off airborne (S_A) at sea level. Using a simulation program, plot the variations of: (1) aircraft climb angle, (2) distance traveled, (3) airspeed, and (4) height as a function of time. Select a time step of 0.01 s, and continue the simulation until a 35 ft obstacle is cleared.

10.7 Consider a business jet aircraft with a maximum take-off mass of 30,000 kg, a wing area of 60 m^2, a wing span of 24 m, and two turbofan engines each generating 50 kN of thrust. Assume the following:

$$C_{D_o} = 0.022,\ e = 0.88,\ V_s = 90\,\text{knot},\ V_{\max} = 550\ \text{knot}.$$

Construct the hodograph for this aircraft for sea level. From the graph, determine the maximum rate of climb and the maximum climb angle.

10.8 Consider a fighter jet aircraft with a maximum take-off mass of 25,000 kg, a wing area of 50 m^2, a wing span of 12 m, and two turbofan engines each generating 100 kN of thrust. Assume the following:

$$C_{D_o} = 0.024,\ e = 0.7,\ V_s = 120\,\text{knot},\ V_{\max} = 700\,\text{knot}.$$

Construct the hodograph for this aircraft for sea level. From the graph, determine the maximum rate of climb and the maximum climb angle.

10.9 Consider a jet transport aircraft with a maximum take-off mass of 260,000 kg, a wing area of 400 m^2, a wing span of 50 m, and three turbofan engines each generating 250 kN of thrust. Assume the following:

$$C_{D_o} = 0.018,\ e = 0.92,\ C_{L_{\max}} = 2.2,\ V_{\max} = 600\ \text{knot}.$$

Calculate and plot the maximum rate of climb versus altitude. Then, identify the absolute ceiling from the graph.

10.10 Consider a fighter jet aircraft with a maximum take-off mass of 20,000 kg, a wing area of 40 m^2, a wing span of 10 m, and two turbofan engines each generating 180 kN of thrust. Assume the following:

$$C_{D_o} = 0.017,\ e = 0.84,\ C_{L_{\max}} = 2,\ V_{\max} = 800\,\text{knot}.$$

Calculate and plot the maximum rate of climb versus altitude. Then, identify the absolute ceiling from the graph.

10.11 Consider a business jet aircraft with an absolute ceiling of 50,000 ft and a maximum rate of climb of 4,000 ft/min. Plot the variations of altitude versus time, and then calculate the minimum time to climb the absolute ceiling. Select a height-step of 100 ft.

10.12 Consider a fighter jet aircraft with an absolute ceiling of 60,000 ft and a maximum rate of climb of 10,000 ft/min. Plot the variations of altitude versus time, and then calculate the minimum time to climb the absolute ceiling. Select a height-step of 100 ft.

10.13 Consider a prop-driven GA aircraft with an absolute ceiling of 20,000 ft and a maximum rate of climb of 1,200 ft/min. Plot the variations of altitude versus time, and then calculate the minimum time to climb the absolute ceiling. Select a height-step of 100 ft.

10.14 A transport aircraft is employed in a zero-gravity flight. The flight is started at 9,000 m with a velocity of 200 m/s and lasts about 20 s. Plot the variations of (1) height; (2) vertical velocity; (3) total velocity; and (4) descent angle as a function of time. Ignore the drag in the z-direction.

10.15 A large transport aircraft is employed in a zero-gravity flight. The flight is started at 10,000 m with a velocity of 190 m/s and lasts about 25 s. Plot the variations of (1) height; (2) vertical velocity; (3) total velocity; and (4) descent angle as a function of time. Ignore the drag in the z-direction.

10.16 Consider a semi-acrobatic GA aircraft with a maximum take-off mass of 5,000 kg, a wing area of 28 m^2, and a dive speed of 320 m/s. Assume the following:

$$+C_{L_{\max}} = 1.9, -C_{L_{\max}} = -0.9,\ n_{\max} = +5.8,\ -n_{\max} = -2.4$$

Plot the *V-n* diagram for sea level altitude.

10.17 Consider a transport aircraft with a maximum take-off mass of 80,000 kg, a wing area of 125 m^2, and a dive speed of 380 m/s. Assume the following:

$$+C_{L_{\max}} = 2.8, -C_{L_{\max}} = -1.6,\ n_{\max} = +3,\ -n_{\max} = -1.4$$

Plot the *V-n* diagram for sea level altitude.

10.18 Consider a fighter aircraft with a maximum take-off mass of 20,000 kg, a wing area of 28 m^2, and a dive speed of 450 m/s. Assume the following:

$$+C_{L_{\max}} = 2.3, -C_{L_{\max}} = -1.3,\ n_{\max} = +8,\ -n_{\max} = -2.5$$

Plot the *V-n* diagram for sea level altitude.

Appendix A
Standard Atmosphere, SI Units

$\rho_o = 1.225\,\text{kg/m}^3$, $T_o = 15°\text{C} = 288.15\,\text{K}$, $P_o = 101,325\,\text{N/m}^2$,

$a_o = 340.29\,\text{m/s}$, $\mu_o = 1.785 \times 10^{-5}$ kg/m/s

Altitude (m)	T (K)	P (N/m²)	ρ (kg/m³)
0	288.15	101,325	1.225
1,000	281.65	89,876	1.1117
2,000	275.15	79,501	1.007
3,000	268.67	70,121	0.9093
4,000	262.18	61,660	0.8193
5,000	255.69	54,048	0.7364
6,000	249.20	47,217	0.6601
7,000	242.71	41,105	0.590
8,000	236.23	35,651	0.526
9,000	229.74	30,800	0.467
10,000	223.26	26,500	0.413
11,000	216.78	22,700	0.365
12,000	216.66	19,399	0.312
13,000	216.66	16,579	0.267
14,000	216.66	14,170	0.228
15,000	216.66	12,112	0.195
16,000	216.66	10,353	0.166
17,000	216.66	8,850	0.142
18,000	216.66	7,565	0.122
19,000	216.66	6,467	0.104
20,000	216.66	5,529	0.089
21,000	216.66	4,727	0.076
22,000	216.66	4,042	0.065
23,000	216.66	3,456	0.056
24,000	216.66	2,955	0.047
25,000	216.66	2,527	0.041

Appendix B
Standard Atmosphere, English Units

$\rho_o = 0.002378\,\text{slug/ft}^3$, $T_o = 518.7°\text{R}$, $P_o = 2116.2\,\text{lb/ft}^2 = 14.7\,\text{psi}$,

$a_o = 1116.4\,\text{ft/s}, \mu_o = 3.737 \times 10^{-7}\ \text{slug/ft} \cdot \text{s}$

Altitude (ft)	T(°R)	P(lb/ft²)	ρ(slug/ft³)	Altitude (ft)	T(°R)	P(lb/ft²)	ρ(slug/ft³)
0	518.7	2116.2	0.002378	**31,000**	408.3	601.6	0.000858
1,000	515.12	2040.9	0.002308	**32,000**	404.7	574.6	0.000827
2,000	511.5	1,967.7	0.002241	**33,000**	401.2	548.5	0.000796
3,000	508	1,896.7	0.002175	**34,000**	397.6	523.5	0.000767
4,000	504.43	1,827.7	0.002111	**35,000**	394.1	499.3	0.000738
5,000	500.86	1,761	0.002048	**36,000**	390.5	476.1	0.000710
6,000	497.3	1,696	0.001987	**37,000**	390	453.9	0.000678
7,000	493.7	1,633.1	0.001897	**38,000**	390	432.6	0.000646
8,000	490.2	1,572.1	0.001868	**39,000**	390	412.4	0.000616
9,000	486.6	1,513	0.001811	**40,000**	390	393.1	0.000587
10,000	483	1,455.6	0.001755	**41,000**	390	374.7	0.00056
11,000	479.5	1,400	0.001701	**42,000**	390	357.2	0.000533
12,000	475.9	1,346.2	0.001648	**43,000**	390	340.5	0.000509
13,000	472.4	1,294.1	0.001596	**44,000**	390	324.6	0.000485
14,000	468.8	1,243.6	0.001545	**45,000**	390	309.5	0.000462
15,000	465.2	1,195	0.001496	**46,000**	390	295	0.00044
16,000	461.7	1,147.5	0.001448	**47,000**	390	281.2	0.00042
17,000	458.1	1,101.7	0.001401	**48,000**	390	268.1	0.0004
18,000	454.5	1,057.5	0.001355	**49,000**	390	255.5	0.000381
19,000	451	1,014.7	0.001311	**50,000**	390	243.6	0.000364
20,000	447.4	973.3	0.001267	**51,000**	390	232.2	0.000347
21,000	443.9	933.3	0.001225	**52,000**	390	221.4	0.00033
22,000	440.3	894.6	0.001184	**53,000**	390	211	0.000315
23,000	436.8	857.3	0.001143	**54,000**	390	201.2	0.0003
24,000	433.2	821.2	0.001104	**55,000**	390	191.8	0.000286
25,000	429.6	786.3	0.001066	**56,000**	390	182.8	0.000273
26,000	426.1	752.7	0.00103	**57,000**	390	174.3	0.00026
27,000	422.5	720.3	0.000993	**58,000**	390	166.2	0.000248
28,000	419	689	0.000958	**59,000**	390	158.4	0.000236
29,000	415.4	658.8	0.000923	**60,000**	390	151	0.000225
30,000	411.9	629.7	0.00089	**61,000**	390	144	0.000215

Appendix C
Performance Characteristics of Several Aircraft [9,65]

TABLE C.1
Performance Characteristics of Several Piston-Prop Aircraft

No.	Aircraft	Manufacturer	Type	m_{TO} (kg)	P (hp)	V_{max} (knot)	Ceiling (ft)	Range (km)	ROC (fpm)	S_{TO} (m)	V_s (knot)
1.	PA-23-25-Aztec	Piper	Transport	2,360	2×250	187	18,950	2,445	1,400	517	59
2.	Cessna 180 Skywagon	Cessna	GA	1,270	171.5	148	19,600 Service	470	1,090	367	48
3.	BN-2A MK III-2 Trislander	Britten–Norman	Transport	4,536	3×260	156	15,600	1,610	980	594	—
4.	Beech Bonanza A36	Beechcraft	Utility	1,633	285	187	17,800	1,425	1,015	383	52.5
5.	Speed Canard—B	Gyroflug	GA	680	116	146	14,500 Service	1,350	985	700	57
6.	Epsilon	Aerospatiale	Military trainer	1,250	300	205	23,000 Service	—	1,850	640	62
7.	PL-12 Airtruk	Transavia	Agriculture	1,925	300	106	12,500	—	514	329	39
8.	A-135 Tangava II	Aerotech	Trainer	960	200	136	20,000	800	1,400	270	48
9.	Optica Scout	Brooklands	Surveillance	1,315	260	120	14,000	926	810	335	51
10.	NAC1 Freelance	NAC	Agriculture	3,855	750	143	—	1,482	955	419	60
11.	Slingsby T-67B	Slingsby	Sport	862	116	115	12,000	835	660	537	46
12.	Performance 2000	Cagney	Trainer	680	108	118	13,125	800	690	350	38
13.	Lederin 380-1	France	Home-built	600	90	109	12,000	885	900	122	26
14.	Microflight Spectrum	England	Ultralight	356	40	61	12,000	322	800	65	25
15.	Silver Eagle	USA	Ultralight	251	23	55	12,000	243	640	69	24

TABLE C.2
Performance Characteristics of Several Turboprop Aircraft

No.	Aircraft	Manufacturer	Type	m_{TO} (kg)	P (hp)	V_{max} (knot)	Ceiling (ft)	Range (km)	ROC (fpm)	S_{TO} (m)	V_s (knot)
1.	Turbo commander 690A	Rockwell	Transport	4,649	2×700	285	33,000	2,725	2,849	675	77
2.	Super King Air 200	Beechcraft	Transport	5,670	2×850	289	31,000	3,497	2,450	592	75
3.	Fairchild SA227-AC	Fairchild	Passenger	6,577	3×1,000	278	27,500	1,610	2,370	991	87
4.	DO 128-6	Dornier	Transport	4,350	2×400	183	32,600	1,825	1,260	554	38
5.	G-222	Aeritalia	Transport	29,000	2×4,860	310	25,000	2,500	1,705	1,000	84
6.	Atlantique	Dassault	Maritime	45,000	2×6,100	320	30,000	9,075	2,000	1,840	90
7.	P180 Avanti	Piaggio	Transport	4,767	2×800	400	41,000	3,335	3,650	736	78
8.	C-130 Hercules	Lockheed	Transport	79,380	4×4,508	325	34,700	7,876	1,900	1,573	100
9.	Pucara	Fama	Reconnaissance	6,800	2×978	270	32,800	3,710	3,543	705	78
10.	EMB-120 Brasilia	Embraer	Transport	11,500	2×1,800	328	29,800	2,983	2,120	1,420	87
11.	DCH-8 Dash 8-100	De Havilland	Transport	14,968	2×1,800	268	25,000	1,650	2,070	948	72
12.	ATR 42	ATR	Transport	16,150	2×1,800	267	25,000	1,666	2,100	1,010	73
13.	Cessna 208	Cessna	Utility	3,629	600	175	27,600	1,797	1,215	507	60
14.	Jetstream 31	BAE	Transport	6,950	2×940	263	25,000	1,296	2,080	975	86

TABLE C.3
Performance Characteristics of Several Jet Aircraft

No.	Aircraft	Manufacturer	Type	m_{TO} (kg)	T (kN)	V_{max} (knot)	Ceiling (ft)	Range (km)	ROC (fpm)	S_{TO} (m)	V_s (knot)
1.	F-5A	Northrop	Strike-fighter	9,379	2×18.5	Mach 1.4	50,000	2,594	28,700	1,113	128
2.	MiG-29	Mikoyan	Fighter	40,700	2×219.6	Mach 2.3	59,000	1,570	65,000	250	—
3.	Hawker Siddeley 125-600	Hawker Siddeley	Transport	11,340	2×16.7	280	12,500	2,890	4,900	1,341	83
4.	Boeing 737-200	Boeing	Transport	56,472	2×18.2	462	35,000	5,970	1,800	2,027	102
5.	Boeing 747-200B	Boeing	Transport	371,945	4×229.5	523	45,000	11,397	3,800	3,170	120
6.	B-52G	Boeing	Bomber	221,350	8×61.2	516	55,000	6,500	6,270	3,050	—
7.	Skyfox	Boeing	Trainer	9,070	2×16.5	505	50,000	3,360	7,500	670	97
8.	Cessna Citation III	Cessna	Transport	9,979	2×16.2	472	51,000	4,679	3,700	1,581	97
9.	Learjet 55	Gates Learjet	Transport	8,845	2×16.5	477	51,000	3,982	4,560	1,384	103
10.	F-16A	General Dynamics	Strike-fighter	11,094	111.2	>Mach 2	50,000	3,890	>50,000	—	110
11.	A-6	Grumman	Attack-bomber	27,397	2×41.4	560	42,400	4,410	7,620	1,390	98
12.	An-124	Antonov	Transport	405,000	4×229.5	467	39,000	4,500	—	3,000	110
13.	IL-76T	Ilyushin	Cargo	190,000	4×117.7	459	50,850	6,700	—	850	105
14.	Microjet 200B	Microjet	Trainer	1,300	2×1.3	250	30,000	870	1,705	850	72
15.	AMX	International	Close support	12,500	49.1	Mach 0.86	42,650	3,150	10,000	1,525	—
16.	Tornado ADV	Panavia	Strike-fighter	14,500	2×40	Mach 2.2	50,000	1,390	15,000	915	104
17.	Eurofighter	Europe	Fighter	23,500	2×60	Mach 2	65,000	29,00	62,000	700	—
18.	AS-39 Gripen	Saab	Fighter	14,000	54	Mach 2	50,000	32,00	50,000	800	—
19.	Rafale	Dassault	Fighter	24,500	2×50	1,032	50,000	+37,00	60,000	400	—
20.	Mig-35	Mikoyan	Fighter	29,700	2×53	Mach 2.25	57,400	2,000	65,000	400	—

TABLE C.4
Performance Comparison between the U.S. and Russian Military Aircraft

Aircraft	Manufacturer	Type	m_{TO} (kg)	T (kN)	V_{max} (Mach)	Ceiling (ft)	Range (km)	ROC (fpm)	Radius of Action (km)	No. of Seats	First Flight
USA											
B-52H	Boeing	Bomber	229,066	8×75.7	0.95	55,000	20,120	6270	4,630	6	1,961
F-14A	Grumman	Fighter	33,724	2×93	2.4	50,000	3,000	30,000	1,230	2	1,970
F-15C	McDonnell Douglas	Fighter	30,845	2×106.5	2.3	63,000	3,135	50,000	1,100	1	1,972
F-16A	General Dynamics	Fighter	16,060	106	2.02	52,000	4,080	62,000	885	1	1,974
F/A-18	McDonnell Douglas	Fighter	25,400	2×70.3	1.8	50,000	4,627	60,000	1,150	1	1,978
U-2C	Lockheed	Reconnaissance	7,835	49	850 km/h	80,000	6,440	9000	—	1	1,955
F-111F	McDonnell Douglas	Fighter	45,360	2×111.7	2.2	60,000	6,115	43,000	2,000	2	1,962
SR-71A	Lockheed	Reconnaissance	77,110	2×151.3	3	106,000	4,800	12,000	—	2	1,964
F-22 Raptor	Lockheed Martin	Fighter	38,000	2×116	Mach 2.42	>65,000	3,220	69,000	852	1	1,997
F-35	Lockheed Martin	Multirole fighter	31,751	125	1.6	40,000	2,800	—	1,239	1	2,006
Russia											
MiG-25	Mikoyan	Fighter	35,000	2×120.6	2.8	79,000	2,575	41,000	950	1	1,969
MiG-27	Mikoyan	Fighter	20,400	80	1.6	56,000	2,800	—	800	1	1,973
MiG-29	Mikoyan	Fighter	40,700	2×219.6	2.3	59,000	1,570	65,000	800	1	1,980
MiG-35	Mikoyan	Fighter	24,500	2×52	2.25	52,000	2,100	65,000	1,000	1 or 2	2,016
Su-24	Sukhoi	Fighter	39,500	2×112.8	2	53,000	6,000	35,000	1,700	2	1,970
Su-35	Sukhoi	Fighter	34,500	2×86.3	Mach 2.25	59,000	3,600	55,000	—	1	2,008
Su-57	Sukhoi	Multirole fighter	35,000	2×88.3	1.3	66,000	4,500	—	—	1	2,010
Tu-28	Tupolev	Reconnaissance	38,500	2×108	1.65	53,000	3,200	—	1,250	—	1,959
Tu-26	Tupolev	Bomber	11,000	2×211	2	56,000	8,000	27,500	2,600	3	1,972
Tu-95	Tupolev	Bomber	188,000	P=4× 15,000 hp	0.7	45,000	15,000	2,000	—	6	1,956
Tu-160	Tupolev	Bomber	275,000	4×137.3	2.05	52,000	12,300	14,000	2,000	4	1,981

Appendix D
Flight Records

TABLE D.1
Flight Records for Aircraft with Piston-Prop Engine

No.	Competition	Aircraft	Manufacturer	Pilot	Record	Unit	Date of Flight	Place or Itinerary
1.	Range at straight line and close loop	Voyager	USA	Dick Rutan and Jeana Yeager	40,312	km	December 14–23, 1986	Earth circumference
2.	Ceiling	Caproni Ca-161	Italy	Mario Pezi	56,046	ft	October 22, 1983	—
3.	Maximum speed	F8F Bearcat	USA	Lyle Shelton	850.25	km/h	August 21, 1989	Las Vegas, NV

TABLE D.2
Flight Records for Aircraft with Turboprop Engine

No.	Competition	Aircraft	Manufacturer	Pilot	Record	Unit	Date of Flight	Place or Itinerary
1.	Range at straight line	HC-130H Hercules	USA	Al Ellison	14,052.95	km	February 20, 1982	—
2.	Range at a closed loop	RP-3D Orion	USA	Philip Height	10,103.51	km	November 4, 1972	—
3.	Ceiling	Eggrett-1	USA	Invar Envoldson	53,573	ft	September 1988	Grenville, TX
4.	Maximum speed in straight line	P-3C Orion	USA	Donald Lilienthal	806.1	km/h	January 27, 1971	In a 15.25 km route
5.	Maximum speed in closed loop	TU-114	USSR	Ivan Sofomlin	877.212	km/h	April 9, 1960	5,000 km loop

TABLE D.3
Flight Records for Aircraft with Jet Engine

No.	Competition	Aircraft	Manufacturer	Pilot	Record	Unit	Date of Flight	Place or Itinerary
1.	Range – single pilot- round-the-world without refueling	GlobalFlyer	Scaled composite	Steve Fossett	41,467	km	11 February 2006	Cape Canaveral, Florida, Ireland, Florida
2.	Range in straight line	B-52H	USA	Clyde Evilly	2,016.78	km	January 10–11, 1962	Okinawa to Madrid
3.	Range in closed loop	An-124	Ukraine	Vladimir Tereski	20,150.92	km	May 6–7, 1987	Moscow-Tashkand-Bigal-Shakut-Marmensk-Moscow
4.	Ceiling	MiG-25	Ukraine	Alexander Fedotev	123,523	ft	August 31, 1977	—
5.	Maximum speed in straight line	SR-71A	USA	Olden Gorses and George Morgan	3,529.56	km/h	July 28, 1976	Beale AFB, CA
6.	Maximum speed in 1,000 km closed loop	SR-71A	USA	Aldolfs Bolts and John Fuller	3,367.221	km/h	July 27, 1976	Beale AFB, CA
7.	Maximum speed in a 3 km route at limited altitude	F-104RB	USA	Daryl Greenmamayer	1,590.45	km/h	October 24, 1977	Nevada
8.	Maximum speed in 100 km closed loop	MiG-25	Ukraine	Alexander Fedotev	2,605.1	km/h	April 8, 1973	—
9.	Maximum speed in 500 km closed loop	MiG-25	Ukraine	Em Komarof	2,981.5	km/h	October 5, 1967	Moscow
10.	Greatest payload to a height of 2,000 m	An-225 Mryia	Antonov, Ukraine	Aleksandr Galunenko	253,820	kg	September 11, 2001	Ukraine
11.	Speed – single pilot, round-the-world without refueling	GlobalFlyer	Scaled composite	Steve Fossett	297	knot	11 February 2006	From Salina, KS

(*Continued*)

TABLE D.3 (*Continued*)
Flight Records for Aircraft with Jet Engine

No.	Competition	Aircraft	Manufacturer	Pilot	Record	Unit	Date of Flight	Place or Itinerary
12.	Ceiling when launched from mother aircraft	X-15A-3	USA	R. White	314,750	ft	July 17, 1962	Edward AFB, CA

TABLE D.4
Flight Records for Amphibian Aircraft

No.	Competition	Aircraft	Manufacturer	Pilot	Record	Unit	Date of Flight	Place or Itinerary
1.	Range in straight line	Mercury	England	D. Bent and A. Harvey	9,652	km	October 6–8, 1938	Scotland to South Africa
2.	Ceiling	M-10	USSR	George Burianof	49,088	ft	September 9, 1961	Azouf Sea
3.	Maximum speed in straight line	M-10	USSR	Nicolai Androsky	912	km/h	August 7, 1961	Jakofski to Petrofskof

TABLE D.5
Flight Records for Gliders

No.	Competition	Aircraft	Manufacturer	Pilot	Record	Unit	Date of Flight	Place or Itinerary
1.	Range in straight line (one seat)	ASW-12	Germany	Hans grouse	14,608	km	April 25, 1972	—
2.	Ceiling (one seat)	G-102	USA	Robert Harris	49,009	ft	February 17, 1986	—
3.	Range in straight line (two seats)	ASH-25	France	Gerard Herbed and Jin Herbed	1,383	km	April 17, 1992	Venin (France) to Fez (Morocco)
4.	Ceiling (two seats)	PR-G1	USA	Lawrence Edgar and Harold Clifford	44,256	ft	March 19, 1952	Bishop, CA

TABLE D.6
Flight Records for Ultralight Aircraft

No.	Competition	Aircraft	Manufacturer	Pilot	Record	Unit	Date of Flight	Place or Itinerary
1.	Ceiling	U-2 Superwing	USA	Richard Rowley	25,940	ft	September 17, 1983	—
2.	Range in straight line	Quickie	USA	Norman Howl	1,249.52	km	April 9, 1987	—
3.	Maximum speed in straight line	Moni	USA	David Green	189.21	km/h	October 23, 1985	km route

TABLE D.7
Flight Records for Helicopters

No.	Competition	Aircraft	Manufacturer	Pilot	Record	Unit	Date of Flight	Place or Itinerary
1.	Range in straight line	YOH-6A	USA	R. Ferry	3,561.55	km	April 6–7, 1966	—
2.	Ceiling	SA 315B Lama	France	Jin Bolt	40,820	ft	June 21, 1972	—
3.	Maximum speed in straight line	Lynx	England	Trevor Eginton and Derek Clouse	400.87	km/h	August 11, 1986	15.25 km route
4.	Maximum speed in 1,000 km closed loop	Mi-6	USSR	Boris Galtisky	340.15	km/h	August 26, 1964	Moscow
5.	Maximum speed in 500 km closed loop	S-76A	USA	Tomas Devil	345.74	km/h	February 8, 1982	Palm Beach, FL

TABLE D.8
Flight Records for Autogyros

No.	Competition	Aircraft	Manufacturer	Pilot	Record	Unit	Date of Flight	Place or Itinerary
1.	Ceiling	WA-121/MC	England	K. Wallis	18,516	ft	July 20, 1982	—
2.	Range in straight line	WA-116/F	England	K. Wallis	847.32	km	September 28, 1975	Lirta airport (Scotland)

(*Continued*)

TABLE D.8 (*Continued*)
Flight Records for Autogyros

No.	Competition	Aircraft	Manufacturer	Pilot	Record	Unit	Date of Flight	Place or Itinerary
3.	Range in closed loop	WA-116/F	England	K. Wallis	1,002.75	km	August 5, 1988	—
4.	Maximum speed in straight line	WA-116/F	England	K. Wallis	193.6	km/h	September 18, 1986	3 km route

TABLE D.9
Flight Records for Free Balloons

No.	Competition	Aircraft	Manufacturer	Pilot	Record	Unit	Date of Flight	Place or Itinerary
1.	Endurance	Cameron R-77	USA	Richard Ebrosor and Terry Bradley	144.25	h	September 16–22, 1992	Bangor (USA) to Sidi Emralkadmiri (Morocco)
2.	Range in straight line	Cameron R-150	USA	Estefan Foust	8,748.11	km	February 22, 1995	Seoul to Canada
3.	Ceiling	Lee Lewis memorial	USA	M. Ross and V. Prather	113,740	ft	May 4, 1961	—

TABLE D.10
Flight Records for Hang Gliders

No.	Competition	Pilot	Record	Unit	Date of flight	Place or itinerary
1.	Straight distance	Dustin B. Martin	764	km	2012	Zapata, Texas
2.	Altitude record for a balloon-launched	Judy Leden	38,800	ft	25 October 1994	Wadi Rum, Jordan
3.	Gain of height	Judy Leden	13,025	ft	1992	

References

Second Edition

1. Lutgens, F. K. and Tarbuck, E. J., *The Atmosphere: An Introduction to Meteorology*, 9th edition, Prentice Hall, Hoboken, NJ, 2004.
2. Aguado, E. and Burt, J. E., *Understanding Weather & Climate*, 2nd edition, Prentice Hall, Hoboken, NJ, 2001.
3. The US Standard Atmosphere, US Government Printing Office, Washington, DC, 1976.
4. Paine, S., *The Am Atmospheric Model*, Smithsonian Astrophysical Observatory, Cambridge, MA, 2014.
5. Stinton, D., The Anatomy of the Airplane, BSP, UK, 1989.
6. Federal Aviation Regulations, US Department of Transportation, Federal Aviation Administration, www.faa.gov.
7. Houghton, E. L. and Carruthers, N. B., *Aerodynamics for Engineering Students*, 5th edition, Elsevier, Oxford, UK, 2003.
8. Mizner, R. A., Champion, K. S. W., and Pond, H. L., *ARDC Model Atmosphere, 1959*, AFCRC-TR-59-267, Air Force Surveys in Geophysics No. 11, Bedford, MA, 1987.
9. Jackson, P., *Jane's All the World's Aircraft*, Jane's Information Group, Coulsdon, UK, 2020.
10. Shevell, R. S., *Fundamentals of Flight*, 2nd edition, Prentice Hall, Hoboken, NJ, 1989.
11. Anderson, J. D., *Introduction to Flight*, 7th edition, McGraw-Hill, New York, 2012.
12. Gurjen Giesen, Physics and Astronomy, Germany, 2007, http://www.jgiesen.de/SME/.
13. Cengel, Y. A. and Cimbala, J. M., *Fluid Mechanics: Fundamentals and Applications*, 3rd edition, McGraw Hill, New York, 2013.
14. Potter, M. C. and Somerton, C. W., *Thermodynamics for Engineers*, McGraw Hill, New York, 1993.
15. El-Rabbany, A., *Introduction to GPS: The Global Positioning System*, 2nd edition, Artech House Publishers, Norwood, MA, 2006.
16. Fisher, F. A. and Plumer, J. A., *Lightning Protection of Aircraft*, NASA Reference Publication 1008, Pittsfield, MA, 1977.
17. Moorhouse, D., MIL-F-8785C, Military Specification: Flying Qualities of Piloted Airplanes, US Department of Defense, OH, 1980.
18. Military Handbook MIL-HDBK-1797, US Air Force, Revised 1997.
19. NASA Sounding Rocket Program Overview, NASA Goddard Space Flight Center, Wallops Flight Facility, Wallops Island, VA, July 2015.
20. American Institute of Aeronautics and Astronautics, *Daily Launch*, March 4, 2013.
21. Roskam, J., *Airplane Flight Dynamics and Automatic Flight Control, Part I*, DAR Corporation, Lawrence, KS, 2007.
22. Stevens, B. L. and Frank, L. L., *Aircraft Control and Simulation*, John Wiley, Hoboken, NJ, 2003.
23. Anderson, J., *Fundamentals of Aerodynamics*, 3rd edition, McGraw-Hill, New York, 2005.
24. Walters, J. M. and Sumwalt, R. L., *Aircraft Accident Analysis: Final Reports*, McGraw-Hill, New York, 2000.
25. Kimberlin, R. D., *Flight Testing of Fixed-Wing Aircraft*, AIAA, Reston, VA, 2003.
26. Crash During Experimental Test Flight, Gulfstream G650, N652GD, NTSB/AAR-12/02, PB2012-910402, National Transportation Safety Board, April 2, 2011.

27. Rizzi, A., Jirásek, A., Lamar, J. E., Crippa, S., Badcock, K. J., and Boelens, O. J., Lessons Learned from Numerical Simulations of the F-16XL Aircraft at Flight Conditions, *Journal of Aircraft*, *46*(2), 423–441, 2009.
28. Cavallok, B., Subsonic Drag Estimation Methods, Report no. NADCAW-6604, US Naval Air Development Center, 1966.
29. Nicolai, L. and Garichner, G., *Fundamentals of Aircraft and Airship Design, Vol. I-Aircraft Design*, AIAA, Reston, VA, 2010.
30. Hoak, D. E., USAF Stability and Control DatCom, Air Force Flight Dynamics Laboratory, Wright-Patterson Air Force Base, Dayton, OH, 1978.
31. Kuchemann, D., *Aerodynamic Design of Aircraft*, Pergamon Press, Oxford, UK, 1978.
32. Abbott, I. H. and Von Doenhoff, A. E., *Theory of Wing Sections*, Dover, Mineola, NY, 1959.
33. Roskam, J., *Airplane Design*, Vol. VI, DAR Corp., Lawrence, KS, 2004.
34. Ross, R. and Neal, R. D., Learjet model 25 drag analysis, *Proceeding of the NASA-Industry-University GA Drag Reduction Workshop*, Lawrence, KS, July14–16, 1975.
35. Horner, S. R., *Fluid-Dynamic Drag*, Midland Park, New Jersey, 1965.
36. McCormick, B. W., *Aerodynamics; Aeronautics; and Flight Dynamics*, John Wiley, Hoboken, NJ, 1995.
37. Smith, A. and Kaups, K., Aerodynamics of surface roughness and imperfections, SAE Technical Paper 680198, Society of Automotive Engineers, New York, 1968. doi: 10.4271/680198.
38. Vorburger, T. V. and Raja, J., Surface finish metrology tutorial, NISTIR-4088, U.S. Department of Commerce, Gaithersburg, MD, 1990.
39. Katz, J. and Plotkin, A., *Low-Speed Aerodynamics*, 2nd edition, Cambridge University Press, Cambridge, UK, 2001.
40. Bolkcom, C., Air force aerial refueling methods: Flying boom versus hose-and-drogue, CRS Report for Congress, Congressional Research Service, Washington, DC, 2006.
41. American Institute of Aeronautics and Astronautics, *Daily Launch,* April 21, 2020.
42. AIRLINERS, www.airliners.net.
43. Lan, E. C. and Roskam, J., *Airplane Aerodynamics and Performance*, DAR Corp., Lawrence, KS, 2003.
44. Anderson, J., *Modern Compressible Flow*, 3rd edition, McGraw-Hill, New York, 2005.
45. Moony Airplane Company, Inc., *Moony Pilot's Operating Handbook and Airplane Flight Manual,* Moony Airplane Company, Inc., Kerrville, TX, 2008.
46. Gunston, B., *Piston Aero Engines*, PSL, Patrick Stephens Ltd, Somerset, UK, 1999.
47. Raymer, D. P., *Aircraft Design: A Conceptual Approach*, AIAA, Reston, VA, 2006.
48. Mattingly, J. D., *Elements of Propulsion: Gas Turbine and Rockets*, AIAA, Reston, VA, 2006.
49. American Institute of Aeronautics and Astronautics, Daily Launch, Reston, VA, February 20, 2014.
50. Flack, R. D., *Fundamentals of Jet Propulsion*, Cambridge Aerospace Series, Cambridge University Press, Cambridge, UK, 2005.
51. FlightGlobal, *Flight International*, Weekly Magazine, Reed Business Publication, January7–13, 1998.
52. Kroes, M. J. and Wild, T. W., *Aircraft Powerplants*, 7th edition, McGraw-Hill, New York, 1995.
53. Hill, P. and Peterson, C., *Mechanics and Thermodynamics of Propulsion*, 2nd edition, Addison Wesley, Reading, MA, 1992.
54. Farokhi, S., *Aircraft Propulsion*, Wiley, Hoboken, NJ, 2009.
55. Avco Lycoming O-320, *Operator's Manual*, Avco Corporation, Williamsport Division, Delaware, Greenwich, CO, 1973.
56. Anderson, J., *Aircraft Performance and Design*, McGraw-Hill, New York, 1999.

57. Anonymous, *Cherokee Arrow Pilot's Operating Manual*, Piper Company, Vero Beach, FL, 1973.
58. Dorf, R. C. and Svoboda, J. A., *Introduction to Electric Circuits*, 9th edition, Wiley, Hoboken, NJ, 2013.
59. Phillips, W. F., *Mechanics of Flight*, 2nd edition, John Wiley, Hoboken, NJ, 2010.
60. Freeman, H. B., Comparison of full-scale propellers having R.A.F.-6 and Clark Y airfoil sections, NACA Report No. 378, Inglewood, CA, 1932.
61. Hartman, E. and Biermann, D., The aerodynamic characteristics of full-scale propellers having 2, 3, and 4 blades of Clark Y and R.A.F. 6 Airfoil Sections, NACA Report No. 640, Inglewood, CA, 1938.
62. Naftel, J. C., *NASA Global Hawk: Project Overview and Future Plans*, NASA Dryden Flight Research Center, Palmdale, CA, 2011.
63. Gulfstream Aerospace Corporation. *Flight Operations, Operating Manual Supplement for G350, G450, G500 and G550 Airplanes*, Gulfstream Aerospace Corporation, Atlanta, GA, 2012.
64. Virgin Atlantic GlobalFlyer, Steve Fossett's adventure challenges, 2008, http://www.strangebirds.com/Steve-Fossett.html.
65. Krivinyi, N., *Taschenbuch der Luftflotten 1994/95 Warplanes of the Worlds*, Bernard & Graefe Verlag, Bonn, Germany, 1994.
66. Hale, F. J., *Introduction to Aircraft Performance, Selection and Design*, John Wiley, Hoboken, NJ, 1984.
67. Carson, B. H., Fuel efficiency of small aircraft, AIAA-80-1847, AIAA Aircraft Meeting, Anaheim, CA, August 4–6, 1980.
68. American Institute of Aeronautics and Astronautics, *Daily Launch*, January 1, 2018.
69. Spiegel, M. R., *Schaum's Mathematical Handbook of Formulas and Tables, Schaum's Outlines*, 2nd edition, McGraw-Hill, New York, 1998.
70. Aircraft Commerce, *Aircraft Operator's & Owner's Guide: ERJ-135/-140/-145*, Nimrod Publications Ltd, West Sussex, UK, 2009.
71. Menon, P. K., Study of Aircraft Cruise, *Journal of Guidance, Control and Dynamics*, *12*(5), 631–639, 1989.
72. Airbus Industries, Airbus A318/A319/A320/A321 Flight Crew Operating Manual, Blagnac, France, 2008.
73. Werner, D., *FAA Struggles to Control Small Drone Rollouts*, Aerospace America, American Institute of Aeronautics and Astronautics, Reston, VA, 2014, pp. 39–43.
74. Ardema, M. D. and Asuncion, B. C., Flight path optimization at constant altitude, Chapter 2, in: Buttazzo, G. and Frediani, A. (eds.), *Variational Analysis and Aerospace Engineering*, Springer Optimization and Its Applications (pp. 21–32), Springer, Berlin, Germany, 2009.
75. American Institute of Aeronautics and Astronautics, *Daily Launch*, Piper Company Publication, Vero Beach, FL, June 12, 2013.
76. Pilatus Aircraft Ltd, PC-9 M Factsheet, Pilatus Aircraft Company Publication, Stans, Switzerland, 2002.
77. Beechcraft/Raytheon Aircraft, Beech Starship 1 Model 2000 Airplane, Flight Manual, Beechcraft/Raytheon Aircraft, Wichita, KS, 1993.
78. NAVAIR, Lockheed C-130 Hercules, Standard Aircraft Characteristics, Commander of the Naval Air System Command, Saint Mary, MD, 1967.
79. Cessna 172, *Pilot's Operating Handbook*, Cessna Aircraft Company, Wichita, KS, 1978.
80. Roberson, W. and Johns, J. A., Fuel conservation strategies: Takeoff and climb, *AERO Magazine*, Boeing, 2007.
81. U.S. Department of Transportation, Federal Aviation Administration, *Airplane Flying Handbook*, FAA-H-8083-3A, US Department of Transportation, Federal Aviation Administration, Washington, DC, 2004.

82. Kreshner, W. K., *The Instrument Flight Manual*, Iowa State University Press, Ames, IA, 1991.
83. Beer, F., Johnston, R., Mazurex, D., Cornwell, P., and Eisenberg, E., *Vector Mechanics for Engineering: Statics & Dynamics*, 9th edition, McGraw-Hill, New York, 2009.
84. Zhang, X. and Zerihan, J., Off-Surface Aerodynamic Measurements of a Wing in Ground Effect, *Journal of Aircraft*, *40*(4), 716–725, 2003.
85. Anonymous, *Flying Qualities of Piloted Airplanes*, Air Force Flight Dynamic Laboratory, WPAFB, Dayton, OH, 1990.
86. Anonymous, *P180 II Avanti Specification and Description*, Piaggio Aero Industries, Genoa, Italy, 2005.
87. Federal Aviation Administration, Federal Aviation Regulations, Part 23: Airworthiness standards for airplanes in the normal, utility, aerobatic, and commuter categories, 1984.
88. U.S. Department of Transportation, *Federal Aviation Administration, Flight Instrument Flying Handbook, Standards Service, FAA-H-8083-15B*, US Department of Transportation, Federal Aviation Administration, Washington, DC, 2012.
89. Aircraft Operations, *Doc 8168 (PANS-OPS)*, 5th edition, International Civil Aviation Organization, Montréal, Quebec, Canada, 2006.
90. Anonymous, MIL-F-1797C, Flying qualities of piloted airplanes, Air Force Flight Dynamic Laboratory, WPAFB, Dayton, OH, 1990.
91. Agard WG19, Operational agility, AGARD AR-314, April 1994.
92. Blaye, P. L., Agility: History, definitions and basic concepts, Defense Technical Information Center, Report ADPO10448, WPAFB, Dayton, OH, 2000.
93. Joyce, D. A., *Flying Beyond the Stall: The X-31 and the Advent of Supermaneuvrability*, NASA, Washington, DC, 2014.
94. Eden, P., *The Encyclopedia of Modern Military Aircraft*, Amber Books, London, UK, 2004.
95. Paul, M. B., Genesis of the F-35 Joint Strike Fighter, *Journal of Aircraft*, *46*(6), 1825–1836, 2009.
96. Gertler, J., F-35 Joint Strike Fighter (JSF) Program, Congressional Research Service 7–5700, Congressional Research Service, Washington, DC, 2014.
97. Advisory Group for Aerospace Research and Development, Current concepts on G-protection research and development, LS-202, AGARD, Neuilly-sur-Seine, France, 1995.
98. Federal Aviation Administration, Federal Aviation Regulations, Part 25: Airworthiness standards for airplanes in the transport category, 1984.
99. Attaway, S., *MATLAB: A Practical Introduction to Programming and Problem Solving*, 3rd edition, Butterworth-Heinemann, Burlington, MA, 2013.
100. Moler, C. B., *Numerical Computing with MATLAB*, Society for Industrial & Applied Mathematics, Philadelphia, PA, 2012.
101. MATLAB 15; R2015a, The MathWorks Inc., Natick, MA, 2015.
102. Gilat, A., *MATLAB: An Introduction with Applications*, 5th edition, John Wiley & Sons, Hoboken, NJ, 2014.
103. Chapman, S. J., *MATLAB Programming for Engineers*, 5th edition, CL Engineering, New Delhi, India, 2015.
104. MathWorks®, http://www.mathworks.com.

Index